ENGINEERING DIVISION LIBRARY

Property of
Flood Control District of MC Library
Please Return to
2801 W. Durango
Phoenix, AZ 85009

PREPRINTS OF THE INTERNATIONAL RIPRAP WORKSHOP

THEORY, POLICY AND PRACTICE OF EROSION CONTROL USING RIPRAP, ARMOUR STONE AND RUBBLE

FORT COLLINS
COLORADO
UNITED STATES
12 - 16 JULY 1993

VOLUME I

PRODUCED BY:
DELFT GEOTECHNICS
P.O. BOX 69
2600 AB DELFT
THE NETHERLANDS

Sponsored by

Colorado State University
Department of Civil Engineering
United States

Construction Industry Research and Information Association
United Kingdom

Delft Geotechnics
The Netherlands

Rijkswaterstaat
The Netherlands

University of Nottingham
Department of Geography
United Kingdom

Organizing committee

Colin R. Thorne
University of Nottingham
United Kingdom

Steven R. Abt
Colorado State University
United States

Frans B.J. Barends
Delft Geotechnics
The Netherlands

Krystian Pilarczyk
Rijkswaterstaat
The Netherlands

Stephen T. Maynord
US Army Corps of Engineers
United States

Garry Stephenson
Construction Industry
United Kingdom

CONTENT Page

J. Aguirre-Pe, R. Fuentes
Stability and weak motion of riprap at a channel bed 6

A.F. Ahmed, F. El-Gamal, M.M. Gasser
Deterministic and probabilistic design approaches of riprap as bank protection 37

J.P. Ahrens
Design considerations for dynamic revetments 55

G.J. Akkerman, E. Berendsen
Experimental validation of stability criteria for the design of rockfill closure dams 77

N.W.H. Allsop
Stability of rock armour and riprap on coastal structures 99

K.J. Bakker, M.B. de Groot, H.J. Verheij
A simple design relation for geometric open filters in bed protections 120

F.B.J. Barends
Geotechnical stability of riprap structures 125

N.G. Bhowmik
Evaluation and utilization of biotechnical techniques and willow posts for stabilizing eroding streambanks 163

R.E.A.M. Boeters, F.C.M. van der Knaap, H.J. Verheij
Behaviour of armour layers of riprap bank protections along navigation channels 193

K. Bruxvoort
Use of the 1991 Corps of Engineers riprap design procedure in mine reclamation 207

F.W. Chamberlin, M.S. Meyers
A case study of the use of riprap in Rochester, Minnesota 219

CONTENT Page

B.A. Christensen
Optimum design of riprap protected trapezoidal channels 239

A.J. Combe, C.W. Soileau
Mississippi River - Gulf outlet, tests of riprap bank stabilization 257

E.A. Dardeau Jr, K.J. Killgore Jr, A.C. Miller
Using riprap to create or improve riverine habitat 258

M.L. Dove
Standardized riprap gradations 274

K.K. Duskaev
Principles of stone stability and the probability of stone break 275

A. El-Fiky, A. El-Mongy, A.M. Talaat, M.M. Anwar
Wave energy dissipation by composite breakwater 288

A.A. El-Sayad, E.A. Abdel-Hafiez, A.M. Talaat
Effect of flow on riprap protected beds 305

A. Franken, R.E. Jorissen, H.E. Klatter
Design rules for the use of riprap in closure works 315

V.J. Galay, M. Zaki Abo El Fotouh, M. El Moattassem
Pilot project for bank protection along the river Nile 326

D.H. Gray, R.D. Hryciw
Biotechnical stabilization of coastal landforms 341

M.B. de Groot, J. Lindenberg
Pore pressures in riprap structures due to non-stationary loads 357

M.B. de Groot, P. Meijers
Wave induced sliding of revetments 375

D.J. Hagerty, A.C. Parola
Seepage effects in riprap armored embankments 381

CONTENT Page

J. Haltiner, P. Williams & Associates Ltd
Environmentally sensitive approaches to river channel management 398

F. Heezen
Risk analysis of a closure design: A case study 416

J.E. Hite
Design, repair, and rehabilitation of scour protection. Downstream from Inland. Navigation dam stilling basins 437

J. van 't Hoff, M. Lindo, W.H. Tutuarima
Construction aspects of rock structures 459

R.E. Jorissen, D.P. De Wilde, E. Berendsen
Design of the bed protection of the Rotterdam storm surge barrier 480

G.J. Laan
Quality and quality control of stone for hydraulic structures 494

R.J. Larson, G.A. Nicholson
Durability index for protection stone: A concept 526

J.P. Latham, G.G. Gauss
The drop test for armourstone integrity 527

STABILITY AND WEAK MOTION OF RIPRAP AT A CHANNEL BED

J. Aguirre-Pe and R. Fuentes
Laboratorio de Hidráulica, facultad de Ingeniería
Universidad de Los Andes
Apartado 45, Mérida 5101-A, Venezuela

ABSTRACT

This paper is first concerned with the initiation of motion of big particles at the bed of a channel. Because the authors have previously demonstrated that the Shields criterion is not applicable when the ratio of flow depth to bed particle diameter is less than 10 (macro-rough flow), they here propose a critical Froude number of the particles, based on a critical mean velocity of flow, as a suitable criterion for the initiation of motion. Critical Froude numbers of the particles were obtained after calibration with available laboratory data. The proposed criterion is compared with other formulations which consider critical shear stress, critical mean velocity or critical discharge. Experimental weak transport of large sediment particles, initially at rest and at the bed of a laboratory flume under torrential flow is then presented. A weak transport predictor is obtained as a function of parameters that define macro-rough flow. The proposed relationship is tested against riprap data. It is found that it exhibits a better behavior than other transport predictors.

INTRODUCTION

The stability of riprap on margins and beds of channels and rivers has been commonly considered to be a function of the threshold shear stress required to initiate motion of individual particles (Simons and Sentürk, 1976). Even though the concept of threshold or critical shear stress gained a solid support with the study and solution by Shields (1936), it is known that in most experiments conducted to obtain critical shear stress, fine particles corresponding to sand diameters were used. Shear stress is related to the relative thickness of the laminar sublayer of the boundary layer, but boundary layer theory loses physical meaning on boundaries with large

relative roughness of say d/D < 10 in which d is the mean depth of flow, and D a characteristic diameter of particles at the bed.

Breusers (1982) conducted a comprehensive review of equations proposed to predict the critical mean velocity Uc required to move stones. In general, these relationships may be rewritten to express a critical Froude number of the particles $F_c^* = Uc / (g \Delta D)^{1/2}$, as a function of d/D, with g being the acceleration due to gravity, and $\Delta = \rho_s/\rho - 1$, where ρ_s is the density of the solid particles and ρ the fluid density.

As the mean velocity of flow is related to bed resistance, it is convenient to consider which are the appropriate resistance functions that might be applied to flow on a riprap bed.

After discussing the resistance and initiation of motion problems, this paper analyzes different formulations to estimate transport of large particles. A comparison of the most appropriate relationships to estimate sediment discharge in macro-rough flow is also presented. Formulations by Meyer-Peter and Müller (1948), Ackers and White (1973), Smart and Jaeggi (1983), Bathurst *et al.* (1983), Van Rijn (1987) and Mora *et al.* (1990) are considered. Formulae are compared against gravel and riprap experimental transport for flows with high relative rugosities ($d/D_{50} <\simeq 10$). For the highest relative rugosities ($d/D_{50} <\simeq 6.5$), sediment discharge relationships tend to overestimate experimental transport. Because of this, a calibration of transport relationships was performed for two riprap sizes and an equation for weak riprap transport was obtained as a function of discharge in excess of critical discharge. Formation of antidunes and massive sediment transport result to be a function of dimensionless discharge and of the slope of the energy line.

FLOW RESISTANCE

The Nikuradse's sand-roughness standard --normally used to describe roughness and resistance in pipes --was extended to open-channel by Keulegan (1938) and others (*e.g.*, Einstein, 1944; Simons and Sentürk, 1976). The corresponding boundary layer theory, however, is not adequate for describing resistance to flow in channels for which the size of roughness elements is comparable to mean depth.

Among the most used formulations for flow resistance of macro-rough flows are those that express resistance as a function of the logarithm of

relative roughness D/d or of D/R, in which R is the hydraulic radius. These formulations may be expressed in the general Keulegan's form as:

$$\frac{U}{u^*} = C^* = \left[\frac{8}{f}\right]^{1/2} = 5.75 \log\left[\frac{a\,R}{\alpha\,D}\right] \qquad (1)$$

in which U is the mean velocity of flow, u* the mean shear velocity at the boundaries, C^* the dimensionless Chezy coefficient, f the Darcy-Weisbach friction factor, a a function of channel or river shape varying from 11.1 for hydraulically wide shapes to 13.5 for semicircular sections, and α is a texture factor that depends on the characteristic diameter selected for the functional relationship. The product α D in Eq.1 plays the same role as Nikuradse's standard k_s in Keulegan's equation. In Table 1 texture factors obtained from relationships recommended by different authors are provided for high gradient channel flow on macro-rough boundaries. Specific formulations by Kamphuis (1974), Hey (1979), Griffiths (1981) and Jaeggi (1983) were obtained for riprap consisting of gravel or crushed stone particles.

Eq.1 does not show the influence which the form and distribution of particles spread on the bed exert on friction factors. This explains why different values of α may be obtained for the same characteristic diameter of bed particles and why other structures for resistance equations have been proposed.

Indeed, Maynord (1991) conducted a comprehensive analysis of resistance equations applicable to riprap boundaries and found that the theoretical coefficient 5.75 in Eq.1 would transform into 3.92 for the best fit logarithmic equation. Thompson and Campbell (1979), studying a temporary boulder-bed spillway, introduced a corrective factor in Eq.1 which takes into account blocking effects on flow caused by protruding particles. Their experimental relationship is given as:

$$\left[\frac{8}{f}\right]^{1/2} = 5.66\left[1 - \frac{0.1\,k_s}{R}\right]\log\left[\frac{12\,R}{k_s}\right] \qquad (2)$$

in which $k_s = 4.5\,D_{50}$. Bathurst (1978) proposed a different relationship given by:

$$\left[\frac{8}{f}\right]^{1/2} = \left[\frac{R}{0.365\,D_{84}}\right]^{2.94}\left[\frac{W}{d}\right]^{(7Lo-0.56)} \qquad (3)$$

where W is the water surface width and Le the ratio of the frontal cross-sectional area of elements to the area of the bed. In practical terms, Bathurst related roughness concentration to relative submergence as:

$$Le = 0.039 - 0.139 \log \left(\frac{R}{D_{84}} \right) \qquad (4)$$

for $R/D_{84} < 1.2$ in high slope and shallow water rivers (Bathurst, 1982).

Other researchers have calibrated relationships based on a power form of the resistance equations. Bray (1979, 1982) presented Kellerhals' (1967) functional relationship for paved gravel-bed rivers as:

$$f^{1/2} = c \left(\frac{d}{D} \right)^{m} \qquad (5)$$

in which c and m are numerical coefficients that depend on the characteristic diameter. In Table 2, values of c and m for Kellerhals and Bray functional relationships are provided.

Manning coefficient n may substitute Darcy-Weisbach friction factor considering that:

$$\left(\frac{8}{f} \right)^{1/2} = \frac{K R^{1/6}}{n g^{1/2}} \qquad (6)$$

in which K is a constant that takes the value of 1 in the International Unit System and of 1.486 in the British Unit System. It is clear then that there are as many functional relationships for n as there are for f. Jarret (1984) obtained channel roughness by the Manning formula from 75 current-meter measurements of discharge at 21 high-gradient natural stream sites. In particular, Limerinos' equation (1970) has been used for gravel bed rivers and for riprap boundaries; this equation is expressed as:

$$n = \frac{a_1 d^{1/6}}{1.16 + 2.00 \log(d/D_{84})} \qquad (7)$$

where the mean depth replaces the hydraulic radius originally used by Limerinos, a_1 being equal to 0.113 if d is given in feet, and to 0.0927 if d is measured in meters.

Equations for macro-rough flow may generate deviations of up to 30% when

applied to rivers but of less than 15% when applied to well aligned channels. Discrepancies between experiments and formulae arise because resistance to flow is related to randomness of the pattern and spacing of those roughness elements that protrude from the mean bed and produce additional drag to that of uniform beds.

To introduce additional calibration elements in the logarithmic relationships for resistance, Aguirre-Pe and Fuentes (1990) took into account the fact that in the lower portion of flow in steep rough streams close to the bed, there is a wake zone that modifies the logarithmic profile as was suggested by Montes (1968) and later corraborated by Aguirre-Pe *et al.* (1986a) and Schreider (1988). Two zones are identified in the flow field: In the first zone, close to the top of the roughness elements and containing the overlapping wakes generated by them, the velocity u_i in the direction of the flow is taken to be essentially constant, as shown in Figs.1 and 2. This zone is first assumed to be of a thickness proportional to the diameter D of the roughness elements by a linear factor --herein called the wake factor-- denoted by β. A sketch defining the flow in the two zones is shown in Fig.2. In the second zone, located above the first one, the velocity distribution can be described in terms of a power law which is approximated by a logarithmic profile. This bestows some practical importance to the approach and allows comparisons with other commonly used formulations. Provided that the flow below the top of the roughness is negligible, the mean velocity is given by:

$$U = \frac{u_i \beta D}{d} + \frac{1}{d}\int_{\beta D} u\,dy \qquad (8)$$

in which dy is differential of height for which u is defined. The integral term corresponds to the logarithmic zone for which:

$$\frac{u}{u^*} = \frac{1}{\kappa} \ln \frac{y}{\alpha D} + B \qquad (9)$$

where B is an additive function that approaches 8.5 for high shear velocity Reynolds numbers and κ the universal Von Kármán constant. Combining Eqs.8 and 9 yields:

$$C^* = \frac{1}{\kappa} \ln \frac{d}{\alpha D} + B - \frac{1}{\kappa} + \frac{\beta D}{\kappa d} + \frac{\beta D}{d}\left[\frac{u_i}{u^*} - \frac{1}{\kappa} \ln \frac{\beta D}{\alpha D} - B\right] \qquad (10)$$

But, since $u = u_1$ for $y = \beta D$, Eq.10 reduces to:

$$C^* = \frac{1}{\kappa} \ln \frac{d}{\alpha D} + B - \frac{1}{\kappa} + \frac{1}{\kappa} \frac{\beta D}{\kappa d} \qquad (11)$$

and

$$C^* = C_o^* + \frac{1}{\kappa} \frac{\beta D}{d} \qquad (12)$$

in which:

$$C_o^* = \left(\frac{8}{f_o} \right)^{1/2} = \frac{1}{\kappa} \ln \frac{d}{\alpha D} + B - \frac{1}{\kappa} \qquad (13)$$

where C_o^* is the dimensionless Chezy coefficient for a flow without the wake effect related to the Darcy-Weisbach friction factor f_o for low-scale roughness. Eq.13 shows that for high relative roughness, C^* is different from C_o^*.

Laboratory experiments that test the validity of Eq.11 for riprap boundaries have previously been carried out: On the one hand, Aguirre-Pe *et al.* (1990) conducted flume experiments for riprap roughness and for two types of gravel, and on the other, data for sand and gravel beds obtained by Olivero (1984), Kamphuis (1975), Bathurst *et al.* (1984) and Picón (1991) have also been used to test the validity of that equation. Experimental values of the coefficients α and β in Eq.11 may be obtained in the following way:

1. From the known hydraulic parameters, experimental values of $C^* = U/(g\ R\ S)^{1/2}$ are calculated.
2. From an assumed value of α, Eq.13 provides C_o^* values.
3. By linear regression, an equation for the straight line $C^* - C_o^* = f_1\ (D/d)$ is determined.
4. If $C^* - C_o^* \approx 0$ at $D/d = 0$ for this equation, then the assumed value of α is correct and β/κ is given by its slope.
5. If $C^* - C_o^*$ is significantly different from 0 for $D/d = 0$, a new value of α is assumed and the procedure is repeated.

A summary of data for different rugosity patterns with corrected wall effects is presented in Table 3 in which mean values of α and β for D_{50} in

several riprap layers are α_r = 3.2 and β_r = 0.7.

For composite macro-rough flow with varying roughness patterns along the wetted perimeter, Fuentes and Aguirre-Pe (1991) assumed uniform flow in bands of uniform roughness in which conservation of momentum and matching of shear stresses between two successive bands allowed the determination of the friction factor for each roughness through successive iterations. If velocity is assumed uniform in the whole transversal section, then the mentioned algorithm reduces to Einstein's method (1942) that may be written in the general form:

$$P f = \sum P_i f_i \qquad (14)$$

where P and f are the total wetted perimeter and the bulk friction factor respectively, and where P_i, f_i represent the wetted perimeter and the friction factor for each of the different rugosities.

RIPRAP STABILITY AT THE BED OF A CHANNEL

The equilibrium of a particle on a stream bed is governed by the balance of destabilizing drag and lift forces and the stabilizing forces of gravity and particle interlock. As early as 1753, Brahms observed a one-sixth power relationship between mean flow velocity and the weight of a particle whose motion had just started.

The best known relationship which describes the initiation of motion was proposed by Shields (1936) who, in order to define critical shear stress by extrapolating to zero the transport of solid particles, correlated rates of sediment transport with mean bed shear stress. He related dimensionless critical shear stress to a particle Reynolds number which was in turn related to the relative thickness of the laminar sub-layer of the boundary layer. But the boundary layer, as considered by the familiar theory, loses physical meaning in steep streams with large relative roughness of, say, d/D < 10.

The one sixth power law by Brahms corresponds to a relationship of the form $Uc \approx D^{1/2}$, where Uc is the critical mean velocity. Breusers (1982) pointed out that some of the equations that predict a critical mean velocity of flow to move stones, $F_c^* = Uc / (g \Delta D)^{1/2}$, are expressed as functions of log(d/D) or of (d/D) to a power.

Flow in steep rough streams being a stochastic problem of macroturbulent

flow, several difficulties arise when attempts are made to define the critical conditions for the initiation of motion. One of them is related to the definition of threshold of particle motion. Another problem lies in the definition of depth when steep rough flows occur. The first problem may be solved by extrapolating the mean sediment discharge to zero or to a constant small value. The second problem can be avoided (cf. Bathurst *et al.*, 1983) by considering the dimensionless critical discharge as a function of slope only. A different approach consists in defining the depth as the distance from the top of the mean bed particles to the free surface, and to assume that a simple model proposed by Aguirre-Pe and Fuentes (1990) holds valid for a wake region close to the bed.

INITIATION OF PARTICLE MOTION

Critical conditions for the motion of the particles are established when the moment due to the acting forces F of the moving fluid is equated with the moment due to the body forces W around some point (see Fig.2).

Considering the existence of a wake zone close to the bed of constant velocity u_1, the critical conditions on the particle of diameter D_o will be established precisely when:

$$\frac{\rho\, \delta_1\, u_{1c}^2\, D_o^3}{(\rho_s - \rho)\, \delta_2\, g\, D_o^4\, \cos\theta\, (\tan\phi - \tan\theta)} = 1 \qquad (15)$$

where θ is the longitudinal angle of the bed channel, ϕ the friction angle of bed particles, δ_1 and δ_2 factors that depend on the flow velocity near the bed and the shape of the particles. The velocity is supposed to follow the Prandtl-von Kármán logarithmic law for $y \geq \beta D$. Thus, it can be shown, from Aguirre-Pe and Fuentes' wake model (1991), that for $y = \beta D$, we will have:

$$\frac{u_{1c}}{u^*_c} = \frac{1}{\kappa} \ln \frac{\beta D}{\alpha D} + B \qquad (16)$$

where B = 8.5 at high Reynolds numbers of the particles, u^*_c is the critical shear velocity that can be expressed as Uc/C_c^*, and C_c^* the dimensionless critical Chézy coefficient. Substitution of Eq.16 by Eq.15 leads to:

$$F_c^* = \frac{Uc}{(g\ \Delta\ D_o \cos\theta\ (\tan\phi - \tan\theta))^{1/2}} = \frac{(\frac{\delta_2}{\delta_1})^{1/2}}{\frac{1}{\kappa} \ln \frac{\beta}{\alpha} + B} C_c^* \qquad (17)$$

in which α, β and δ_1, δ_2 depend on the shape, the relative size of the elements and the flow conditions.

Since, according to Eq.11

$$C^* = 5.75 \log(\frac{d}{\alpha D}) + 6.0 + 2.5 \frac{\beta D}{d}, \qquad (18)$$

a formulation for the critical Froude number of the particles F_c^* should be given by the functional relationship:

$$F_c^* = \frac{Uc}{(g\ \Delta\ D_o \cos\theta\ (\tan\phi - \tan\theta))^{1/2}} = f_1\ (d/D,\ FF) \qquad (19)$$

where FF are shape factors that describe the particles.

Critical conditions for initiation of motion of riprap particles have been recorded for a relatively long period of time by Aguirre-Pe (1975) and Aguirre-Pe *et al.* (1986b, 1991 and 1992). These experiments as well as the data from Neill (1967), Ashida and Bayazit (1973), Olivero (1984) and Bathurst *et al.* (1983, 1984) for, large relative roughness in the range $0.2 < d/D < 30$ are given in Fig.3.

Classical Shields plots (1936) of dimensionless critical shear stresses are given in Fig.4 for the indicated data. Dimensionless critical shear stresses τ_c^* = d S / Δ D --where S is the mean slope of the energy line-- are presented against critical Reynolds numbers of the particles $R_c^* = \tau_c^{*1/2} D^{*3/2}$, where $D^* = D(g\ \Delta/\ \nu^2)^{1/3}$ in which ν is the kinematic viscosity of fluid. Supporting theoretical considerations, this graph shows that, beyond any doubt, for steep slopes and low relative submergences a constant value for the dimensionless critical shear stress does not exist. Experiments indicate, as was also observed by Bathurst et al. (1983, 1984), that τ_c^* increases as slopes and submergence d / D increase. In fact, as can be seen on Fig. 4, for $D^* \simeq 560$, an experimental variation of τ_c^* between 0.035 and 0.090 is observed, and for $D^* = 1933$ a value as low as $\tau_c^* = 0.02$ is obtained.

In contrast, by inserting Eq.18 into Eq.17, an explicit relationship for F_c^* is obtained. As was discussed above, the particle coefficients involved in Eq.17 are not constant. Accepting minor scatter, the following equation

represents fairly well the experimental data:

$$F_c^* = 0.9 + 0.5 \ln\left(\frac{d}{D_o}\right) + 1.3\,\frac{D_o}{d} \qquad (20)$$

Fitness of Eq.20 may be appraised in Fig. 3. In fact, Eq.20 represents Eq.17 for mean values of $\alpha = 1.8$, $\beta = 2.6$ and $(\delta_2/\delta_1)^{1/2} = 1.9$. This implies that Eq.17 and Eq.20 can be written in the more compact form:

$$F_c^* = \frac{1}{5}\,C_c^* \qquad (21)$$

The critical Froude number of the particles and the dimensionless critical shear stress, modified by the factor $\cos\theta\,(\tan\phi - \tan\theta)$ for steep slopes, are related by the identity:

$$F_c^* = \tau_c^{*1/2}\,C_c^* \qquad (22)$$

In Fig.5 a graph of F_c^* versus d/D is given for $\tau_c^* = 0.04$ and $C_o^* = 2.5 \ln(d/k_s) + 6.0$ as obtained from the classical Keulegan expression (1938), for $k_s = 2D$. Comparison of Eqs.21 and 22 implies that the critical Shields stress $\tau_c^* \simeq$ constant should by modified by the factor $(C_o^*/C^*)^2$ for steep macro-rough flow.

Critical mean velocities for the stability of stones on dams, in revetments, and for riprap beds have been presented by Breusers (1982) and Maynord (1988) as having, for $\cos\theta(\tan\phi - \tan\theta) \cong 1$, the form of:

$$F_c^* = m_1 \log\left(m_2\,\frac{d}{D}\right) \qquad (23)$$

or the form:

$$F_c^* = m_3\left(\frac{d}{D}\right)^{m_4} \qquad (24)$$

where m_1, m_2, m_3 and m_4 are constants which take different values according to different authors. Neill (1967) proposed a safe design curve to avoid scour of coarse uniform bed-material, given in Fig.5 as Eq.24, for $m_3 = 1.58$ and $m_4 = 0.10$. A relationship obtained by Maza and García (1978) can be transformed into Eq.24, taking $m_3 = 1.50$ and $m_4 = 0.15$.

Based on previous work by Schoklitsch (1962) and Bettes (1984), Bathurst *et al.* (1987) found that, for flume data, the non-dimensional critical discharge per unit width $q_c^* = q_c/(g\ D^3)^{1/2}$ --where q_c is the critical discharge per unit width-- is a function of slope, given by:

$$q_c^* = \frac{q_c}{(g\ D_{50}^3)^{1/2}} = 0.15\ S^{-1.12} \qquad (25)$$

which applies to uniform sediment for the slope range $0.0025 < S < 0.20$, with D_{50} being the size of particle median axis. Taking into account that $q_c = U_c\ d$ and $U_c = (g\ d\ S)^{1/2} C^*$, Eq.25 may be rewritten in terms of the critical Froude number of the particles, for $\Delta = 1.65$ and $\cos\theta\ (\tan\phi - \tan\theta) \cong 1$, as:

$$F_c^* = 0.481\ C^{*0.691}\ \left(\frac{d}{D_{50}}\right)^{0.037} \qquad (26)$$

This relationship is presented in Fig.5.

INCIPIENT AND WEAK MOTION

After the critical conditions for the initiation of particle motion are surpassed in a bed formed by loose particles --either because of an increment of slope or depth and the corresponding increment of the mean velocity-- transport of bed particles is established. Two different patterns of transport may be distinguished. The first one occurs at relatively low transport rates for mean velocity of flow not exceeding the mean critical velocity in more than fifty percent. For this condition the bed remains flat and the mode of gravel or riprap transport is for individual grains to roll and jump. This first transport mode may be named as weak or incipient transport. For the second pattern, most of the particles at the bed move and pavement breaks up. Massive displacements of particles in the form of avalanches are produced, and antidunes that travel upstream are generated. This transport mode is present for velocities higher than 1.5 U_c.

In order to analyze the behavior of different existing transport relationships, experimental data for low relative submergences $d/D \leq 10$, obtained by different authors from measurements in laboratory channels were selected from Brownlie's compilation of information (1981) on sediment discharge in open channels. Additional data of gravel and riprap transport

from Smart and Jaeggi (1983), Bathurst *et al.* (1984), and Mora *et al.* (1990) were used. Information regarding analyzed experimental data is displayed in Table 4.

Formulae with mechanical and theoretical basis calibrated for different experiments are chosen. Sediment transport in volume per unit time and unit width q_s may be written in dimensionless form as:

$$\Phi^* = \frac{q_s}{D\,(g\,\Delta\,d)^{1/2}} \qquad (27)$$

in which Φ^* is the Einstein's transport parameter (1942).

Then, the Meyer-Peter and Müller's sediment transport relationship (1948) may be written as:

$$\Phi^* = 8\left(\lambda\,\tau^* - \tau_c^*\right)^{3/2} \qquad (28)$$

in which λ is a numerical factor that depends on sediment and flow conditions, and τ^*, τ_c^* are the Shields parameter and the critical Shields parameter as previously defined.

In its general form, Ackers and White's functional relationship (1973) is given as:

$$\Phi^* = K_1 \left\{ \frac{1}{A} \frac{\tau^{*\,n_1-2}\,F^{*\,1-n_1}}{C_o^{*\,1-n_1}} \sqrt{\frac{D_{50}}{D_{35}}} - 1 \right\}^m C_o^{*\,n_1} \frac{D_{35}}{D_{50}} F^* \qquad (29)$$

where F^* is the densimetric Froude number, K_1, A, m and n_1 are empirical functions of the specific Reynolds number of the grains also called dimensionless diameter D^*. This number is expressed as:

$$D^* = D_{35} \left\{ \frac{\Delta\,g}{\nu^2} \right\}^{1/3} \qquad (30)$$

The dimensionless Chezy coefficient in Ec.29 corresponds to that of a flat bed for high submergence and is given by:

$$C_o^* = \sqrt{32}\,\log\left[\frac{a\,d}{D_{35}}\right] \qquad (31)$$

in which a is a coefficient equal to 10 for flat beds without transport.

Smart and Jaeggi's transport equation (1983) may be expressed by the functional relationship:

$$\Phi^* = 4 \left[\frac{D_{90}}{D_{30}} \right]^{0.2} S^{0.6} C^* \tau^{*0.5} \frac{d}{R} [\tau^* - \tau^*_{cj}] \qquad (32)$$

where τ^*_{cj} is given by:

$$\tau^*_{cj} = \tau^*_c \cos (\arctan S) \left[1 - \frac{S}{\tan \phi} \right] \qquad (33)$$

As may be observed, relationships by Smart and Jaeggi correspond to a more complete version of Meyer-Peter and Müller transport equation.

Van Rijn (1987) proposed the functional relationship:

$$\Phi^* = \frac{0.053}{D_*^{0.3}} \left[\frac{F^{*2}}{C_o^{*2} \tau^*_c} - 1 \right]^{2.1} \qquad (34)$$

in which:

$$C^*_o = 5.75 \log \left[\frac{12 R}{3 D_{90}} \right] \qquad (35)$$

Bathurst *et al.* (1987), considering the structure of former Schoklitsch's relationship (1962), showed that sediment transport may be expressed as a function of slope and of discharge in excess of the critical discharge. In a dimensionless form, in terms of common variables, it may take the form of:

$$\Phi^* = \frac{2.5 S^{3/2}}{(\Delta+1) D_{50} (g \Delta D_{50})^{1/2}} \left[q - q_c \right] \qquad (36)$$

in which q is discharge of water per unit width..

A different transport function based on the concept that sediment transport is a function of the excess of stream power above the critical stream power, was proposed by Mora *et al.* (1990) as calibrated from data mentioned in Table 4. This relationship is given by:

$$\Phi^* = 0.0072\ S\ C^*\ (F^{*2} - F_c^{*2})^{3/2} \qquad (37)$$

In order to compare the performance of the different equations in relation with the data (see Table 4), a statistical analysis was performed to obtain the percentage of the total number of experiments that each formula interprets with an error smaller than a given value. The deviation in percentage is defined as:

n = # of data

$$Dev = 100\ \frac{|\Phi^*_{exp}/\Phi^*_{eq} - 1|}{n}. \qquad (38)$$ (?)

If Pd is the percentage of data, then the mean deviation $\overline{Dev}$ may be represented by a function f_1 of Pd and by the corresponding equation (Eq.) which is being analyzed, *i.e.*,:

$$\overline{Dev} = f_1\ (\ Pd,\ Eq.) \qquad (39)$$

Performance of Eq.39, as may be observed in Fig. 6, is acceptable and comparable to, but not better than, those of Smart and Jaeggi, Bathurst *et al.*, and Ackers and White.

Fig. 6 indicates that the best performance of transport relationships in decreasing order of applicability are those of Smart and Jaeggi (Eq.32), Bathurst *et al.*(Eq.36), Ackers and White (Eq.29), Mora *et al.* (Eq.37), Van Rijn (Eq.34) and Meyer-Peter and Müller (Eq.28).

Eq.36 by Bathurst *et al.* exhibits an important feature: In macro-rough flow, it is easier from a practical point of view, to measure discharge than to measure depths or to estimate shear stresses. Because of this, Picón (1991) and Aguirre-Pe *et al.* (1992) calibrated Bathurst *et al.*'s transport relationship (1987) for the condition of weak motion for small submergences $1.5 < d/D < 6.5$ on mean flat beds composed of riprap particles slopes ranging from 0.02 to 0.06. To take into account the effect of the internal friction angle ϕ and of the slope, the definition of Einstein's transport function (1942) may be modified to the form Φ^*_r given as:

$$\Phi^*_r = \frac{\Phi^*}{(\cos\theta(\tan\phi - \tan\theta))^{1/2}} \qquad (40)$$

The best fit relationship for weak riprap transport on flat beds, as a

function of Bathurst *et al.*'s parameter given as the dimensionless liquid discharge in excess to the critical discharge is given by:

$$\Phi_r^* = 88 \left[\frac{2.5\ (q-q_c)\ S^{1.5}}{(\Delta + 1)\ D_{50}\ (g\ \Delta\ D_{50})^{1/2}} \right]^{5/2} = 88\ B_T^{5/2} \qquad (41)$$

Eq.41 for riprap exhibits an arithmetic mean error of 36% for tested data, and an absolute mean error, $\sum 100\ abs\ (\phi exp/\phi calc-1)$, of 65%. Both errors are smaller than those obtained using other relationships.

In Fig.7, experimental values of transport and the best fit functional relationship corresponding to Eq.41 are given. Abscissa B_T in Fig.7 corresponds to the term between bracketts in Ec.41. For the highest experimental points in Fig.7, antidune bed forms began to develop.

CONCLUSIONS

This study confirms that, for flows in steep rough channels ($S > \approx 1\%$ and $d/D < \approx 10$), the criterion of a constant critical bed-shear stress associated with particle motion is not valid.

A criterion is proposed for determining the critical mean velocity associated with initiation of particle motion in steep rough streams. It is found that F_c^*, critical Froude number of the particles corresponding to Uc, varies strongly for $d/D_{50} < \cong 2$, being the relationship one of proportionality of F_c^* to D/d. For relative submergences $d/D > \approx 4$, F_c^* varies slowly with log(d/D). For relative submergences in the range of 2 to 4, F_c^* has a near constant value of 2.

The concept of a critical Froude number of the particles was first compared with the concept of a critical shear stress. It was found that for $\tau^*_c = 0.04$ and $d/D > 40$, both yield similar results, but that they strongly diverge for low relative submergences .

Criteria of mean critical velocity developed by others tend to describe fairly well the critical conditions for $d/D > 1$. Relatively low values of F_c^* given by Neill's equation for higher d/D are due to the introduction of a safety factor for design purposes.

The critical discharge concept as presented by Bathurst et al. yields values similar to those obtained in the present formulation.

Different relationships for the prediction of sediment transport at low

submergences and high slopes were tested against several data banks and their performance were compared. At very low submergences, d / D < 6.5, on mean flat beds a new relationship is proposed for weak sediment transport.

ACKNOWLEDGEMENTS

The authors wish to acknowledge the support given by the "*Consejo de Desarrollo Científico, Humanístico y Tecnológico*" (CDCHT) of *Universidad de los Andes*" through Grant I-330-90. They are indebted to Dr. Françoise Meyer who proofread the manuscript and to Francisco Rivas who did most of the typing.

REFERENCES

Ackers, P and White, W. R. (1973). "Sediment Transport: New Approach and Analysis", *J. Hydr. Div.*, ASCE, 99, No HY11, 2041-2060.

Aguirre-Pe, J. (1975). "Incipient Erosion in High Gradient Open Channel Flow with Artificial Roughness Elements", *Proc. 16th Congress of the Int. Assoc. for Hydr. Res.*, Sao Paulo, Brazil, 2, 173-180.

Aguirre-Pe, J., Fuentes, R., and Oliveros, M. L. (1986a). "Una Fórmula para la Fricción en Escurrimientos Macrorugosos a Superficie Libre", *Proc., 12th Latin American Congress of the Int. Assoc. for Hydr. Res.*, Sao Paulo, Brazil, 1, 86-95.

Aguirre, J., Fuentes, R. and Olivero, M. L. (1986b). "Influencia de la Rugosidad Relativa y La Densidad Relativa de las Partículas sobre la Velocidad Crítica de Sedimentos Diseminados", *Proc., 13th Latin American Congress of the Int. Assoc. for Hydr. Res.*, La Habana, Cuba, 1, 55 - 66.

Aguirre-Pe, J. and Fuentes, R. (1990). "Resistance to flow in Steep Rough Streams", *J. Hydr. Engrg.*, ASCE, Vol.116, No.11, 1374-1387.

Aguirre-Pe, J., and Fuentes, R. (1991). "Movement of Big Particles in Steep, Macro-rough Streams", *Proc. 24th Congress of the Int. Assoc. for Hydr. Res.*, Madrid, Spain, A, 149-158.

Aguirre-Pe, J., Fuentes, R., Picón, G. and Moncada, A. (1992). "Estudio Experimental de Transporte de Sedimentos Gruesos", *Proc., 15th Latin American Congress of the Int. Assoc. for Hydr. Res.*, Cartagena, Colombia, 3, 129-139.

Ashida, K., and Bayazit, M. (1973). "Initiation of Motion and Roughness of Flows in Steep Channels", *Proc. 15th Congress of the Int. Assoc. for Hydr. Res.*, Istambul, Turkey, 1, 475-484.

Bathurst, J. C. (1978). "Flow Resistance of Large Scale Roughness", *J. Hydr. Div.*, ASCE, 104(12), 1587-1603.

Bathurst, J. C. (1982). "Flow Resistance in Boulder-bed Streams", Chapter 16 of *Gravel-bed Rivers*, Edited by R. D. Hey, J. C. Bathurst and C. R. Thorne, John Wiley and Sons ltd, New York, 443-465.

Bathurst, J. C., Graf, W. H., and Cao, H. H. (1983). "Initiation of Sediment Transport in Steep Channels with Coarse Bed Material", *Mechanics of Sediment Transport*, Edited by Sumer, B. M., and Müller, A., Balkema, Rotterdam, The Netherlands, 207-213.

Bathurst, J. C., Cao, H. H., and Graf, W. H. (1984). "The Data from the EPFL Study of Hydraulics and Sediment Transport in a Steep Flume", EPFL *Report CH-1015*, Lausanne, Switzerland, pp.64.

Bathurst, J. C. (1985). "Flow Resistance Equation in Mountain Rivers", *J. Hydr. Engrg.*, ASCE, 111(4), 1103-1122.

Bathurst, J. C., Graf, W. H., and Cao, H. H. (1987). "Bed Load Discharge Equations for Steep Mountain Rivers", Chapter 15, *Sediment Transport in Gravel-bed Rivers*, Edited by Thorne, C. R., Bathurst, J. C., and Hey, R. D., John Wiley and Sons Ltd., New York, 453-491.

Bettes, R. (1984). "Initiation of Sediment Transport in Gravel Streams", *Proc. Inst. Civ. Engrs.*, 77, 2, 79-88.

Bray, D. I. (1979). "Estimating Average Velocity in Gravel-bed Rivers", *J. Hydr. Div.*, ASCE, 105(9), 1103-1122.

Bray, D. I. (1982). "Flow Resistance in Gravel-bed Rivers", Chapter 6, *Gravel-bed Rivers*, Edited by R. D. Hey, J. C. Thorne, John Wiley and Sons Ltd., New York, 109-137.

Breusers, H. N. C. (1982). *Lecture Notes on Sediment Transport*, International Course in Hydraulic Engineering, Delft, The Netherlands.

Brownlie, W. R. (1981). "Compilation of Alluvial Channel Data: Laboratory and Field", Report No. KH-R-43B, California Institute of Technology, Pasadena, California, U.S.A.

Einstein, H.A. (1942). "Formulas for the Transportation of Bed Load", *Transactions*, ASCE, Vol. 107, Paper 2140, 251-573.

Fuentes, R., and Aguirre-Pe, J. (1991). "Resistance in Composite, Macro-rough Flow", *Proc. 24th Congress of the Int. Assoc. for Hydr. Res.*, Madrid, Spain, A, 243-252.

Graf, W. H. (1984). "Flow Resistance for Steep Mobile

Channels", Semminary "Idraulica del Territorio Montano", Brixen, Italy.

Griffiths, G. A. (1981). "Flow Resistance in Coarse Gravel Bed Rivers", *J. Hydr. Div.*, ASCE, 107(7), 899-918.

Hey, R. D. (1979). "Flow Resistance in Gravel-bed Channels", *J. Hydr. Div.*, ASCE, 105(4), 365-379.

Jaeggi, M. (1983). "Alternierende Kiesbänke", *Mitteilung der Versuchsanstalt für Wasserbau*, Hydrologie und Glaziologie, ETH, Zürich, No. 62.

Jarret, R. D. (1984). "Hydraulics of High-gradient Streams", *J. Hydr. Engrg.*, ASCE, 110(11), 1519-1539.

Kamphuis, J. W. (1974). "Determination of Sand Roughness for Fixed Beds", *J. Hydr. Res.*, ASCE, 12(2), 193-203.

Kellerhals, R. (1967). "Stable Channels with Gravel-Paved Beds.", *J. Wtrways, Harbors and Coast.*, ASCE, No. WW1, 63-84.

Keulegan, G. H. (1938). "Laws of Turbulent Flow in Open Channels", *J. Res. at the Nat. Bureau of Standards, 21, Research Paper RP 1151*, 707-741.

Leopold, L. B., Wolman, M. G. and Miller, J. P. (1964). *Fluvial Processes in Geomorphology*, Freeman, San Francisco, U.S.A., 522 pp.

Limerinos, J. T. (1970). "Determination of the Manning Coefficient for Measured bed Roughness in Natural Channels", Water Supply Paper 1849-B, United States Geological Survey, Washington D. C., U.S.A.

Maynord, S. T. (1988). "Stable Riprap Size for Open Channel Flows", Technical Report HL-88-4, U.S. Army Engrg. Waterways Experiment Station, Vicksburg, Miss., U.S.A.

Maynord, S. T. (1991). "Flow Resistance of Riprap", *J. Hydr. Engrg.*, ASCE, 117(6), 687-696.

Maza, J. A., and García, M. (1978). "Velocidades Medias para el Inicio del Movimiento de Partículas", *Proc., 8th Latin American Congress of the Int. Assoc. for Hydr. Res.*, Quito, Ecuador, 195-206.

Meyer-Peter and Müller, R. (1948). "Formulations of the Bed-load Transport", *2th Congress of the Int. Assoc. for Hydr. Res.*, Stocolm, Sweden, 39-64.

Montes, S. (1968). "Una Nueva Teoría acerca del Escurrimiento Bidimensional sobre un Contorno con Rugosidad Artificial", *Proc., 3rd Latin American Congress of the Int. Assoc. for Hydr. Res.*, La Plata, Argentine, 1, 100-118.

Mora, E., Aguirre-Pe, J. and Fuentes, R. (1990). "Fórmulas de Gasto Sólido para Flujo Macrorugoso", *Proc., 14th Latin American Congress of the Int. Assoc. for Hydr. Res.*, Montevideo, Uruguay, 3, 1537-1548.

Neill, C. R. (1967). "Mean Velocity Criterion for Scour of Coarse Uniform Bed-material", *12th Congress of the Int. Assoc. for Hydr. Res.*, Fort Collins, Colorado, 3, 46-54.

Olivero, M. L. (1984). "Movimiento Incipiente de Partículas en Flujo Torrencial", *Application Report for Associate Professor*, Universidad de los Andes, Mérida, Venezuela, 169 pp.

Picón, G. A.(1991). " Estudio Experimental de Transporte de Sedimentos en Ríos de Montaña", M.Sc. Thesis, Universidad de Los Andes, Mérida, Venezuela, 221 pp.

Schoklitsch, A. (1962). *Handbuch des Wasserbaues*, 3rd edn., Springer-Verlag, Vienna, Austerich.

Schreider, M. I. (1988). "Estimación de la Resistencia en Escurrimientos Macrorugosos", M.Sc. Thesis, Universidad de Los Andes, Mérida, Venezuela, 345 pp.

Shields, A. (1936). "Anwendung der Aehnlichkeitsmechanik der Turbulenzforchung auf die Geschiebebewegung", *Mitt. der Preuss.* Versuchsanstalt für Wasserbau und Schiffbau, Berlin, Germany.

Simons, D. B., and Sentürk, F. (1977). "Sediment Transport Technology", Water Resources Publications, Fort Collins, Colorado 80522, U.S.A., 807 pp.

Smart, G. M. and Jaeggi, M. (1983). "Sediment Transport on Steep Slopes", V.A.W., Mitteil 64, Hidrologie und Glaziologie, E.T.H., Zurich, Switzerland, 191 pp.

Thompson, S. M., and Campbell, P. L. (1979). "Hydraulics of a Large Channel Paved with Boulders", *J. Hydr. Res.*, ASCE, 17(4), 341-354.

Van Rijn, L. C. (1987). "Mathematical Modelling of Morphological Processes in the Case of Suspended Sediment Transport", Delft Hydraulics Communication No. 382.

NOTATION

A constant

a function of channel shape

a_1 constant in Limerinos-Manning equation

B additive function in semilogarithmic velocity distribution

B_T dimensionless excess of discharge, $B_T=2.5(q-q_c)S^{1/5}/((\Delta+1)D_{50}(g\Delta D_{50})^{1/2})$

C^* dimensionless Chézy coefficient

C_o^* dimensionless Chézy coefficient for flow without wake effect

C_c^* dimensionless critical Chézy coefficient

c numerical coefficient

D characteristic diameter of particles at the bed

D_o particle diameter subject to critical conditions

D^* dimensionless diameter of particles

D_{ev} desviation in percentage

$\overline{D_{ev}}$ mean desviation

D_{30} 30th percentile diameter size

D_{35} 35th percentile diameter size

D_{50} mean sediment diameter

D_{80} 80th percentile diameter size

D_{84} 84th percentile diameter size

D_{90} 90th percentile diameter size

d depth of flow

dy differential of heigh for which u is defined

F acting forces

F^* densimetric Froude number

F_c^* critical densimetric Froude number

FF shape factors that describe the particles

f Darcy-Weisbach friction factor

f_o Darcy-Weisbach friction factor for low-scale roughness

f_i friction factor of a band

f_1 function

g acceleration of gravity

K constant in Manning equation

K_1 constant in Ackers and White transport relationship

ks Nikuradse standard grain size

Le concentration of exposed roughness elements

m constant numerical coefficient

m_1 constant numerical coefficient

m_2 constant numerical coefficient

m_3 constant numerical coefficient

m_4 constant numerical coefficient

n Manning coefficient

n_1 empirical constant in Ackers and White transport relationship

P total wetted perimeter

Pd percentage of data

P_i wetted perimeter of a band

q unit discharge of water

q_c critical unit discharge

q_c^* non-dimensional critical unit discharge

q_s volumetric sediment transport per unit width

R hydraulic radius

R_c^* critical Reynolds number of the particles

S longitudinal stream slope

U mean flow velocity

Uc critical mean velocity

u local flow velocity

u_1 assumed constant-flow velocity in wake zone

u_{1c} assumed critical velocity in wake zone

u_* mean shear velocity [$u_* = (gRS)^{1/2}$]

u_{*c} critical mean shear velocity

W water-surface width

y local vertical distance

α texture factor related to Nikuradse standard by $k_s = \alpha D$

α_r texture factor for riprap

β wake factor

β_r wake factor for riprap

Δ apparent relative density ($\Delta = \rho_s/\rho - 1$)

δ_1, δ_2 factors that depend on flow velocity and on particle's shape

Φ_r^* Einstein transport parameter for riprap

Φ_*^* Einstein transport parameter

Φ_{*xp}^* experimental Einstein transport parameter

Φ_{*q}^* Einstein transport parameter as obtained from equations

ϕ friction angle of the bed particles

κ universal Von Kármán constant ($\kappa = 0.407$)

λ numerical factor that depends on sediment and flow conditions

ν kinematic viscosity of fluid

θ longitudinal angle of the bed channel

ρ fluid density

ρ_s density of solid particles

τ^* Shields parameter

τ^*_c critical Shields parameter

Fig.1. Velocity Distributions in Flow Over Cobble Beds

Fig.2. Velocity Distribution and Particle Motion in a Steep Rough Channel

Fig.3. Critical Froude Number of the Particles for the Initiation of Particle Motion

Fig.4. Critical Shear Stresses in Steep Rough Channels

Fig.5. Comparison of Criteria for the Initiation of Particle Motion

Fig.6. Discrepancies of Transport Relationship for Analyzed Data

Fig.7. Weak Riprap Transport

Table 1

Texture Factors α in Eq. 1

Author	D	α	R/D or d/D
Keulegan (1938)	k_s	1	
Leopold *et al.*(1964)	D_{84}	3.57	0.8< d/D <16
Limerinos (1970)	D_{84}	2.98	1< d/D <50
Kamphuis (1974)	D_{90}	2.00	d/D <10
Hey (1979)	D_{84}	3.50	0.8-100
Griffiths (1981)	D_{50}	5.00	5≤ R/D ≤200
Graf (1984)	D_{50}	3.01	R/D <100
Graf (1984)	D_{84}	2.24	R/D <100
Bathurst (1985)	D_{84}	2.24	0.3< d/D <6
Jaeggi (1983)	D_{90}	2.00	10< d/D

Table 2

Power Form of the Friction Factor for Gravel Beds

Author	D	c	m	d/D
Kellerhals (1967)	D_{90}	2.30	0.250	2-200
Bray (1979)	D_{50}	1.36	0.281	2-200
Bray (1979)	D_{65}	1.48	0.276	2-200
Bray (1979)	D_{90}	1.78	0.268	2-200

Table 3

Summary of Data Used to Test Eq. 11 for Riprap.

Author (1)	Channel Width (m) (2)	Type of roughness (3)	Height of roughness (4)	Texture Factor α (5)	Wake Factor β (6)
Kamphuis (1975)	0.38	Gravel $D=D_{90}$	0.005-0.046	2.0	3.0
Olivero (1984)	0.10	Gravel $D=D_{90}$	0.01-0.023	2.5	3.0
Bathurst *et al.*(1984)	0.60	Gravel $D=D_{50}$	0.022	3.8	0.7
Bathurst *et al.*(1984)	0.60	Gravel $D=D_{50}$	0.044	3.3	0.5
Aguirre-Pe *et al.*(1990)	1.00	Cobbles $D=D_{50}$	0.064	1.0	1.0
Aguirre-Pe *et al.*(1990)	1.00	Gravel $D=D_{50}$	0.0464	1.0	0.6
Picón (1991)	1.00	Riprap $D=D_{50}$	0.0175	3.0	0.9
Picón (1991)	1.00	Riprap $D=D_{50}$	0.0386	2.5	0.5

Table 4

Transport at Low Submergences

Experiments	Number of Data	Reference
Gilbert	32	Brownlie (1981)
Bogardi and Yen	47	Brownlie (1981)
Mavis, Liu and Soucek	41	Brownlie (1981)
Bathurst, Cao and Graf	64	Bathurst *et al.*(1984)
Smart and Jaeggi	37	Smart and Jaeggi (1983)
Meyer-Peter and Müller	36	Meyer-Peter, Müller(1948)
Aguirre-Pe	59	Mora *et al.*(1990)

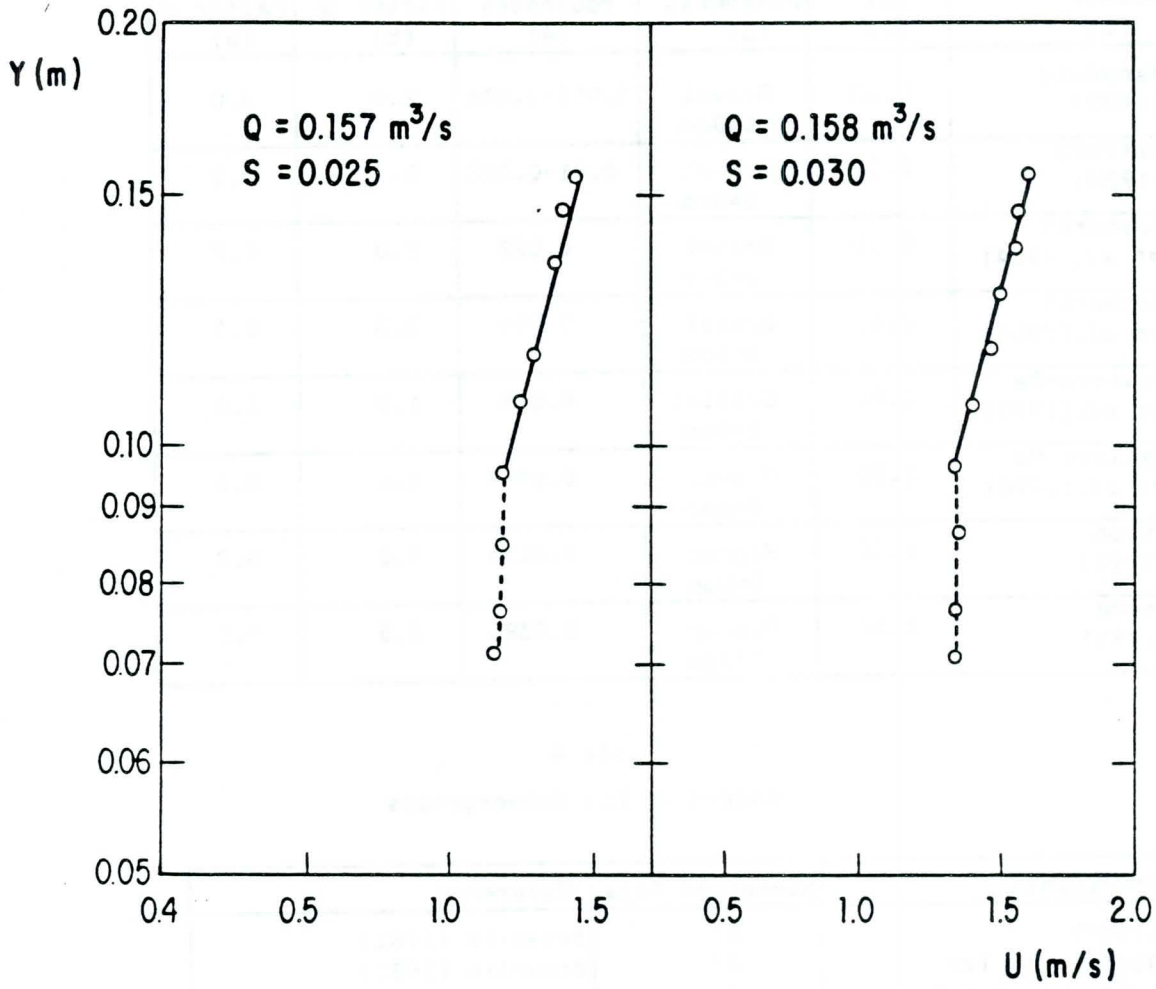
Y (m)
0.20
0.15
0.10
0.09
0.08
0.07
0.06
0.05
Q = 0.157 m³/s
S = 0.025
Q = 0.158 m³/s
S = 0.030
0.4
0.5
1.0
1.5
0.5
1.0
1.5
2.0
U (m/s)

Figure 1.

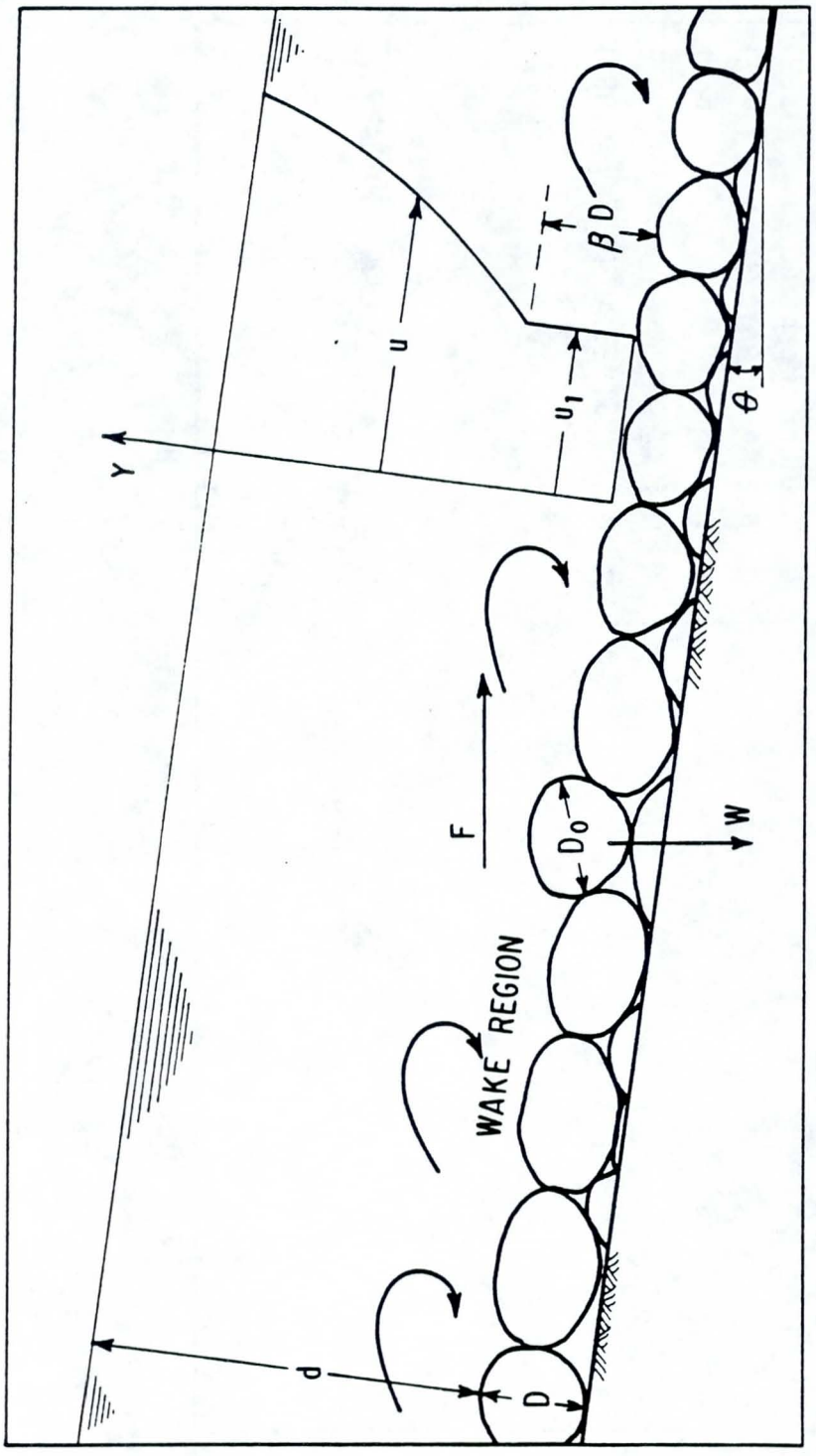

Figure 2.

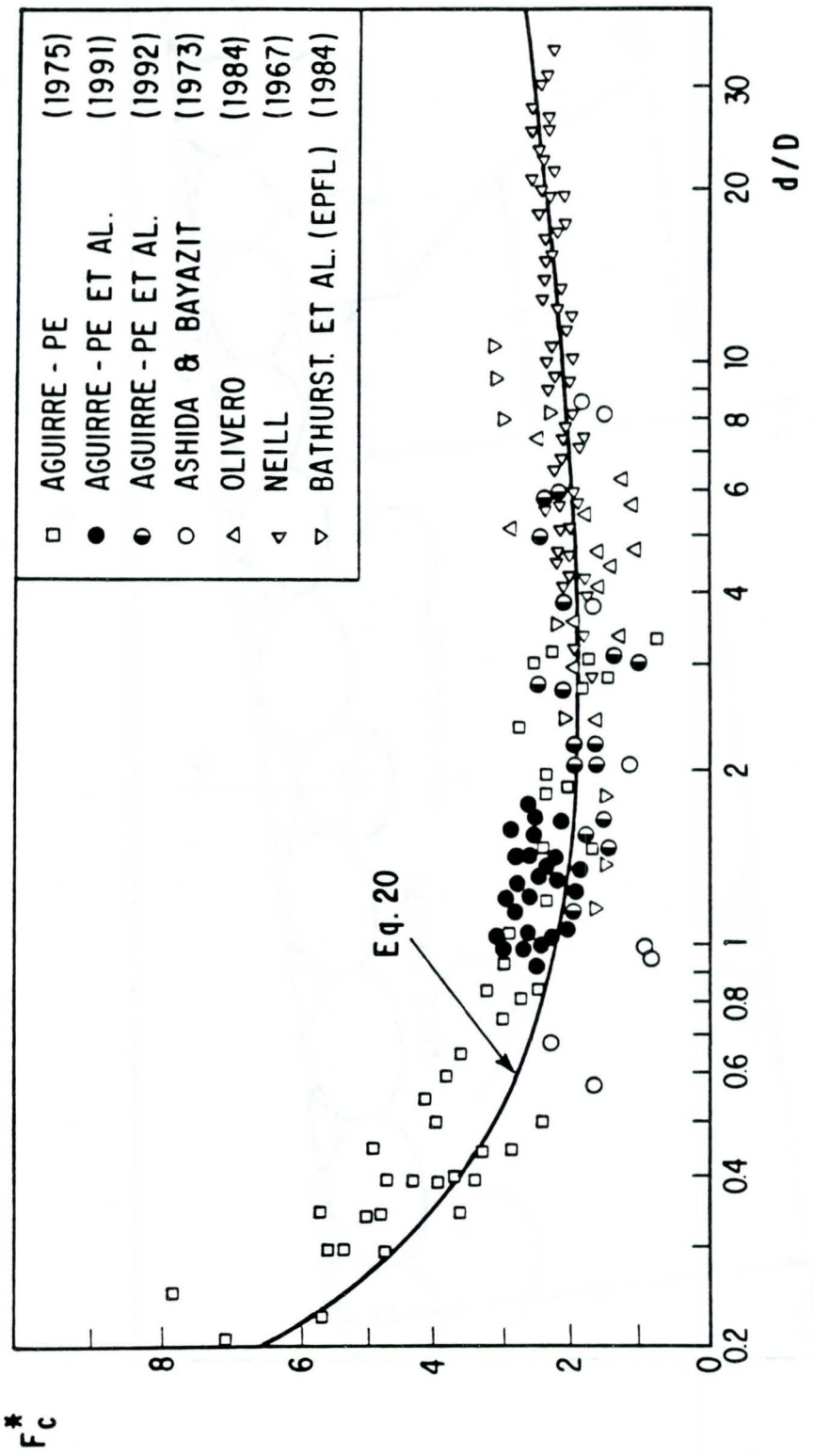
AGUIRRE - PE (1975)
AGUIRRE - PE ET AL. (1991)
AGUIRRE - PE ET AL. (1992)
ASHIDA & BAYAZIT (1973)
OLIVERO (1984)
NEILL (1967)
BATHURST. ET AL. (EPFL) (1984)
Eq. 20
F_c^*
d/D
0
2
4
6
8
0.2
0.4
0.6
0.8
1
2
4
6
8
10
20
30

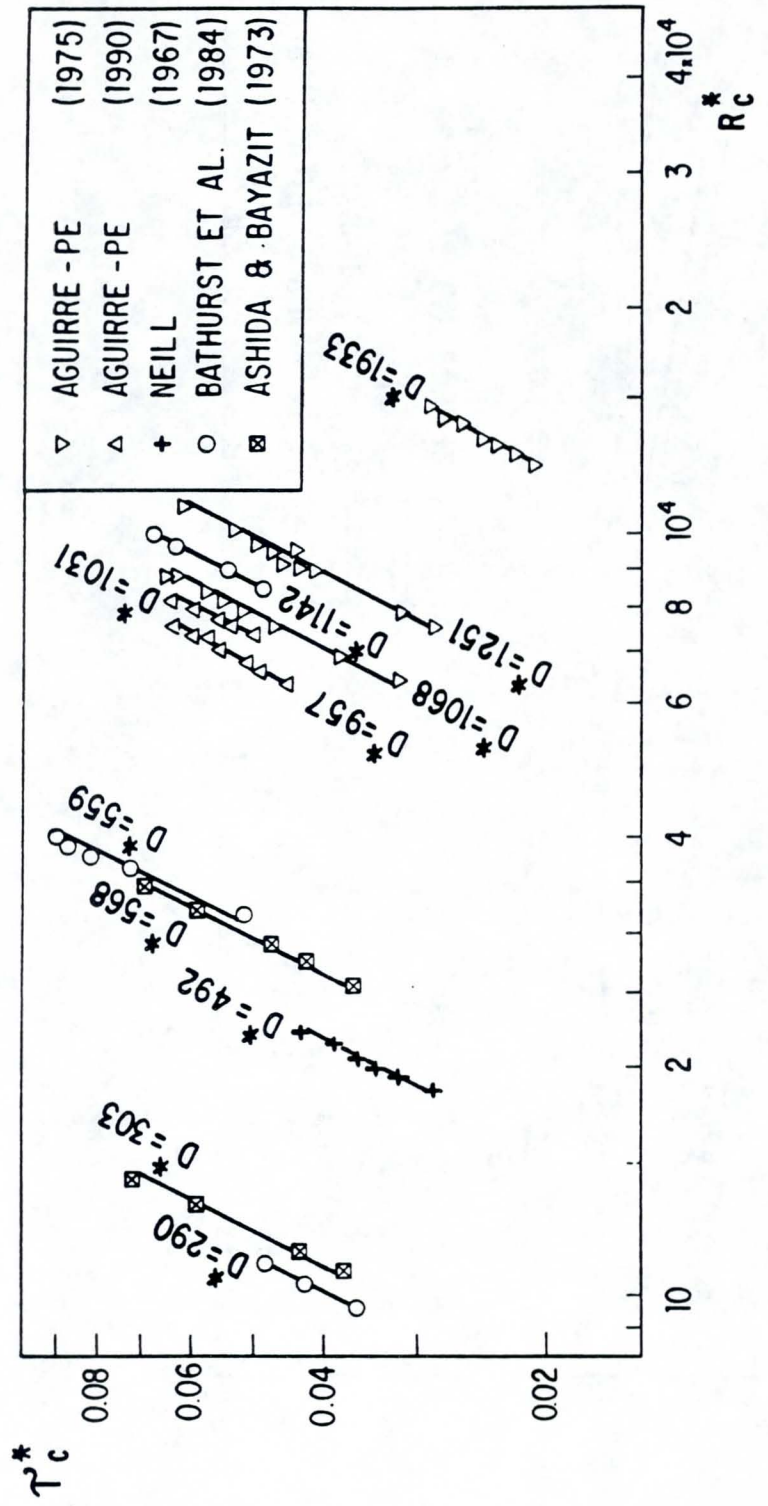
AGUIRRE-PE (1975)
AGUIRRE-PE (1990)
NEILL (1967)
BATHURST ET AL. (1984)
ASHIDA & BAYAZIT (1973)
D*=1933
D*=1251
D*=1068
D*=1142
D*=957
D*=1031
D*=559
D*=568
D*=492
D*=303
D*=290
0.08
0.06
0.04
0.02
10
2
4
6
8
10^4
2
3
4x10^4
τ*c
R*c

Figure 4.

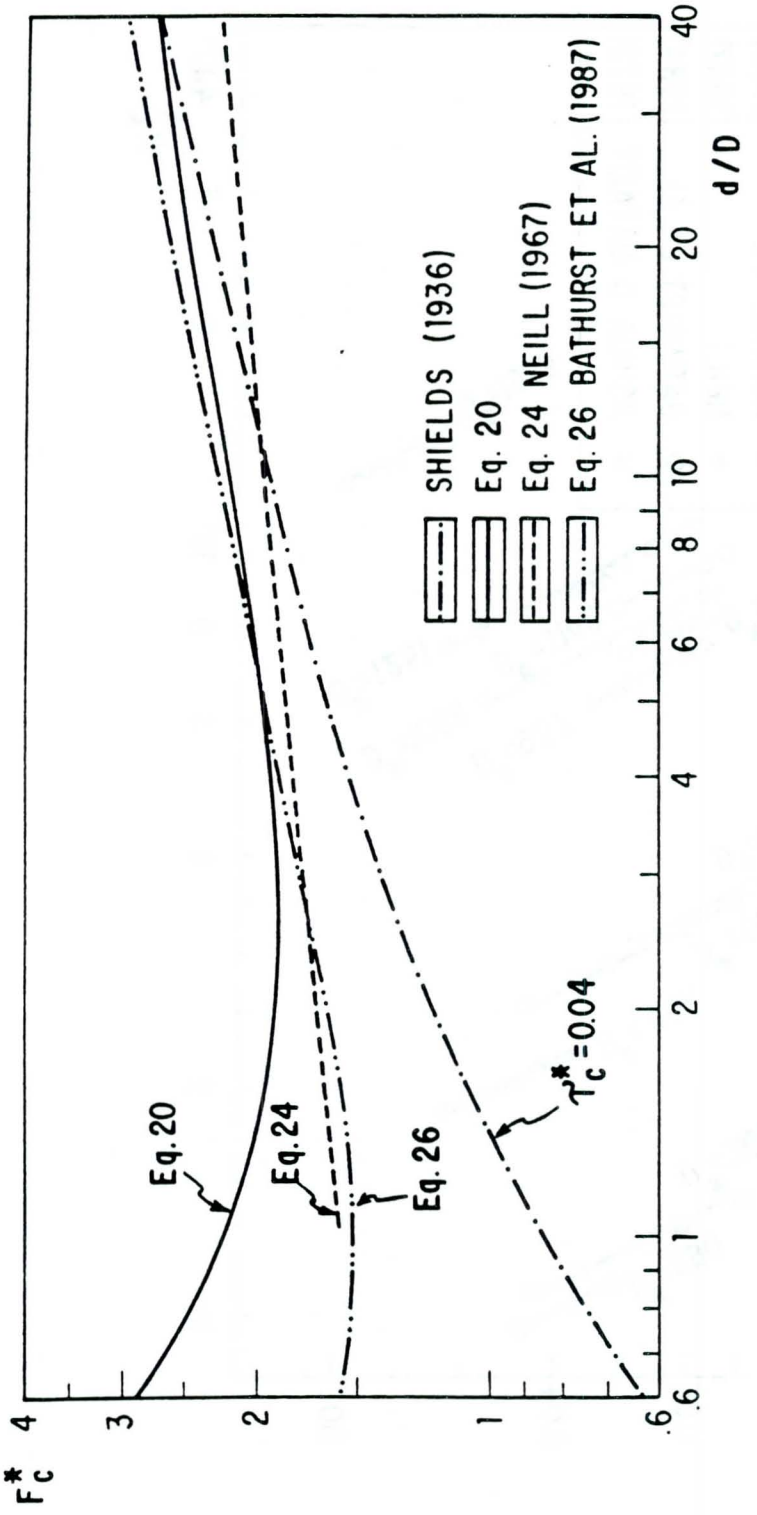
SHIELDS (1936)
Eq. 20
Eq. 24 NEILL (1967)
Eq. 26 BATHURST ET AL. (1987)
Eq.20
Eq.24
Eq.26
τ_c^*=0.04
F_c^*
d/D
.6
1
2
3
4
6
8
10
20
40

Figure 5.

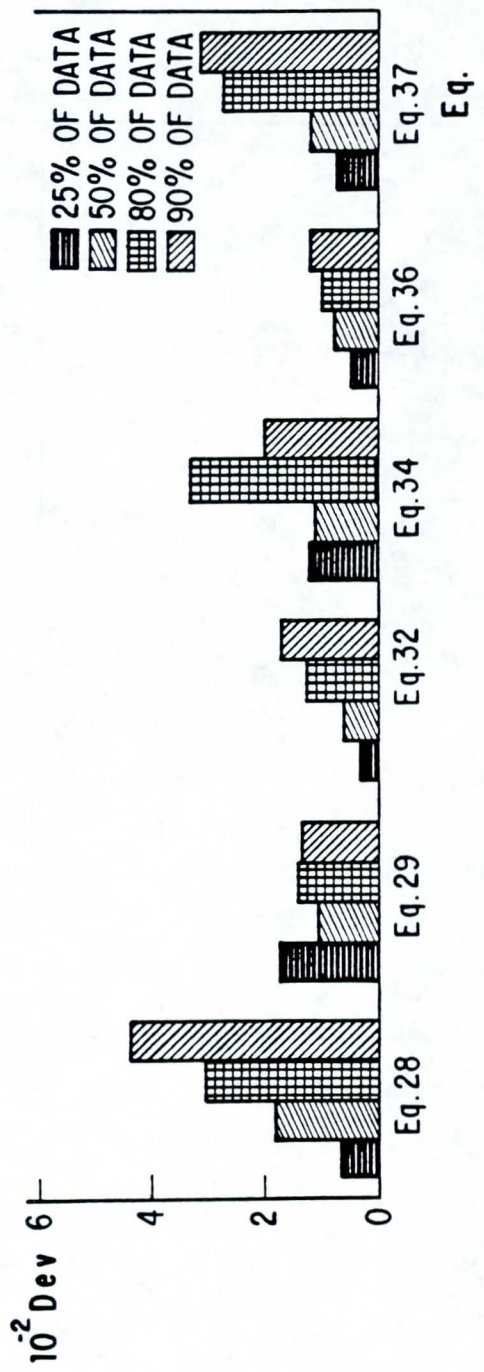
25% OF DATA
50% OF DATA
80% OF DATA
90% OF DATA
Eq.28
Eq.29
Eq.32
Eq.34
Eq.36
Eq.37
Eq.
10^{-2} Dev
0
2
4
6

Figure 6.

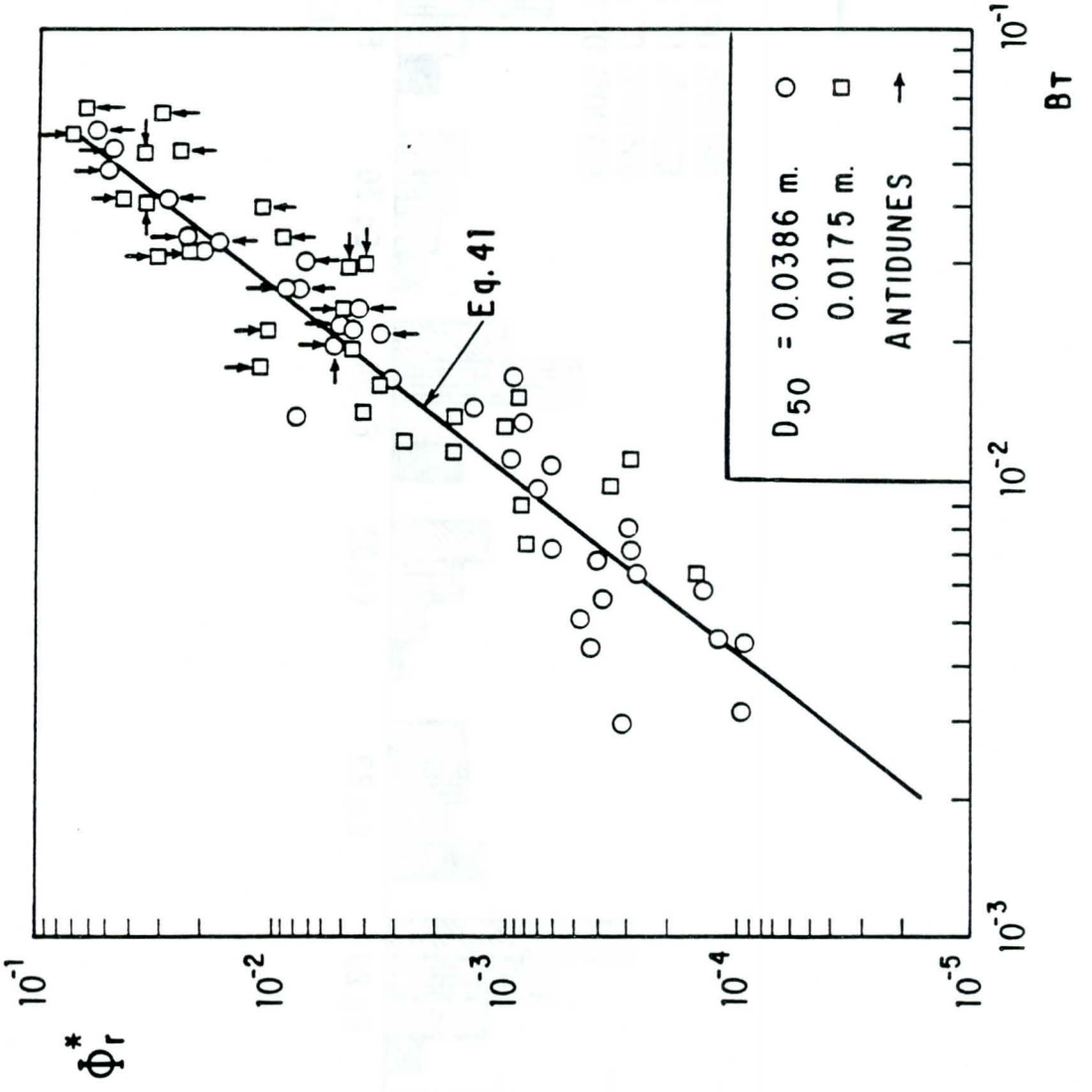
10^{-1}
10^{-2}
10^{-3}
10^{-4}
10^{-5}
Φ_r^*
10^{-1}
10^{-2}
10^{-3}
BT
Eq. 41
D_{50} = 0.0386 m.
0.0175 m.
ANTIDUNES

Figure 7.

DETERMINISTIC AND PROBABILISTIC DESIGN APPROACHES OF RIPRAP AS BANK PROTECTION

A.F. Ahmed, F. El-Gamal and M.M. Gasser
The Hydraulics and Sediment Research Institute
Delta Barrages, Egypt

ABSTRACT

Rock riprap as a protection against erosion is immensely used for a very wide range of hydraulic structures. The available knowledge of the hydrodynamic forces, lift and drag, acting on a side slope riprap particle are mainly based on laboratory measurements and it has been inadequate for the purpose of developing a suitable design criterion. This is due to the numerous factors that influence the stability, and the definite probabilistic natures of the acting forces which may, for certain period of time, be significantly in excess of mean values and consequently causing movement.

In this study two design criteria, namely deterministic and probabilistic, for sizing riprap for side slope protection are developed. Those approaches were formulated on the basis of laboratory measurements that took place at the Chilworth Hydraulic Laboratory at the University of Southampton, England. The hydrodynamic forces acting on a representative particle of the side slope protective layer were measured. Assessment of the applicability of the two approaches and the existing sizing methods were tested using the laboratory data. The results revealed the preference of the two methods developed in this study.

1. INTRODUCTION

There are a large number of design criteria for sizing riprap (e.g., *U. S. Army Corps of Engineers 1966; Anderson et al. 1970 and California Division of Highways 1970*). Recently, two types of designing methods for sizing riprap have been developed. The first one was derived by relating the flow characteristics, and the properties of the slope and particles to stability of individual particle and is referred to as the deterministic approach (e.g., *Stevens and Simons 1971; Stevens et al. 1976; Li et al. 1976; Samad 1978 and Li and Simons 1979*). In the second method, which is referred to as the probabilistic approach, the fluctuating nature of the hydrodynamic forces acting on an individual particle were considered (e.g., *Li et al. 1976; Samad 1978 and Li and Simons 1979*). This method enables the designer to interpret the stability of riprap by checking its probability of adequacy under design conditions rather than indicating a factor of safety.

2. THEORITICAL CONSIDERATIONS

The forces acting on a single particle resting on the side slope of a trapezoidal channel are shown in Fig.(1). This particle is exposed not only to a drag force F_D acting in the flow direction, but also to a component of the particle weight W acting down the side slope, and lift force F_L acting perpendicular to the side slope plane. The resultant force is a combination of those forces which tends to dislodge the particle out of the riprap layer and it is called the driving force F_{DR}. The force resists movement is the component of the particle weight acting downwards perpendicular to the side slope plane and is called the resisting force F_{RE}. Those forces can be expressed as :

$$F_{DR} = (W^2 sin^2\theta + F_D^2)^{1/2} \qquad (1)$$

$$F_{RE} = (W \cos\theta - F_L) \tan\phi \quad (2)$$

In which

$$W = \frac{\pi}{6} D_{50}^3 \rho g (S_s - 1) \quad (3)$$

$$F_D = 1/2 \; C_D \; \rho \; u^2 \; D_{50}^2 \quad (4)$$

$$F_L = 1/2 \; C_L \; \rho \; u^2 \; D_{50}^2 \quad (5)$$

Where W is the submerged weight of the particle; θ is the angle of the side slope of the channel; S_s is the particle specific gravity; F_D and F_L are the mean drag and lift forces; C_D and C_L are the drag and lift coefficients; u is some characteristic velocity; D_{50} is the representative diameter of the particle; ρ is the mass density of the water; g is the gravitational acceleration and Φ is the angle of repose in degrees.

The factor of safety SF against movement of a particle may be defined as the ratio of the resisting force, F_{RE} to the driving force, F_{DR} on a representative particle size of the protective layer and can be expressed as

$$SF = \frac{(W \cos\theta - F_L) \tan\phi}{(W^2 \sin^2\theta + F_D^2)^{1/2}} \quad (6)$$

2.1. Deterministic Approach

The conventional approach to the stability of a single particle is based on the consideration that the forces acting on the particles are invariant quantities. This can be obtained by considering the mean value of drag and lift forces given in Eq.(6) as $\bar{F}_D$ and $\bar{F}_L$. Thus the mean or conventional safety factor $\bar{SF}$ is defined as

$$\bar{SF} = \frac{(W \cos\theta - \bar{F}_L) \tan\phi}{(W^2 \sin^2\theta + \bar{F}_D^2)^{1/2}} \quad (7)$$

When $\overline{SF} = 1$, the rock protection is considered to be at the critical condition; if $\overline{SF} > 1$, the rock protection is safe and if $\overline{SF} < 1$, the rock protection is considered unsafe and failure may be established.

2.2. Probabilistic Approach

Due to the fact that the hydrodynamic forces acting on the side slope particles are randomly varying, therefore the probability of adequacy for the riprap protection can be determined as :

$$P_a = \text{probability } [\ F_{RE} > F_{DR}\ ] \tag{8}$$

$$P_a = P\ [\ F_{RE} > F_{DR}\ ] \tag{9}$$

$$P_a = f(SF) \tag{10}$$

In which P[.] is the probability of the specified event.

In this method the probability of adequacy for the riprap particles at the critical condition (SF=1) is considered equal to 0.5. This implies that there is a 50% chance of adequacy (P_a) if the riprap is designed according to the conventional safety factor of 1.0. Accordingly if $P_a > 50$ %, the particle is said to be stable, and if $P_a < 50$%, the particle will be displaced. According to the assumption recommended by *Li et al.(1976) and Smith (1986)*, the drag force F_D was considered to be proportional to the boundary shear stress τ , and the lift force F_L was considered to be related to drag force F_D, i.e.

$$F_D = \delta\tau \tag{11}$$

and

$$F_L = \beta F_D = \delta\beta\tau \tag{12}$$

Where δ is the proportionality parameter. Therefore, substitute Eqs.(11 and 12) into Eq.(6) to obtain

$$SF = \frac{(W \cos\theta - \beta\delta\tau)\ \tan\phi}{(W^2 \sin^2\theta + \delta^2\ \tau^2)^{1/2}} \qquad (13)$$

For an existing riprap Structure, the critical shear stress τ_c can be determined using Eq. (13) with $\tau = \tau_c$ when SF = 1, to obtain:

$$(W \cos\theta - \beta\delta\tau_c)\tan\phi = (W^2 \sin^2\theta + \delta^2\ \tau_c^2)^{1/2} \qquad (14)$$

Eq.(14) is a quadratic equation in τ_c, and its Solution was derived by *Samad (1978) as*

$$\tau_c = \frac{(A_1^2 + W^2\ A_2\ A_3)^{1/2} - A_1}{\delta\ .\ A_2} \qquad (15)$$

in which

$$A_1 = \beta\ W \cos\theta\ \tan^2\phi \qquad (16)$$

$$A_2 = 1 + \beta^2 \tan^2\phi \qquad (17)$$

$$A_3 = \cos^2\theta\ \tan^2\phi - \sin^2\theta \qquad (18)$$

3. EXPERIMENTAL TESTS

Six modelled trapezoidal channels, each 10-m long and having 1.5 H : 1 V side slopes protected with a 20.1-mm diameter rock layer 1.5 diameters thick, were constructed (Fig.2). Each model was tested under different flow discharges to investigate the failure mode of the riprap protective layer, and to identify the hydraulic parameters at the threshold and failure flow conditions. Those results were utilized to assess the applicability of the available deterministic and probabilistic approaches for sizing riprap for side slope protection (*Ahmed 1988 and 1989*).

Furthermore, laboratory tests, to measure the hydrodynamic forces acting on a representative spherical particle of side

slope, were carried out in 21.4 m long recirculating flume (Fig.3). Such measurements were previously made on a bed particle under uniform flow conditions over both uniform spherical and hemispherical particles, (*Einstein and El-Samni 1949; Chepil 1958; Coleman 1967 and Cheng and Clyde 1972*). This revealed that no attempt has been made to measure forces acting on side slope particles. For this reason, direct measurements have been made of the acting hydrodynamic forces on 20.1-mm spherical particle placed within the riprapped side slope. Preliminary experiments were conducted to establish the appropriate sphere diameter and its location at level of maximum wall shear. A load beam cell (Fig. 4) was devised to acquire simultaneous stresses which were transformed into simultaneous values of lift and drag forces. Twelve runs covering a wide range of flows were performed. For each run the hydrodynamic lift and drag forces acting on a simulated spherical particle as well as the necessary information of the flow condition were recorded (*Ahmed 1988 and 1991*).

4. RESULTS

Summary of the constructed models and results obtained are illustrated in the following table :

Model No.	Bed slope	Bed material	Filter type	Riprap material	Max. flow (m^3/s)	Threshold flow (m^3/s)	Failure flow (m^3/s)
1	0.005	Riprap	Granular	Uniform	0.219	-	-
2	0.008	"	"	"	0.216	-	-
3	0.008	Geotextile	"	"	0.222	-	-
4	0.0125	"	"	"	0.179	0.149	0.179
5	0.0125	"	Geotextile	"	0.142	0.130	0.142
6	0.0125	"	"	Graded	0.130	0.104	0.130

Based on the experimental results, judgement of riprap stability for each model was considered from the stand point of the following eight deterministic methods :

Method No. (1) : *Lane (1955)*
Method No. (2) : *Stevens and Simons (1971)*
Method Nos. (3 & 4) : *Stevens et al. (1976)*
Method No. (5) : *Li et al. (1976)*
Method No. (6) : *Li and Simons (1979)*
Method Nos. (7 & 8) : *Samad (1978)*

On the other hand, the probability of adequacy for the side slope of the tested models was considered from the stand point of the following four probabilistic approaches:

Method No. (I): *Li et al.(1976)*
Method No. (II): *Li and Simons (1979)*
Method Nos. (III & IV) : *Samad (1978)*

The results obtained concluded that the side slope protective layer was much more stable than the prediction of the applied methods. In addition some of the applied methods always predict failure whatever the particle size. This consequently implied that those methods underestimate the stability that occurs when riprap is placed on channel side slopes. More details of the laboratory tests and sample of numerical examples for the sizing methods applied are presented by (*Ahmed 1988 and 1989*).

Due to the irregularity of the particles composing the riprap layer, non of the local velocities at any location above the particle could be adequately used as a characteristic velocity, so this value was evaluated as the average flow velocity and the hydrodynamic forces was calculated using eqs. (4 and 5). Summary of the results obtained from the force measurements are illustrated in the following table.

Run No.	Flow rate (m^3/s)	Flow depth (m)	F_D X 10^3 (N)	C_D X 10^3	F_L X 10^3 (N)	C_L X 10^2	F_L/F_D ratio
1	0.036	0.073	0.979	8.016	4.218	3.452	4.31
2	0.050	0.090	1.092	7.706	4.537	3.202	4.16
3	0.058	0.099	1.148	7.544	4.629	3.042	4.03
4	0.065	0.107	1.209	7.494	4.793	2.972	3.97
5	0.070	0.111	1.269	7.630	4.910	2.952	3.87
6	0.078	0.119	1.289	7.305	4.947	2.803	3.84
7	0.089	0.128	1.353	7.186	5.123	2.722	3.79
8	0.100	0.137	1.421	7.066	5.292	2.632	3.73
9	0.107	0.143	1.471	7.016	5.459	2.603	3.71
10	0.120	0.152	1.495	6.683	5.531	2.472	3.70
11	0.132	0.159	1.622	6.865	5.815	2.462	3.59
12	0.143	0.167	1.683	6.814	5.965	2.414	3.54

The recorded forces for all runs revealed that the lift and drag are randomly fluctuating around mean values and their distributions were found to be approximately normal. Moreover, the relationships developed either for the variation of the lift and drag coefficients, and the ratio of lift to drag, confirmed the correlation between these coefficients and the relative roughness parameter (R/D_{50}). The result of the force measurements found to be defined by a simple power equation of the following forms:

$$C_D = 0.011\ (R/D_{50})^{-0.27} \quad (19)$$

$$C_L = 0.063\ (R/D_{50})^{-0.56} \quad (20)$$

$$\beta = 5.861\ (R/D_{50})^{-0.29} \quad (21)$$

$$u/u_* = 8.47\ (R/D_{50})^{0.03} \quad (22)$$

In which R is the hydraulic radius; β is the ratio of lift to drag forces and u_* is the shear velocity.

5. NEW METHODOLOGY

As a consequence of the preceding findings, one may conclude that derivation of a design criterion on the basis of the stability of a single particle can be achieved as long as the result is confirmed experimentally. For this reason the relationships derived from the force measurements will be utilized to formulate the following deterministic and probabilistic design methods for sizing riprap :

5.1. Deterministic Method

Considering the mean values of lift and drag forces, the conventional safety factor of the riprap side slope can be predicted. For a given values of D_{50}, R, ϕ, θ, u, ρ and S_s, $\overline{SF}$ can be calculated using the following procedure :

Step 1 : Use Eq.(3) to obtain the value of W
Step 2 : Use Eqs.(19 and 4) to determine the value of $\overline{F_D}$.
Step 3 : Use Eqs.(20 and 5) to obtain the value of $\overline{F_L}$.
Step 4 : Applying Eq.(7), the safety factor $\overline{SF}$ is obtained

5.2. Probabilistic Method

This can be used to predict the chance of movement of an individual particle of the side slope which accordingly enables the designer to establish the stability of the whole riprap layer. In order to evaluate the parameter δ in Eq.(11), the expression $\tau = \rho u_*^2$ was utilized and substituted in Eq. (11) to derive the following formula

$$\frac{\delta}{D_{50}^2} = \left(\frac{u}{u_*}\right)^2 \cdot \left(\frac{C_D}{2}\right) \qquad (23)$$

The term (δ / D_{50}^2), was plotted against (R/D_{50}) and the result was

$$\delta = 0.386\ D_{50}^2\ (R/D_{50})^{-0.21} \tag{24}$$

The above formula implies that δ does not have a constant value as suggested by *Li et al. (1976) and Li and Simons (1979)*. On the other hand, the value of SF in Eq.(13) will be less than or equal to 1.0 when τ is greater or equal to τ_c. Thus, the probability of adequacy of riprap structure can be expressed as:

$$P_a = probability\ [\tau_c \geq \tau] \tag{25}$$

$$P_a = P\ [\tau_c \geq \tau] \tag{26}$$

$$P_a = F\ (\tau_c) \tag{27}$$

At the critical condition Eqs.(11 and 12) can be written as

$$F_{CD} = \delta \tau_c \tag{28}$$

$$F_{CL} = \delta \beta \tau_c \tag{29}$$

In which F_{CD} and F_{CL} are the drag and lift forces respectively at the case of the critical shear stress. Therefore, as the lift and drag forces are perpendicular to each other, the mean and critical resultants can be obtained as

$$\overline{F} = (\overline{F_L^2} + \overline{F_D^2})^{1/2} = \delta \overline{\tau}\ (\beta^2 + 1)^{1/2} \tag{30}$$

$$F_c = (F_{CL}^2 + F_{CD}^2)^{1/2} = \delta \tau_c\ (\beta^2 + 1)^{1/2} \tag{31}$$

In which $\overline{F}$ and F_C are the mean and critical resultant forces respectively.

As a result of the laboratory measurements, it was concluded that the lift force is normally distributed with relative intensity LI equal to

$$LI = \frac{\sigma_L}{\overline{F}_L} = 0.554 \tag{32}$$

Where σ_L is the standard deviation of the lift force. Substituting for $\overline{F}_L$ into Eq.(5) to obtain

$$\sigma_L = 0.554\ C_L\ \rho\ \overline{u^2}\ D_{50}^2/2 \tag{33}$$

Therefore, one can evaluate the quantile point q_n as

$$q_n = \frac{F_c - \overline{F}}{\sigma_L} \tag{34}$$

and

$$f\ (F_c) = f(\tau_c) = \phi(q_n) \tag{35}$$

In which ϕ (.) is the cumulative distribution function for the normalized distribution curve, and then the probability of adequacy is

$$P_a = \phi(q_n) \tag{36}$$

The probability of adequacy for the side slope riprap particles can be derived for the given values of D_{50}, R, ϕ, θ, u, ρ *and* S_s as follows:

Step 1 : From Eq.(3) particle submerged weight W is determined

Step 2 : The value of β is evaluated from Eq.(21)

Step 3 : δ is determined from Eq.(24)

Step 4 : τ_c is determined from Eq.(15)

Step 5 : $\overline{F}$ is determined from Eq.(30)

Step 6 : F_C is determined from Eq.(31)

Step 7 : C_L is determined from Eq.(20)

Step 8 : σ_L is determined from Eq.(33)

Step 9 : q_n is determined from Eq.(34)

Step 10: The probability of adequacy ϕ (q_n) is expressed as acumulative distribution function for the normalized distribution curve which can be obtained from a standard normal table.

6. VERIFICATION

To establish the applicability of the two approaches developed in this study, three different tests were conducted by utilizing the results obtained in the laboratory experiments. The first test was carried out by applying the flow conditions at the maximum attainable flow rate for the first three models, where no substantial movement resulted, the predictions of the side slope safety factor and probability of adequacy were as follows:

Model No.	1	2	3
SF	1.056	1.038	1.033
P_a	98.0 %	79.7 %	78.3 %

This principally confirms the laboratory results which were materially different from the predictions of all other recognized approaches.

In the second test, the two developed approaches were utilized to predict the failure discharge for the case of Model 4. The corresponding probability of adequacy of the results obtained from the four failure tests conducted on this model were also determined as follows :

Test No.	Flow rate (m^3/s)		P_a %
	Actual failure	Predicted failure	
1	0.1794	0.1815	50.20
2	0.1825	0.1815	49.90
3	0.1853	0.1815	49.64
4	0.1769	0.1815	50.43

These results are in accord with the failure discharges in the laboratory tests, and confirm the applicability of the developed models.

During the third test a comparison between the two derived approaches and all the existing methods was made utilizing the available data of Model 4. This mathematical test was conducted by considering the flow to be uniform with both energy and bed slopes equal to 0.0125. In this study, judgement of side slope riprap stability was considered from the stand point of the previously mentioned eight deterministic methods and four probabilistic approaches. The results obtained from this test are plotted in Figs.(5 and 6) for the deterministic and probabilistic approaches respectively. Bearing in mind that the failure occurred in Model 4 at a flow rate of 0.179 m^3/s. This implied that the failure discharges predicted by applying the two developed methods were very close to that obtained from the experimental work than that with other methods. This revealed that the other existing methods for sizing riprap for side slope are a little more conservative than the approaches developed in this study.

7. SUMMARY

Based on the laboratory measurements of the hydrodynamic lift and drag forces acting on a representative spherical particle of side slope protective layer, two design methods were formulated. The first is the deterministic method of riprap design which was

developed on the basis of stability of a single particle. The second is the probabilistic method which enables the designer to interpret the stability of the riprap structure and takes into account the fluctuating nature of the hydrodynamic forces that act on the particles. Assessment of the applicability of the two approaches with the laboratory tests as well as the existing deterministic and probabilistic methods were made and the results revealed the preference of the two developed methods. This also leads to the conclusion that the two developed approaches in this study are practical and more economic than the other mentioned methods.

8. REFERENCES

Ahmed, A.F. (1988)."Stability of Riprap Side Slopes in Open Channels," Thesis presented to University of Southampton, U.K., in partial fulfillment of the requirements for the degree of Doctor of Philosophy.

Ahmed, A.F. (1989). "Model Study of Side Slope Riprap, " Proc. of ASCE, Int. Symposium of Sediment Transport Modeling, New Orleans, Louisiana, USA, 14-18 Aug., pp.233-241.

Ahmed, A.F. (1991)."Experimental Determination of the Hydrodynamic Forces Acting on Riprap Side Slope," The XXIV IAHR Congress for Study of Streams and Watersheds of High Hydraulic Irregularity, Madrid - Spain, 9-13 Sep., pp. A.511-A.519.

Anderson, A.G., Paintal, A.S. and Davenport, J.T.(1970)." Tentative design Procedure of Riprap-Lined Channels," Project Report No. 96. St. Anthony Falls Hyd. Lab., Minneapolis, Minnesota.

California Division of Highway, (1970)." Bank and shore Protection in California Highway Practice," Dept. of Public Works, Sacramento, California.

Campbell, F.B. (1966)."Hydraulic Design of Rock Riprap," Misc. Paper No. 2-777, Office of Chief of Engineers, U.S. Army, Waterways Experiment Station, Vicksburg, Mississippi.

Cheng, E.D.H. and Clyde, C.G. (1972)."Instantaneous Hydrodynamic Lift and Drag Forces on Large Roughness Element in Turbulent

Open Channel Flow," Chapter 3 in SHEN, H.W. (Ed.), "Sedimentation", Water Resources, Fort Collins, Colorado.

Chepil,W.S. (1958)."The Use of Evenly Spaced Hemispheres to Evaluate Aerodynamic Forces on a Soil Surface," Trans. American Geophysical Union, 39 (3), 397-404.

Coleman, N.L. (1967)." A Theoretical and Experimental Study of Drag and Lift Forces Acting on a Sphere Resting on a Hypothetical Stream Bed," Proc. of the 12th Congress of IAHR, Vol. 3, Fort Collins, c22-1-c22-8.

Einstein,H.A. and El-Samni, E.A. (1949)." Hydrodynamic Forces on a Rough Wall," Review of Modern Physic, 21 (3), 520-524.

Lane, E.W.(1955)."Design of Stable Channel". Trans. ASCE, Vol.120,pp.1234-1260.

Li, R.M. and Simons, D.B. (1979)." Failure Probability of Riprap Structures," ASCE Convention and Exposition, Atlanta, 1-21.

Li, R.M., Simons, D.B., Blinco, P.H. and samad, M.A. (1976). "Probabilistic Approach to Design of Riprap for River Bank Protection," Symposium on Inland Waterways for Navigation, Flood Control and Water Diversions, 2, 1572-1591.

Samad, M.A. (1978)." Analysis of Riprap for Channel Stabilization," Thesis presented to Colorado State University, Fort Collins, Colorado, in partial fulfillment of the requirements for the degree of Doctor of Philosophy.

Smith, K.V.H. (1986). " Probabilistic Approach to the Stability Analysis of Rock Protection for Earth Weirs", Proc. of Inst. of Civil Eng., Part 2, Vol.81, pp.243-253.

Stevens, M.A. and Simons, D.B. (1971)."Stability Analysis for Coarse Granular Material on Slopes," Chapter 17 in SHEN, H.W. (Ed.) "River Mechanics, Vol. 1," Fort Collins, Colorado, 17.1-17.27.

Stevens, M.A., Simons, D.B., and Lewis, G.L.(1976)."Safety Factors of Riprap Protection," Proc. Hyd. Div., ASCE, 102 (5).

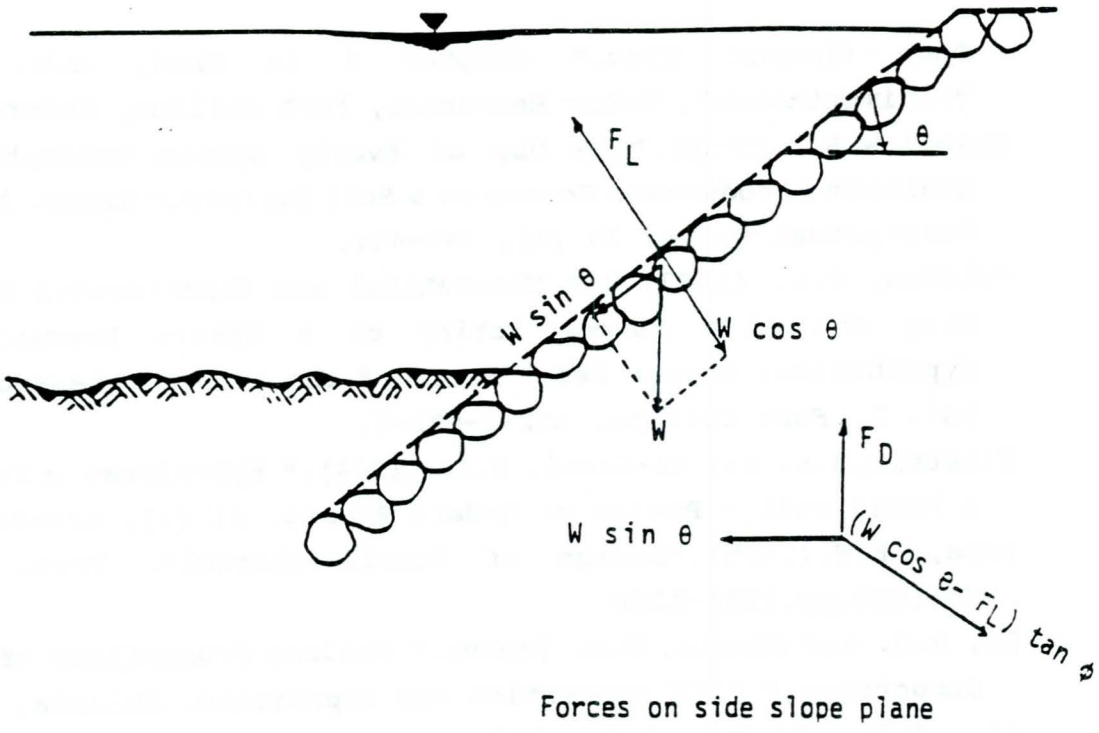

Fig. 1: Forces acting on a side slope particle.

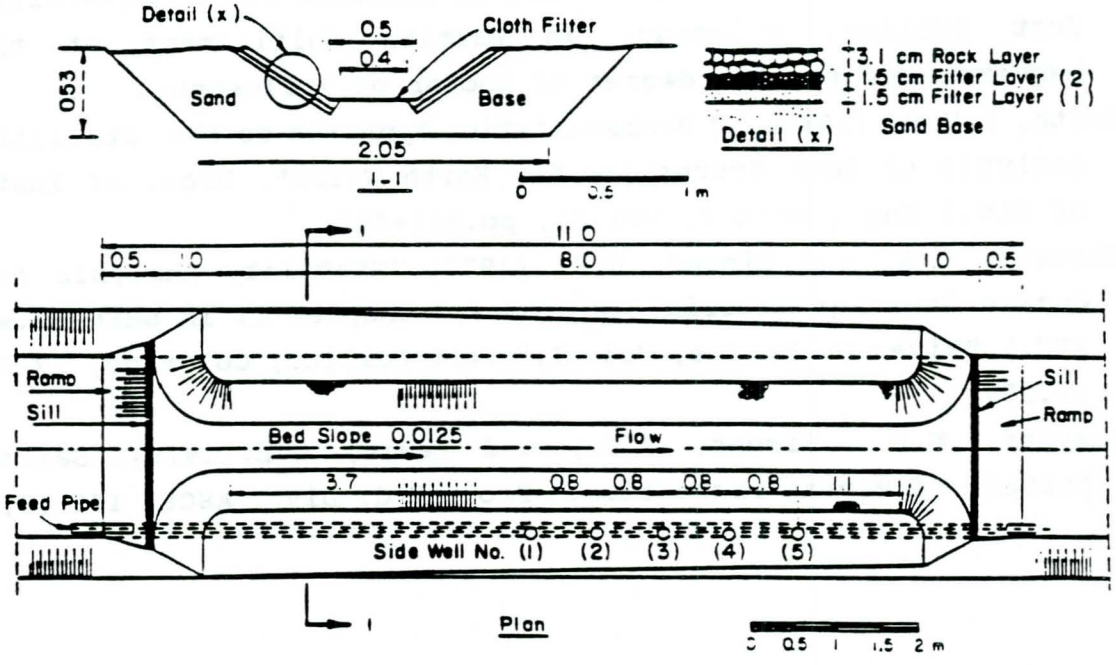

Fig. 2: Details of the model No. 4.

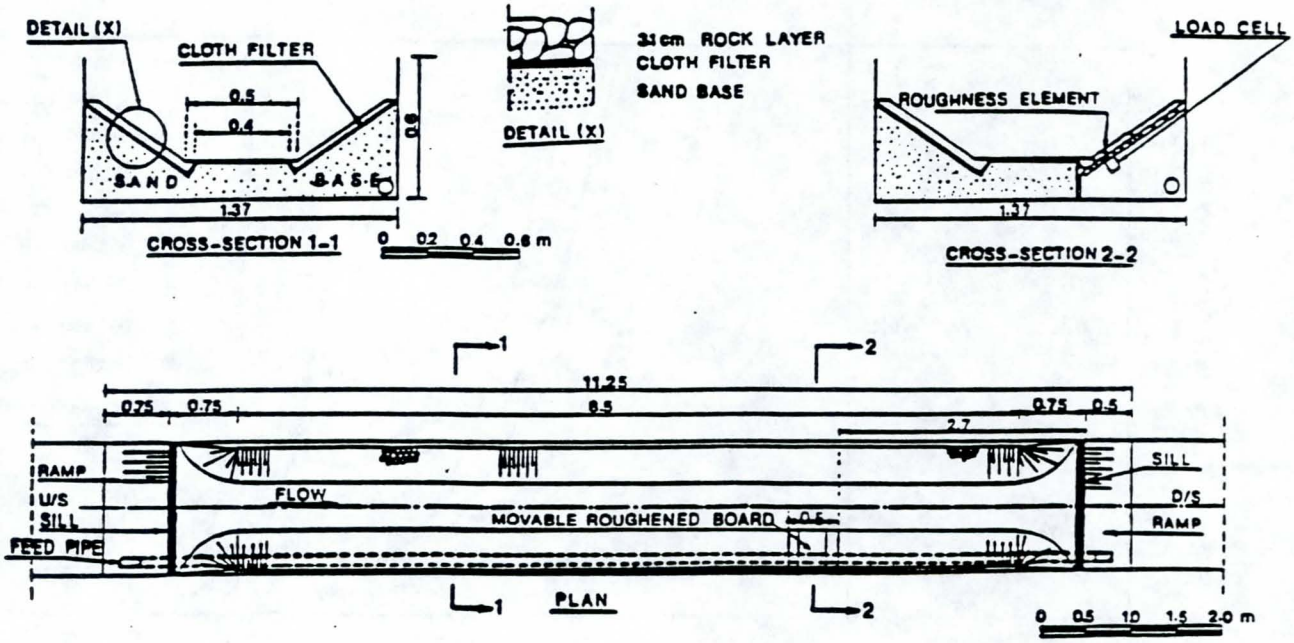

Fig. 3: Model alignment during force measurements.

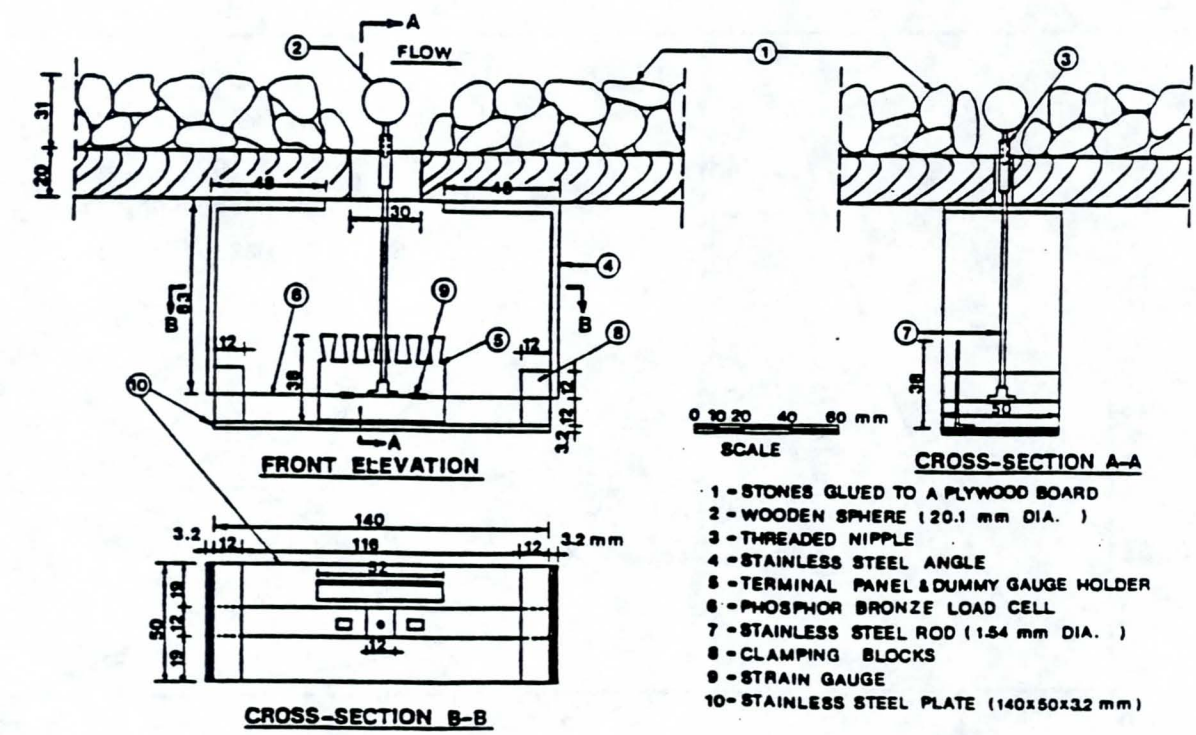

Fig. 4: Details of the load beam assembly.

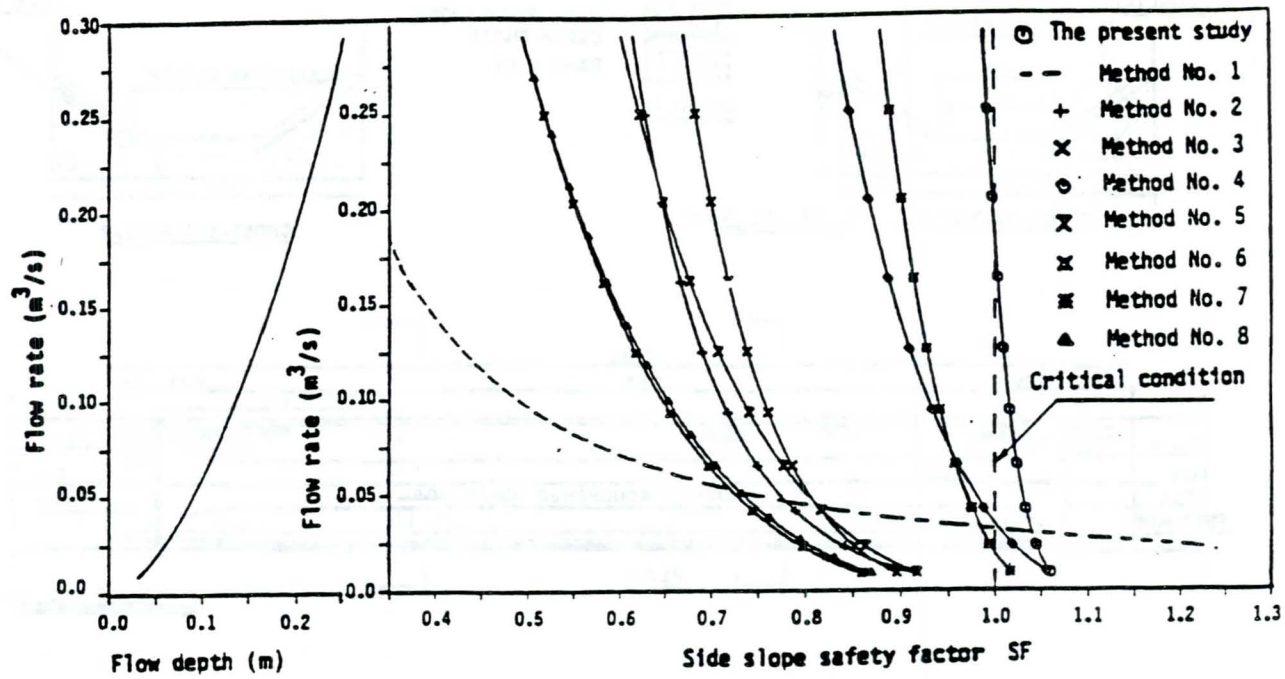

Fig. 5: Comparison of conventional safety factor.

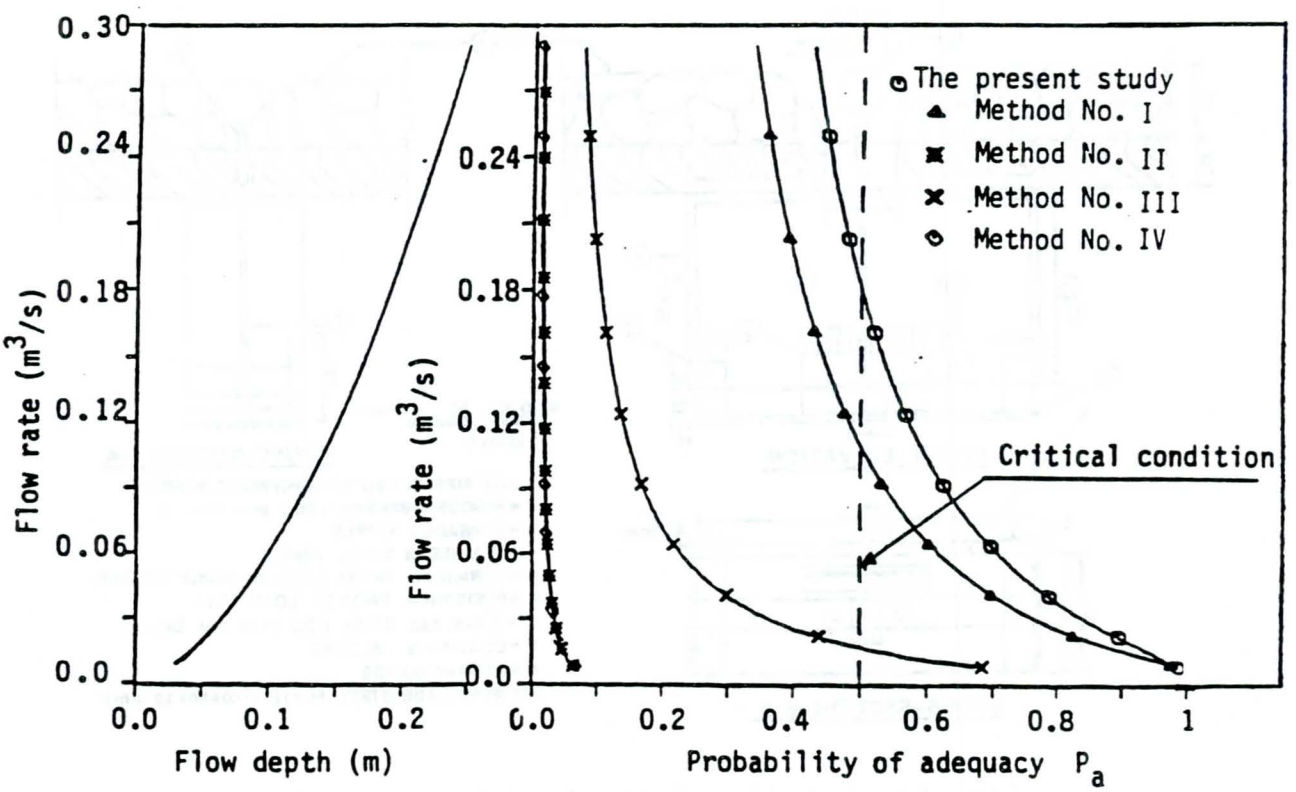

Fig. 6: Comparison of probability of adequacy.

DESIGN CONSIDERATIONS FOR DYNAMIC REVETMENTS

J.P. Ahrens
NOAA Seagrant, Silver Spring, Maryland

ABSTRACT

Dynamic revetment refers to the use of engineered gravel and/or cobble berms for shoreline protection. These "structures" are dynamic, since the stone size is small compared to the armor stone size used in traditional statically stable riprap revetments. Wave action is expected to shape and reshape a dynamic revetment as it defends the shoreline. The gravel or cobbles can be used in conjunction with a seawall, bulkhead, groins, or without a complementing structural component. Recent interest in dynamic revetments reflects recognition of their engineering advantages, economic advantages, and environmental acceptability for a number of situations.

The most conspicuous feature of a dynamic revetment, or a gravel/shingle beach is the high berm crest which terminates the foreshore. This feature is easy to recognize and can be accurately measured. On a mature slope, the berm crest is built and maintained by the extreme conditions of wave uprush and, therefore, it is an approximate measure of the maximum runup. Based on analysis of laboratory data, this paper will show that the berm crest height is a function of the wave steepness and the extent of truncation of the incident wave height distribution. It will also be shown that the size of a dynamic revetment required for stability (critical mass) can logically be scaled by the predicted berm crest height.

INTRODUCTION

Dynamic revetments fill an interesting conceptual niche for shore protection, between traditional statically stable riprap revetments and beach nourishment. From a coastal geomorphology perspective, a dynamic revetment could be called an engineered gravel or cobble berm, as used by Galvin and Ahrens (1993). Development of design criteria for dynamic revetments has been encouraged by the observation that gravel and shingle beaches provide very effective shore protection. A typical berm profile for coarse sediment is shown in Figure 1.

Conventional revetments are designed to be statically stable; that is, no motion of the armor stone is anticipated. Stones in the armor layer are sized and placed such that their weight and interlocking will preclude movement during wave attack. In contrast, a dynamic revetment is designed to allow wave action to rearrange the stones into an equilibrium profile. Because stones are allowed to move, a smaller size of stone can be used than is needed by a statically stable riprap revetment. An approximate size range for stone that can be used in a dynamic revetment is from 0.5 cm to 30 cm. However, even though smaller material may be used, a dynamic revetment will require a larger quantity of material to protect a given length of shoreline than a traditional riprap revetment. Generally, the cost of additional material is offset by the lower costs of smaller stone and, because size is less critical, a more cost-effective use may be made of quarry output. In addition, smaller stone is less expensive to handle, and since initial placement is not critical, dynamic revetments may be dumped in place rather than the stones being individually placed, Ward and Ahrens (1992). In common with beach nourishment, the amount of material required to defend the coast is a quite important design consideration for dynamic revetments. This paper will give definitive guidance, based on physical model tests, for determining the volume of stone required per unit length to provide effective shoreline protection.

BACKGROUND

Field Studies

Downie and Saaltink (1983) discuss the use of an engineered cobble beach about 600 m long to protect the base of an eroding sand cliff, near Vancouver, British Columbia. Deep water wave heights, generated in the Strait of Georgia, of about 3 meters have a return period of one year. Erosion and damage potential is increased, in this area, by the presence of large logs and compounded by a large tide range of over 4 meters. Although severe erosion threatened several buildings on the University of British Columbia campus at the top of the cliff, considerable effort was expended to develop an environmentally acceptable design for the protection. Groins were used to reduce the rate of longshore drift of the cobbles. This protection has continued to function effectively up to the present, Downie (1992).

Zenkovich and Schwartz (1987) discuss the extensive efforts to nourish gravel beaches on the Black Sea. Part of this effort was accomplished by dumping gravel from barges in water depths of 4 to 6 m. It was found that these submerged mounds of gravel would migrate shoreward during storms and, in a year or so, would nourish both the submerged and above sea level portions of the beach.

Johnson (1987) found that gravel beaches and dumped rubble are frequently cost-effective alternatives to using sand for beach nourishment and placed stone for revetments, respectively. These findings were obtained from extensive experience on Lakes Michigan and Superior where fluctuating water levels create enormous problems for conventional shoreline protection. Dynamic revetments are not vulnerable to toe scour, overtopping, or flanking based on Johnson's observations. Specific advantages of gravel sized material include a long residence time, an ability to stay near the water line, ease of placement, and usually lower unit costs than armor stone.

Research on equilibrium beach profile characteristics overlaps the sediment size range considered for dynamic revetments. Dean (1991) shows that coastlines with sediment particle sizes in the range of 15 to 30 cm have profiles which fit closely to the power law relation commonly used for sand beaches. Application of this research to dynamic revetments will be discussed below.

Da Costa, et al. (1992) designed a gravel and cobble beach to protect severely eroding shoreline on Flathead Lake, Montana. The site has a fetch of about 36 km, wave heights are up to 1.5 m, and water levels on the lake vary over the year by about 3 m. Initial placement of coarse material proved to be insufficient and considerable material was added before the second erosion season. The authors regard the project as a success with the additional material in place.

Laboratory Studies

Laboratory tests of gravel beach response to wave action were conducted in the Netherlands by van Hijum and Pilarczyk (1982). The conditions investigated by van Hijum and Pilarczyk were for much greater relative water depths at the toe of the structure than would be appropriate for dynamic revetments. Results from van Hijum and Pilarczyk's study were incorporated into the larger and more general investigation of both dynamic and static rubble structures of van der Meer (1988). Unfortunately the more general treatment of van der Meer still did not specially address the design of dynamic revetments in shallow water. van der Meer found that the berm crest height was a function of the deep water wave steepness and the number of waves and not a function of the stone size. For the latter finding to be correct the stone size and void spaces would have to be large enough for the wave uprush to be free draining through the foreshore slope, which was the case for the Dutch research.

In the United Kingdom, laboratory tests of the response of shingle beaches to wave action were studied by Powell (1988). These tests were conducted because it was realized that it would be useful to develop engineering design criteria that took advantage of the ability of shingle beaches to provide effective and environmentally acceptable shore protection for a variety of situations. Powell found that the prominent berm crest formed by wave uprush was overtopped on an equilibrium beach by about only 1 to 2% of the waves. In addition, Powell also found that the berm height was not a function of the size of the shingle, which is consistent with Dutch findings.

CERC Laboratory Study

The purpose of the study conducted at the Coastal Engineering Research Center (CERC) was to determine how dumped stone might be used to protect a vertical bulkhead in shallow water, and particularly to provide a means of calculating the minimum quantity of stone necessary to provide adequate protection (the "critical mass").

Laboratory tests were conducted in a wave tank using a nominal 1:16 (model:prototype) undistorted Froude scale. Twenty-two tests used gravel having a median sieve diameter of 8.1 mm and four tests used gravel with a median diameter of 5.6 mm, about 13 cm and 9 cm prototype respectively. Wave conditions were divided between those with a nominal period of peak energy density, T_p, of 1.75 and 2.50 seconds, or 7.0 and 10.0 seconds prototype respectively. The zero moment wave height, H_{mo}, ranged from 3.7 to 10.3 cm in the model and, the initial water depths at the toe of the model dynamic revetment, ranged from 10.5 to 15.9 cm. Stone near the water line becomes mobilized by wave action when stability numbers exceed about 2.5. Stability numbers for this study ranged from three to 10. Water depths at the wave generator range from about 58 to 67 cm and waves propagated from deep water to the toe of the structure over a one to 30 (vertical to horizontal) slope. A wide range of berm widths were tested to provide information on the minimum quantity of gravel required to protect the bulkhead. Typical initial and equilibrium dynamic revetment profiles are shown in Figure 2. Considerable detail about the test setup, conditions, and procedures, and data collection and analysis is given in Ward and Ahrens (1992).

In all 26 tests, the structures were categorized, based on their response to the waves, as safe, intermediate, or failure. When wave conditions were severe in relation to the quantity of stone in the revetment, wave action would erode the rubble by carrying it over the bulkhead until the waves would impact directly against the bulkhead. This response category was designated failure and a typical profile for this category is shown in Figure 3. When the amount of stone in the revetment was large in relation to the wave conditions, the berm crest could develop to its fullest extent and neither water or stone were carried over the bulkhead. This response category was designated safe and is illustrated in Figure 2. The third category fell between failure and safe and occurred when the berm crest buildup extended far enough landward to reach the bulkhead. For this situation, there would be some minor overtopping of the bulkhead by water and stone. This intermediate category is shown in Figure 4.

Some additional laboratory tests were also conducted to investigate the movement of a submerged mound of gravel, Ahrens and Camfield (1989). The results were similar to the field experience of Zenkovich and Schwartz (1987). At prototype scale the mound was about 1.5 m high in a water depth of about 3.0 m. As soon as wave generation commenced, the mound started moving landward. The mound continued moving landward, without hesitation, until it reached the highly reflective bulkhead, then mounded up against the wall; and finally, wave overtopping of the wall carried substantial quantities of gravel over the wall. At prototype scale, the waves had a zeroth moment wave height of about 2.0 m and a peak period of 10 sec, and sediment had a median diameter of about 13 cm.

PREDICTING THE BERM CREST HEIGHT

When the relative berm crest height data of van Hijum and Pilarczyk (1982) is compared to data of

Model and Variable Comparisons

general form $h_c = C_o + C_1 X_1$, $\bar{h}_c = 18.5$ cm

Model No.	Variable X_1(cm)	C_o(cm)	C_1	R^2
1	H_{mo}	11.5	1.06	0.599
2	$(H_{mo}L_o)^{1/2}$	8.04	0.150	0.873
3	$(H_{mo}L_p^2)^{1/3}$	3.87	0.200	0.916
4	$(H_{mo}L_o d_s)^{1/3}$	3.61	0.370	0.917
5	R_c*	2.12	0.869	0.914

* R_c defined by Equation 2

Table 1

Ward and Ahrens (1992), they have relatively similar values when plotted versus the deep water significant wave height. Figure 5 shows h_c/H_{so} versus H_{so}/L_o for the two studies, where h_c is the berm crest height, H_{so} is the deep water significant wave height, and L_o is the deep water wave length calculated using the period of peak energy density, T_p, of the incident wave spectrum. The comparison shows that on the basis of deep water conditions the two studies yielded approximately equivalent berm crest heights.

Scrutiny of the data of Ward and Ahrens (1992) indicates that the water depth at the toe of the structure has a noticeable influence on the berm crest height. The influence is such that the greater the depth, the greater the berm crest height, suggesting that the truncation of the wave height distribution is an important effect. Table 1 shows the importance of different variables used in a simple, linear form to predict berm crest height. The following discusses the models in Table 1:

Model 1 uses only H_{mo} to predict h_c; both the small percent of variance explained, R^2, and the large constant term, C_o, show that Model 1 is not satisfactory. In the simple model used in Table 1, a large value for the constant term demonstrates a problem with the model as it indicates an effect without a cause, eg. a finite berm crest height for a wave with zero height.

Model 2 uses both H_{mo} and T_p to predict h_c; R^2 is much higher than Model 1 but the constant term is still large. Model 2 is similar to the model proposed by van der Meer (1989) for predicting the berm crest height for the data of van Hijum and Pilarczyk (1982), but would not be suitable for the data of Ward and Ahrens (1992).

Model 3 represents an improvement over Model 2 by using the local wave length rather than the deep water wave length. By using the local wave length, Model 3 brings in some of the necessary influence of water depth, but the physical rationale for Model 3 is not clear and use of the local wave length is not convenient. Model 3 is similar to the model recommended by Ward and Ahrens to calculate berm crest heights.

In Model 4, the water depth is introduced directly into the prediction of h_c. Model 4 provides good predictions of h_c and is simple but the physical justification for the form of Model 4 is not apparent.

Model 5 is an improved version of Model 4 where the water depth is included in a physically realistic way through the variable, R_c, which is the estimated value of the berm crest height as developed in the analysis given below.

In both the data sets of van Hijum and Pilarczyk (1982) and Ward and Ahrens (1992) the relative berm crest height, h_c/H is strongly proportional to the square root of the wave steepness, where H represents either H_{mo} or H_s. This suggests a relationship similar to that between relative runup and the surf parameter on statically stable riprap revetments. In addition, the data of Ward and Ahrens also show a strong influence of water depth, which is consistent with the influence of truncation of the wave height distribution. Truncation of the wave height distribution would not be expected to have much influence on h_c in the data of van Hijum and Pilarczyk because the relative wave heights, H_s/d_s, are small in their study. Research by Stive (1986) on wave height distributions in shallow water indicate that the parameter, $(1+H_{mo}/d_s)^{1/3}$, would be a good variable to characterize the truncation of the wave height distribution. Using the two variables suggested above a number of regression models were fit to the data of Ward and Ahrens. From this analysis the best regression model is:

$$\frac{h_c}{H_{mo}} = \frac{0.536(L_o/H_{mo})^{1/2}}{1.0+0.649(L_o/H_{mo})^{1/2}[(1.0+H_{mo}/d_s)^{1/3}-1.0]} \qquad [1]$$

The form of Equation 1 is consistent with a number of runup equations that use the surf similarity parameter as the independent variable and have been fit to laboratory data collected on rough, porous coastal structures, eg. Ahrens and Heimbaugh (1988). Solving Equation 1 for h_c, the following definition is useful:

$$R_c \equiv H_{mo}(\text{RHS Eq. 1}) \qquad [2]$$

where, RHS Eq. 1, indicates the right hand side of Equation 1. The purpose of Equation 2 is to make a distinction between the observed and predicted berm crest height. R_c is treated like an independent variable in Model 5 in Table 1. Figure 6 shows a scatter plot of h_c versus the predicted value given by Eq.2; both the figure and Model 5 in Table 1 indicate that Eq.2 does a good job of predicting the berm crest height.

R_c was found to range from 10% less to 5% greater than the maximum runup on riprap revetments predicted by the method of Ahrens and Heimbaugh (1988). The comparison was made using the standard surf parameter with a riprap revetment slope of 1 : 1.5 (vertical : horizontal), which corresponds to a typical average dynamic revetment foreshore slope. Wave conditions in the comparison were regarded as severe H_{mo}/d_s = 0.6, Hughes (1984), wave periods ranged from 4.0 to 12.0 seconds, and water depths from 1.0 to 3.0 meters. It is felt that the comparison strongly supports the method of estimating the berm crest height given by Eq.1 and Eq.2, since the two method were developed from entirely different data sets.

DESIGN CRITERIA

Critical Mass for Vertical Seawalls and Bulkheads

Not only is the berm crest height strongly correlated to the estimated berm crest height, R_c, but so is the cross sectional area, A_f, of a dynamic revetment under the foreshore slope, i.e. the area between the still water line (SWL) and the berm crest and above the still water level. Figure 7 is a plot of A_f versus R_c^2 and shows the strong correlation between A_f and R_c.

The estimated berm crest height can also be used to determine the amount of material in the dynamic revetment required to be stable, i.e. critical mass. Figure 8 shows the category of the response of a dynamic revetment to wave attack as a function of V_t/R_c^2, where V_t is the total cross sectional area of the dynamic revetment. It can be seen in Figure 8 that the variable V_t/R_c^2 does a perfect job of discriminating among the three response categories; all the safe category tests have high values of the variable, all the failure category tests have low values of the variable, and all the intermediate category response tests fall in between without overlap! This analysis then allows the establishment of the following values of the dimensionless volume V_t/R_c^2 of 3.25 and 5.0 as being the transition between failure and intermediate, and intermediate and safe response categories respectively.

The estimated berm crest height, R_c, is a measure of the severity of wave conditions near the shoreline and therefore a logical variable to normalize the volume of coarse, protective material. However, if there are observed berm crest heights for suitable material and wave conditions near a project they could be used to estimate or check the volume of material required for protection.

Critical Mass for Protective Beaches

Dean's (1991) research on beach equilibrium profiles includes sediment sizes from fine sand to cobbles and boulders. This research has been extensively evaluated and used by other researchers, eg. Kriebel, Kraus, and Larson (1991), and provides a logical method of connecting the findings discussed above with the design of protective beaches with coarse material.

The basic beach profile used by Dean (1991) is given by,

$$d = AX^{2/3} \qquad [3]$$

where d is the depth at a distance offshore X from the water line for the design water level, and A is the sediment characteristic parameter. Figure 9 is a definition sketch for Dean type profiles, where one curve characterizes an erosion profile and has a relatively small value of the sediment characteristic parameter and the other curve is the profile of the coarse material used to protect the shoreline and has a relatively large value of the sediment characteristic parameter. The water depth at the intersection of the two profiles in Figure 9 is regarded as the toe water depth, d_s, for the protective "structure." Values of the sediment characteristic parameter can be determined for various sized particles in Moore (1982) or Dean (1991).

The volume of coarse material below the design water depth is the foundation volume, V_f, and can be calculated by,

$$V_f = \frac{3d_s(X_1-X_2)}{5} \qquad [4]$$

where, $X_1 = (d_s/A_1)^{3/2}$

and, $X_2 = (d_s/A_2)^{3/2}$

It is convenient to define a foundation length X_f as,

$$X_f = X_1 - X_2 \qquad [5]$$

The volume of coarse material required above the design water level to build the berm crest can be estimated by assuming that the average foreshore slope is 1 on 1.5 and landward slope is 1 on 1, about the angle of repose for gravel. These slopes require a dimensionless volume of $V_p/R_c^2 = 1.25$, and a foundation length of $X_f = 2.5\ R_c$, see Figure 9. The total volume is then given by,

$$V_t = V_p + V_f = 1.25\ R_c^2 + \frac{3\ d_s\ (2.5\ R_c)}{5} \qquad [6]$$

For severe wave conditions, i.e. $H_{mo}/d_s = 0.6$, Eq.6 can be converted into the same form as developed for estimating the volume of coarse material needed to protect a seawall or bulkhead, by using Eq.1; this

Volume of Coarse Material Used for Protective Beaches in Two Field Studies

Study	Volume of Protection $V_t(m^3/m)$	Berm Crest Height $h_c(m)$	V_t/h_c^2	Protection Status
Johnson (1987)	21.0	2.5-3.0*	2.3-3.4	Satisfactory
Da Costa et al. (1992)	2.5	1.3	1.5	Unsatisfactory
Da Costa et al., (1992)	10.0	1.3	5.9	Satisfactory

*Typical berm crest height in area of study Johnson (1992)

Table 2

procedure yields,

$$\frac{V_t}{R_c^2} = 1.8 + 3.6\,(d_s/L_o)^{1/2} \qquad [7]$$

Two field studies support Eq.7 as providing reasonable design guidance for the volume of material for protective beaches. Johnson (1987) indicates that 12 tons of coarse material per foot of shoreline is satisfactory protection for locations on Lakes Michigan or Superior. Da Costa, et. al (1992) demonstrates that one cubic yard of gravel per foot of shoreline is inadequate for Flathead Lake, but when this inadequate protection is supplemented by three cubic yards per foot, the protection is quite satisfactory. Information from these two studies is put into the context of this paper and summarized in Table 2.

When Eq.7 is solved for water depths from 1.0 to 3.0 m and wave periods from 4.0 to 12.0 sec., the dimensionless volume ranges from 2.0 to 3.0. This range is relatively consistent with the range of dimensionless volumes that provide satisfactory shoreline protection, as shown in Table 2.

Alongshore Transport Considerations

Much of the discussion above was from a two-dimensional perspective, but gravel and cobble-sized material can also move alongshore in response to oblique wave attack. Based on field observations by Johnson (1989), the littoral transport relation of Kamphuis, et. al (1985) accounts quite well for the relative movement of sand through gravel sized sediment particles. Kamphuis indicates that transport rates are inversely proportional to the square root of the particle diameter. For coarse material that might have particle diameters anywhere from ten to a thousand times greater than sand the transport rates would be

from 3.2 to 32 times smaller than sand.

If the alongshore loss of gravel and cobble size material needs to be reduced, short high groins can be used, Johnson (1989). The groins can be short since there is little tendency for coarse material to move offshore, but the groins need to be high to contain the high berm crest.

Wave Reflection and Energy Dissipation

For seawalls and bulkheads fronted by coarse material where, $V_t/R_c^2 \geq 3.25$, Ward and Ahrens (1992) found the reflection coefficient, K_r, can be calculated by,

$$K_r = \frac{1.0}{1.0+23.4\,(d_{50}/L_o)^{0.312}\exp[-0.00374(L_o/H_{mo})]} \quad [8]$$

The percent energy dissipation, %D, can be calculated by,

$$\%D = (1.0 - K_r^2)\ 100 \quad [9]$$

The dynamic revetments tested by Ward and Ahrens dissipated between 75 and 92% of the incident wave energy. Powell (1988) found for wave steepnesses greater than 0.02, i.e. breaking wave conditions, that reflection coefficients were about 0.10. This means that Powell's protective shingle beaches were dissipating 99% of the incident wave energy!

SUMMARY AND CONCLUSIONS

This paper shows that the berm crest height formed by coarse material under wave attack can be used to scale the size of a dynamic revetment or a protective beach. The berm crest height provides a logical measure of the severity of wave action on these types of "structures." Equation 2 will give accurate estimates of the berm crest height.

Both field and laboratory studies show that coarse material dumped offshore will migrate landward and build protective beaches or dynamic revetments. More research is required to define the conditions for which this method of placement will work.

Dimensionless volumes, V_t/R_c^2, of 3.25 and 5.0 are the transition values between failure and intermediate, and intermediate and safe response categories for dynamic revetments respectively. These values give the critical mass required to front a seawall or a bulkhead. Johnson (1992) notes that dynamic revetment designs can be based on the intermediate response category if material lost to the system can be replaced readily.

Research on dynamic revetments and studies of equilibrium beach profiles by Dean (1991), can be

combined to provide criteria for protective beaches composed of coarse material. Equation 7 estimates the critical mass for protective beaches. Field studies provide some support for the use of Equation 7, but more research is needed.

ACKNOWLEDGEMENTS

The author thanks Don Ward and Johnny Heggins of CERC for finding data and other information from the CERC study of dynamic revetments. Phil Keillor of Wisconsin Sea Grant and Charley Johnson of the North Central Division of the U.S. Army Corps of Engineers provided background information on the behavior of gravel beaches in the Great Lakes. Cyril Galvin, coastal engineer, provided conceptual insight on the response of coarse sediment to wave action. Bill Seelig, Naval Facilities Engineering Command, helped put together several of the figures. Sue Borda, National Sea Grant Office, put the text, figures, and graphs together into a paper.

REFERENCES

Ahrens, J.P., and Heimbaugh, M.S., "Irregular Wave Runup on Riprap Revetments", Technical Note, ASCE Journal of Waterways, Port, Coastal, and Ocean Engineering, Vol. 114, No. 4, July 1988, pp 524-530.

Ahrens, J.P., and Camfield, F., "Dynamic Revetments", The CERCular, Information Exchange Bulletin, Vol. CERC-89-2, Coastal Engineering Research Center, Vicksburg, MS., Sept. 1989.

Da Costa, S.L., Scott, J.L., and Simpson, D.P., "Gravel Equilibrium Beach Design for Arresting Shore Erosion at Flathead Lake, Montana", ASCE Conference on Coastal Engineering Practice, Long Beach, CA. March 1992, pp 154-169.

Dean, R.G., "Equilibrium Beach Profiles: Characteristics and Applications", Journal of Coastal Research, Vol 7, No. 1, Winter 1991, pp 53-84.

Downie, K.A., and Saaltink, H., "An Artificial Cobble Beach for Erosion Control", ASCE Conference Coastal Structures '83, Arlington, VA., March 1983, pp 846-859.

Downie, K.A., personal communication to Cy Galvin, 1992.

Galvin, C.J. and Ahrens, J.P., "Cross-Section of Engineered Gravel and Cobble Berms Fronting Seawalls", submitted to the ASCE Journal of Waterways, Port, Coastal, and Ocean Engineering, June 1992.

van Hijum, E., and Pilarczyk, K.W., "Gravel Beaches: Equilibrium Profile and Longshore Transport of Coarse Material under Regular and Irregular Wave Attack", Delft Hydraulics Laboratory Publication No. 274, Delft, the Netherlands, July 1982.

Hughes, S.A., "The TMA Shallow-Water Spectrum, Discription and Applications", U.S. Army Corps of

Engineers, Waterways Experiment Station, Technical Report CERC-84-7, Vicksburg, MS., Dec. 1984,

Johnson, C.N., "Rubble Beaches Versus Rubble Revetments", Proceedings Conference on Coastal Sediments' 87, ASCE, New Orleans, La. 1987, pp 1216-1231.

Johnson, C.N., personal communication, 1992.

Kamphuis, J.W., Davies, M.H., Nairn, R.B., and Sayao, O.J., "Calculation of Littoral Sand Transport Rate", Journal of Coastal Engineering, No.10, 1986, pp 1-21.

Kriebel, D.L., Kraus, N.C., and Larson, M., "Engineering Methods for Predicting Beach Profile Response", Proceedings Coastal Sediments '91, ASCE, Seattle, Wa., June 1991, pp 557-571.

van der Meer, J.W., "Rock Slopes and Gravel Beaches under Wave Attack", PhD Thesis, Dept. of Civil Engineering, Delft Technical University, April 1988.

Moore,B.D., "Beach Profile Evolution in Response to Changes in Water Level and Wave Height", Masters Thesis, Dept. of Civil Engineering, U. of Delaware, June 1982.

Powell, K.A. "The Dynamic Response of Shingle Beaches to Random Waves", Proceedings 21st Conference on Coastal Engineering, Malaga, Spain, June 1988, pp 1763-1773.

Stive, M.J.F., "Extreme Shallow Water Wave Conditions", Delft Hydraulics Internal Report H533, 1986.

Ward, D.L., and Ahrens, J.P., "Laboratory Study of a Dynamic Berm Revetment", U.S. Army Corps of Engineers, Waterway Experiment Station, Technical Report CERC-92-1, Vicksburg, MS, Jan. 1992.

Zenkovich, V.P.and Schwartz, M.L., "Protecting the Black Sea-Georgian S.S.R. Gravel Coast" Journal of Coastal Research, 3 (2), pp 201-211, 1987.

FIGURE CAPTIONS

Figure 1. Typical berm profile for a beach with coarse sediment.

Figure 2. Typical dynamic revetment profile for the safe response category.

Figure 3. Dynamic revetment profile for the failure response category.

Figure 4. Dynamic revetment profile for the intermediate response category.

Figure 5. Comparison of the relative berm crest height, as a function of deep water wave steepness, for Delft and CERC data.

Figure 6. Predicted, using Equation 2, berm crest height versus observed berm crest height.

Figure 7. Cross sectional area of a dynamic revetment under the foreshore slope as a function of the square of the predicted berm crest height.

Figure 8. Response category of a dynamic revetment as a function of the discrimination variable, A_t/R_c^2.

Figure 9. Definition sketch for an erosional shoreline protected by coarse material using Dean type profiles.

Table 1. Berm crest height, models and variables comparison.

Table 2. Volume of coarse material used for protective beaches in two field studies.

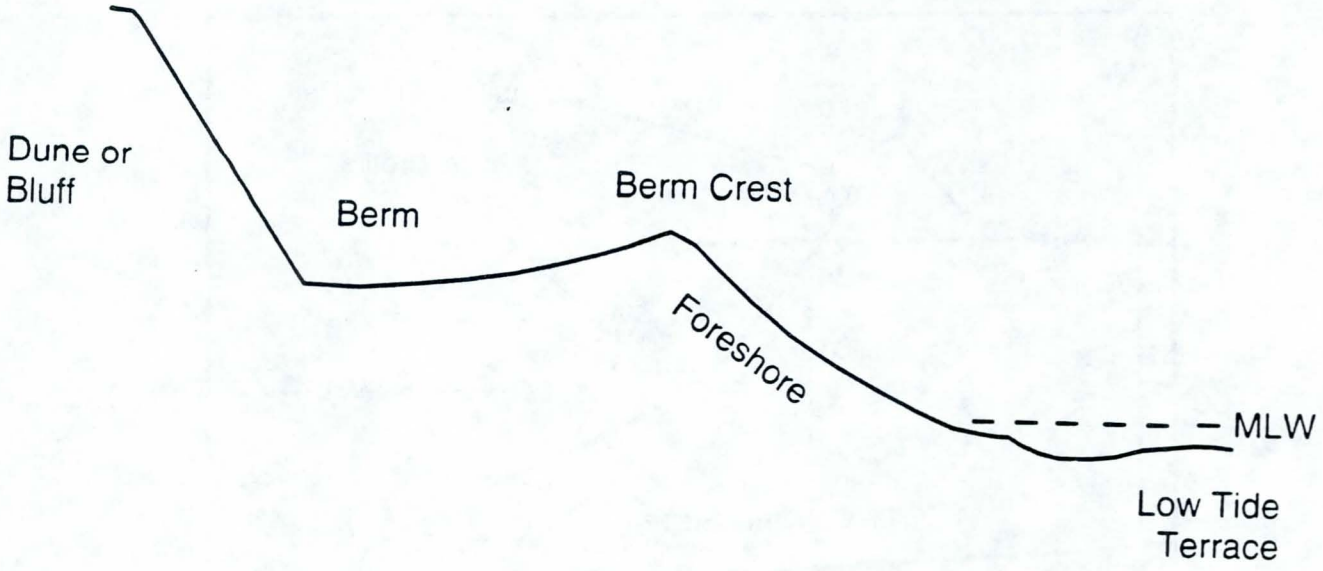
Dune or
Bluff
Berm
Berm Crest
Foreshore
MLW
Low Tide
Terrace

Figure 1.

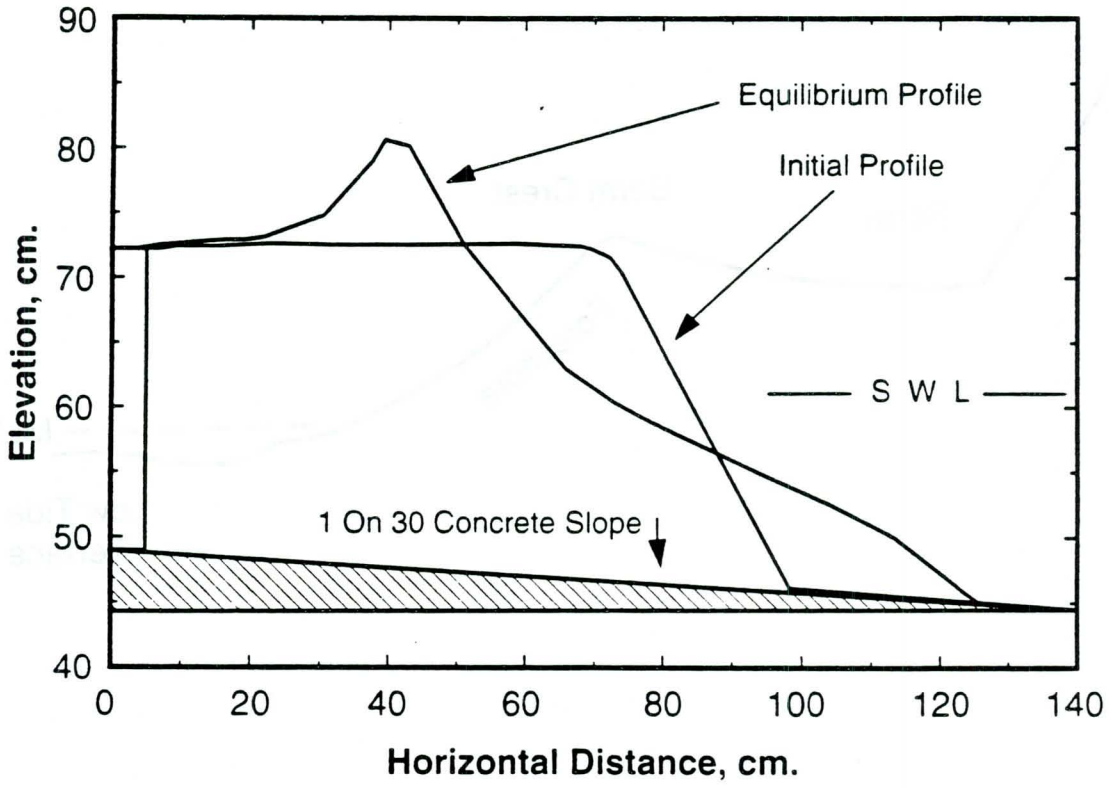
90
80
70
60
50
40
Elevation, cm.
0
20
40
60
80
100
120
140
Horizontal Distance, cm.
Equilibrium Profile
Initial Profile
S W L
1 On 30 Concrete Slope

Figure 2.

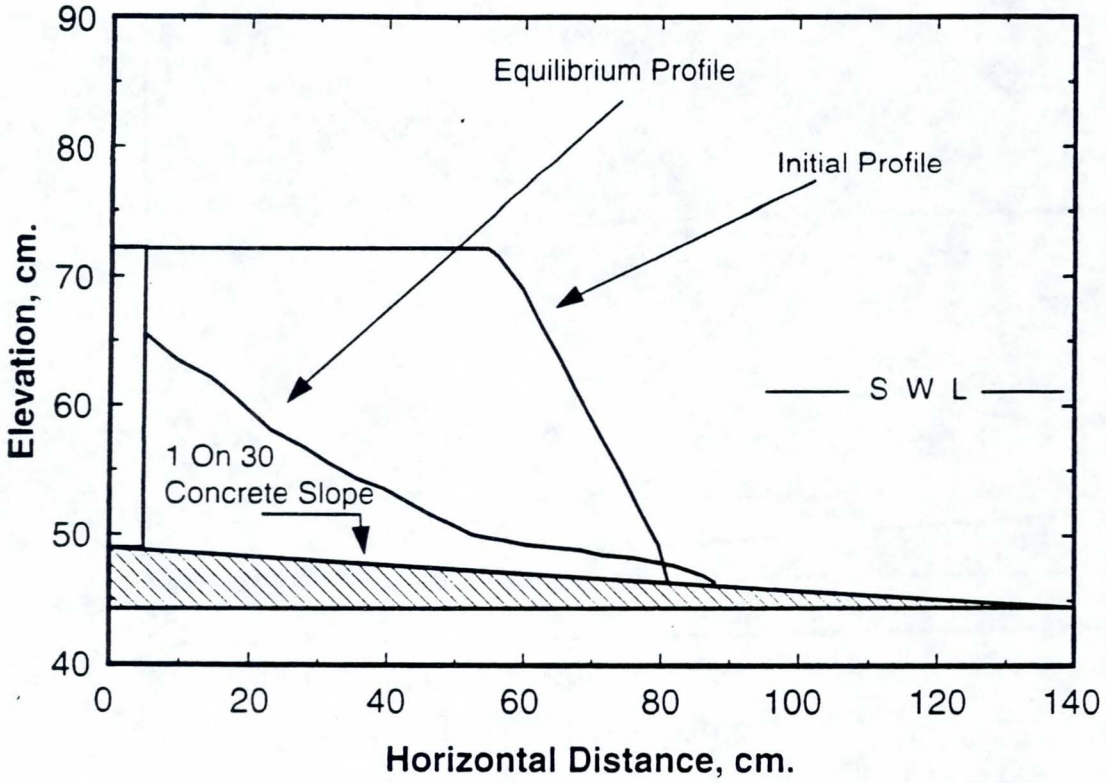
90
80
70
60
50
40
Elevation, cm.
Equilibrium Profile
Initial Profile
S W L
1 On 30
Concrete Slope
0
20
40
60
80
100
120
140
Horizontal Distance, cm.

Figure 3.

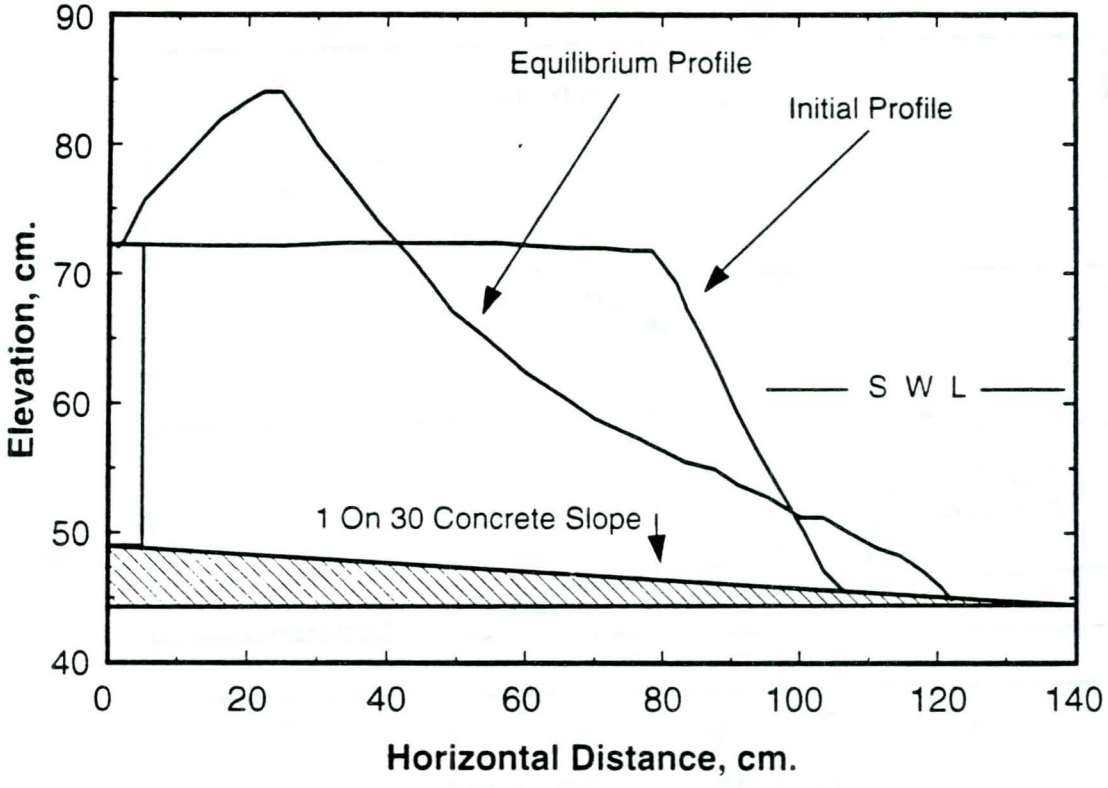
90
80
70
60
50
40
Elevation, cm.
Equilibrium Profile
Initial Profile
S W L
1 On 30 Concrete Slope
0
20
40
60
80
100
120
140
Horizontal Distance, cm.

Figure 4.

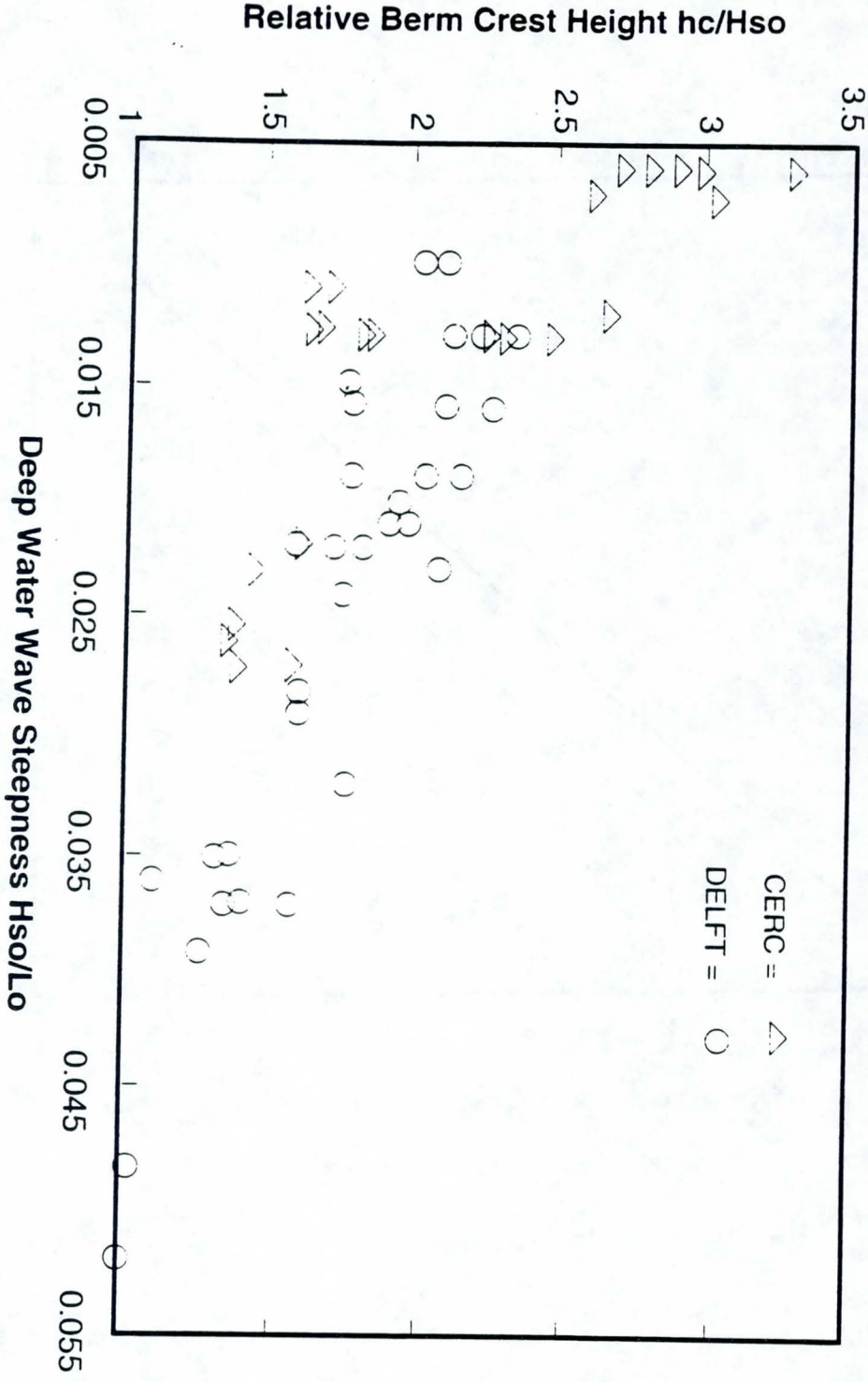
Relative Berm Crest Height hc/Hso
1
1.5
2
2.5
3
3.5
0.005
0.015
0.025
0.035
0.045
0.055
Deep Water Wave Steepness Hso/Lo
CERC =
DELFT =

Figure 5.

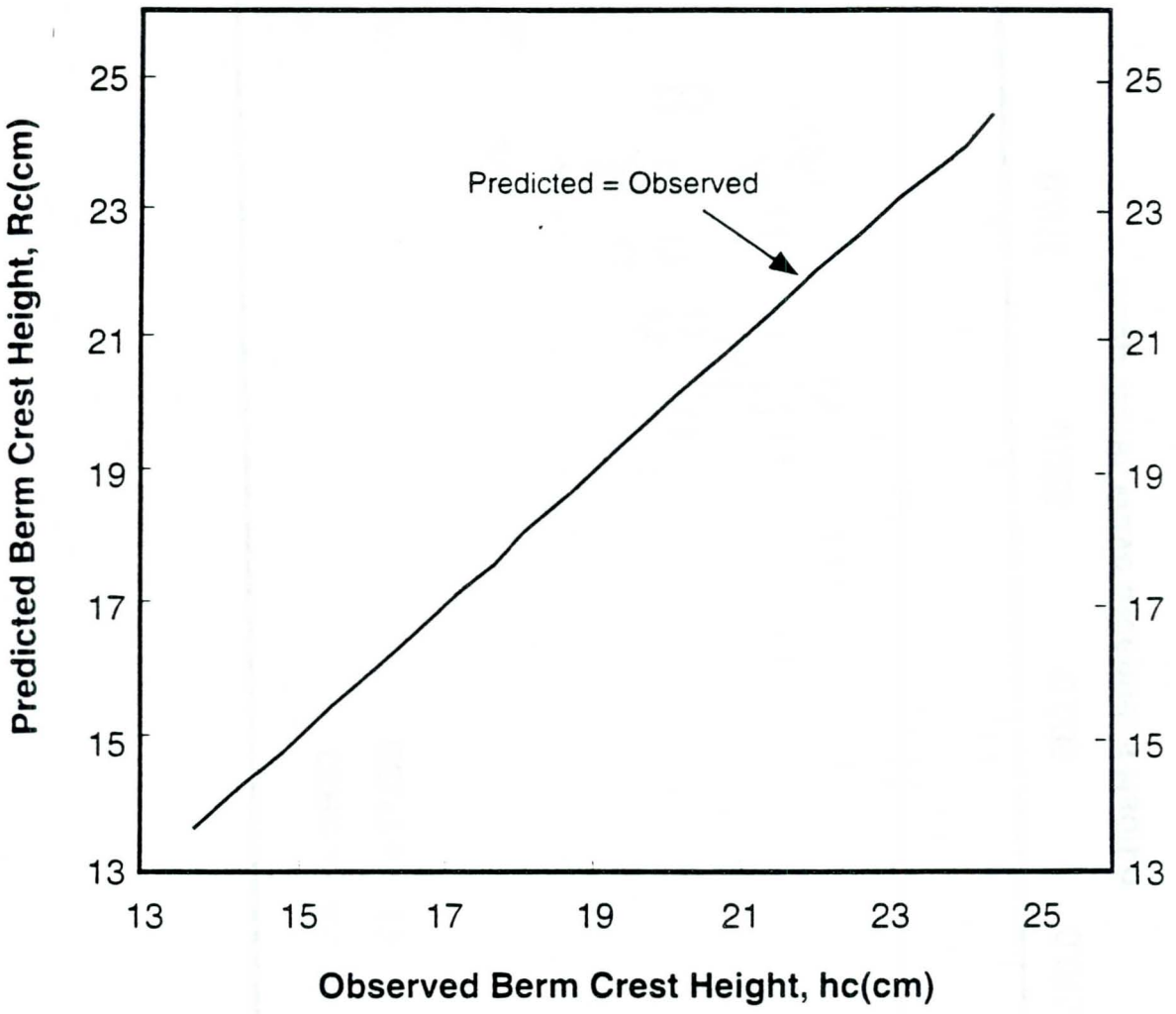
Predicted = Observed
Predicted Berm Crest Height, Rc(cm)
Observed Berm Crest Height, hc(cm)
13
15
17
19
21
23
25

Figure 6.

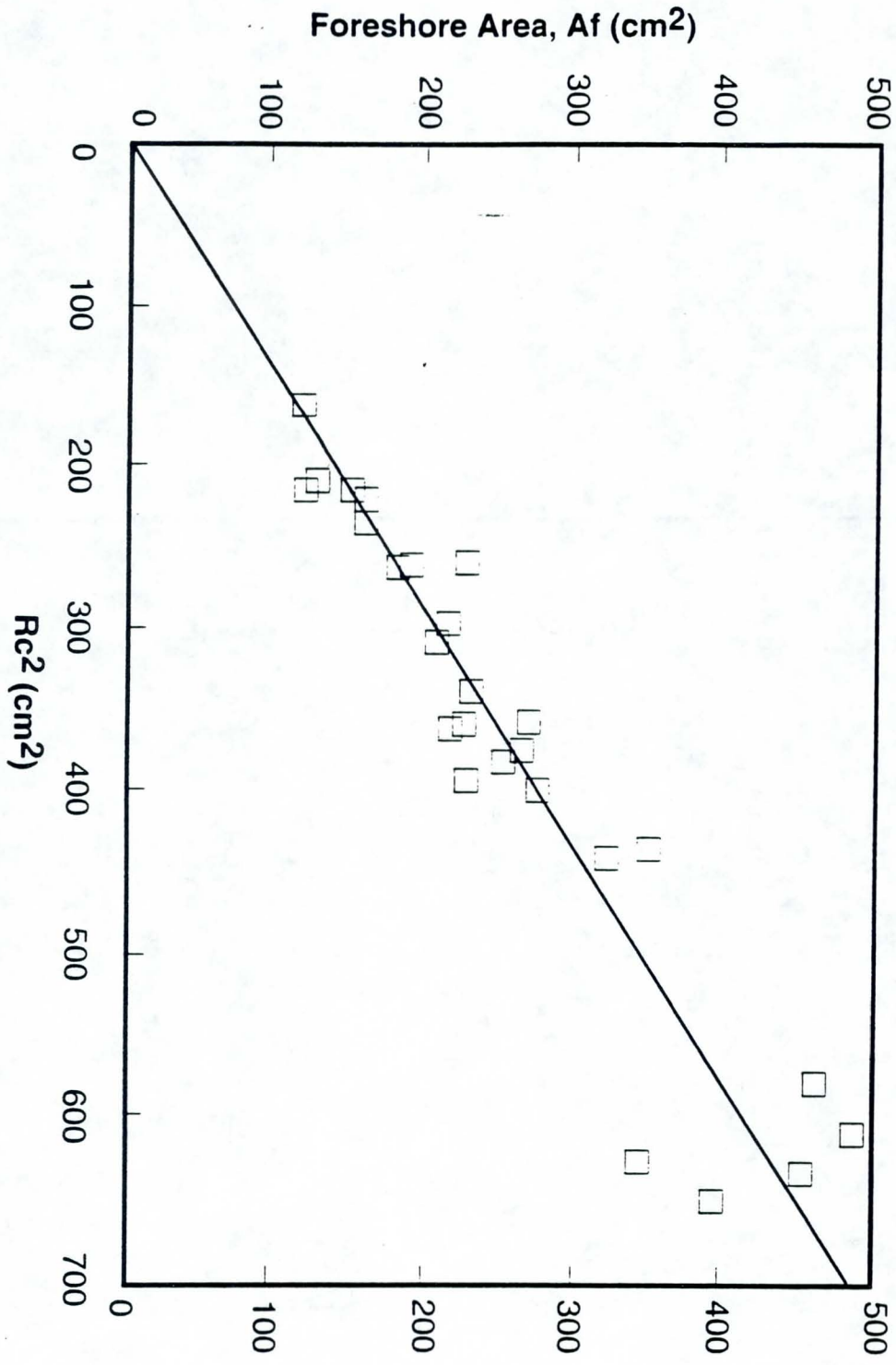
Foreshore Area, Af (cm2)
0
100
200
300
400
500
Rc2 (cm2)
0
100
200
300
400
500
600
700

Figure 7.

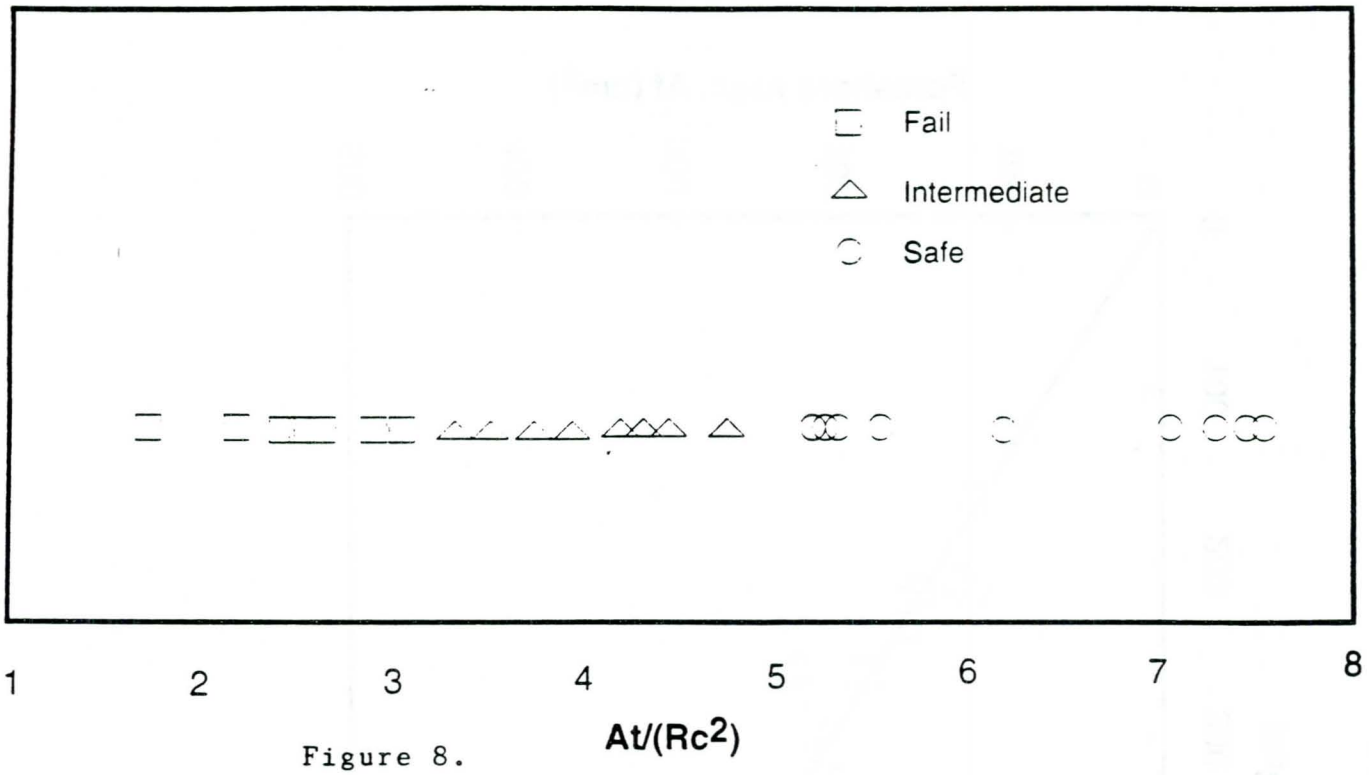

Figure 8.

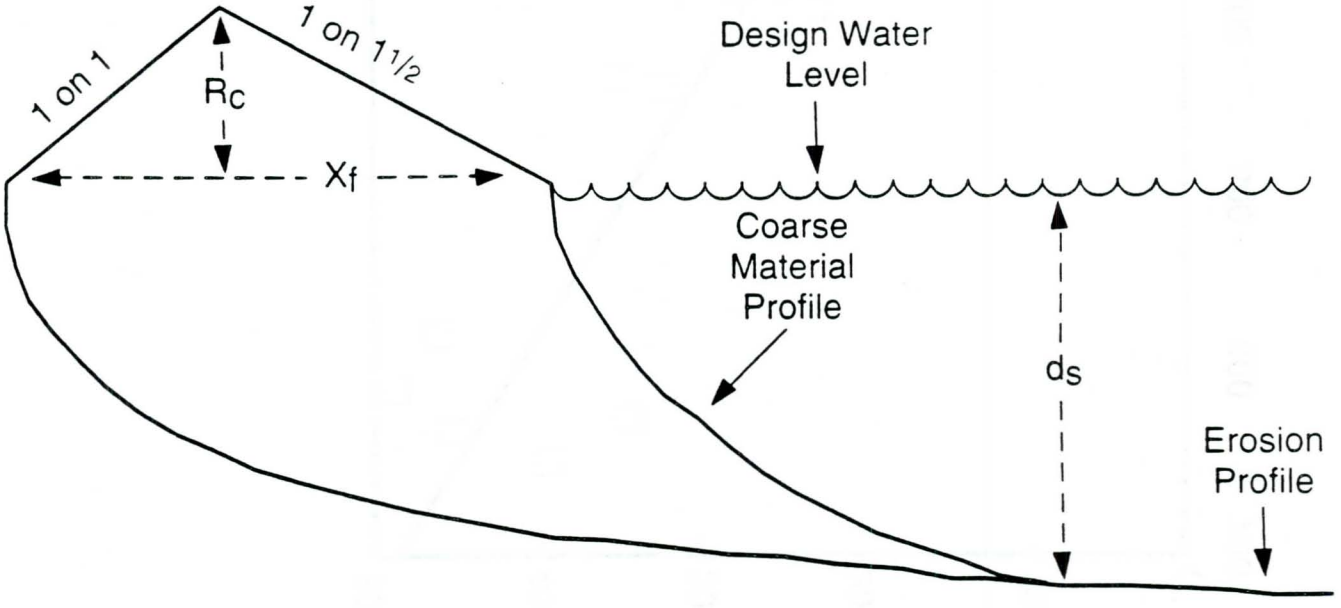

Figure 9.

EXPERIMENTAL VALIDATION OF STABILITY CRITERIA FOR THE DESIGN OF ROCKFILL CLOSURE DAMS

G.J. Akkerman
Delft Hydraulics, P.O. Box 152, 8300 AD Emmeloord,
The Netherlands

E. Berendsen
Road and Hydraulic Engineering Division, Rijkswaterstaat,
P.O. Box 5044, 2600 GA Delft, The Netherlands

ABSTRACT

A physical model investigation was carried out to verify the applicability of stability criteria for rockfill closure dams for combined closure (vertically and horizontally). These criteria have been implemented in a computer program (CLODES). The results of the computations and measurements are compared. The results confirmed the applicability of the criteria for combined closure.

INTRODUCTION

Within the framework of the Dutch Delta Works, experience was obtained in predicting the dimensions of rockfill closure dams under tidal circumstances. As regards the elaborate design procedure for time-dependent conditions, a computer program (CLODES) was developed. This program focussed on the vertical-closure method, i.e. dams that were raised more or less vertically during construction. More recently the program was also adapted for horizontal closure (end-tipping) and combined closure. This paper deals with a scale-model investigation in which the criteria used in this program were validated for a wide variety of closure dam lay-outs. In this paper the predictions rendered by the computer program are compared to those measurements and conclusions on the validation of the criteria used are drawn.

STABILITY CRITERIA FOR ROCKFILL CLOSURE DAMS

Dam-crest stability

For overflow dams, i.e. dams with a more or less horizontal crest, ample experience was obtained in the Netherlands within the framework of the closures of the Delta Project. Early attempts to increase the applicability of this specific experience for general dam geometries and for a wide range of conditions failed. However, in an evaluation study (Akkerman et al., 1985) two general criteria were derived for vertical-closure dams. One of the criteria relates the overtopping height H (water level upstream of the closure dam, relative to the dam crest) to the relative downstream water depth h_d (also relative to the dam crest). The other criterion involves the specific discharge through the closure gap.

The overtopping height criterion, denoted H-criterion, reads as follows:

$$\frac{H}{\Delta D} = c_0 + c_1 \frac{h}{\Delta D} + c_2 \left(\frac{h}{\Delta D}\right)^2 + c_3 \left(\frac{h}{\Delta D}\right)^3 + c_4 \left(\frac{h}{\Delta D}\right)^4 \qquad (1)$$

The coefficients $c_0 \ldots c_4$ have been derived from polynomial curve fitting through all relevant data, see Figure 1. These data comprised vertical-closure dams for a wide range of conditions and various dam shapes, stone dimensions and porosities.
For a wide range of $H/\Delta D$ values, inbetween -4.5 (negative overtopping height) and 15.9, the values values of $c_0 \ldots c_4$ were found to be: $c_0 = 2.00061$; $c_1 = 0.75595$; $c_2 = 0.05705$; $c_3 = -0.00353$; $c_4 = 0.00007$.

The discharge criterion, denoted q-criterion, reads as:

$$\frac{q}{g^{0.5}(\Delta D)^{1.5}} = c_0^1 + c_1^1 \frac{h}{\Delta D} + c_2^1 \left(\frac{h}{\Delta D}\right)^2 + c_3^1 \left(\frac{h}{\Delta D}\right)^3 + c_4^1 \left(\frac{h}{\Delta D}\right)^4 \qquad (2)$$

Also the coefficients $c_0^1 \ldots c_4^1$ were derived from polynomial curve fitting through data of the same set of investigations, see Figure 2.

For the range of H/ΔD values inbetween -3.5 and 15.9 the values of $c_0^1 \ldots c_4^1$ were found to be: $c_0^1 = 1.99952$; $c_1^1 = 1.06866$; $c_2^1 = 0.13884$; $c_3^1 = -0.00234$; $c_4^1 = -0.00002$.

Criteria to assess separate coefficients for various dam-geometry parameters (porosity, crest width, downstream slope angle), obtained by parametric analysis, are also enclosed in the computer program; however, in general, predictions using these criteria do not show improvement, probably due to a lack of systematic data. Therefore, the validation focused on the general criteria outlined in the above.

Dam-face stability

For end-tipped closure dams, i.e. dams that restrict the waterway in a horizontal sense, data of (Naylor, 1976) have been elaborated in such a way that a more convenient and generally applicable criterion was obtained (Akkerman, 1986). This criterion related to the mean gap velocity, see Figure 3. It must be said that this criterion is valid for end-tipped dams only, i.e. without the presence of a vertically raised sill in the remaining closure gap.
The critical velocity criterion, denoted u-criterion, for the most endangered place of the end-tipped dam (somewhat upstream of the advancing dam face) can simply be expressed as:

$$\frac{u_{gap}}{\sqrt{F \Delta g D}} = \log\left(3 \frac{h_c}{D}\right) \qquad (3)$$

where u_{gap} = critical mean gap velocity (m/s) at the damage location derived from the mean specific discharge divided by the local depth Z, with $Z = (2H + h_c)/3$, F = enlargement factor for extreme roughness (-), Δ = specific stone density (-), g = gravitational constant = 9,81 (m/s^2), D = nominal stone diameter, h_c = control water depth (see below).
The enlargement factor F is derived from (Ashida et al.,1976) and reads for $h_c/1.5D$ inbetween 1.0 and 5.2:

$$F = 0.8 \exp\left[\frac{1.174}{h_c/(1.5D)}\right] \quad (4)$$

For $h_c/1.5D > 5.2$: $F = 1$ and for $h_c/1.5D < 1.0$: F is 2.7.

The control water depth for supercritial flow h_c is defined according to (Naylor, 1976):

$$h_c = 0.4H(1-1.5p+\sqrt{1+2p+2.25p^2}) \quad (5)$$

where:
p = contraction coefficient = b_0 /H(cotg β_1 + cotg β_2), with b_0 = width between the toe of the advancing banks and β_1 and β_2 being the slope angles of both advancing bankfaces.
For subcritical flow $h_c = h_d$.

For combined closures, i.e. end-tipped dams in combination with a horizontal sill in the closure gap, no prediction method was available. This method is expected to be economical in many situations as, compared to end-tipping only, bed-protection works may remain modest.
It was reasoned that both methods for dam-crest stability and for dam-face stability might still be applicable if for the end-tipped dam face(s) the bed level was assumed to be at the sill-crest height. For the sill (i.e. the verically erected dam section) in the closure gap it was reasoned that the influence of the advancing dam abutments might be negligible. This reasoning was substantiated as the damage region of the dam face, lying somewhat upstream of the dam-axis, is far away from the downstream dam-crest of the sill. Furthermore, local increase of the flow velocity over the crest due to flow contraction was assumed to be small as well as regards the nicely rounded end-tipped dam face.
The present model investigation was aimed at checking these assumptions, as well as validating the elaborated criterion for the dam-face stability based on (Naylor, 1976).

PHYSICAL MODEL INVESTIGATION

The model investigation was performed in a 2 metre wide circulation flume, depth approx. 0.8 m, flow capacity 0.25 m^3/s, see Figure 4. The flume was equipped with an electronic profile-sounding probe which registrated displacements of stones very accurately, without disturbing the stone arrangement. This measuring procedure allowed for a small length scale as compared to the normal procedure with coloured bands (labour-intensive repair afterwards when done on a small scale). An arbitrary length scale of 40 was adopted, so as to facilitate practical interpretation (the downstream water depth of 0.5 m thus corresponding to 8 m in reality). Processing of the sounded levels, measured in closely spaced cross-sections all over the dam crest of the sill and the end-tipped dam face, was effected by a data-processing program which determined the damaged volume and number of stones. For each situation successive damage steps were performed by increasing the discharge step-by-step at a constant downstream depth during a flow time per step of approx. 0.25 hr (corresponding to approx. 1.5 hr in reality). After each step the contours of the dam face and the dam crest of the sill were sounded. After processing of the data the boundary conditions (discharge, water levels) were determined from interpolation to a reference damage volume.

After careful selection the cross-sectional reference damage area per metre dam section for the dam crest (averaged over half of the closure gap) was defined at 0.15 m^2 on true scale, being a practical measure for initiation of stone displacement. Depending on the stone sizes used (mean diameters: 0.19 m, 0.34 m and 0.54 m on true scale) the reference numbers of displaced stones thus varied between 14 and 0.5).
For the dam face a reference damage volume for the whole embankment face was set at 10 m^3 on true scale. This figure may look somewhat large but at this deformation rate the stones are mainly displaced within the boundaries of the advancing dam profile, so there is hardly any loss of material during subsequent construction; in addition, this damage matched the criterion of (Naylor, 1976) very well.

For situations with a large narrowing of the closure gap, i.e. a high-level sill in combination with approaching end-tipped dam sections, the measured model discharge had to be corrected for flow through the adjoining completed dam sections. This was necessary as the completed dam sections were uniformly built up with the stone class used in the stability tests, whereas for the assessment of the specific discharge only the flow through the closure gap had to be known. The correction was done according to the method developed by (Ikeya, 1992), as outlined below. In order to check the correctness of this method, the specific discharge was also determined directly from the water-level measurements, taking into account a discharge coefficient of 0.9 in the well known discharge relation:

$$q = \mu h_d \sqrt{2gz} \qquad (6)$$

In this:
$z = H - h_d$ for subcritical flow in the closure gap, and
$z = 2/3\ h_d$ for supercritical flow in the closure gap

The prediction of throughflow can be done as follows (Ikeya, 1992), (for notation see Figure 4):

$$q = \sqrt{\frac{K}{3l}\left(h_{upstr}^3 - h_{downstr}^3\right)} \qquad (7)$$

with:
K = permeability coefficient = $n^2 g D_{50}/C$,
n = porosity = 0.45 (-)
g = 9.81 (m^2/s)
D_{50} = mean sieve diameter (m)
C = shape model parameter = 3.1 for angular rocks (-)

l = characteristic seepage length =
= $B + (d - h_{upstr})\cot\alpha + (d - h_{downstr})\cot\beta$

This discharge was computed for the dam sections adjoining the closure gap with exclusion of the cones of the end-tipped dam faces. Next, this discharge was subtracted from the total measured model discharge.

After correcting the model discharge with the predicted throughflow, a mean discharge coefficient of 0.9 was also observed, see Figure 5, thus giving confidence in the corrected discharge figures. It must be said that the correction was only relevant for the critical discharge method and substantial deviation from the total measured discharge was only observed at approaching dam sections (75 and 85% contraction ratio, see further). In the following the discharges directly derived from the water-level measurements have been presented.

A straightforward comparison of the accuracy of the criteria mentioned before, was obtained by computing the critical stone dimensions using the CLODES program for the reference damage condition and subsequent comparison with the stone sizes applied in the model.

ANALYSIS OF RESULTS

Dam-crest stability results

The accuracy of the sounding method is illustrated in Figure 6 for the dam-crest, for a typical initial damage pattern somewhat larger than the reference damage.

Typical results, i.e. predicted stone dimensions versus measured dimensions (on true scale), are presented in Figure 7. Herein the stone dimensions, expressed as ΔD, are plotted against the dimensionless downstream water depth over the sill crest in the closure gap $h_d/(\Delta D)$. This parameter $h_d/(\Delta D)$ also denotes the construction stage of the closure gap sill (large value corresponds to low sill height, and vice versa). It should be remarked that the ΔD used in $h_d/(\Delta D)$ refers to the measured stone dimensions (and not the computed dimensions).
Figure 7 refers to a contraction ratio of 50 %. The contraction ratio is defined as the percentage of horizontal blockage of the flume (total

width on true scale 80 m) by the presence of the dam abutments at a level above the sill crest, see notation in Figure 4. At a contraction of 50 % the dam faces are rather wide apart, the relative distance b_0/L being approx. 1.4 (toe width at the sill level b_0 divided by the sill crest width L).
In this situation, the predictions with the q-criterion are very close to the measurements, even for high-level sills (close to the downstream water level). At a low sill level, the predictions are slightly unsafe (<1.0); this can be attributed to the damage-reference level which is very sharp for this situation. In fact, there will be a large safety margin and damage will be spread more evenly over the crest than for high-level sills. In addition, it can be stated that no differences were observed along the sill crest in the longitudinal direction of the dam. This observation confirmed the expectation that flow contraction over the sill due to the presence of the dam abutment faces might be small.

The H-criterion is over 50% too safe for all sill levels. This can be explained by the wide sill crest which exceeded those of dams analysed in earlier investigations (Akkerman et al., 1985). The wide sill causes friction losses and hence reduces the effective overtopping height H, the reduction of which is not accounted for in the H-criterion. The specific discharge is not sensitive for this friction effect.

In Figure 8 the dam-crest stability is plotted for various stages of horizontal closure.
Figure 8 refers to two (interpolated) relative sill heights: a medium-level sill with $h_d/(\Delta D) = 6$ and a high-level sill with $h_d/(\Delta D) = 2$ for widely varied horizontal closure stages, i.e. inbetween no dam abutments at all (contraction ratio 0%), and the moment that the toes of the dam-faces do almost meet (contraction ratio 85%).
From Figure 8 it follows that only in the final stage of approach of the abutments (upon a contraction ratio of 75%) the actual stability of the sill is slightly increased, resulting in a safer prediction. For the q-criterion this margin goes up to about 50%, whereas the H-criterion reaches over 100% additional safety. The more favourable condition for the sill during the last stage of closure of the end-tipped dams, may be

attributed to interference of the flow around the dam faces and the sill crest.

Dam-face stability results

Figure 9 shows the validity of the dam-face stability approach for the presence of a dam sill in the closure gap. With no sill at all, i.e. for $h_d/(\Delta D) = 13.8$, the result is rather close to 1.0 for all contraction stages. Taking into account the ample margin for failure, the predictions do confirm the u-criterion of (Akkerman, 1986) for the stability of end-tipped dams only.
In the case of a sill, the assumption of a bed level at the height of the sill level, seems justified as long as the approaching dam abutments are not too close. For 50% contraction the predictions are even somewhat too optimistic; at 75% contraction the computations do show a fair agreement. Only at the largest contraction (85%, at which the toes do almost meet) the predictions according to the u-criterion are too unsafe, even in the case of a low sill, resulting in an underestimation of some 30 to 40% of the stone dimensions.

Comparison of dam-crest and dam-face stability

The stability of dam-crest and dam-face can be compared directly, by plotting the critical overtopping height H at both dam sections for their respective reference damage levels. The results are rather striking, see Figure 10. From this figure it can be seen that, in general, the critical overtopping height is somewhat higher for the dam face than for the dam crest at a high sill level, whereas for a low sill level there is high resemblance. The margin is rather small, even for the final closure stages. This implies that, in a practical sense, in the case of combined closure the stone size at the end-tipped dam abutments can be chosen the same as for the dam sill, even up to final closure. It is advised to perform computations for the dam crest (q-criterion) as a reference, rather than for the dam face as regards computational accuracy.

Failure damage margin for the dam crest

Some tests were performed up to damage leading to failure. Although this damage could only be defined rather arbitrarily, the results give an indication of the failure damage margin relative to the reference damage. This is illustrated in Figure 11, in which the ratio of corresponding specific discharges is shown (the arrows indicating complete failure). In spite of the scatter it can be seen that the margin is some 25% for low sill heights and increases up to 50% or more for high-level sills, with no distinct influence of the contraction ratio.
This result shows that for the limited construction time for rockfill closures additional safety may be sought in this damage margin when computing the stone dimensions with the criteria for reference damage indicated in the above. Although not investigated here, it is known from literature and practice that a considerable margin also exists for the dam-face stability.

CONCLUSIONS

Based on the experimental results for validation of stability criteria for rockfill closure dams, the following conclusions can be drawn:

- The critical discharge criterion (q-criterion) for the dam-crest stability of a sill in a closure gap applies very well for all kind of stages of combined closure.
- The dam-face stability criterion can also be applied for all stages of sill construction, apart from the stages where the dam faces are approaching closely. A simpler approach is, to take the same stone class for the dam faces as for the dam crest (computed with the q-criterion); this is also valid for the final closure stages.

ACKNOWLEDGEMENT

This study was commissioned to DELFT HYDRAULICS by the Dutch Public Works Department, Road and Engineering Division and the Construction Engineering Division.

REFERENCES

Akkerman, G.J.; Konter J.L.M. (1985); Hydraulic design criteria for rockfill closure of tidal gaps, Vertical closure method, DELFT HYDRAULICS, M1741-IV, evaluation report.

Akkerman, G.J. (1986); Hydraulic design criteria for rockfill closure of tidal gaps, Horizontal closure method, DELFT HYDRAULICS, S861/Q438, evaluation report.

Ashida, K.; Bayazit, M.; Initiation of motion and roughness of flow in steep channels, IAHR Istanbul, paper A58.

Ikeya, T. (1992); An analytical estimate of the discharge through rockfill dams, DELFT HYDRAULICS, internal note.

Naylor, A.M. (1976); A method for calculating the size of stone needed for closing end-tipped rubble banks in rivers, CIRIA report 60.

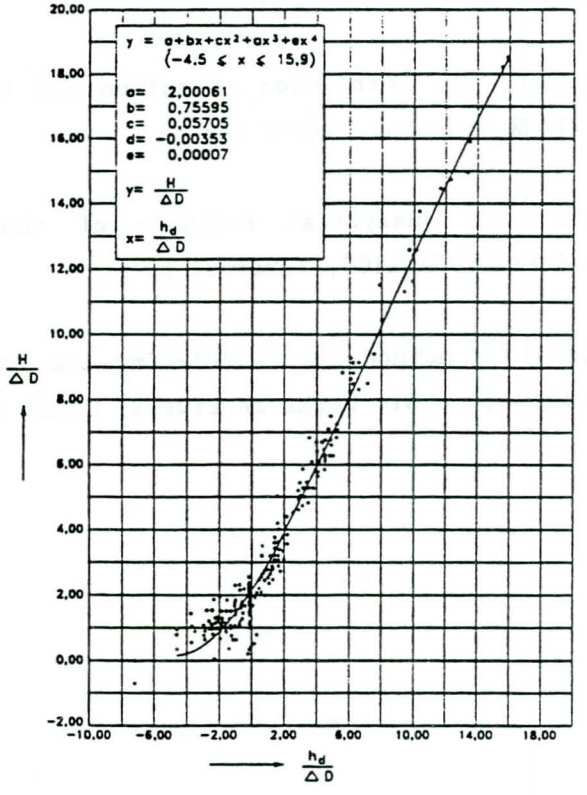

Figure 1: H-criterion for dam-crest stability

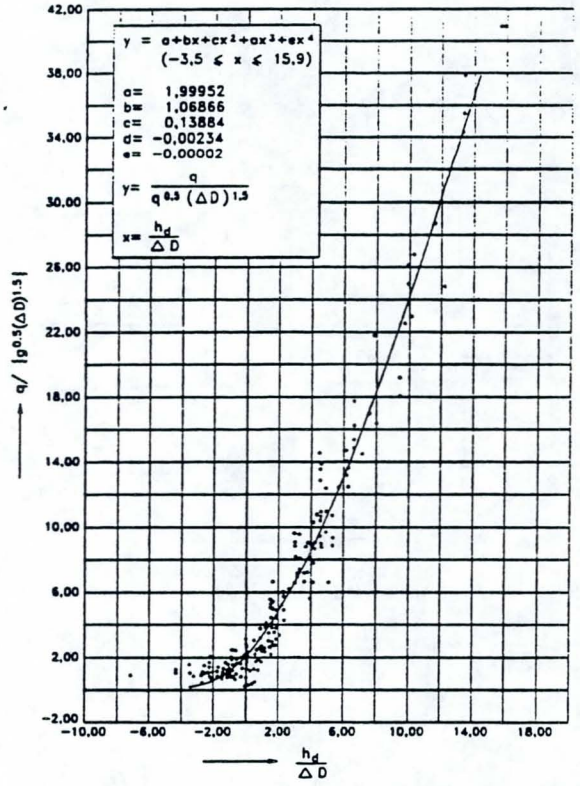

Figure 2: q-criterion for dam-crest stability

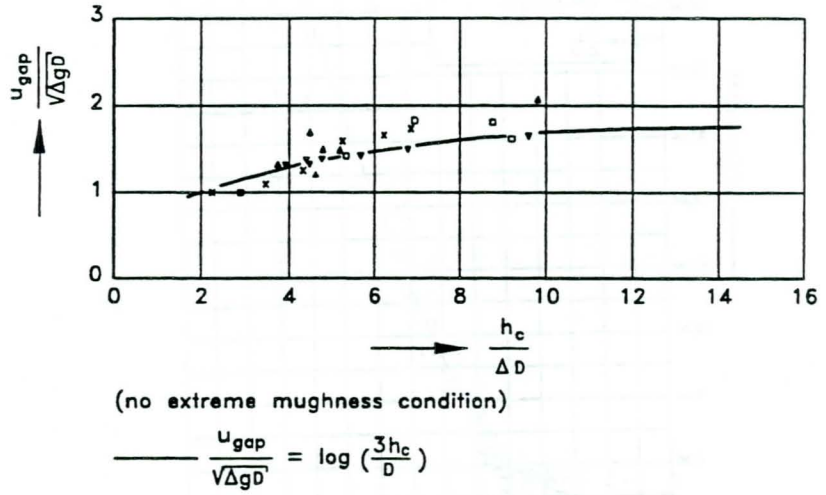

Figure 3: u-criterion for dam-face stability (based on Naylor's (1976) data)

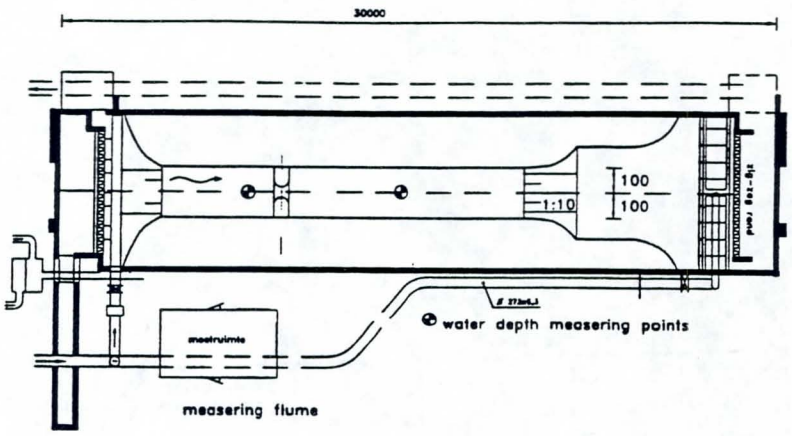

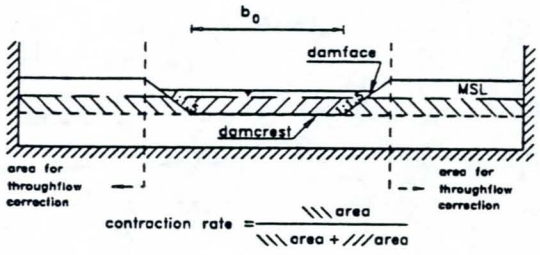

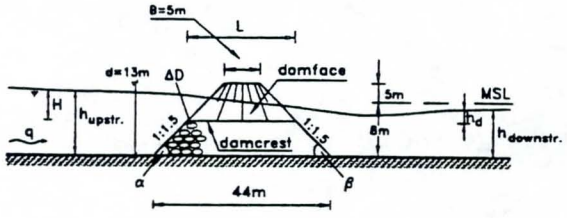

Figure 4: Model set-up and denotation

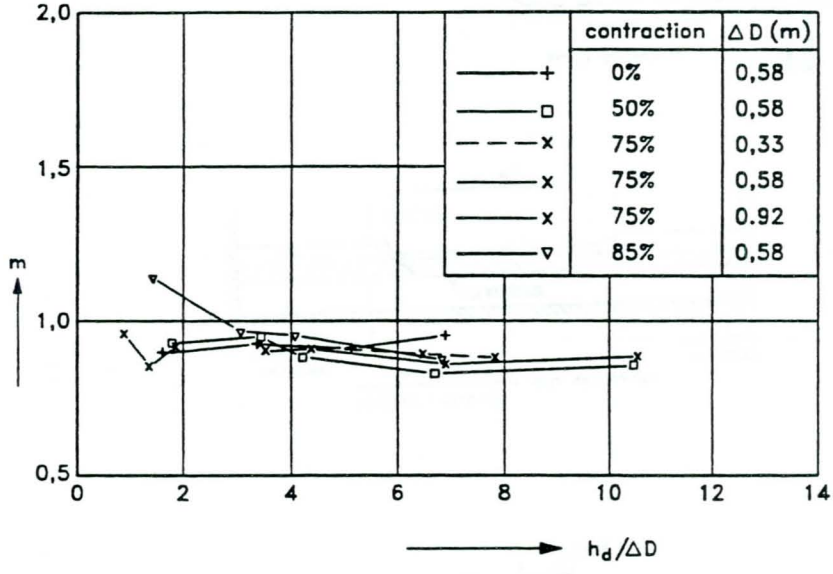

Figure 5: Discharge coefficient at critical condition dam crest

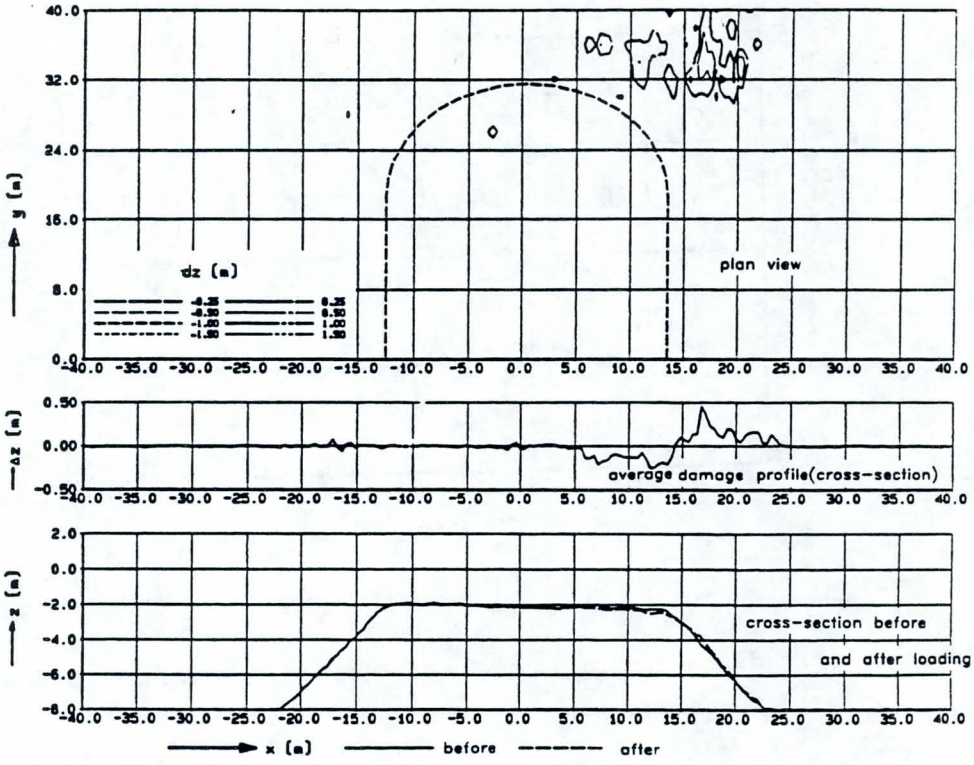

Figure 6: Example of sounding results initial damage dam crest

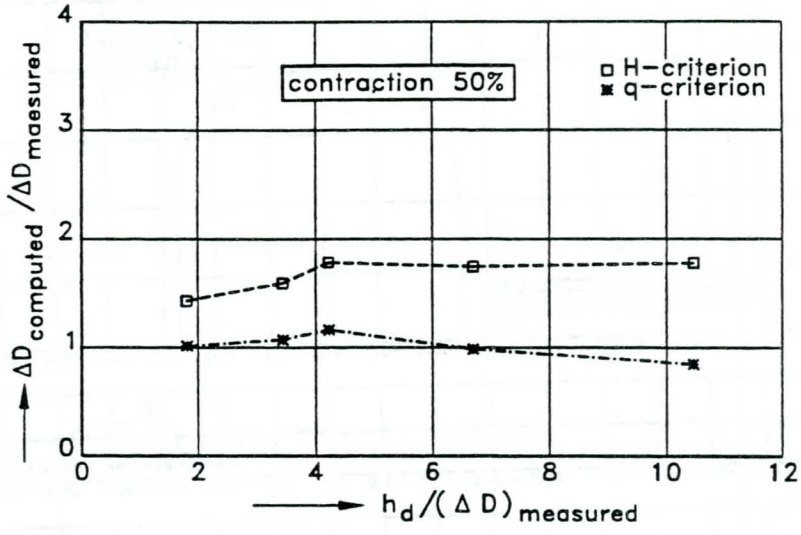

Figure 7: Predicted and measured critical stone dimensions dam crest at 50 % contraction

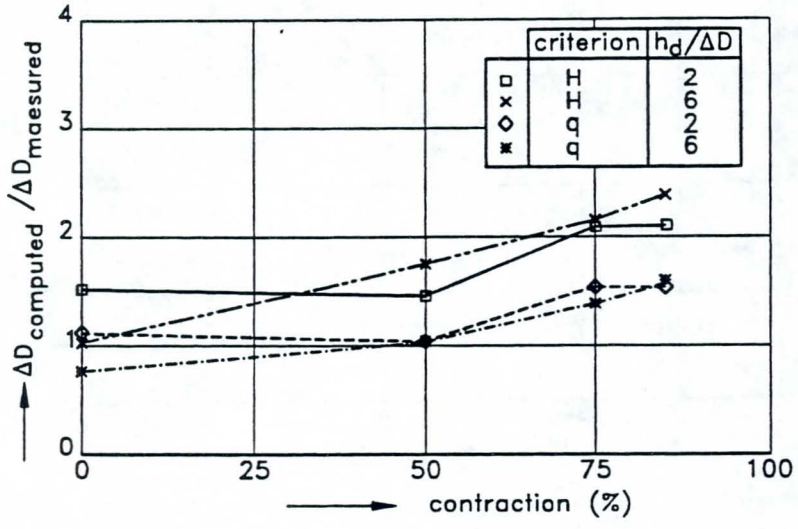

Figure 8: Dam-crest stability results as a function of contraction ratio

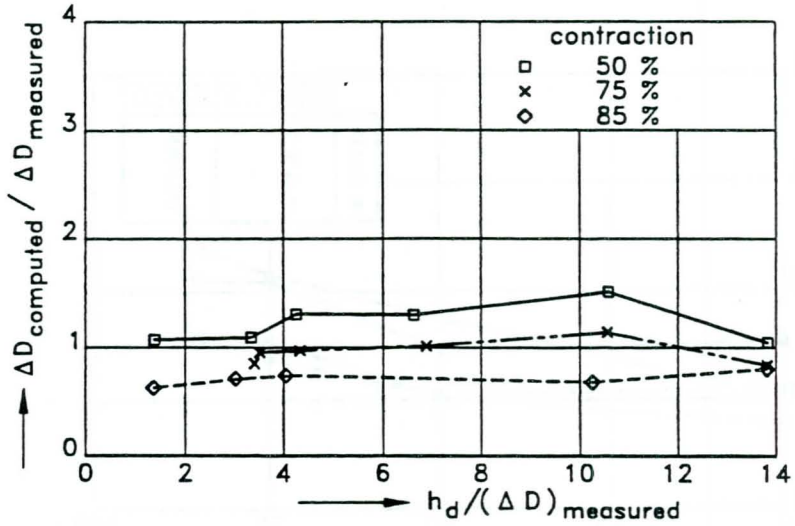

Figure 9: Predicted and measured critical stone dimensions dam face (ΔD = 0.58 m)

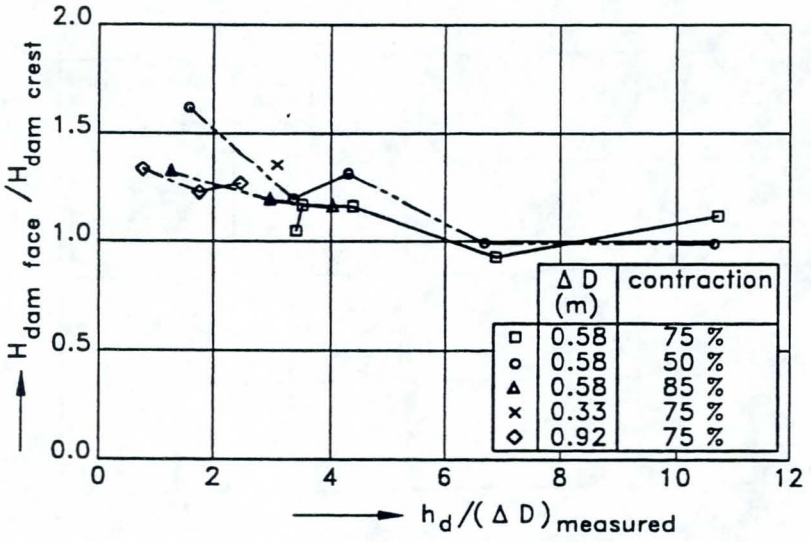

Figure 10: Comparison of critical overtopping heigth of dam crest and dam face

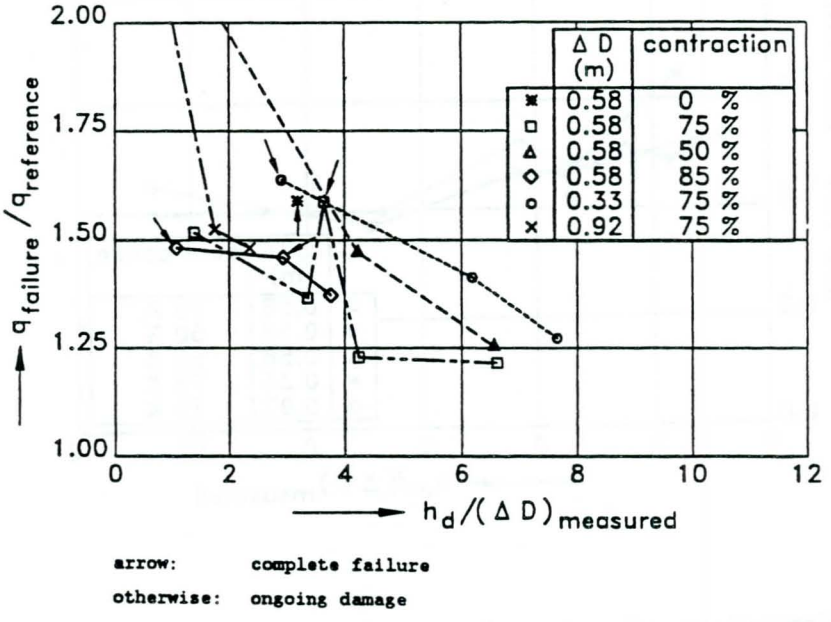

Figure 11: Failure margin for specific discharge dam-crest stability

STABILITY OF ROCK ARMOUR AND RIPRAP ON COASTAL STRUCTURES

N.W.H. Allsop and R.J. Jones
Hydraulic Research, Wallingford, OX10 8BA England

Abstract

This paper identifies the principal methods available to calculate the unit size of rock or rip-rap armour to be used to protect rubble mound breakwaters; sea walls; coastal and reservoir revetments against erosion by wave attack. It describes the results of recent studies to provide better data both on the stability of armour of shapes and gradings outside of the limits commonly accepted, and on the stability of armour placed on structures that differ from the simplified configurations for which most design methods have been developed. The paper also discusses the influence of variabilities in the design formulae and the input parameters on the safety of the final results. Where appropriate the paper draws on design information compiled for the CIRIA / CUR manual on rock structures (Ref 1).

1 Introduction

1.1 Background

The principal purposes of coastal or shoreline structures such as breakwaters, sea walls, groynes and revetments, are to reduce direct and indirect effects of wave action, particularly erosion and/or overtopping. Such structures may be constructed using quarried rock to form a series of rough and permeable layers, within the pores of which wave energy is dissipated. These classes of structures are often termed rubble mounds or rubble revetments. In absorbing a significant proportion of the incident wave energy, the structures themselves should not suffer excessive re-shaping or damage to the outer layers, although some re-adjustment of the armour is an inherent feature of this class of structure, and is implicit in the development of the design formulae.

In designing such structures to give acceptable structural responses, the principal variables to be selected are the unit armour mass, usually M_{50}, or the equivalent nominal diameter, D_{n50}. The armour, often laid in thicknesses equivalent to $t_a = 2.0$ to $2.5D_{n50}$, resists wave forces principally by its weight and interlock. The armour mass required for stability is generally proportional to the incident wave height cubed, H^3. The main other structural variables, such as seaward slope angle α, and crest height R_c, are principally set by hydraulic requirements such as limits on wave overtopping and reflections, although it will be seen later that these and other parameters also influence the armour size needed.

The design methods for calculating armour size are principally empirical formulae, themselves based on results from hydraulic model tests on idealised cross-sections. The test data available, and hence the design methods, are limited almost entirely to simple mounds subject to normal wave attack, $\beta=0°$, and to narrow graded rock of generally cubic shape. Quarried rock however occurs in many shapes, sizes and gradings, and such structures are seldom subjected only to normal wave attack. Remarkably little guidance has been available on the influence of these variables on armour stability. Some recent experimental studies have indicated the influence of some of these parameters, but have not yet been fully reflected in design methods or specifications.

This paper describes some of the recent extensions to the design formulae available, and presents example results from recent and continuing research on the design of rock armoured shoreline structures.

1.2 Use of rock in armoured structures

1.2.1 Types of structures

Rubble mound structures to resist wave action are frequently used in those areas of the world where rock may be quarried and handled in appropriate sizes, in sufficient quantities, and of acceptable potential durability. The principal types of structures that may be formed in this way are summarised below, although many other types of have been devised:

Harbour breakwaters - formed to limit wave action within a specified area so that ships or small vessels may be operated, moored, and /or anchored without disruption to the required (commercial) activities, and without damage to the vessel or harbour structures;

Sea walls or shoreline revetments - to halt coastal erosion and/or to restrict wave overtopping and hence flooding, and to limit the degree of wave reflections;

Armour layers to embankment dams - protecting the dam core and filter layers against direct or indirect wave attack, and restricting any wave overtopping of the dam crest to an acceptable minimum;

Coastal defence breakwaters - constructed to encourage the development or maintainance of a beach or beaches in their lee, and/or to limit wave action at the coastline;

Beach control structures including groynes - to assist in the retention of adequate beaches which themselves limits any coastal erosion and/or flooding.

1.2.2 Rock armour

In some areas, rock armour may be extracted and handled in unit sizes up to about 25 tonnes, having a nominal diameter D_n of approximately 2.1m. Armour layers formed from such sizes may resist substantial wave attack, perhaps up to significant wave heights of 6 -7 metres. In other areas, the rock available is substantially smaller, and may only be used to resist relatively small waves. In some cases, where the rock available is small and/or the waves are large, concrete armour units will be used. The design of concrete armour units has become a substantial subject area in its own right, and is not discussed further in this paper.

As first blasted in the quarry, the rock will be highly variable in unit size. In the design of most rubble structures, and/or in the quarrying operation itself, care will be taken to optimise the use of different rock sizes. Very small sizes will be used in the production of aggregate materials for concrete, roadstone, or similar uses. Sizes up to about 0.3 to 0.5m will often be crushed to be used as aggregate etc. Above about 0.5m, the rock may be useful to form under- or filter layers, and or armour layers where wave attack is slight.

Most rock armour is prepared in narrow size or weight bands, eg. nominally 3 to 6 tonne. This material is generally handled individually, and placed in armour layers of about 2 stones thickness. Rock to be used as such armour must therefore be carefully sorted in the quarry, often requiring specialist plant for the handling, and weighing if needed. Once prepared in this way, the rock is carefully controlled, and is relatively easy to measure before placement and on the structure.

An alternative material is rip-rap: a wide graded rock which has not been sorted to the same extent as rock armour, if at all. Rip-rap is handled and placed in bulk, and because of its wider range of sizes, must be laid in relatively thicker layers. Over much of the range of sizes, these materials respond to wave action in relatively similar ways, but will differ significantly at the extremes. Single sized rock armour can be used to form quite steep slopes, perhaps up to 1:1.25, although such a steep slope is seldom recommended. When placed at steep slopes, rock armour is at risk of damaging suddenly, with a relatively brittle failure mode. Wider-graded material will not naturally sit at such steep slopes, but when placed on shallower slopes, say 1:2 to 1:4, will generally damage more gradually, even when nearing its failure limit.

1.3 Historical context

A full understanding of the use of present design methods requires some knowledge of their derivation. The most widely known design formula is that developed by Hudson at the Waterways Experiment Station (WES) and now used in the Shore Protection Manual (Ref 2). This method is based on the results of regular wave studies in the early 1950s at the Waterways Experiment Station, Vicksburg, USA. A simple formula was developed to relate the armour unit weight to the structure slope angle, armour unit density, and (regular) wave height.

In 1975, Thompson & Shuttler at Wallingford completed some of the earliest random wave tests on rock armoured slopes in a study for the Construction Industry Research and Information Association in the UK (CIRIA). The tests were directed to the stability of rip-rap protection for embankment dams on inland reservoirs. The results of these tests were used to derive a design method for rock armour of grading up to $D_{85}/D_{15} = 2.25$ on a long slopes with an impermeable core. The model test results were published as an HRS report, and as a design guide by CIRIA, Report 61 (Ref 3).

Between 1983 and 1988, a comprehensive series of studies were conducted by van der Meer and co-workers at Delft Hydraulics in the Netherlands to extend the validity of Thompson & Shuttler's tests to give the armour response for a wide range of armoured structures, including breakwaters, sea walls, and revetments. The test procedures extended those used by Thompson & Shuttler, and included a wider range of hydraulic and structure parameters. Van der Meer included the CIRIA results with the new data. The analysis of the extended data set generated new stability formulae (Ref 4) covering the wider range of input parameters.

In 1987, further model tests were conducted at HR Wallingford in the UK with Queen Mary and Westfield College (QMW) to explore the effect of particle shape on the armour response (Refs 5, 6).

Then in 1988, a project was initiated to compile a new design manual on the use of rock in coastal engineering jointly by CIRIA in the UK, and the Centre for Civil Engineering Research, Codes and Specifications in the Netherlands (CUR) (Ref 1). A short series of hydraulic model tests were conducted at Wallingford to identify the general level of the influence of wide grading on armour response (Ref 7).

All the studies above were confined to 2-dimensional wave attack on relatively simple cross-sections. In 1992, Jones & Allsop conducted a series of tests at Wallingford for the UK Ministry of Agriculture, Fisheries, and Food (MAFF) to explore the use of these simple methods to rock armoured groynes and related beach control structures (Ref 8). These tests addressed the stability of rock on armoured structures on steep shingle beaches. The results of this work were also combined with data from the Spanish laboratory CEPYC on the stability of rock armoured groynes on shallow beach slopes.

Between 1990 and 1993, research within a European-wide project, G6-S Coastal Structures supported by national funds and the EC MAST programme, has explored the influence of wave obliquity and short-crestedness on armour stability. Data has also been collected from the main European laboratories on armour responses on site specific structures that have been model tested. The full implications of the results of this work are still being considered, but some initial results will be used here.

Finally in this context, continuing research in the UK on risk assessment and probabalistic design methods has confirmed the importance of assessing the influence of uncertainties in the design methods used, and the variabilities of the main input parameters, on the overall safety of the resulting structures.

2 Present design practice

2.1 General philosophy

Armoured rubble structures may fail by the removal of many individual armour units, precipitating erosion of the layers beneath; the structural failure of individual units, and hence local failure of the armour layer; or by a geotechnical failure of part of the structure, or of its foundation, see Figure 1. Of these failure modes, that accorded most attention has historically been the displacement of armour units by direct wave action, and it is this failure mode which is principally addressed by the design methods covered in this paper.

On rock armoured structures, the placement of the armour, and the shape and size of the armour units themselves, are seldom entirely regular. In many ways regular and close placement of rock armour is undesirable as it can lead to a relatively smooth or "paved" surface, with low armour layer porosity. This often therefore reduces the capacity of the armour for energy dissipation, increasing wave run-up levels and/or overtopping, and wave reflections. The variablities in armour placement, coupled with the stochastic or random nature of waves themselves, mean that the response of the armour layer to wave action will vary along the structure and in time.

Under wave action approaching the design level, rock armour may be expected to adjust position, often settling or bedding down a little and increasing its resistance to wave action. A few armour units may be displaced, especially those that were originally placed loosely. This displacement of armour, often termed "damage", should be relatively small for waves up to and including the design storm condition. Historically a level of displacement or damage of up to N_{od}=5% at the design wave condition has been accepted for many coastal structures and, where the design wave condition has been correctly determined, this has allowed the successful design, construction, and use of many rock armoured structures worldwide.

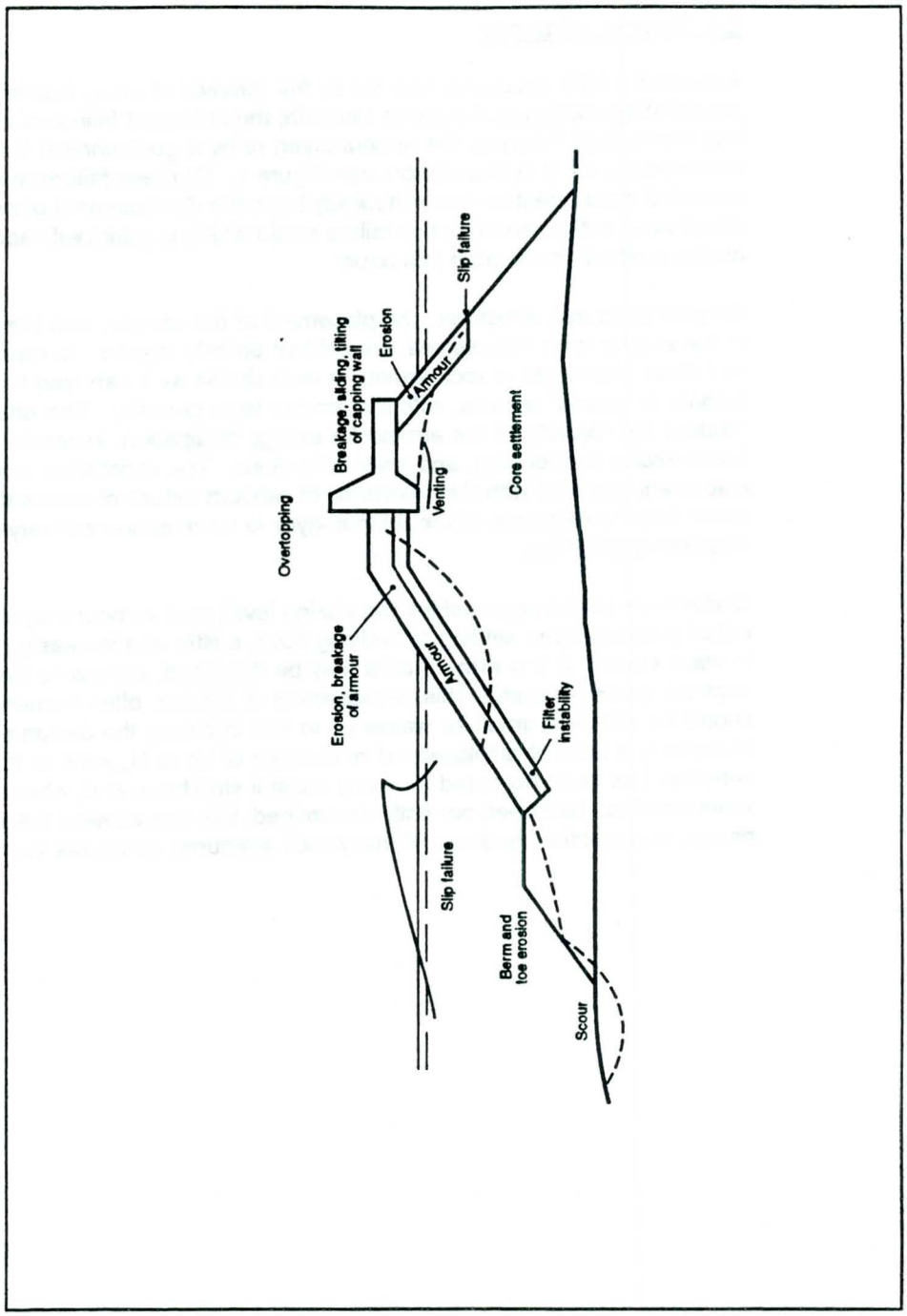

Figure 1 Failure modes for armoured structures, after Burcharth

Where the structure is of higher importance; the wave conditions less certain; or the consequences of any damage more severe; more conservative design criteria may be applied, perhaps restricting armour movement to N_{od}=1%. Such restrictions generally result in increases to the relative armour size, and often to the overall structure volume and hence cost. It is however seldom realistic to design rock armour for no armour movement at all, hence the wide acceptance of "no damage" criteria falling in the range N_{od}=1-5%.

Most designs of coastal structures are based on a deterministic approach in which formulae are used to determine a single value for a particular input parameter for each of the required responses. In recent years it has become possible to use probabilistic methods to asses the levels of risk of different failure conditions, taking account of the variabilities of the structure; environmental conditions; and of the prediction formulae themselves. These methods are under development, and will be discussed in future reports. A brief example will be discussed later in this paper.

2.2 Design methods

Design methods for rock armour focus principally on the calculation of the median armour unit mass, M_{50}, or the nominal median stone diameter, D_{n50}, defined in terms of M_{50} and the rock density, ρ_r:

$$D_{n50} = (M_{50}/\rho_r)^{1/3} \qquad (1)$$

The two most commonly used methods are:

a) the Hudson formula, as used in the Shore Protection Manual, (SPM);
b) van der Meer's equations.

2.2.1 Hudson's formula, regular waves

Hudson developed a simple expression for the minimum armour weight required to resist a given (regular) wave height. The formula was originally written in terms of the individual armour unit weight and the weight density, but may now be re-written in terms of the median armour unit mass, M_{50}, relevant mas densities, and the wave height, H:

$$M_{50} = \rho_r H^3 / K_D \cot\alpha \, \Delta^3 \qquad (2)$$

where
ρ_r = mass density of rock armour (kg/m^3)
Δ = bouyant density of rock, = (ρ_r/ρ_w)-1
ρ_w = density of sea water
α = slope angle of the structure face;

and K_D is a stability coefficient to take account of the other variables. For wide graded rock or rip-rap, values of a coefficient K_{RR} were substituted for K_D.

Values of K_D were derived from model tests at Vicksburg, using regular waves with permeable cross-sections subject to little or no wave overtopping. The armour stability was studied under a range of wave heights and periods. In each case, the design value of K_D chosen was that corresponding to the wave height giving worst stability. Some re-arrangement of the armour was expected, and values of K_D

suggested for design correspond to a "no damage" condition where up to 5% of the armour units may be displaced. Values of K_D for "no damage" were determined for breaking and non-breaking wave conditions at the structure:

Armour	Waves	K_D
Rough stone	Non-breaking	4.0
	Breaking	2.0
Smooth stone	Non-breaking	2.4
	Breaking	1.2

Other values for increasing levels of damage are tabulated in the SPM (Ref 2).

It is often convenient to re-arrange the Hudson equation in terms of a stability number N_s:

$$N_s = H_s/\Delta D_{n50} = (K_D \cot\alpha)^{1/3} \quad (3)$$

This stability number is re-used by van der Meer, see section 2.2.2, and is also used in calculations of toe armour sizes using methods in the SPM.

2.2.2 Van der Meer's formulae, random waves

Van der Meer has derived formulae which include the effects of random waves, a wide range of core / underlayer permeabilities, and distinguish between plunging and surging wave conditions. The formulae relate the incident wave conditions, and the level of damage that may be allowed, to the dimensionless stability number, $H_s/\Delta D_{n50}$. For plunging waves:

$$H_s/\Delta D_{n50} = 6.2\ P^{0.18}\ (S_d/\sqrt{N})^{0.2}\ \xi_{sm}^{-0.5} \quad (4)$$

and for surging waves:

$$H_s/\Delta D_{n50} = 1.0\ P^{-0.13}\ (S_d/\sqrt{N})^{0.2}\ \sqrt{\cot\alpha}\ \xi_{sm}^{P} \quad (5)$$

where the parameters not previously defined are:

P	notional permeability factor, see Figure 2
S_d	design damage number = A_e/D_{n50}^2
A_e	erosion area from profile
N	number of waves
ξ_{sm}	Iribarren number = $\tan\alpha/s_m^{1/2}$
s_m	wave steepness for mean period = $2\pi H_s/gT_m^2$
T_m	mean wave period;

and the transition from plunging to surging waves is calculated using a critical value of ξ_{sm} :

$$\xi_{sm} = (6.2\ P^{0.31}\ (\tan\alpha)^{0.5})^{1/(P+0.5)} \quad (6)$$

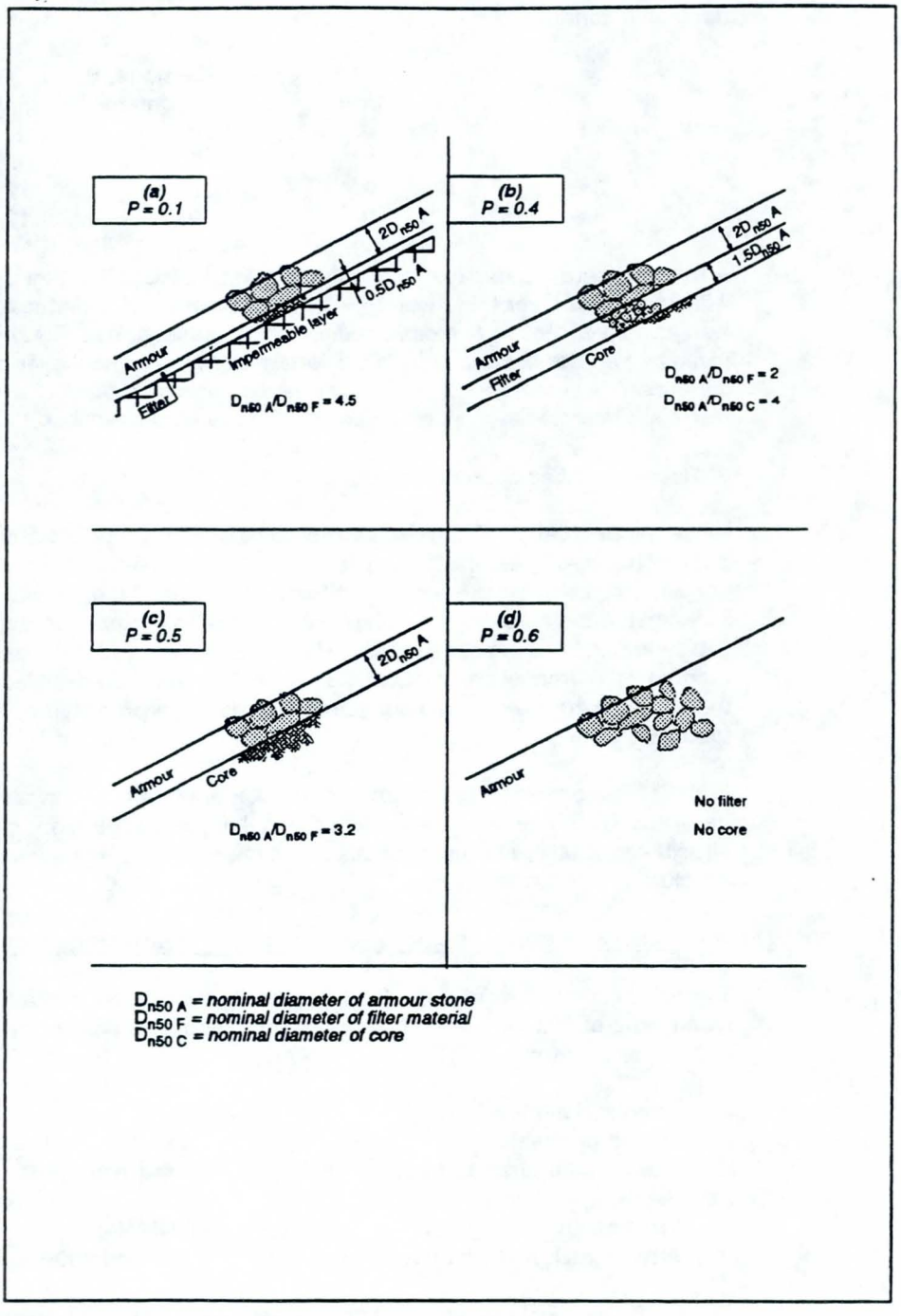

Figure 2 Permeability factor, P, for van der Meer's stability formulae

Recommended values of the damage parameter, S_d, are given for each of three damage criteria:

Slope	Damage, S_d		
	Initial	Moderate	Failure
1 : 1.5	2	-	8
1 : 2	2	5	8
1 : 3	2	8	12
1 : 4-6	3	8	17

A range of core / underlayer configurations were used in the test programme, each with an armour layer thickness, $t_a = 2.2D_{n50}$. A value of a permeability factor, P, was assigned to each of these structure configurations, see Figure 2. Values of P given by van der Meer vary from 0.1 for armour on an underlayer over an impermeable embankment, to 0.6 for a homogeneous mound of armour size material. Intermediate values of 0.4 and 0.5 are also described.

3 Recent studies on rock armour stability

Since the publication of van der Meer's equations, a range of further studies have been conducted to extend the application of these equations to other armour specifications and structure configurations. The first of the studies at Wallingford investigated the influence on stability of changes to the armour unit shape; the layer thickness; and the armour grading. The model tests used the 2-dimensional random wave framework of Thompson & Shuttler and van der Meer. Damage measured in these tests was compared with damage predicted by van der Meer's formulae.

Further tests on 3-dimensional models of rock armoured breakwaters and groynes have also been conducted to explore the stability of rock armour on beach control structures. Analysis of these results is not yet complete, but preliminary conclusions are drawn here.

3.1 Influence of armour shape, layer thickness and armour grading

Two model studies were carried out to quantify the influence of armour shape and placement; and of very wide armour grading. Structure parameters common to both studies were:

Armour slope (cot α)	2.0
Mound permeability	Impermeable, P = 0.1
Water depth at structure (h_s)	0.5m (model)
Bed approach slope	1:50
Spectral shape	JONSWAP
Armour rock and water densities	2710 and 1000 kg/m3

During the joint HR / QMWC tests investigating the effects of armour shape and layer thickness, all test sections were constructed with a constant median rock weight and armour grading of $D_{85}/D_{15}=1.25$. Armour layers were constructed in two layers with individual placement of armour stones. This method of construction was selected as typical of the construction of narrow graded rock armour. In previous

studies, armour had generally been placed in bulk, rather than stone by stone.

3.1.1 Influence of layer thickness on stability

In the preliminary analysis of the HR / QMWC results, each set of damage measurements was compared with damage predicted using van der Meer's formulae. In virtually all cases the formulae under-predicted the damage recorded. Further analysis and comparison of the results revealed some important variations.

The procedure adopted for construction of the armour layers in the HR / QMWC study was typical of methods used for the construction of two layer armouring to sea walls and breakwaters, but was different from that used in the earlier studies. In many practical cases armour layers may be formed of thickness less than $2.2D_{n50}$, and the average achieved in these tests was $t_a=1.5\text{-}1.7D_{n50}$. This represents a 30% reduction with respect to earlier studies, and it was felt that this reduction alone could account for the increase in damage.

Relatively little data on this effect were available, as essentially only one layer thickness of $t_a=1.5\text{-}1.7D_{n50}$ had been studied. The damage to armour of thickness $t_a=1.6D_{n50}$ was compared with that predicted by van der Meer's equations for $t_a=2.2D_{n50}$. A simple adjustment of the power coefficient of $(S_d/\sqrt{N})$ in Equations 4 & 5 from 0.2 to 0.25 gave a better description of the damage for the thinner armour layers. The modified equations then become, for plunging waves:

$$H_s/\Delta D_{n50} = 6.2\ P^{0.18}\ (S_d/\sqrt{N})^{0.25}\ \xi_m^{-0.5} \qquad (8)$$

and for surging waves:

$$H_s/\Delta D_{n50} = 1.0\ P^{-0.13}\ (S_d/\sqrt{N})^{0.25}\ \sqrt{\cot\alpha}\ \xi_m^{P} \qquad (9)$$

Initially these changes seem to be counter-intuitive, in that the rate of damage with wave height reduces from H^5 to H^4. However it should be noted that for most realistic cases, values of $S_d/\sqrt{N}$ will vary between 0.15 and 0.03, so the overall effects of the modified equations are to increase damage with decreasing layer thickness. This may be illustrated by considering the armour size needed on a 1:2 slope against waves of $H_s=2m$, $T_m=6s$, N=1500 waves, and a structure of P=0.4. For the "standard" or thicker layer, $t_a=1.6D_{n50}$, an armour unit mass of $M_{50}=0.85$ tonne is needed for a damage level $S_d=2$. If the armour is laid to form the thinner layer, $t_a=2.2D_{n50}$, an armour unit mass of $M_{50}=1.3$ tonne is needed for the same damage level.

3.1.2 Influence of armour shape on stability

The main purpose of the joint HR / QMWC studies had been to investigate the influence of armour unit shape on stability. Five classes of rock were prepared, each of similar grading and unit size, but falling into different shape classifications:

Fresh	Selected to be representative of most rock armour used in the UK;
Equant	Chosen to be as near cubic as practical, typical of the most cubic material available in UK;
Semi-round	Rounded slightly by tumbling in an old concrete mixer drum to

	simulate abrasion wear;
Very round	Rounded more significantly to simulate the effects of severe abrasion;
Tabular	Flat or elongate material, shapes normally rejected for armour.

The damage to test sections using each of the armour shapes tested was compared with damage calculated using van der Meer's formulae, taking account of the effects of layer thickness by using Equations 8 & 9. As expected, very round rock suffered more damage than any of the other shapes. The performances of the fresh and equant rock were broadly similar. Surprisingly, the tabular rock exhibited higher stability than other armour shapes.

A regression analysis was carried out on the test results for each of the armour shapes. Values of new stability coefficients C_{pl}' and C_{su}' were calculated for the shapes tested in this study, and for layer thicknesses of $t_a=1.6D_{n50}$, to replace the coefficients **6.2** and **1.0** in the modified plunging and surging formulae (Equations 8 and 9). These revised coefficients are summarised In Table 1.

Table 1. Revised coefficients for "non-standard" armour shapes

Rock shape class	Plunging C_{pl}'	Surging C_{su}'
Fresh	6.32	0.81
Equant	6.24	1.09
Semi-round	5.96	0.99
Very round	5.88	0.81
Tabular	6.72	1.30

The modified formulae for the thinner armour layers then become, for plunging waves:

$$H_s/\Delta D_{n50} = C_{pl}' \, P^{0.18} \, (S_d/\sqrt{N})^{0.25} \, \xi_{om}^{-0.5} \qquad (10)$$

and for surging waves:

$$H_s/\Delta D_{n50} = C_{su}' \, P^{-0.13} \, (S_d/\sqrt{N})^{0.25} \, \sqrt{\cot\alpha} \, \xi_{om}^{P} \qquad (11)$$

A simple comparison of the relative performance of armour shapes can be made. The change in damage due to the use of very round rock rather than equant material suggests, for plunging waves:

$$\text{Damage}_{(\text{very round})} = 1.4 \, \text{Damage}_{(\text{equant})} \qquad (12)$$

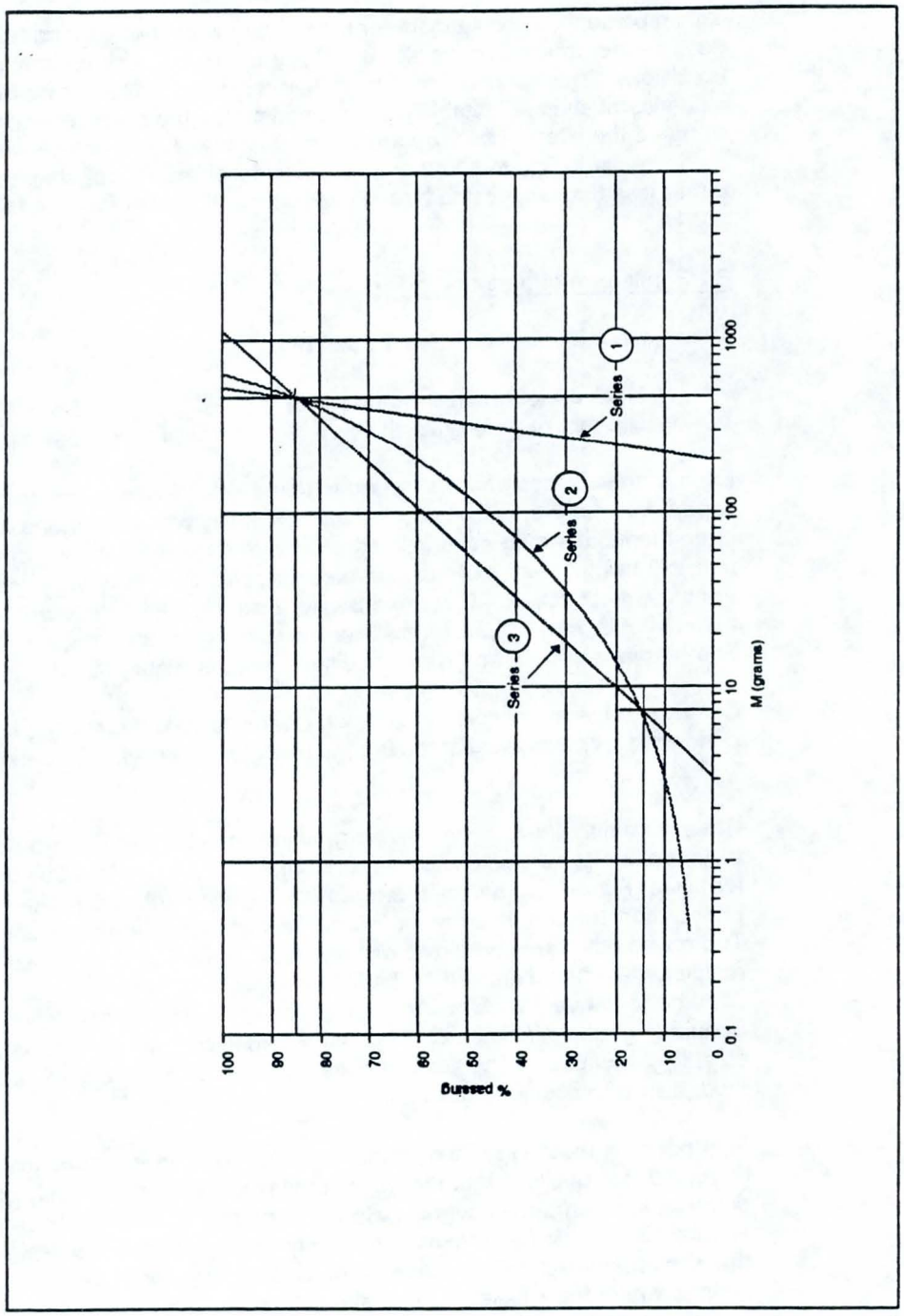

Figure 3 Comparative gradings of very wide-graded rock

This represents a requirement for the median weight of very round rock to be about 30% greater to achieve the same stability as equant rock under plunging wave conditions. This simple comparison may represent an over-simplification of the influence of shape on stability, but demonstrates the potential dangers of under-design if the effects of shape are ignored. It may however be useful to note that the increase in D_{n50} required by these new formulae for constant damage levels is rather less than suggested by the decrease in K_D given for round rock in section 2.2.1.

3.1.3 Influence of armour grading

Most armour in common use falls into one of 2 classes:

Rock armour, narow-graded	$D_{85}/D_{15} < 1.5$
Rip-rap, or wide-graded	$D_{85}/D_{15} < 2.25$

Each of these types of armour require some selection, and this may be quite expensive where the sizes needed are not easily produced in the quarry. There are often therefore strong economic attractions in reducing the level of selection, possibly using "all-in" material. Two specifications of "very wide graded" rock armour with $D_{85}/D_{15} = 4.0$, termed Series 2 and 3, were tested against conventional material of $D_{85}/D_{15} = 1.25$, termed Series 1, in the studies described in Reference 7. The gradings are shown (in model dimensions) in Figure 3.

Damage to the narrow graded armour, Series 1, constructed to $t_a = 2.2D_{n50}$ performed as predicted, confirming the use of van der Meer's formulae for $t_a=2.2D_{n50}$.

Results from the tests on very wide graded armour showed more scatter than other tests, generally exhibiting slightly more damage than predicted by van der Meer's formulae, Figure 4. The scattered results may be attributed to the wide variation in armour construction, in terms of the median armour size along the sample length. There was noticeable preferred movement of smaller rock in Series 2 and 3, resulting in reduced support to the larger rocks in the armour layers. Analysis of damage to the very wide-gradings prepared to the log-linear (Series 3) and Schuman gradings (Series 2) indicated no significant differences when the median size, D_{n50} was used. The scatter in the results did not permit any further modification to design formulae.

In conducting these tests, it became clear that very wide-graded material is difficult to control rigorously, in that the median mass will vary significantly along any practical structure, even over a quite short length. It is therefore very difficult to ensure that the median armour size locally remains above the design limit, implying that the armour will then damage more than allowed for in the design over those lengths where the smaller material predominates.

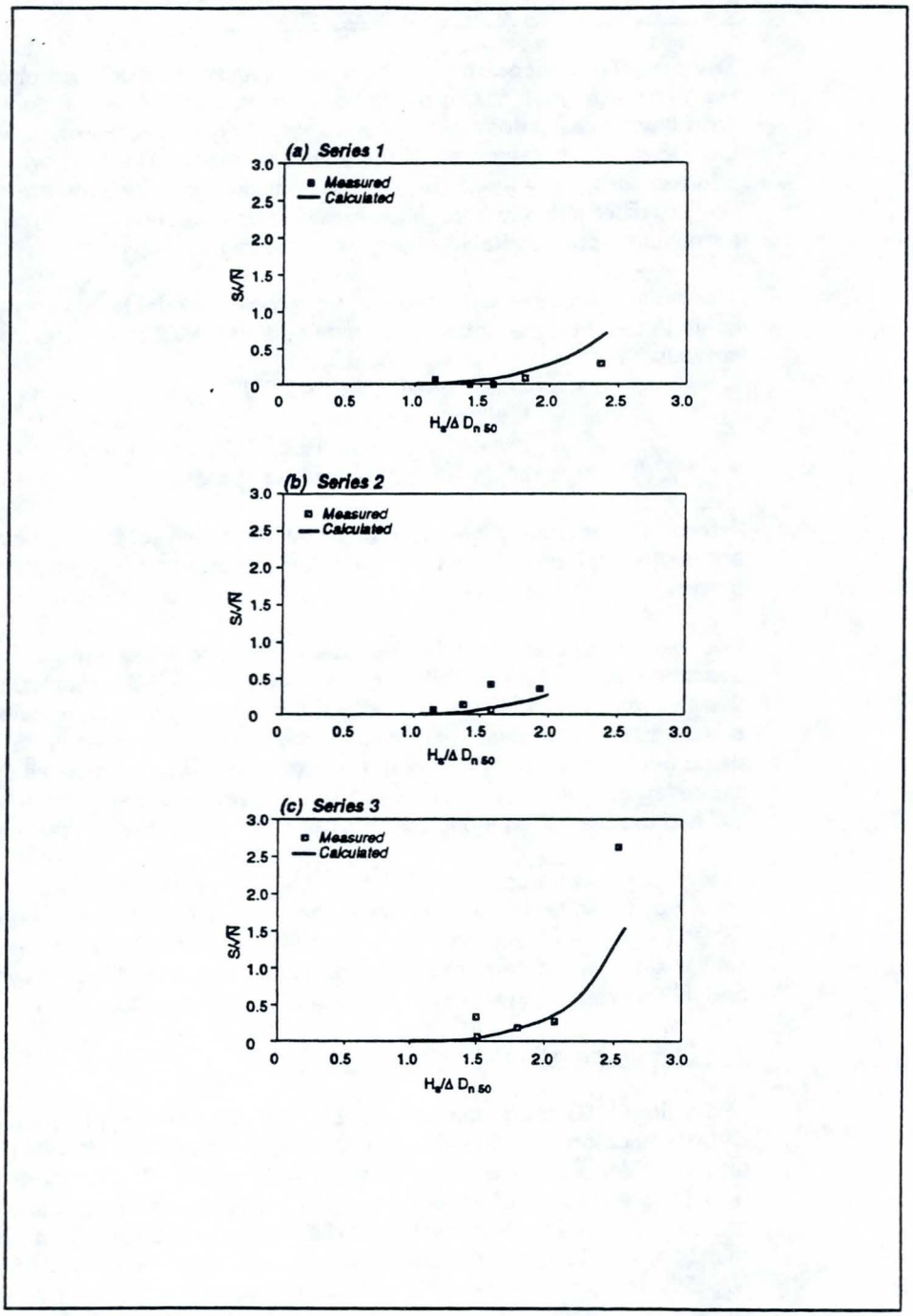

Figure 4 Influence of armour grading on stability

3.2 Stability of rock armoured rubble groynes

The control of beaches for coast protection and/or sea defence often requires the use of rock groynes or shore-detached breakwaters. A very recent series of model tests have investigated the armour stability on typical rock armoured sea defence and beach structures on a 1:7 slope shingle beach. The tests were intended to address particularly those parts of the structures for which the armour stability is likely to differ strongly from those idealised configurations for which the standard formulae for armour stability have been derived.

The study used three-dimensional (3-d) physical model tests in a random wave basin to describe the armour response on four typical rock armoured beach control structures built in a 1:7 shingle beach:

a) a bastion groyne, CIRIA / CUR Type 2;
b) an L-shaped groyne, formed from (a) above;
c) an inclined groyne, CIRIA / CUR Type 1; and
d) a simple 1:2 rubble seawall slope.

Armour displacements were quantified by measuring profile lines over selected areas of each model. The measured damage was compared with damage predicted by Van der Meer's equations for simple trunk sections.

The test results confirmed that Van der Meer's prediction formulae adequately describe damage for the rock armoured sea wall subject to normal wave attack, but that they may seriously under-predict the degree of damage sustained on non-standard structures such as groynes or breakwater roundheads. In general the damage on the curved parts of the bastion and L-shaped groynes substantially exceeded that predicted for simple trunk sections. Damage to the armour on the inclined groyne varied along the groyne, and also exceeded that predicted.

It has not yet been possible to identify whether the significant increase in damage shown by these tests is due solely to the plan configurations of the structures tested, or was also exacerbated by the relatively steep beach slope. Analysis of a similar set of test data from the Spanish laboratory CEPYC on groynes on 1:100 and 1:30 slopes is underway to try to clarify these effects.

3.3 Stability of rock under oblique attack

Under the MAST programme of the EC, studies within the project G6-S Coastal Structures co-ordinated by the author have addressed the stability of breakwater armour under oblique and short-crested wave attack. Tests reported by Galland (Ref 11) give results of armour damage measurements on rock and concrete armour subjected to long-crested waves at approach angles from $\beta = 0°$ to 75°. The results are subject to some qualification, but seem to indicated that for damage N_{od}<5%, there is relatively little reduction in damage to rock armoured slopes for wave attack angle up to about 60°. At β=75° rock armour damage was significantly reduced.

The results of the matching tests on the rock armoured slope using short-crested waves reported by Canel & de Graauw (Ref 12) gave rather more confusing results. Generally the trend appeares to be for slightly less damage to the rock armour as

the degree of spreading increases from 0° up to 20° for β=0°. At β=30 or 45°, the damage seems to increase with increasing spreading.

3.4 Stability of rock on breakwater roundheads

Remarkably little data is available on the stability of armour on breakwater roundheads. Historically, designers have used modified values of K_D taken from the Shore Protection Manual (Ref 2), and/or the results of site specific tests. Generally these have led designers to increase the armour unit mass by up to 2-fold, or to reduce the slope angle, say from 1:1.5 to 1:2.5. Under the MAST project G6-S Coastal Structures, analysis by Allsop & Franco (Ref 13) has tried to identify any particular trends from the results of previous site specific tests conducted at the major European laboratories. These data have again shown considerable variation, with some breakwater roundheads appearing to be more stable than would be predicted for the equivalent trunk section, whilst others showed substantially more damage. These uncertainties have not yet however been resolved.

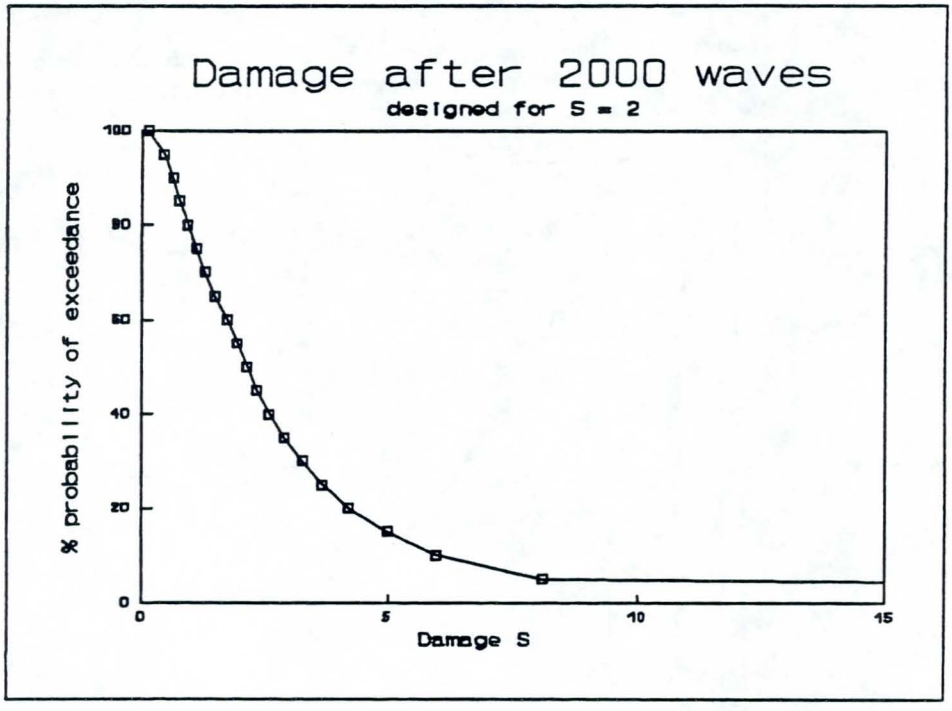

Figure 5 Variability of damage S_d, when designed for $S_d = 2$: $\mu(S_d) = 3.0$, and $\sigma(S_d) = 3.7$

3.5 Influence of variability on armour damage

All of the design methods discussed up to now in this paper are entirely deterministic, using single value input parameters, and calculating single value results. In reality all parameters will suffer from variability which will, more or less, influence the final result. The structure itself will probably differ significantly from

the idealised sections for which the prediction formulae have been derived. Even when the design formulae can be applied directly to the particular structure configuration, there will be some uncertainty in the empirical coefficients used to fit the (simple) formula to the test data. The effects of these stochastic variations may be illustrated by calculations of their influence for the simple case of rock armoured revetment slopes, varying slightly in geometry, and subject to varying wave conditions. We have also taken account of the variability of the prediction formulae, in this case Equation 4. The variables used may be summarised below:

Input parameter	**Distribution**	**Standard deviation**	**Mean**
H_s	Normal	10%	3.0m
Wave steepness, s_m	Normal	10%	0.05 limit 0.07
Slope angle, cot α	None	0%	2.0
Rock density, ρ_a	Normal	5%	2650kg/m^3
D_{n50}	Normal	5%	1.3m (1.08m)
Permeability, P	None	0%	0.1
parameter, a	Normal	10%	6.2
parameter, b	Normal	10%	0.18

The results of the simulations are shown in Figure 5 for a design where the mean values of each parameter were set to give S_d=2, and in Figure 6 where the mean values were set to give S_d=5.

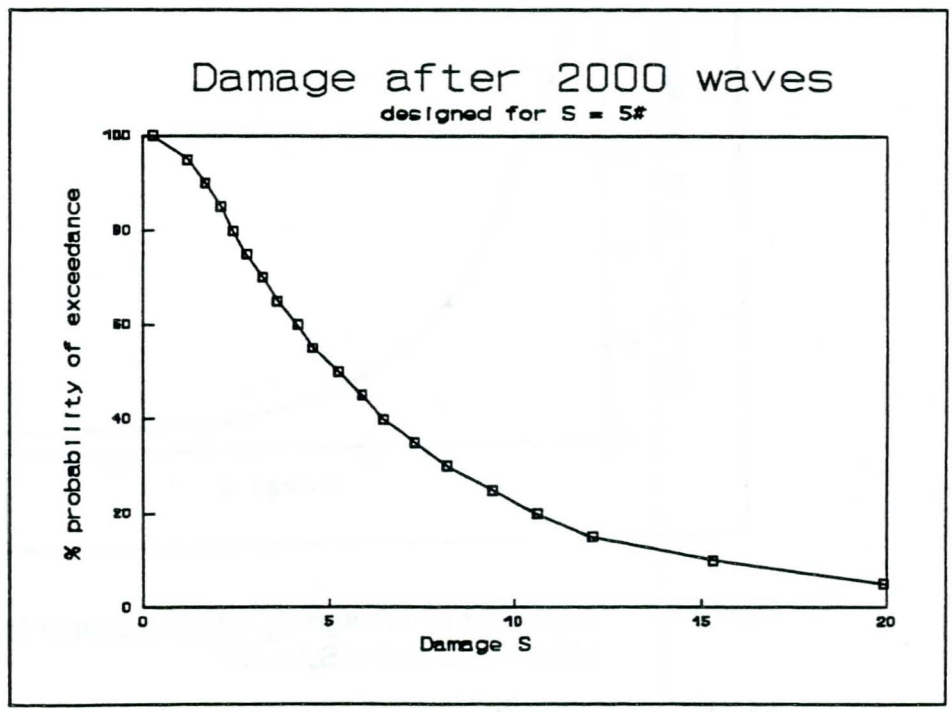

Figure 6 Variability of damage S_d, when designed for S_d = 5: $\mu(S_d)$ = 7.35, and $\sigma(S_d)$ = 7.25

Both sets of results present a similar picture. In each instance the mean damage exceeds the target damage, S_d= 2 or 5, by about 50%. Failure of the structure, taken as being given by S_d>12 over a length of 20-40m, may occur at a 5% risk level if the structure is actually designed for S_d=2, and at a 15% risk level if designed for S_d=5.

4 Conclusions and recommendations

4.1 Effects of layer thickness, armour shape and grading

Van der Meer's equations give a good description of rock armour damage, for armour laid in thicknesses of at least $2.2D_{n50}$, equivalent to k_Δ=1.1, but damage will be greater for thinner armour layers. For a thickness of t_a=$1.6D_{n50}$, equivalent to k_Δ = 0.8, damage is better described by the modifications to van der Meer's equations proposed by Bradbury et al (Ref 4), and given here in equations 8 and 9. The results of tests conducted to examine the effects of rock armour shape on stability were compared with predictions by van der Meer's formulae. New stability coefficients are suggested in Table 1 above as modifications to equations 8 and 9 for plunging and surging wave conditions. These confirm that rounded rock is less stable than equant rock of equivalent weight. The performance of flat slabby rock was however better than expected from previous work.

Model tests on a 1:2 slope with an impermeable core were conducted to identify whether the use of rock armour of grading wider than D_{85}/D_{15} = 2.25 will lead to armour performance substantially different from that predicted by van der Meer's equations. The test results confirmed the validity of van der Meer's formulae for rock of narrow grading. Very wide gradings, such as D_{85}/D_{15} = 4.0, may in general suffer slightly more damage than predicted for narrower gradings. On any particular structure, there will be greater local variations in the sizes of the individual stones in the armour layer than for narrow gradings. This will increase spatial variations of the damage, giving a higher probability of severe local damage. Considerable difficulties will be encountered in measurement and checking such wide gradings.

4.2 Beach control structures

Damage to areas of these structures can be substantially higher than predicted by the formulae available for normal wave attack on simple sections. Designers will certainly need to consider increases in the armour unit mass of up to double the mass predicted for simple slopes using van der Meer's formulae. Even so, damage in some circumstances, particularly on steep shingle beach slopes, may be further increased.

4.3 Oblique attack and roundheads

Remarkably little reliable information is available on the influence of non-standard geometry on the armour response. Some example results of recent research are discussed here. It appears that damage does not reduce significantly with oblique attack up to β=60°. On breakwater roundheads the armour performance is even less well-defined, and it is clear that only a systematic series of model studies will give reliable data for design.

4.4 Risk assessment

This is an area of active research, but relatively little information is available from monitoring of actual structures. Equally, data from model tests has generally omitted to analyse the variability of data test by test, or compare the results of site specific tests with the simple prediction methods. Information on these aspects is urgently needed if risk analysis methods are to be of use.

4.5 Recommendations for future work

Present design methods are valid for the placement densities and patterns used in the model tests on which the design method was based. Unfortunately it is possible, and may often occur, that armour layers are formed to a lower thickness than anticipated. This will be compounded if "non-standard" armour shapes are used. Tests described here have shown that these thinner armour layers damage more rapidly than layers of $t_a = 2.2D_{n50}$. Further research should identify more completely the effects of placement pattern and porosity / layer thickness on armour stability.

Tabular rock, when placed with random orientation, would appear to be more stable than indicated hitherto. In some areas of the world it is quite common to fit flat rock together, forming a paved surface, with the expectation that this will increase the armour stability, albeit with attendant reductions in the hydraulic performance. The data available in this study is not sufficient alone to support a change in design practice. Armour placement, preferred orientation and grading are likely to have a very significant effect on the stability performance of tabular or cubic rock, particularly where the stones are placed closely or fitted together. The practical limitations on handling and placement of tabular rock need to be identified. Then hydraulic model studies should be carried out to quantify possible stability increases.

The stability of armour on the curved parts of beach control structures and on the outer roundheads of harbour and coast protection breakwaters will often be substantially less than on simple slopes. The influence of local beach slope on armour stability on beach control structures may be more important than appreciated hitherto, and should be investigated further.

5. Acknowledgements

This paper summarises results from studies funded in the UK by the Construction Policy Directorate of Department of the Environment; the Ministry of Agriculture, Fisheries and Food; the Science and Engineering Research Council; and the Construction Industry Research and Information Association. Additional support for parts of this work has been given by Queen Mary and Westfield College, the European Community's MAST programme, and by HR Wallingford.

The author gratefully acknowledges the assistance of colleagues at HR Wallingford: Rob Jones, Tony Williams, Ian Meadowcroft, and Jonathan Simm; Claudio Franco from the University of Rome; Jean-Charles Galland from Electricite de France; Max Canel of Sogreah; and HR Wallingford for support in the preparation and presentation of this paper.

6. References

1. Simm JD "Manual on the use of rock in coastal and shoreline engineering" CIRIA Special Publication 83 / CUR Report 154, November 1991.

2. Coastal Engineering Research Centre. "Shore Protection Manual", Vols I-II, US Gov Printing Off, Washington, 4th edition 1984

3. Thompson DM & Shuttler RM. "Design of riprap slope protection against wind waves" Report 61, CIRIA, London 1976.

4. Van der Meer JW. "Rock slopes and gravel beaches under wave attack", PhD thesis Delft University of Technology, April 1988. (available as Delft Hydraulics Communication 396)

5. Bradbury AP, Allsop NWH, Latham J-P, Mannion MB & Poole AB. "Rock armour for rubble mound breakwaters, sea walls and revetments: recent progress", Report SR 150, HR Wallingford, March 1988.

6. Latham J-P, Mannion MB, Poole AB, Bradbury AP & Allsop NWH. "The influence of armourstone shape and rounding on the stability of breakwater armour layers" Queen Mary College, University of London, September 1988

7. Allsop NWH "Rock armouring for coastal and shoreline structures: hydraulic model studies on the effects of armour grading" Report EX 1989, HR Wallingford, June 1990

8. Jones RJ & Allsop NWH "Stability of rock armoured beach control structures" Report SR 289, HR Wallingford, March 1993

9. Bradbury AP, Latham J-P, & Allsop NWH. "Rock armour stability formulae: influence of stone shape and layer thickness" 22nd ICCE, Delft, July 1990 (available as HR Published Paper 39)

10. Bradbury AP & Allsop NWH "Stability of rock armour under random wave attack: performance of non-standard rock shapes and gradings" Proc Workshop on Quarried Rock for Rubble Mound Structures, Cleveland, ASCE, May 1991 (available as HR Published Paper 58)

11. Galland J-C "Rubble mound breakwater stability under oblique waves" Paper to Final Overall Workshop, MAST G6-S Coastal Structures, Lisbon, November 1992

12. Canel M & de Graauw A "Rubble mound breakwater stability with multi-directional waves" Paper to Final Overall Workshop, MAST G6-S Coastal Structures, Lisbon, November 1992

13. Allsop NWH & Franco C. "Performance of rubble mound breakwaters: singular points" Paper to Final Overall Workshop, MAST G6-S Coastal Structures, Lisbon, November 1992

A SIMPLE DESIGN RELATION FOR GEOMETRIC OPEN FILTERS IN BED PROTECTIONS

K.J. Bakker
Public Works and Water Management, P.O. Box 20.000,
3502 LA Utrecht, The Netherlands

M.B. de Groot
Delft Geotechnics, P.O. Box 69, 2600 AB Delft,
The Netherlands

H.J. Verheij
Delft Hydraulics, P.O. Box 152, 8300 AD Emmeloord,
The Netherlands

1 INTRODUCTION

Design criteria for filters in current attacked bed protections are usually based on a geometric criterion; the size of the pores of any filter layer must be smaller than the grain size of the base material to be protected. The consequent small relation between the diameters of two subsequent layers of the filter results in a large number of filter layers: from fine gravel to protect the sandy bed, via coarse gravel, fine and/or light graded rock to large stones in the cover layer (See figure 1). From experience it was known that several circumstances allow for the reduction of the number of layers. However, although general design rules for geometric open filters were developed during the last ten years, de Graauw et al (1983), no design rule existed for a current loaded bed protection. Recently these general rules have been applied to develop such a design rule, which is the subject of this paper.

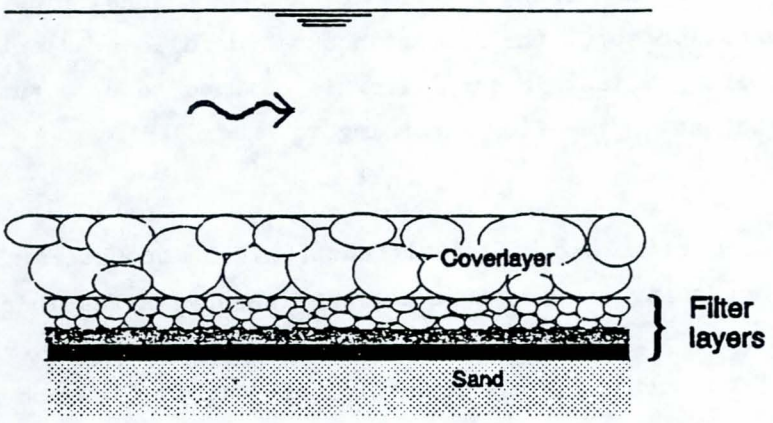

Figure 1 Geometric filter in a bed protection

Geometric open, stable filters are based on the assumption that the base material underneath a filter layer remains stable as long as the current velocity in the pores of the filter does not exceed a critical value. And as this velocity is related with the hydraulic gradient, as long as the hydraulic gradient does not exceed a critical value. These critical values have been determined as a function of the grain size characteristics of both base material and filter material.

2.0 THEORY

The theory developed, is based on the design philosophy that both cover layer and filter must be dimensioned such that they are just stable under the design load. As a chain is as strong as it's weakest link, there is no reason to make the filter layer stronger than the top layer. The stability of the cover layer can be described as a function of the current velocity with the Shields relation. According to Klein Breteler, (Bezuijen et al 1987), the stability of the filter, as a function of the pore velocity or the hydraulic gradient, in a filter can be estimated with a Shields type relation too. The filter stability is determined by

the instantaneous hydraulic gradient rather than by the average gradient. The theory about the turbulence in open channel flow was used to yield information about the instantaneous hydraulic gradient. The maximum hydraulic gradient in the filter is assumed to be a function of the global gradient in the flow according to;

$$\hat{I}^f = C_0 \bar{I}^f \qquad [1]$$

Here C_0 is introduced as a coëfficiënt(function) to account for the differences. According to the aforementioned theory, a feasible range for C_o values is 6 - 100 with an average of 15 (Bakker et al 1993).

This will be valid, for the situation of uniform flow and a boundary layer developed for the full water depth, as is the case in long straight canals, or in a long flume. By approximation this will also be valid for rivers and estuaries, if not downstream of a construction or a groyne. Combining this with the relations for the critical situation of a top layer element, and that for the critical hydraulic situation in the filter, yields a relation for the critical filter ratio.According to;

$$\frac{D_{f15}}{d_{b50}} = f(\psi,\Delta,e)\,\frac{R}{D_{t50}} \qquad [2]$$

where

$$f(\psi,\Delta,e) = \frac{2.2\ \psi_b\ \Delta_b}{C_o\ e^2\ \psi_t\ \Delta_t} \qquad [3]$$

Here ψ is the Shields parameter, Δ is the relative density and e is a coëfficient accounting for the differences between the stability in a filter and in an open channel. R is the hydraulic radius of the stream; the water depth. It occurs that $f(\psi,\Delta,e)$, varies not much. Therefore we see, as is observed in practice, that for a large D_{t50}, the filter ratio tends to a small value, where for a small D_{t50}, a much higher filter ratio is allowed, as is observed in practice.

3.0 EVALUATION

A comparison is made with the results published by Wörman (1989) where he describes his experiments concerning the stability of a non sand tight filter around a pier under stream conditions. The relationship he found for the filter ratio, expressed in the notation we apply, reads;

$$\frac{D_{f15}}{d_{b85}} = 6.25 \frac{(1-n)}{n} \frac{d}{R} \frac{\Delta_b}{\Delta_t} \frac{R}{D_{t85}}$$

where d is the layer thickness of the (one layer) filter material, and n is the filter porosity; According to the figures in Wörmans paper $D_{t85}/D_{t50} \simeq 1.25$ whereas the ratio $d_{b85}/d_{b50} \simeq 1.3$. The filter porosity n, was approximately 0,38. Wörman varied water depth between 0.30 m and 0.40 m and the thickness d between 10 and 100 mm. If we assume the hydraulic radius R equals the water depth, than the ratio d/R varies between 0.025 and 0.33. If we assume an average value for d/R of 0.10 then Wörmans relation yields:

$$\frac{D_{f15}}{d_{b50}} = 1.06 \frac{\Delta_b}{\Delta_t} \frac{R}{D_{t50}}$$

Application of the relationship put forward from our research, equation [2], to Wörman's situation yields nearly the same result: Wörman used base material in the range of 0.45 - 1.15 mm for which $\psi_b \simeq 0.03$ and the filter material lies in between 6 and 36 mm for which $\psi_f \simeq 0.07$. As e $\simeq$0.24 and C_0 is assumed to be 15. this would lead to a filter ratio of;

$$\frac{D_{f15}}{d_{b50}} = 1.09 \frac{\Delta_b}{\Delta_t} \frac{R}{D_{t50}}$$

Though the starting point of Wörman's work is quite different than ours, flow around a pie is much more turbulent than the conditions we assume, the results tend in the same direction

4 CONCLUDING REMARKS

The experiments reported by Wörman and experiments conducted by the authors, but not yet reported, confirm the theoretically found relationship presented here [2]. Further experimental research is needed to widen the field of applicability

The relationship derived enables bed protections with one or two filter layers less than using the traditional geometric tight filter criterion. Especially if the diameter of the top layer is relatively small.

REFERENCES

Bakker, K.J., Verheij, H.J., Groot. M.B.d. (1993)
A design relation for filters in bed protections
submitted for publication

Bezuijen A, Klein Breteler M. and Bakker K.J. (1987)
Design criteria for placed block revetments and granular filters.
Proc. II Int. Conf. Coast&Port Eng.in Dev. Countries, Beijing

Graauw, A. de, Meulen T. van der, Does de Bye, M v.d., (1983)
Design Criteria for granular filters.
Delft Hydraulics, Publication No. 287, january

Konter, J.L.M. (1988)
Priorities between research proposals for CUR-committee C54
Utrecht november, Note C54-92, Private communication

Shields, A (1936)
Anwendung der Ähnlichkeitsmechanik der Turbulenzforschung auf die Geschiebewegung.
Mitt. der Preuss. Versuchsanstalt für Wasserbau und Schiffbau, Berlin, Heft 26

Wörman, A, (1989)
Riprap Protection without Filter Layers
Journal of Hydraulic Engineering., ASCE, 115(12) december

GEOTECHNICAL STABILITY OF RIPRAP STRUCTURES

F.B.J. Barends
Delft Geotechnics, Delft, The Netherlands
Technical University Delft, Civil Engineering,
Delft, The Netherlands

1. INTRODUCTION

Geotechnical aspects of hydraulic rockfill structures concern the mechanical behaviour of the rockfill and the subsoil being subjected to gravitation, to seepage forces, to pore pressures, to accelerations by wave or earthquake loading, and to weathering. Relevant information must be collected about material properties, about loading forces and about the actual state of stress and porous flow. This information is input for simulation models and formulas, and with engineering experience the functioning of the structure under various conditions is assessed. The design loading essential for geotechnical stability is usually the maximum loading occurring during the structure's lifetime. For a realistic evaluation the degradation of the structure with time should be taken into account. An example of such a situation is presented in Figure 1 which shows the pore pressures during a maximum wave on a rockfill structure tested in a large wave flume. If different critical situations are to be considered, a consistent evaluation can be obtained by applying probabilistic methods (CIAD PG Breakwaters, 1985; PIANC PCTII WG12, 1990).

A decennium ago, the principles of soil mechanics were rarely applied in the design of rockfill structures, except in relation to the subsoil. The attention was focussed on the local stability of rock units under hydraulic forces due to free water motion and due to seepage forces. For example, Stephenson (1979) describes in his book "Rockfill in Hydraulic Engineering" the stability of rockfill in water engineering and focuses on generalized equations for the porous-flow process using dimensionless parameters and practical design graphs.

The failure of some large structures in the late seventies and the early eighties, and the need to apply medium-quality rock and widely graded riprap inspired a new interest in geotechnical aspects involved in hydraulic rockfill structures.

2. STATE OF THE ART

Hydraulic rockfill structures are commonly designed by hydraulic engineers. Hydraulic aspects concerning waves, hydraulic stability of the armour and scour are considered. Practical formulas mostly based on empirical research are available (Stephensen, 1979).

Geotechnical aspects were usually limited to standard subsoil investigation and recommendations about settlements and static stability. Thorpe (1985) gives a review of the common foundation problems involved in this field. Hedges (1985) describes the commonly used design methods for the core and underlying layers. The importance of a thorough geotechnical investigation is emphasized by some dramatic accidents. The Sibari Breakwater, for example, disappeared due to subsoil squeezing just after completion (Romiti et al., 1986). Dinardo (1992) mentions the massive collapse of a rubble mound structure on soft mud at Rhu Marina in Scotland.

The threshold of the movable gates of the storm surge barrier at the Eastern Scheldt in the Netherlands completed in 1986 is founded on a rubble mound sill, the composition of which was investigated in the period 1974-1978. The sill can be conceived as a submerged breakwater withstanding a relatively large fall of 9m steady and 4m cyclic water head. The stability of various coarse filter structures under turbulent porous flow conditions was studied investigated. Since the subsoil consists of loose sand with a high liquefaction potential, the stabilization of the seabed received much attention. Delft Geotechnics

performed the major part of the geotechnical investigations which were extensively reported. Two- and three-dimensional models were developed and applied to evaluate the dynamic gradients in the sill and to establish the filter stability under turbulent seepage forces (Barends & Thabet, 1978). At present the knowledge about dynamic filter stability is well documented, and new design formulas which include dynamic gradients are available (Bezuijen et al., 1987; Bakker et al., 1990; CUR-CIRIA Rock Manual, 1991). The unsteadiness plays a major role in the wave-induced porous flow field. Numerical simulation models are developed, but their applicability is limited. The latest improvements will be discussed.

The dramatic failure of once the world's largest breakwater in Sines, Portugal (Figure 2) gave the start to investigate geodynamical aspects in a comprehensive way. The geotechnical analysis gave insight in the applicability of standard geomechanical methods under static (weight), semi-dynamic (waves) and dynamic (impacts, earthquakes) conditions. The results of this comprehensive study provided some practical suggestions and gave qualitative information concerning the causes and importance of dynamic geotechnical failure modes (Barends et al., 1983). This approach was applied and further extended during various breakwater studies (Barends, 1986). In the last series of four breakwater conferences held in UK in 1983, 1985, 1988 and 1991, most of the progress in geomechanical engineering of rockfill structures is published. A survey of the research in the last 8 years and the missing knowledge is presented by Burcharth (1991).

Recently, the conference Geocoast 91 in Yokohama shed new light on soft-soil foundation and seabed liquefaction, and the ICCE conference in Delft (1990) shows that progress is gained on permeability formulas, block-revetment stability and dynamic pore pressures.

In the CUR-CIRIA Manual on the Use of Rock in Coastal and Shoreline Engineering (1991) the state of the art in Europe is compiled. For geotechnical aspects reference is made to chapter 5.2 and appendix 5.

The last three years a consortium of European research institutes and technical universities combined efforts under the EC-funded MAST program in order to develop a physically based numerical formulation of the water motion on and in a porous rockfill structure. Some aspects will be discussed here.

In general, one can state that standard methods for geotechnical stability and deformation (settlement and squeezing) are applicable with modifications related to effects of dynamic gradients. Cyclic liquefaction of the seabed can be assessed taking into account drainage and preshearing; for two-dimensional problems promising progress is made.
The assessment of the mechanical behaviour under dynamic conditions is, however, still far from being practical. Robust physical concepts related to dynamic response of hydraulic rockfill structures have to be developed. There is a general shortage of well-instrumented in-situ tests for validation.

3. GEOTECHNICAL ASPECTS

An outline is given about the general principles applied in the geotechnical evaluation of hydraulic rockfill structures. Some of the concepts uncommon in conventional geotechnical engineering will be discussed in more detail. The recent progress is discussed. For other aspects the reader is referred to the literature.

3.1 Geotechnical functioning

From a geotechnical viewpoint a hydraulic rockfill structure consists of the following elements: subsoil, surface bed, filter, core, toe, slope and superstructure. Geotechnical aspects are important in those circumstances when one or more of these elements do not function properly (malfunctioning or failure). The manner in which such a state occurs is called a failure mechanism. Three failure mechanisms are considered, each involving various aspects.

- *slip failure of slope and subsoil* (slope geometry, internal friction, pore pressures, rock-structure interaction, accelerations);
- *settlement of the core and subsoil* (rockfill densification, subsoil-layer compaction, squeezing, cavity collapse);
- *erosion of filters and core materials* (filter gradation, change of properties, fatigue, dynamic gradients).

The assessment of these geotechnical failure mechanisms includes proper data-acquisition and calculations applying a variety of facilities, from simple empirical formulas to sophisticated numerical models. Experimental model testing is unusual due to difficulties in coping with nonlinear behaviour and scale effects. A promising facility to alleviate this deficiency is geocentrifuge testing.
On the other hand the mathematical description of the mechanical process is not complete, which limits the applicability of the numerical models.
Because of the multi-phase (air, water, rock/soil) and dynamic character of the response of hydraulic rockfill structures the approach may differ from standard static geotechnics. Sometimes a static method applies with minor adaptation. The behaviour of the water and rockfill can occasionally be separated, which simplifies the analysis.

3.2 Geomechanic principles

The response of hydraulic rockfill structures to gravitation, waves and earthquakes involves intergranular stresses, seepage forces, pore pressures, accelerations, velocities and deformations, which affect the mechanical stability. The in-situ state (actual stresses and material properties), which is usually not known, is important, particularly for nonlinear behaviour which is typical for rock and soil. This lack on information restricts a quantitative evaluation. Therefore, many practical methods are more or less empirical and mostly applied in a qualitative sense. The explicit interpretation is based on experience and engineering intuition to a large extent.
Since in rockfill three phases exist (air, water, riprap), granular stress σ' and pore pressure p (air or water) interact. Together they balance the loading (total stress σ). Differences in pore pressure cause flow, which in turn changes the pore pressure in time. Effective stress will also vary to compensate for this change. Deformations are, therefore, indirectly related to porous flow. In a dynamic environment the inertia (acceleration) plays a role in this process. The coherence of these various processes can be presented in the following graph.

numerical model *physical model*
mechanical description *scaling rules*

state of stress
accelerations

flow *deformation*
saturation *stability*
drainage/dissipation *rigidity*

The evaluation of a failure mechanism with respect to malfunctioning depends on the character of the process, whether it is self-healing or progressive. The success of rockfill structures depends to a large extent on the self-healing character. A certain amount of deformation is acceptable, and in many cases will not directly lead to a catastrophe (casualties). Reshaping of the slope by natural processes may provide a more stable profile (Van Der Meer, 1988). Slip failure along a slope is in principle self-healing, if no vulnerable elements become unprotected (Figure 3). Hydraulic lifting of individual rock units is self-healing (Figure 4). This is the reason of the stability of nicely paved revetments (Burger et al., 1988). It does not apply for artificial highly porous armour units. Liquefaction of the surface bed may be self-healing when suitable precautions are taken, such as shown in Figure 5 where the filter is extended in order to stop the progress after initial start. With a proper understanding of these processes it is possible to make more flexible and economical designs.

3.3 Geodynamics

The wave loading on a porous rockfill structure is a dynamic process. It can be described by a two equations: the mass balance (storage) and the momentum balance (equilibrium). For moderate waves the dynamic behaviour involves consolidation and unsteady porous flow controlled by phreatic storage (moving boundary). It is, in fact, a quasi-dynamic process. Inertia effects related to turbulent porous flow and free surface waves are considered. It is studied extensively in the last years. A complication for coarse rockfill is the nonlinear character of the wave-induced porous flow and for sand the cyclic liquefaction.

For short or breaking waves and wave impacts the dynamic behaviour is described in similar way, but now the inertia terms are important. Here, the energy dissipation by dilatational waves (compression) and distortional waves (shear) is considered. In a response to wave loading the solid phase and the fluid phase interact by friction and by inertia. For the friction (the interaction by relative velocity) a flow law is used (Darcy or Forchheimer). For the inertia the relative acceleration is considered. The effect that the other phase is present, can be expressed by a virtual-mass coefficient.

The theory of the dynamic behaviour of a two-phase porous medium is described by Biot (1956) and De Josselin de Jong (1956). The equations involved are complicated, and only in few cases a comprehensive solution can be found. The theory predicted special effects, of which some are verified recently in laboratory tests (Van der Grinten, 1987; Smeulders, 1991). Some aspects of the dynamic behaviour are not fully understood. The main points of the theory will be outlined for a one-dimensional situation. The solid units are rigid. The equilibrium of the fluid (equation of motion) is described by:

$$np_{,x} + n\rho_f \dot{u} + n^2 \frac{\mu}{k}(u-v) = 0 \qquad (3.1)$$

It states that the inertia force and the friction force make equilibrium with the force related to the pressure gradient. Here, u is the *fluid velocity*, k is the *intrinsic permeability*, and μ the *dynamic viscosity*. It is important to notice that the friction is expressed relatively to the *soil-skeleton velocity* v.

The inertia term can be postulated as follows (after Biot):

$$\dot{u} = u_{,t} + \lambda u \cdot u_{,x} + (\zeta-1)(u-v)_{,t} \qquad (3.2)$$

where, the first term on the right-hand side is the local time rate, the second is the convective term, the third term is the mass effect due to the relative acceleration between both phases. The factor ζ, the *coefficient of dynamic dispersion*, depends on tortuosity of the pore geometry. the coefficient λ is related to the averaging from micro to macro scale. At micro scale the tortuosity of the porous structure causes irregular velocities and accelerations, some water is adhered to the solid phase or moves independently (vortices). Kowalski

(1992) describes a concept of two porosities, one the common *volumetric porosity n* and the other an effective surface porosity related to the actual relative flow, referred to by *structural permeability e*, and he obtains for the dynamic dispersion coefficient $\zeta = n^2/e$. This can be extended to:

$$\zeta = (1+\xi)n^2/e \qquad (3.3)$$

where ξ includes the effects of vortices at pore-size dimension.
The equilibrium equation for the solid phase (equation of motion) is:

$$\sigma'_{,x} + (1-n)p_{,x} + (1-n)\rho_s \dot{v} - n^2\frac{\mu}{k}(u-v) = 0 \qquad (3.4)$$

Here σ' is the horizontal *intergranular stress*, which represents the intergranular forces averaged over the bulk area. The inertia term includes:

$$\dot{v} = v_{,t} + \lambda v \cdot v_{,x} - \frac{n\rho_f}{(1-n)\rho_s}(\zeta-1)(u-v)_{,t} \qquad (3.5)$$

In the design of hydraulic rockfill structures the dynamic behaviour of the solid part is usually not considered, except for rocking and moving of individual units at the surface (dynamic stability). If, for the time being, the convective effect is disregarded, and the soil skeleton is assumed to be rigid ($v=0$), then one obtains for the equations of motion for the water and the solid:

$$np_{,x} + n\zeta\rho_f u_{,t} + n^2\frac{\mu}{k}u = 0 \qquad (3.6a)$$

$$\sigma'_{,x} + (1-n)p_{,x} - n\rho_f(\zeta-1)u_{,t} - n^2\frac{\mu}{k}u = 0 \qquad (3.6b)$$

This set can be reformulated into:

$$p_{,x} + \zeta\rho_f u_{,t} + n\frac{\mu}{k}u = 0 \qquad (3.7a)$$

$$(\sigma' - p)_{,x} + n\rho_f u_{,t} = 0 \qquad (3.7b)$$

In equation (3.7a) ζ and $n\mu/k$ remind of the fact that a porous fluid is considered. The factor ζ resembles the virtual-mass coefficient, familiar in hydraulics. Together with the mass conservation for the pore fluid:

$$(n\rho_f)_{,t} + (n\rho_f u)_{,x} = 0 \qquad (3.8)$$

a solution for p and u can be found, and it can be applied to determine the corresponding effective stress σ', employing equation (3.6b). In this hypothetical situations the deformations in the skeleton are disregarded. In reality the solid skeleton responds to the loading and deforms, and this has implications for the mass-conservation equation for the fluid and the solid skeleton.
Therefore, the rockfill itself plays a significant part in the dynamic process. In fact, the major part of wave energy is transferred to the solid phase by friction and acceleration. In equation (3.7a) the pressure gradient is balanced by a viscous term (friction) and an inertia term. The relative importance of these terms depends on the character of motion. If a sudden pressure change is imposed (shock), the response is described by:

$$\zeta\rho_f u_{,t} + n\frac{\mu}{k}u = 0 \qquad (3.9)$$

which has a solution according to:

$$u = u_o exp(-(n\mu/\zeta\rho_f k)t) = u_o exp(-(ng/\zeta K)t) = u_o exp(-\omega t) \qquad (3.10)$$

where $K=k\rho g/\mu$ is the *hydraulic permeability*. The order of magnitude of the *critical frequency* $\omega=ng/\zeta K$ is for sand: 50.000 1/s. This implies that for loading frequency of 50 kHz mobilizes the inertia term and the viscous term in equal intensity. For lower frequencies the viscous term dominates. A common viscous flow law (Darcy or Forchheimer) applies. For higher frequencies the viscous area at micro scale (boundary layer) decreases, and inertia effects in the fluid in the pore become dominant. The critical frequency is investigated by Johnson (1989), who describes a significant change in the dynamic permeability due to this effect. It is not clear whether the common flow laws still apply in the high frequency range.

For (coarse) rockfill the critical frequency ω is much lower, in the order of 1 to 10 Hz. Hence, for rockfill subjected to moderate waves the inertia is less important. For short waves and wave impacts the inertia is of significant importance. The phenomena correspond then to the high frequency range, and the validity of applying rules and laws known from the low-frequency range must be reconsidered.
Comprehensive studies on the dynamic two-phase response of coarse rockfill structures are rare. One example is shown in Figure 6 which represents the calculated dynamic two-phase elasto-plastic response of a breakwater to a large wave impact (Barends, 1983). The permeability is important for the development of the relative acceleration, and the in-situ stress for the development of plastic zones, which occur parallel to the slope geometry (shallow dynamic shear planes).
Recently, a promising numerical algorithm is suggested for more-dimensional two-phase dynamics, which allows for long term behaviour and nonlinear skeleton behaviour (Hölscher & Barends, 1993).
Proper field investigations are required to improve the state of the art with respect to true dynamic behaviour of rockfill structures. Otherwise the theoretical efforts remain qualitative and design methods empirical.

3.4 Permeability

The permeability is not always a constant, such as in very fine pores at low gradients, in unsaturated porous media and in coarse porous media where inertia effects are significant. The virtual mass effect due to variations in the acceleration is in principle not included in the expression for the permeability. The momentum equation for porous flow is (3.1) and (3.2) yield:

$$np_{,x} + np_f(\zeta u_{,t} + \lambda u \cdot u_{,x} - (\zeta-1)v_{,t}) + n^2\frac{\mu}{k}(u-v) = 0 \qquad (3.11)$$

With the introduction of the *filter velocity* $q=n(u-v)$, the hydraulic permeability $K=\rho gk/\mu$, and the *gradient* I: $\rho_f g I = p_{,x}$ this becomes:

$$-ngI = cq_{,t} + ngq/K + (\lambda/n)q \cdot q_{,x} \qquad (3.12)$$

with $$c = \zeta + n(v/q)_{,t} \qquad (3.13)$$

The last term expresses the effect due to solid accelerations. It has never been considered yet, and its importance is unknown. However, Figure 6 shows that this term can be important in coarse-porous media. It is a probable reason that the measurement of the *coefficient of unsteadiness* c is not successful. Tests on medium-coarse rockfill ($D_{s0}<0.06m$) suggest a value for c varying between 1 and 5, but also higher values are found. There is still little knowledge about this effect in coarse rockfill.

Next, omitting the convective term, and introducing $K=1/(a+b|q|)$ yields:

$$-I = (c/ng)q_{,t} + (a+b|q|)q \qquad (3.14)$$

The coefficient a is related to linear flow (Darcy, 1856) and b is related to turbulent flow (Forchheimer, 1901). It is validated for one-dimensional flow by many tests, reported in literature (Bear, 1972; Hannoura & Barends, 1981; Van Gent, 1992). The investigations with regard to the coefficients a, b, and c reveal that the formulation in terms of fundamental material properties is not complete (Williams et al., 1992; Burcharth & Andersen, 1992). This is attributed to the following reasons. As shown in equation (3.12) some aspects are omitted. The description of the unsteadiness by a single term may not be sufficient because of nonlinearity (c may be different for positive and negative acceleration, and varying in time). The one-dimensional flow is at micro-scale, in fact, more-dimensional. For more-dimensional flow the nonlineairity causes so-called *induced anisotropy*. The choice of $|q|$ in stead of the vector q is purely a matter of mathematical convenience; there is no physical justification. The induced anisotropy is observed in tests.

The common idea to assign one type of flow for a specific type of rockfill - b.e. turbulent flow for coarse rockfill - is not correct for time-variant flow, because the type of porous flow is characterized by the local gradient, both in time and place. Therefore, numerical modelling should, preferably, be two-dimensional, and proper physical scale modelling is not possible due to scaling inconsistency.

The coefficient a is related to the hydraulic permeability: $a=1/K$. The *hydraulic permeability* K comprises properties of the pore water and the skeleton: $K = k\rho g/\mu = kg/\nu$. The *intrinsic permeability* k can be expressed by the following relation:

$$k = D^2 n^3/((1-n)^2\alpha) \qquad (3.15)$$

where D^2 represent a mean cross-sectional conductivity. D is usually identified with a specific grainsize, b.e. D_{10} (Hazen, 1892). The coefficient α is dimensionless and it was measured extensively. Various empirical formulas are available. Bear (1972) reports a value between 10 and 2000 depending on the type of soil. Den Adel (1991) reports for fine sands to coarse granular media:

$$\alpha = (75<160<350) \qquad (3.16)$$

where 75 and 350 are the 95% confidence values and 160 is the most probable value. Shih (1990) mentions a formula which includes the shape of the grainsize distribution:

$$\alpha = (1680 + 0.00312\ [g/\nu]^{2/3}\ D_0^2) \qquad (3.17a)$$

with: $$D_0 = D_{15}\ \sqrt{[\frac{D_{50}}{D_{15}}]}\ \sqrt{[\frac{D_{50}D_{50}}{D_{15}D_{85}}]} \qquad (3.17b)$$

For a lognormal distribution $ln[D_{50}/D_{15}]$ is the variance, and the skewness $\sqrt{[D_{50}D_{50}/D_{15}D_{85}]}$ is equal to 1.

The coefficient b is related to (steady) turbulent flow. It can be expressed by:

$$b = \beta/(gD_{15}) \qquad (3.18)$$

The coefficient β is dimensionless. Measurements on uniform coarse grains (gravel) show (De Lara, 1955):

$$\beta = 1.4\ (1/n^5) \qquad (3.19)$$

Den Adel verified a wider range of materials and he reports:

$$\beta = (0.9<2.2<5.3)\ (1/n^3) \qquad (3.20)$$

Shih reports:

$$\beta = (1.71 + 1.57\ exp[-0.0051(g/\nu^2)D_0])\ (1-n)/n^3 \qquad (3.21)$$

Above formulas are valid for relatively round materials. McCorquadale et al. (1978) incorporate the shape and roughness of the rockfill (see also Hannoura & Barends, 1981).
The dynamic hydraulic permeability is in practice usually measured as a result of a linearization applied to observed gradients and fluxes. The empirical character of the permeability causes usually deviations in measured values. An accuracy with a variation of 200% is not uncommon. Since the effects of porous flow at micro-scale on the mechanical stability are not completely understood, it is questionable if further refinement in the current porous-flow laws will bring any significant improvement.

3.5 Wave-induced porous flow: an engineering tool

The assessment of wave-induced porous flow is a subject of research since many years, and a long list of valuable published contributions is available. Hall & Hettiarachchi (1992) give a summary of models, which describe the transmission of waves through a porous structure, varying from linearized porous flow to Navier-Stokes in schematized pore systems. In most of the models limiting assumptions are adopted in order to obtain practical solutions. Some models use numerical techniques, and they provide velocities and pressures, which determine the dynamic stability of units and of the entire structure. The usual boundary conditions are the dynamic pressures and the corresponding fluctuating water table at the outer slope and the lee side. Such a model is the HADEER code, which was developed at Delft Geotechnics through a cooperation between Hannoura and Barends in 1980. It describes laminar and turbulent friction and inertia of the porous flow. It was compared to flume tests and used in various projects (Barends, 1986; Barends & Hölscher, 1988)).

The wave-induced free-water motion on an impervious rough slope can be simulated by using numerical techniques. A popular one-dimensional model is developed by Kobayashi et al. (1987) suitable for long waves. Koutitas (1982) tried to couple the free-water motion to the a linear porous-flow model. In a recently completed EC-funded project in the MAST-program (Marine Structures) Delft Geotechnics coupled the Kobayashi model to the HADEER model to obtain a comprehensive engineering tool. The result is the model MBREAK. Van Gent developed a slightly different model, called ODIFLOCS. Both models are based on a one-dimensional schematization, they are userfriendly, and run on a PC. The calculation is shown on screen simulating the water motion in a realistic fashion. Because different assumptions are adopted - particularly the coupling of wave run-up and rush-down to internal seepage surface fluctuations is critical - a comparison and validation is made by Yamazaki at Delft Geotechnics. Some of the results are mentioned here.

The physical background of the models can be described with the one-dimensional momentum-conservation and mass-conservation equations.

The following essential assumptions are applied:

- the solid phase is completely rigid,
- the horizontal flow is uniform,
- the vertical pressure distribution is hydrostatic.

For the porous-flow equation (3.1) and (3.2) provide:

$$n\rho_f(\zeta u_{,t} + \lambda u \cdot u_{,x}) + np_{,x} + n^2\frac{\mu}{k}u = 0 \qquad (3.22)$$

The pressure is related to the actual height of the water:

$$n\zeta u_{,t} + n\lambda u \cdot u_{,x} + ngh_{,x} + n^2\frac{g}{K}u = 0 \qquad (3.23)$$

Introduction of the *filter velocity* $q=nu$ and Forchheimer's law yields:

$$\zeta q_{,t} + (\lambda/n)q \cdot q_{,x} + ngh_{,x} + ng(a+b|q|)q = 0 \qquad (3.24)$$

The general mass balance equation states:

$$(n\rho_f)_{,t} + (n\rho_f u)_{,x} = 0 \qquad (3.25)$$

The *porosity n* is constant. For the one-dimensional flow the density is related to the mass in a unit section with *height h*, which yields:

$$nh_{,t} + (hq)_{,x} = 0 \qquad (3.26)$$

The turbulent unsteady porous flow is described by equations (3.24) and (3.26). The solution with an explicit second order finite difference method provides the water table changes (h) and the average horizontal filter velocity (q) as a function of x and t. Next, a quasi-steady two-dimensional approach can be applied for each time step using a finite element method, in order to determine approximately the two-dimensional velocity and pressure field. Calculation according to this method requires little time, and provides sufficient accuracy (Höscher et al., 1988).

The equations for open channel flow on an inclined slope (*angle* θ) are (Chow, 1959):

$$u_{,t} + u \cdot u_{,x} + gH_{,x} + g\tan\theta + \tfrac{1}{2}f|u|u/H = 0 \qquad (3.27a)$$

$$H_{,t} + (Hu)_{,x} = 0 \qquad (3.27b)$$

which are similar to those for the porous flow provided the parameters are adjusted accordingly. The *height* H is the height of the free water, and f is a friction factor.

The coupling can be achieved in different ways (Figure 7). In the model MBREAK point B, the "beginning" of the phreatic surface, is coupled to point A, the "end" of the free water surface (run-up and rush-down), which is defined by the waterfilm thickness Δ. This coupling includes the *disconnection* of water heights in and outside, i.e. a *positive seepage surface*, as the wave rush-down is faster than the phreatic surface can follow, and a *negative seepgae surface*, as the wave run-up is faster. The importance of the disconnection is shown in tests (Barends & Hölscher, 1988), and it complicates the coupling seriously. The *discharge* Q passing through the interface between both flow fields is incorporated by considering the gradient of the phreatic watertable at the coupling point; it covers phreatic outflow during rush-down and infiltration during run-up.

In the model ODIFLOCS both flow fields are coupled along the entire slope by introducing vertical mass transport w (filter velocity) accross the interface and by including a momentum transport $w(u-q)$, which expresses that the mass from the porous-flow field is be accelerated to suite the free-flow field, and vise versa. The equations describing the free-flow field are:

$$u_{,t} + u \cdot u_{,x} + gH_{,x} + g\tan\theta + \tfrac{1}{2}f|u|u/H + w(u-q) = 0 \qquad (3.28a)$$

$$H_{,t} + (Hu)_{,x} = w \qquad (3.28b)$$

and the equations for the porous-flow field are:

$$\zeta q_{,t} + (\lambda/n)q \cdot q_{,x} + ngh_{,x} + ng(a+b|q|)q + w(q-u) = 0 \qquad (3.29a)$$

$$nh_{,t} + (hq)_{,x} = -w \qquad (3.29b)$$

The value of w is related to q by (3.29b) along the submerged part of the slope, which yields:

$$w + q\tan\theta = 0 \qquad (3.30)$$

In the area where the free flow field (run-up) exceeds the internal phreatic flow the value of q is determined by infiltration. In the area where the free flow field (rush-down) is faster than the internal phreatic flow the value of q should be absorbed in the rush-down. In both models these aspects ares only approximately covered. By using proper values for the maximum phreatic run-up and rush-down and a certain waterfilm limit (Δ) of the free-water motion on the slope a realistic simulation can be achieved. The proper values can be determined by comparison with experiments. Field tests are best; scale tests should not be too small in order to limit the scaling effects for turbulent flow and air intrusion effects.

The validation by Yamazaki provides the following recommendations. The infiltration during run-up and the momentum transport in ODIFLOCS should be improved. Run-up and rush-down simulated by ODIFLOCS are too low. The rush-down and the corresponding phreatic response in MBREAK should be improved. MBREAK does not include the momentum transport in

the coupling. The coupling in ODIFLOCS is more flexible than in MBREAK, and more time consuming; MBREAK calculations are about ten times faster than ODIFLOCS. MBREAK can handle more filter layers and different conditions at the lee-side. In Figure 8 the run-up situation of both models are presented for a typical case, and in Figure 9 the rush-down. The models can calculate many waves successively. The graphic display shows a dynamic simulation (moving pictures), which elucidates effects of internal set-up and transmission. It is advised to combine ODIFLOCS and MBREAK in one model with a new algorithm, in such a way that advantages are combined.

3.6 Geotechnical stability

In hydraulic rockfill engineering two types of stability are distinguished. *Hydraulic stability* refers to the stability of individual units under hydraulic loading; particles are conveyed by flow. *Geotechnical stability* refers to stability of a coherent mass of particles, for which beside hydraulic forces also geomechanical forces (effective stress, friction, acceleration) are involved.
The stress state in the rockfill is a tensor (*normal stresses* σ' and *shear stresses* τ), represented by the Mohr circle. The slip in the matrix will occur along critical planes (Figure 10). Where exactly these slip planes develop, depends on in-situ stresses (geometry, material properties), loading, and deformation (dilatancy).
The conventional approach (Bishop's method) assumes a circular slip plane (kinematic admissible), which simplifies the analysis drastically. The assumed stress state is, however, not realistic. This uncertainty is covered by a (fancy) safety factor. The long experience with this practical method made it valuable up to today.
In hydraulic rockfill structures this method can be applied as well, if some adaptations with respect to the wave-induced porous flow field and the internal friction are made (Barends, 1986). From various calculations it appears that the geotechnical slope stability factor determined by a slip-circle analysis decreases up to 25% under storm-wave conditions, and the internal friction depends on rock type and porosity, but also on matrix strength and local effective stress level (Barton & Kjaernsli, 1981). In the slip-circle analysis this can be incorporated easily (CUR-CIRIA Manual on Rock, 1991).

In granular media the deformation may occur arbitrarily along two different directions (slide planes on micro-scale), which is referred to as *double sliding* (de Josselin de Jong, 1971; Teunissen, 1991). It promotes flexibility during failure (different failure modes), particularly for stratified rockfill structures and for superstructures (Figure 10). The double-sliding phenomenon causes the failure load to be less than the conventional Mohr-Coulomb approach.
The geotechnical stability of stratified rockfill on a slope depends on the dynamic gradients, on the corresponding pore pressure and effective stress, and on the local shear resistance (mechanical friction). If the top layer is draining well, excess pore pressures will hardly build up. Graphs for slip-circle stability for homogeneous slopes under rapid drawdown are presented in various textbooks (Stephensen, 1979). For inhomogeneous slopes the *interface friction angle* (between different layers) and the *artificial cohesion* (intertangling) (Kobayashi et al., 1987) are less. This causes that slip predominantly develops along such interfaces. A rough estimate for the interface friction angle δ is $\delta=2\phi/3$, which, according to Figure 11, implies a reduction by $\tan\delta/\tan\phi$, in the order of 60%.
If the top layer is less pervious, because it is a paved block revetment or because of biological growth of deterioration by weathering, the pore pressures accumulate at the interface, and the frictional resistance reduces accordingly. The same may happen during overtopping at the lee side, when water accumulates in the core. The failure mechanism changes from circular slip through the core to planar slip along the interface, depending on the permeability difference. In this case the transmissivity/storativity of the underlying layers in relation to the drainage capacity (leakage length) of the top layer is essential. The same aspect is discussed by Bezuijen & Klein-Breteler (1992) for oblique wave loading on block revetment structures.

The permeability of different layers in a stratified rockfill structure plays an important role, since gradients developed in a wave-induced porous flow at the interfaces contribute to the local stability (*internal migration*, *filter stability*) and the corresponding pore pressure build up may jeopardize the total stability,

particularly during rapid drawdown and continual overtopping. Hedges (1986) reports on the slope stability of a rockfill structure under horizontal and parallel seepage forces. The direction of seepage changes drastically during wave loading (see Figure 2), and the effect on the stability is significant (Figure 11).

The state of the art of the hydraulic stability of rockfill filters is described in the CUR-CIRIA Manual. Criteria based on hydrodynamic limits rather than geometric limits are developed, including the use of geotextile. Bakker et al. (1990) describe experiments, which verify the theory and underscore the applicability of the suggested formulas, compiled in practical design graphs (Bezuijen et al., 1987).

A typical phenomenon in the deformation of granular structures is dilatancy. Due to rearrangements in the granular skeleton the volume of an assembly of particles may decrease or increase under shear deformation. The corresponding pore volume changes, influencing the local pore pressure, and hence the stress state. Ultimately, the induced pore pressure may exceed the effective stress, so that a state of liquefaction occurs, referred to as *deviatoric liquefaction*. The granular skeleton looses almost all shear resistance, which may trigger collapse of the structure. Deviatoric liquefaction can be caused by waves and earthquakes. It may start locally, and may extend rapidly in time. A physically consistent description of this phenomenon is not yet available. For one-dimensional situations a practical procedure exists (Rahman & Jaber, 1986). Recent improvements are made with respect to dissipation and preshearing (densification), which render the method more realistic (De Groot et al., 1991; Barends, 1991). For two-dimensional situations a promising method is suggested by Oka et al. (1993).

When air bubbles occur in the pore fluid, it becomes more compressible. The compressibility of an air-fluid mixture is 100 to 1000 times larger than the compressibility of pure water. The permeability is affected by the presence of air(bubbles), which may block pores or show a tendency to rise, and, hence, opposing or stimulating porous flow depending on its direction. Tests have shown that unilateral confined cyclic loading of loose sand deposits may generate pore-pressure build up. The air entrainment seems to play an essential role (Zen & Yamazaki, 1990). The large compressibility due to air-bubble breathing, and the corresponding variation in

permeability causes a steady pore-pressure build up; at high pressure (crest of wave) infiltration is easier than dissipation at low pressure (trough of wave).
During wave loading on coarse-rockfill slopes air intrusion is obvious. The pore water is partly saturated. The effect of dynamic pore-pressure build up due to huge waves during rush down may liquefy the rockfill in one single cycle. This *dynamic liquefaction* as such is observed in real storms. A physical description of air effects in the dynamic stability of rockfill slopes under wave attack is a subject of research.

4. CONCLUDING REMARKS

The empirical character of the permeability causes large deviations in measured values. The effects of porous flow at micro-scale on the mechanical stability are not well understood, and it is questionable if further refinement in the current porous-flow laws will bring any significant improvement.
The coupling of one-dimensional free flow and one-dimensional porous flow under wave loading is feasible; the empirical parameters, such as wave run-up and rush-down, phreatic run-up and rush-down velocities, the minimum waterfilm on the slope, which control the numerical calculation, have to be determined by experiments. With the insight gained by the validation a new and better model can be composed.
Proper field investigations are required to improve the state of the art with respect to true dynamic behaviour of rockfill structures. This requires measurements of accelerations of the porous flow field and the solid skeleton. Otherwise, theoretical efforts remain qualitative and design methods mainly empirical.
It is worthwhile to put effort in a proper physical description of air(bubble) effects in the dynamic stability of rockfill slopes under wave attack.

5. ACKNOWLEDGEMENT

The information concerning the dynamic permeability and the one-dimensional models for wave-induced coupled flow on and in rockfill structures is collected from the achievements of the EC-funded MAST-I project, in which, amongst others, Delft Geotechnics, Delft Hydraulics and Delft Technical University participated. The effort of Marcel van Gent, Sjoerd Spierenburg, Franc Engering and Henk den Adel is kindly acknowledged, and the validation of the models by Hiroyuki Yamazaki from Port and Harbour Research Institute in Yokosuka is greatly appreciated.

6. REFERENCES

Bakker K.J., Klein-Breteler M., Den Adel H. (1990) New criteria for granular filters and geotextile filters under revetments. Proc 22d ICCE Delft, (ed. B.L. Edge), ASCE 2:1524-1537.

Barends F.B.J. (1991) Interaction between ocean waves and sea-bed. GEOCOAST 91 (general report) 2:1091-1108.

Barends F.B.J., Hölscher, P. (1988) Modeling interior process in a breakwater. Proc BREAKWATERS 88, Thomas Telford, p:49-58.

Barends F.B.J. (1986) Geotechnical aspects of rubble mound breakwaters. Proc Conf BREAKWATERS 85, Thomas Telford, London, 6:155-174.

Barends F.B.J., van der Kogel H., Uijttewaal F.J., Hagenaar J. (1983) West Breakwater - Sines; Dynamic-geotechnical stability of breakwaters. Proc Conf Coastal Structures 83, ASCE:31-44.

Barends F.B.J., Thabet R. (1978) Groundwater flow and dynamic gradients. Proc. Int Symp Foundation Aspects of Coastal Structures Delft 2(VI)1.

Barton N., Kjaernsli B. (1981) Shear strength of rockfill. J1. ASCE, GT7(7):...-...

Bear J. (1972) Dynamics of flow in porous media. Am. Elsevier, New York, pp:672

Bezuijen A., Klein-Breteler M. (1992) Oblique wave attack on block revetments. Proc 23d ICCE Venice, to be published.

Bezuijen A., Klein-Breteler M., Bakker K.J. (1987) Design criteria for placed block revetments and granular filter. Proc 2nd Conf Coast & Port Eng in Devel Countries Beijing, p:1852-1866.

Biot M.A. (1956) Theory of propagation of elastic waves in a fluid-saturated porous solid. Part 1 & 2, Jrnl Am Acoustic Soc, 28(2):155-164.

BREAKWATERS 83, Design and construction. Thetford Press, Norfolk, pp:187.

BREAKWATERS 85, Development in breakwaters. Thomas Telford, London, pp:329.

BREAKWATERS 88, Design of breakwaters. Thomas Telford, London, pp:406.

BREAKWATERS 91, Coastal structures and breakwaters. Thomas Telford, London, pp:581.

Burcharth H.F. (1992) Desing innovation including recent research contributions. Proc BREAKWATERS 91, Thomas Telford, London, p:55-94.

Burcharth H.F. (1992) Introduction of partial coefficients in the design of rubble mound breakwaters. Report PIANC PTCII WG12, Proc BREAKWATERS 91, Thomas Telford, London, p:543-565.

Burcharth H.F., Andersen O.H. (1992) On the 1D unsteady porous flow equation. Proc ICCE 92 Venice, to be published.

Burger A.M., Klein-Breteler M., Banach L., Bezuijen A., Pilarczyk K.W. (1988) Analytical design method for relatively closed block revetments. Proc 21st ICCE at Malaga, p:525-544.

Chow V.T. (1959) Open channel hydraulics. McGraw Hill, NY, pp:660.

CIAD PG BREAKWATERS (1985) Computer-aided evaluation of the reliability of a breakwater design. (ed Barends), CIAD Assoc Zoetermeer, The Netherlands, pp:116.

CUR-CIRIA (1991) Manual on the Use of Rock in Coastal and Shoreline Engineering. Spec Publ 83, Bell & Bain Ltd, Glasgow, pp:607.

Darcy H.P.G. (1856) The public fountains of the city Dijon (French). Victor Dalmond, Paris.

De Groot M.B., Lindenberg J., Meijers P. (1991) Liquefaction of sand used for soil improvement in breakwater foundations. Pos GEOCOAST 91 Yokohama, Port and Harbour Research Inst Japan, p:555-560.

De Lara, G.C. (1955) Coefficient of conductivity in porous media based on the hydrodynamic equilibrium of a mass (French). La Houille Blanche 2:167-176.

Den Adel (1991) priv comm.

Dinardo C. (1992) Investigation into the collapse of the rubble mound breakwater over soft soil muds seabed at Rhu Marina, Scotland. Porc BREAKWATER 91, Thomas Telford, London, p:351-364.

Forchheimer P.H. (1901) Water motion through soils (German). Zeitschrift des Vereines Deutcher Ingenieure 45:1782-1788.

Hall K.R., Hettiarachchi S. (1992) Mathematical modelling of wave interaction with rubble mound breakwaters. Proc BREAKWATERS 91, Thomas Telford London, p:123-147.

Hannoura A.A. (1978) Numerical and experimental modelling of unsteady flow in rockfill embankments. Ph-D Thesis, Univ of Windsor, Ont. Canada, pp:270.

Hannoura A.A., Barends F.B.J. (1981) Non-Darcy flow; a state of the art. Proc Euromech 143 Delft, Balkema PC,p:37-52.

Hazen A. (1892) Some physical properties of sands and gravels with special reference to their use in filtration. 24th Annual Rp, Mass State Board of Health.

Hedges T.S. (1986) Geotechnics (workshop D). Proc BREAKWATERS 85, Thomas Telford, London, p:301-308.

Hölscher P., Barends F.B.J. (1993) Mixed FEM for dynamic analysis of fluid-saturated porous media, Conf SDEE, Trondheim, to be published.

Hölscher P., De Groot M.B., Van Der Meer J.W. (1988) Simulation of internal water movement in breakwaters. Proc SOWAS Delft, Balkema PC, p:427-433.

Johnson D.J. (1989) scaling fucntion for dynamic permeability in porous media. Phys Rev Letters 63(580).

De Josselin de Jong G. (1956) What happens in soil during pile driving (Dutch). De Ingenieur 68, B77-B88.

De Josselin de Jong G. (1971) The double sliding, free rotational model for granular assemblies. Géotechnique 21:155-163.

Kobayashi M, Masaak T., Takahashi K. (1987) Bearing capacity of a rubble mound supporting a gravity structure. Rp Port and Harbour Res Inst Vol 26(5).

Kobayashi N., Otta A.K., Roy I. (1987) Wave reflection and run-up on rough slopes. Jrnl WPC&OE, ASCE 113(3):282-298.

Koutitas C. (1982) A numerical model for rubble mound breakwater stability. Proc Symp Eng in Marine Environment, Brugge, KVIV 2:1-6.

Kowalski S.J. (1992) On the motion of a fluid-saturated porous solid. Jrnl Transport in Porous Media 9(1&2):39-48.

McCorquodale J.A., Hannoura A.A., Nasser M.S. (1978) Hydraulic conductivity of rockfill. Jrnl Hydr Res IAHR 16(2):...-...

PIANC PCTII WG12 BREAKWATERS 1990: reference Burcharth (1992).

Oka F., Yashima A., Shibata T., Kato M., Uzuoka R. (1993) FEM-FDM coupled liquefaction analysis of a porous ground using an elasto-plastic model. To be published in Jrnl Appl Scient Research.

Rahman M.S., Jaber W.Y. (1986) A simplified analysis for wave-induced liquefaction in ocean-floor sands. Jl.Soils and Foundations 26(3):57-68.

Romiti G., Noli A., Franco L. (1986) The Italian experience in composite breakwaters. Proc BREAKWATERS 85, Thomas Telford, London, p:211-228.Shih W.K. (1990) Permeability characteristics of rubble material - new formulae. Proc 22nd ICCE 90 Delft 2:1499-1512.

Smeulders D.M.J. (1992) On wave propagation in saturated and partially saturated porous media. Ph-D Thesis Techn Univ Eindhoven, The Netherlands, pp:131.

Stephensen, D. (1979) Rockfill in hydraulic engineering. Developments in Geotechnical Engineering Vol 27Elsevier Sc.PC, Amsterdam, pp:215.

Terzaghi K. (1925) Soil mechanics based on physical principles (German). Wiley & Sons, New York.

Teunissen J.A.M. (1991) Analysis of plasticity and non-coaxiality in geomaterials. Dr-Thesis, Technical University Delft, pp:128.

Thorpe W.R. (1984) Foundation problems. Porc BREAKWATERS 83, Thomas Telford, London, p:65-70.

Van Der Grinten J.G.M., Sniekers R.W.J.M., Van Dongen M.E.H., Van Der Kogel H. (1988) An experimental study of shock-induecd wave propagation in dry, watr-saturated and partly saturated porous media. Conf SOWAS Delft, Balkema PC Rotterdam, p:469-478.

Van Der Meer J.W. (1988) Rock slopes and gravel beaches under wave attack. Ph-D Thesis Techn Univ Delft, also Delft Hydraulics Communication 396, pp:152.

Van Gent M.R.A. (1992) Formulae to desribe porous flow. Comm Hydr & Geot Eng, ISSN 0169-6548:92(2), Univ Delft.

Williams A.F., Burcharth H.F., Den Adel H. (1992) The permeability of rubble mound breakwaters; new measurements and new ideas. Proc 23d ICCE 92 Venice, to be published.

Zen K., Yamazaki H. (1990) Oscillatory pore pressuresand liquefaction in sea-bed induced by ocean waves. Jl. Soils and Foundations 30(4):147-161.

LIST OF VARIABLES

α	coefficient related to linear porous flow	[1]
β	coefficient related to turbulent porous flow	[1]
Δ	waterfilm thickness	[m]
ϕ	angle of internal friction	[rad]
θ	angle of bed slope	[rad]
λ	coefficient for averaging on micro scale	[1]
ρ	density	[kg/m^3]
μ	dynamic viscosity; $\mu=\rho\nu$	[Ns/m^2]
ν	kinematic viscosity	[m/s^2]
σ'	effective stress	[N/m^2]
ζ	coefficient of added mass	[1]
ξ	coefficient of added mass (vortices at micro scale)	[1]
ω	critical frequency of permeability	[rad]
a	coefficient of linear steady porous flow	[s/m]
b	coefficient of turbulent steady porous flow	[s/m^2]
c	coefficient of unsteadiness of porous flow	[1]
D_{15}	grain size; 15% grains is smaller than D_{15}	[m]
e	structural permeability	[1]
f	index referring to fluid phase	-
f	friction factor	[1]
g	gravity acceleration	[m^2/s]
h	height of porous water	[m]
H	height of free water	[m]
I	pressure head gradient	[1]
k	intrinsic permeability	[m^2]
K	hydraulic permeability; $K=k\rho g/\mu$	[m/s]
n	volumetric porosity	[1]
p	pressure	[N/m^2]
q	filter velocity; $q=n(u-v)$	[m/s]
s	index referring to solid phase	-
t	time	[s]
u	horizontal water velocity	[m/s]
v	horizontal solid-skeleton velocity	[m/s]]
w	vertical filter velocity between porous and free water	[m/s]
x	space coordinate	[m]

LIST OF FIGURES

Figure 1. The Arzew Breakwater under maximum wave loading
Figure 2. Porous flow in the Sines West-Breakwater
Figure 3. Selfhealing, circular slip failure
Figure 4. Selfhealing, lifting surface unit
Figure 5. Selfhealing, partial liquefaction at a toe structure
Figure 6. Geodynamics in the Sines West-Breakwater
Figure 7. Methods of coupling inner and outer wave-induced flow
Figure 8. MBREAK/ODIFLOCS simulation; moment of maximum run-up
Figure 9. MBREAK/ODIFLOCS simulation; moment of maximum rush-down
Figure 10. Double sliding failure mechanism
Figure 11. Slope filter stability under seepage forces

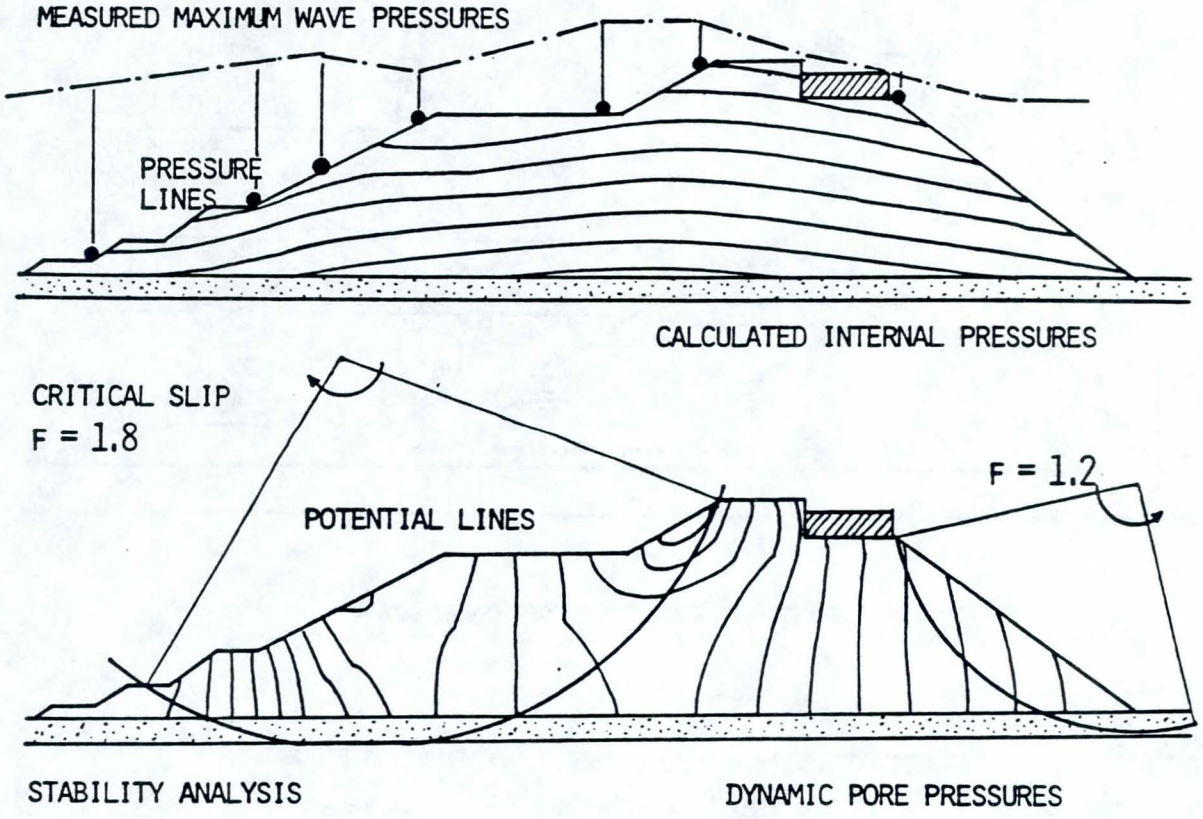

COMPUTER ANALYSIS OF BREAKWATER STABILITY UNDER WAVE ATTACK

Figure 1. The Arzew Breakwater under maximum wave loading

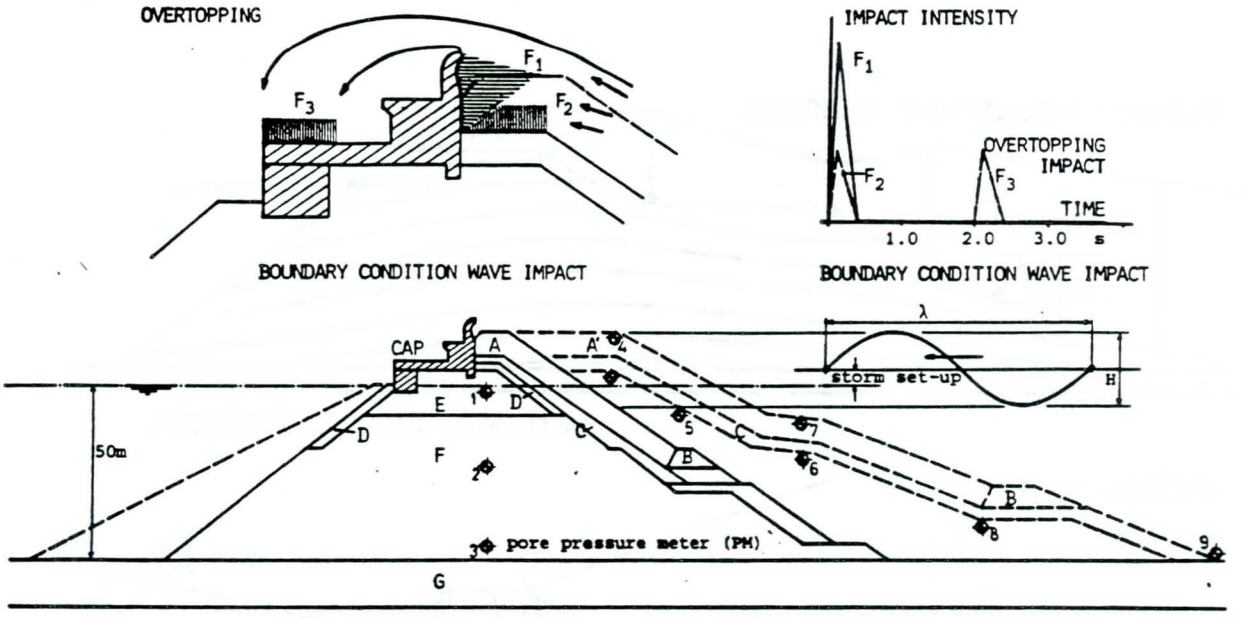

GEOMETRY AND COMPSITION OF A RELEVANT CROSS-SECTION OF THE WEST BREAKWATER

LAYER	TYPE	WEIGHT TF	MASS TF/M3	POR.	DIAM. M	ROUGHN. MM	SHAPE
A ARMOR	DOLOS	42	2.4	.53	3.20	1.65	1.20
A'ARMOR	ANTIFER	90	2.4	.42	4.00	1.65	1.20
B TOE	ROCK	9-20	3.0	.39	2.00	2.00	1.25
C FILTER 1	ROCK	3- 6	3.0	.38	1.40	2.35	1.30
D FILTER 2	ROCK	1- 3	3.0	.37	1.00	2.80	1.45
E SELECTED	ROCK	- 3	3.0	.34	0.50	4.50	1.50
F CORE	ROCK	- 3	3.0	.32	0.35	5.40	1.55
G SEA BED	SAND/ROCK	-	2.6	.36	.001	-	-

COMPARISON BETWEEN MEASURED AND CALCULATED FLOW. MEASURMENTS IN DELTA FLUME BY DYNAMIC PORE PRESSURE METERS (PM). CALCULATION BY THE HADEER AND SEEP CODE.
subjective choice of incident wave top and trough

COMPARISON	PHYSICAL MODEL SCALE 1:12 / NUMERICAL MODEL SCALE 1:1			
	WAVE TOP		WAVE TROUGH	
PM	PHYSICAL	NUMERICAL	PHYSICAL	NUMERICAL
1	0.95	10.0	0.60	5.0
2	2.50	25.0	2.15	20.0
3	4.10	39.0	3.80	35.0
4	0.05	0.0	free	-
5	1.40	15.5	0.65	6.5
6	2.05	21.0	1.45	14.0
7	1.00	12.5	0.25	2.5
8	2.80	27.0	2.80	38.0
9	3.45	35.0	3.60	36.0

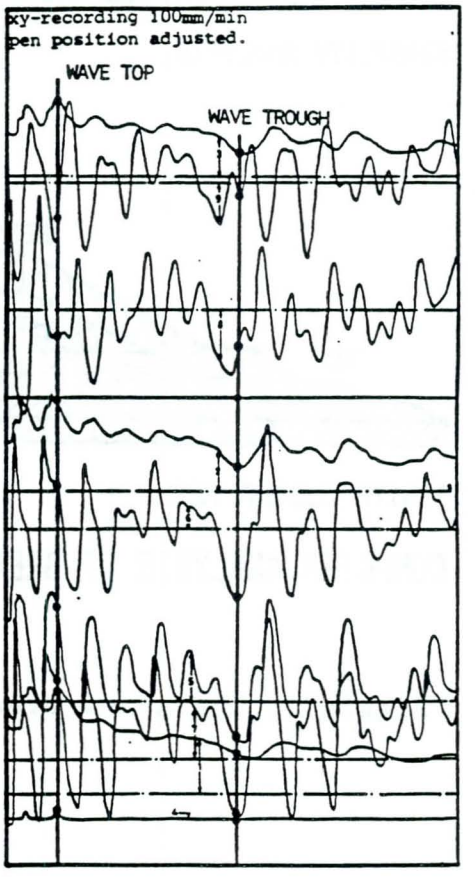

Figure 2a. Porous flow in the Sines West-Breakwater

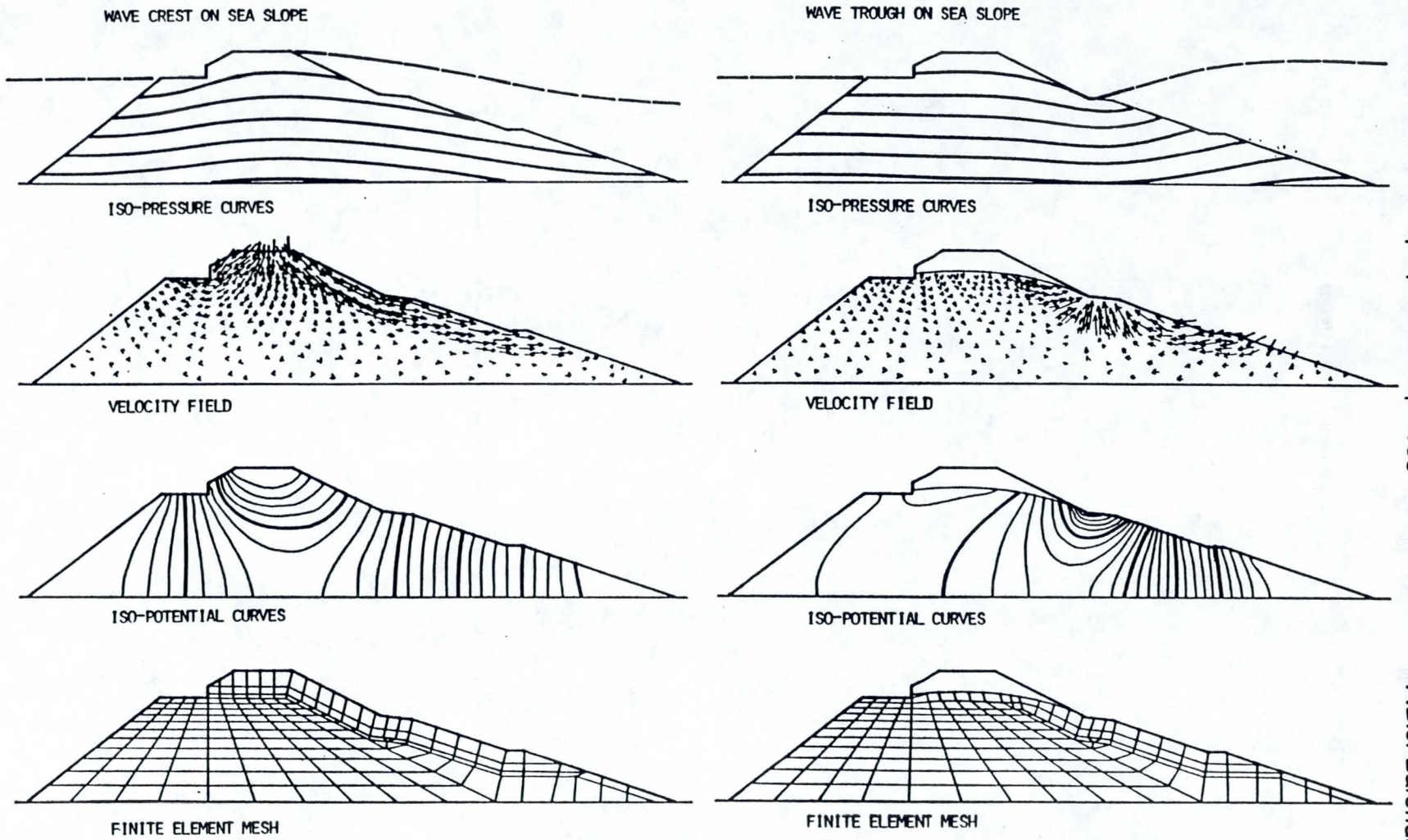

Figure 2b. Porous flow in the Sines West-Breakwater

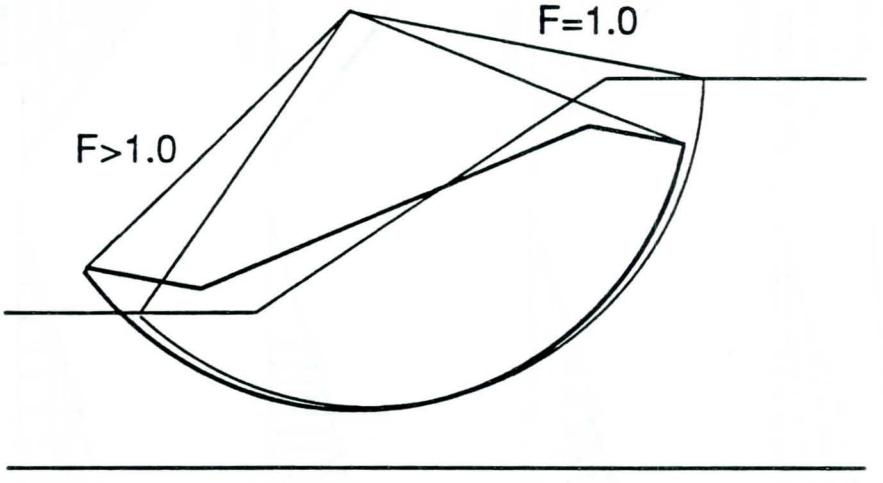

Figure 3. Selfhealing, circular slip failure

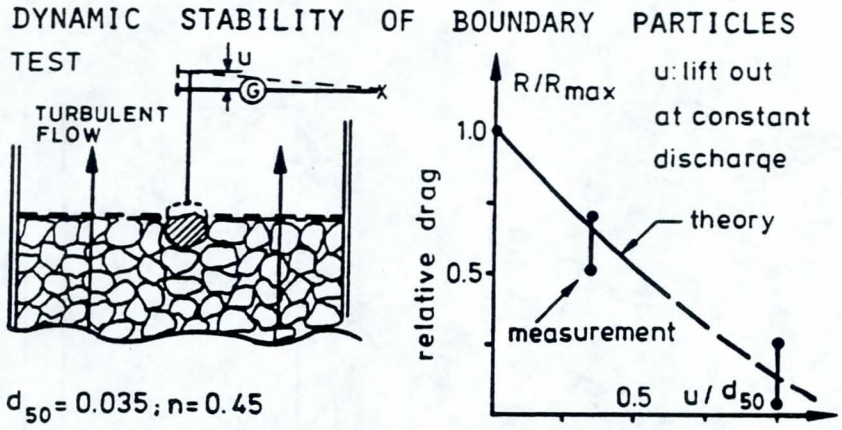

LOCAL STABILITY OF A BOUNDARY PARTICLE UNDER TURBULENT POROUS OUTFLOW CONDITIONS TAKING INTO ACCOUNT THE EFFECT CAUSED BY THE MOTION OF THE PARTICLE INDUCED BY THE OUTFLOW

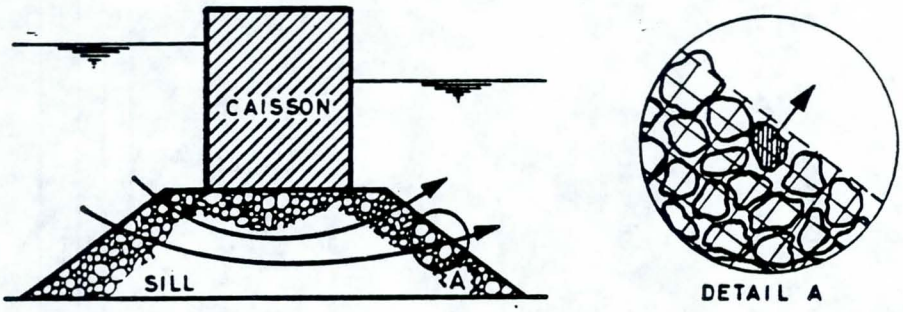

Figure 4. Selfhealing, lifting surface unit

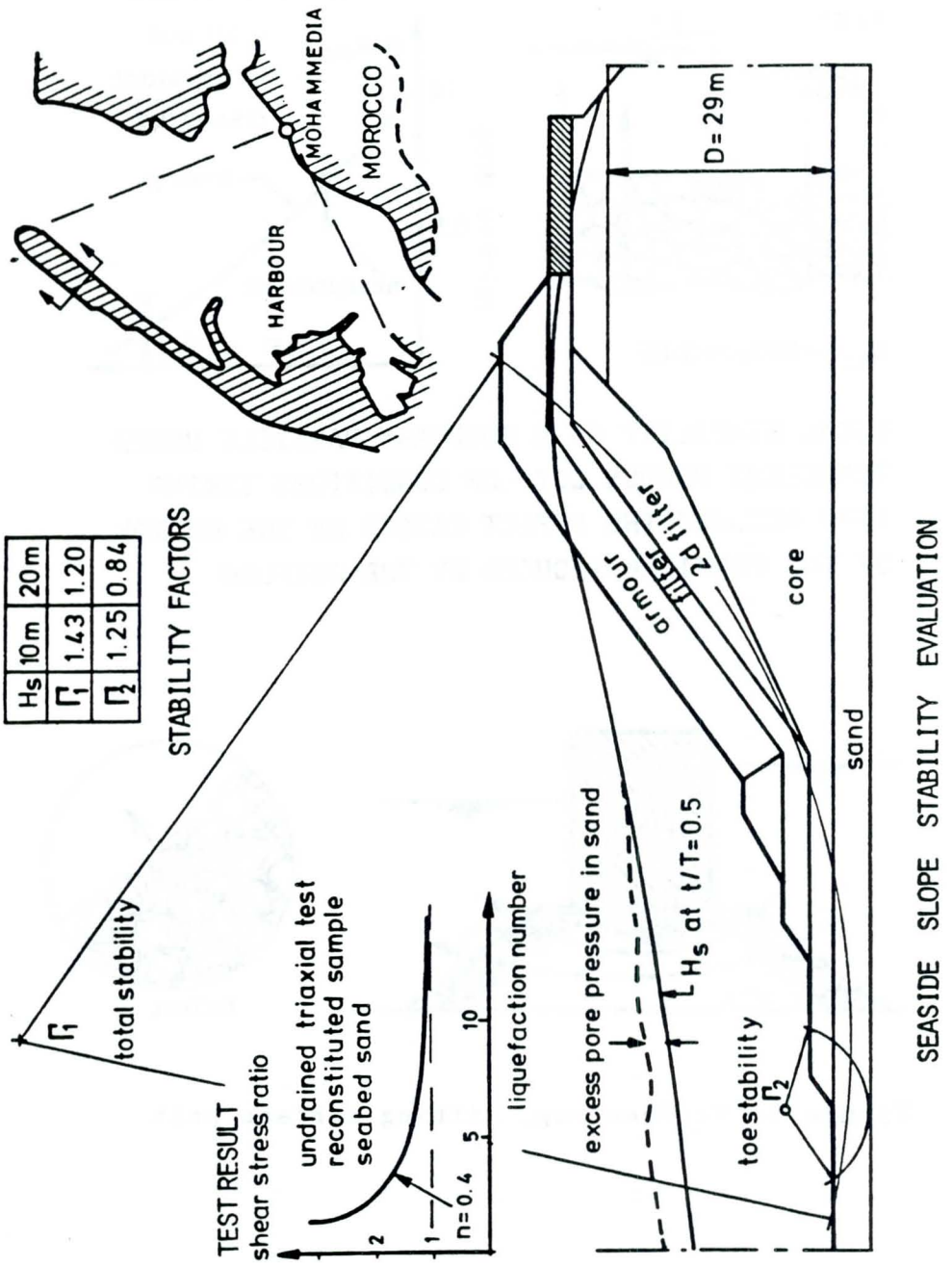

Figure 5. Selfhealing, partial liquefaction at a toe

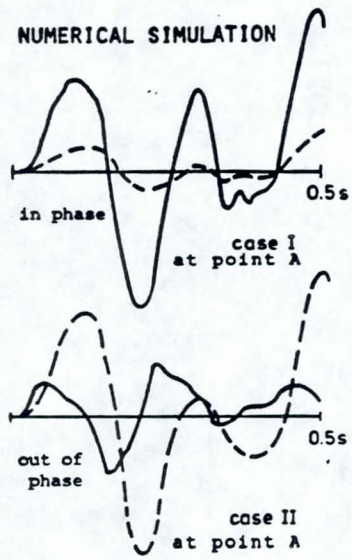

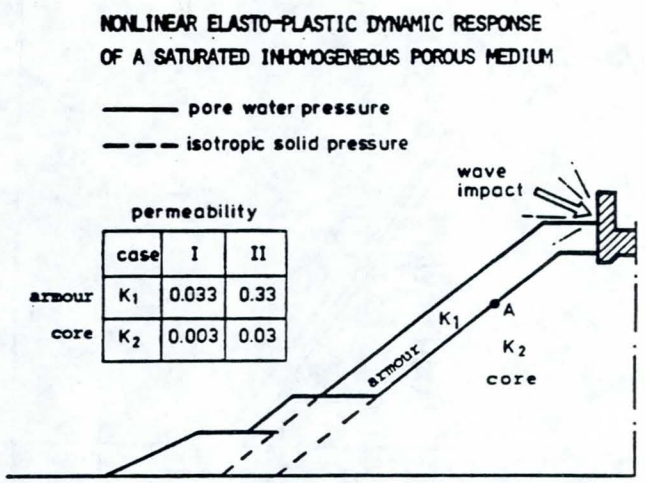

THE EFFECT OF PERMEABILITY IN PORO-HYDRO-DYNAMICS

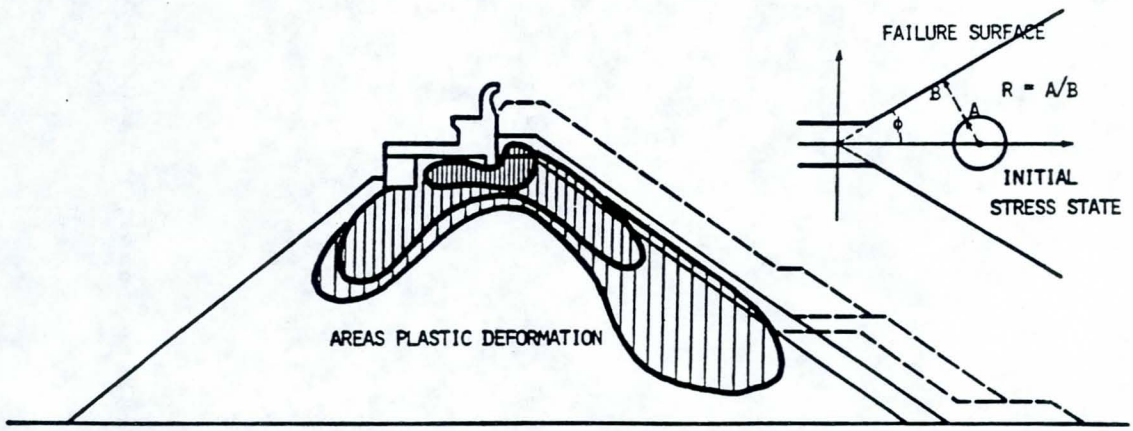

DEVELOPMENT OF PLASTIC ZONES DEPENDENT ON INITIAL STRESS STATE.

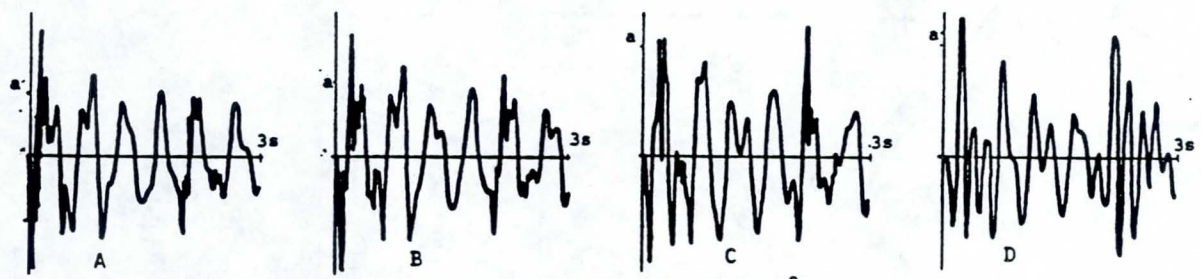

CALCULATED HORIZONTAL ACCELERATIONS DUE TO WAVE IMPACT ($a = 0.5\ m/s^2$)

SAFETY FACTOR DUE TO WAVE IMPACT

SLOPE	3/4	2/3
φ 40°	0.8	1.0
φ 45°	-	1.2

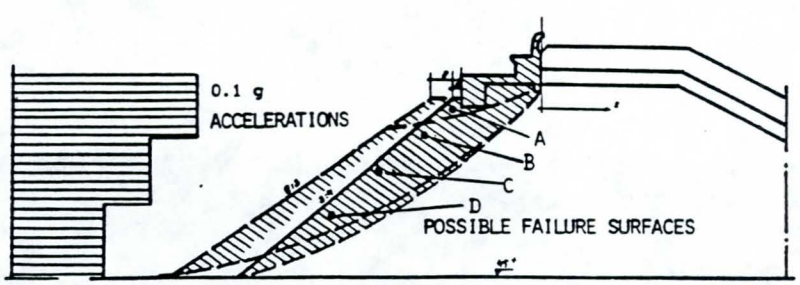

GEOTECHNICAL STABILITY OF THE LEE-SIDE SLOPE UNDER IMPACT LOADING.

Figure 6. Geodynamics in the Sines West-Breakwater

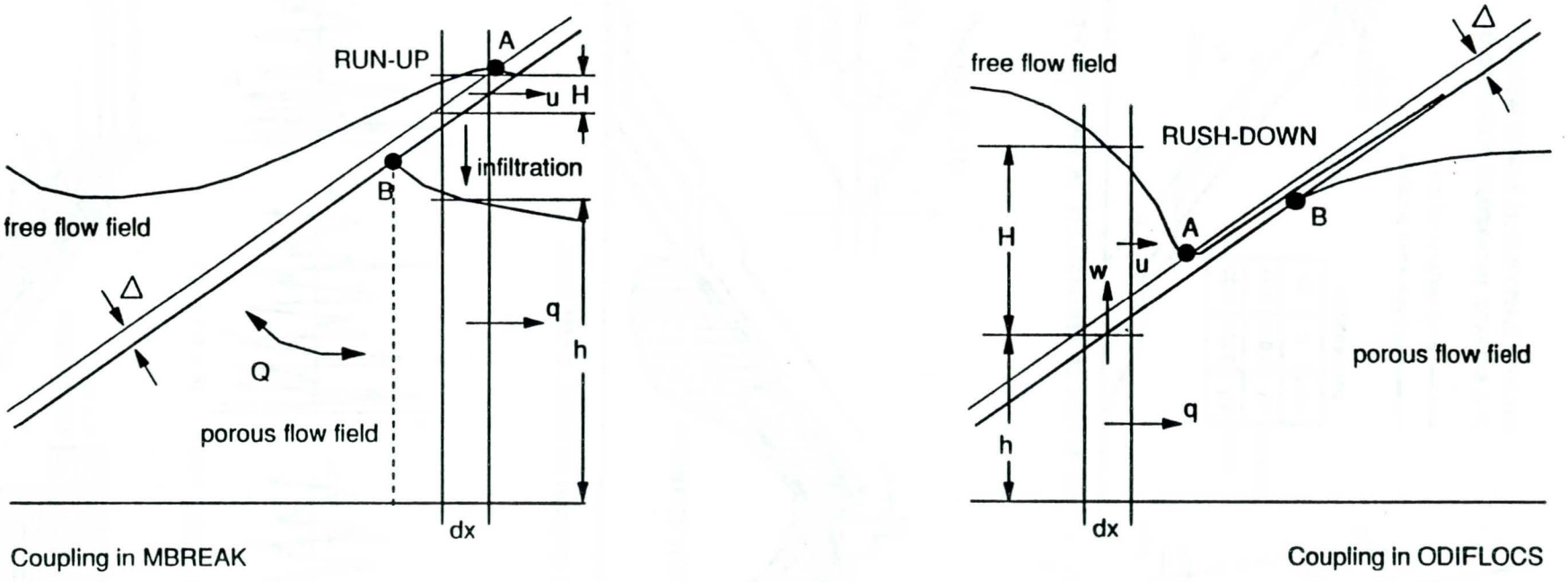

Figure 7. Methods of coupling inner and outer wave-induced flow

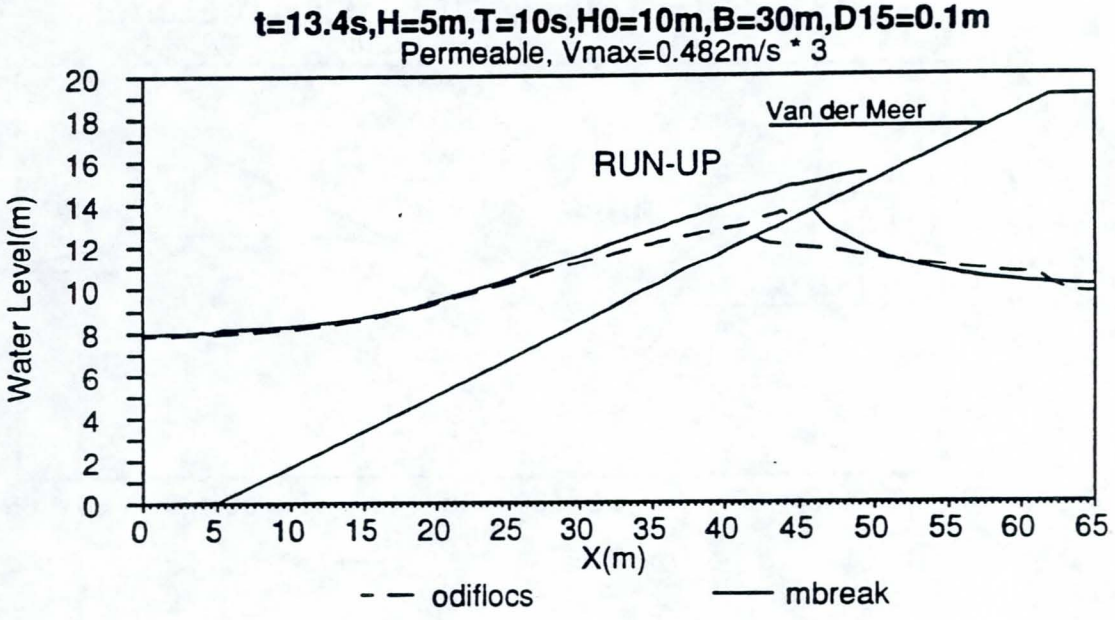

Figure 8. MBREAK/ODIFLOCS simulation of maximum run-up

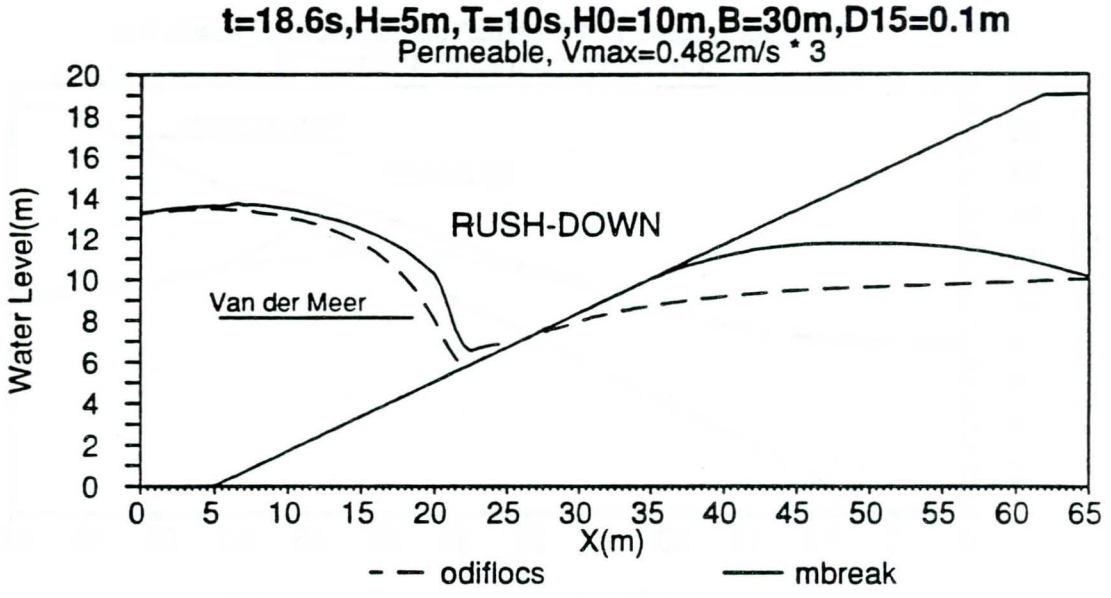

Figure 9. MBREAK/ODIFLOCS simulation of maximum rush-down

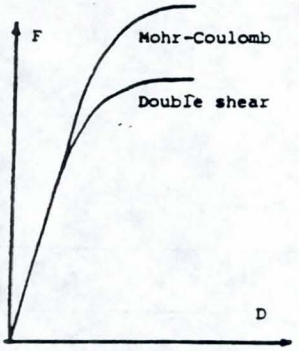

Load deformation diagram

Mohr-Coulomb

$\psi = 0$

$\lambda = 0$

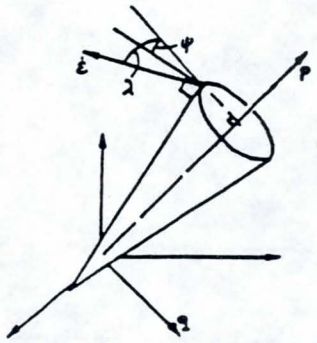

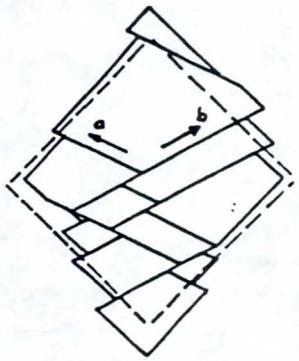

Double sliding model of De Josselin de Jong

$\tan\psi = \sin\phi$

$\tan\lambda = (a-b)\tan\phi/(a+b)$

Effect of constitutive models on deformation behaviour

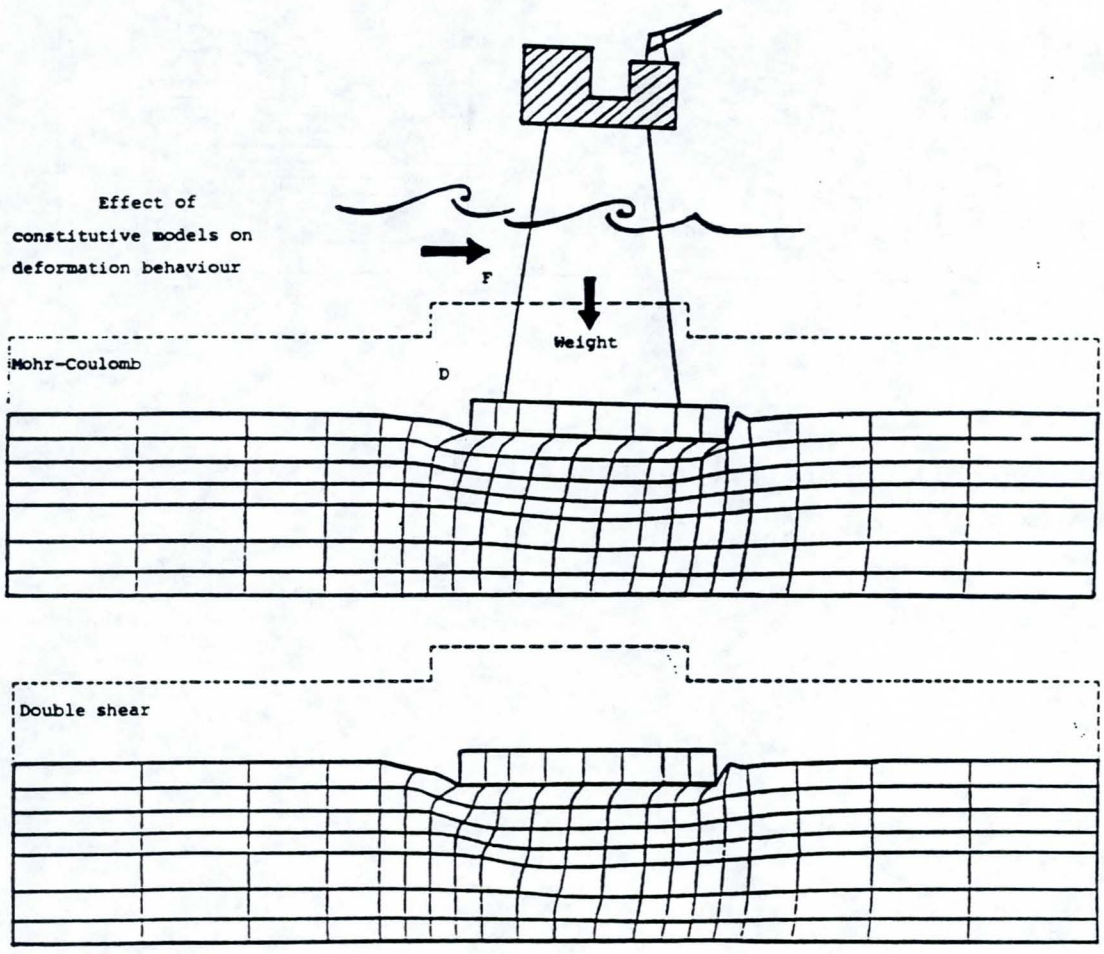

Figure 10. Double sliding failure mechanism

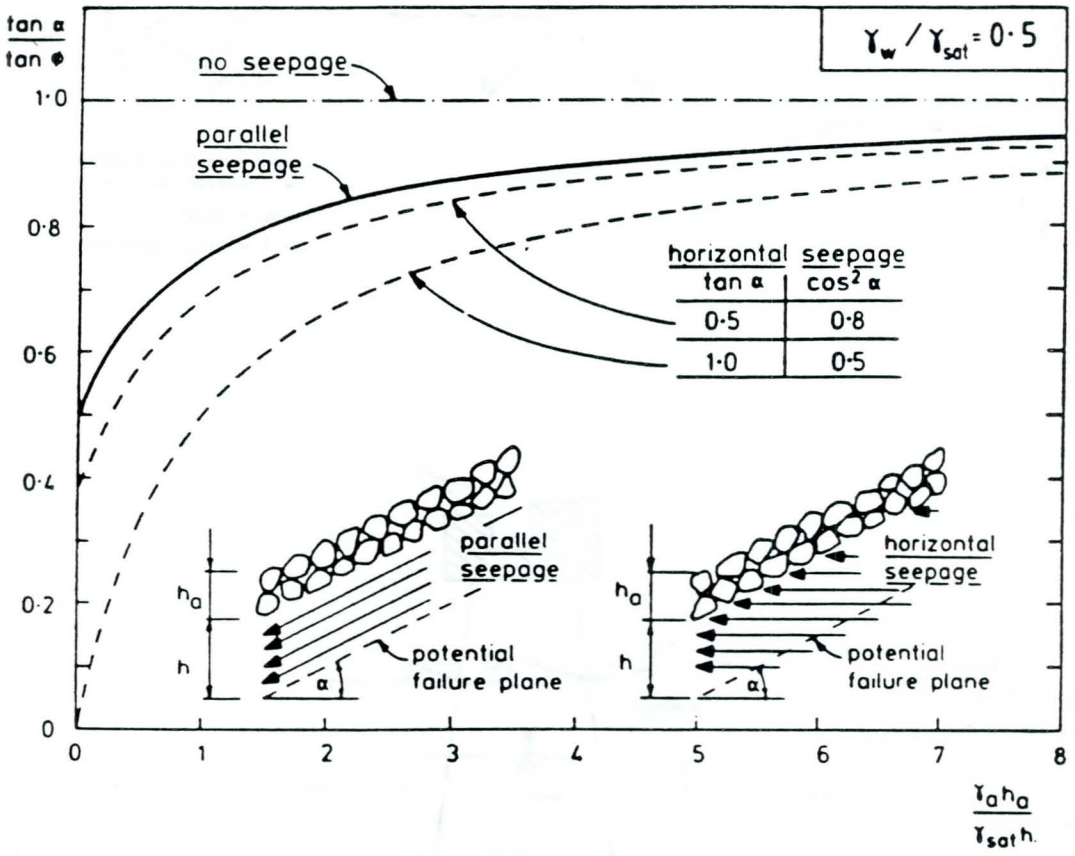

Figure 11. Slope filter stability under seepage forces (Hedges, 1986)

EVALUATION AND UTILIZATION OF BIOTECHNICAL TECHNIQUES AND WILLOW POSTS FOR STABILIZING ERODING STREAMBANKS

N.G. Bhowmik
Illinois State Water Survey, Hydrology Division,
Champaign, Illinois, USA

ABSTRACT

Erosion of the streambanks is a natural process. However, in many instances bank erosion could be quite extensive requiring not only an evaluation of the bank erosion processes but also developing and implementing bank stabilization techniques that are expected or assumed to be effective for a long time. Structural treatments such as riprap, stone or concrete revetment, etc. have been and will be utilized extensively to stabilize eroded streambanks. In recent times, application of biotechnical methods for small- to medium-sized streams has been tried quite successfully. Biotechnical streambank stabilization not only affords bank stability, but could also enhance aquatic and in some cases terrestrial habitats. This paper summarizes some of the principles utilized in biotechnical applications and case studies on willows, tree revetments, and others that were applied in the Midwest to stabilize eroded streambanks.

INTRODUCTION

Erosion and sedimentation of streams and rivers are natural processes that cannot be completely stopped or eliminated. However, excessive erosion of streambanks can be controlled by utilizing various structural and nonstructural techniques. Numerous examples and technical papers, articles, etc. including those presented in this workshop showed how structural techniques such

as riprap are quite valuable in the stabilization of eroding streambanks. The present paper will essentially concentrate on the biotechnical aspect of streambank erosion control methods and how these techniques can be valuable, not only in controlling the bank erosion but also in providing additional benefits to the fish and wildlife and aesthetics of the environment.

Even though erosion is a natural process due to the actions of water and wind, excessive erosion could still be caused by a variety of actions, some of which are natural and some human-induced. Caution must be exercised in applying a stop-gap measure to control a site-specific bank erosion problem without evaluating or understanding the basic and fundamental causes of the erosion. Erosion at a specific location along a stream course may have been initiated as a result of the instability of the stream, either because of increased stream gradient due to channelization, decrease in sediment load following the construction of an impounding reservoir or the paving of the watershed, increased flow concentration and flooding due to land-use changes, or the lowering of the base level of the river due to sediment removal, and so on. All these actions may precipitate streambank erosion or bed scour. In all these cases the stream is essentially attempting to reach a new dynamic equilibrium consistent with its gradient, sediment supply, bed and bank materials, water discharge and topographical features. Unless the main cause of the bank erosion is addressed, stabilizing the streambank at one specific location may essentially shift the problem at another location.

It is imperative that the entire watershed be evaluated, to determine the cause of excessive bank erosion before stabilization work is initiated. Once this information has been gathered and analyzed, then corrective measures can be initiated. It should be noted here that even if the root cause of the bank erosion cannot be addressed, a thorough knowledge of the causative factors will enable the stream managers to understand and appreciate the limiting factors of the bank stabilization techniques implemented and anticipate the success or failure of the work to be done. Various techniques that could be utilized in the stabilization of an eroding bank have been briefly described by Bhowmik (1983). A major portion of the present paper has been presented as a talk in a workshop by Bhowmik and Roseboom (1993) during the 24th Annual Conference and Trade Exposition of the International Erosion Control Association (IECA). However, the paper has not been published by the IECA.

The streambank stabilization work should be preceded by the following steps:

1. Evaluate the watershed to determine any recent or historical changes.
2. Evaluate the stream planform to determine recent changes, such as diversion, channelization, etc.
3. Determine the cause of the instability.
4. Evaluate streambank material, its consistency, composition, etc.
5. Analyze the streambank stability, utilizing concepts outlined in the companion paper in this session.
6. Determine appropriate method or techniques for stabilizing the eroding bank.
7. Determine if biotechnical methods will be appropriate.
8. Design and construct method or methods that would offer maximum protection against erosive forces. This may include a combination of structural and nonstructural techniques.
9. Provide adequate support for monitoring the implemented technique to determine its relative success or failure in preventing further erosion or stabilizing the bank.

The following section will briefly describe the basic concepts in the stabilization of streambanks utilizing biotechnical methods.

BIOTECHNICAL PRINCIPLES

Plants and live materials reinforce soil because their root systems create stability within the eroding banks. Nature has developed a built-in mechanism to protect against erosion similar to its ability to erode a streambank or a watershed.

Roots by nature will bind the soil and increases its strength against shear forces. This is essentially similar to the use of reinforced rods in concrete or flexible fibers used in some structure. Bache and MacAskill (1984) has included a discussion and an evaluation of the principles involved in the analyses of a soil-root mass system against shear failure. The following materials are essentially to those given by Bache and MacAskill (1984).

Figure 1 shows a conceptual drawing of an idealized single strand of a root within a horizontal shear zone on flat bed. This simplistic approach and the associated model was

developed by Wu et al. (1979). Original orientation of the root is normal to the shearing surface and deformation of the soil mass will be resisted by the tangential forces that will develop along the root as shown by T in figure 1. The ultimate resistance will be provided by the tensile strength of the root. Assuming that the internal angle of friction Ø is not effected by the root, Wu et al. (1979) developed the following relationship.

$$\Delta S_R \approx 1.15\, t_R \tag{1}$$

where ΔS_R is the increase of shear strength due to the presence of the root, and t_R is the average tensile strength of the root fibers per unit area of the soil. The average tensile strength per unit are of the soil is given by Equation 2.

$$t_R = T_R \left[\frac{A_R}{A}\right] \tag{2}$$

where T_R is the tensile strength of the root, A_R is the total fiber cross-sectional area and A is the total shear cross-sectional area. For a mass of roots, the value of t_R is obtained by summing the individual value for all root sizes and their strengths. Bache and MacAskill (1984) indicated that it may be advisable to represent the 'root area ratio in terms of the root concentration'.

The same authors also represented an equation for the determination of the total shear strength S of the soil root system in the Coulomb expression by adding the added shear strength increase, ΔS_R. This equation is given as follows.

$$S = (S_S + \Delta S_R) + \sigma \tan \varnothing \tag{3}$$

where S_S is the shear strength of the root-free soil and σ is the effective normal stress. This model indicates that high concentration of roots with high tensile strength will increase the strength of a soil-root system.

Bache and MacAskill (1984) reviewed the research done in the areas of root strengths of various trees. Based on this evaluation, they indicated that for fresh tree roots, tensile strength is a function of the diameter of the root and that the roots growing uphill is stronger than those growing downhill. Root strength also varies based on season having higher strengths in the fall. When trees are felled, root numbers and tensile strength decrease with age. Tensile strength also varies from species to species with higher values for alders and poplars compared to that for willows. In general and for similar root diameters, the strength of the tree roots are usually 1.5 to 3 times greater than those present for grasses, Bache and MacAskill (1984).

The discussion presented so far indicates that the vegetation with roots could not only reduce the flow velocity close to the bank but also offers added stability to the root-soil mass through its tensile strength and penetration to the banks. The following observation could thus be made for vegetation on a streambank as far as the erosion prevention is concerned.

- Dissipating the kinetic energy of the falling raindrop.
- Increasing surface roughness and reducing velocity close to the bank, which reduces the transport capacity of the flowing stream near the bank at that location.
- Reinforcing the bank through the root system, thus increasing the shear strength of a potential eroding site.
- Reducing surface runoff due to increased retention of water on the surface and assisting in the increase of groundwater recharge.
- Deflecting high-velocity flow away from the unstable bank.

Two types of vegetation could be used to protect an eroding bank grasses and woody plants. For immediate protection of streambanks against low velocities, grasses may be perfectly all right, but normally they are not suitable for high-velocity flows. Parsons (1963) indicated that the reduction in stream velocity due to the presence of grasses is directly related to the length, width, and density of the blades, and the areal density and depth of the root systems. Keown et al. (1977) indicated that a well-established grass system could reduce the velocity at the boundary layer by as much as 90 percent.

Research by Ree (1949) and Ree and Palmer (1949) has shown that the presence of Bermuda grass can effectively reduce flow velocity at and above the interface of the grass blades. Figure 2 shows the distribution of velocity in an experimental flume where Bermuda grass 0.2 meters (m) or 8 inches long was present. Comparable velocity distribution within a bare channel is also given in this figure. It is clear that in the channel and close to the bed, the reduction in velocity with Bermuda grass (dormant) is quite significant Moreover, the rate of change of velocity with depth within the grass channel is much smaller than the rate of change of velocity in a bare channel. This observation indicates that the shear stress near the soil surface should also be smaller in the grass channel, significantly reducing the erodibility of the flowing water.

The information presented in Figure 2 or similar information could be utilized to evaluate the stability of an eroding bank. If bed and bank materials are such that critical velocity (with due consideration for the bank slope and cohesion of the bank materials) is less than the expected range of velocities, then the bank could be considered stable.

Another factor that should be kept in mind relates to the types of vegetation that are suitable at certain locations within a stream, and stream and floodplain cross-sections. Seibert (1968) has shown that flow duration and water level in a river can be correlated with the type of vegetation that could be expected to survive or thrive at various locations. Seibert's conceptual division of a stream cross-section and its relationship with the bank and shore vegetation is reproduced in Figure 3

In hydrological terms, bankful discharges are defined as the flow that normally has a frequency of occurrence of approximately 2.33 years. Figure 3 shows that Seibert's mean water level, and/or the next higher water level, approximately correspond to the bankful discharge in a stream. Thus stabilization of the zone at or below the low-water level should only be attempted with aquatic plants. The zone of bank slope between the low-water level and the bankful stages could sustain reed-type vegetation and some soft woods. For any portion of the bank above the bankful stage, only hardwood-type vegetation should be utilized.

The type of plants that can survive at various submersions during the normal cycle of low, medium, and high stream flows is important to the design and implementation of biotechnical bank stabilization techniques. Installation of soft wood within the reed zones or

hardwood in the reed and soft-wood zone would probably result in a failure of the technique, simply because of the incompatibility of the vegetation habitat with the hydraulic and hydrologic factors. Thus before any riparian vegetation is used for stabilizing an eroded bank, the hydrologic and stream cross-section-related factors should be considered and evaluated.

Erosion at many streambank sites is due to the removal of the toe of the bank due to fluvial action. Stabilization here can be accelerated by the utilization of inert materials at the toe, followed by appropriate vegetation as shown in Figure 3. A conceptual design technique is shown in Figure 4 after Seibert (1968) for a stream at an eroding bank site.

Materials discussed so far concentrate on the general topic of biotechnological methods for protecting streambanks. Some of the specific applications for protecting an eroding bank will now be described including a detailed description of the willows that were utilized to stabilize an eroding site on Richland Creek, a tributary of Peoria Lake along the Illinois River, Slowikowski et al. (1992).

BIOTECHNICAL METHODS

Grass

Hydraulic engineers, geotechnical engineers, stream managers, and homeowners have long been aware of the utility of grass as a stabilizing natural barrier in waterways and other erodible areas. Research such as that by Ree (1949), Ree and Palmer (1949), and Whitehead et al. (1976) has shown how grass can provide resistance to flow and stability to a potentially eroding surface. Whitehead et al. (1976) indicated that well-chosen grass can withstand a velocity of 2 meters per second (m/s) for up to ten hours, a velocity of 3-4 m/s for several hours, and a velocity of up to 5 m/s for one to two hours.

Grass must be selected after thorough evaluation of soil type, hydraulic and erosion suitability, maintenance requirements, and the surface expected to be exposed for a prolonged period of time. Grass is normally utilized for the bank that is exposed during the low-flow period. The grass strip (turf) can be installed in a diagonal bond pattern and should be pinned down or covered with a biodegradable netting. On exposed surfaces, grass seeds can also be planted through hydroseeding. However, it should be noted that grass cover could break down due to a variety of factors (Hydraulics Research Station, 1980; Whitehead et al., 1976).

In all streambank stabilization work with vegetation such as grasses, it should be remembered that vegetation will normally assist in stabilizing an eroding bank where bank velocity is in the range of 1 m/s or less, but it probably will not cure the erosion problem (Faguay, 1972).

Reed Clumps

Reed clumps have been utilized for bank protection for a long time (Schiechtl, 1980). Root clumps of reed plants are placed along the bank line, interspaced with rocks and other types of revetments. Fertile soil is needed for the proper spread of rhizomes. Normally about three clumps are needed for every running meter of shoreline.

Planting should be done during the dormant period. Depending upon the species, planting can be located both below and above the normal water line. Clumps such as these could accelerate the deposition of sediment, reduce the flow velocity, dissipate wave energy, and stabilize the shores with root systems. Reed clumps do not provide immediate bank protection and are not suitable for streams with fairly high velocities. Reed clumps can, in some instances, assist in the stabilization of wet slopes or where seepage is a problem.

Reed Rolls or Swamp Sod Rolls

A combination of ground support with driven poles; and longitudinal gravel-filled rolls of wire mesh, with reed clumps attached to the mesh, are used as a single entity to stabilize an eroding bank. This type of construction is possible when the water level is below the eroding face of the bank. For below-water construction, dead branches or large rocks are used for installing such reed rolls (Schiechtl, 1980). Tree branches are normally preferred because of their effectiveness in reducing the velocity and the associated deposition of suspended sediment loads. Again, all the construction is done during the dormant period. This technique can provide bank protection immediately after construction, while reed clumps may require two to three growing seasons before they become effective in stabilizing the banks. This type of bank protection is effective for streams where flows are normally controlled, thus limiting the fluctuation of water levels.

Live Fascines

Live fascines are normally placed in previously dug shallow trenches at the interface of the low to medium water lines (Schiechtl, 1980). The fascines should be secured with live or dead pegs. Fascines can be used in river banks to protect against washout. Fascines, when installed on brush layers with brushes sticking to the bank, can also provide protection against wave action. Fascines become effective after they take root and start to grow. This type of bank protection is also effective where water level fluctuation is small and other bank protection techniques, such as brush mattresses, sodding, and even structural techniques such as ripraps, are used to protect the bank above the water line. Incorporation of live fascines into booms for bank protection along Crow Creek was successfully applied in 1987 (Roseboom et al., 1991).

Live Wooden Baffles

According to Schiechtl (1980), live wooden baffles are normally utilized for protecting the banks of mountainous streams where the water level fluctuation is very high and the streams carry sizable amounts of small-grained bed load. Live branches such as willow are placed between the wooden logs laid longitudinally along a bank. The bank should consist of rich soils. This technique should afford a reasonable amount of protection against the erosive action of the flow. Construction can also be done like a crib wall. Concrete or other inert materials such as riprap can also be used with live branches instead of the wooden logs.

Tree Revetments

Revetment materials normally provide greater resistance to flow, have higher critical velocity, accelerate the deposition of sediments, and provide stability to an eroding bank. Revetment are made of piles, concrete, brickwork, blocks, riprap, gabions, branch mattresses, live branch packing, sods, newly felled trees and other materials. Use and application of trees as revetments will now be briefly described.

Palmiter (Institute of Environmental Sciences, 1982) recommended the use of felled trees anchored at their bases and placed strategically at or near the toe of the eroding bank for protecting against further erosion. Placing the trees at the eroding bank, which in most cases is on the concave side of the bend, also should deflect the high-velocity flow from the bank toward

the center of the channel. This deflection of flow should also resuspend the sediment that may have deposited as point bars, thus making the channel hydraulically efficient. Materials for such stream stabilization work are normally obtained from the surrounding land and watersheds. Willeke and Baldwin (1984) have indicated that the Palmiter technique of bank stabilization showed positive biological impacts in Ohio.

Tree revetments have been used extensively in a number of streams by the Missouri Department of Conservation (MDC). MDC (undated) has published a brochure outlining the proper construction of a tree revetment for the protection of eroding banks and the enhancement of fisheries habitats. Tree selection for revetment construction is an integral part of the success of such a revetment. The following factors are taken from the MDC publication:

- The more limbs and fine branches a tree has, the better it will reduce the velocity and trap silt in a tree revetment. For this reason, eastern red cedar is usually the best choice. Cedar trees have the added advantage of good resistance to decay. Hardwood trees with brushy tops (like pin oak) will also work.
- Trees growing in uncrowded conditions are usually the best choice because their branches are denser. When growing in close competition with other trees, even cedars can have sparse tops.
- It is best to cut live trees for revetments; trees that have been dead for some time are usually brittle and may break apart as they are moved into place and anchored.
- Tree size is important. The diameter of the tree's crown should be about two-thirds the height of the eroding bank. A large tree covers more bank than a small one, and isn't much more difficult to move into place. Both time and money can be saved by using the biggest trees available. Trees that are more than 6 m tall are best for most streambanks.
- After felling trees, it is best to cut off any trunk at the bottom of the tree that is without limbs. The tree limbs are what protects the bank — any excess trunk is simply extra weight that makes it more difficult to move the tree into place.

Figure 5 shows a conceptual technique that could be utilized in the construction of a tree revetment. Construction of the revetment should start at the downstream end and proceed in the

upstream direction. Trees should be placed at the toe of the bank with the tree butt pointed upstream and anchored at both ends with T-posts. Trees must be held tightly against the eroding bank. Subsequent trees are placed so that the top of the second tree overlaps the butt of the first tree and so on. The top of each subsequent tree should be anchored with the butt of the previous tree. The technique is similar to attaching shingles on rooftops. The idea is to deflect the flow away from the bank without allowing an opening where high-velocity flow or the component of the secondary current can attack the bank and undermine the toe or erode the bank.

The tree revetment shown in Figure 5 should also facilitate the deposition of sediment next to the trees. This sediment most probably consists of washloads in a river, which are essentially topsoil in the midwestern parts of the country. These topsoils are extremely fertile and they should assist in the revegetation of the eroding bank. Even though cottonwood, sycamore, and willow may appear naturally, planting of seedlings or cuttings can accelerate the process of revegetation.

Tree revetments may not work in a stream that is unstable because of a drastic change in its gradient, land-use attenuation, or other human or natural catastrophic acts or events. Small and medium streams will probably be suitable candidates for such a bank stabilization technique. MDC also recommends that tree revetments should not be used when the eroding bank is more than 3.6 m in height. Other factors that should be kept in mind in the design and construction of a tree revetment include: a) not significantly constricting the flow, b) not allowing the tree revetment to be completely under the normal water line, c) not leaving any gaps between the trees, and d) establishing a wooded corridor on the bank, probably 30-40 m wide, where no cattle grazing is allowed.

Establishment of tree revetments in a number of Missouri streams has shown that not only are the streambanks protected against the erosive action of the flow, but the revetments also assisted in the restoration of fish habitats (Gough, 1990). Gough reported results from 33 revetment sites with additional data from six of those sites on cross-sectional changes and fish habitat determination. This research has shown that cross sections in those reaches treated with tree revetments became narrower and deeper. It should be noted that the tree revetments were placed mostly on the outside bank of the bend where the velocity is highest, superelevation is largest, and probably the traverse component of the velocity (secondary circulation) is also

greatest. Obviously, placing the tree revetments at these locations deflected the core of the high velocity away from the bank, which in turn eroded the bed of the channel in order to maintain the needed conveyance. Gough's data have also shown that in the sampled revetment sites, both minnows and game fish were present when the fish community was sampled.

Palmiter implemented a series of tree revetments on bank erosion sites in a 3-4.8 km reach of Court Creek (Roseboom and White, 1990). Palmiter tree revetments were effective on bank erosion sites with annual erosion rates of less than 1 m. However, on several erosion sites, the Knox County Soil and Water Conservation District added tree revetments with Laconia earth anchors where the Palmiter revetments had washed out. These remained in place and reduced the rates of bank erosion on 11 bank erosion sites when compared to 4 sites in the upstream and downstream controls (Roseboom and White, 1990). However even with small willow slips, the reduced erosion rates still prevented revegetation of the bank.

This discussion shows that a tree revetment is a viable alternative for stabilizing small- to medium-size streams, but these should not be substituted for a thorough evaluation of the stream hydraulics, stream morphology, and geotechnical properties of the bank materials to identify the main cause of the bank instability.

Willows

A 1925 *Engineering News Record* carried an article showing the use of live willow poles for stabilizing eroding streambanks. The technique described in this article was essentially the same one used in a number of other works since 1934 including the Cook Creek watershed in southwestern Wisconsin (Fry, 1938).

Fry indicated that under favorable conditions, live willows did not have any difficulty in sprouting and/or growing. But newly planted willows had to be protected against floods. In the Cook Creek watershed, live willow planting preceded the establishment of brush-rock wing dams, piling, timber cribs and bulkheads in the upstream area.

The technique found to be effective on Cook Creek consists of grading the eroding bank to 1:1 slope and planting the willows in dug trenches at 1.2-1.5 m intervals along the slope of the bank. Then the willows were fastened to the bank with stakes. The exposed areas between the willows were thatched with bundles of willows. The willow poles and thatch were covered

with wires and tied with stakes and posts. The use of mats and willow posts afforded immediate bank protection, similar to riprap. After about two growing seasons, the sprouts from the willows were about 2 m high and could withstand the erosive action of the flow. Fry also indicted that willow mattresses could possibly be utilized to stabilize the banks without the use of the willow poles. However, he cautioned that in this type of stream stabilization technique, the toes of the banks must also be protected by structural means such as riprap. Protection of the live willows against immediate flood flows and ice floes can be attained by the construction of fences, wing dams, etc.

Utilization of willows for streambank stabilization have also been described by Dupre (1948) for streams in Ohio, by Carlson and Preston (1976) in northeastern USA after tropical storm Agnes, and by Workman (1974) in Montana. Workman (1974) also indicated that in the Prickly Creek watershed, where clearing was necessary to construct a portion of an interstate highway, live willow planting and natural seeding have brought the population of rainbow and brown trout to their preconstruction levels. Workman (1974) was quick to point out that in any and all reconstruction projects, the goal should be to reconstruct a channel that approximately equals the original channel.

Vegetative streambank stabilization technique was utilized in Illinois to stabilize eroded banks and also to enhance aquatic habitats, Roseboom et al., (1992). As a result of the limited success of the Palmiter tree revetments, the willow post technique (York, 1984) was adapted for two sites on Court Creek in 1987. In the willow post technique, dormant willow posts are placed in holes below the maximum scour depth along the eroding bank. The willows grow root systems and branches in early spring. No erosion has occurred in the succeeding five years. The willow posts must be placed below the maximum depth of channel scour and near the groundwater level. Willow posts increase the stability of the bank after the first year when the root systems grow and interlock.

As a result of willow post stabilization trials on Court Creek, the Illinois River Soil Conservation Task Force installed a series of test sites on tributaries to the Illinois River. The task force was formed to reduce the rate of sedimentation in Peoria Lake, which has one of the highest rates of sedimentation in Illinois (Demissie and Bhowmik, 1985, 1987). These

investigators pointed our the Peoria tributaries deliver a disproportionate amount of sediment to the lake compared to their relatively small drainage areas.

On the Richland Creek site a series of monumented stream transects were installed to document stream channel configuration in 1988, Slowikowski et al. (1992). On Richland Creek the following treatments were applied: willow posts (3 m or longer) on site 1, willow stakes (1 m long) on site 2, and willow slips (0.4 m long) on site 3, and grasses on site 4. Sites 1, 3, and 4 were monitored to determine the changes that occurred with time.

A drought in 1988 and 1989 caused the loss of all vegetation except for the longer willow posts, which were placed closer to groundwater level. The willow posts were placed in holes formed with a 1.83 m ram, while the willow stakes were placed in shorter holes formed with tile probes or short steel bars.

With the 1988 survey data from the Soil Conservation Service, Slowikowski et al. (1992) resurveyed the stream during 1990 and 1991. Figure 7 shows the plan form changes and the thalweg profiles on the south fork of Richland Creek, where willows survived the 1988 drought. Cross-sectional data from these reaches including an outline of the bank profiles have been collected three to four times from November 1988 through November 1991. From 1988 through 1991, some erosion of the banks took place at site 3 and downstream but on the opposite bank of the treated site. Thalweg profiles between these intervening years shows a gradual aggradation of the bed within this reach. The cross-sectional elevations at three sections, 36, 36, and 34, Figure 6, are shown on Figure 8. For this upper reach, where the bank erosion took place, the width and cross-sectional area of the stream increased. On the other hand, within more stable stream cross-sections, the cross-sectional area showed a net decrease.

Similar to the South Fork (Figure 7) the thalweg at this site also aggraded between 1988 and 1991 (Figure 9). The variations in cross-sectional profiles at sections 23, 20B, and 20A between 1988 and 1991 are given in Figure 10. Again, only three cross-sections are shown here. Sections 20B and 20A are outside of the willow post treated site, and all the erosion took place on the downstream side opposite of the treated bank.

Both the cross-sectional area and the top width at this erosion site also increased after 1988. Cross sections 27 through 24 (Figures 6 and 9), were fairly stable with a slight decrease in cross-sectional area.

The results presented above show the changes that occurred for a period of about three years. Further data on the stabilized site and changes in the downstream reaches, if any, will certainly be helpful in determining the main causes of bank erosion on this stream, even though the willow posts have helped to reduce the erosion at the treated sites.

Further work on willow post and tree revetment bank stabilization work has continued on the Richland Creek by the Illinois State Water Survey. Within this creek and also at difficult sites, the bank is sloped and cedar tree revetments are placed along the toe of the streambank. Contractors excavate the post holes with steel ram or a hydraulic auger. When private contractors are utilized and willow posts are purchased, the technique cost ranges from $4.00 to $8.00 per linear foot (0.305 m), Bhowmik and Roseboom (1993). Cost will depend on the extent of bank sloping and the proximity of the willow post supply. Willow posts and cedars provide both the structural component and the vegetative component of bank stabilization.

Lunker Habitat Stabilization

In the lunker technique, willow post stabilization can be enhanced with the addition of wooden platforms below the waterline. These lunkers are usually 2.44 m and are held in place with rebars. Riprap is placed beneath the water to provide additional stability and rocky cobble enhancing habitats for smallmouth bass. In Franklin Creek State Park (Roseboom et al., 1992), the population of young smallmouth bass increased 300 percent while the numbers of smallmouth bass above 0.5 pound increased 50 percent

When willow posts stabilize the earth bank above normal waterline, the amount of required riprap is greatly reduced in lunker construction. Therefore bank stabilization costs can be reduced by 50 percent. The lunker costs was $25.00 per 0.3 m in rural areas. The willow posts were normally cut by the second season when prairie grasses became established.

COSTS OF BIOTECHNICAL TREATMENTS

Data on costs of various biotechnical treatments are not readily available. Moreover, since most of the cost in this type of treatments is labor, they normally change from year to year and will certainly increase in the future. Roseboom and White (1990) have presented some data on costs of various techniques. Presently, costs have been estimated as follows.

Table 1. Costs of Bank Stabilization Practices

Method	Cost per linear foot (0.305 m)
Tree Revetments	$3-$16
Willow Posts	$3-$9
Lunkers (rural)	$25-$35
Lunkers (urban)	$50
A-Jacks (urban)	$45

REPAIRING DAMAGED BANKLINES AND SHORES

The techniques identified previously could be utilized to repair a damaged shoreline or an eroding bank. Repairs could be accomplished at two or three different levels. Either a single treatment such as willow posts or a combination of treatments such a tree revetments and willow posts and other live planting can accomplish the desired results. Schiechtl (1980) described clearly how rock-fill with live branch layering can be used to stabilize a stream reach. The main concept here is to reduce the velocity near the eroded area and force the flowing stream to drop its sediment load. In low-flow season, this would or could establish vegetation due to natural seeding.

Another technique described by Schiechtl (1980) consists of the construction of log-brush barriers at eroded sites with the ultimate goal of reducing velocity and forcing the stream to drop its sediment loads. Both of these techniques are variations of the method originally proposed by Prueckner (see Schiechtl, 1980) for stabilizing washout areas. Schiechtl also mentioned that tree branches could be packed into a washout zone to stabilize the site and encourage sediment deposition.

SUMMARY

This paper presented several biotechnical methods that could be utilized to stabilize eroding banks of medium- to small-size streams. Biotechnical methods alone probably will not stabilize a stream with very high velocity, but these could be utilized in combination with other structural means such as riprap, wing dams, piles, fences, etc.

Biotechnical methods that could be utilized consist of grass, reed clumps, reed rolls, live fascines, wooden baffles, tree revetments, willow posts, and lunkers. In general, costs of biotechnical treatment are much smaller than the structural techniques, provided that materials for biotechnical treatments are available locally. In some instances, biotechnical methods could be utilized to stabilize a washout section of a stream. All streambank stabilization work will require regular maintenance to make certain that it works out as designed. Bank stabilization and the establishment of a set-back zone where grazing, cattle movement, and other concentrated use is eliminated or avoided, should enable a stream manager to establish and maintain viable and stable streambanks.

Biotechnical treatments, if applied properly and maintained on a regular schedule, will enhance aquatic habitats such as fisheries.

In all streambank stabilization work, caution must be exercised so that measures are not instituted at one site, while the problem of stream instability simply shifts to another location. An evaluation of stream hydraulics, hydrology, and watershed land uses, along with streambank and bed material analyses should precede the stabilization work. This evaluation will enable the managers to determine the main causes of the bank instability and anticipate the relative success of the implemented work.

ACKNOWLEDGEMENTS

Materials presented in this paper are based on work done by the authors and others in the general area of streambank stabilization or management. Most of these materials were presented at a workshop during the 24th Annual Meeting of the International Erosion Control Association in Indianapolis in February 1993 by the author and Don Roseboom of the Illinois State Water Survey. A special thanks goes to Steve Gough of Steve Gough & Associates, Champaign, IL, for his extensive assistance in the preparation of this paper and also for providing some the reference materials. The camera-ready copy of the paper was prepared by Lori Nappe, graphics were done by Linda Hascall, and Laurie Talkington edited the paper. Partial support for some of the work reported in this paper was provided by the U.S. Army Corps of Engineers through the EMP for the Upper Mississippi River System. The Environmental Management Technical

Center of the U.S. Fish and Wildlife Service, Onalaska, Wisconsin, served as the project coordinator with Ken Lubinski as the project manager.

REFERENCES CITED

Bache, D.H., and I.A. MacAskill. 1984. *Vegetation in Civil and Landscape Engineering.* Granada Publishing Ltd., London.

Bhowmik, N.G. 1983. *Streambank Stabilization Techniques.* Proceedings, National Symposium on Surface Mining, Hydrology, Sedimentology, and Reclamation, November 17-December 2, University of Kentucky, Lexington, KY.

Bhowmik, N.G., and D.P. Roseboom. 1993. *Streambank Stabilization with Biotechnical Techniques.* Workshop talk, 24th Annual Conference and Trade Exposition, The International Erosion Control Association, Indianapolis, February 23-26, not published.

Carlson, J.R., and J.O. Preston. 1976. Stream Co Purple Osier Willow. *American Nurseryman,* 144(2): 12, 73.

Demissie, M., and N.G. Bhowmik. 1985. *Peoria Lake Sediment Investigation.* Illinois State Water Survey Contract Report 371, Champaign, IL.

Demissie, M., and N.G. Bhowmik. 1987. Long-Term Impacts of River Basin Developments on Lake Sedimentation: The Case of Peoria Lake. *Water International,* 12: 23-32.

Dupre, D.D., Jr. 1948. Willow Mats Economical for Bank Protection. *Roads and Streets*, 91(2): 92-94.

Engineering News Record. 1925. *Protecting Steep Banks by Planting Live Willow Poles.* 94(20): 822-823.

Faguay, G.A. 1972. *Bank Erosion on Low-Velocity Streams.* In International Commission on Irrigation and Drainage, Eighth Congress, Varna, R 29, Trans., Vol. 5, Questions 29.1, pp. 29.1475-29.1493.

Fry, J.R. 1938. Willows for Streambank Control. *Soil Conservation,* IV(5), November.

Gough, S. 1990. *Stream Fish Habitat Response to Restoration Using Tree Revetments.* Proceedings of the Symposium on Restoration of Midwestern Streams, Randy Sauer, ed., 52nd Midwest Fish and Wildlife Conference, December 4-5, Minneapolis, MN.

Hydraulics Research Station. 1980. *Report on Bank Protection in Rivers and Canals.* Prepared by C.H. Dobbi & Partners for Hydraulics Research Stations, Wallingford, Oxfordshire, England.

Institute of Environmental Sciences. 1982. *A Guide to the George Palmiter River Restoration Techniques.* Miami University, Oxford, Ohio, prepared for U.S. Army Corps of Engineers, WRSC, Ft. Belvoir, VA.

Keon, M.P., N.R. Oswalt, E.B. Perry, and E.A. Dardeau, Jr. 1977. *Literature Survey and Preliminary Evaluation of Streambank Protection Methods.* U.S. Army Corps of Engineers, Waterways Experiment Station, Vicksburg, MI, Tech. Rept. H-77-9.

Missouri Department of Conservation. (Undated) *Tree Revetments for Streambank Stabilization.* Streams for the Future, Fisheries Division, Missouri Dept. of Conservation, Jefferson City, MO.

Parsons, D.A. 1963. *Vegetative Control of Streambank Erosion.* Proceedings of the Federal Inter-agency Sedimentation Conference. U.S. Dept. of Agr. Misc. Publ. 970, pp. 130-136.

Ree, W.O. 1949. Hydraulic Characteristics of Vegetation for Vegetated Waterways. *Agr. Engin.*, 30(4): 184-187.

Ree, W.O., and V. J. Palmer. 1949. Flow of Water in Channels Protected by Vegetative Linings. *U.S. Dept. Agr. Tech. Bulletin,* 967:115 pp.

Roseboom, D.P. and W. White. 1990. *The Court Creek Restoration Project.* Erosion Control: Technology in Transition, Proceedings of XXI Conference of the International Erosion Control Association, Washington, DC, p. 25-40.

Roseboom, D., W. White, and R. Sauer. 1991. *Streambank and Habitat Strategies along Illinois River Tributaries.* Governor's Conference of the Management of the Illinois River, p. 112-122.

Roseboom, D., R. Sauer, D. Day, and J. Lesnack. 1992. *Value of Instream Habitat Structures to Smallmouth Bass.* Illinois State Water Survey Misc. Publication 139, Peoria, Il, 86 pp.

Schiechtl, Dr. H. 1980. *Bioengineering for Land Reclamation and Conservation.* The University of Alberta Press. 404 pp.

Seibert, P. 1968. *Importance of Natural Vegetation for the Protection of the Banks of Streams, Rivers, and Canals.* In Freshwater. European Committee for the Conservation of Nature and Natural Resources, Nature and Environmental Series.

Slowikowski, J.A., W.C. Bogner, and N.G. Bhowmik. 1992. *An Evaluation of Streambank Stabilization Work on Richland Creek.* Illinois Dept. of Energy and Natural Resources, IENR/RE-WR-92/05, 80 pp.

Whitehead, E., Nickersons of Rothwell. 1976. *A Guide to the Use of Grass in Hydraulic Engineering Practice.* CIRIA Tech. Note 71.

Willeke, G.E., and A.D. Baldwin. 1984. *An Evaluation of River Restoration Techniques in Northwestern Ohio.* Miami University of Ohio, prepared for U.S. Army Corps of Engineers, WRSC, Ft. Belvoir, VA, 80 pp.

Workman, D.L. 1974. *Improvements on Prickly Pear Creek, 1971-1973.* Final report, Montana State Fish and Game Commission, Great Falls, MT.

Wu, T.H., W.P. McKinnell, and D.N. Swanston. 1979. *Strengths of Tree Roots and Landslides on Prince of Wales Island, Alaska.* Canadian Geotechnical Journal, 16: 19-33.

York, J.C. 1985. *Dormant Stub Planting Techniques.* Proceedings of the First North American Riparian Conference, University of Arizona, Tucson, AZ.

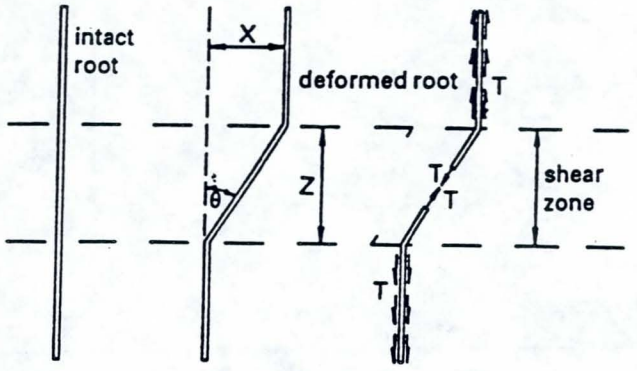

Fig. 1. Conceptual model of a flexible vertical root extending through a horizontal shear zone on flat bed (after Bache and MacAskill, 1984).

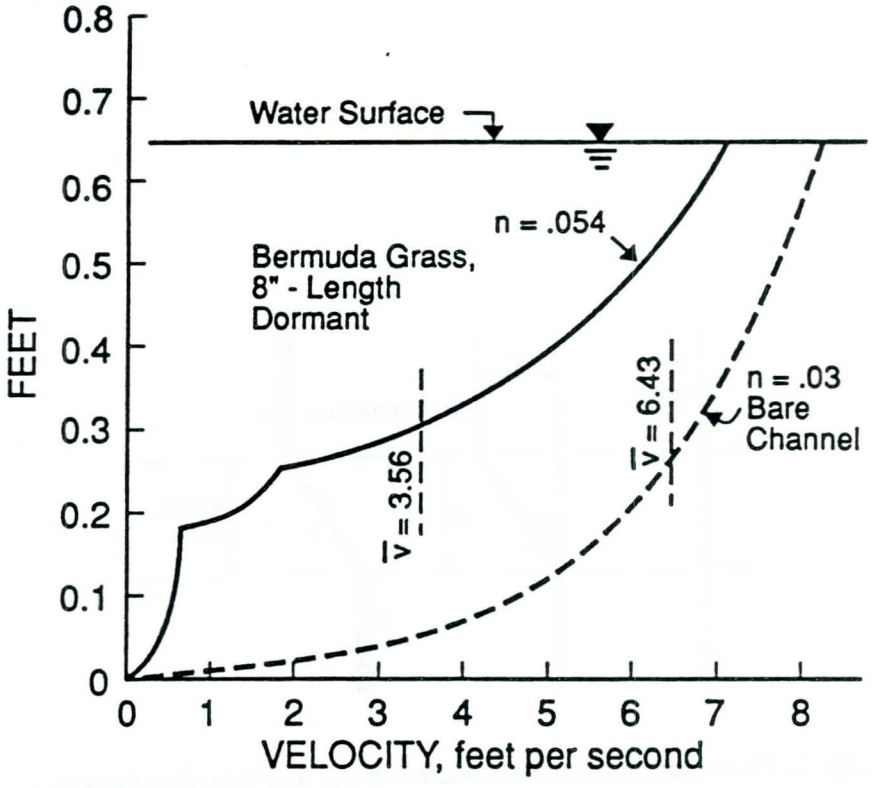

Fig. 2. Flow through vegetation (after W.O. Ree, 1949).

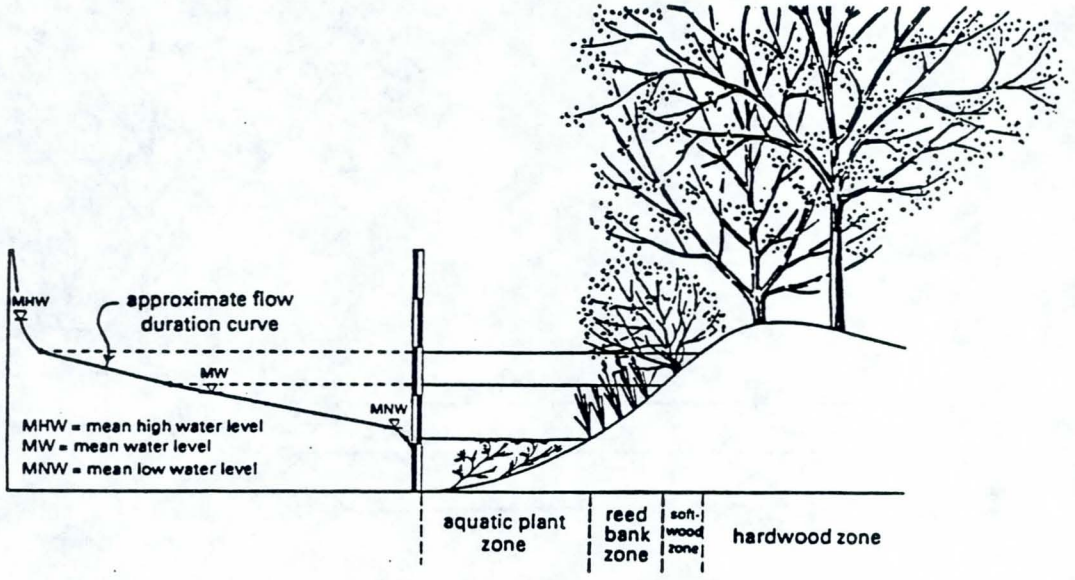

Fig. 3. Annual curve of water-levels, showing duration of the different levels, correlated with the graduation of vegetation at the same location (after Seibert, 1968).

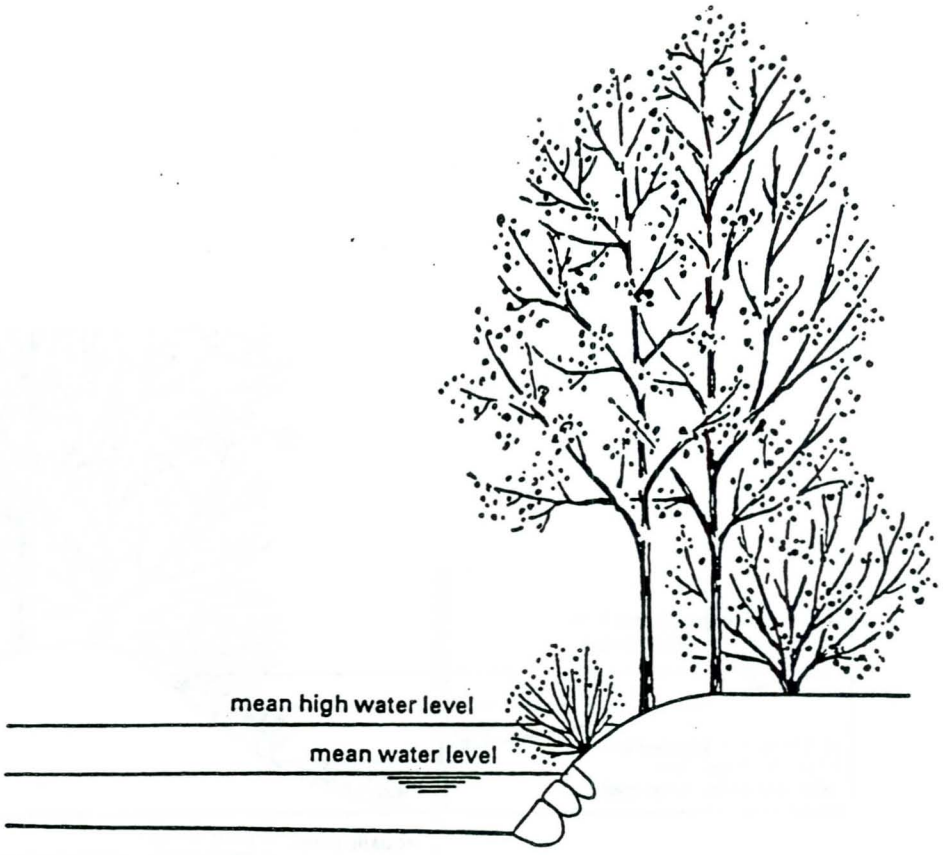

Fig. 4. Plan for a stand of trees on a river bank (after Seibert, 1968).

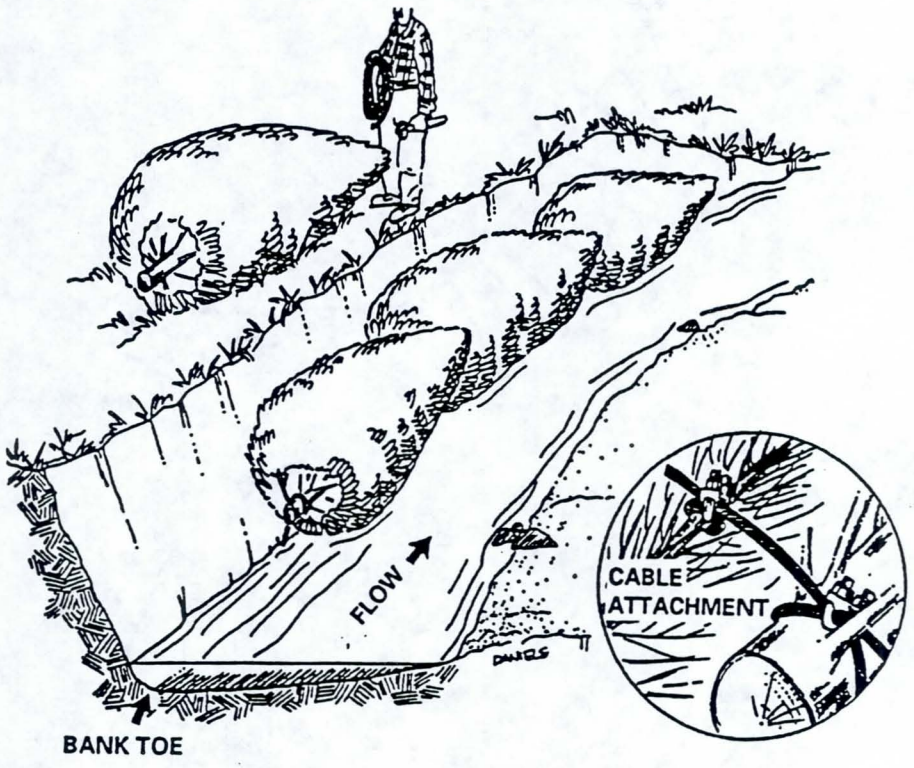

Fig. 5. Construction of a tree revetment (after Missouri Department of Conservation).

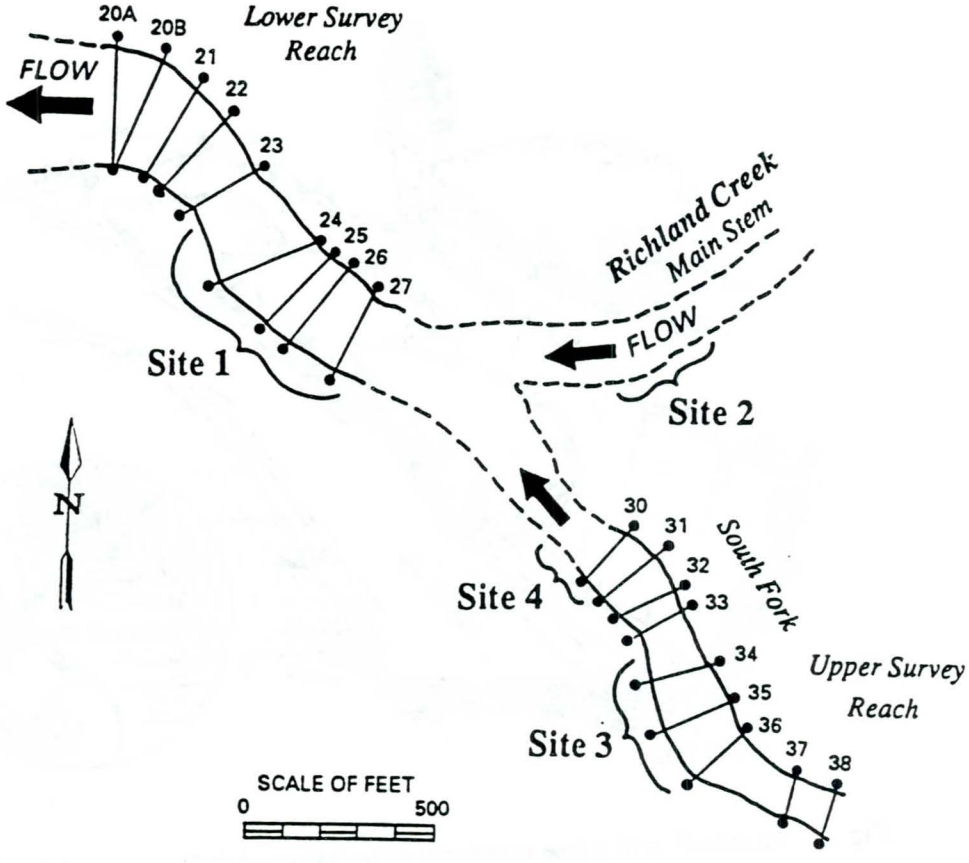

Fig. 6. Richland Creek study area (after Slowikowski et al., 1992).

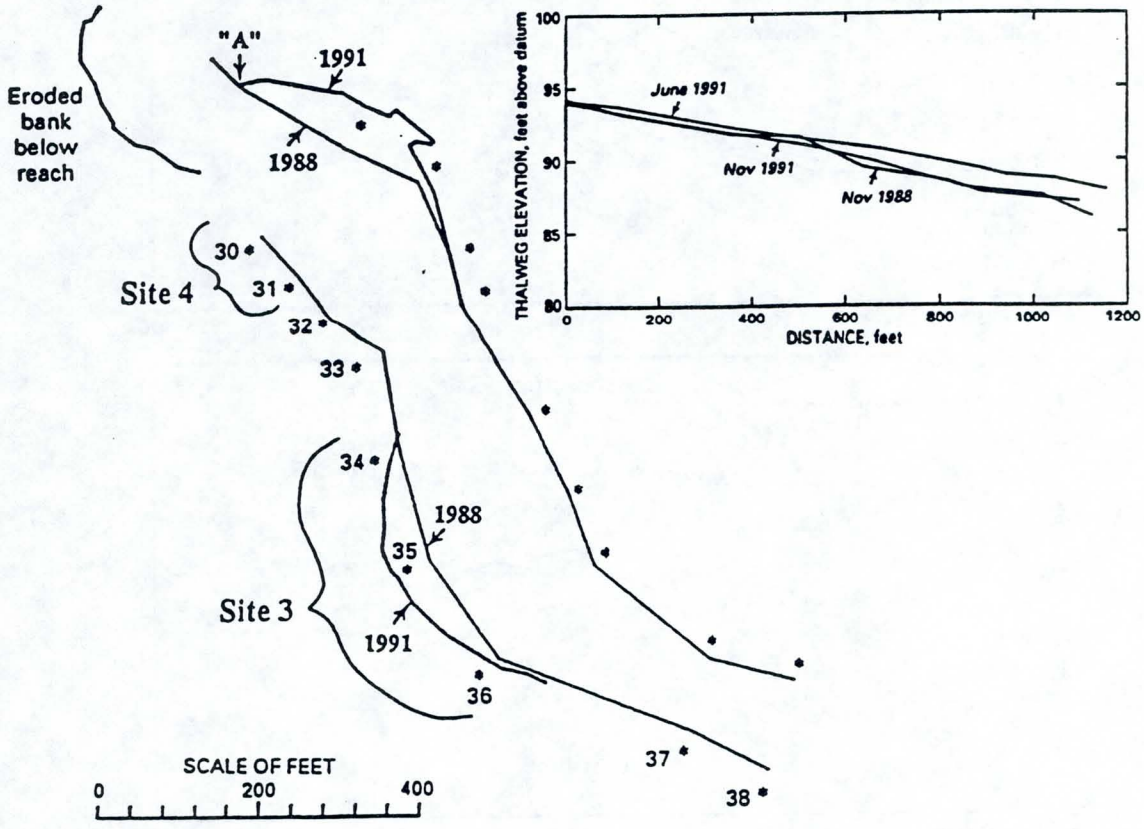

Fig. 7. Plan form changes and thalweg profile of the South Fork of Richland Creek, 1988-1991 (after Slowikowski et al., 1992).

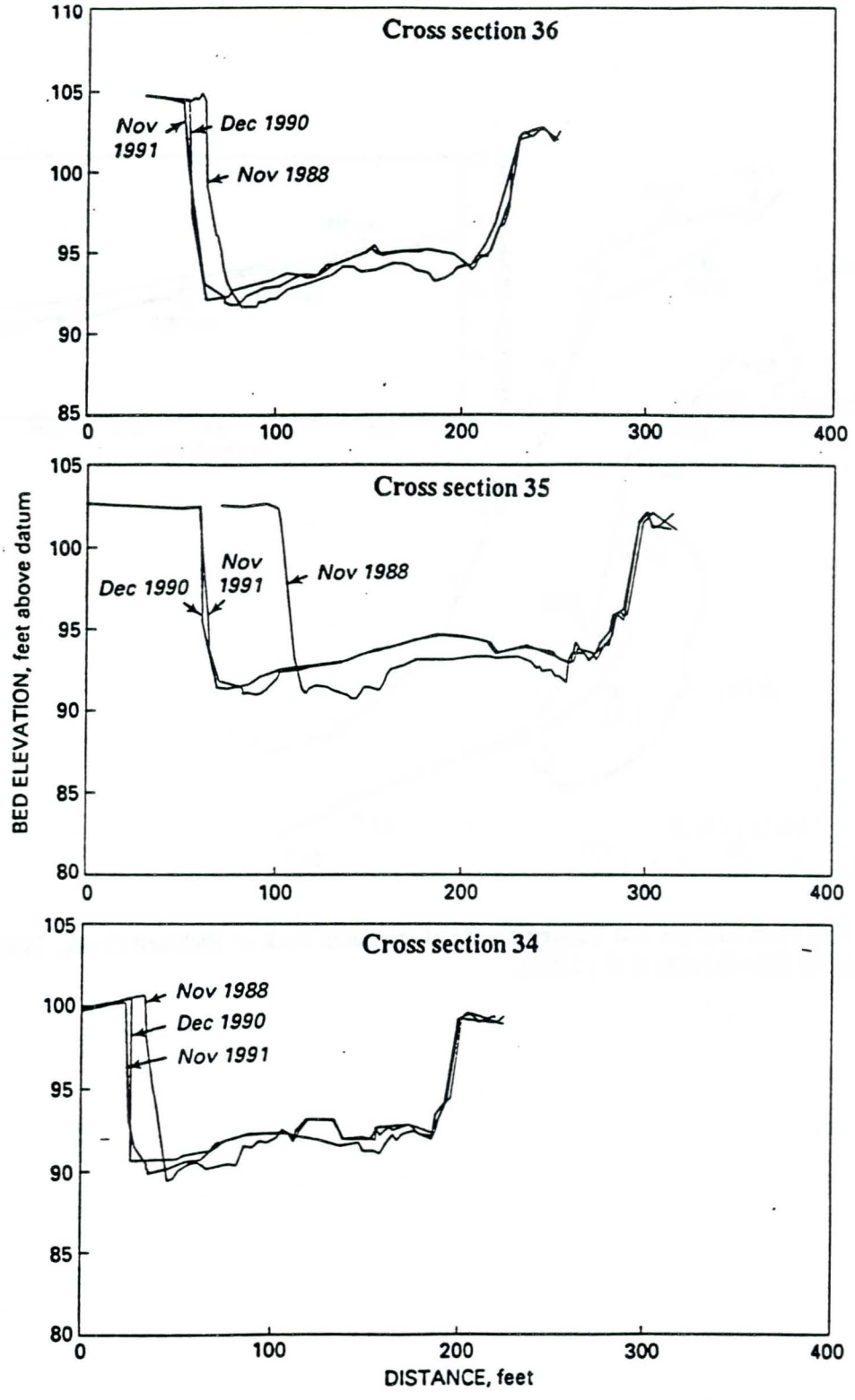

Fig. 8. Variation in cross-sectional shapes within the South Fork of Richland Creek (Slowikowski et al., 1992).

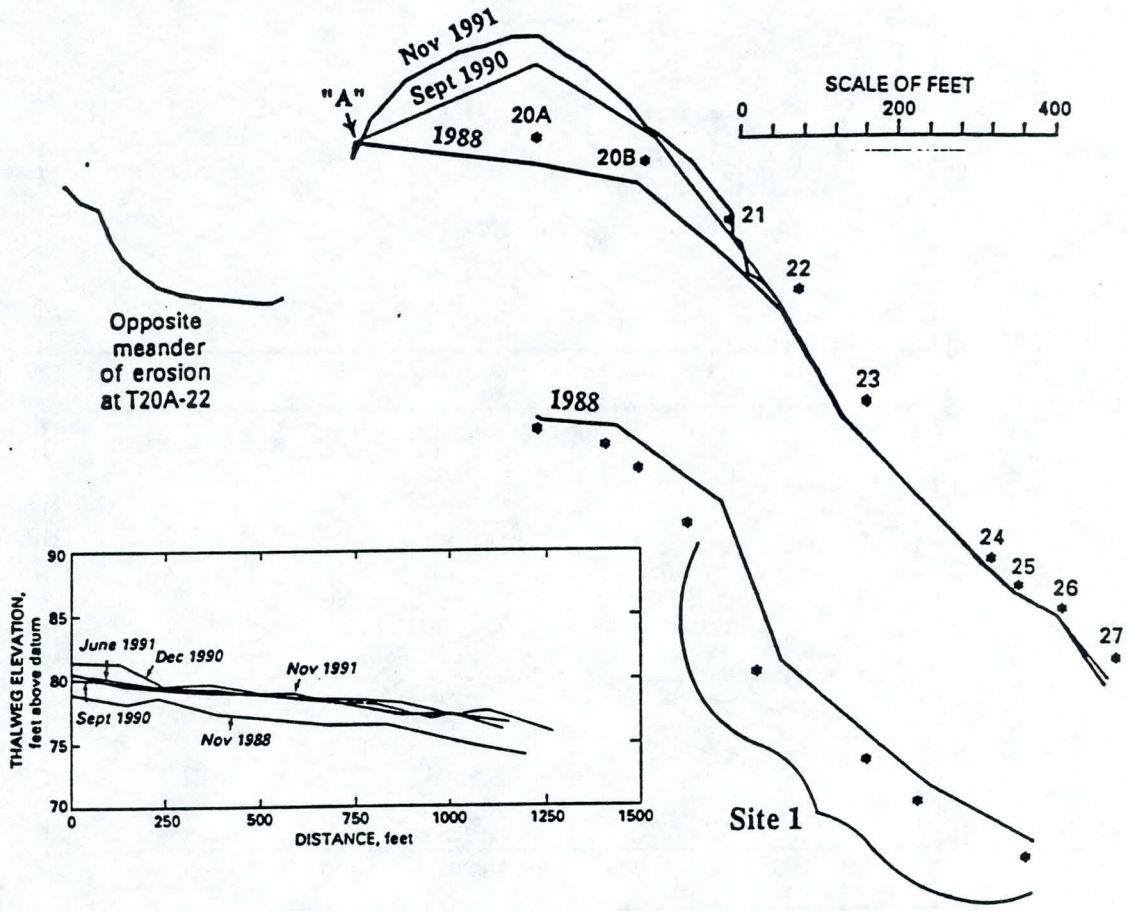

Fig. 9. Plan form and thalweg profile changes of Richland Creek, 1988-1991 (after Slowikowski et al., 1992).

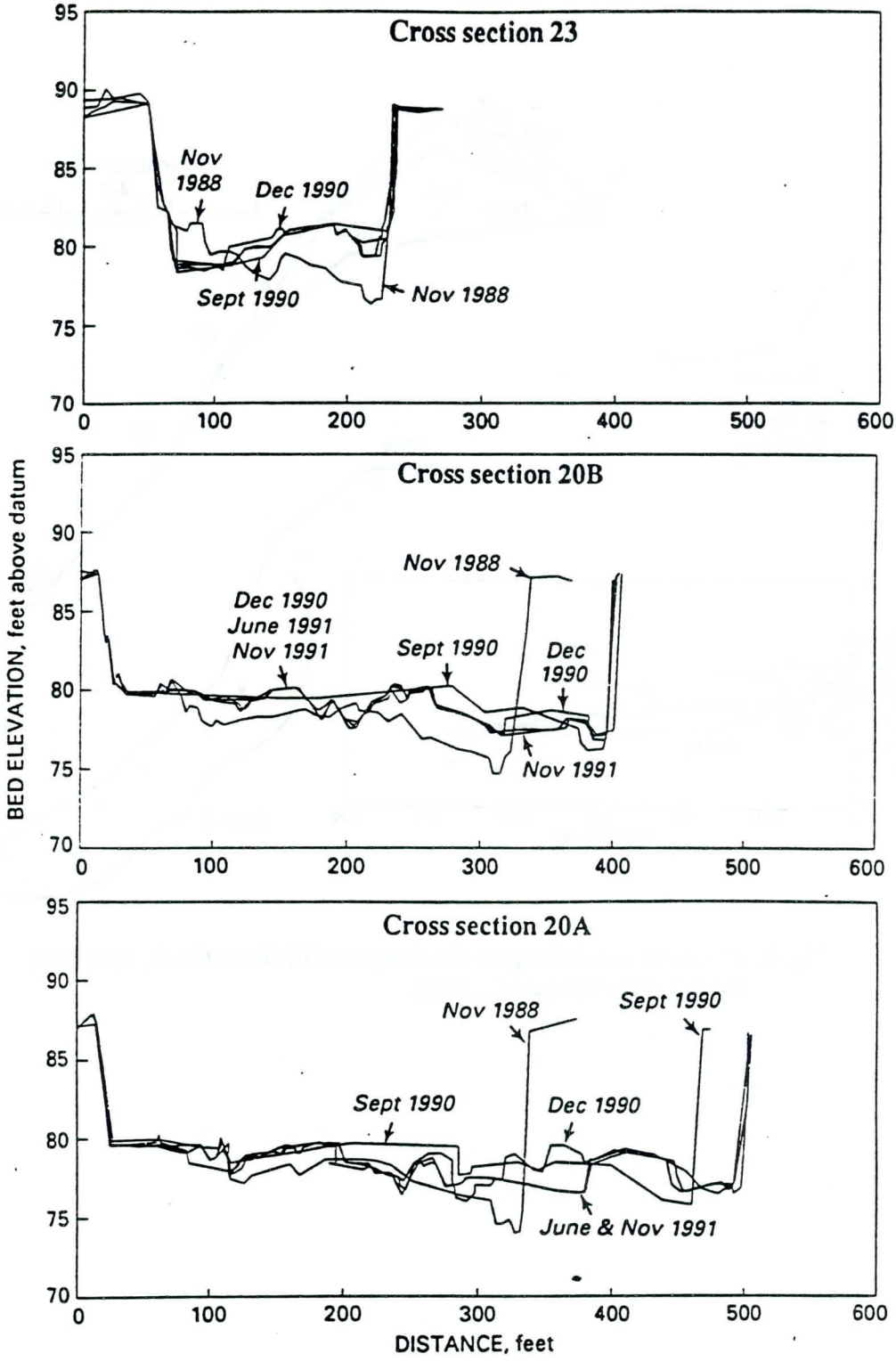

Fig. 10. Variation in cross-sectional profiles in Richland Creek (after Slowikowski et al., 1992).

BEHAVIOUR OF ARMOUR LAYERS OF RIPRAP BANK PROTECTIONS ALONG NAVIGATION CHANNELS

R.E.A.M. Boeters
Public Works and Water Management, Road and Hydr. Eng. Division,
Delft, The Netherlands
F.C.M. van der Knaap, H.J. Verheij
Delft Hydraulics, De Voorst Branch, Emmeloord, The Netherlands

Abstract

Model tests have been carried out to determine the damage that may occur to a riprap armour layer along a navigation channel, for instance because of the increase in ship-induced hydraulic loads compared to the initial design load. The executed model tests at Delft Hydraulics have been set up with the assumption that the occurrence and development of damage to armour layers caused by ship-induced waves are similar to the behaviour of breakwater armour layers under wind waves. In a European Class IV waterway sections with different riprap sizes have been tested. Profile measurements have been carried out several times after a number of ship passages, the maximum of which being 300. The analysis of the results has shown that the development of damage to an armour layer along a navigation channel can indeed be predicted with a mathematical model similar to that for breakwaters. The derived model can be used to predict the behaviour of riprap bank protections as a function of time.

1. Introduction

Armour layers of riprap protecting banks along fairways, are often designed by taking into account a maximum characteristic hydraulic load and calculating a stone size that ensures that the applied riprap protection will be absolutely stable. Design rules developed by Iribarren and Hudson are used in this respect.

Still, damage of the riprap protection occurs. Possible reasons for this are the increase in hydraulic loads and the displacements of smaller stones, inducing instability of the larger ones.

The ways in which damage to riprap armour layers of breakwaters develops, caused by the attack of wind waves and the number of these waves, has been extensively studied by Van der Meer (Van der Meer, 1988). Secondary waves induced by shipping are very much similar to wind waves. Therefore the idea arose to investigate the possibility of using the formulas of Van der Meer to describe and predict the damage to riprap bank protections, caused by ship-induced hydraulic loads, as a function of the number of loads exerted.
When indeed the formulas of Van der Meer can be applied to riprap protections along fairways, the opportunity occurs to predict damage to these protections as a function of time, since there is a direct dependence between the number of ship-induced loads and the number of passages, during a year for instance. The prediction of damage as a function of time can be very useful when planning maintenance of a protection.

In this paper the study of the applicability of Van der Meer's formulas to riprap bank protections is described. The investigations (Van der Knaap e.a., 1992) consisted of a series of model tests on a length scale of 1 to 10.5 and an analysis of the characteristics of secondary ship waves in comparison to wind waves.

2. Aims of the research and approach

The main goal of the research was to develop a predictive model for time-dependent development of damage to different types of riprap bank protections along fairways. Because of the similarity between armour layers of quarry stone of bank protections and of breakwaters on the one hand, and between wind waves and secondary ship waves on the other, it was considered that the most efficient way to develop such a predictive model was to focus on the predictive models derived by Van der Meer, which are valid for breakwaters attacked by wind waves. This means that the already existing formula of Van der Meer, giving the relationship between development of damage, properties of the protection, and the number and magnitude of waves, provided the framework for the investigations to be carried out. The general form of Van der Meer's formula is as follows:

$$\frac{H_s\sqrt{\xi}}{\Delta D_n} = C\, P^{0.18} \left(\frac{S}{\sqrt{N}}\right)^{0.2} \qquad (1)$$

In which

H_s	significant wave height [m]
ξ	tan α / $\sqrt{}$ (H_s/L), surf similarity parameter [-]
α	angle of the slope [°]
L	wave length [m]
Δ	relative mass density [kg/m^3]
D_n	nominal stone diameter [m]
C	coefficient [-]
P	permeability coefficient of the armour layer [-]
S	damage level, $A/(D_{n50})^2$ [-]
N	number of waves [-]
A	erosion area [m^2]

An explanation of the damage level S is given in figure 1.

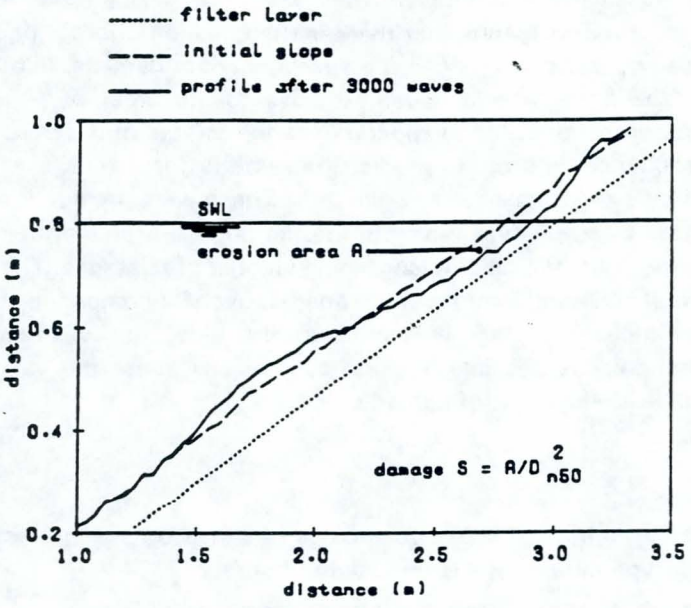

Figure 1. Damage level S, based on erosion area A

In order to check the validity of this type of formulation of damage prediction for bank protections surcharged by ship-induced waves, a physical model was installed in a flume, in which all the relevant variables could be varied. This meant that different riprap protections, varying in stone size (D_n) and permeability (P), had to be applied. The waves were generated by a small, fast sailing ship. The sailing speed of a ship determines the height and length of the waves that are generated, so by varying the speed, different combinations of wave height (H) and length (L) could be achieved. Each run with a specific sailing speed was repeated a great many times, in order to get a large number of waves (N). By measuring the damage profiles of the different protections for each combination of wave height and length, at regular intervals of the number of ship passages, sets of data were obtained that could be fitted in the form of Van der Meer's formula. When this should prove to be possible, one might conclude that the assumptions about the validity of Van der Meer's formulation for the development of damage to a riprap bank protection along a fairway were correct and a similar mathematical description could be derived.

Of course, it was realised that there are differences between wave loads caused by wind and generated by ships, and between the circumstances under which damage occurs to a breakwater and to a riprap bank protection.
First of all, wind waves exist almost continuously, while ship-induced waves only occur when a ship passes by. In a wave field caused by a storm, there is a rather large variety in the wave heights and lengths that occur, and the properties of such a wave field have to and can be statistically described by a Rayleigh distribution. The secondary waves induced by a ship show a more or less fixed pattern, with one or two high waves, followed by four to six decreasing waves, strongly intercorrelated. Therefore it was decided that a statistical analysis had to be made of the ship-induced secondary wave field, in order to make a comparison with the Rayleigh distributed wind waves and to be able to choose a characteristic waveparameter, like the significant wave height, which is used in Van der Meer's original formula.
Secondly, damage to a breakwater will only occur in a storm with a certain probability of occurrence, which depends on the technical life-time of the structure, for example once in a hundred years.

In navigation channels, the possibility exists every day that the design load occurs and consequently, that damage appears. This means that there is the question of order of succession in the occurrence of wave loads and, subsequently, in the development of damage. In other words, is the occurring distortion of the riprap armour layer sensitive to the order of appearance of different heights of wave loads, or is it possible to superimpose the effects of different classes of wave loads, neglecting their sequence, in order to predict the same distortion?
This problem was investigated by using both sides of the model. These were provided with exactly the same riprap protections. One side however, was put into its original profile after each series of tests with a specific combination of wave height, length and number of passages. The other side was left untouched for several of the combinations mentioned above. By comparing the damage level of this side with the superimposed damage levels of the other side, that was reconstructed after every series of tests, it should be possible to draw conclusions about the validity of the principle of superposition for the development of damage.

3. Description of the model and testseries

At Delft Hydraulics a model has been built of a European Class IV canal, on a length scale of 1 to 10.5. A transsection with prototype dimensions is depicted in figure 2.

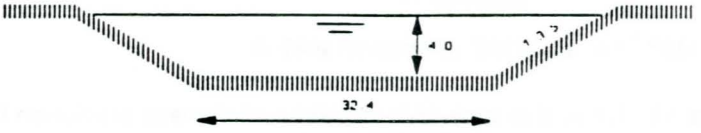

Figure 2. Transsection of the modelled navigation channel (prototype dimensions)

The total length of the model was 35 meters, plus at each side 20 meters of acceleration and deceleration zone for the model vessel. In the center of the model, at each side, four sections of 5 meters wide were provided with riprap protections with different stone sizes and layer thicknesses. Almost in the middle of each 5 meters wide section, a space of 1 meter wide was prepared to execute measurements of the displacements of the stones. Figure 3 gives a bird's eye view of the model.

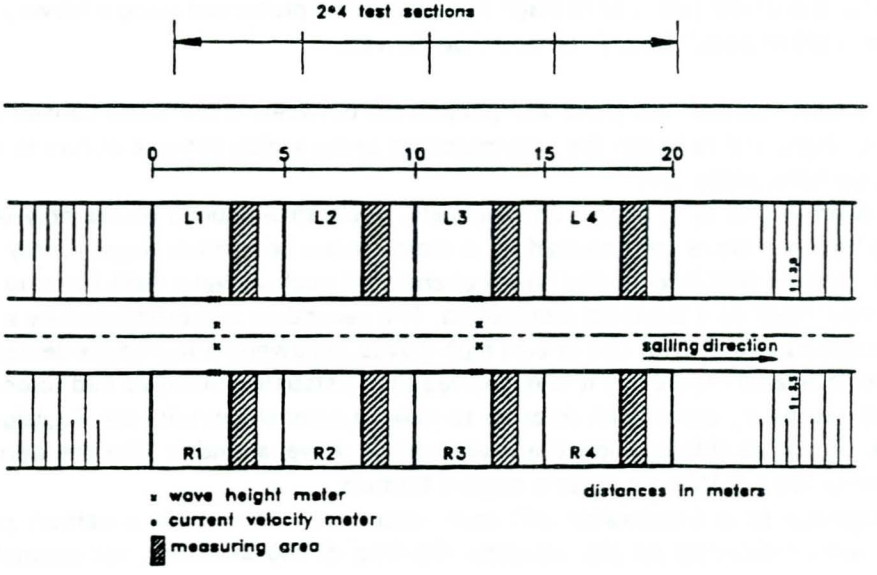

Figure 3. Bird's eye view of the model

Table 1 shows the four different types of riprap protection that have been installed.

Table 1. Riprap protections applied in the model.

Section	layer thickness	D_{50} in prototype (m)	D_{50} in the model (mm)	D_{85}/D_{15} (model)
1	$1*D_{50}$	0.20	19.51	2.10
2	$2*D_{50}$	0.12	11.50	2.21
3	$2*D_{50}$	0.08	8.94	2.04
4	$10*D_{50}$	0.06	6.46	1.72

The model vessel "Rixt", used in the test, had the shape of a small tugboat. Its dimensions (in meters, prototype):

Length	12.20
Width	3.15
Draught	1.20

This vessel was pulled through the water, it had no power installed aboard.
The course of the vessel was in the centre of the simulated channel, thereby ensuring that at both sides the attack by the ship-induced waves was the same.
In table 2 a summary is given of the velocities with which the ship was pulled through the water and the number of passages after which the profiles of the test sections were measured.

Table 2. Sailing velocities of the model ship and number of passages

Series	Vessel speed (m/s) (model)	Vessel speed (m/s) (proto -type)	number of passages between measurements of profile						Total number of passages
			first	second	third	fourth	fifth	sixth	
T1	1.30	4.20	10	20	30	40	30		130
T2	1.40	4.55	5	5	10	20	60	60	160
T3	1.45	4.70	5	15	60	220			300
T4	1.50	4.85	10	30	60				100

The sections on the left side were restored after each test series. The sections on the right side were restored after series T1 plus T2 and after series T3 plus T4, in order to investigate the validity of the principle of superposition of damage levels.

Measurements of the distortion of the armour layers were executed by means of a profile follower, mounted in a specially designed frame, that could be placed over the measuring section, each time in the exact and same position. Measurements were taken in eight rows per section. To be able to use the profile follower, the waterlevel had to be raised temporarily to the toplevel of the sides of the model.

4. Testresults

In figures 4 and 5 two examples are shown of the damage profiles that were the result of the runs with the model vessel. In each figure the test section and the number of passages are mentioned.

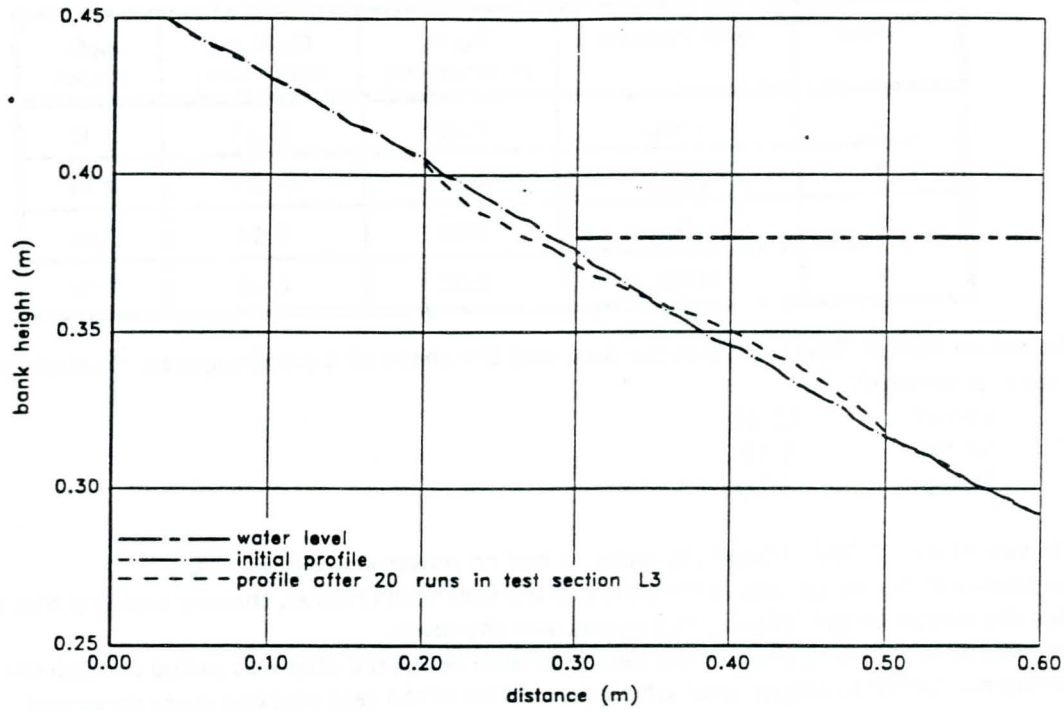

Figure 4. Damage profile in test section L3 after 20 runs

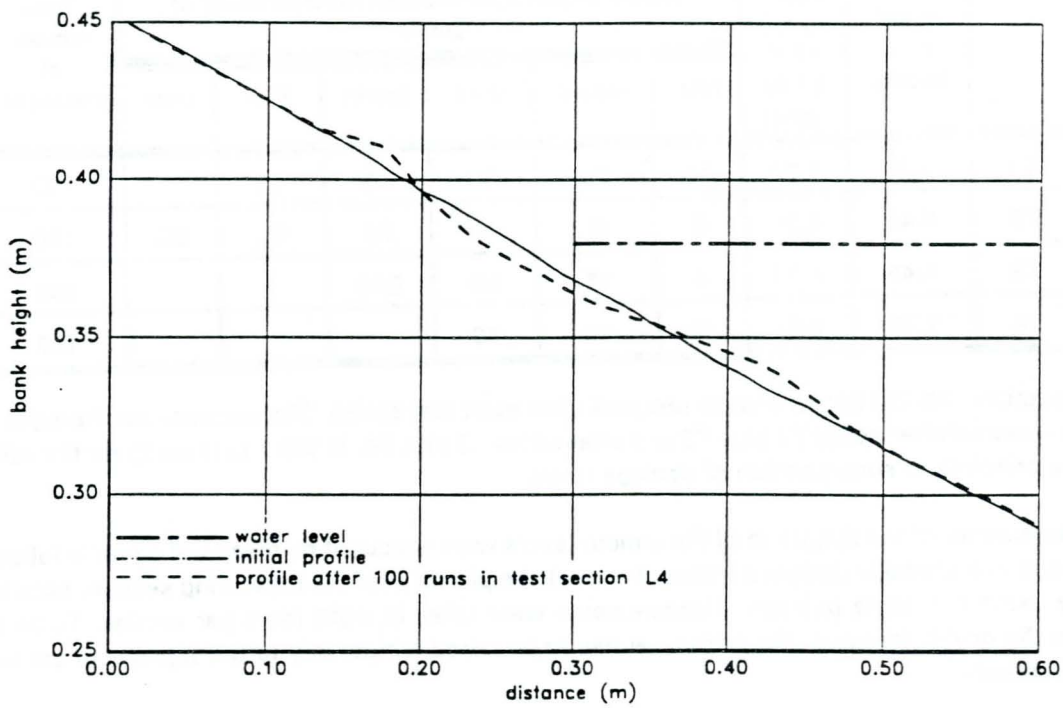

Figure 5. Damage profile in test section L4 after 100 runs

As already mentioned, eight profiles were measured in each testsection. To derive the values of the damage level S, two methods were applied:

1. By composing an average damage profile out of the registered eight profiles, and calculating the damage level for this profile (S1).
2. By calculating the damage levels for all eight measured profiles and taking the average of these values (S2).

As it appeared, there was little difference between S1 and S2. In the analysis, S1 has been used.

At several places in the model, waves were registered. See figure 3 for the exact locations. Figure 6 shows an example of such a registration.

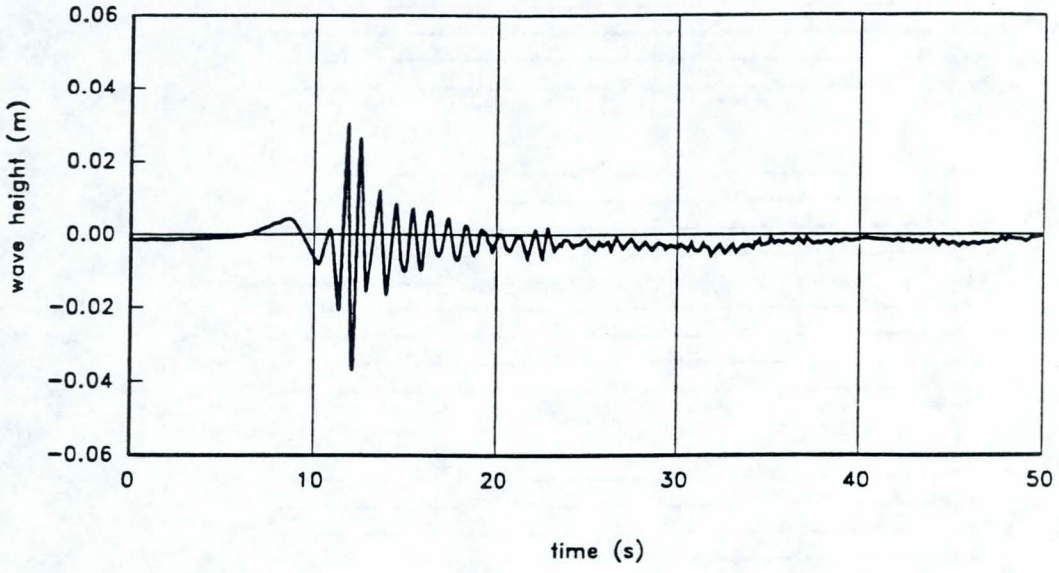

Figure 6. Example of a measured secondary wave pattern

Table 3 summarizes the maximum wave heights and average wave periods that have been registered in each test series, at the toe of each slope. The values are translated into prototype wave heights and periods.

Table 3. Registered wave heights and periods

Series	sailing speed (m/s) (model)	sailing speed (m/s) (prototype)	Model		Prototype	
			max. wave height (m)	wave period (s)	max. wave height (m)	wave period (s)
T1	1.30	4.20	0.055	0.68	0.58	2.20
T2	1.40	4.55	0.065	0.69	0.68	2.24
T3	1.45	4.70	0.074	0.74	0.78	2.40
T4	1.50	4.85	0.084	0.78	0.88	2.53

5. Analysis

5.1 Secondary ship waves compared to wind waves

To make a statistical analysis of the secondary ship-induced waves, a number of five runs have been made with the model vessel having a fixed speed. This has been done for five different speeds (1.2 to 1.6 m/s). All registrations have been combined into one long series of wave registrations and this has been statistically analysed, using a same method as applied to wind waves. Figure 7 shows the combined registrations and table 4 gives the result of the analysis.

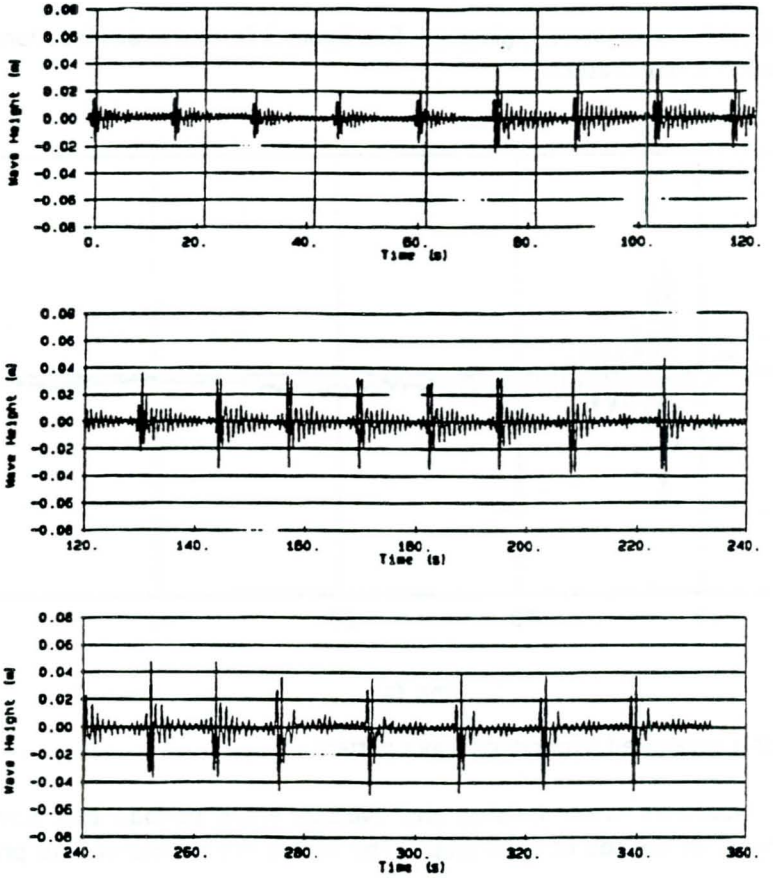

Figure 7. Combined registrations of secondary waves, generated by the model vessel

Table 4. Statistical parameters of the secondary wave field

	WHM005
number of waves	437
Wave height $H_{1/3}$ (m)	0.0310
Wave height $H_{1/10}$ (m)	0.0568
Wave height H_{m0} (m)	0.0420
Average wave period (s)	0.806
Peak period (s)	0.890
Spectral density (m^2/Hz)	0.213

It appears that secondary ship waves have different ratios between the characteristic wave heights that describe a wind-generated wave field, which represent the Rayleigh distribution, $H_{1/3}$, $H_{1/10}$ and H_{m0}. So one may conclude that secondary ship waves do not fit the Rayleigh-distribution. This is confirmed by the graph in figure 8, that shows the probability of exceedance, derived for the registered waves, plotted against the probability according to a Rayleigh-distribution.

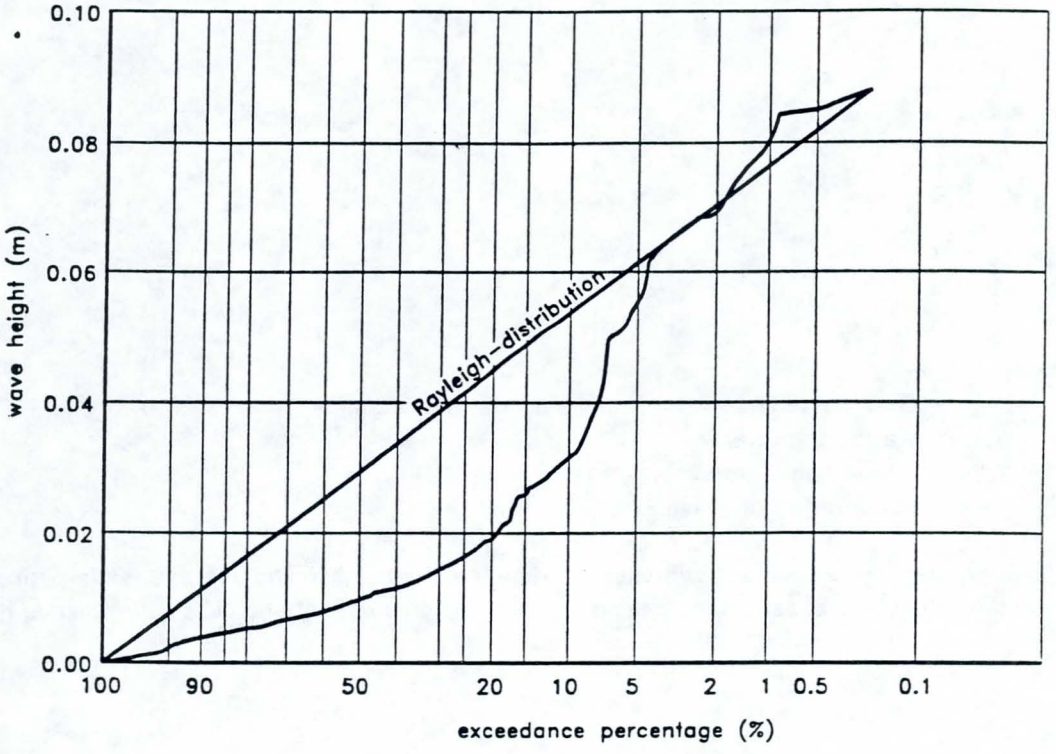

Figure 8. The probability of exceedance of secondary ship waves plotted against the same probability according to a Rayleigh-distribution

Van der Meer has shown that in case of broken waves on a shallow foreshore, which are also not Rayleigh-distributed, distortion of riprap armour layers of breakwaters could be predicted by using $H_{2\%}$. Based on this and on the graph in figure 8, one may conclude that in a predictive model for damage caused by secondary ship waves, some kind of $H_{2\%}$ should be used, meaning more or less the maximum wave height.

5.2 Derivation of the predictive model

In order to get a proper description of a model that predicts damage to a riprap bank protection, caused by secondary ship waves, a kind of "short cut" analysis has been carried out. Because of the similarity, it was assumed that the model should have the same form and terms as Van der Meer's formulation for breakwaters attacked by wind waves, see section 2, formula (1).
The above means that the analysis of the data could be constrained to four items:

a. Wave parameters ($H/\sqrt{\xi}$)
b. Number of waves (N)
c. Permeability (P)
d. Coefficient (C)

a. Wave parameters

Earlier investigations (Verheij and Bogaerts, 1988) have resulted in a set of equations with which

the maximum secondary wave height (H_l), the average wave period (T_l) and wavelength (L_l) can be calculated. The equations are:

$$\frac{H_l}{h} = \left(\frac{s}{h}\right)^{-0.33} \left(\frac{V_s}{\sqrt{gh}}\right)^4 \quad (2)$$

$$T_l = 5.1 \frac{V_s}{g} \quad (3)$$

$$L_l = g \frac{T_l^2}{2\pi} \quad (4)$$

With:

s	distance between the ship's side and the secondary waves (m)
h	waterdepth (m)
V_s	sailing speed (m/s)
g	acceleration of gravity (m^2/s)

In figure 9 a comparison is made between maximum wave heights and average wave periods, as measured during the test series and calculated with the given equations. The resemblance is very good.

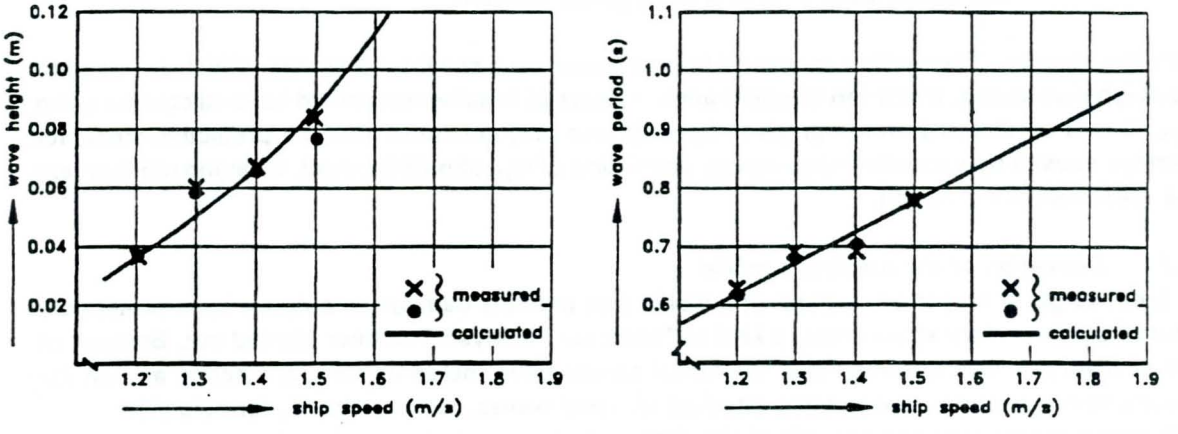

Figure 9. Comparison between measured and calculated secondary wave heights and periods (model data)

As stated in section 5.1, the choice of the maximum wave height to be applied in the damage prediction model, looks very appropriate. Since the given equations can be applied to a large variety of ship-fairway combinations, it was decided to use in the predictive model the wave parameters that follow from these equations.

b. Number of waves

By choosing the maximum wave height as a governing parameter in the model, the number of waves can be directly translated into the number of passages. Furthermore, as can be seen in figure 7, secondary waves have a more or less fixed pattern, with one or two high and four to six smaller waves. So with a known number of passages, the number of waves is also known.
Now the question remains whether the relationship between the measured damage levels and the number of passages is a function of the root of the latter.
In the graph of figure 10 two examples are shown of this relationship.

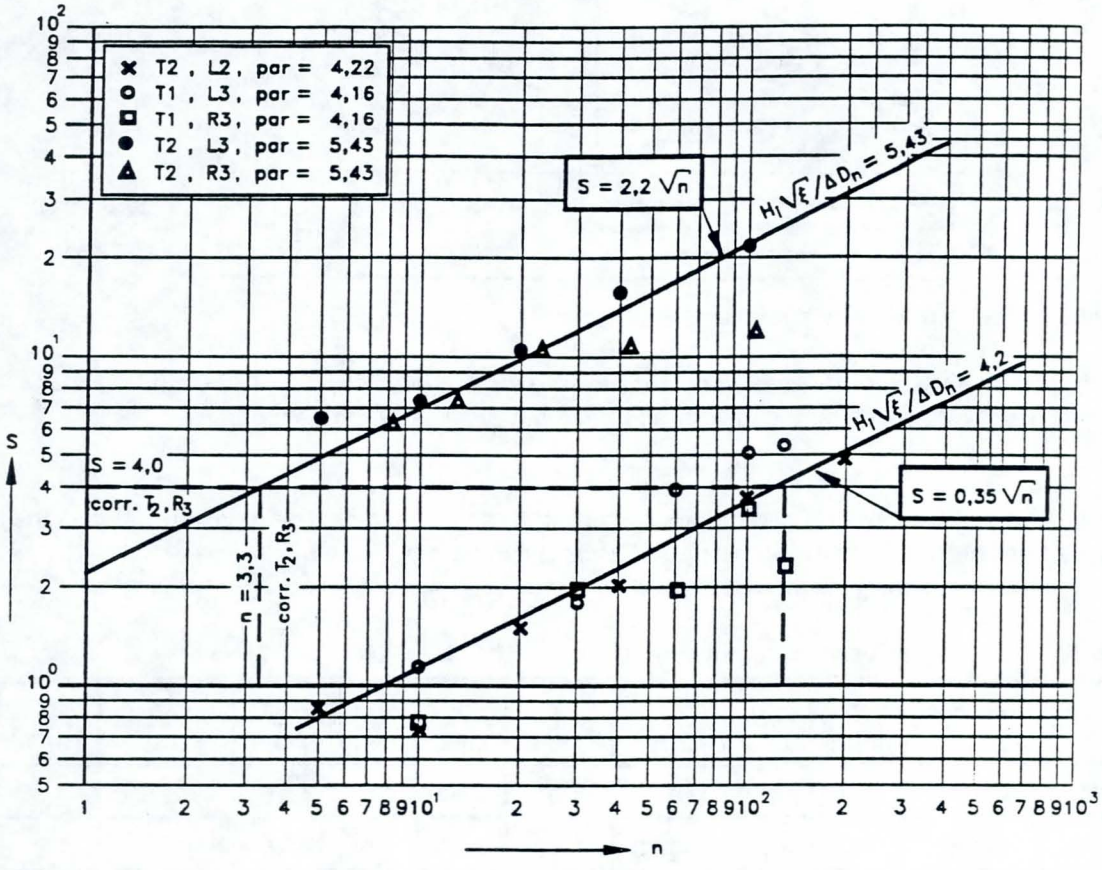

Figure 10. Relationship between S and n, test series T1 and T2

Based upon an analysis of the graphs of this kind for all test series, it could be concluded that the root of the number of passages is highly correlated with the damage levels S.

c. Permeability

Van der Meer has given an overview of different types of riprap armour layers and connected values for the permeability P, see figure 11.

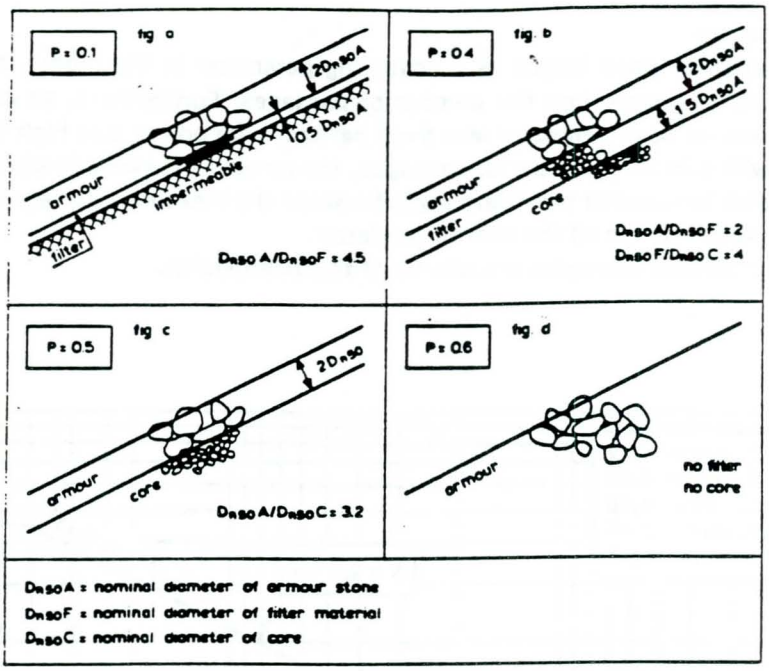

Figure 11. Permeability coefficient P

Based on this, a value of 0.1 has been chosen for test sections 2 and 3, and 0.5 for sections 4. Sections 1 showed hardly any damage, and have not been taken into account.

d. Coefficient

Having chosen all the relevant parameters and using the same functional relationship between these as in Van der Meer's formulation, the coefficient C can be determined.
Table 5 gives a summary of the result.

Table 5. Values used in determining C

Series	Sections	V_s (m/s)	H_i (m)	L_i (m)	ξ (-)	D_n (mm)	P (-)	$\frac{H\sqrt{\xi}}{\Delta D_n}$	$S/\sqrt{n}$ (-)	C (-)
T1	L3, R3	1.3	0.05	0.73	1.09	7.42	0.1	4.16	0.35	7.8
T1	L4, R4	1.3	0.05	0.73	1.09	5.36	0.5	5.76	0.4	7.8
T2	L2	1.4	0.068	0.84	1.00	9.55	0.1	4.22	0.35	7.9
T2	L3, R3	1.4	0.068	0.84	1.00	7.42	0.1	5.43	2.2	7.0
T2	L4, R4	1.4	0.068	0.84	1.00	5.36	0.5	7.51	1.95	7.4
T3	L2, R2	1.45	0.078	0.90	0.97	9.55	0.1	4.76	0.57	8.2
T3	L3, R3	1.45	0.078	0.90	0.97	7.42	0.1	6.12	1.58	8.7
T3	L4, R4	1.45	0.078	0.90	0.97	5.36	0.5	8.47	2.5	8.0
T4	L3, R3	1.5	0.089	0.97	0.94	7.42	0.1	6.88	1.34	9.9
T4	L4, R4	1.5	0.089	0.97	0.94	5.36	0.5	9.53	2.5	9.0
										C = 8.2

So for C an average value of 8.2 could be determined (standard deviation 0.8). It is interesting in this respect to mention the value of the same coefficient, found by Van der Meer in his formula for damage levels caused by the already mentioned $H_{2\%}$ (see section 5.1), being 8.7.

5.3 The validity of superposition

Proof of the fact that superposition of damage, caused by different levels of hydraulic loads, is allowed, can be detected from the results of test sections 3 and 4 after series T1 and T2. Figure 12 shows testresults for sections 4 after T1 and T2.

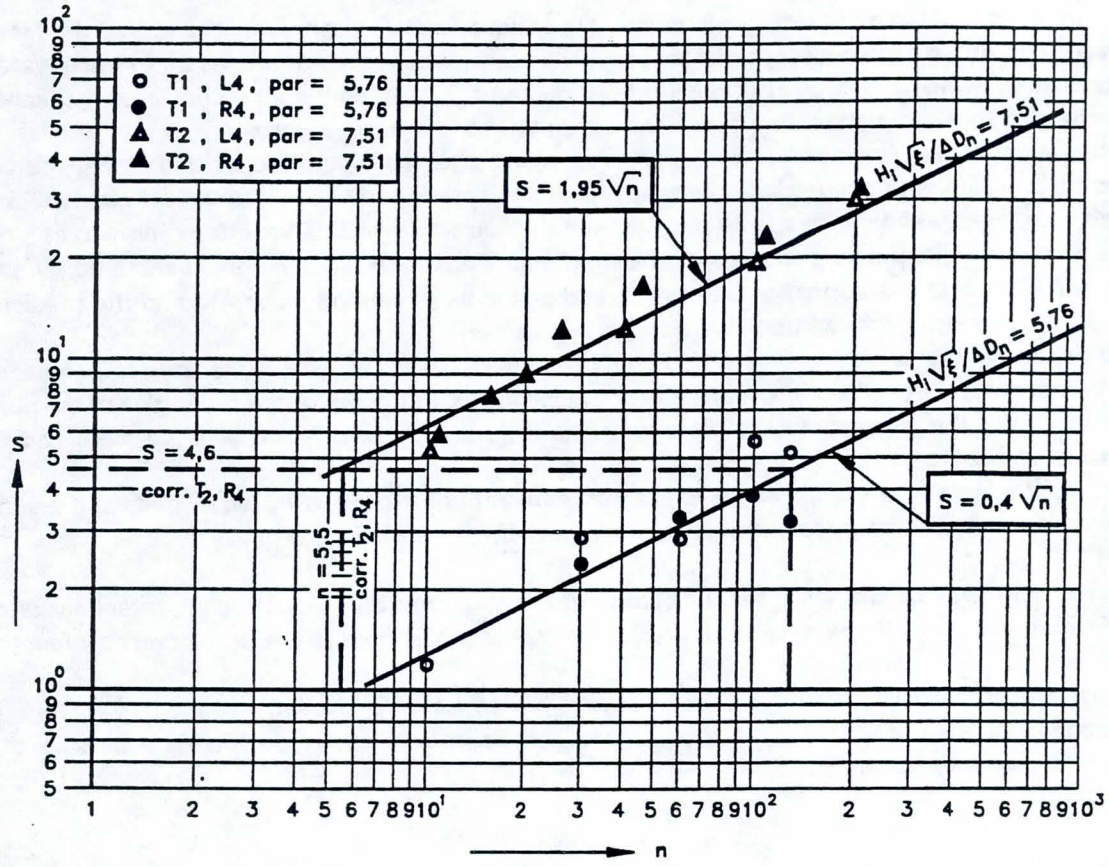

Figure 12. Test results for sections 4 after T1 and T2

The lower graph gives the relationship between damage levels S and the number of passages n, for both the left as well as the right side of section 4, as a result of test series T1. After this series, the left side has been put in its original state. The right side however, has been left in its distorted state. Before the start of T2, both profiles have been measured to act as a reference for the damage caused by the wave loads, generated in this series. In order to get the upper graph of figure 12, the damage levels measured on the already distorted right side have been corrected by adding the damage level, found after T1 (S=4.6). Also the number of passages has been corrected, by adding a fictive number of passages, that has been derived from the damage level after T1, as though it has been the result of test series T2 (n=5.5). As it appears, the thus corrected damage levels, measured during test series T2 at the right side, agree rather well with the damage levels measured at the left side. (The same applies to testsections 3, where an identical correction has been carried out for the damage levels measured at the right side, see figure 10.) Based upon this agreement, one may draw the conclusion that an already existing distortion of the riprap protection, casu quo damage, caused by a specific number of wave loads, does not affect

the damage, caused by a number of higher wave loads. This implies that the effects of different combinations of wave loads and numbers of waves, on the damage to a riprap bank protection are independent of each other, which allows the superposition of the separate, corresponding damage levels.

6. Conclusions

By means of tests in a physical scale model, the assumption has been verified that Van der Meer's description of a mathematical model that predicts damage to stone armour layers of breakwaters, attacked by wind waves, is also applicable to riprap bank protections along navigation channels, surcharged by secondary ship waves. The assumption proved to be correct.
A statistical analysis of a set of secondary ship waves showed that these have an energy density spectrum which is in shape similar to that of wind waves. However, the statistical distribution of secondary ship waves differs from the Rayleigh distribution, which is valid for wind waves.
The analysis indicated that the use of the maximum secondary wave height, generated by each passing ship, and the corresponding length and period as governing parameters in the predictive model for damage to riprap bank protections, is appropriate.
The predictive mathematical model that could be derived from the test results and earlier research by Van der Meer, describes the development of damage as a function of the properties of the riprap armour layer, the maximum secondary wave height and length for each ship passage, and the number of passages.
Test results indicated that damages caused by different combinations of wave loads and number of waves, casu quo passages, may be superimposed.

The mathematical model describes the behaviour of riprap armour layers of bank protections along navigation channels. It can be used to predict the maintenance state of the protection as a function of time.
To be able to do this, shipping on the fairway has to be well known, in terms of number of passages per year and average sailing speed and course of each specific type of ship that frequently sails the channel.

References

J.W. Van der Meer, 1988
Rock slopes and gravel beaches under wave attack (Thesis); Delft Hydraulics Communication No. 396

F.C.M. Van der Knaap, D.H. Wilkens, H.J. Regeling, 1992
Models to predict the behaviour of riprap bank protections; report of model investigations (in Dutch)

H.J. Verheij, M.P. Bogaerts, 1988
Ship waves and the stability of armour layers protecting slopes; Paper presented at the nineth International Harbour Congress, Antwerp

USE OF THE 1991 CORPS OF ENGINEERS RIPRAP DESIGN PROCEDURE IN MINE RECLAMATION

K. Bruxvoort, B.L. Carlson and T.A. Shepherd
Shepherd Miller Inc., Fort Collins, Colorado

1. INTRODUCTION

Shepherd Miller, Inc. (SMI) prepared a reclamation plan for a gold mining facility in Nevada, USA. The reclamation plan was submitted to the Nevada Division of Environmental Protection in May, 1992. The site is located in a cool, high desert environment with annual precipitation of approximately 325 mm, at an elevation of approximately 2100 m. The area is sparsely populated with the nearest town located about 20 km away. The site is currently operating.

The reclamation plan was developed to return the mine site to a condition that will support wildlife habitat and domestic grazing, dispersed recreation, mineral exploration, and aesthetic value. Other purposes of the reclamation include ensuring public safety, minimizing environmental degradation to surrounding surface and ground water sources, and re-establishment of stable topographic conditions.

The plan has been approved by the State of Nevada and by the U.S. Bureau of Land Management. Interim reclamation will occur during the summer of 1993. The initial steps of final reclamation will commence in approximately 1995.

The reclamation plan addresses regrading of the waste rock and heap leach piles to stable slopes, revegetation of disturbed surfaces, and detoxification of the heap leach pad. Trapezoidal diversion channels will also be part of the reclamation plan. The diversion channels are intended to reduce the amount of erosion which may occur on the reclaimed site and limit runoff from surrounding basins from flowing onto, and subsequently through, mineralized materials.

The channels will be lined with riprap where appropriate. Approximately 2710 m of diversion channel will be lined with riprap.

2. SITE DESCRIPTION

2.1 General

The site features an open pit mining method, with a mining-milling-leaching complex for the processing of gold ore. Figure 1 shows the site facilities, including the mill, heap leach pad, tailings impoundment, open pit and waste rock pile. The site is located on a drainage divide. A spring is located to the north of the divide, below the waste rock pile and an ephemeral stream

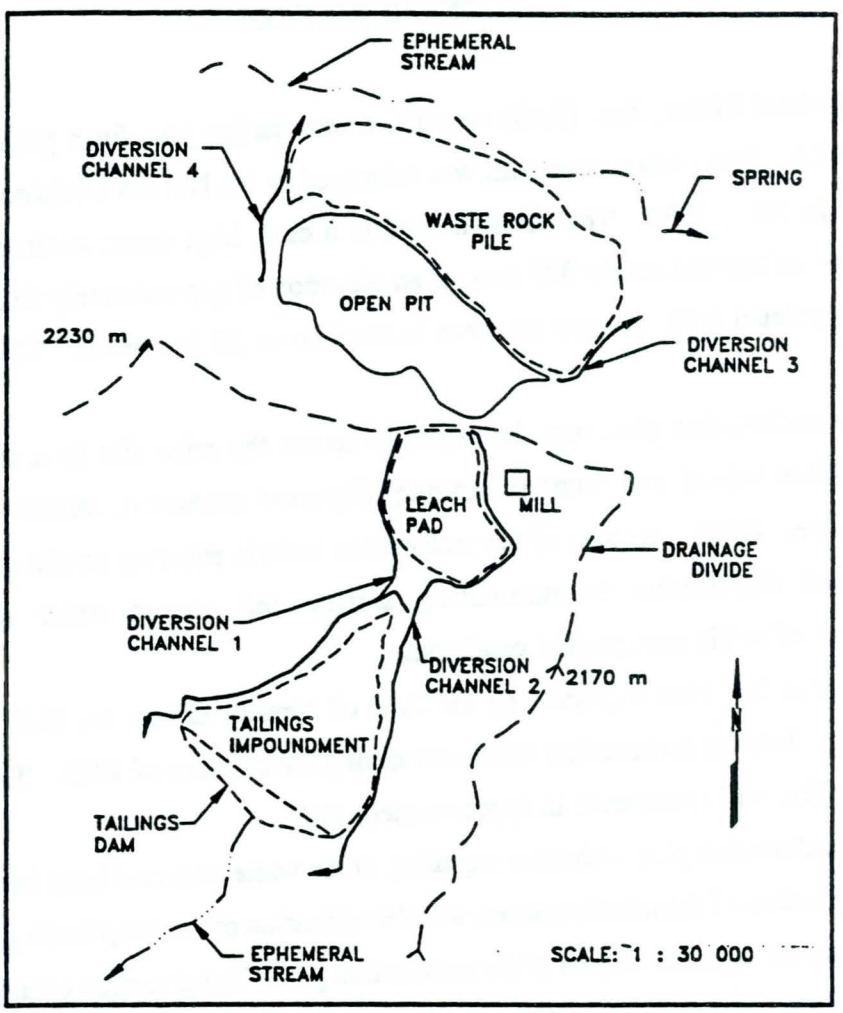

Figure 1. Site map

flows to the south of the divide. This stream valley is blocked near its top by the tailings dam and associated tailings impoundment.

The site soils are characterized as a gravelly clay loam. The native vegetation at the site is typically sage brush, moderately dense, with sparse desert grasses. Land use for the area is characterized as range land. Ephemeral stream bottoms show no differentiation in channel materials beyond that found in the rest of the basin; stream bottoms are composed of gravelly silt and clay soils with scattered native vegetation.

2.2 Diversion channels

Figure 1 also shows the locations of four diversion channels designed to capture and convey the design event around reclaimed site features. Channel 1 is located to the west of the leach pad and tailings impoundment; Channel 2 is located to the east of the leach pad and tailings impundment; Channel 3 is located at the southeast toe of the waste rock pile; and Channel 4 is located above the open pit and along the northwest portion of the waste rock pile. The channels vary in gradient from 0.2% to nearly 40%.

3. DESIGN INPUTS

3.1 Hydrology

The design event for the diversion channels is the 100-year, 24-hour precipitation. For the site, this quantity is 71 mm. The channel discharges associated with this storm were determined through application of the U.S. Army Corps of Engineers (COE) hydrologic model, HEC-1. The U.S. Soil Conservation Service (SCS) method for determining runoff from small watersheds was employed within HEC-1 to determine the runoff peaks.

Basins contributing runoff to the channels were delineated and HEC-1 inputs for each basin were determined, including basin physiography and SCS curve number and lag time. Corresponding channel reaches were defined on the basis of changes in discharge and slope. The peak discharge results of the hydrologic modeling are presented in Table 1 for each reach of the diversion channels.

3.2 Solution procedure

An iterative procedure was used in determining the riprap size for each channel reach. The equations used in estimating channel hydraulics and in sizing riprap are detailed below. First, a rock diameter was assumed. Then an appropriate equation was used to determine Manning's n, as a function of rock diameter. Normal depth hydraulic characteristics of each reach were then determined using Manning's equation. Given the hydraulic characteristics, the riprap size was determined using the COE (1991) riprap sizing procedure, and the resulting riprap size was compared to that originally assumed. Iteration was performed until the assumed riprap diameter equalled the calculated diameter.

TABLE 1. Inputs to diversion channel riprap sizing.

Channel ID	Peak discharge (m^3/sec)	Minimum slope (m/m)	Maximum slope (m/m)	Mannings n	Radius of curvature (m)
1a	0.88	0.077	0.111	0.045	600
1b	1.10	0.014	0.1	0.044	240
1c	0.11	0.007	0.007	0.029	60
1d	1.93	0.002	0.002	0.029	105
1e	3.34	0.002	0.002	0.029	600
1f	4.73	0.002	0.002	0.029	90
1 outlet	5.04	0.1	0.1	0.045	n/a
2a	0.79	0.027	0.027	0.033	600
2b	1.47	0.005	0.005	0.031	75
2c	2.18	0.012	0.125	0.049	150
2d	2.61	0.002	0.002	0.029	600
2e	2.89	0.002	0.002	0.029	600
2f	3.26	0.002	0.002	0.029	600
2 outlet	3.40	0.2	0.2	0.052	n/a
3	1.81	0.071	0.2	0.054	600
4a	0.28	0.014	0.035	0.032	400
4b	0.28	0.156	0.357	0.055	240
4c	0.59	0.135	0.217	0.052	275

n/a: not applicable

3.3 Flow resistance

Two equations for determining Manning's n were employed, depending on the slope of the reach. Abt et al. performed flume studies of resistance to flow provided by riprap on steep slopes. The authors studied slopes varying from 1 to 20 percent with riprap median diameters of 25 to 150 mm (1 to 6 inches). They developed a relationship between Manning's n and riprap size and embankment slope. This relationship is

$$n = 0.0456\ (d_{50} * S)^{0.159} \qquad (1)$$

where: n = Manning's n,
d_{50} = median rock diameter, inches, and
S = channel slope, ft/ft.

For reaches with slopes flatter than 1 percent, the equation developed by Anderson et al. (1970) was used. Anderson et al. defined Manning's n as a function of rock diameter only. This relationship applies to gradients up to 2 percent and is given by

$$n = 0.0395\ (d_{50})^{1/6} \qquad (2)$$

where: d_{50} = median rock diameter, feet.

Manning's n values for the riprap-lined channel segments in this case varied from 0.031 to 0.054. Table 1 summarizes the Mannings n values for each reach and other hydraulic inputs.

4. RIPRAP SIZING

4.1 Riprap model

The COE (1991) model was used to determine riprap sizing in each reach of the diversion channels. The model applies to open channels not immediately downstream of stilling basins or other turbulent areas, and channel slopes less than 2 percent (COE, 1991). Several diversion channel reaches have slopes in excess of 2 percent. The COE method was applied for these reaches, however, because judgement indicated this method was still suited for this application. (Further discusssion is provided in Section 5). The basic equation in the COE model, in either SI or non-SI units, is

$$D_{30} = S_f C_s C_v C_T d \left[\left(\frac{\gamma_w}{\gamma_s - \gamma_w} \right)^{1/2} \frac{V}{\sqrt{K_1 g d}} \right]^{2.5} \quad (3)$$

where:
- D_{30} = rock diameter of which 30 percent is finer,
- S_f = safety factor,
- C_s = stability coefficient,
- C_v = vertical velocity distribution coefficient,
- C_T = thickness coefficient,
- d = local depth of flow,
- γ_w = unit weight of water,
- γ_s = unit weight of rock,
- V = average velocity,
- K_1 = side slope correction factor, and
- g = gravitational constant.

Factor K_1 is defined by

$$K_1 = \sqrt{1 - \frac{\sin^2\theta}{\sin^2\phi}} \quad (4)$$

where:
- θ = angle of the side slope with the horizontal, and
- ϕ = angle of repose of the rock material.

The safety factor and stability, thickness, and vertical velocity distribution coefficients increase the resulting riprap diameter as site conditions require. For the reclamation plan, two safety factors were used. Where the slope of a channel reach was less than 2 percent, the basic safety factor of 1.1 was used. Where channel slopes exceeded 2 percent, a safety factor of 1.3 was used.

A stability coefficient of 0.30, corresponding to angular rock was used. A thickness coefficient of 1.0 was used since the designed riprap layer thickness was twice the d_{50}, or approximately the d_{100}. The vertical velocity distribution coefficient for the outside of bends is defined by

$$C_v = 1.283 - 0.2 \log(R/W) \quad (5)$$

where: R = radius of curvature, and
W = channel topwidth.

The vertical velocity distribution for straight channels (R/W > 26) and for the inside of bends is 1.0. The radius of curvature for each reach is listed in Table 1. The specific gravity was assumed to be 2.65 and the angle of repose was assumed to be 40 degrees. The side slopes of the riprap-lined channel reaches were 3H:1V.

4.2 Riprap sizing results

A size gradation was selected for the riprap such that the d_{50} is about 1.4 times the d_{30}. The resulting d_{50} from application of the COE model for each diversion channel reach is listed in Table 2. Required median riprap diameters ranged from less than 50 mm to 380 mm.

Several of the diversion channel reaches have low design discharges or flat slopes, resulting in low velocities, even during the peak discharge of the design storm. For reaches with channel velocities below 1.5 m/sec, with an unlined Mannings n value of 0.025, erosion protection will be provided by vegetation rather than riprap. The channel reaches which will not be lined with riprap are 1c through 1f, 2b, and 2d through 2f.

To minimize cost, five riprap size classes were selected for the reaches requiring riprap: 75, 150, 230, 305 and 380 mm. Table 2 summarizes the selected riprap median diameters to be placed in each reach. Overall, 2710 m of diversion channel will be lined with riprap.

A smooth size distribution for the riprap was chosen so that the d_{100} is approximately twice the d_{50} and the d_{20} is about half the d_{50}. This type of distribution allows the interstices of the larger stones to be filled with smaller stones, minimizing turbulence around the larger stones. The thickness of the riprap layers was specified to be twice the d_{50} (equal to the d_{100}).

Dimensions of the trapezoidal diversion channels were then determined using Mannings equation based on the lining material to be used and the minimum slopes in each reach.

TABLE 2. Results of COE (1991) riprap sizing procedure

Channel ID	Required riprap d_{50} (mm)	Selected riprap d_{50} (mm)	Reach length (m)
1a	188	230	160
1b	203	230	640
1c	15	n/a	230
1d	28	n/a	150
1e	38	n/a	670
1f	48	n/a	365
1 outlet	226	230	30
2a	84	150	175
2b	56	n/a	295
2c	307	380	595
2d	33	n/a	380
2e	36	n/a	535
2f	38	n/a	150
2 outlet	267	305	30
3	374	380	365
4a	71	75	220
4b	226	230	165
4c	246	305	330

5. DISCUSSION

The COE (1991) states that its procedure is applicable for slopes less than 2 percent. Two other riprap methods were also investigated to determine which of the three may be used for steep slope applications. The former COE (1970) and the Safety Factor (Richardson, et al., 1975) procedures were examined. The COE (1970) established relationships between the boundary shear a particle is subjected to and the shear at which incipient motion begins, defined by the Shields curve (1936, and presented in Simons and Senturk, 1977). The Safety Factor method is similarly shear-based but was derived in a different manner. It is a theoretically-derived procedure relating the forces causing motion to those resisting motion. For brevity,

these two procedures are not described here in detail.

Table 3 summarizes the results of application of these two procedures and compares the results to the later COE (1991) procedure. Where the required riprap size exceeds 380 mm (15 inches), rock is not economically available for the site. For these cases, therefore, grouted riprap would be employed.

TABLE 3. Comparison of riprap design procedures

Channel ID	COE (1991) riprap d_{50} (mm)	COE (1970) riprap d_{50} (mm)	Safety Factor riprap d_{50} (mm)	Maximum slope (m/m)
1a	188	230	305	0.111
1b	203	230	380	0.1
1c	15	<50	<50	0.007
1d	28	<50	<50	0.002
1e	38	<50	50	0.002
1f	48	<50	50	0.002
1 outlet	226	150	686*	0.1
2a	84	75	75	0.027
2b	56	<50	75	0.005
2c	307	380	610*	0.125
2d	33	<50	50	0.002
2e	36	<50	50	0.002
2f	38	<50	50	0.002
2 outlet	267	230	1070*	0.2
3	374	380	1370*	0.2
4a	71	50	75	0.035
4b	226	**	1070*	0.357
4c	246	230	760*	0.217

* Riprap size too large to be economically available.
** No solution obtained.

For diversion channel reaches with slopes less than about 4 percent, the three procedures yield similar results. For steeper slopes, however, the results begin to diverge. For these reaches, the Safety Factor procedure yields much larger riprap diameters than do either of the COE procedures. The required riprap diameters from the Safety Factor procedure for steep reaches are much too large to be economically available. For Channel 4b, the COE (1970) procedure cannot provide a rock size which is stable.

For an explanation of why the three procedures give such different results at large slopes, one must review hydraulic principles. The total resistance to flow in a stream channel (and hence shear and energy slope) can be described as consisting of two elements (Taylor and Brooks, 1962, and others): 1) the resistance due to boundary effects induced by the channel particles (small-scale, or micro-effects) and 2) the resistance induced by channel form (large-scale, or macro-effects, including bed forms such as dunes in sand-bed streams and step sequences in gravel- and boulder-bed streams). This can be represented in equation form for slope by

$$S = S' + S'' \tag{6}$$

where: S = overall energy slope,
S' = portion of energy lost due to boundary effects, and
S" = portion of energy lost due to form effects.

The equation for shear then can be represented as

$$\tau = \gamma RS' + \gamma RS'' \tag{7}$$

The shear acting on a particle results from the force resisted by boundary effects (or, $\tau = \gamma RS'$). At large slopes, the effects of form resistance represent a larger portion of the total energy loss and shear equations based on the overall slope can over-predict the amount of particle shear. The Safety Factor method is based on $\tau = \gamma RS$ and therefore over-predicts shear for large slopes.

The COE (1991) method is velocity-based and is applicable where velocity is adequately defined. It is generally accepted to be an improvement over the earlier COE method and was found to be more conservative for this case. The equation for Mannings n developed by Abt et al. was developed for coarse bed material and large slopes, similar to that experienced for this case. The velocities estimated in this manner were therefore determined to adequately reflect expected hydraulic conditions.

Given the shortcomings of shear-based methods in steep slope conditions and the adequacy of the estimated velocities for the site's steep slopes, it was determined that the COE (1991) method was an appropriate procedure for application at the site.

6. SUMMARY

A reclamation plan was developed for a gold mining operation in Nevada, USA. Four diversion channels will be built as part of the plan to collect and route runoff around a waste rock pile, leach pad and tailings impoundment. The hydrologic model HEC-1 was used to define 100-year, 24-hour runoff in the diversion channels. An iterative procedure was used to define site hydraulics. Rock size was assumed and the equations for Mannings n developed by Anderson et al. and Abt et al. were used to estimate channel hydraulics. Given channel hydraulics, the COE (1991) procedure was used to determine the required riprap size to protect the channels from erosive velocities. The calculated riprap size was then compared to that assumed and iteration was performed if necessary.

Five riprap size classes were selected for reaches with unlined velocities exceeding 1.5 m/sec: 75, 150, 230, 305 and 380 mm. Approximately 2710 m of the diversion channels will be lined with riprap. The remaining reaches will be lined with natural vegetation.

Although the COE (1991) procedure is stated to be applicable only where slopes are less than 2 percent, this velocity-based procedure was determined superior to the previous COE procedure and to the Safety Factor procedure. The Safety Factor procedure is shear-based and subject to over-sizing riprap on steep slopes.

REFERENCES

Abt, S.R., R.J. Wittler, J.F. Ruff, and M.S. Khattak, 1988. Resistance to Flow Over Riprap in Steep Channels, *Water Resources Bulletin*, Vol. 24, No. 6.

Anderson, A.G., A.S. Paintal, and J.T. Davenport, 1970. "Tentative Design Procedure for Riprap Lined Channels," *NCHRP Report No. 10.*

Chow, V.T., 1959. *Open Channel Hydraulics*, McGraw, Hill Book Company, Inc., New York.

Richardson, E.V., et al., 1975. "Highways in the River Environment - Hydraulics and Environmental Considerations," U.S. Department of Transportation. Available from Publications Office, Engineering Research Center, Colorado State University, Fort Collins, Colorado, 80523.

Shields, A., 1936. "Anwendung der Aenlichkeitsmechanik und der Turbulenzforschung auf die Geschiebebewegung," *Mitteilungen der Preussischen Versuchsanstalt fur Wassrbau und Schiffbau*, Berlin, Germany. Translated to English by W.P. Ott and J.C. van Uchelen, California Institute of Technology, Pasadena, California, 1936.

Simons, D.B. and F. Senturk, 1977. *Sediment Transport Technology*, Water Resources Publications, Littleton, Colorado.

Taylor, R.H., Jr. and N.H. Brooks, 1962. Discussion of "Resistance to Flow in Alluvial Channels," *Transactions*, ASCE, Vol. 127, Part I, Paper No. 3360.

U.S. Army Corps of Engineers (COE), 1970. *Hydraulic Design of Flood Control Channels*, EM 1110-2-1601, Washington, D.C.

U.S. Army Corps of Engineers, 1990. *Flood Hydrology Package, HEC-1*, Washington, D.C.

U.S. Army Corps of Engineers, 1991. *Hydraulic Design of Flood Control Channels*, EM 1110-2-1601, Washington, D.C.

U.S. Soil Conservation Service (SCS), 1985. *National Engineering Handbook*, Section 4, Hydrology, Water Resources Publications, Littleton, CO.

A CASE STUDY OF THE USE OF RIPRAP IN ROCHESTER, MINNESOTA

F.W. Chamberlin
US Army Corps of Engineers, Hydraulic Design Section,
St. Paul, Minnesota, USA
M.S. Meyers
US Army Corps of Engineers, Geotechn. Design Section,
St. Paul, Minnesota, USA

ABSTRACT

The US Army Corps of Engineers is regularly involved in flood control projects throughout the nation. Inherent features of these projects are measures to control erosion. Since riprap is often readily available and economical, erosion control usually involves extensive use of riprap. Projects are often located in urban environments resulting in local concern for project design. Because the Corps of Engineers is committed to being a leader in customer care, the hydraulic design of flood control projects must result in a safe, efficient, reliable, cost effective project with appropriate consideration for environmental and social aspects (ER 1110-2-1405, 1982). This paper focuses on these elements and their relationship to the use of riprap in an urban area. This is accomplished by presenting a case study of the use of riprap for an on-going flood control project by the St. Paul District. Current Corps guidance and the development of new methodologies to address local concerns regarding the use of riprap is discussed. Also included is a presentation of design details and the construction procedures required. The paper is concluded with a discussion of lessons learned from observations made during and after construction.

BACKGROUND

The US Army Corps of Engineers, St. Paul District is currently involved in the design and construction of a 10 stage $100 million urban flood control project in Rochester, Minnesota (South Fork Zumbro River GDM, 1982). Rochester

is home to the Mayo Clinic which attracts people from around the world. The city has a population of about 60 000 and is located in southeastern Minnesota at the confluence of the South Fork Zumbro River, Bear Creek, Cascade Creek, and Silver Creek. The project consists of deepening and widening seven miles of the South Fork Zumbro River and four miles of its tributaries. The only portion of the Corps project that lies outside the city limits is the mitigation area. Features include a continuous pedestrian and bicycle trail with bridge underpasses, complex wall systems, and grade control structures.

The geology of the Rochester area is extremely variable with the channel bottom changing from soil to bedrock in numerous places. Generally the excavated channel has existing soil or bedrock along the channel bottom and riprap protection along the side slopes which vary from 1V:2.5H to 1V:3H. The toe of the riprap extends to the anticipated maximum scour depth or is keyed into the bedrock. The design event varies from 1 to 0.5 percent exceedence (100-to 200-year event) flow. Channel velocities range from 2 to 3 mps (6 to 9 fps), whereas velocities at the drop structures range from 3.5 to 4.5 mps (12 to 15 fps).

The project design calls for seven Types of riprap gradations and four Types of bedding material. Total riprap and bedding quantities are approximately 190 000 m^3 (250 000 cy) and 76 500 m^3 (100 000 cy) respectively at a total cost of $6.5 million. Riprap used on the project has a specific weight of about 2640 kg/m^3 (165 pcf). The following table shows the various riprap Types and their gradations:

Table 1
Riprap Types and Gradations

	% Lighter by Weight in lb							% Lighter by Weight in kg						
	d_{100}	100		50		15		d_{100}	100		50		15	
Type	inch	Max	Min	Max	Min	Max	Min	meter	Max	Min	Max	Min	Max	Min
A	12	86	35	26	17	13	5	0.30	39	16	12	17	6	2
B	18	292	117	86	58	43	18	0.46	132	53	39	26	20	8
C	21	400	160	169	80	84	25	0.53	181	73	77	36	38	11
D	24	691	276	205	138	102	43	0.61	313	125	93	63	46	20
F	27	984	394	292	197	146	62	0.69	446	179	132	89	66	28
G	36	2331	933	691	467	346	146	0.91	1057	423	313	212	157	66
H	28	1098	439	463	220	232	69	0.71	498	199	210	100	105	31

Project construction began in September of 1987 and is scheduled to be completed by 1996. As of March 1993 approximately 80 000 m^3 (105 000 cy) of riprap has been placed.

SAFETY

Riprap in Park Areas

The uneven riprap surface, combined with placement on a slope, poses a potential hazard to people. Therefore, exposed riprap was minimized in areas where the potential was greatest. This was accomplished in the Bear Creek park areas by providing a two stage channel with a low-flow channel and high-flow berms. The design concept was to reduce design flow velocities along the high-flow berms and side slopes such that riprap protection would not be required. The resulting design consists of a riprap lined low-flow channel with 1V:2.5H side slopes and a grass covered high-flow channel with 1V:3H side slopes. The high-flow side slopes were flattened to 1V:3H so they could be maintained safely by mowing. The low-flow channel has a 20 percent exceedence (5-year) flow capacity and design flow velocities of 2.6 mps (8.5 fps), whereas design flow velocities along the high-flow channel are 1.6 mps (5.4 fps). Analysis of the outside channel bends showed design flow velocities along the high-flow channel increased to be about 2.1 mps (6.8 fps), thus requiring riprap protection. As a safety concern, the riprap in these areas was covered with topsoil and sod. The design analysis of the topsoil and sod is discussed in 'Environmental and Social Aspects, Land Use'.

Riprap Adjacent to Bicycle Paths

As mentioned in the project background, the path system for the Rochester project is designed to be a multipurpose system for use by pedestrians and bicycles. In order to maintain a continuous path system along as much of the project as possible, the paths were designed to pass under the bridges. The underpasses are set at an elevation which allows for a clearance of approximately ten feet below the low steel elevation of the bridge, but at an elevation which minimizes frequent inundation of the path. The paths approach the underpasses at a maximum five percent slope and use sight distance requirements to determine the geometric layout of the path. The paths are constructed of concrete with thickened edges below the design water surface elevation.

Since the path is below the design water surface elevation, riprap was placed landward of the path, as shown in Figure 1. Placing riprap immediately adjacent to the path creates a safety hazard should a bicycle leave the path for some reason. The voids in the riprap next to the path were choked with bedding, which was covered with aggregate base coarse. This strip of material allows an

errant biker to recover without getting the wheels of the bike caught in the voids of riprap, falling, and injuring himself on the sharp angular edges of the riprap.

EFFICIENCY

Operation and Maintenance

The stone was properly sized to withstand shear stresses imposed by flood flows and therefore will require little maintenance. Regular inspection is however, continually made for failures, vandalism, and the presence of large woody vegetation growing in the riprap. Design measures to prevent failure are briefly discussed under 'Reliability'.

Vegetation

Vegetation is inimical to riprap installations. When sediment deposits on the riprap, vegetation usually occurs. Corps guidance allows vegetation on low flow berms provided the roots do not penetrate the riprap, failure does not jeopardize project purposes, and the presence of vegetation does not significantly reduce the channel discharge capacity. Figure 2 shows vegetation that has developed over a 2 year period. Vegetation control with defoliants and periodic removal of large woody vegetation by hand will be an annual maintenance cost.

Because of concerns for aesthetics in residential areas, riprap above the 5 percent exceedence (20-year) flowline was covered with topsoil and seeded. This portion of the channel side slope is 1V:3H to facilitate maintenance by mowing. This procedure is in accordance with EM 1110-2-1601. For channel reaches with design flow velocities of about 1.8 mps (6 fps), riprap above the 20 percent exceedence (5-year) flow was covered with topsoil and seeded. While this procedure slightly increases the potential for sediment deposition downstream there are major benefits in the form of increased aesthetic quality and ease of maintenance.

The local sponsor had previous experience with riprap, especially maintenance mowing at the top of the riprap slope or at other locations where grass is adjacent to riprap protection. Based on this previous experience, the local sponsor requested that the Corps of Engineers develop a mowing strip detail. Figure 2 illustrates the appearance of the mowing strip over a large distance of one of the project reaches. The development of this detail is discussed further under 'Design and Construction Details'.

Vandalism/Theft

Experience at other locations has shown that in areas where riprap is not readily available, theft can occur. For example, riprap was stolen by cutting the gabion baskets used to protect the shoreline along the Mississippi River near New Orleans, Louisiana. Because riprap is readily available in the Rochester area, the occurrence of theft was not considered and vandalism was assumed to be of minimal concern.

As part of the first stage of construction 600 linear meters (2000 ft) of channel was enlarged and a 0.3 m (12 in) layer of Type A riprap was placed on the side slopes. As shown in Table 1 the W_{50} (min) for Type A riprap is 7.7 kg (17 lb). This gradation exceeded stability requirements for design flow velocities and was assumed sufficient to address concerns for vandalism. Shortly after placement, field observations showed that 'vandals' had dislodged several of the smaller stones from the slope protection and had thrown them into the channel and onto the pedestrian pathway and had also used them to break nearby lighting fixture globes. This vandalism disrupted use of the pathway, increased the maintenance cost of the lighting system, and given time, could jeopardize the integrity of the slope protection. Therefore, a 0.46 m (18 in) layer of Type B riprap with a W_{50} (min) of 26 kg (58 lb) was selected as an alternative. From Table 1 it can be seen that there is a much smaller quantity of 'throwable' rock. As of March 1993, 3000 linear meters (10 000 ft) of this type of erosion protection is in place and vandalism to the riprap has not shown to be a serious problem. An example of Types A and B riprap are shown on Figures 2 and 13 respectively.

Recent Corps guidance (EM 1110-2-1601, 1991), suggests 'a W_{50} (min) of 36 kg (80 lb) should help prevent theft and vandalism'. A riprap gradation meeting this requirement (see Table 1) would have a maximum stone diameter of 0.53 m (21 in) and weight of about 180 kg (400 lb). Based on the success of the Type B riprap, a riprap of similar gradation should be considered when guarding against vandalism.

RELIABILITY

Riprap is the most widely used nonvegatative type of bank protection and has a long life expectancy. If properly designed and installed, failure rates are relatively low. Because of its long period of use, skills and abilities required for riprap design and construction are widely available (TR E-85-3,

1985). The stone should be sized to withstand shear stresses imposed by design flood flows and a bedding material should be placed beneath the riprap to prevent the in situ soils from migrating upward into the riprap.

Stone Size

For this project, stone was sized for three types of design work; channel, grade control, and bridges. Hydraulic Design Criteria (HDC, 1988) developed by the Waterways Experiment Station (WES), Corps manual EM 1110-2-1601, 'Hydraulic Design of Flood Control Channels' (1970, 1991), and Technical Report TR 2-650 'Stability of Riprap and Discharge Characteristics, Overflow Embankments, Arkansas River, Arkansas (1966) were used to size the stone. The presentation of detailed design procedures is beyond the scope of this paper. In general, the following table shows the design parameters used to size stone:

Table 2
Stone Size - Design Parameters

Design For:	Depth Averaged Local Velocities Obtained From:	Turbulence	Design Theory
Channel			
Low Flow	HEC-2 w/Reduced Manning 'n'	Low	Isbash
High Flow	Alpha Method	Low	Brater & King
Grade Control			
Embankments	Unit Discharge		WES Model Tests
Approach	HEC-2 w/Reduced Manning 'n'	Low	Isbash
Exit	Conjugate Depth Tailwater	High	US Bureau of Reclamation
Bridge Piers	HEC-2 w/Reduced Manning 'n'	High	WES Recommendation

Froude number was also considered to size stone for the high turbulent conditions at the bridge piers. WES personnel recommended a curve between that developed by US Bureau of Reclamation and the Isolated Cube method for Froude numbers between 0.3 and 1.0.

Bedding Material

The gradation of the bedding material is designed to meet filter design criteria set forth in Appendix E of EM 1110-2-1913, 'Design and Construction of Levees' (1978). As a result of the filter criteria, the gradation of the bedding material prevents the in situ soils from migrating upward into the riprap and the gradation of the riprap prevents the bedding material from being pulled through the riprap during high velocity flows. Because of the pervious nature

of the in situ sands on the Rochester project, the stability criteria were considered to be of greater importance than the permeability criteria.

COST EFFECTIVENESS

Construction costs for riprap lined channels depends on local availability of proper stone size and quality. Because quality riprap is readily available from the three quarries located in the Rochester area, little consideration to alternatives to riprap was given. Cost comparisons however, were made for alternatives to sod over riprap. The results showed sod over riprap to be more cost effective. The following are brief examples of other cost effective uses of riprap for the project.

Embankments

Because the channel was deepened, side channel inlets require some means of conveying flow from the side channel inlets to a lower elevation. To perform this function, riprap embankments were used in place of concrete structures. Hydraulic model tests were conducted by WES on overflow embankments to be located on the Arkansas River (TR 2-650, 1964). Stability test for three riprap gradations with varying unit discharge and varying headwater-tailwater conditions were made. Based on the limits of stability for the particular design parameters present, a riprap gradation and unit discharge were determined. The crest length of the embankment was adjusted to produce the desired unit discharge. The overflow embankments modeled by WES had a crest width of about 6.7 m (22 ft); therefore, crests widths of 6.7 m (22 ft) were used. Based on model test failures it appears further cost savings could be made by reducing the crest width to 3.0 m (10 ft).

Bridge Replacement

Several bridge replacements were avoided by the practice of combining riprap and concrete scour protection. At those locations the channel is lowered to a depth below the bridge pier footings. To prevent scour near the bridge piers, concrete is to be placed around the pier footings. The concrete extends to the depth of bedding material as shown Figure 3.

Channel Bottom

A sedimentation study for the flood control project was performed by WES. Based on the maximum scour depths determined, riprap lining of the channel bottom was eliminated by extending the riprap side slope protection to the scour depth.

Obviously this is only cost effective when the channel bottom width is much greater than the maximum scour depth. While this method proved cost effective, it also served as a mitigation feature for loss of instream habitat.

Consistent Riprap Types

Another cost effective measure used on the Rochester project is the use of consistent riprap and bedding Type gradations throughout the ten stages of the project. Once a riprap or bedding Type gradation has been used on the project, that gradation is not used for another Type of riprap or bedding. Required riprap and bedding gradations for a given area are checked against gradations Types already developed for the project. If the required gradations are relatively close to a Type gradation which has already been developed, that Type gradation is used to minimize the number of riprap and bedding Types required for the project or stage. For example, the gradation of Type A riprap or Type 1 bedding is the same on all stages of the project on which it is used. The major advantage of this practice is that once a riprap or bedding Type has been used on the project, the pits or quarries producing the materials are set up to produce that Type on the later stages of the project, leading to lower and consistent costs for these materials. A secondary advantage is the minimizing of riprap and bedding Types used on the project.

ENVIRONMENTAL AND SOCIAL ASPECTS

Water Habitat

Loss of instream habitat of the South Fork Zumbro River was mitigated in part by constructing a meandering low-flow channel and future placement of large riprap along the low-flow channel to provide instream habitat. The random placement of large riprap will produce localized downstream scour holes and zones of reduced velocity. The large riprap is to be placed when the low-flow channel stabilizes.

Some portions of the channel improvement required riprap across the entire channel section. Armor layers that develop by selective removal of fine sediments in natural streams provides good habitat for macroinvertebrates and fish spawning (TR E-85-3, 1985); therefore, riprap lining of the channel should perform similarly.

Land Use

Portions of the channel improvement pass through residential neighborhoods, parks, and a golf course. Concerns in the residential and park areas are mainly for safety and aesthetics, whereas in the golf course, exposed riprap on the wide benched channel would provide a large unwanted golf hazard. Therefore, topsoil and grass mixtures were designed for its particular use. Corps design guidance for this concept is limited. EM 110-2-1601 'Design of Flood Control Channels' (1991) states that 'planned use of vegetation with riprap should serve some justifiable purpose, be accounted for in capacity computations, be controllable throughout the project life, have a strengthened riprap design that will withstand the additional exigencies, and account for increased difficulty of inspection'. While the use of vegetation with riprap was certainly justifiable, the following design parameters had to be considered:

1. Selection of the most suitable type of grass cover.
2. Topsoil specifications to promote good grass stand.
3. Proper thickness of topsoil to establish a good root system.
4. Prevention of migration of topsoil into the riprap.

Grass Cover

Design of the sod grass mixture for the golf course differed from that for the park and residential areas. Both grasses had to be tolerant to design flow velocities; however, the golf course required a mixture that would prevent a contrast between existing grass features and the proposed sod. Therefore, the following grass mixtures were selected:

Residential & Park Areas		Golf Course Fairways	
Common Name	Mixture %	Common Name	Mixture % by Weight
Kentucky Bluegrass	75 (min)	Ram I Bluegrass	20
Acceptable Varieties	0 - 25	Adelphi Bluegrass	20
Park, Newport, Glade		Parade Bluegrass	20
Nugget, Touch Down,		Rugby Bluegrass	20
Rugby and Parade		Merit Bluegrass	20

The use of sod over riprap in the golf course is illustrated in Figures 4 and 5 and sod over riprap in a park area is illustrated on Figure 7. Figure 6 shows a comparison of sod over riprap and exposed riprap.

Topsoil

The selection of topsoil mix was important in producing a good grass stand with a deep root system. Consultation with turf specialist at the University

of Minnesota (U of M) and the Minnesota Department of Transportation (MnDOT) led to the development of a sandy topsoil mixture. A silty soil would lead to a shallow root system with a depth of about 25 mm (1 in). A shallow root system would not be able to sustain design flow velocities and also would not be very drought tolerant. A sandy soil mixture allows the percolation of water through the soil thus promoting a deep root system. Therefore, a select topsoil mixture developed by MnDOT was modified for project use. The following Select and Common topsoil mixtures were developed for areas requiring a higher grade topsoil (e.g. parks and golf course), and for all other areas (e.g. residential) respectively:

	MnDOT Spec		Select Spec		Common Spec	
	Min.	Max.	Min.	Max.	Max.	Min.
Material Passing #10 sieve	90%	--	90%	--	85%	--
Clay	5%	30%	5%	20%	5%	30%
Silt	10%	70%	10%	50%	10%	70%
Sand	20%	70%	40%	70%	40%	70%
Organic Matter	3%	20%	3%	20%	3%	20%
pH	6.1	7.5	6.1	7.5	6.1	7.8
Soluble Salts (Mho)		1.5		1.5		
Extractable Phosphorous (lb/Ac)	30		30			
Exchangeable Potassium (lb/Ac)	150		150			

Through discussions with the U of M, it was determined that 0.15 m to 0.3 m (6 to 12 in) of topsoil would be adequate to produce a suitable grass stand. Because of local concerns for rapid drainage of the soil and to account for variations in placement, a layer thickness of 0.3 m (12 in) was selected. Figure 8 shows the placement of topsoil in the golf course.

Migration of Topsoil

A further use of the bedding was to prevent mass migration of the topsoil into the underlying riprap. This was accomplished by simply choking the surface of the riprap on which the topsoil was to be placed with the same bedding Type which was required for that riprap Type. For example, if a Type A riprap was to be covered with topsoil, and the Type A riprap required a Type 1 bedding, the surface of the riprap would also be choked with Type 1 bedding material. This choking material was given the formal name of 'riprap surface treatment'.

The use of bedding as a riprap surface treatment material came about after trying several other material types, such as sand and aggregate base coarse. In both instances, the relatively finer gradations of these two materials

required large volumes of riprap surface treatment material, especially in the larger riprap gradations. Since the bedding material is designed to be filtered by the riprap, it seemed appropriate to use the bedding as a riprap surface treatment material to minimize the volume of material per unit area of riprap to be chinked. It is estimated that approximately 0.12 m^3 of riprap surface treatment material is required for each square meter (0.4 ft^3/sq ft area) of riprap surface to be choked.

In the golf course reach of the project, the local sponsor was very concerned about maintaining a sufficient topsoil depth to establish and maintain a high quality playing surface where topsoil and sod were placed over riprap. In this area, a further precaution to the loss of topsoil via downward migration was included by adding a layer of nonwoven geosynthetic material on top of the riprap surface treatment prior to placing the topsoil. The nonwoven nature of this material tends to clog and minimize the amount of material from passing through it, while maintaining an adequate percolation rate. The construction of this detail is illustrated in Figure 8.

DESIGN AND CONSTRUCTION DETAILS

Many riprap design and construction details for this project were obtained from EM 1110-2-1601, 'Hydraulic Design of Flood Control Channels'. Other details were modifications to EM 1110-2-1601 or were specifically developed for this project. For example, details in EM 1110-2-1601 addressing riprap toe detail requirements do not have sufficient detail regarding actual construction. Figures 9 through 23 present several engineering drawings and as-built photographs of these same details. Note the nice straight lines indicating the placement of riprap and other materials. The intent of this discussion is that the appearence of details shown on drawings are often quite different from the final product. Several details are discussed further below.

Top of Slope Riprap Detail

Figure 9 shows the engineering drawing of the top of slope riprap detail. Figure 10 shows the constructed detail with no attempt to fill the void between the riprap and adjacent soil. The concerns of the local sponsor with respect to maintenance and safety are readily evident. As the project progressed, the appearance of this detail improved through the use of different materials and construction schemes. Figures 10 through 14 illustrate the evolution of the top

of slope riprap detail. Figure 11 used aggregate lime to fill the void. Figure 12 used aggregate base coarse to fill the void. Figure 13 shows the constructed detail with an attempt to fill the void between a large gradation of riprap and the adjacent soil with aggregate base coarse. Figure 14 used bedding material, as discussed previously, to fill the void. A further refinement of this detail was to use bedding material to fill the void (to minimize the amount of material required to fill the void) and to place aggregate base coarse on top of the bedding material to improve the visual appearance of the detail. Two related details, presented in Figures 15 and 16, occur when sod or turf over riprap changes to exposed riprap at a vertical or horizontal interface. These details also require filling of the riprap voids adjacent to the sod to prevent migration of topsoil materials into the riprap and to provide a mowing strip.

Riprap Toe Details in Soil

Figure 17 presents the engineering drawing of a riprap toe detail in soil. This detail was selected from Method A, Plate 37, Appendix III of EM 1110-2-1601. However, note that excavation of a triangular area of soil is required to construct this detail. This area of excavation must also be backfilled. In the St. Paul District, the construction contractors are allowed to excavate and place riprap and bedding in the wet. Since the excavation is not visible in the wet, a volume measurement of the required excavation and backfill is almost impossible to obtain. Therefore, a bid item referred to as 'toe backfill' was created. This item is bid per lineal foot of toe backfill.

Figure 18 presents the engineering drawing of an alternate riprap toe detail in soil. This detail was selected from Method B, Plate 37, Appendix III of EM 1110-2-1601. This detail has been modified in that the riprap is placed to the elevation of the channel bottom instead of recessed as shown in the EM, thus minimizing excavation quantities.

Riprap Toe Details in Rock

Figure 19 presents the engineering drawing of a riprap toe detail in rock. This detail was selected from Method E, Plate 37, Appendix III of EM 1110-2-1601. This detail is typically constructed in the wet, but is difficult to construct even in the dry. The rock encountered on the Rochester project is typically thin to medium bedded. The thin slab like nature of the rock makes the excavation of this detail extremely difficult. Several methods of excavation have been attempted. On one reach of the project, the construction contractor

attempted to blast the rock to the shape of the key. This failed to produce satisfactory results because the contractor did not utilize controlled blasting. A hoe ram attached to a hydraulic excavator proved to be the most successful method of achieving the controlled excavation required for a detail such as this, but was not entirely successful. The depth of excavation at the toe of the slope, normal to the slope, was not able to be achieved, especially in the wet, because of the nature of the rock formation. Figure 20 presents a photograph of this detail as constructed. Note that the depth of the toe key is obviously less than required by the detail.

Maintenance Paths at the Top of Slope

Maintenance access paths were placed at the top of slope when a multipurpose path was not used, as shown on the engineering drawing in Figure 21. The riprap extends overbank some distance at the top of the slope, requiring the voids in the riprap to be filled with bedding and covered with aggregate base course as the maintenance path material. Figure 22 presents a photograph of this detail as constructed.

Increased Thickness of Materials for Underwater Placement

As discussed previously, the St. Paul District allows the placement of riprap and bedding materials in the wet. This eliminates the construction of temporary cofferdams to provide placement in the dry and the risk of overtopping of these cofferdams. To insure that the proper thickness of material is being properly placed underwater, the required thicknesses of the riprap and bedding materials are increased 50 percent. The thickened section is carried approximately one foot above the anticipated water surface elevation at the time of construction. A sketch of this typical detail is presented in Figure 23.

CONCLUSIONS

A combination of theoretical applications, engineering judgement, and practicality can be used to strike a balance between function, aesthetics, and cost. Design methodologies developed specifically for this project to address concerns for safety, efficiency, and environmental and social aspects led to cost saving measures that can be employed on future projects. Lessons learned during construction has led the development of improved design and construction details.

This project has shown that riprap can be safely used to provide a reliable, efficient, and cost effective means to control erosion.

REFERENCES

1. US Army Corps of Engineers, St. Paul District, St. Paul, Minnesota, 1982: Design Memorandum No.1, Phase 2, General Project Design, Flood Control, South Fork Zumbro River, Rochester, Minnesota.

2. US Army Corps of Engineers, Washington, D.C., 1970 & 1991: Engineering Manual EM 1110-2-1601, 'Hydraulic Design of Flood Control Channels'.

3. US Army Corps of Engineers, Washington, D.C., 1882: Engineering Regulation ER 1110-2-1405, "Hydraulic Design for Flood Protection Projects'.

4. US Army Corps of Engineers, Hydraulic Engineering Center (HEC), 1982 and 1990: Generalized Computer Program, 'Water Surface Profiles'.

5. US Army Corps of Engineers, Washington D.C., 1978: Engineering Manual EM 1110-2-1913, 'Design and Construction of Levees'.

6. Waterways Experiment Station (WES), Vicksburg, Mississippi, 1983: Miscellaneous Paper HL-83-7, 'Sedimentation Study for the Rochester, Minnesota, Flood Control Project'.

7. Waterways Experiment Station (WES), Vicksburg, Mississippi, 1985: Technical Report TR E-85-3, 'Incorporation of Environmental Features in Flood Control Channel Projects'.

8. Waterways Experiment Station (WES), Vicksburg, Mississippi, 1966: Technical Report TR 2-650, 'Stability of Riprap and Discharge Characteristics, Overflow Embankments, Arkansas River, Arkansas'.

9. Waterways Experiment Station (WES), Vicksburg, Mississippi, 1988: 'Hydraulic Design Criteria', Volumes 1 and 2.

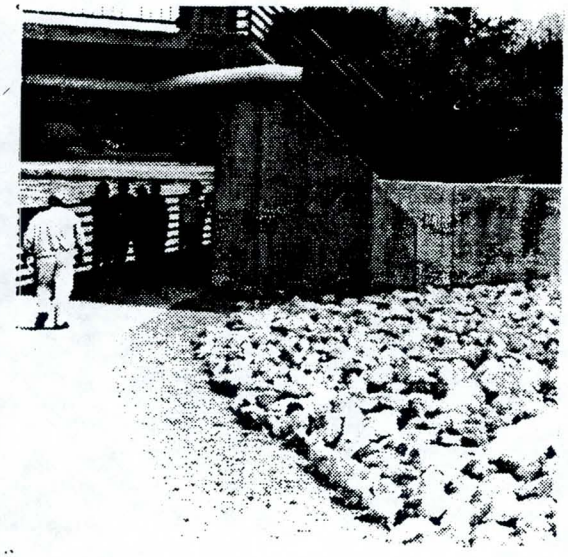

Figure 1. Riprap Placed Adjacent to Concrete Path.

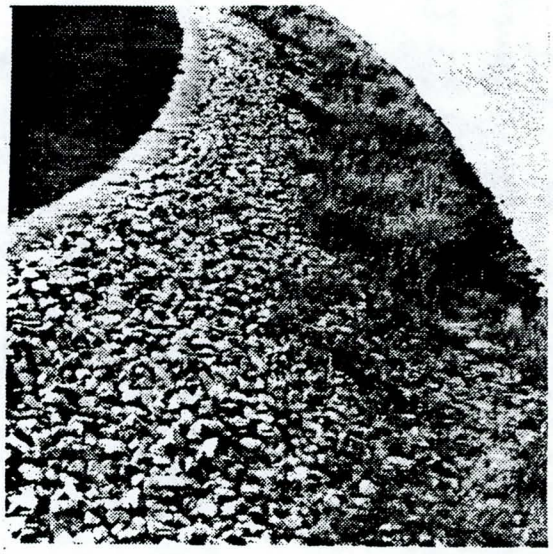

Figure 2. Mowing Strip and Vegetation in Riprap.

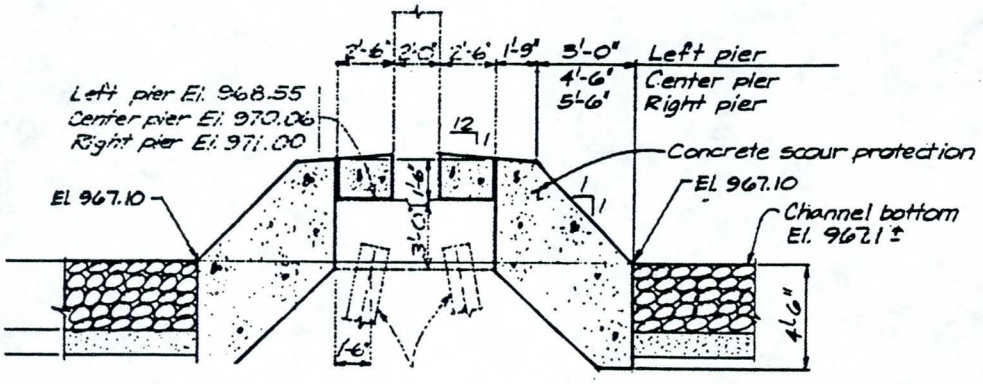

Figure 3. Concrete Bridge Scour Protection.

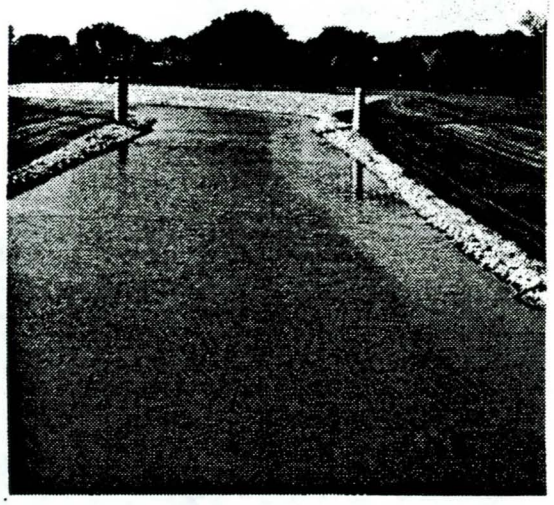

Figure 4. Sod Over Riprap in Golf Course.

Figure 5. Sod Over Riprap in Fairway 5.

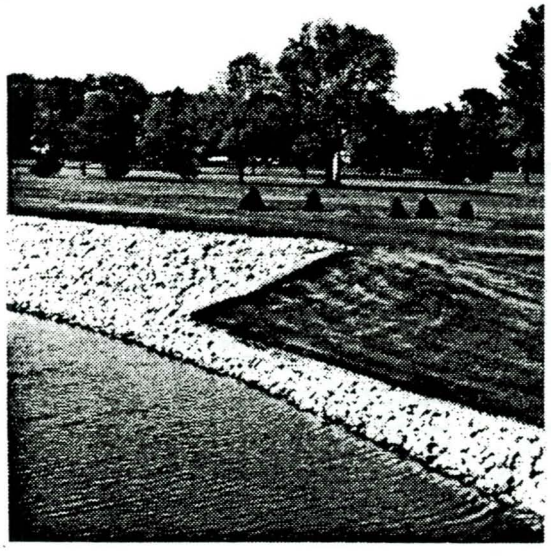

Figure 6. Sod Over Riprap Adjacent to Exposed Riprap.

Figure 7. Sod Over Riprap in a Park Area.

Figure 8. Topsoil, Filter Fabric, Riprap Construction in Golf Course.

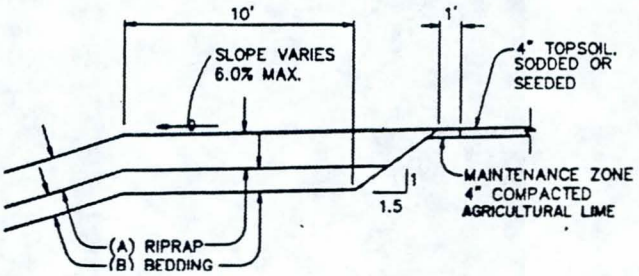

Figure 9. Top of Slope Detail.

Figure 10. Top of Slope Detail - No Fill.

Figure 11. Top of Slope Detail with Agricultural Lime Fill.

Figure 12. Top of Slope Detail with Aggregate Base Course Fill.

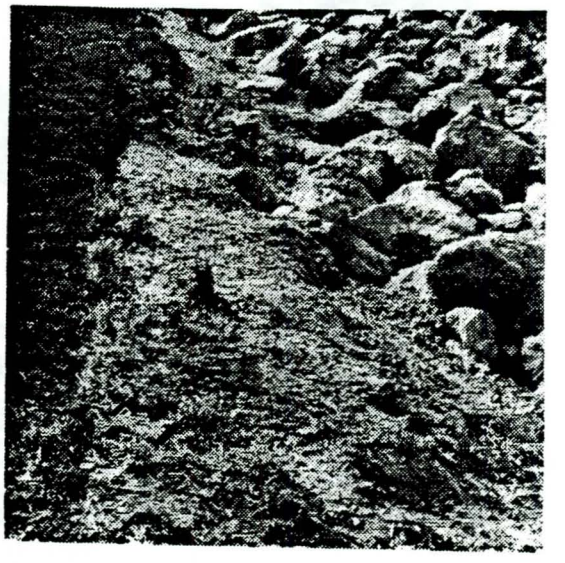

Figure 13. Top of Slope Detail - Aggregate Base Course in Large Riprap.

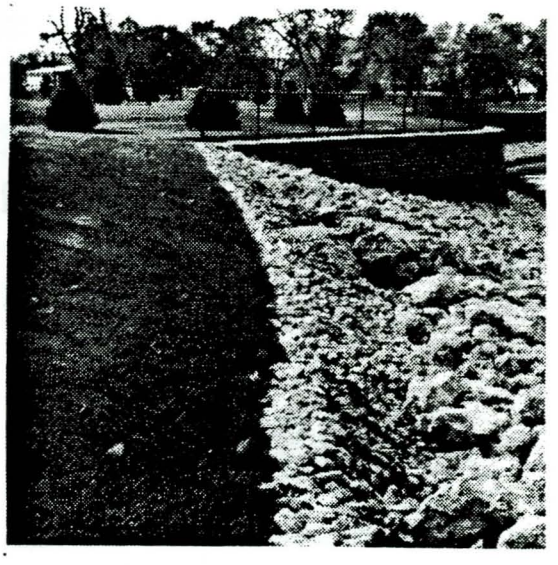

Figure 14. Top of Slope Detail with Bedding Fill.

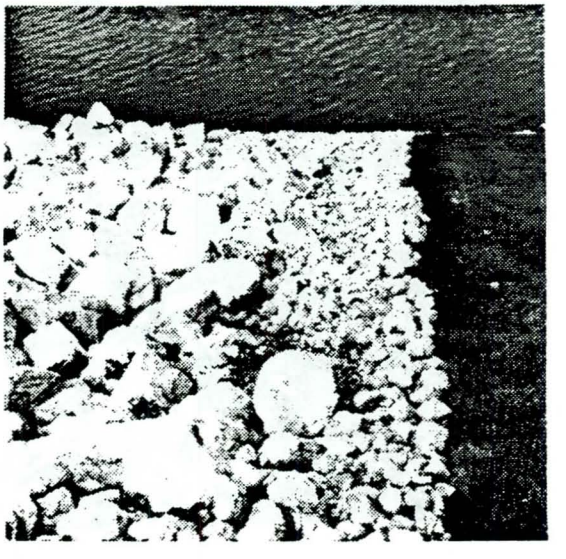

Figure 15. Sod/Riprap Interface on Channel Side Slope.

Figure 16. Sod/Riprap Interface at Bottom of Slope.

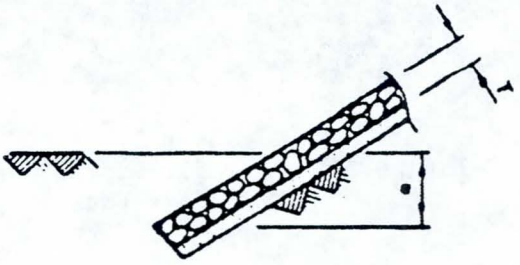

Figure 17. Riprap Toe Key Detail in Soil.

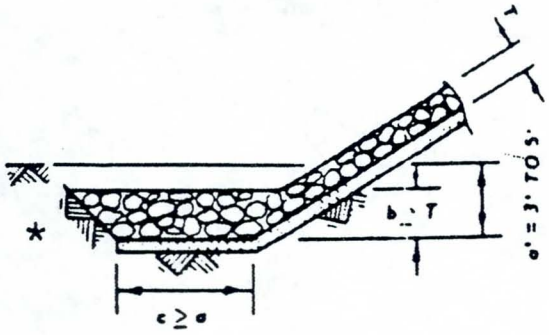

Figure 18. Alternate Riprap Toe Kep Detail in Soil.

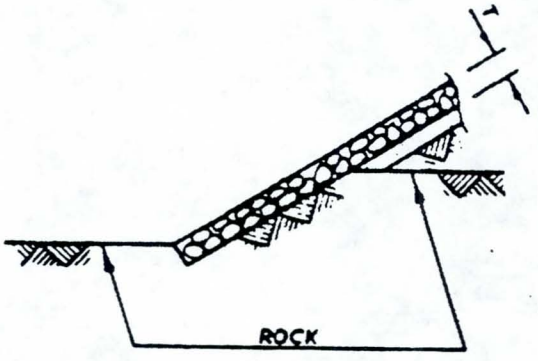

Figure 19. Riprap Toe Key Detail in Rock.

Figure 20. As-Built Riprap Toe Key Detail in Rock.

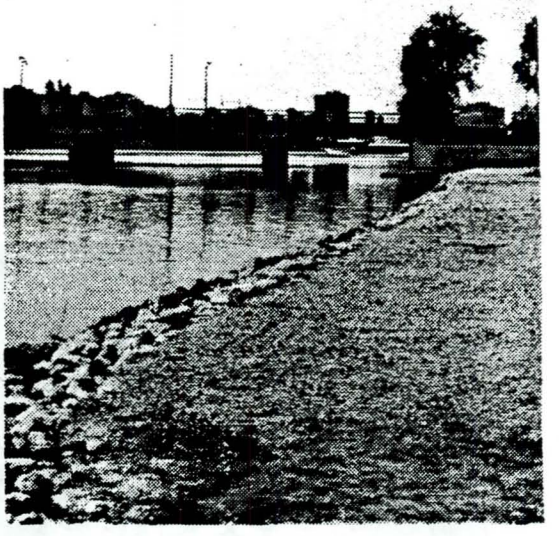

Figure 21. As-Built Maintenance Path Over Riprap Detail.

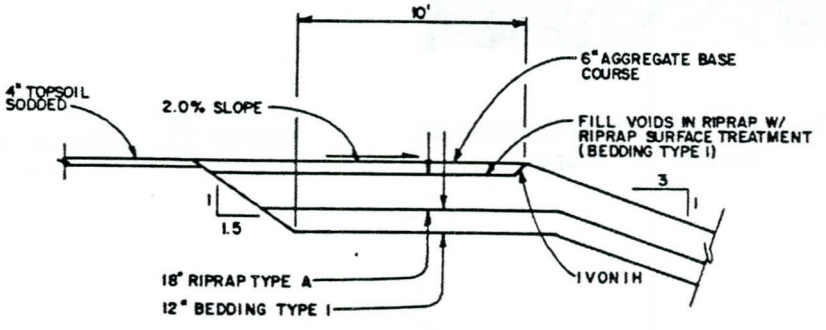

Figure 22. Maintenance Path Over Riprap Detail.

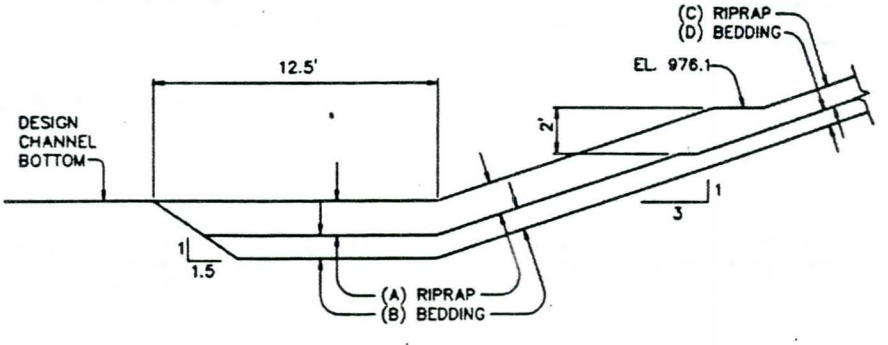

Figure 23. Thickened Riprap/Bedding Detail.

OPTIMUM DESIGN OF RIPRAP PROTECTED TRAPEZOIDAL CHANNELS

B.A. Christensen
University of Florida, Gainsville, FL 32611, USA

ABSTRACT

Rock riprap is a commonly used material for the protection of canals against flow induced erosion. Block size is usually determined by a buoyant weight versus drag force consideration in a canal already designed for the discharge and bedslope in question by use of an old standby, the Manning formula based on the cross-section's hydraulic radius. A safety factor is applied to take uncertainties in flow, Manning's n and block size distribution into consideration. Another approach to sizing the blocks is to require that the shear stress on the trapezoid's banks is equal to or less than the local critical shear stress determined by multiplying the critical shear stress of a horizontal bed made up of the same riprap by a correction factor taking the influence of bank slope on critical shear stress into consideration. Usually, the US Bureau of Reclamation formula for the correction factor is used. This formula does not take the hydrodynamic lift on the individual blocks into consideration, which makes the approach somewhat unsafe. This shortcoming is usually overcome by application of a more or less arbitrary safety factor.

An abundance of formulas, charts and nomograms reflecting the above-mentioned approaches may be found in the relevant literature. What they all have in common is that they actually separate erosion prevention from conveyance design. Economy is not always considered and if it is, it is done by minimizing the flow area of the channel not including cost of land, riprap protection and the extra excavation cost involved in providing the necessary freeboard of the canal and room for riprap.

The present paper develops an integrated procedure for determination of channel depth, bottom width, and the necessary block size that will make the total cost of the canal per unit length minimum.

INTRODUCTION

Sizing riprap blocks for protecting man-made channels against the erosive forces of rapidly flowing water is a quite well researched area. Individual parts of the design such as block sizing, selection of the geotextile on which the blocks are placed, or designing a stone filter instead of the geotextile are described in detail in the literature.

American practice is described in recent publications from the US Army Corps of Engineers [1,2] usually in connection with procedures for design of structures such as spillways, flood control channels, bridge abutments, etc. Maynard [3] discusses the sizing of stable riprap specifically for open channel flows. The area of transportation research contributes also to the riprap literature. For instance, the Bureau of Public Roads [4] provides guidelines for use of riprap for bank protection already in the sixties. Brown and Clyde [5] introduce recent design procedures for riprap revetments.

European experience is presented in a state-of-the-art publication by Pilarczyk et al. [6] discussing Dutch practices in general, while van der Knaap et al. [7] introduce the reader to the design of geotextiles and de Graauw et al. [8] give design criteria for granular filters.

Most of these contributions to the riprap design literature consider only one of the many parts related to successful riprap design. However, an integrated approach is needed to optimize the design. It must be required that the riprap is stable and that the conduit conveys the design discharge at the given bedslope with the roughness characteristics dictated by the block size of the riprap. Last but certainly not least the total cost of the considered channel including excavation cost, land cost, and cost of the riprap protection must be minimum. A design procedure satisfying these three requirements is developed in the following.

CRITICAL SHEAR STRESS AND CORRECTION FOR BANK SLOPE

Two basic criteria for incipient motion of the moveable bed prevail in the literature. The critical velocity approach discussed by Hjulström [9] among others and the critical shear stress approach due to Shields [10] used here stating that erosion is initiated when the time-mean bed shear stress $\overline{\tau_o}$ is in excess of a critical value given by

$$\overline{\tau}_{cr.h} = E_h(\gamma_s - \gamma)\, d_e \qquad (1)$$

for a horizontal or nearly horizontal bed. In Eqn. (1) E_h = a dimensionless entrainment function which is constant in the turbulent rough flow range, d_e = block size, and γ_s and γ

= unit weight of block material and water, respectively. Due to the stochastic nature of the turbulent flow generating the bed shear stress, E_h must be a function of the probability of erosion p. High probabilities correspond to low E_h-values and vice versa. Christensen [11] shows that E_h may be written

$$E_h = [(\beta_2/\beta_1) \cdot (1 + s_u^2)/(\cot\phi + (\overline{\lambda}/\overline{\tau_o}))]/(1 + ts_u)^2 \qquad (2)$$

in which β_1 = (bed area associated with one block)/d_e^2, β_2 = (block volume)/d_e^3, s_u = standard deviation of turbulent velocity fluctuation near bed divided by the corresponding time-mean velocity, s_u is a constant = 0.164, t = normalized abscissa of the Gaussian probability density curve corresponding to the chosen probability of erosion, and ϕ = angle of repose of the bed material (riprap in this case). $\overline{\lambda}$ and $\overline{\tau_o}$ are the time-mean values of the hydrodynamic lift per unit bed area and the bed shear stress, respectively. Using Einstein's observations of $\overline{\lambda}$ the lift/shear stress ratio is shown to be

$$\overline{\lambda}/\overline{\tau_o} = 0.556\,[\ln(1 + (10.4/r)]^2 \qquad (3)$$

where r is the roughness grain-size ratio defined as Nikuradses roughness k divided by block size d_e. It is noted that $\overline{\lambda}/\overline{\tau_o} \to 0$ for $r \to \infty$ corresponding to a very irregular pattern of the topmost layer of grains.

On a sloping channel bank the critical shear stress $\overline{\tau}_{cr.b}$ must be smaller than $\overline{\tau}_{cr.h}$ on the corresponding horizontal bed since gravity amplifies the flow induced shear stress. A correction factor K_b (<1) may be developed so that

$$\tau_{cr.b} = K_b \tau_{cr.h} = K_b E_h (\gamma_s - \gamma) d_e \qquad (4)$$

where

$$K_b = \frac{(s^2\tan^2\phi - 1)(\cot\phi + (\overline{\lambda}/\overline{\tau_o}))}{(\overline{\lambda}/\overline{\tau_o})s\tan^2\phi + \sqrt{\left((s^2 + (\overline{\lambda}/\overline{\tau_o})\tan^2\phi - 1\right)}} \cdot \frac{1}{\sqrt{(1 + s^2)}} \qquad (5)$$

still referring to Christensen [11].

For $r \to \infty$, i.e., disappearing lift, Eqn. (5) approaches

$$K_b = \sqrt{(1 - (\sin^2\theta/\sin^2\phi))} \qquad (6)$$

where $\theta = \cot^{-1}s$ = inclination of banks with respect to horizontal. Eqn. (6) is the conventional US Bureau of Reclamation formula for K_b, which neglects the influence of lift and therefore may be on the unsafe side.

BOUNDARY SHEAR STRESS DISTRIBUTION AND FLOW FORMULA

Conventionally, the time-mean value of the boundary shear stress $\overline{\tau_o}$ of an open channel is evaluated is by the formula

$$\overline{\tau_o} = \gamma R S_{EGL} \tag{7}$$

in which R = hydraulic radius, and S_{EGL} = slope of the energy grade line. The latter is equal to the bedslope S_b when the flow is uniform. This assumes that the shear stress is constant along the wetted perimeter P, or Eqn. (7) may be said to give the average boundary shear stress if that assumption is not made.

To get a better idea of the true shear-stress distribution along P consider Fig. 1 showing a typical open channel cross-section of arbitrary shape. A curved m-axis is located along the wetted perimeter with m = 0 at the left shoreline and m = P/2 at the centerline. Isovels, i.e., curves passing through points having the same flow velocity v are shown. Two adjacent orthogonals to the isotachs are drawn. These orthogonals intersect the wetted perimeter at points located the short distance dm from each other. The area between the two orthogonals is dA.

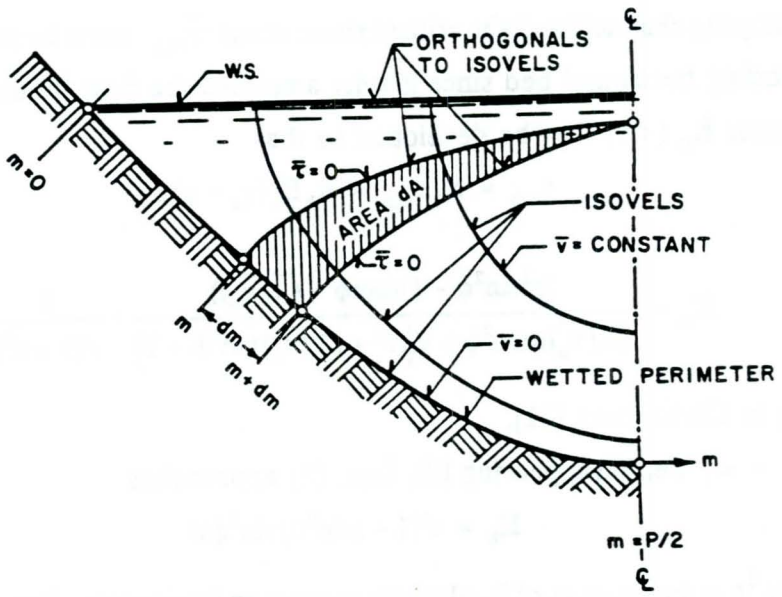

Fig. 1. Typical Open Channel Section with Isovels and Orthogonals to Isovels.

Along the orthogonals the shear stresses in the direction of flow must be zero since the velocity gradient normal to the orthogonals must be zero. From the equilibrium principle applied to uniform flow in this section it is therefore seen that

$$\overline{\tau}_o = \gamma \frac{dA}{dm} S_b \tag{8}$$

at this location. Using only one area element located between the two orthogonals represented by the free water surface leads to Eqn. (7) since dA = A and dm = P in this case.

In the symmetrical trapezoidal section with depth d_o, bottom width b and inverse bank slope s shown in Fig. 2 the isovels may be assumed to be parallel with the wetted perimeter. This assumption leads to the $\overline{\tau}_o$-distribution shown in the right half of Fig. 2 with the maximum shear stress

$$\overline{\tau}_{o\,max} = \gamma d_o S_b \tag{9}$$

occurring on the bank and on the horizontal bed as indicated.

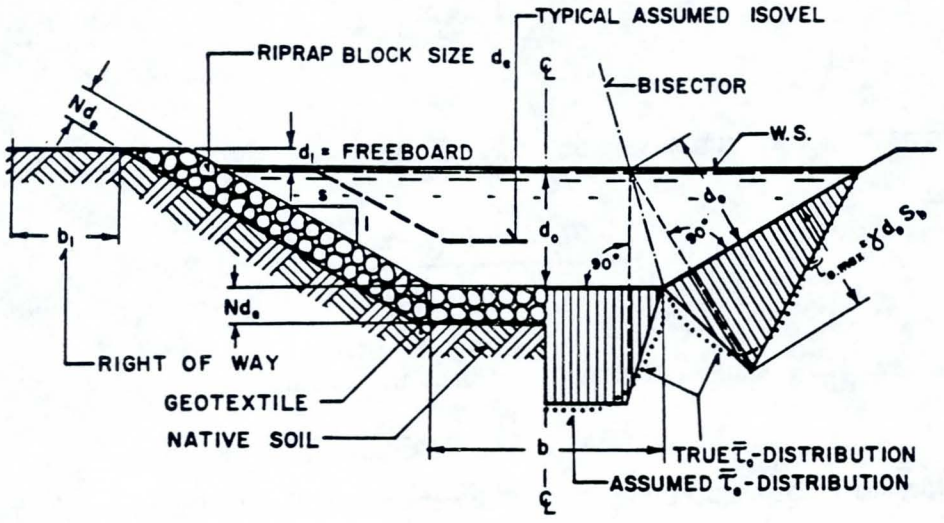

Fig. 2. Trapezoidal Channel Section With Assumed Isovels and Boundary Shear Stress Distribution

The nonuniform boundary shear stress distribution implied by Eqn. (8) also makes it necessary to replace the hydraulic radius R conventionally used in the Manning formula by another parameter, here called the conveyance radius R_N. Since the flow oriented shear stresses along the orthogonals to the isovels are zero it may be concluded that the discharge in area element dA is

$$dQ = M\left(\frac{dA}{dm}\right)^{2/3}\sqrt{(S_b)}\,dA \tag{10}$$

assuming that the Manning formula is valid, i.e., that flow is in the turbulent rough range, that the inverse relative roughness R/k is between 5 and 300 and

$$M = 8.25\sqrt{(g)}/k^{1/6} \tag{11}$$

stands for 1/n (or 1.486/n in English units), Christensen [12]. From Eqn. (10) it is seen that the total discharge must be

$$Q = \int_o^P M\left(\frac{dA}{dm}\right)^{2/3}\sqrt{(S_b)}\,dA = AMR_N^{2/3}\sqrt{(S_b)} \tag{12}$$

From which the general expression for the conveyance radius R_N is found to be

$$R_N = \left[\frac{1}{A}\int_o^P\left(\frac{dA}{dm}\right)^{2/3}dA\right]^{3/2} \tag{13}$$

In the symmetrical trapezoidal section of Fig. 2 this gives

$$R_N = \left[\frac{b + [(5/4)s - (\sqrt{(1+s^2)}/2)]\,d_o}{b + s\,d_o}\right]^{3/2} d_o \tag{14}$$

See Christensen [13]. This concept is to be used in the following.

MINIMUM COST REQUIREMENT

In the design of a riprapped trapezoidal channel the conveyance requirement, scour protection and, last but not least, minimum cost of the completed canal must be considered in order to obtain a satisfactory engineering solution. Consider for instance the symmetrical trapezoidal channel shown in the left hand half of Fig. 2. This channel's inverse bank slope s is determined by the stability of the native soil. The block size d_e of the riprap is unknown

but the number of block layers N may be prescribed. The riprap is placed on a geotextile, but could just as well be located on a properly designed stone filter.

This channel is to be designed for uniform flow with the constant discharge Q and bedslope S_b. Its free board is d_1, and space for right of ways of width b_1 along the channels sides must be provided.

The Lagrangean method for finding the minimum of a function of several variables, that also must satisfy certain constraints, is used to find the optimum values of d_o, b and d_e.

The total cost per unit length of the channel may be written

$$C = \underbrace{c_1[b(d_o+d_1) + s(d_o+d_1)^2 + (b+2(d_o+d_1)\sqrt{(1+s^2)})Nd_e]}_{\text{Excavation cost per unit channel length}} + \underbrace{c_2[2b_1 + 2s(d_o+d_1+Nd_e) + b]}_{\text{Land cost per unit channel length}} + \underbrace{c_3(b + 2(d_o+d_1)\sqrt{(1+s^2)})Nd_e}_{\text{Lining cost per unit channel length}} \quad (15)$$

in which c_1 = excavation cost per unit volume, c_2 = land cost per unit area and c_3 = cost of placed riprap per unit volume. The cost of the geotextile or filter is included in c_3. Consistent units are used for c_1, c_2 and c_3. The decision variables are d_o, b and d_e.

The first constraint is expressing that there should be no erosion, or rather incipient erosion, at the point of maximum shear stress on the channel's banks. The assumed boundary shear stress distribution is shown in the right hand side of Fig. 2. It corresponds to linear isovels parallel to the section's wetted perimeter. Expressing equilibrium between gravity forces in direction of flow and boundary shear, leads to the maximum shear stress on the channel banks

$$\bar{\tau}_{o.max} = \gamma d_o S_b \quad (9)$$

This must be equal to the critical shear stress of the banks riprap $\bar{\tau}_{cr.b}$. Hence,

$$\bar{\tau}_{o.max} = \gamma d_o S_b = K_b E_h(\gamma_s - \gamma) d_e \quad (16)$$

in which the correction factor K_b and the value of Shields' entrainment function E_h may be found from Eqns. (5) and (2). Introducing the first auxiliary constant

$$K_1 = S_b/[K_b E_h\{(\gamma_s/\gamma)-1\}] \quad (17)$$

Eqn. (16), i.e., the first constraint, may be written

$$d_e = K_1 d_o \tag{18}$$

relating stone size to maximum flow depth.

The second constraint expresses that the channel must convey the discharge Q at the bedslope S_b with the roughness dictated by the block size. The latter may be related to the equivalent sand roughness k by

$$k = r d_e \tag{19}$$

in which r, the roughness/grain-size ratio is a measure of the orderliness of the placing of the blocks. A perfect placing of the blocks; i.e., a placing similar to the arrangement of the roughness elements (sand) used in Nikuradses classic experiments, corresponds to r = 1, r = 5 represents a fairly good and realistic placing without any vegetation, and r = 100 is a poor placing with plenty of vegetation in between the individual blocks.

Using the flow area $bd_o + sd_o^2$ and the conveyance radius given by Eqn. (14) instead of the hydraulic radius, the Manning formula may be written

$$\frac{Q}{bd_o + sd_o} = \frac{8.25\sqrt{(g)}}{k^{1/6}} \cdot \frac{b + [5s/4 - \sqrt{(1+s^2)}/2]d_o}{b + sd_o} d_o^{2/3}\sqrt{(S_b)} \tag{20}$$

In Eqn. (20) 1/Manning's n (or 1.486/n in English units) is replaced by $8.25\sqrt{(g)}/k^{1/6}$ where k of course may be replaced by rd_e. See for instance Christensen [12].

Introducing the second auxiliary function

$$K_2 = Qr^{1/6}K_1^{1/6}/(8.25\sqrt{(g\,S_b)}) \tag{21}$$

Eqn. (20) may be presented in the form

$$\psi = K_2 - bd_o^{3/2} - [5s/4 - (\sqrt{(1+s^2)}/2)]d_o^{5/2} = 0 \tag{22}$$

This is now the only constraint since one of the original three decision variables, d_e, is eliminated by use of Eqn. (18).

The block size d_e may of course also be eliminated from the objective function by introduction of Eqn. (18) in Eqn. (15) giving

$$\frac{C}{c_1} = b(d_o + d_1) + s(d_o + d_1)^2 + NK_1(bd_o + 2(d_o^2 + d_o d_1)\sqrt{(1 + s^2)})$$

$$+ \frac{c_2}{c_1}[2b_1 + 2s(d_1 + (1 + NK_1)d_o) + b]$$

$$+ \frac{c_3}{c_1}(bd_o + 2(d_o^2 + d_o d_1)\sqrt{(1 + s^2)})NK_1 \qquad (23)$$

where c_1 of course is constant.

Eqn. (23) is now the final objective function, d_o and b the only decision variables, and Eqn. (22) the only constraint.

Application of the Lagrangean method yields

$$\frac{\partial(C/c_1)}{\partial d_o} + \lambda\frac{\partial\psi}{\partial d_o} = 0 \qquad (24)$$

and

$$\frac{\partial(C/c_1)}{\partial b} + \lambda\frac{\partial\psi}{\partial b} = 0 \qquad (25)$$

or by elimination of the Lagrangean multiplier λ

$$\frac{\partial(C/c_1)}{\partial d_o} \Big/ \frac{\partial(C/c_1)}{\partial b} = \frac{\partial\psi}{\partial d_o} \Big/ \frac{\partial\psi}{\partial b} \qquad (26)$$

which must be satisfied to get a minimum cost design.

The four partial derivatives in Eqn. (26) may be developed from Eqns. (15) and (22) and introduced resulting in an equation that may be solved for the bottom width/depth ratio b/d_o

$$\frac{b}{d_o} = 2 \cdot \frac{(K_3/K_4) - K_7 + [(K_5 - (K_6/K_7))/K_4]/d_o}{1 + (3K_6/K_4)/d_o} \qquad (27)$$

in which the additional five auxiliary constants are

$$K_3 = 2s + 4NK_1\sqrt{(1 + s^2)}[1 + (c_3/c_1)] \qquad (28)$$

$$K_4 = 1 + NK_1[1 + (c_3/c_1)] \qquad (29)$$

$$K_5 = 2d_1(s + NK_1\sqrt{(1 + s^2)}[1 + (c_3/c_1)]) + 2s(c_2/c_1)(1 + NK_1) \qquad (30)$$

$$K_6 = d_1 + (c_2/c_1) \tag{31}$$

and

$$K_7 = (5/2)(5s/4 + (\sqrt{(1 + s^2)}/2)) \tag{32}$$

The constraint, Eqn. (22), may also be solved for b/d_o giving

$$b/d_o = -(2/5)K_7 + K_2/d_o^{5/2} \tag{33}$$

Combining this equation with Eqn. (27), i.e., eliminating b/d_o, results in an equation in which d_o is the sole unknown. It must be solved by iteration. An iterative form of this equation is

$$d_o = \left\{\frac{K_2K_4d_o + 3K_6K_2}{(2K_3 - (8/5)K_7K_4)d_o + 2K_5 - (4/5)K_6K_7}\right\}^{2/5} \tag{34}$$

into which $d_o = 0$ may be introduced as a first estimate to initiate the iterative solution.

Once the depth d_o is found the corresponding bottom width is simplest found from Eqn. (33) and the block size from Eqn. (18). This block size may be reduced on the horizontal part of the section where the correction factor K_b must be unity at least with the small bedslopes that are normal. Hence the reduced block size for the horizontal bed $d_{e.h}$ is obtained from Eqns. (17) and (18) with $K_b = 1$

$$d_{e.h} = d_oS_b/[E_h\{(\gamma_s/\gamma)-1\}] \tag{35}$$

The resulting shift of the d_o- and b- values giving minimum cost per unit channel length is so minor that it safely may be neglected.

NUMERICAL EXAMPLE

Application of the method proposed in this paper is illustrated by the following numerical example

Given:

Discharge: $Q = 11.5\ m^3s^{-1}$

Bedslope: $S_b = 0.00375$

Inverse bank slope: $s = 1.75$

Free board: $d_1 = 0.75m$

Roughness/grain-size ratio: $r = k/d_e = 1.5$

Angle of repose of riprap: $\phi = 40°$

Riprap shape factors: $\begin{cases} ß_1 = 0.95 \\ ß_2 = 0.75 \end{cases}$

Normalized turbulent velocity fluctuation: $s_u = 0.164$

Probability of erosion: $p = 10^{-4}$

Specific gravity of blocks: $\gamma_s/\gamma = 2.65$

Acceleration due to gravity: $g = 9.81\ ms^{-2}$

Number of block layers: $N = 5$

Unit costs:
$$\begin{cases} \text{Excavation: } c_1 = 10\ \$\ m^{-3} \\ \text{Land: } c_2 = 7500\ \$\ ha^{-1} = 0.75\ \$\ m^{-2} \\ \text{Riprap: } c_3 = 20\ \$\ m^{-3} \end{cases}$$

Note that the constant width b_1 of the right of way is not needed since it drops out in the optimization process.

Find: d_o, b and d_e giving minimum total cost per unit length of the channel

Procedure: First calculate the lift shear stress ratio from Eqn. (3)

$$\overline{\lambda}/\overline{\tau_o} = 0.556[\ell n(1+(10.4/1.5)]^2 = 2.385$$

The value of Shields' entrainment function may now be found from Eqn. (2). The normalized velocity fluctuation corresponding to probability of erosion $p = 10^{-4}$ is found from Gaussian probability tables to be $t = 3.75$. Hence

$$E_h = \frac{0.75}{0.95} \cdot \frac{1 + 0.164^2}{\cot 40° + 2.385} \cdot \frac{1}{(1 + 3.75 \cdot 0.164)^2} = 0.0869$$

The correction factor for inverse bank slope is found from Eqn. (5)

$$K_b = \frac{(1.75^2 \tan^2 40° - 1)(\cot 40° + 2.385)}{2.385 \cdot 1.75 \tan^2 40° + \sqrt{((1.75^2 + 2.385)\tan^2 40° - 1)}} \cdot \frac{1}{\sqrt{(1 + 1.75^2)}} = 0.444$$

With these values the seven auxiliary constants K_1 through K_7 can now be found from Eqns. (17), (21), (28), (29), (30), (31) and (32)

$$K_1 = \frac{0.00375}{0.444 \cdot 0.0869 \cdot (2.65 - 1)} = 0.0589$$

$$K_2 = \frac{11.5 \cdot 1.5^{1/6} \cdot 0.0589^{1/6}}{8.25\sqrt{(9.81 \cdot 0.00375)}} = 4.850\ m^{5/2}$$

$$K_3 = 2 \cdot 1.75 + 4 \cdot 5 \cdot 0.0589 \cdot \sqrt{(1 + 1.75^2)} \cdot \left(1 + \frac{20}{10}\right) = 10.623$$

$$K_4 = 1 + 5 \cdot 0.0589 \cdot \left(1 + \frac{20}{10}\right) = 1.884$$

$$K_5 = 2 \cdot 0.75 \cdot \left(1.75 + 5 \cdot 0.0589 \cdot \sqrt{(1 + 1.75^2)} \cdot \left(1 + \frac{20}{10}\right)\right)$$

$$+ 2 \cdot 1.75 \cdot \frac{0.75}{10} \cdot (1 + 5 \cdot 0.0589) = 5.636\,\text{m}$$

$$K_6 = 0.75 + \frac{0.75}{10} = 0.825\,\text{m}$$

$$K_7 = \frac{5}{2}\left(\frac{5}{4} \cdot 1.75 - \frac{\sqrt{(1 + 1.75^2)}}{2}\right) = 2.949$$

Next the needed combinations of the seven auxiliary constants are calculated

$$K_2K_4 = 4.850 \cdot 1.884 = 9.137\ \text{m}^{5/2}$$

$$3K_6K_2 = 3 \cdot 0.825 \cdot 4.850 = 12.004\ \text{m}^{7/2}$$

$$2K_3 - (8/5)K_7K_4 = 2 \cdot 10.623 - (8/5) \cdot 2.949 \cdot 1.884 = 12.357$$

$$2K_5 - (4/5)K_6K_7 = 2 \cdot 5.636 - (4/5) \cdot 0.825 \cdot 2.949 = 9.326\ \text{m}$$

Introduction of these values in Eqn. (34) yields the equation

$$d_o = [(9.137 \cdot d_o + 12.004)/(12.357 \cdot d_o + 9.326)]^{2/5}$$

from which d_o is found by a simple iteration procedure.

Using $d_o = 0$ as a first estimate (seed value) yields the following convergent sequence of d_o-values

$$d_o = 0\ \text{m} \rightarrow 1.106\ \text{m} \rightarrow 0.984\ \text{m} \rightarrow 0.991\ \text{m} \rightarrow 0.990\ \text{m}$$

The corresponding bottom width is found from Eqn. (33)

$$b = 4.850/(0.990^{3/2}) - (2/5) \cdot 2.949 \cdot 0.990 = 3.756\ \text{m}$$

and the stone size from Eqn. (18)

$$d_e = 0.0589 \cdot 0.990 = 0.058\ \text{m} \cong 6\ \text{cm}$$

The bottom width/depth ratio

$$b/d_o = 3.756/0.990 = 3.794 > 2\sqrt{(1+1.75^2)} - 2 \cdot 1.75 = 0.531$$

as assumed in the development of the procedure.

Since the critical shear stress of a horizontal bed is higher than the critical shear stress of a sloping bank of the same material it is possible to use a smaller block size,

namely equal to $K_b d_e = 0.444 \cdot 6$ cm = 2.7 cm, on the horizontal part of the wetted perimeter. In this case the resulting savings are hardly worth considering.

For the Manning formula to be applicable in this example as assumed, the Reynolds' number, Re, based on mean velocity $v_{m.o}$ and hydraulic radius R_o must be in excess of 2300/4 = 575 to assure turbulent flow; the Wall Reynolds' number, Re_w, based on friction velocity $v_{f.o}$ and roughness $k = rd_e$ must be greater than 70 for the flow to be in the rough range. Finally, the inverse relative roughness, R_o/k, must be less than 300 but greater than five. In this numerical example the flow area is

$$A_o = bd_o + sd_o^2 = 3.756 \cdot 0.990 + 1.75 \cdot 0.990^2 = 5.434 \text{ m}$$

corresponding to the wetted perimeter

$$P_o = b + 2d_o\sqrt{(1+s^2)} = 3.756 + 2 \cdot 0.990\sqrt{(1+1.75^2)} = 7.747 \text{ m},$$

the mean velocity

$$v_{m.o} = Q/A_o = 11.5/5.434 = 2.116 \text{ ms}^{-1}$$

and the hydraulic radius

$$R_o = A_o/P_o = 5.434/7.747 = 0.701 \text{ m}.$$

The friction velocity may be found as

$$v_{f.o} = \sqrt{(gR_oS_b)} = \sqrt{(9.81 \cdot 0.701 \cdot 0.00375)} = 0.1606 \text{ ms}^{-1}$$

The three parameters are therefore

$$Re = v_{m.o}R_o/\nu = 2.116 \cdot 0.701/(1.3 \cdot 10^{-6}) = 1.141 \cdot 10^6 > 575$$

$$Re_w = v_{f.o}k/\nu = 0.1606 \cdot 1.5 \cdot 0.058/(1.3 \cdot 10^{-6}) = 1.074 \cdot 10^4 > 70$$

assuming a water temperature of about 10°C,

and $$5 < R_o/k = 0.701/(1.5 \cdot 0.058) = 8.1 < 300$$

confirming that the flow truly is in the range where the Manning formula applies.

REFERENCES

[1] US Army Corps of Engineers, "Hydraulic Design of Spillways," EM 1110-2-1603, Department of the Army, Washington, DC, 1990.

[2] US Army Corps of Engineers, "Hydraulic Design of Flood Control Channels," EM 1110-2-1601, Department of the Army, Washington, DC, 1991.

[3] Maynard, S. T., "Stable Riprap Size for Open Channel Flows," Technical Report HL-88-4, US Army Engineer. Waterways Experiment Station, Vicksburg, Mississippi, 1988.

[4] Bureau of Public Roads, "Use of Riprap for Bank Protection," Hydraulic Engineering Circular No. 11, US Department of Commerce, Washington, DC, 1967.

[5] Brown, S. A. and E. S. Clyde, "Design of Riprap Revetment, Hydraulic Engineering Circular 11, FHWA, US Department of Transportation, Washington, DC, March 1989.

[6] Pilarczyk, K. W., Havinga, H., Klaassen, G. J., Verhey, H. J., Mosselman, E., and Leemans, J.A.A.M., "Control of Bank Erosion in the Netherlands. State-of-the-Art," Publication No. 442, 32 pp. Delft Hydraulics, Delft, Holland, 1990.

[7] van der Knaap, Breteler, M. K. and van der Meulen, T., "Design Criteria for Geotextiles Beyond the Sand Tightness Requirement," Proceedings of the Third International Conference on Geotextiles, 6 pp.,Vienna, Austria, 1986.

[8] de Graauw, A., van der Meulen, T. and van der Does de Bye, M., "Design Criteria for Granular Filters," Publication No. 287, 25 pp., Delft Hydraulics, Delft, Holland, 1983.

[9] Hjulström, F., "The Morphological Activity of Rivers as Illustrated by River Fyris," Bull. Geol. Inst. Uppsala, Vol. 25, Uppsala, Sweden, 1935.

[10] Shields, A., "Anwendung der Ähnlichkeitmechanik und Turbulenzforschung auf die Geschiebebewegung," Mitteil. Preuss. Versuchsaust. Wasser, Erd, Schiffbau, No. 26, Berlin, Germany, 1936.

[11] Christensen, B. A., "The Mechanism of Sea Flow Erosion," Proc. of World Dredging Congress 1983, pp. 263-82, BHRA, Singapore, 1983.

[12] Christensen, B. A., Discussion of "Interaction of Flow and Incrustation in the Roman Aqueduct of Nimes," by G.F.W. Hauck and R.A. Novak, Journal of Hydraulic Engineering, Vol. 113, No. 2, ASCE, New York, NY, 1987.

[13] Christensen, B. A., "Replacing Hydraulic Radius in Manning's Formula," in "Channel Flow Resistance: Centennial of Manning's Formula," Ben Chie Yen, editor, Water Resources Publications, Littleton, Colorado, 1992.

SYMBOLS

The symbols used in this paper are defined where they first appear and in the following list

A	cross-sectional area
A_o	cross-sectional area corresponding to uniform flow
b	bottom width of trapezoidal cross section
b_1	width of right of way strips along channel
C	total cost per unit length of the channel
c_1	excavation cost per unit volume
c_2	land cost per unit area
c_3	cost per unit volume of placed riprap (including cost of geotextile or filter)
d_e	individual block size
$d_{e.h}$	individual block size on horizontal bed
d_o	normal depth in trapezoidal channel
d_1	free board
E_h	Shields entrainment function for horizontal bed
g	acceleration due to gravity
k	Nikuradses equivalent sand roughness
K_b	correction factor for bank slope
K_1, K_2, K_3, K_4, K_5, K_6, K_7	auxiliary constants
m	abscissa measured along wetted perimeter
M	roughness coefficient = $8.25\sqrt{(g)}/k^{1/6}$
n	Manning's n
N	number of layers of riprap blocks
p	probability of erosion

P	wetted perimeter
P_o	wetted perimeter corresponding to uniform flow
r	roughness/grain-size ratio = k/d_e
R	hydraulic radius = A/P
R_o	hydraulic radius corresponding to uniform flow = A_o/P_o
R_N	conveyance radius
s	inverse bank slope = $\cot\theta$
s_u	standard deviation of turbulent velocity fluctuation near bed normalized by local time-mean velocity
S_b	bed slope of channel
S_{EGL}	slope of energy gradeline in channel
t	normalized velocity fluctuation near bed corresponding to the probability p of exceeding
$\bar{v}$	time-mean velocity
$v_{f.o}$	friction velocity corresponding to uniform flow
$v_{m.o}$	cross sectional mean velocity corresponding to uniform flow
β_1	shape factor = (bed area associated with one block)/d_e^2
β_2	shape factor = (block volume)/d_e^3
γ	unit weight of water
γ_s	unit weight of block material
θ	inclination of channel bank with respect to horizontal
λ	Lagrangean multiplier
$\bar{\lambda}$	time-mean of hydrodynamic lift per unit bed area
ν	kinematic viscosity of water
$\bar{\tau}_{cr.h}$	critical shear stress of a horizontal bed, a time-mean value
$\bar{\tau}_{cr.b}$	critical shear stress of a sloping channel bank, a time-mean value
$\bar{\tau}_o$	time-mean bed shear stress
$\bar{\tau}_{o.max}$	time-mean value of maximum bed shear stress
ϕ	angle of repose of riprap material in place
ψ	constraint function

FIGURE CAPTIONS

Fig. 1. Typical Open Channel Section with Isovels and Orthogonals to Isovels.

Fig. 2. Trapezoidal Channel Section With Assumed Isovels and Boundary Shear Stress Distribution

KEY WORDS

Riprap, Erosion, Trapezoidal Channel, Hydraulic Radius, Critical Shear Stress, Optimum Design, Lagrange Method

MISSISSIPPI RIVER - GULF OUTLET TESTS OF RIPRAP BANK STABILIZATION

A.J. Combe and C.W. Soileau
US Army, Engineer District, New Orleans, USA

ABSTRACT

To develop the most cost effective structure to protect the toe of 11.5 miles of hurricane protection levee, New Orleans District tested four stone dike sections and two cellular concrete block revetments. The toe of the levee berm was being eroded by ship waves. The structures would be subject to wave action from the passage of ocean going vessels. The area has poor to very poor soil strengths. Thus a lighter structure that survives the wave action will be less subject to settlement. Each concrete block device and half the linear extent of the largest and smallest stone section was laid on a filter fabric (geotextile) as a separation between the armor units and the *in situ* material. The remaining stone sections were laid on a shell bedding layer. The performance of each structure is described using photography.

USING RIPRAP TO CREATE OR IMPROVE RIVERINE HABITAT

E.A. Dardeau, Jr., K.J. Killgore, Jr., A.C. Miller
US Army Engineer Waterways Experiment Station,
3909 Halls Ferry Road, Vicksburg, Mississippi, USA

ABSTRACT

Riprap is the oldest and most common construction material for river engineering projects. It is used to protect streambanks and streambeds from erosion, to build dikes used in river training, to provide grade control, and to fill gabions used for erosion control. In addition to its engineering use, riprap can improve riverine habitat quality, regardless of rock type, diameter, or length-width ratio. Invertebrates (such as caddisflies, midges, and freshwater mussels) and fishes of commercial and recreational importance can benefit from the use of riprap. Case studies illustrate the habitat value of riprap, which is particularly pronounced in alluvial river systems dominated by soft substrates.

1. INTRODUCTION

Many different methods and construction materials are used in river engineering (Dardeau 1981, Fischenich and Baxter 1992, Hemphill and Bramley 1989, Henszey et al. 1989, Keown et al. 1977). By far, the most common material chosen for protection is riprap, defined as "natural cobbles, boulders, or broken stone placed on a bank or filter as an armor against erosion" (Keown et al. 1977), as opposed to man-made materials (e.g., construction rubble or broken concrete) that have similar physical attributes. Man-made materials may offer needed protection, but they do not provide project aesthetic or recreational objectives, and they can cause deleterious environmental consequences (e.g., degradation of water quality). Riprap has also been successfully used in river training dikes, in grade-control structures, and as fill for gabions.

Increased demands placed on lotic ecosystems have intensified the need for habitat improvement and restoration. Restoration of altered habitats can

compensate for habitat altered by construction and operation of water resource projects. In riverine ecosystems, the placement of rock along the bank or in the channel can increase invertebrate production, provide rearing habitat for fishes, and create velocity refugia for fishes and invertebrates within the interstitial spaces. Riprap can also be used in riverine habitat creation. Cooperation of engineers and environmental scientists ensures that a project that achieves engineering objectives and provides habitat benefits for aquatic biota. This paper provides examples of habitat value of riprap for invertebrates and fishes.

2. HABITAT BENEFITS

Use of riprap in river engineering projects (e.g., rock dikes or sills or stone revetments) results in the creation or improvement of riverine habitat especially in soft substrates of alluvial river systems. Before the 1970s, habitat benefits of such construction were incidental to engineering objectives, such as flood protection, increased conveyance, or erosion protection. Because both environmental and engineering benefits must be addressed in project planning, design, construction, and maintenance, environmental scientists and engineers must work cooperatively in all project phases. Riprap is used to create or improve slackwater areas, low-flow channels, and artificial riffles; to modify or restore meandering alignments; and to control reconnection of flows between backwater areas and main channels.

Numerous riverine and riparian management and enhancement techniques that use riprap include installation of in-channel structures and sediment basins; streambank stabilization; and substrate manipulation (Shields and Hoover 1991, Wesche 1985). Placement of gravel, cobble, or boulders along the bank or in the channel promotes invertebrate production and provides additional rearing habitat and cover for fishes. Riprap can slow or halt bank erosion, thereby allowing recovery of natural vegetation (Wesche 1985), which also offers riparian and riverine habitat benefits. The most important characteristic of these features is the creation of depth, velocity, and substrate diversities to form food-producing areas, spawning and rearing areas, and instream and overbank cover to maintain reproductive populations (Wesche 1985).

3. INVERTEBRATE HABITAT

Riprap provides hard substrate for invertebrates, which is especially important in alluvial river systems where this material is scarce or absent (Mathis et al. 1982). Both larval insects and thin-shelled mussels can benefit from the placement of riprap on the banks or in the channels of such river systems.

Payne et al. (1989) studied the annual production of caddisflies (Tricopterae) and midges (Chironomidae) on the lower Mississippi River near Vicksburg, Mississippi. These authors reported that annual production of dominant populations of such organisms was slightly greater than 10 g/m^2 on riprap. This level of annual production is comparable to an average of 13 g/m^2 observed in high density populations of caddisflies on natural stone riffles in relatively pristine upper midwestern streams (Mackay and Waters 1986). Water quality in the lower Mississippi River can be considered moderate to good, although it usually has a high suspended-sediment load (Keown et al. 1986).

In the summer of 1987, Miller and Mauney (1993) collected freshwater mussels (Unionidae) in riprap in the St. Francis Floodway, Arkansas. Mussels are usually found in stable deposits of gravel, sand, or silt in large rivers or backwaters. Collections were made in 65- to 115-m sections of riprap protecting bridge supports at River Miles 22.0, 28.0, 31.0, and 33.0, in St. Francis and Lee Counties. These bridges and the associated riprap bank protection were constructed in the late 1950s and early 1960s. Live mussels were collected under and between large stones and then identified and counted. Twenty species were found on riprap, including high concentrations of a thin-shelled species, the fat pocketbook (*Potamilus capax*) listed as endangered by the U.S. Fish and Wildlife Service (1991).

The mussel fauna in the riprap was dominated by thin-shelled species such as fragile papershell (*Leptodea fragilis*) (63.6 percent), bleufer (*P. purpuratus* (13.4 percent), and fat pocketbook (6.2 percent). Three thick-shelled species, threeridge (*Amblema plicata plicata*), washboard (*Megalonaias nervosa*), and pimpleback (*Quadrula pustulosa pustulosa*), comprised only 9.86 percent of the fauna in the riprap (Figure 1).

During the summer and fall of 1987, Jenkinson and Ahlstedt (1988), using techniques similar to those of Miller and Mauney (1993), collected mussels at 252 sites with fine-grained sediments in the St. Francis River, the floodway,

and adjacent ditches. The thin-shelled species that Miller and Mauney (1992) found to be common to abundant in riprap were comparatively uncommon in fine-grained sediments. Conversely, Jenkinson and Ahlstedt (1988) reported that thick-shelled species, such as threeridge and washboard, were most common in fine-grained sediments (Figure 1).

Immature mussels are likely to be swept into riprap and trapped among the stones. A stable matrix composed of stone, gravel, sand, and detritus provides good habitat for thin-shelled bivalves that might not survive in shifting sand and gravel. In the St. Francis Floodway, thin-shelled species, including the endangered fat pocketbook, were more common among riprap than in fine-grained sand or silt. Although its principal purpose is to maintain navigation channels, the value of riprap for freshwater mussels should not be overlooked.

4. FISH HABITAT

Many freshwater fish species prefer and will seek out a hard substrate, particularly for reproduction and feeding. Rocks and other coarse-grained material can provide velocity shelters, predator refugia, and feeding areas for all life stages of a fish. Lithophils are fish that deposit their eggs on rocks or gravel (Balon 1984) and include important commercial and recreational fishes such as sturgeon (*Scaphirhynchus spp.*), paddlefish (*Polyodon spathula*), striped bass (*Morone saxatilis*), walleye (*Stizostedion vitreum*), and various species of suckers. Many species of larval fish also associate with hard substrates (Wallus et al. 1990).

Studies have reported an improvement in fish habitat following installation of riprap (Swales 1989). The variable size rocks used in revetment create slackwater areas in interstitial spaces can be used as resting and feeding sites. Riprap can harbor many species of fish, particularly those species that require swift water and hard substrate to complete one of more life stage. For example, Baker et al. (1991) listed 23 species of fish in the lower Mississippi River that are typically found associated with revetment (Table 1) and suggested that these habitats could harbor larger numbers of fish than currently indicated. The difficulty in sampling riprap placed in swift water hinders accurate assessment of its habitat value.

Substrates in channelized rivers usually consist of clay, silt, or sand.

Channelization often eliminates coarse-grained habitats, such as gravel bars, with a concomitant decrease in species diversity and abundance of fishes (Brookes 1988). Riprap may be the only hard substrate available to fishes in rivers that have been channelized or highly eroded, particularly alluvial rivers where natural coarse-grained habitats are rare.

Studies in the Yazoo River system, Mississippi, provide an example of the importance of riprap to fishes where naturally derived coarse-grained substrate is limited. Channel modifications have been implemented in the basin during the past 50 years, and the substrate consists of clay, sand, and silt. The only form of instream structure is fallen trees, which are sporadically scattered along the stream margins. With the exception of a few isolated gravel bars, riprap is the only type of coarse-grained substrate in the main stem rivers (Yazoo, Tallahatchie, Yalobusha, and Coldwater rivers), occurring downstream from the four flood control reservoirs (Arkabutla, Sardis, Enid, and Grenada), along bridge abutments, and along banks of highly populated areas.

Fish were sampled in the Upper Yazoo River system from 1989 to 1991 (Figure 2). Hoop net and electroshocking samples were collected in main stem rivers at four habitats: sandbars, banks with cover (submerged woody structure), banks without cover, and riprapped banks. The riprapped tailwater channels downstream from the four flood control reservoirs were also sampled (Killgore and Hoover 1986).

Mean catches from hoop nets (number of fish/net-night) for all species combined at the tailwater sites were considerably higher than for main stem river sites (Figure 3). Catches at riprapped sites within the main stem proved to be equivalent to those of banks with natural cover and greater than those for all other habitat categories. Fish often concentrate in tailwaters to feed on an abundant food supply released from the reservoir (Walburg et al. 1971). Most tailwaters are riprapped, which combined with high water velocities can attract fish that prefer swiftwater, coarse-grained habitats. Paddlefish and blue sucker (*Cycleptus elongatus)* are two such species that were collected at the tailwater sites in the Yazoo River system. Their abundance has declined in the lower Mississippi River valley partly due to a loss in spawning habitat (Dillard et al. 1986, Robison and Buchanan 1988). Riprap may be one of the few areas in which lithophils can successfully spawn.

Although there has not been direct observation of spawning, young-of-the-year blue suckers were collected over a flooded gravel road.

Catches from hoop nets in the main stem sites were variable among each habitat, suggesting that many of these fish move among habitats with no decided preference. Seasonal differences were evident, however. Flathead (*Pylodictis olivaris*) and blue catfish (*Ictalurus furcatus*) used banks with cover and riprapped banks in the summer (Figure 4). These two species spawn in June and July (Robison and Buchanan 1988).

River levels in the Yazoo system are usually low in the fall and winter, and much of the woody debris is above the elevation of the water surface. Submerged riprap can thus become a primary structural feature during low-water periods, as is exemplified by the relatively high abundances of three species of fish at main stem riprap sites during the fall and winter. Mean electroshocking catch for bluegill (*Lepomis macrochirus*), brook silverside (*Labidesthes sicculus*), and freshwater drum (*Aplodinotus grunniens*) was two to three times higher at riprap sites and banks with cover than other habitats sampled during low-water periods (Figure 5).

5. RIVERINE HABITAT COMPENSATION

Riprap has been used to compensate for lost riverine habitat. One recent example is the Upper Yazoo Projects (UYP), designed to address flood control in the alluvial floodplain of the Yazoo River Basin (called "the Delta"). Construction began in 1976 but was halted by court order with continuation subject to findings of the UYP Reformulation Study (U.S. Army Engineer District, Vicksburg 1989). The Reformulation Study was conducted to determine habitat losses in the Delta expected to result from the project and to evaluate the engineering, real estate, and management alternatives that will yield both the required project conveyance and compensation objectives (Dardeau et al. 1992).

The Habitat Evaluation Procedure (U.S. Fish and Wildlife Service 1980) was used to quantify changes in fish habitat for pre- and post-project habitat conditions. Killgore and Hoover (1992) determined habitat units for six target species of fish characteristic of the Delta: blacktail shiner (*Cyprinella venusta*), smallmouth buffalo (*Ictiobus bubalus*), channel catfish (*Ictalurus furcatus*), flathead catfish, largemouth bass (*Micropterus salmoides*), and white crappie (*Pomoxis annularis*). Habitat units are

composite measures of habitat quality and quantity calculated by multiplying a Habitat Suitability Index (HSI) value that ranges from 0.0 (unusable habitat) to 1.0 (optimum habitat) by the areal extent of that habitat). Loss of riverbank structure habitat will result from the removal of logs, woody debris, and live trees growing along the bank. Killgore and Hoover (1992) reported a habitat loss of 52 habitat units for the six target species.

To compensate for habitat losses, 5.3 ha of restored bank habitat will be required (Killgore and Hoover 1992). One mitigation alternative is the placement at or below the elevation of the 2-year-frequency flood of a mixture of 20 percent riprap, 20 percent gravel[2], and 60 percent logs, trees and woody debris (Dardeau et al. 1992). The riprap is quarry run limestone having a diameter range of between 20 (4.5-kg unit weight) and 38 cm (63.5-kg unit weight). Specified revetment thickness is 36 to 53 cm. The trees, logs, and woody debris will be constructed as a revetment of overlapping elements (crowns oriented downstream) placed below the elevation of mean low water. This design will ensure that the revetment will last at least as long as the 50-year project life.

6. CONCLUSIONS

Riprap is used primarily to maintain navigation channels; however, its value as riverine habitat is important when planning, designing, constructing, and operating a water resource project. Stable riprap provides habitat for invertebrates, such as aquatic insects and thin-shelled mussels that is of particular value when natural coarse-grained subtrate is scarce or absent.

This material can harbor many species and different life history stages of fish including those of commercial and recreational value. Stone placed on banks can provide areas for fish to feed, avoid predators, and find shelter from high currents. Riprap can be used to compensate for loss of riverbank habitat resulting from a water resource project while providing erosion protection for the banks, channel, project features (e.g., water control structures, levees, water intakes, or outfalls), or existing critical assets in the project area (e.g., bridges).

---

[2] Gravel placement is planned for backwater areas that are at or below the 2-year flood-frequency elevation.

7. RECOMMENDATIONS

Five general recommendations are that

(1) a team approach to project planning, design, construction, and maintenance that involves not only engineers but also habitat specialists be used to ensure that both the engineering objectives and environmental benefits are met.

(2) quantitative pre-project field surveys of existing hard substrate be conducted to determine both initial conditions and the amount of substrate loss expected to occur as a result of the project; in areas where substrate is lacking or losses are anticipated, riprap would have relatively high value for habitat compensation.

(3) riprap specified for a project should be well-graded and sized to withstand shear forces expected to occur at a given location.

(4) placement of riprap for riverine habitat purposes not be considered in areas of high sediment deposition.

(5) effectiveness of riprap placement be monitored to quantify changes in population or species composition.

8. REFERENCES

Baker, J. A., Killgore, K. J., and Kasul, R. L. 1991. Aquatic habitats and fish communities in the Lower Mississippi River. Critical Reviews in Aquatic Science, Vol 3, pp 313-356.

Balon, E.K. 1984. Patterns in the evolution of reproductive styles in fishes. Fish Reproduction: Strategies and Tactics (G. W. Potts and R. J. Wooton, eds.). Academic Press, London, pp 13-34.

Brookes, A. 1988. Channelized rivers: perspectives for environmental management. John Wiley and Sons, New York, 326 pp.

Dardeau, Elba A., Jr. 1981. Supplementary literature survey of streambank-protection methods. Supplementary report to technical report H-77-9, literature and preliminary evaluation of streambank-protection methods. US Army Engineer Waterways Experiment Station, Vicksburg, MS, 15 pp, 2 tables, 24 figures, appendices a-e. (also published as appendix a, part II. Final report to Congress, Streambank Erosion Control Evaluation and Demonstration Act of 1974, Section 32, Public Law 93-251).

Dardeau, Elba A., Jr., Fischenich, J. Craig, Olin, Trudy J., and Landin, Mary C. 1992. Upper Yazoo Projects Reformulation Study: environmental engineering design and mitigation considerations. Technical appendix to environmental impact statement. US Army Engineer District, Vicksburg, Vicksburg, MS, 54 pp, 20 tables, 19 figures (prepared by US Army Engineer Waterways Experiment Station, Vicksburg, MS).

Dillard, Joe G., Graham, L. Kim, and Russell, Thomas R., eds. 1986. The paddlefish: status, management, and propagation. Special publication 7, American Fisheries Society, North Central Division, Columbia, MO.

Fischenich, J. C., and Baxter, B. E. 1992. Colorado erosion control manual. Colorado Department of Natural Resources and Colorado Water Conservation Board, Denver, 90 pp, 5 appendices (prepared by US Army Engineer District, Omaha).

Hemphill, R. W., and Bramley, M. E. 1989. Protection of river and canal banks: a guide to selection and design. Construction and industry research information association report. Butterworths, London and other cities.

Henszey, Robert J., Wesche, Thomas A., and Skinner, Quentin D. 1989. Evaluation of state-of-the-art streambank stabilization. Wyoming Department of Environmental Quality, Cheyenne, WY, 224 pp.

Jenkinson, J. J., and Ahlstedt, S. A. 1988. A search for additional populations of *Potamilus capax* in the St. Francis and Cache River watersheds, Arkansas and Missouri. Tennessee Valley Authority, Office of Natural Resources and Economic Development, Knoxville, TN, 304 pp.

Keown, Malcolm P., Dardeau, Elba A., Jr., and Causey, Etta M. 1986. Historic trends in the sediment flow regime of the Mississippi River. Water Resources Research, Vol 22, No. 11, pp 1555-1564.

Keown, Malcolm P., Oswalt, Noel R., Perry, Edward B., and Dardeau, Elba A., Jr. 1977. Literature and preliminary evaluation of streambank-protection methods. Technical report H-77-9. US Army Engineer Waterways Experiment Station, Vicksburg, MS, 94 pp, 5 tables, appendices a-d (republished 1981 as appendix a, part I. Final report to Congress, Streambank Erosion Control Evaluation and Demonstration Act of 1974, Section 32, Public Law 93-251).

Killgore, K. Jack, and Hoover, Jan Jeffrey. 1992. Evaluation of the aquatic resources associated with the upper Yazoo River system, Mississippi. Technical appendix to environmental impact statement. US Army Engineer District, Vicksburg, Vicksburg, MS, 89 pp, 27 tables, 31 figures, 1 appendix (prepared by US Army Engineer Waterways Experiment Station, Vicksburg, MS).

Mackay, R. J., and Waters, T. F. 1986. Effects of small impoundments on hydropsychid caddisfly production in Valley Creek, Minnesota. Ecology, Vol 67, pp 1680-1686.

Mathis D. B., Bingham, C. R., and Sanders, L. G. 1982. Assessment of implanted substrate samplers for macroinvertebrates inhabiting stone dikes of the lower Mississippi River. Miscellaneous paper E-82-1. US Army Engineer Waterways Experiment Station, Vicksburg, MS.

Miller, A. C., and Mauney, M. 1993. Suitability of riprap in the St. Francis Floodway, Arkansas, as habitat for thin-shelled freshwater mussels (Mollusca: Unionidae). The Nautilus (in press).

Payne, Barry S., Bingham, C. Rex, and Miller, Andrew C. 1989. Life history and production of dominant larval insects on stone dikes in the lower Mississippi River. Lower Mississippi River Environmental Program report 18. Mississippi River Commission, Vicksburg, MS, 23 pp, 10 tables, 8 figures.

Robison, H. W., and Buchanan, T. M. 1988. Fishes of Arkansas. The University of Arkansas Press, Fayetteville, AR.

Shields, F. Douglas, Jr., and Hoover, Jan Jeffrey. 1991. Effects of channel restabilization on habitat diversity, Twentymile Creek, Mississippi. Regulated Rivers: Research and Management, Vol 6, pp 163-181.

Swales, S. 1989. The use of instream habitat improvement methodology in mitigating the adverse effects of river regulation on fisheries. Alternatives in regulated river management (J.A. Gore and G.E. Petts, eds.), CRC Press, Inc., Boca Raton, FL, pp 185-188.

US Army Engineer District, Vicksburg. 1989. Flood control, Mississippi River and tributaries, Yazoo River Basin, Yazoo Headwaters Project. General design memorandum 41, supplement 1. Vicksburg, MS.

U.S. Fish and Wildlife Service. 1980. Habitat Evaluation Procedures. ESM 102, Washington, DC.

US Fish and Wildlife Service. 1991. Endangered and threatened wildlife and plants. Federal Register, 15 July 1991. 50 CFR 17.11 & 17.12.

Walburg, Charles R., Kaiser Gerald L., and Hudson, Patrick L. 1971. Lewis and Clark tailwater biota and some relations of the tailwater and reservoir fish populations. Reservoir fishes and limnology (Gordon E. Hall, ed.). Special publication no. 8, American Fisheries Society, Washington, DC, pp 449-467.

Wallus, R., Simon, T. P., and Yeager, B. L. 1990. Reproductive biology and early life history of fishes in the Ohio River drainage. Volume 1: Acipenseridae through Esocidae. Tennessee Valley Authority, Chattanooga, TN.

Wesche, T. A. 1985. Stream channel modifications and reclamation structures to enhance fish habitat. The Restoration of rivers and streams (J. A. Gore, ed.), Butterworth Publishers, Boston, MA, pp 103-163.

Table 1. Fishes commonly associated with riprap in the lower Mississippi river (from Baker et al. 1991).

FAMILY	COMMON NAME	GENUS AND SPECIES
Acipenseridae	Shovelnose sturgeon	*Scaphirhynchus platorynchus*
Lepisosteidae	Longnose gar	*Lepisosteus osseus*
	Shortnose gar	*L. platostomus*
Clupeidae		
	Skipjack herring	*Alosa chrysochloris*
	Gizzard shad	*Dorosoma cepedianum*
	Threadfin shad	*D. petenense*
Cyprinidae	Common carp	*Cyprinus carpio*
	Mississippi silvery minnow	*Hybognathus nuchalis*
	Silver chub	*Macrhybopsis storeriana*
	Emerald shiner	*Notropis atherinoides*
	River shiner	*N. blennius*
	Silverband shiner	*N. shumardi*
	Mimic shiner	*N. volucellus*
Catostomidae	River carpsucker	*Carpiodes carpio*
	Blue sucker	*Cycleptus elongatus*
	Smallmouth buffalo	*Ictiobus bubalus*
Ictaluridae	Blue catfish	*Ictalurus furcatus*
	Channel catfish	*I. punctatus*
	Flathead catfish	*Pylodictis olivaris*
Atherinidae	Inland silverside	*Menidia berylina*
Percichthyidae	White bass	*Morone chrysops*
Percidae	Sauger	*Stizostedion canadense*
Sciaenidae	Freshwater drum	*Aplodinotus grunniens*

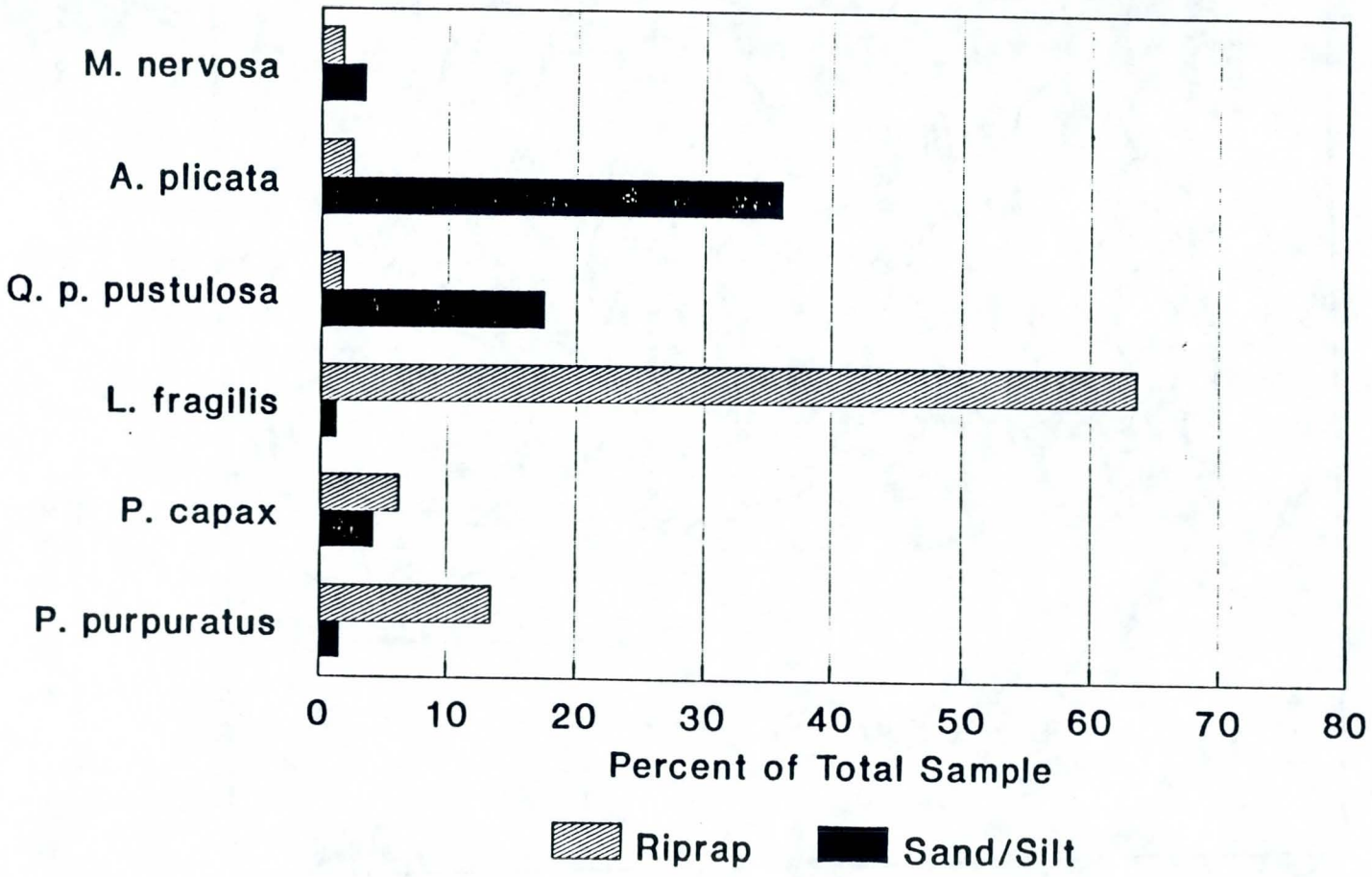

Figure 1. Comparison of thick- and thin-shelled species of mussels collected in fine grained sediments (Jenkinson and Ahlstedt 1988) and riprap (Miller and Mauney 1993) in the St. Francis Watershed, 1987.

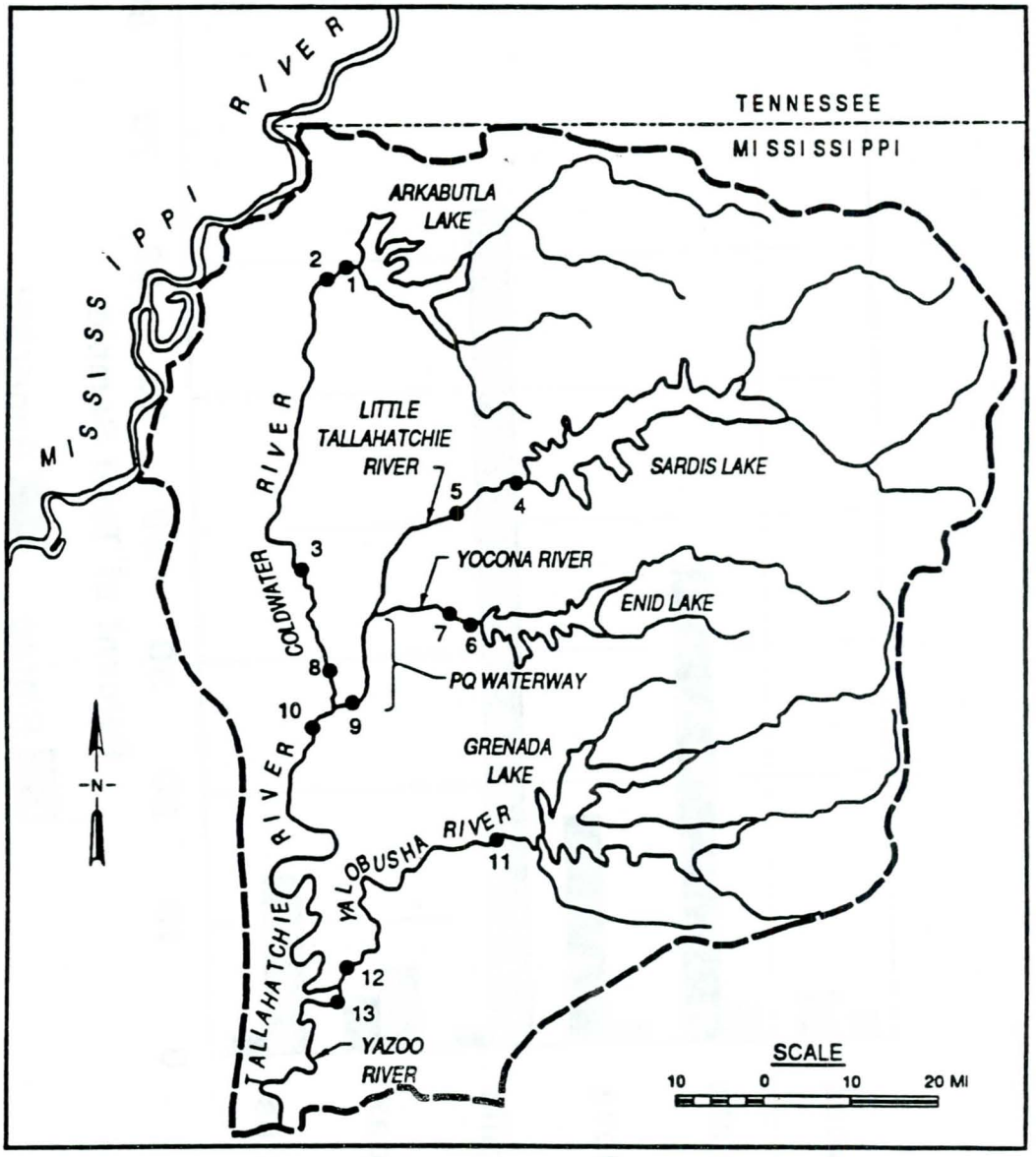

Figure 2. Locations of fish sampling sites, Upper Yazoo River system, 1989-1991 (adapted from Killgore and Hoover 1992).

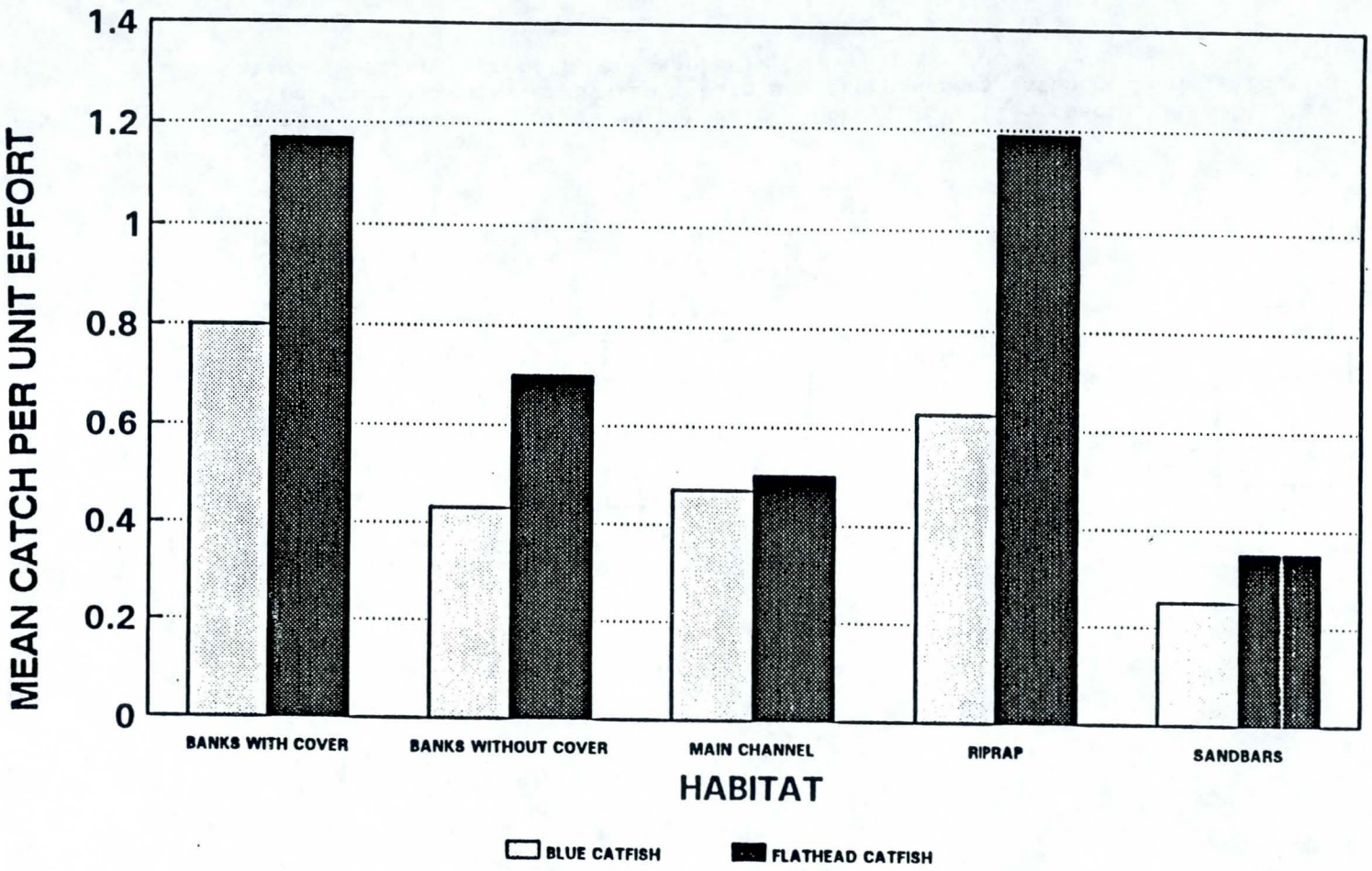

Figure 4. Summer shoreline habitat use by two fishes in the Upper Yazoo River System. Data are expressed as catch per unit effort (mean number/net-night; 373 samples).

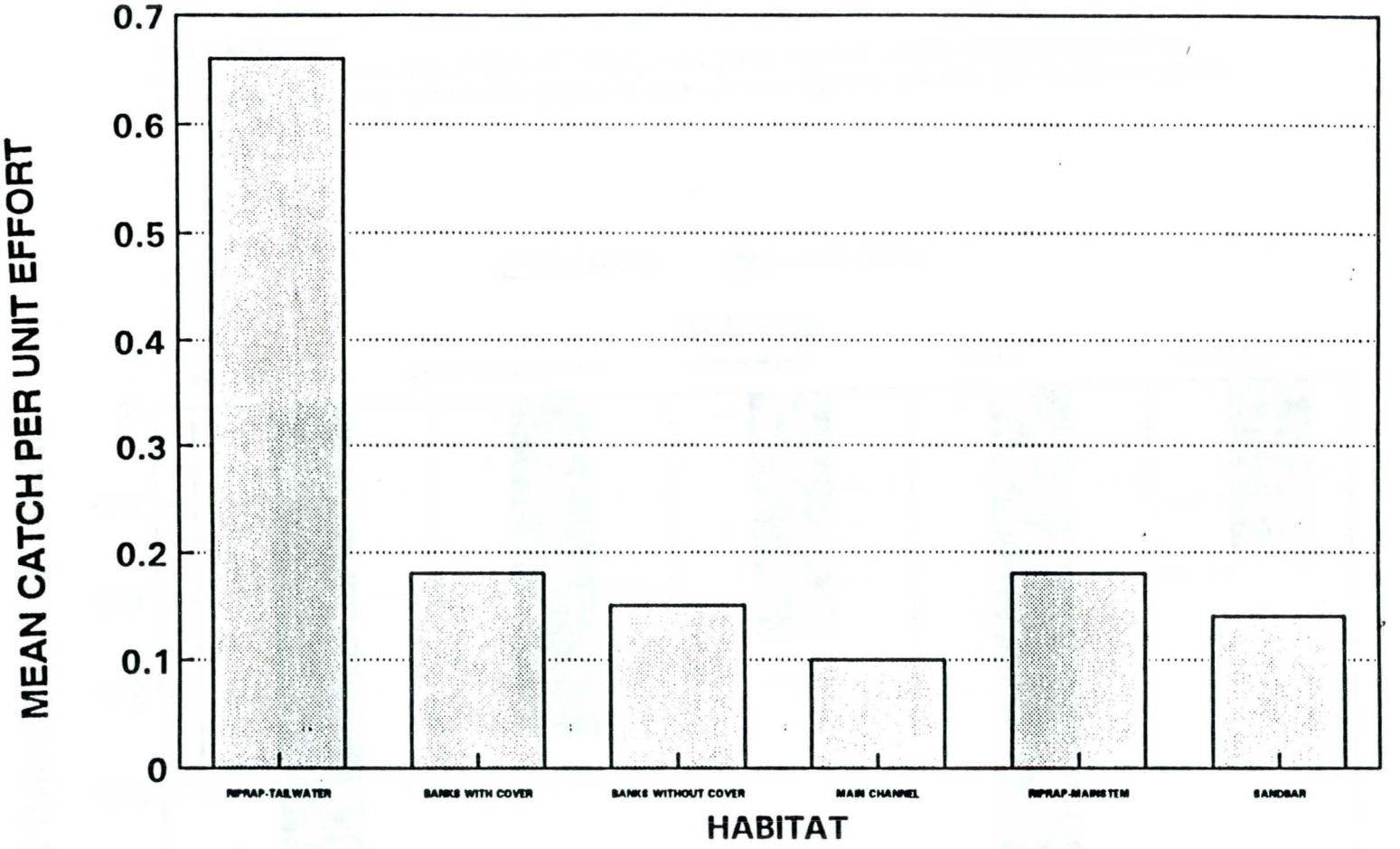

Figure 3. Comparison of catch per unit effort of all fish species at habitats in the Upper Yazoo River System. Data are expressed as catch per unit effort (mean number/net-night; 1,056 samples).

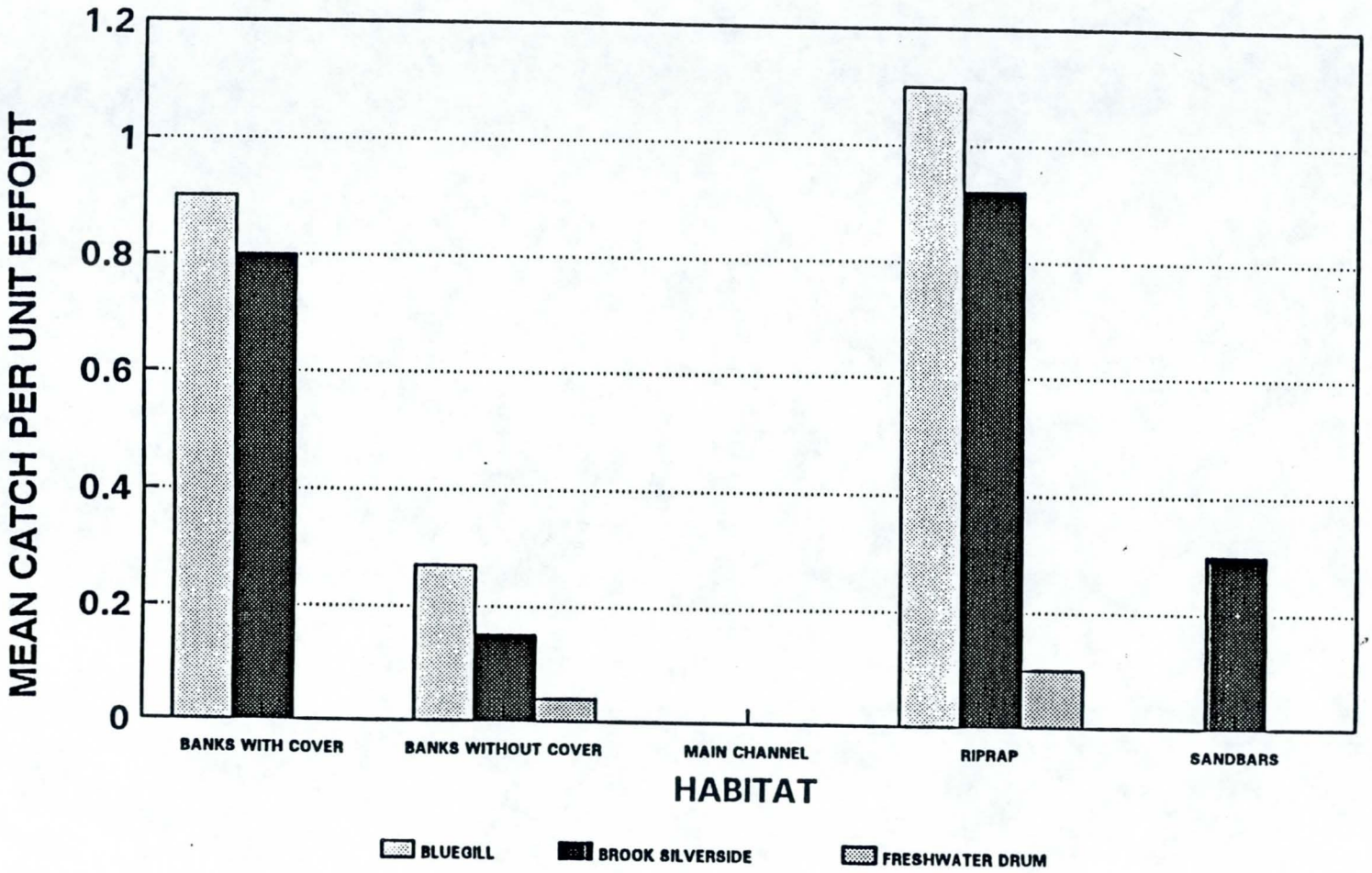

Figure 5. Fall/winter shoreline habitat use by three fishes in the Upper Yazoo River System. Data are expressed as catch per unit effort (mean number/ 10 minutes of electroshocking; 94 samples).

STANDARDIZED RIPRAP GRADATIONS

M.L. Dove
US Army Corps of Engineers, Lower Mississippi,
Valley Division, USA

General guidance for the design of riprap used at U. S. Army Corps of Engineers (Corps) structures and channels within the Lower Mississippi Valley Division (LMVD) is provided in Engineer Technical Letters, Engineering Manuals, and other Hydraulic Design Criteria. Using these criteria, the minimum 50 percent lighter by weight (W_{50}) of a stable layer is computed and a gradation band is specified for a given flow condition, design velocity and water depth. Typically there are a number of different design conditions at a large project and several different gradation bands could be computed. If all were specified, this could create a production problem for the rock quarries. The paper describes this problem and the field review and study undertaken by LMVD to minimize the number of gradations to be specified. For several years, LMVD has used the set of standard gradation curves developed.

PRINCIPLES OF STONE STABILITY AND THE PROBABILITY OF STONE BREAK

K.K. Duskaev
Al-Farabi Kazakh National State University

1. PROBABILITY METHOD OF ESTIMATION OF STABILITY OF PARTICLES OF MATERIAL MAKING RIVER BEDS AND CANALS

Stability of material fractions that river beds and canals consist of depends upon many factors most of them having an accidental character, that is why the probability method is more correct for the calculation of the stability of the beds.

Special research of stability of particles of non-connected material of the river bed has been conducted by the probability method [1].Stability of the fractions at the bottom has been estimated through probability P of break, which is equal to the ratio of quantity of the particles, having left the boundary of the bottom area under examination to the total quantity of the particles in the surface layer of the same area.

In general, value of P is the function of d , ρ , ρ_s , U_* , g , t , values, and of boundary conditions:

$$P = f(d, \rho, \rho_s, \nu, U_*, t, \text{ boundary conditions}) \quad (1.1)$$

The criterion equation has been derived using Buckingham's π -theory:

$$P = f\left(A_z, Re_*, Sh, \text{ boundary conditions}\right), \quad (1.2)$$

where $A_z = \frac{g d^3}{\nu^2}\left[\frac{\rho_s - \rho}{\rho}\right]$ - Archimedes number;

$Re_* = \frac{U_* d}{\nu}$ - dynamic Reynolds number;

$Sh = \frac{d}{U_* t}$ - Struhal number.

In order to exclude influence of observed area dimensions on the time of probability P realization, dependence $P = f(1/Sh)$ is given in the form of $P = f(1/Sh_*)$, where

$$1/Sh_* = \frac{U_* t}{d N} \quad (1.3)$$

$$N = \frac{F k}{\omega_i} \quad (1.4)$$

where ω_i is the area of projection of one particle.

The dependence (1.2) has the advantage over the dependence (1.1). This advantage is in that all its criteria have definite physical meanings: the criterion Re_* characterizes the flow, A_z characterizes the material of the bed, $Sh\,(1/Sh_*)$ characterizes the time of the flow influence on the particles.

As a result of experimental work it has been determined that there are two kinds of maximum velocity characterizing different stages of particles stability at the bottom:

1) maximum uneroding velocity U_o, when particles at the bottom are practically fixed and the probability P of their break is minimum and approaches zero. One can assign the value of U_o according to the problem solved and in accordance with the class of hydrotechnical construction strength, because practically to any velocity U (even to the smallest one) corresponds its own break probability P different from zero;

2) maximum eroding velocity U_e, exceeding of which leads to full destruction and flowing out of surface layer of the examined area. Steady transport of alluviums begins.

There exists some probability P_i of break of separate particles for the velocity, $U_o<U_i<U_e$ and this probability lies within $0<P_i<P_{max}$ (P_{max}= 7 - 10%). Moreover, to every velocity U_i corresponds quite definite value of P_i, and when this value is achieved particles break ceases irrespective of the duration of observation (automodel region for parameter $1/Sh_*$ at the given value of P).

Processing of experimental data for the automodel region for $1/Sh_*$ gives the following dependence of possibility of particles break from the bottom of a flow as:

$$P = A\left(\frac{Re_*}{\sqrt{A_z}}\right)^m \qquad (1.5)$$

In the region where $1/Sh_* < 1/Sh_{*B}$, the dependence for evaluation of P_i' has the next form:

$$P_i' = P_i \left[1 - e^{-0.06 (1/Sh_*)} \right] \qquad (1.6)$$

In its turn the value of $1/Sh_{*b}$ is determined by:

$$1/Sh_{*b} = \beta + \alpha P \qquad (1.7)$$

The procedure of calculation of bank fortification with stone heaps taking into account stone break probability has been worked out using observed results [2].

2. CALCULATION OF BANK FORTIFICATION WITH STONE HEAPS TAKING INTO ACCOUNT STONE BREAK PROBABILITY

2.1 General Cases of Calculation

One can encounter the next cases when calculating bank fortification.

a) The next values are given: U , H , d , k , dimensions F of the bed area intended for being protected, and flow influence time t. The time is a flood duration with consumption Q , corresponding to given velocity U . Stone break probability P (quantity of fortification material washed away) is to be calculated.

In this case equivalent roughness d_e is determined using known diameter d of bed particles. For this one can use the dependence proposed in [3].

$$d_e = 1.4 d^{0.75} \qquad (2.1)$$

Hydraulic resistance coefficient λ is calculated then. The value of λ for quadratic resistance region can be calculated using A.P. Zegda's formula:

$$1/\sqrt{\lambda} = 4\lg\left(\frac{R}{d_e}\right) + 4.25 \qquad (2.2)$$

After that U_* is determined using the connection of dynamic velocity with mean flow velocity:

$$U_* = U\sqrt{\lambda/2} \qquad (2.3)$$

Then using expressions (1.3) and (1.4) the value of $1/Sh_*$ is calculated. This value is compared with boundary value of $1/Sh_{*B}$, calculated by (1.7). In case when $1/Sh_* < 1/Sh_{*B}$ the value of P is calculated by the formula (1.6), and in case $1/Sh_* > 1/Sh_{*B}$ it is calculated by the formula (1.5).

b) Stone break probability P, values of d, H, k, F, and t are given. Flow velocity U (water consumption Q) corresponding to given stone break probability P should be determined.

As it has been mentioned above the value of P is assigned according to the class of the construction strength. The procedure of calculation of flow velocity U is as follows.

The value of A_z is calculated and the value of U_* is found for the given value of P by the formula (1.5). Further, velocity U is determined using relationships (2.1), (2.2), and (2.3). Then, comparing the values of $1/Sh_*$ and $1/Sh_{*B}$ one can establish whether the given value t is sufficient for realization of the given probability P on the area F.

c) The value of U . P . H . k . F. and $\pm$ are given. Size of fortification material is to be determined.

In this case the value U_* of is determined using expressions (2.2) and (2.3). Then Archimedes value A_z is determined using expressions (1.5) or (1.6) depending on $1/Sh_* > 1/Sh_{*B}$ or $1/Sh_* < 1/Sh_{*B}$. After that the size of particles corresponding to the given stone break probability is determined.

These are the most general cases in calculation of river bank fortification. Now, the case b), i.e., calculation of stone size in connection with its break probability will be considered.

2.2. Stone Size Computational Procedure

The equation for the initial stage of particles movement at the bottom of a flow in case of uniform motion is derived in the paper [4].

$$R_{e_*} = \alpha A_z^{n} \qquad (2.4)$$

where α and n are the parameters depending on the region of resistance (hydraulically smooth, transitional, or of quadratic resistance), and also on the form of particles.

In accordance with [4] the dependence (2.4) has the form of:

$$R_{e_*} = 0.162\, A_z^{0.5} \qquad (2.5)$$

for quadratic region of resistance, appearing when $d > 1 - 2\ 10^{-3}$ m.

Putting (2.5) into (1.5) gives $P = 0.037$. Consequently, we may state that probability of particles break equal to 3.7% corresponds to the velocity, given in paper [3].

Dependence (2.4) is used for development of stone size calculation procedure in case of bank fortification with stone heaping up (5). Dependences has been derived allowing to determine stone size in the center of a slope, at its foot, and at a water level. Taking into account casual character of the process of fortification erosion one can present these dependences in the form:

* for determination of stone size in the center of a slope d_m :

$$\left(\frac{d_m}{H}\right)^{0.61} = A' F_z \frac{K_2}{K_1} \qquad (2.6)$$

* for determination of maximum stone size at the foot of the slope when d_m is known:

$$\frac{d_{max}}{H_0} = A' F_z \frac{K_3}{K_1}\left(\frac{d_m}{H_0}\right)^{0.39} \qquad (2.7)$$

* for determination of minimum stone size at the water level:

$$\frac{d_{min}}{H_0} = A' F_z \frac{K_4}{K_1}\left(\frac{d_m}{H_0}\right)^{0.39} \qquad (2.8)$$

where K_1 , K_2 , K_3 , K_4 are the coefficients, derived from special formulae and nomograms [5].

Using experimental data, formulae (1.5) and (2.4) allow to establish relationship between probability P, parameters α and A' (Figs.1 and 2). Having this relationship and using formulae (2.6 - 2.8) one can determine stone size in the center of a slope, at its foot, and at the water level with given probability of stone break. But in this case probability P of stone break should be assigned, and this probability in its turn should be put in correspondence with designed probability of flood consumption excess.

2.3. Choice of Designed Probabilities of Stone Break and of Provision of Flood Consumption

Designed probability of flood consumption excesses is assigned in accordance with the class of a construction strength. For example, for railways of the first and the second categories the designed P_d probability of consumptions excesses and of water levels in rivers corresponding to these excesses is taken to be 1%. But incidentally constructions of these categories should be tested for the case of passing through the river the consumption having maximum probability P_{max} of excess equal to 0.33%. Apparently, the problem should have an optimal decision because the smaller is the probability of stone break the bigger is the stone size with given designed value of water consumption in a river. In this case the interval of the construction operation without a crash becomes greater. And on the contrary, if having the same conditions to increase the probability of stone break, stone size will be smaller and the interval of the construction operation without a crash will be smaller too. Thus, the problem is to find an optimal decision. Below we give one of the possible ways of its realization.

First of all, permissible value of stone break probability $P=P_p$ is assigned, moreover P_p = 5 - 7% (with reserve coefficient of 1.5 regarding the maximum value P_{max} = 7 - 10%) velocity U_d corresponding to this assigned value. Then, according to the procedure described in 2.2, necessary stone size is determined using given probability of stone break, and water consumption corresponding to the designed probability P_d of exceeding of water consumption. After that, the stone size is tested for the probability P of break, when the consumption in the river $Q=Q_{Pmax}$. When the probability P of break appears to be greater than

7 - 10%, it means that the construction will be destroyed with a flood having $Q_{p\,max}$. In this case recalculation of stone size should be done with the same probability P_p of stone break and of water consumption of $Q_{p\,max}$.

All further calculations should be made by a construction maintenance department. Having data about floods in the river, knowing stone size laid in the construction it can determine the quantity of stones washed away. Admissible extent of the construction destruction not making it unsafe being assigned, dates of repairs of the construction can be determined

The calculations can be done on the stage of a construction designing using a number of consumptions observed (hydrograph).

One meets great technological difficulties when making a slope fortification with stone of determined size. To make bank fortification with rock mass is easier to a far greater extent.

2.4. Stone Size Calculation in Case of Bank Fortification with Rock Mass

Stone size calculation in this case has no difference from one described above. But in rock mass there should be stone sizes to which probability P of break, smaller than permissible one P_p corresponds ($P<P_p$), when there is a flood in the river having consumption of designed probability Q_{pd} , or, if it is necessary of $Q_{p\,max}$. However, there are some peculiarities of the calculation lying in that there is fine material in rock mass. This fine material will be fully washed out because it has break probability greater than 7 - 10%. Consequently, the volume of the rock mass in a construction body should be greater than it is necessary. The excess of rock mass must be equal

to the volume of small fractions. Some destructions are assumed in such constructions, essentially big ones when designed floods pass through the river. But the process will subside owing to formation of weekly washed out layer of coarse fractions.

Let us assume that as the result of the process subsidence there has been formed a layer of stones of middle size d_m on the slope of the construction. Then the volume of the layer on the area F of the slope is equal to $d_m F$. Suppose, rock mass has X_m particles of size $d \geq d_m$ according to a curve of granulometric composition. Then apparent equality is correct:

$$d_m F = \Delta h F X_m \qquad (2.9)$$

where Δh is the thickness of the layer of the material left in place by the flow (X_m is measured in parts of a unit). Then additional thickness of the rock mass Δh_d on the slope can be found. This additional thickness should be foreseen in a construction design taking into account the fact that after the process of washing out of fine fractions the construction dimensions should correspond to necessary conditions of its reliable maintenance. Considering (2.9) we have:

$$\Delta h_d = \Delta h - d_m = d_m \frac{X_i}{X_m} \qquad (2.10)$$

where X_i is the quantity of particles of size $d < d_m$ in rock mass.

ACKNOWLEDGMENT

The author is grateful to professor M.A. Mihalev for his consultation during the work conduction.

REFERENCES

1. Дускаев К.К. Условия начала трогания и массового движения частиц несвязного крупнозернистого материала. Труды ЛПИ N415. Ленинград, изд ЛПИ, 1986, с. 89-92

2. Дускаев К.К. Расчет берегоукрепления из каменной наброски с учетом вероятности срыва камня. Труды Пятого Всесоюзного гидрологического с'езда, т. 10 кн. 2, Ленинград, Гидрометеоиздат, 1988, с. 260-266

3. Кнороз В.С. Неразмывающая скорость для несвязных грунтов и факторы ее определяющие. Изв. ВНИИГ, 1958, т. 59, с. 62-81

4. Михалев М.А. Материалы по моделированию некоторых видов движения вязкой жидкости. Изв. ВНИИГ, 1975, т. 108, с. 27-39

5. Михалев М.А. Расчет крупности камня при берегоукреплении каменной наброской. Гидротехническое строительство. 1983, N11, с. 32-34

NOTATION

A - parameter in formula for break probability
A' - parameter in formula for stone size calculation
d - diameter of bed particles (stone size), m
ρ_s - density of bed, kg/cubic m
ρ - water density, kg/cubic m

$F_r = \frac{U^2}{gH}$ - Froud number

g - acceleration due to gravity, m/s
U - mean velocity of flow, m/s
U_* - dynamic velocity, m/s
U_o - uneroding velocity, m/s
U_e - eroding velocity, m/s
H - depth of flow, m
k - coefficient of bed porosity
m - index in formula for break probability
N - number of particles in the surface layer of bed
P - probability of break of particles
P_p - permissible probability of particle break
Q - water consumption, cubic m/s

Q_{pd} - consumption of designed probability of excess

Q_{Pmax} - consumption of maximum probability of excess

t - time of flow influence on the particles
λ - coefficient of hydraulic resistance
ν - kinematic coefficient of water viscosity, square m/s
X - quantity of particles in the curve of granulometric composition, measured in parts of a unit

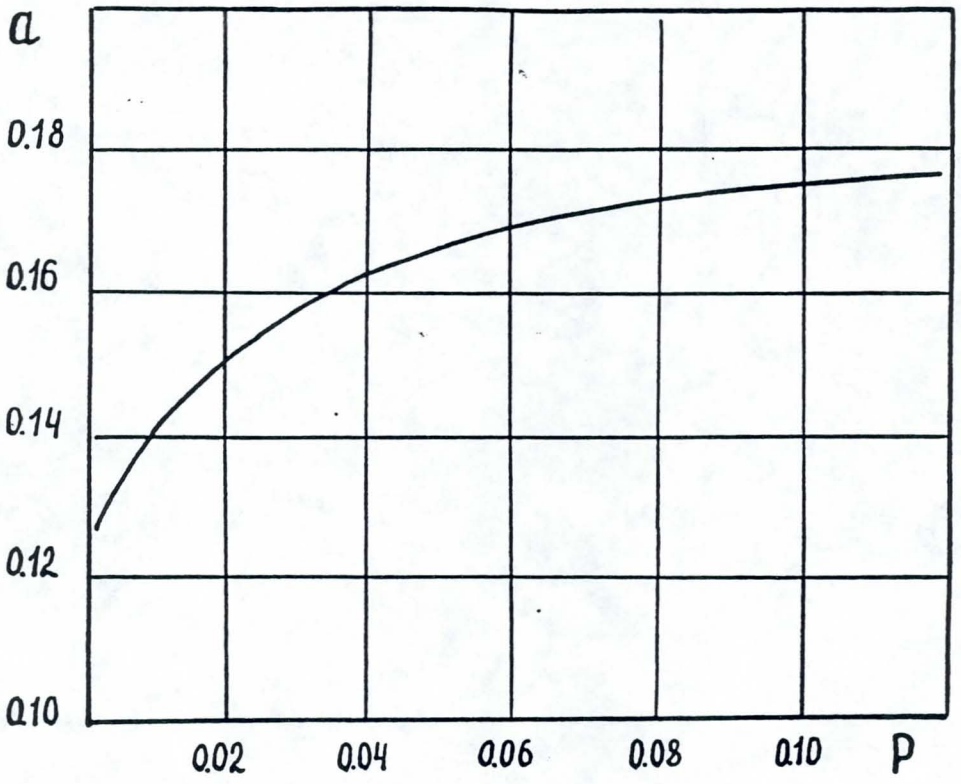

Fig 1. Dependence $a = f(p)$

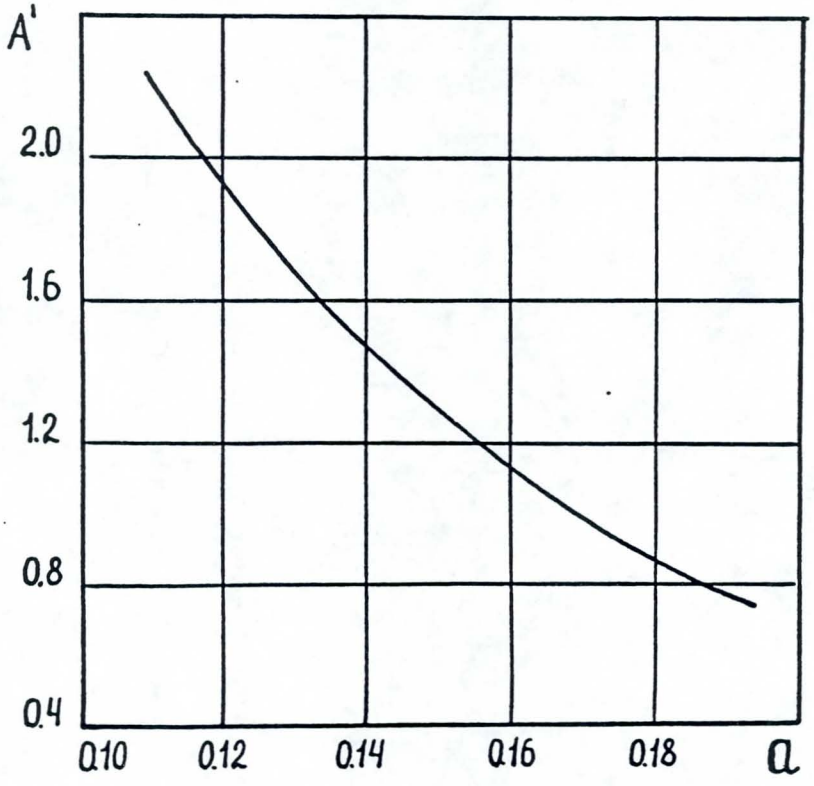

Fig 2. Dependence $A' = f(a)$

WAVE ENERGY DISSIPATION BY COMPOSITE BREAKWATER

A. El-Fiky, A. El-Mongy and M.M. Talaat
Ain Shams University, Faculty of Engineering,
Abbassia, Cairo, Egypt
M.M. Anwar
Helwan University, Faculty of Engineering, Cairo, Egypt

1. INTRODUCTION

Composite breakwater is a permanent structures consisting of a rubble-mound base which mounted by monolithic vertical structure. When waves impact a vertical obstacles, a portion of their momentum is reflected, another portion is transmitted, the rest is lost thoroughly the breakwater by friction and permeability. These portion cause a wave height changes.

The present study aims to obtain empirical formulae for calculating coefficient of transmission "C_t", Coefficient of reflection "C_r", and the amount of energy lost through the modeled composite breakwater, relating all variables to the wave and breakwater characteristics such as wave length (L), wave height (H), total water depth (d), free water depth (d_1) at the toe and toe breadth (B).

Experimental work was conducted at the laboratory of hydraulics and irrigation, Faculty of Engineering, Ain Shams University. Relation between different parameters such as C_r, C_t, E_r/E_i, E_t/E_i, E_L/E_i relating to H/L, B/d, d_1/d were drawn to show the effect of increasing H/L or B/d or d_1/d at the values of C_r, C_t, E_t/E_i, E_r/E_i, E_L/E_i.

Empirical relations were obtained for the calculation of the transmission coefficient "C_t", reflection coefficient "C_r", the percentage of the transmitted energy "E_t/E_i", the percentage of the reflected energy "E_r/E_i" and finally the percentage of energy lost by friction and breaking "E_L/E_i".

2. EXPERIMENTAL WORK

The experimental work was conducted in a wave flume at the hydraulics laboratory of Ain Shams University, Figure 1. It has a reinforced concrete bed rising 0.80 m above the laboratory ground level, its sides are either reinforced or glass panels fixed in aluminum frames, these panels are as follows, beginning from the end at which the motor exists: - 0.30 cm R.C., 2.65 m glass, 3.05 m R.C., 2.95 m glass, and 5.05 m R.C.. The total length of the flume is 14.00 m. The flume width is 0.50 m, and the overall width is 0.82 m. The maximum allowable water width is 0.60 m. The wave flume is equipped with a wave generating machine designed and fabricated locally.

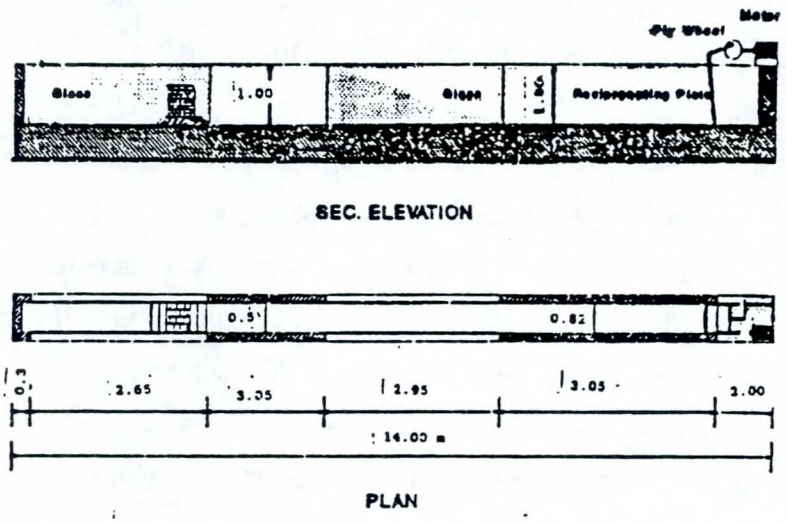

Figure 1. Longitudinal Section and Plan of the Flume

The wave generating machine consists of:-

a) Motor:- which is fixed on a steel plate that rests on a concrete slab of thickness 15 cm, supported on the walls of the flume.

b) Three pulleys:- Pulleys function is similar to that of a gear box. They are responsible of the variation of the motor's speed.

c) Flying wheel:- The flying wheels are two disks of diameter equals to 30.0 cm, each has a groove of length 9.0 cm. The wheels are rotated by shafts that are connected to the motor. They are also connected to wave paddle plate by means of two cranks, the length of each crank is 44.0 cm.

d) Wave paddle:- It is a reciprocating steel plate with length 107.0 cm and width 50.0 cm. The plate's function is to generate waves by its periodical motion which rises from the eccentric fixation of the cranks on the flying wheels. The flume is equipped with two aluminum carriages, each moves on two aluminum rails. On these carriages wave height indicator is fixed. In order to absorb the generated wave behind the reciprocating plate and to prevent its interference with the main front wave a 4:1 gravel slope of 2.00 m length and 0.60 m height was used inside a meshed casing at the back of the plate.

An electrical indicator is used to measure the wave heights generated in the flume and consists of:-

a) Buoy:- It is a floating buoy resting at the water surface and moves vertically up and down due to the variation of the water surface level, this buoy is a hollow foam cube of 15.0 cm side length.

b) Metal bar:- A vertical bronze bar connecting the buoy with the resistance box, its length is 50.0 cm. Its weight is so small that it can be neglected.

c) Resistance box:- A wooden box containing electrical conducting slice, the distance between each of them is 0.50 cm, there are 40.0 conductors, so the maximum wave height that can be measured by this instrument is 20.0 cm.

d) Light board:- It is a board containing 40 small lamps, each of these lamps bright when the metal bar touches the pointer since the electric circuit is completely closed. The accuracy of this indicator is 0.50 cm, so its accuracy is limited.

During the experimental work different parameters were used as mentioned before.

In this study about 550 runs were done. The following steps represent the procedure of one of these runs:

1) The breakwater under investigation is installed near the end of the flume, then the flume is filled to the required height.

2) The motor is operated after adjusting the steel rod at a certain eccentric chosen distance on the flying wheel to give a certain wave condition.

3) The wave period was checked by marking a point on the flying wheel and measuring the time taken by the marked point to revolve 10 revolutions.

$$T = (\text{total time})/10$$

4) The wave celerity (C) is measured by pursuing a wave crest travelling a certain distance "l" in a time "t". C= l/t

5) The wave length L is calculated from the relation:-

$$L = C*T$$

6) The maximum and minimum water levels, at the front surface of the model breakwater are measured to determine the incident and reflected wave heights "H_i", "H_r" where:

$$H_i = \frac{H_{max} + H_{min}}{2} \quad , \quad H_r = \frac{H_{max} - H_{min}}{2} \qquad (2.1)$$

7) The transmitted wave height "H_t" is measured at the rear surface of the model

8) The above experimental measurements were taken in order to calculate the following:-

a) The coefficient of reflection "C_r":-

$$C_r = \frac{H_r}{H_i} \qquad (2.2)$$

c) The percentage of energy dissipated by reflection:-

$$\frac{E_r}{E_i} = \frac{\frac{1}{8}\rho g H_r^2}{\frac{1}{8}\rho g H_i^2} = C^2_r \qquad (2.3)$$

d) The percentage of transmitted energy:-

$$\frac{E_t}{E_i} = \frac{\frac{1}{8}\rho g H_t^2}{\frac{1}{8}\rho g H_i^2} = C_t^2 \qquad (2.4)$$

e) The percentage of energy dissipated by breaking and friction:-

$$\frac{E_L}{E_i} = 1 - C_r^2 - C_t^2 \qquad (2.5)$$

3. ANALYSIS

Measured results were used to calculate several variables. It is for simplification that all types of energies were written in a dimensionless terms relative to the incident energy. Many relations were obtained from the experimental work, and curves were drawn and fitted by means of the exponential regression. These curves relate H/L with each of C_r, C_t, E_r/E_i, E_t/E_i, E_L/E_i. The figures given later show examples of the relations between H/L and each of the above variables for different values of B/d and d_1/d.

More graphical relations were drawn based on the above shown figures, in order to throw a more light on the problem under study. Relations between both B/d and d_1/d and all other parameters are shown in Figures 2 to 17.

From the above figures one can obtain the following general remarks:-

1) As the wave steepness becomes bigger, both of the coefficient of reflection and the amount of the reflected energy decrease.

2) For constant B/d and constant value of H/L as the ratio of d_1/d increases, the value of the coefficient of reflection and the value of the reflected energy decrease.

3) As the wave steepness becomes bigger, both of the coefficient of transmission and the amount of the transmitted energy decrease.

4) For constant B/d and constant value of H/L as the ratio of d_1/d increases the value of the coefficient of transmission and the transmitted energy decrease.

5) The amount of energy lost due to friction and breaking increases with the increase of the wave steepness.

6) As the ratio of d_1/d becomes bigger, the amount of the energy lost by friction and breaking decreases, this happen for constant B/d and H/L.

4. GENERAL EMPIRICAL RELATIONS

To find approximate formulae for the calculation of the transmission coefficient "C_t", reflection coefficient "C_r", the transmitted energy "E_t/E_i", the percentage of the reflected energy "E_r/E_i", and finally the percentage of the energy lost by friction and breaking "E_L/E_i"; these dimensionless parameters were related to the wave height "H", wave length "L", free depth of the water "d_1", total depth of water "d", and breadth of toe at the rubble part of the composite breakwater "B". The effective independent variables

were grouped in a series of dimensionless parameters (H/L, d_1/d, B/d) and an exponential regression was used to fit the data and to determine the constants of the functions relating the dimensionless dependent and independent variables. Different functions were tried and the following empirical formulae gave the best correlation:-

$$C_t = 0.0435676 e^{(20.69396 H/L + 0.649628 d_1/d + 0.20888 B/d)} \quad (4.1)$$

$$C_r = 0.1053265 e^{(19.52178 H/L + 0.041559 d_1/d + 0.287743 B/d)} \quad (4.2)$$

$$\frac{E_t}{E_i} = 0.0018689 e^{(40.2549 H/L + 1.314934 d_1/d - 0.36477 B/d)} \quad (4.3)$$

$$\frac{E_r}{E_i} = 0.011073 e^{(38.8208 H/L + 0.093772 d_1/d + 0.581008 B/d)} \quad (4.4)$$

$$\frac{E_L}{E_i} = 0.4811 e^{(11.96335 H/L + 0.832087 d_1/d - 0.57939 B/d)} \quad (4.5)$$

such that :-

H/L ranged from 0.014 to 0.09

d_1/d ranged from 0.25 to 0.70

B/d ranged from 0.65 to 1.55

5. CONCLUSIONS AND RECOMMENDATIONS

1) From the experimental results and curve fitting we obtained mathematical formulae for the determination of the coefficient of transmission "C_t", and the coefficient of reflection "C_r" for waves attacking composite breakwater. These formulae are:-

$$C_t = 0.0435676 e^{(20.69396 H/L + 0.649628 d_1/d + 0.20888 B/d)} \quad (5.1)$$

$$C_r = 0.1053265 e^{(19.52178 H/L + 0.041559 d_1/d + 0.287743 B/d)} \quad (5.2)$$

These equations proved to be reliable in the range of experiments (i.e. H/L ranges from 0.014 to 0.09, d_1/d ranges from 0.25 to 0.70, and B/d ranges from 0.65 to 1.55). Thus for

design purposes, it seems easy to calculate the values of coefficient of transmission "C_t", and the coefficient of reflection "C_r" when using these general equations.

2) The amount of transmitted or reflected energy increases with the increase of either the ratio between toe breadth and water depth (B/d) or the ratio between free depth of water at the toe and total depth (d_1/d), while it decreases with the increase of wave steepness (H/L). It was noticed also that the transmitted energy increases with the increase of both d_1/d and B/d; but with a rate much lower than that of the reflected energy. Accordingly the amount of the energy lost by friction and breaking decreases with the increase of either the ratio between toe breadth and water depth (B/d) or the ratio between free depth of water at the toe and its total depth (d_1/d), while it increases with the increase of the wave steepness.

3) The sue of the deduced empirical formulae shows that the sum of the dissipated energy by reflection, breaking, and friction together with the transmitted energy is approximately equal to unity with an error 7% for the variation of B/d, 3% for the variation of d_1/d, and 9% for the variation of H/L.

4) The dimensions of the rubble part of the composite breakwater have an important effect:-

effect of breadth:- When toe breadth increases, both of the coefficient of reflection "C_r", and the coefficient of transmission "C_t" increase. Since the rate of change for both the coefficient of reflection and the coefficient of transmission increases rapidly when the value of B/d is more than 0.70, therefore this ratio is considered a suitable value for the design purpose.

effect of thickness:- When the thickness of the rubble layer increases (i.e. the ratio od d_1/d decreases) it causes the decrease of both the coefficient of transmission and reflection. It was found experimentally that when d_1/d becomes greater than 0.40 to 0.50 the coefficient of reflection increases and the coefficient of transmission increases also, in such a way that transmitted waves can have a damaging effect inside the harbor. Consequently, for the design purpose, it is recommended that B/d is not to be greater than 0.70 and d_1/d to be 0.50.

6. REFERENCES

Anwar, M. M. " Wave Energy Dissipation By Composite Breakwaters", M.Sc. Thesis presented to Ain Shams University, Cairo, Egypt, 1992.

Bijker E.W., Massie W.W., and V.D.graaf, " Coastal Engineering Manual" Vol.1, 2, 3, Delft University of Technology, 1985-1986.

Bird, H.W.K. "Wave Interaction With Large Submerged Structures, A two dimensional boundary element approach", M.Sc. University of California, Calif, 1981.

Bovin, R. "Comment On Vertical Breakwaters With Low Coefficient Of Reflection". The dock and harbor authority, 45, June 1960. pp56-61.

Brauhn, Per " Destruction Of Wave Energy By Vertical Walls", Proceeding of american Soc. of Civil Engineering, Vol.82, Journal Waterway Division No.WW1, New York, March 1965, pp 912.

EL-Fiky, A., EL-Mongy, A., Sarhan, E.A., " Experimental study of the effect of geometrical parameters of detached breakwaters on wave energy", Ain Shams University, Eng. bulletin, Vol.25, No.3, Dec., 1990, pp 74-92

EL Serafy, S., "Wave Energy Dissipation By Rubble Mound Breakwaters", M.Sc. thesis presented to Ain Shams University, Cairo, Egypt, 1988.

Kamel, A.M., "Water Wave Transmission and Reflection by Porous Structures", WES. Research Report H-69-1; Oct. 1969.

Kobous, Helmut , "Hydraulic Modelling"; German Association for Water Resources and Land Improvement issued in cooperation with international association for hydraulic research.

Kondo, H. and Toma, S., "Reflection and Transmission for a Porous Structure", Proc.13th Coastal Engineering Conference,Vancouver, Canada, 1972.

Shore Protection Manual, Vol. 1 and 2. Coastal Engineering Center 1984.

Sollitt, Charles K. and Ralph H. Cross III " Wave Reflection and Transmission At Permeable Breakwater", Technical Paper No. 76-8, June 1976.

Yashimi, Goda "Re-analysis of laboratory data on wave transmission over breakwaters", Report of port and harbor research institute, Vol.8, No.3, Sept. 1969.

NOMENCLATURE

B : toe breadth

C : celerity

C_r: coefficient of reflection

C_t: coefficient of transmission

d : total water depth

d_1: free water depth at the toe

E : energy per squared meter in joules

E_i: incident wave energy

E_L: energy lost by friction & breaking

E_r: reflected wave energy

E_t: transmitted wave energy

g : acceleration due to gravity

H : wave height

H_i: incident wave height

H_r: reflected wave height

H_t: transmitted wave height

L : wave height

H/L: wave steepness

T : wave period

ρ : density of salt water

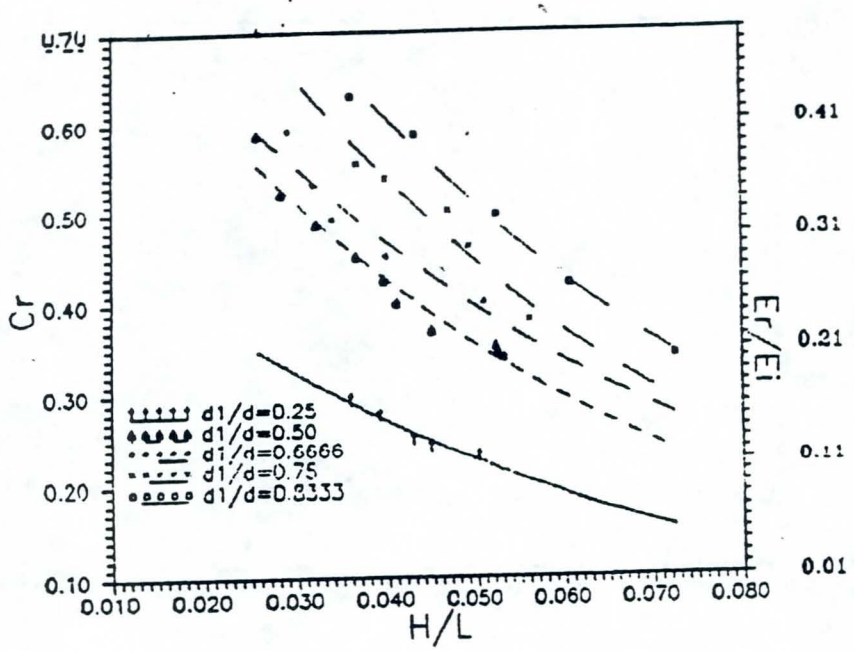

Figure 2. Relation Between H/L & C_r and E_r/E_i at B/d = 1.00

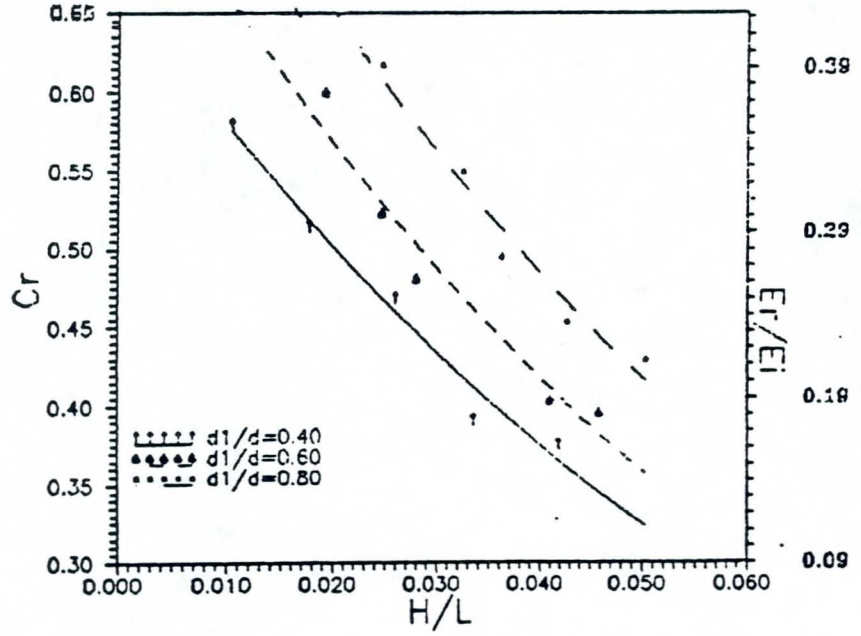

Figure 3. Relation Between H/L & C_r and E_r/E_i at B/d = 1.20

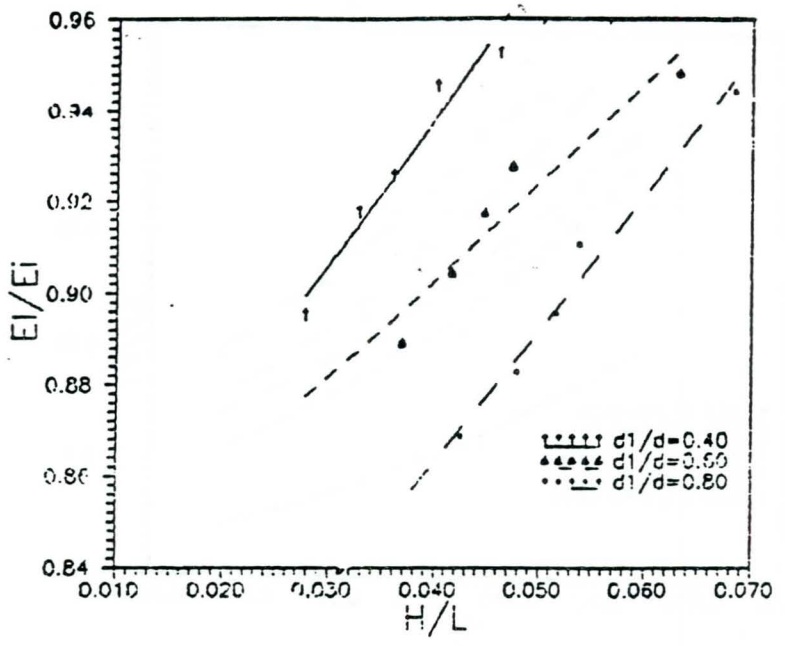

Figure 4. Relation Between H/L and E_r/E_i at B/d = 0.80

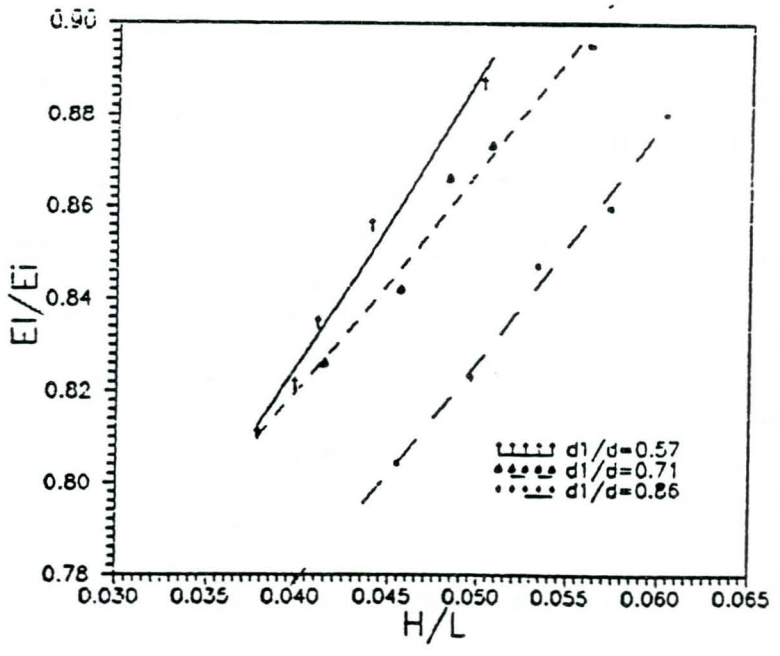

Figure 5. Relation Between H/L and E_r/E_i at B/d = 0.86

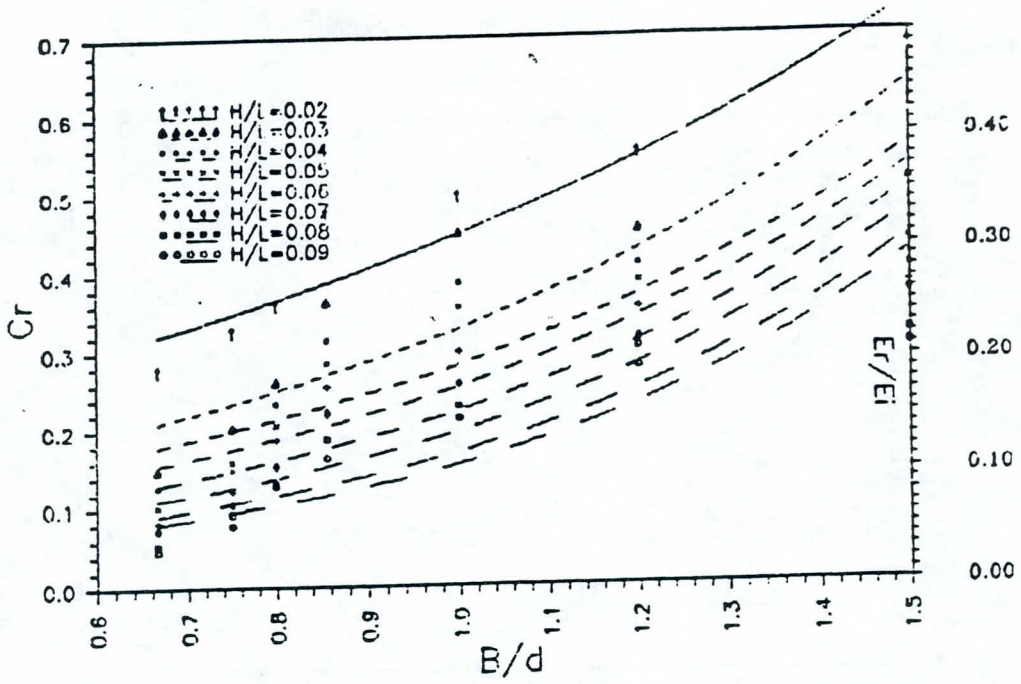

Figure 6. Relation Between B/d & C_r and E_r/E_i at $d_1/d = 0.50$

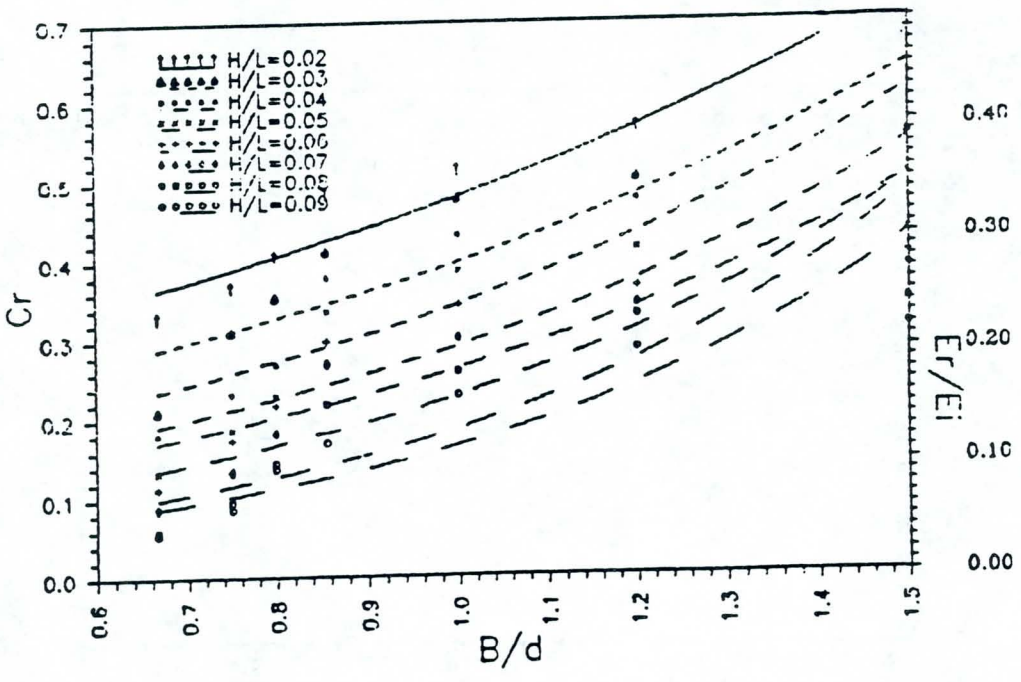

Figure 7. Relation Between B/d & C_r and E_r/E_i at $d_1/d = 0.57$

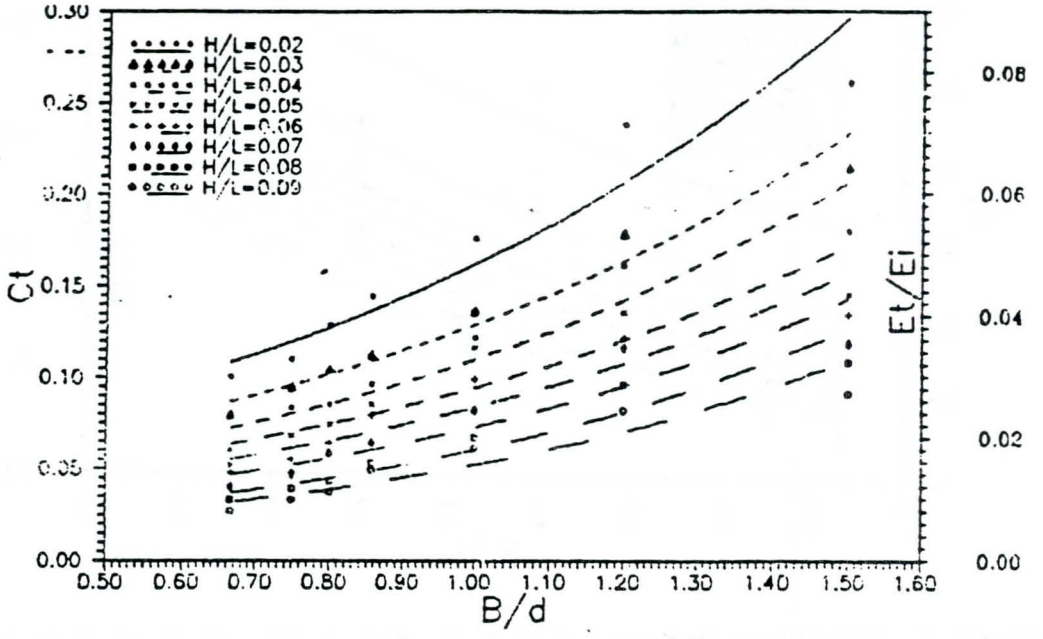

Figure 8. Relation Between B/d & C_t.E_t for $d_1/d = 0.50$

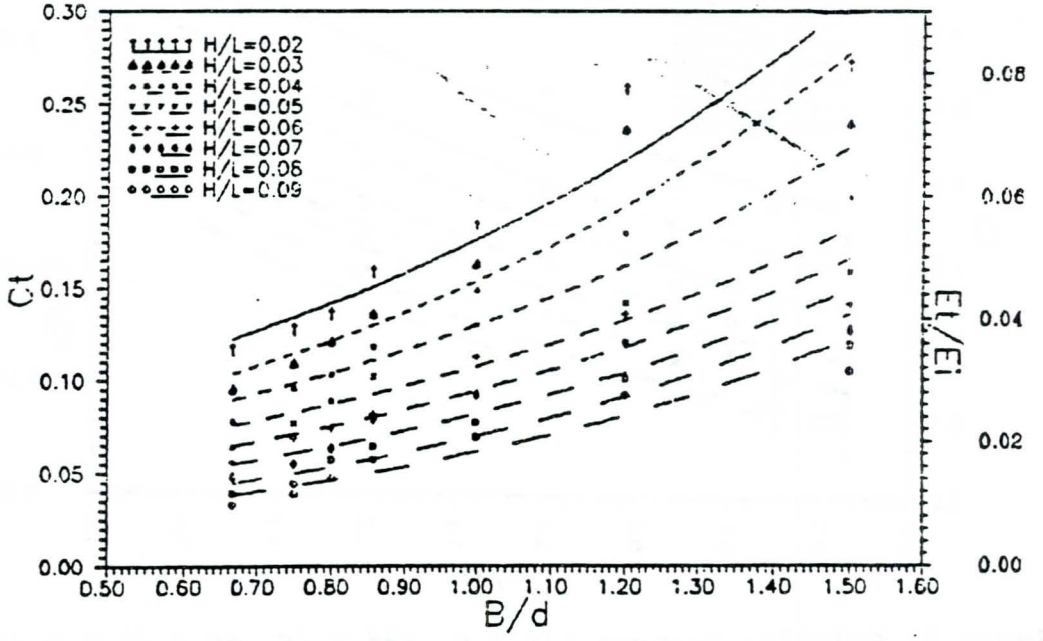

Figure 9. Relation Between B/d & C_t and E_t/E_i at $d_1/d = 0.57$

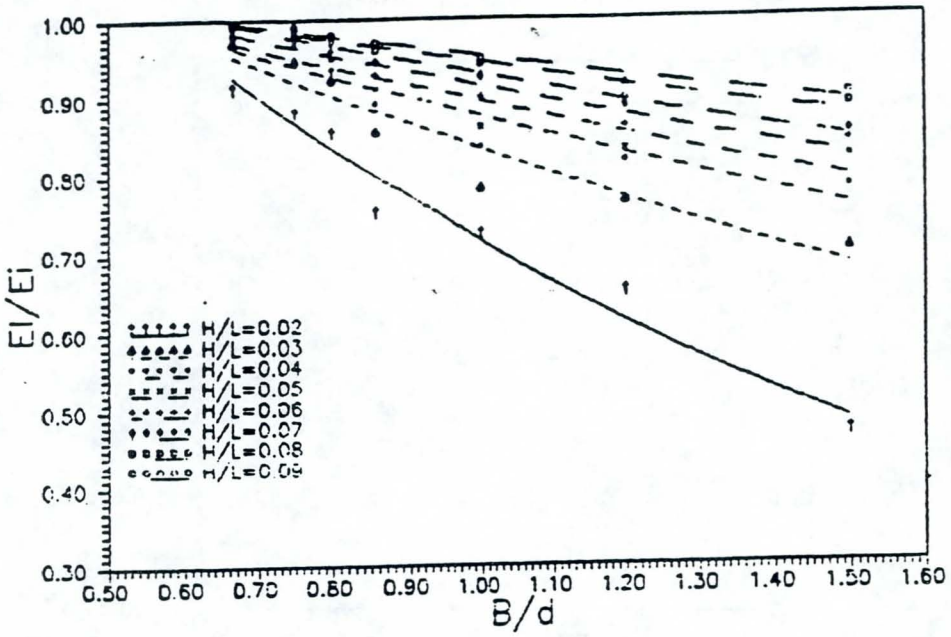

Figure 10. Relation Between B/d & E_1/E_i at $d_1/d = 0.50$

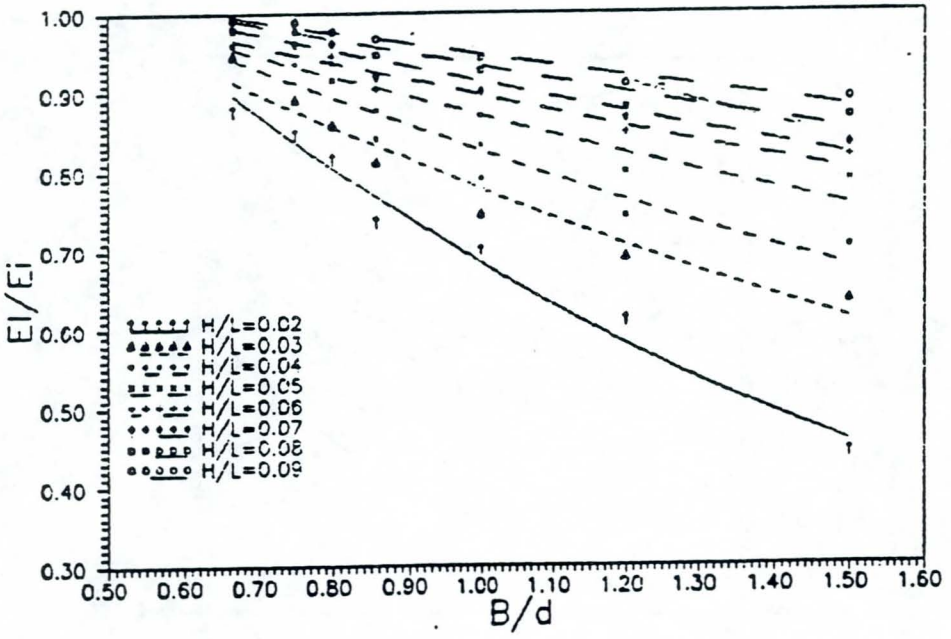

Figure 11. Relation Between B/d & E_1/E_i at $d_1/d = 0.57$

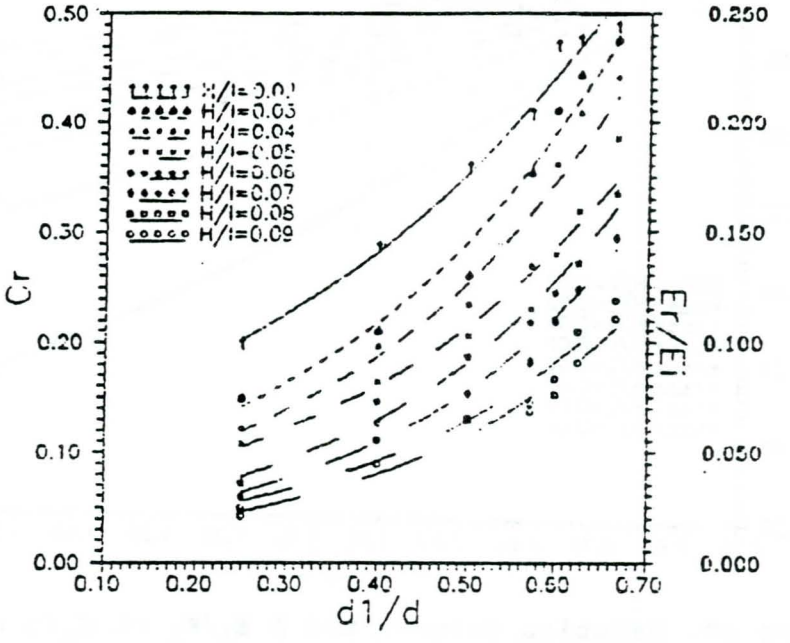

Figure 12. Relation Between d_1/d & C_r and E_r/E_i at B/d = 0.80

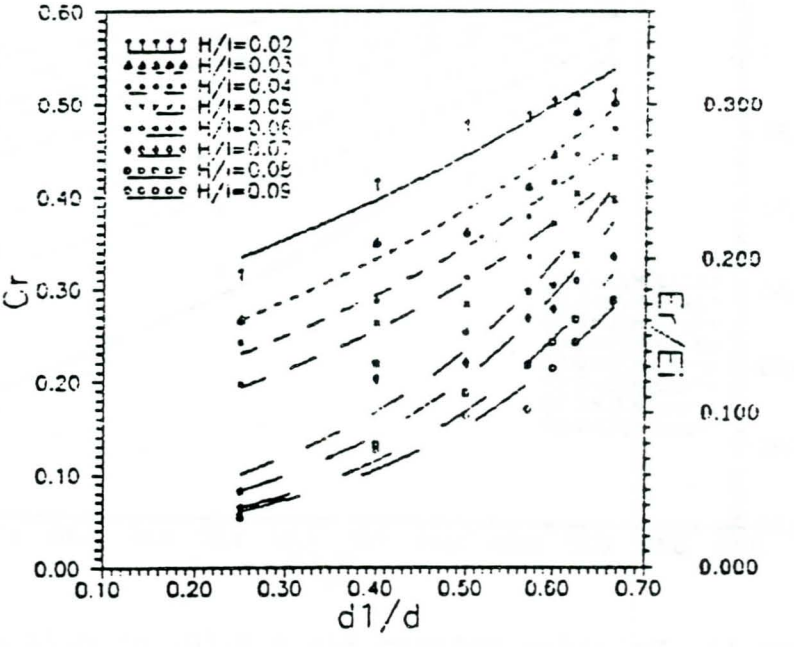

Figure 13. Relation Between d_1/d & C_r and E_r/E_i at B/d = 0.86

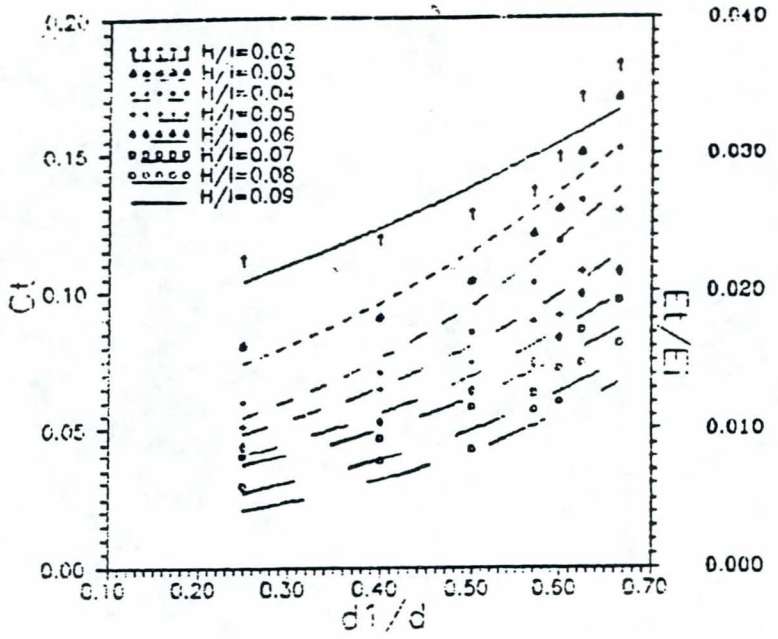

Figure 14. Relation Between d_1/d & C_t and E_t/E_i at B/d = 0.80

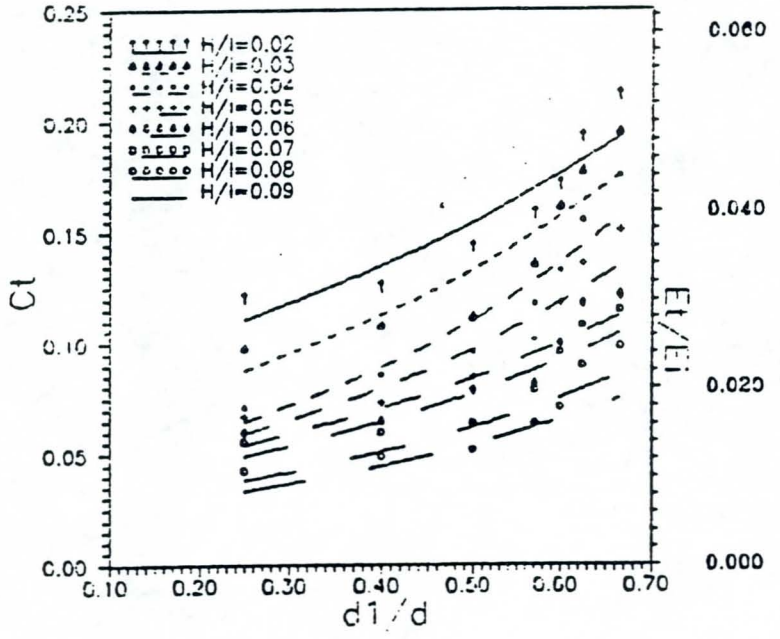

Figure 15. Relation Between d_1/d & C_t and E_t/E_i at B/d = 0.86

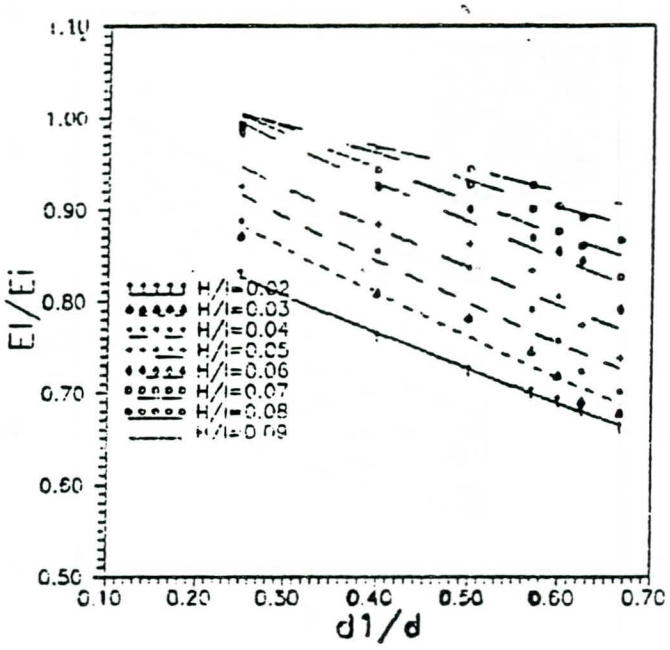

Figure 16. Relation Between d_1/d & E_1/E_i at B/d = 1.00

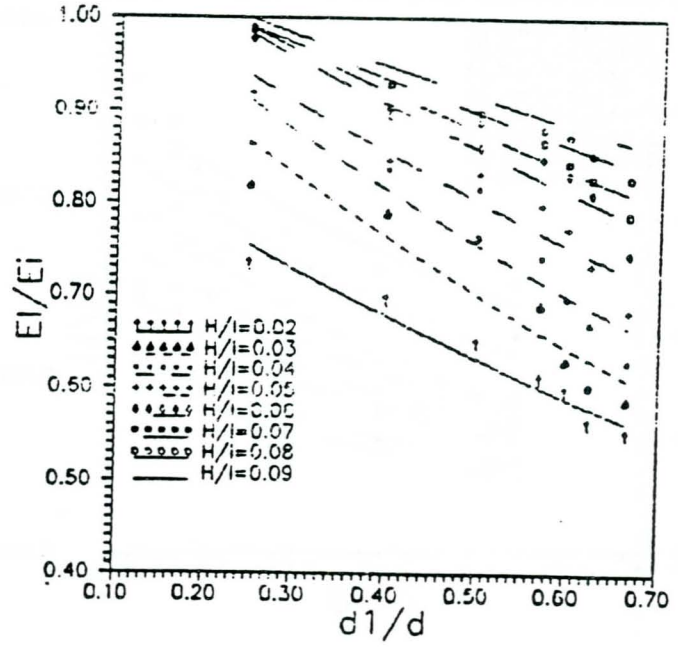

Figure 17. Relation Between d_1/d & E_1/E_i at B/d = 1.20

EFFECT OF FLOW ON RIPRAP PROTECTED BEDS

A.A. El-Sayad
Zagazig University, Water and Water Structures Engineering Dept.,
Faculty of Engineering, Zagazig, Egypt
E.A. Abdel-Hafiez and A.M. Talaat
Ain Shams University, Irrigation and Hydraulic Dept.,
Faculty of Engineering, Cairo, Egypt

1. ABSTRACT

The shear forces acting on the stream bed particles are determined experimentally as a function of the relative roughness, size of particles, and velocity of the stream. A riprap sizing method based on the average flow velocity and the relative roughness of riprap is developed. Also the effects of the gradation and different sizes of grain particles that may be used in the design of the riprap are investigated. Meanwhile, the dimensional analysis is utilized to develop a relationship between the parameters affecting the riprap stability. Design curves for the bottom riprap in rectangular channels are prepared.

2. INTRODUCTION

Beginning and ceasing of sediment motion is of great importance for design of stable channels and riprap protection. Beginning of motion can be related to either the shear stress on the grains or the fluid velocity in the vicinity of the grains. The choice of shear stress or velocity as the main design criteria depends on which one is easier to determine in the field and the type of problem. In riprap design, the critical velocity is commonly used (See *Neill, 1967; Bogardi, 1968; Maynord, 1978; and U.S Army Corps of Engineers, 1982*).

3. THEORETICAL STUDY

Using the principle of dimensional analysis, the functional relationship of relative roughness may be written as,

$$d_{50}/D = \phi\,(F_N,\ d_{85}/d_{15},\ N,\ \phi_s,\ R_e) \qquad (3.1)$$

where

d_{50} diameter corresponds to 50% passing

D average water depth over the tested section

F_N Froude number $\dfrac{U}{\sqrt{gD}}$

U average velocity of the flow (Q/BD)

Q flow rate

d_{85} diameter corresponds to 85% passing

d_{15} diameter corresponds to 15% passing

d_{85}/d_{15} uniformity coefficient of particles (σ_g)

N blanket thickness/d_{50}

R_e Reynolds number

Φ_s shape factor

The method used for calculating the hydraulic radius for both the wall and the bed adopted by *Einstein (1942)* (Ref.*EL-Samni, 1949*) is used here. This method is based on the following assumptions. The entire section can be divided into units that will correspond to similar units of the wetted perimeter, the average velocity is considered to be the same for all units of the cross section, the friction formula is applicable to the entire section and the individual units as well, even if the roughness is of different types. Accordingly, the Manning roughness formula, could be applied to the wall as well as the bed. Therefore, based on Manning's equation, one can write the following formula for calculating the hydraulic radius of the wall.

$$R_w = \left[\frac{n_w U}{1.486\sqrt{S_e}}\right]^{1.5} \qquad (3.2)$$

where

R_w hydraulic radius of the wall = $A_w / P_w = A_w / 2D$

A_w area of the walls

n_w roughness of the wall

P_w wetted perimeter of the wall

S_e slope of the energy line which can be calculated by using the following formula [(*O'Brien 1937*), (*Ref.Fahmy, 1987*)]

$$S_e = S_w - F_N^2 (S_o - S_w) \qquad (3.3)$$

where

S_w water surface slope

S_o bed slope

Equation (3.3) is used for nearly uniform flow. Once the hydraulic radius of the wall is calculated, the hydraulic radius of the bed can be computed using the following formula:

$$A_b = A_T - A_w = BD - 2DR_w \qquad (3.4)$$

where

A_b area of the bed

A_T total area of walls and bed

Then

$$R_b = D\left(1 - 2\frac{R_w}{B}\right) \qquad (3.5)$$

where : R_b hydraulic radius of the bed

In addition to the above relations, the following equations are used to calculate the shear velocity at the bed (U_{*_b}), the critical shear stress over the bed (τ_{cb}), the dimensionless shear stress (τ_{*_b}), and the boundary Reynolds number (R_{*_b}).

$$U_{*_b} = (g R_b S_e)^{0.5} \qquad (3.6)$$

$$\tau_{cb} = \gamma R_b S_e \qquad (3.7)$$

$$\tau_{*_b} = \frac{\tau_{cb}}{d_{50}(\gamma_s - \gamma)} \qquad (3.8)$$

$$R_{*b} = \frac{U_{*b}\, d_{50}}{\nu} \qquad (3.9)$$

where

- γ specific weight of water
- γ_s specific weight of riprap
- ν kinematic viscosity

4. EXPERIMENTAL STUDY

The experimental work was made in a 0.45m deep, 0.30m wide and 12.5m long recirculating flume with vertical glass sides. A sluice gate over rigid apron was used as a control structure to produce the required flow condition. The rock used for riprap model was crushed limestone having a specific gravity of 2.65 gm/cm^3 and angle of repose of 39.7°. The model rock is sieved into the following sizes; 21-14mm, 14-10mm, 10-6.3mm and 6.3-3.35mm as shown in Fig.(1). These four sizes are tested with riprap blanket thickness equal to 21mm for all tested samples. The length of the tested samples is 2.5m.

Under the riprap layer, a cloth filter was placed over the sand to act as a filter to prevent leaching of sand through the riprap. Each test was started with a high tailwater depth. The discharge, which is measured by means of a pre-calibrated orifice meter, was held constant and the tail water was lowered in small increments until the failure of the rock occurred. The boundary of the theoretical bed exists at 0.2 $d_{67.5}$below the top of the roughness as concluded by *El-Samni (1949)*. The number of all runs is 23, 26, 20 and 14 runs for the four samples respectively. Failure was assumed to be the point at which the rock begins movement.

5. ANALYSIS OF RESULTS

A plot of d_{50}/D versus Froude number is shown in Fig.(2). The plotted values represent the tests in which the riprap failed on the channel bottom (at incipient motion condition). A least squares fit of the results of tested cases yields.

$$\frac{d_{50}}{D} = 0.176\,(F_N)^{1.91} \qquad (5.1)$$

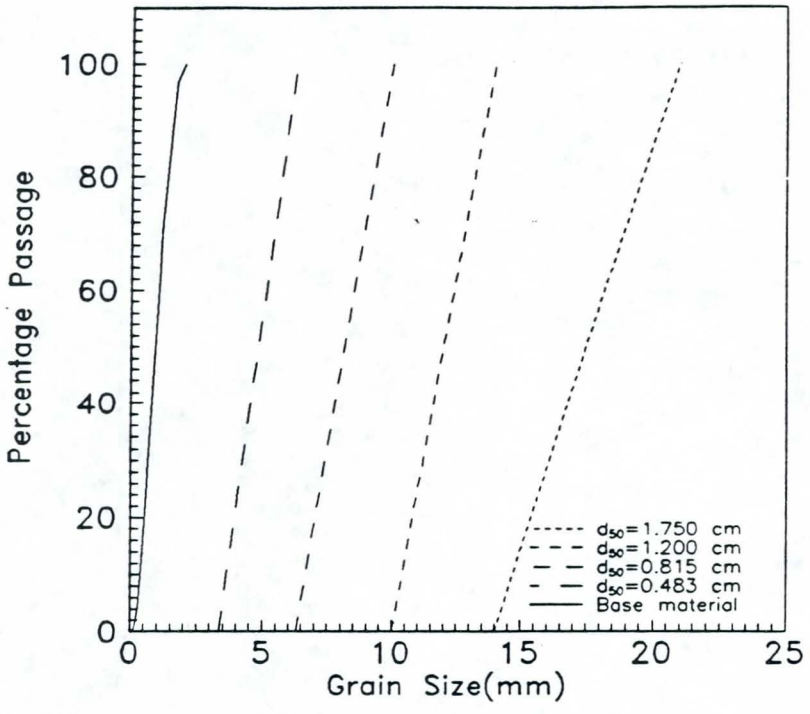

Fig. (1) Grain Size Distribution For The Four Samples and The Base Material

Equation (5.1) is limited for F_N ranges from 0.4 to 1.5 and d_{50}/D ranges from 0.03 to 0.38. The above empirical formula can be used to determine the mean spherical diameter d_{50} for the riprap protection knowing the Froude number and the average flow depth. However, for the safe design a factor of safety (1.5) should be used. Consequently, equation (5.1) becomes:

$$\frac{d_{50}}{D} = 0.264\ (F_N)^{1.91} \qquad (5.2)$$

The permissible tractive force is the maximum unit tractive force that will not cause serious erosion of the material forming the channel bed on a levelled surface. This unit tractive force which is known as the critical tractive force is calculated for all tested samples of riprap. The critical tractive stress (τ_{cb} in gm/m^2) can be calculated by knowing the average particle size of riprap (d_{50} in cm) from the following equation.

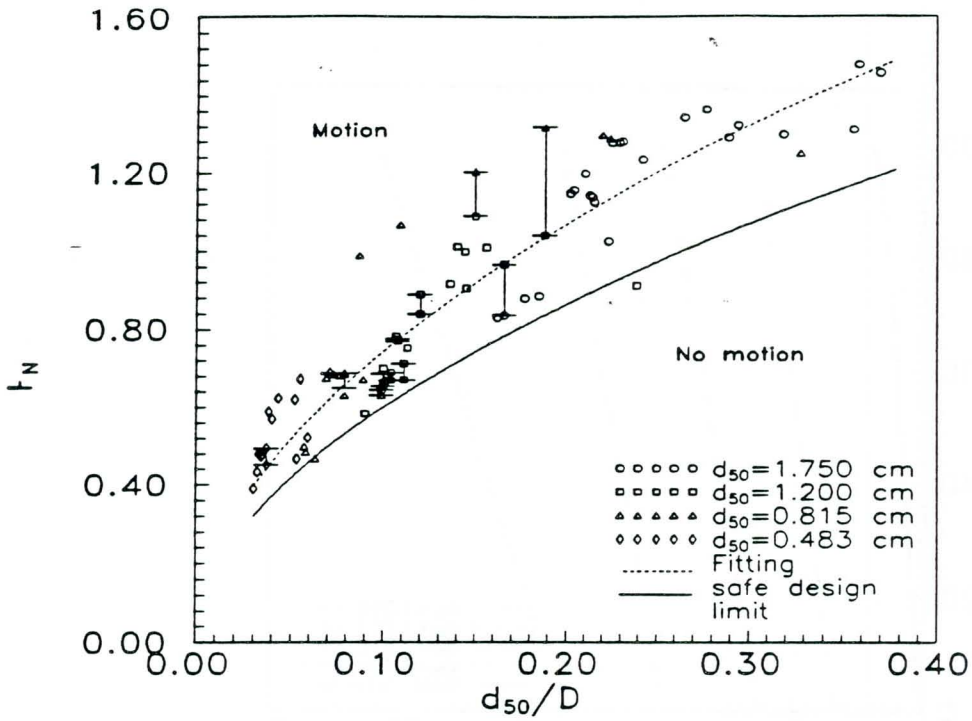

Fig.(2) Relative Roughness Height Versus Froude Number

$$\tau_{cb} = 528.84\, d_{50} + 268.37 \qquad (5.3)$$

This relation is in good agreement with that recommended by Lane (1952) for coarse non cohesive material on channels bed. The relationship between the dimensionless shear stress and the boundary Reynolds number is shown in Fig.(3). This figure shows that the rate of change in dimensionless shear stress increases by decreasing the mean particle diameter d_{50} and does not depend on d_{85}/d_{15} values for the tested range ($\sigma_g \leq 1.55$). The values of τ_{*_b} can be calculated from Fig.(4) which presents the mean values for all the tested samples. From this figure, it is concluded that the present results is in good agreement with that obtained by *Shield's (1936)* and in fair agreement with those of *White (1940)* within the tested range ($R_{*_b} \leq 2500$).

6. ILLUSTRATIVE EXAMPLE

A rectangular channel has a flow rate of 45.0 m^3/s, the water depth through the channel is 3.0 m and the channel width 5.0 m.

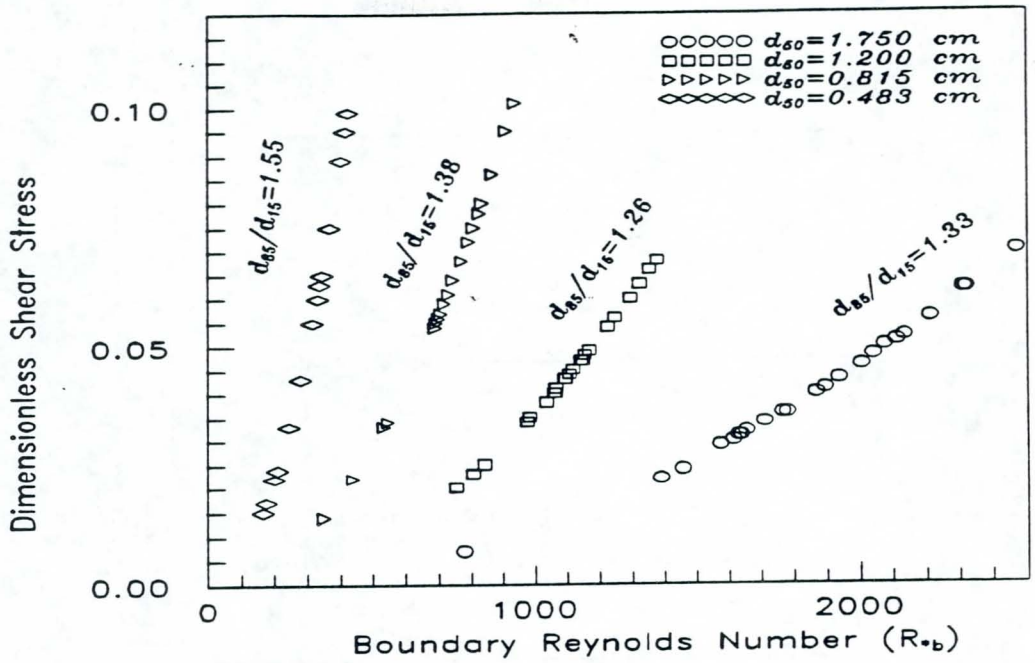

Fig.(3) Dimensionless Critical Shear Stress

determine the average riprap size which required as a protection against scour over channel bed and calculate the shear stress per unit area.

Solution:

The average velocity through the channel

$$U=\frac{Q}{BD}=\frac{45}{3*5}=3.0m/s \qquad (6.1)$$

and the Froude number is

$$F_N=\frac{U}{\sqrt{gD}}=\frac{3}{(9.81*3)^{0.5}}=0.553 \qquad (6.2)$$

from Fig.(2) or equation (5.2) determine the value of d_{50}/D which corresponding to F_N = 0.553

then, $d_{50}/D = 0.0852$

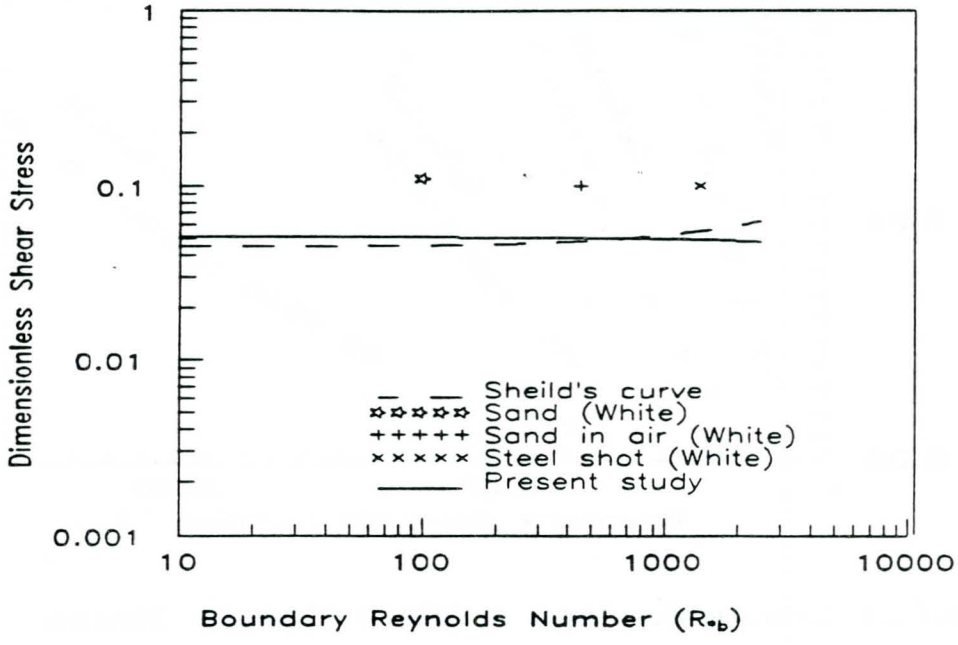

Fig.(4) Coparison Between Present Results and Sheild's Diagram (1936)

and, d_{50} = 0.0852*3.0=0.255 m.

From equation (5.3) calculate τ_{cb} as below,

$$\tau_{cb} = 528.84\, d_{50} + 268.37$$
$$= 528.84 * 25.5 + 268.37 \qquad (6.3)$$
$$= 13778 \ gm/m^2 = 1.3778 \ gm/cm^2$$

7. CONCLUSIONS

A design method for riprap sizing is presented and illustrated by an example. The safe values of the shear stress, τ_{cb}, for course non-cohesive materials such as riprap, is equal to the calculated value from equation (5.3). The gradation coefficient $\sigma_g \leq 1.55$ does not affect the rate of change of τ_{*b} with R_{*b} with the variation between these values increases by increasing d_{50} value as shown in figure (3).

8. REFERENCES

Bogardi, J.L. (1968), "Incipient sediment motion in terms of critical mean velocity", Acta Technica Academiae Scientarium Hungaricae, Budapest, 62 (1-2), 1-24.

Bogardi, J.L. (1978), "Sediment transport in alluvial streams", Academiae Kiado, Budapest.

El-Samni E. (1949)," Hydrodynamic forces acting on particles in the surface of a stream bed", Dissertation submitted in partial satisfaction of the requirements for the degree of Doctor of Philosophy University of California, USA.

Fahmy, A. (1987),"Stability of riprap side slopes in open channels", A thesis submitted for the degree of doctor of philosophy in the Faculty of Engineering, and applied science, University of Southampton.

Gessler, J.B. (1971), "Beginning and causing of sediment motion", River Mechanics, Vol.1, Edited by H.W. Shen, Chapter 7, Fort collins, Colorado, pp.7.1-7.21.

Lane, E.W. (1952), "Progress report on results of studies on the design of stable channels", USBR, Hydraulic laboratory Report No. HYD-352, Denver, Colorado.

Maynord, S.T. (1978), "Practical riprap design", Miscellaneous paper, H-78-7, U.S.Army Corps of Engineers, Waterways Experiment Station, Vicksburg Miss.

Maynord, S.T.,(1987), "Stable riprap size for open channel flows", In partial fulfillment of the requirements for the degree of the Doctor of Philosophy, Colorado State University, Fort Collins, Colorado.

Neill, C.R.(1967), "Mean-velocity criterion for scour of coarse uniform bed-material", International Association on Hydraulic Research, 12th congress, paper C6:3, C6.1 -C6.9.

Shields, A. (1936), "Application of similarity principles and turbulence research to bed-load movement", Mitteilungen der preuss. Versuchsanstalt für Wasserbau und schiffbau, Berlin, no.26 (1936).

U.S. Army Corps of Engineers Division, Lower Mississippi Valley (1982), " Report on standardization of riprap gradations", Vicksburg, Miss.

White, C.M. (1940), "Equilibrium of grains on the bed of a stream", Proc. Royal Society, London, (A), Vol. 174, p.322.

NOTATIONS

A_w	area of the walls
B	channel width
D	average water depth over the tested section
d_{15}	diameter corresponds to 15% passing
d_{50}	diameter corresponds to 50% passing
d_{85}/d_{15}	uniformity coefficient for riprap particles (σ_g)
d_{85}	diameter corresponds to 85% passing
F_N	Froude number ($U/\sqrt{gD}$)
N	blanket thickness/d_{50}
n_w	roughness of the wall
Q	flow rate
R_e	Reynolds number
R_w	hydraulic radius of the wall = $A_w/P_w = A_w/2D$
S_e	energy slope
S_o	bed slope
S_w	water surface slope
U	average velocity of the flow (Q/BD)
Φ_s	shape factor
τ_{cb}	critical shear stress over bed
τ_{*b}	dimensionless shear stress
R_{*b}	boundary Reynolds number
γ	specific weight of water
γ_s	specific weight of riprap
ν	kinematic viscosity

DESIGN RULES FOR THE USE OF RIPRAP IN CLOSURE WORKS

A. Franken, R.E. Jorissen and H.E. Klatter
Ministry of Transport, Public Works and Water Management,
Civil Engineering Division, The Netherlands

ABSTRACT

The closure of a tidal channel can be achieved by several methods and with several kinds of materials. In this paper a design concept will be shown for the use of riprap to close a tidal channel. This concept is based firstly on an uniform definition of hydraulic boundary conditions for each closure method. The hydraulic boundary conditions required for the design concept can be determined quite easily. Secondly these boundary conditions are used in a design formula for riprap stability. This design formula is based on a re-analysis of available riprap stability data. This re-analysis was necessary because the variety of different formulas and parameters used in the past.

Using the presented design concept it has become a relatively easy task to investigate whether a closure with riprap is possible and if so which closure method yields the smallest size of riprap. This is illustrated by a pre-design for a closure in the estuary of Saemankeum in South Korea.

1. INTRODUCTION

Closure works can be subdivided in two different ways (Huis in 't Veld et al, [1]). The geometrical subdivision is based on the closure method, which is used. In figure 1 these methods are shown. Another subdivision is based on the material, which is used to close an estuary. This paper will be based entirely on the geometrical subdivision and the use of the material riprap. Alternative material like sand, gravel or caissons are not treated extensively in this paper.

The horizontal closure method can be executed as a landbased operation simply by dumping rocks at the edges of the final closure gap. As the closure operation continues, the constriction will increase until the closure is completed. In the final stages of the closure operation the current velocities in the closure gap are enormous. However, this current attack is only directed at a small part of the construction and the adjacent bedprotection. The design of a horizontal closure dam is focused on the stability of the rock at the tip of the construction. In most cases instability occurs at the upstream side of the tip of the closure dam and more or less halfway between the bottom level and the water level

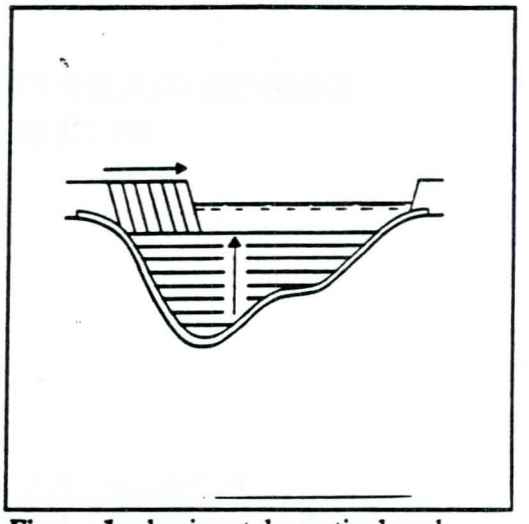

Figure 1 horizontal, vertical and combined closure

The vertical closure method can be executed both as a waterbased operation by dumping rock from a vessel and a landbased operation by the use of a cable way. The first method can only be used in the first stages of the closure operation. The reduced waterdepth above the closure dam limits the use of floating equipment. In this case a horizontal closure method can be used to finish the operation. Furthermore, the use of floating equipment requires restricted current velocities and can only be used around slack tide. By using the vertical closure method the current velocities are limited by the critical discharge situation, which is reached as soon as the damheight is increased to a critical level. In contrast with the horizontal closure method the current will attack along the whole width of the closure gap. The design of a vertical closure is focused on the stability of rock at the downstream edge of the closure dam.
Finally both methods can be used in a so-called combined closure. This combined closure is often applied by constructing a sill of riprap on which caissons can be placed.

The ultimate choice of the closure method depends on the hydraulic circumstances, dimension of the closure gap, the storage area behind, the availibility of material and equipments, etc.

In this paper the attention will be concentrated on the stability of riprap under current attack during the closure operation. Both the horizontal and the vertical closure method will be studied.

2. DESIGN CONCEPT

The design concept is based on the scheme shown in figure 2. This scheme illustrates the two basic steps in the design process of a closure dam. The presented scheme is valid for the closure of a tidal channel. If a river closure is to be designed other aspects as expected peak discharges, diversion channels and storage areas play their role.

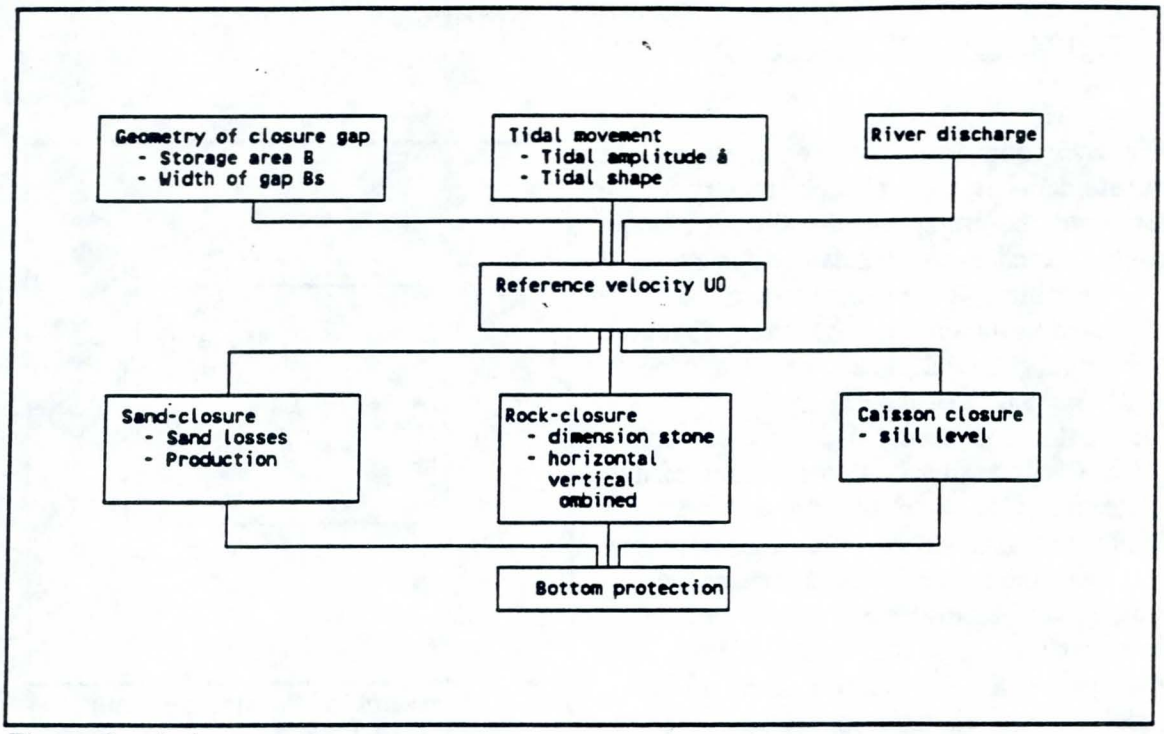

Figure 2 design concept

The first stage in the design process is the characterization of the geometry of the tidal channel and the hydraulic boundary conditions of the area. The geometry is sufficiently characterized by the width of the closure gap (B_s), the sill level (d') and the storage area (B). The relevant hydraulic boundary conditions are the tidal amplitude ($\hat{a}$) and shape of the tidal curve. Based on these five parameters the hydraulic boundary conditions for the closure operation can be calculated easily using a simple hydraulic model.

If the boundary conditions for the closure gap itself are known the properties of the required riprap can be calculated based on the closure method selected. Finally the required bedprotection dimensions can be calculated. If geotechnical instabilities due to scouring and the type of soil are to be expected the dimensions of the bedprotection can be considerable.

In figure 2 also the alternatives for the use of riprap are shown : sand-closure and a closure with caissons. If a sand-closure is applied there is no need for a bedprotection to protect the closure dam itself. However some bedprotection may be necessary to protect adjacent banks of the channel from erosion due to the increased flow velocities. For a closure with caissons the design of the bedprotection is based on the same design rules as applied for the case of a riprap closure.

3. HYDRAULIC BOUNDARY CONDITIONS

The hydraulic boundary conditions at the closure dam itself, which are necessary for the design of the riprap construction, are water levels on each side of the dam, discharges and flow velocities. These parameters can be easily calculated using a hydraulic model. What kind of hydraulic model should be used depends mostly geometry of the estuary.

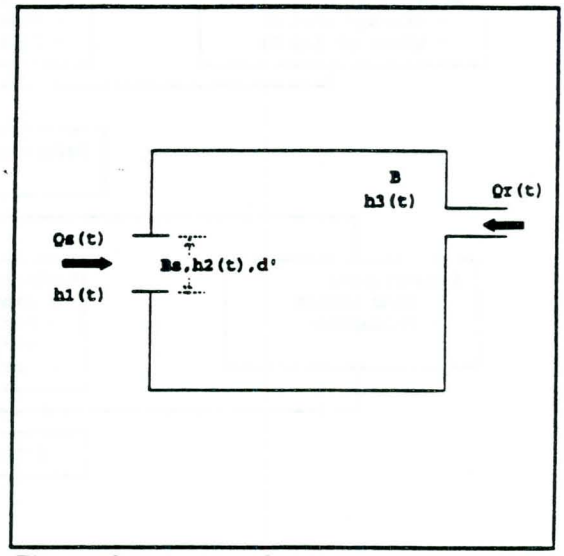

Figure 3 sketch of the storage basin model

The most simple model which can be applied is the (0-dimensional) storage basin model. Neglecting effects of friction and inertia a simple relation between the tidal boundary conditions and the geometrical properties of the estuary and the closure gap can be derived. If the estuary is simply too large or it has a very developed channel pattern a more complex model should be used, for example a (1-dimensional) network channel model. For extremely complicated bathymetries, which do not have a well developed channel pattern, or for detail-study to the closure gap and bottomprotection a 2-dimensional hydraulic model or even a scale model can be used. This improved hydraulic models will yield more accurate hydraulic boundary conditions at the closure gap in the early stages of the closure operation. However these improvements are not very relevant for the most important part of the design : the size of riprap in the final closing stages. In these stages the differences between the results of the mentioned models are very small due to the limited influence of friction and inertia. The hydraulic boundary conditions are dominated by the discharge capacity of the closure gap itself and the tidal boundary conditions. Therefore the hydraulic boundary conditions for the design procedure will be based on calculations with a storage basin model. In figure 3 a definition sketch for this model is shown.

In the estuary shown in figure 3 the following hydraulic parameters are relevant :

- the river discharge into the estuary $Q_R(t)$
- a discharge through the closure gap $Q_S(t)$, determined by the upstream energy level $H_1(t)$, the downstream water level $h_3(t)$ and the discharge relation

In equation (1) the basic storage basin equation is shown.

$$Q = B * \frac{dh_3}{dt} \qquad (1)$$

The discharge relation for submerged flow:

$$Q_s(t) = \mu * A_s * \sqrt{2 * g * (H_1(t) - h_2(t))} \quad (2)$$

$$h_2 = h_3 \quad voor\ h_3 > \frac{2}{3} * H_1 \quad (3)$$

The discharge relation for free flow:

$$Q_s(t) = m * A_s * \sqrt{2/3 * g * (H_1(t))} \quad (4)$$

$$h_2 = \frac{2}{3} * H_1 \quad voor\ h_3 < \frac{2}{3} * H_1 \quad (5)$$

The following symbols are used in the equations (1)..(5).

- Q_S = discharge through closure gap [m^3/s]
- A_s = cross section of closure gap; $B_s * h_2$ [m^2]
- B = plane section of the storage basin [m^2]
- B_s = width of the closure gap [m]
- g = acceleration of gravity [m/s^2]
- H_1 = energy level upstream relative to the sill level d' [m]
- h_2 = water level in the closure gap relative to the sill level d' [m]
- h_3 = water level downstream of closure gap relative to the sill level d' [m]
- d' = sill level relative to the reference level [m]
- μ = discharge coeffcicient for the submerged flow situation [-]
- m = discharge coefficient for the free or modular flow situation [-].

Combining the equation (1)..(5) yields (6)..(8).

$$\mu * A_s * \sqrt{2 * g * (H_1 - h_2)} = B * \frac{dh_3}{dt} - Q_R(t) \quad (6)$$

$$h_2 = h_3 \quad voor\ h_3 > \frac{2}{3} * H_1 \quad (7)$$

$$h_2 = \frac{2}{3} * H_1 \quad voor\ h_3 < \frac{2}{3} * H_1 \quad (8)$$

If the boundary conditions $h_1(t)$ and $Q_R(t)$ are known, the water level in the estuary can be calculated. Flow velocities and head losses at the closure gap can be calculated as well. From equation (6) it follows that only the tidal boundary condition, the ratio between the storage area and the width of the closure gap, the dam height and the discharge coefficients determine the required boundary conditions.

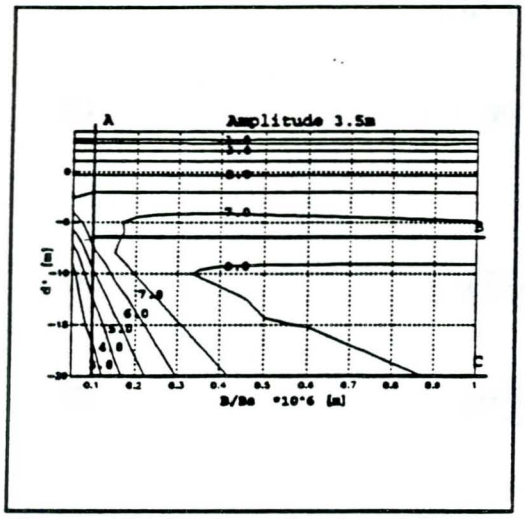

Figure 4 U_0 iso-lines for â = 3.5 m

For a specific tidal boundary condition (â = 3.5 m) equation (6) has been solved for various values of the other mentioned parameters. For the shape of the tidal curve a simple sinuoidal shape has been used with a period of 12 hours and 25 minutes. The effect of this assumption on the final results is negligible. The results are shown in figure 4. This graph is constructed as follows : for each combination of B/B_s and d' equation (6) has been solved. For each combination the maximum velocity during a tidal cycle has been calculated. Figure 4 shows the iso-lines for these velocities. In this graph a closing procedure can be illustrated by starting at a certain dam height d and a certain ratio B/B_s.

A vertical closure increases the dam height while B/B_s remains constant. This is illustrated by the vertical line A. A horizontal closure can be characterized by an increasing ratio B/B_s while d remains constant. This is shown in figure 4 with the horizontal line C. A combined closure is illustrated by line B. For each of these closure procedures the development of the maximum flow velocity during the closure operation is shown in figure 5.

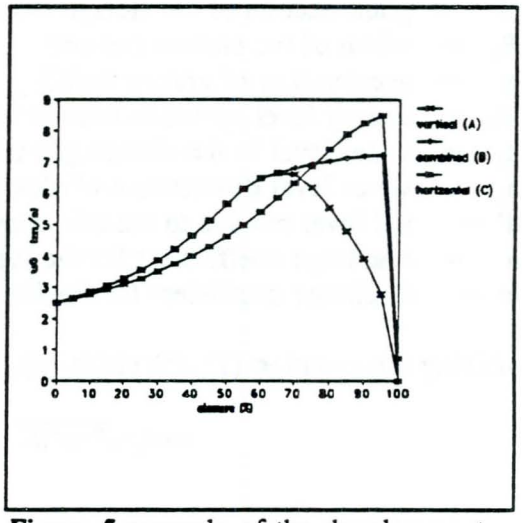

Figure 5 example of the development of the maximum flow velocity during teh closure operation

4. RE-ANALYSIS AVAILABLE DATA

Based on available research data (Akkerman and Konter, [2]) a re-analysis has been carried out. This analysis is based on a uniform definition of parameters used to describe the stability of riprap under current attack. In the figures 6 the definition sketches used in this re-analysis for both the horizontal and vertical closure method are shown.

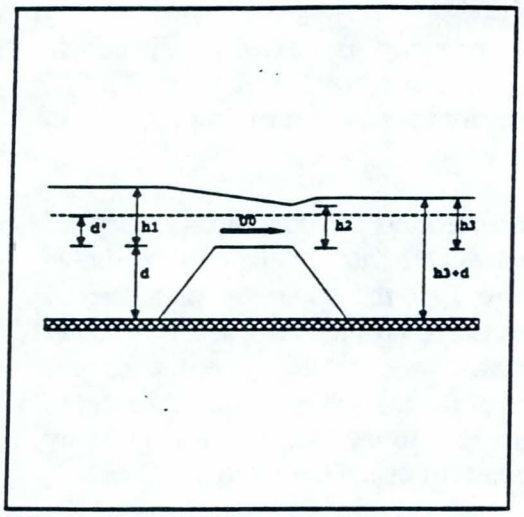

Figure 6a definition sketches for vertical closure

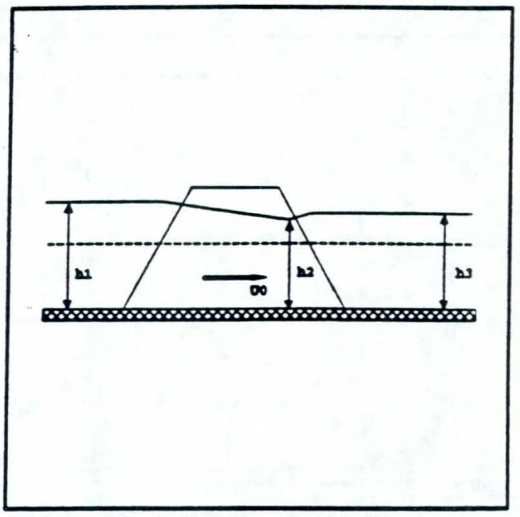

Figure 6b definition sketch for horizontal closure

It is noticed that in case of a horizontal closure the 'damlevel' is equal to the bottomlevel. Starting point of the analysis is the well-known stability relation of Shields, equation (9).

$$\Delta * D_N = \frac{U^2}{C^2 * \Psi} \qquad (9)$$

This relation is valid for uniform flow conditions. The influence of non uniform flow conditions can be introduced by a factor K. At the same time some other parameters are introduced or redefined, see equation (10).

$$\Delta * D_N = \frac{(K * U_0)^2}{C^2 * \Psi} = A * U_0^2 \qquad (10)$$

Δ relative density riprap [-] $= (\rho_s - \rho_w)/\rho_w$
D_N nominal diameter riprap [m] $= \sqrt[3]{(M_{50}/\rho_s)}$
U_0 reference velocity [m/s]
K correction factor [-]
C roughness parameter [$m^{0.5}/s$] $= 25*(h_2/D_N)^{1/6}$
Ψ damage parameter [-]

The most important change compared to earlier investigations is the introduction of the reference velocity U_0. This velocity is defined as :

$$U_0 = \sqrt{2 * g * (H_1 - h_2)} = \frac{U}{\mu} \qquad (11)$$

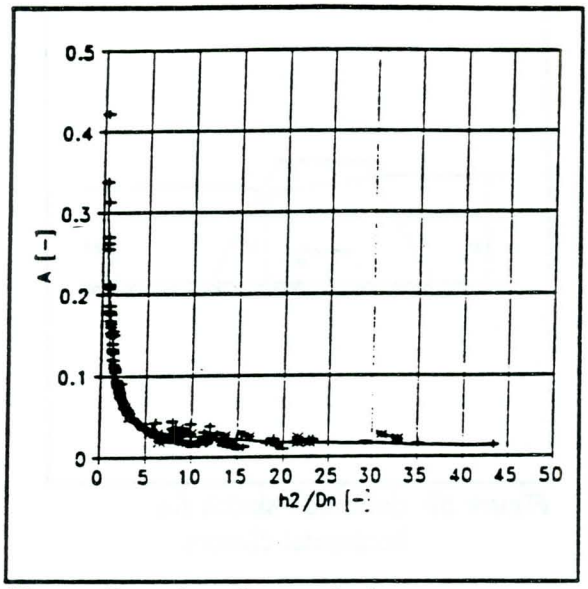

Figure 7 results of re-analysis

The waterlevel h_2 is defined for the critical flow situation ($h_3 < 2/3*H_1$) as $2/3*H_1$, whereas for the non-critical flow situation h_2 is defined as h_3.

These parameters and definitions are applied to the available data and the result is shown in figure 7. In this figure the parameter A from equation (10) is shown as a function of the relative waterdepth h_2 in the control section of the closure dam. All data seem to fit quite well to the line, which is given by equation (10) using $K=1$ and $\Psi=0.04$.

This means that A can simply be expressed as :

$$A = \frac{1}{\Psi * C^2} \qquad (12)$$

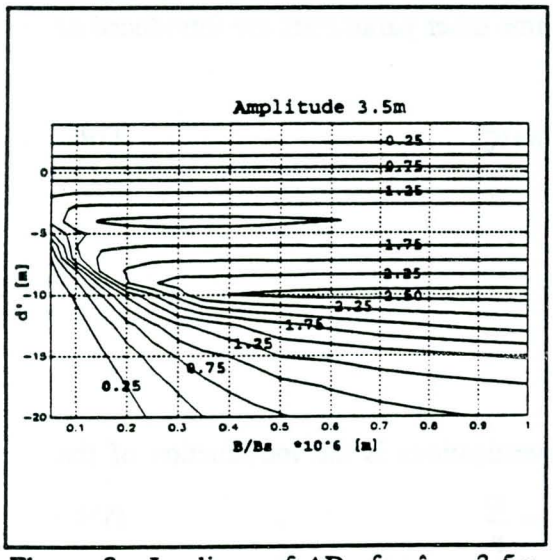

Figure 8 Iso-lines of ΔD_N for $\hat{a} = 3.5$m

For the boundary condition $\hat{a} = 3.5$ m equation 10 has been solved for various combinations of B/B_s and d'. For each combination the maximum value of ΔD_N has been calculated. Figure 8 shows the iso-lines for these stone dimension. In this graph a closing procedure can be illustrated in the same way as done in figure 4.

5. APPLICATION

5.1 introduction

The case-study for a closure is based on the Saemankeum Project. This project features a pre-design of a 400 km² landreclamation at the westcoast of South Korea. The total length of the closure dikes is about 30 km, the average waterdepth is about 5m on the flat areas and 15-25 m in the channels. The tidal amplitude is about 3.5 m during springtides.

The closure can be subdivided into two phases:

- the construction of the closure dikes
- the closure of the three final gaps.

A schematization of the project area is given in figure 9.

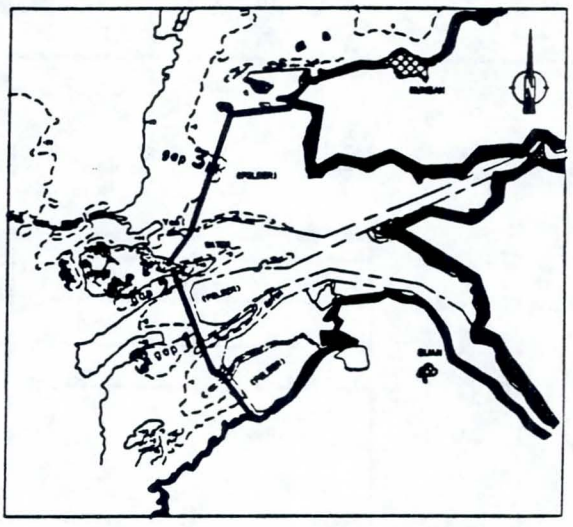

Figure 9 schematization of the project area

5.2 closure-strategy

In table 1 the situation at the start of the closure of the final gaps is given.

	storage area [km²]	Bs [m]	B/Bs [10^6m]	d' [m]
total	400	4100	0.1	
closure gap 1	180	1300	0.15	13.6
closure gap 2	140	1300	0.1	22.5
closure gap 3	80	1500	0.05	9.9

table 1

From figure 4 it can be concluded that the maximum current velocity U_0 is 3-5m/s at the start of this phase and will be increase to 7-8m/s during the closure.
In figure 8 the iso-lines for ΔD_N are given. Both vertical and horizontal closure strategy will lead to a maximum value of ΔD_N between 1.0 and 2.5m for all gaps.

For practical and technical reasons a combined closure strategy has to be chosen; at first in all the three gaps a sill will be constructed (vertical closure). After this, the final gaps will be closed by a horizontal closure strategy.

The sill levels were chosen at respectively MSL-6.0m, MSL -8.0m and MSL -5.5m. Furthermore it was decided to close gap 3 in advance.
Figure 10 shows the time-schedule based on the given production and closure stategy. Each time step concerns a springtide cycle of two weeks

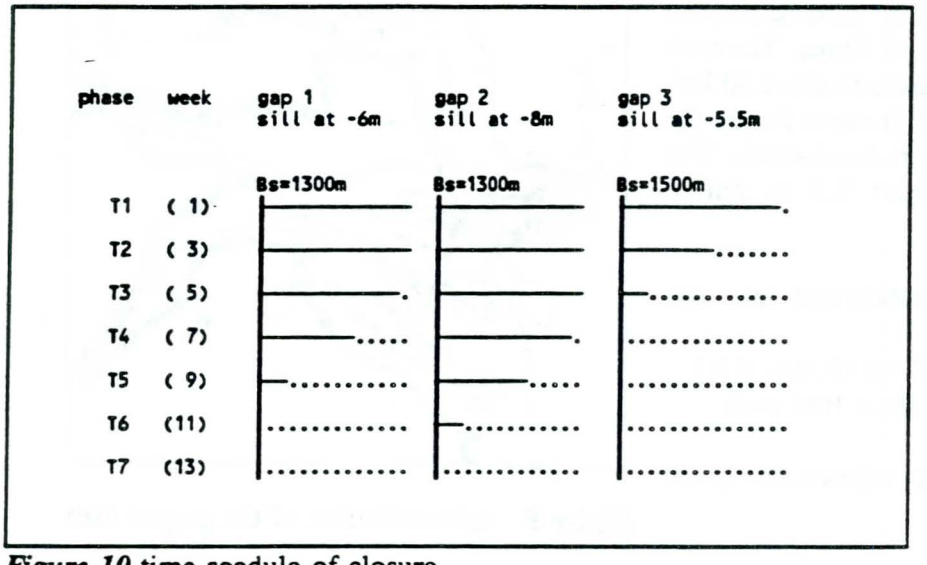

Figure 10 time scedule of closure

5.3 Design of closure gap 3

The closure gap 3 in the north of the estuary was closed before gap 1 and 2. The sill level is at MSL -5.5m; the ratio $B/B_s=0.05$. Neglecting the change in discharge distribution during the closure stage from gap 3 to gap 1 and 2, the acting current velocity and nescessary value of ΔD_N can be determined from figure 4 and 5 (table 2).

phase	Bs [m]	B/Bs [10^6m]	u0 [m/s]	ΔD_N	ΔD_N design
T0	1500	0.05	3	0.75	--
T1	1400	0.06	5	0.90	0.90
T2	800	0.10	6.3	1.35	1.60
T3	200	0.4	7.5	2.1	1.90

table 2 calculated value of ΔD_N compared with the design value

Taken into account the neglecting of the change in discharge distribution the predicted values of ΔD_N fits quite well with the design.

5.4 Design of the closure gap 1 and 2

Gap 1 and 2 are closed simultaneously. Because of the relative small difference in the sill level, gap 1 and gap 2 are taken into account together by the calculation of B/B_s. After the closere

of gap 3 at timestep T3, the whole storage area is connected to gap 1 and 2. Based on figure 4 and 5 the acting current velocity and nescessary value of ΔD_N are determined (table 3). The predicted values fit quite well with the design.

phase	Bs (1+2)	B/Bs [10^6m]	closure gap 1			closure gap 2		
			u0	ΔD_N	ΔD_N design	u0	ΔD_N	ΔD_N design
T0	2600	0.12	3.5	< 0.5	–	< 3.0	< 0.5	–
T1	2600	0.12	6.3	1.3	–	6.0	0.75	
T3	2600	0.15	6.8	1.6	1.5	6.5	1.35	0.9
T4	1700	0.23	7.3	1.8	1.8	7.3	2.0	1.6
T5	800	0.5	7.3	1.9	1.9	7.8	2.3	2.4
T6	200	2.0				7.8	2.3	2.7

table 3 calculated value of ΔD_N for gap 1 and 2 compared with the design value

6. CONCLUSIONS

The re-analysis of the available research data has shown, that the stability relation of riprap under current attack for both the horizontal and the vertical closure method are the same. One should keep in mind however, the uniform definitions which have been used in the presented re-analysis.

The result of this re-analysis does not mean, that the largest size of riprap, which is necessary for the closure of a tidal channel, is the same for both a horizontal and a vertical method. This depends on the value of the reference velocity U_0, which will be higher for a horizontal closure than for a vertical closure.

It is not sufficient to focus the attention completely on the largest size during a closure operation. If a vertical closure is applied this size of riprap is necessary along the entire widht of the tidal channel. If a horizontal closure is applied the largest size of riprap is only necessary in a small section of the tidal channel. This means that the selection of a closure method should be based on the total costs of the operation.

7. REFERENCES

[1] The Closure of Tidal Basins, J.C. Huis in 't Veld et al (editors), Delft University Press 1984, Delft, The Netherlands.

[2] Hydraulic design criteria for rockfill closure of tidal gaps, Akkerman G.J. and Konter J.L.M., Delft Hydraulics, july 1985.

PILOT PROJECT FOR BANK PROTECTION ALONG THE RIVER NILE

V.J. Galay
Northwest Hydraulic Consultants Ltd., Vancouver, Canada
M. Zaki Abo El Fotouh
ECG, Cairo, Egypt
M. El Moatassem
Nile Research Institute, Cairo, Egypt

ABSTRACT

The River Nile, from the High Aswan Dam to the Mediterranean Sea is undergoing bank erosion at a number of locations. Prior to the High Aswan Dam, the river banks that were experiencing erosion were protected by long rock spurs and rock revetments, but after the High Dam, the bank protection changed to short spurs and rock revetment. In 1988, under the River Nile Protection and Development Project (RNPD) a systematic assessment was made of the condition of the river banks and reasons for bank failure were identified. Thereafter, a Bank Protection Pilot Project was initiated with its prime goal to develop cost effective methods of protecting against the various types of river bank failures and to demonstrate the procedures such as planning, design, implementation and maintenance of the works. The Pilot Project undertook construction along three separate reaches of the Nile: at Beni Mazar, at El Monshaa and at Luxor. The Project has developed several simple methods of designing and constructing terraced riprap revetment that also results in recovery of terraced land which is used for growing crops. The revetment also included a substantial toe and a technique for smooth alignment with the main flow channel. The Pilot Project developed two revetment designs, referred to as RNPD Designs A and B, which were more economical and effective than the traditional River Nile revetment. The traditional design used excessive quantities of

rock without adequate toe protection. Also, a design guideline (manual) was developed which set down step-by-step procedures for planning, designing, constructing and maintaining appropriate bank protection revetments. This guideline presents detailed visual examples of construction procedures and design criteria.[1]

1. TYPES OF HISTORICAL BANK PROTECTION ALONG THE RIVER NILE

Prior to the High Aswan Dam, the range of annual water level fluctuation was about 10 m and extensive bank erosion occurred during flows near bankfull necessitating protection of river banks wherever temples, ports or towns were located. For example, Hobson (1987) indicates that the temple of Kom Ombo was constructed during the time of Ptolemy III and that the river bank adjacent to the temple was protected with stone. Some of this protection was eroded over the centuries as noted by the Napoleonic expedition in 1815. Today, the site is still protected by stone revetment as shown in Fig. 1 and the 2,140 year old temple is still at its original location.

In addition to stone revetment, long, high stone spurs were also used to deflect high velocity flows from eroding banks as shown in Fig. 2. These spurs were characterized by long sloping profiles as opposed to an abrupt-end spur and because of the sloped face extensive bank erosion occurred along the river bank just down from the spur as shown in Fig. 3. This sloping spur caused the development of a diving, helicoidal current which resulted in exceptionally deep scour holes and bank erosion. Fig. 3 shows an example of this type of spur and the subsequent downstream bank erosion and a 15 m deep (from bankfull) scour hole. Because of this exceptionally deep scour hole, often the spur would slump into the scour hole resulting in a failed protective structure.

As noted from 1948 maps of the River Nile (Scale 1:25,000) there were about 80 large spurs and approximately 200 km of revetment in existence from the low Aswan Dam to Cairo, which involves about 2,000 km of river bank accounting for both sides.

2. NEED FOR A PILOT PROJECT TO IMPROVE RIVER BANK PROTECTION ALONG THE RIVER NILE

After completion of the High Aswan Dam, the maximum discharge was reduced from a long-term annual monthly peak of 8,430 m^3/s to about 2,550 m^3/s and the range of water levels was reduced to about 2 m. Consequently, the maximum flow velocities were reduced to about 2 m/s. The type of bank protection works were slightly modified to a lower level for the top of revetments and to spurs that were shorter and lower. However, the construction techniques remained as before which involved hand placing of stone along eroding banks and dumping from river-boats for spur construction. The revetment design below water had not changed and there was no toe protection at the base of revetments. Therefore, some of the protective works were failing and a Pilot Project was initiated to assess reasons for failure and to develop methods for improving the design, construction methods and monitoring of river bank protection.

3. PILOT PROJECT PHASES AND SELECTION OF RIVER REACHES

The RNPD Pilot Project commenced within the Nile Research Institute (NRI) by organizing the procedures for development and protection of River Nile banks into four phases:

1. Strategy involved a clear understanding of the river processes such as bank shifting and bed degradation or aggradation.
2. Approach referred to assessment of the basic problems along a river. Tentatively, three distinct types of river problem reaches were identified. These were:
   - constricting reach,
   - expanding reach, and
   - river bends.
3. Design concepts involved setting out preliminary layouts of spurs, revetments or other structures in order to evaluate alternative solutions to the specific problem. Each alternative can be evaluated as to its costs and impacts. One alternative can then be selected for the final design.
4. Detailed design involved field surveys and precise layouts of river structures, dredged channels and/or planting of vegetation.

The institutionalization of the above procedures also included the Nile Protection Directorate staff during planning, field surveys, design, tendering, construction supervision, monitoring and maintenance work. At the same time, NRI retained the role of reviewing designs, training Nile Protection Directorate staff, undertaking special field studies as part of a river research program and updating design guidelines.

In September 1988, preliminary criteria for selection of the pilot reaches for bank protection were proposed. Because the Pilot Project must demonstrate the process of project planning and implementation, criteria were used to select the initial pilot reach. The criteria used for initial selection were as follows:

1. there should be extensive bank erosion within the reach;
2. the navigation channel should be experiencing problems such as shallow crossings and/or moving sand bars;
3. the beginning of the reach should be at a narrow single-channel portion of the river where the banks are relatively stable or where the banks can be stabilized by river works;
4. the upstream approach should be relatively straight in plan alignment;
5. the reach should have islands, flood plains or embayments that can be reclaimed with low dikes and can also serve as an area for disposal of dredge spoil;
6. the reach should avoid sensitive areas where water quality or the environment may be degraded during construction;
7. the reach should have a minimum of infrastructure such as wharfs, bridges and pipelines;
8. the reach should be accessible by road for rapid construction and should not pose problems regarding rights-of-way;
9. the reach should be out of the influence of the backwater effects caused by barrages;
10. the length of the reach should be long enough to allow for alternative treatments of eroding river banks; and
11. the reach should have two or three channels of which any one could be trained to become the main navigation and flow conveyance channel.

After proceeding through the site selection process, including ranking of five possible river reaches according to the above noted criteria, the Beni Mazar reach between km 721 and km 748 was recommended for use as the initial pilot reach. The Beni Mazar reach was approved as the pilot reach in January 1989. In September 1989 El Monshaa was also approved and in August 1990 Luxor was also approved for bank protection.

The map in Fig. 4 shows the three Nile Protection Directorate centers in Upper Egypt, Lower Egypt and Greater Cairo in relation to the three pilot project areas. The lessons learned from the bank protection along the Beni Mazar reach are presented in the remainder of this paper.

4. FINDINGS AND CONCLUSIONS FROM THE BENI MAZAR PILOT PROJECT REACH

The preliminary findings from the Beni Mazar Pilot Project can be grouped into the following categories:

a) materials;
b) designs; and
c) construction methods

At the early stage a variety of erosion resistant materials were investigated and Table 1 compares the cost of the various types of materials. The cheapest materials appeared to be stone and natural vegetation.

A comparison of the materials as used in the traditional bank protection and the two new proposed techniques is summarized in Fig. 5. The traditional design involved dumping of large quantities of stone along an irregular or jagged bankline and utilized large quantities of stone. The irregular bankline generally caused the formation of local eddies resulting in slumping and displacement of the stone which sometimes ended in more bank erosion. Designs A and B both call for a smooth alignment of the toe protection and this was achieved by tracing a smooth toe line on a plan of a surveyed reach of the river bank. This smooth line was subsequently staked out with range rods and dumping of toe stone took place along the surveyed toe line as shown in Fig. 6. The constructed embankment is shown in Fig. 7.

The RNPD designs are less expensive than the traditional design and involve toe stone along with a filter layer of gravel. Also, one advantage is the reclamation of land by the construction of a terrace as shown in Fig. 8. Design B should not be used where bank failures are the result of excessive bank seepage, or where banks are subject to severe wave action at high water levels. The more conservative Design A with a filter should be used in these cases. As limited use has been made of Design B, its application is still being studied and its limitations are being tested under various conditions using alternative toe elevations.

As an outcome of the Pilot Project, a manual has been produced which is referred to as the 'River Nile Bank Protection Guidelines' which is available from the Nile Research Institute, Qanater, Egypt.

REFERENCES

Hobson, C. (1987) - Exploring the World of the Pharaohs, Thames and Hudson, U.K.

Table 1

Comparative Unit Cost of Bank Protection

Protective method of revetment	Average cost per linear meter of bank protected (1989 prices)
• Stone slope revetment with toe and gravel filter (new design)	LE 120 - 160
• Gabion mattress	270 - 300
• Gabion wall	400 - 500
• Concrete blocks	200 - 240
• Soil (or sand-cement) bag	100 - 140
• Big stone toe only	50 - 80
• Vegetative terraces with small stone toe	30 - 60

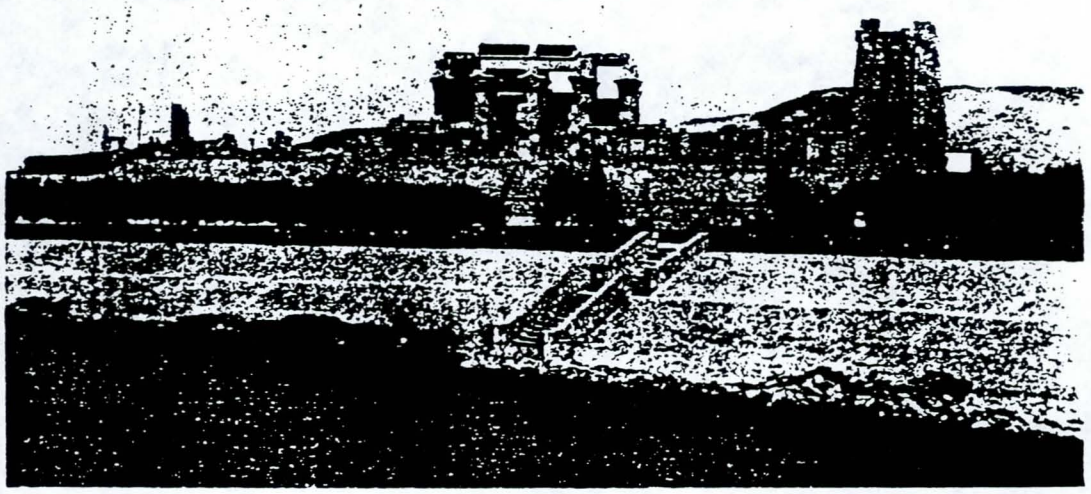

1 Kom Ombo Temple Along the River Nile. The bank is now protected with grouted stone and portions of the revetment are being undermined by erosion at the toe.

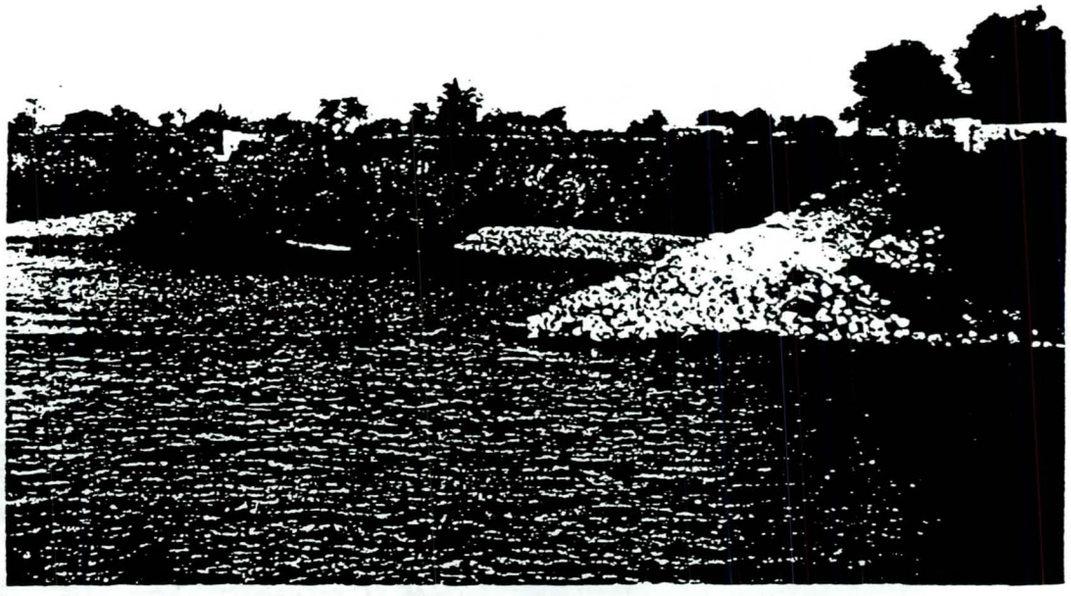

2 Long, sloping spurs constructed in the 1940's to protect the bank of the River Nile.

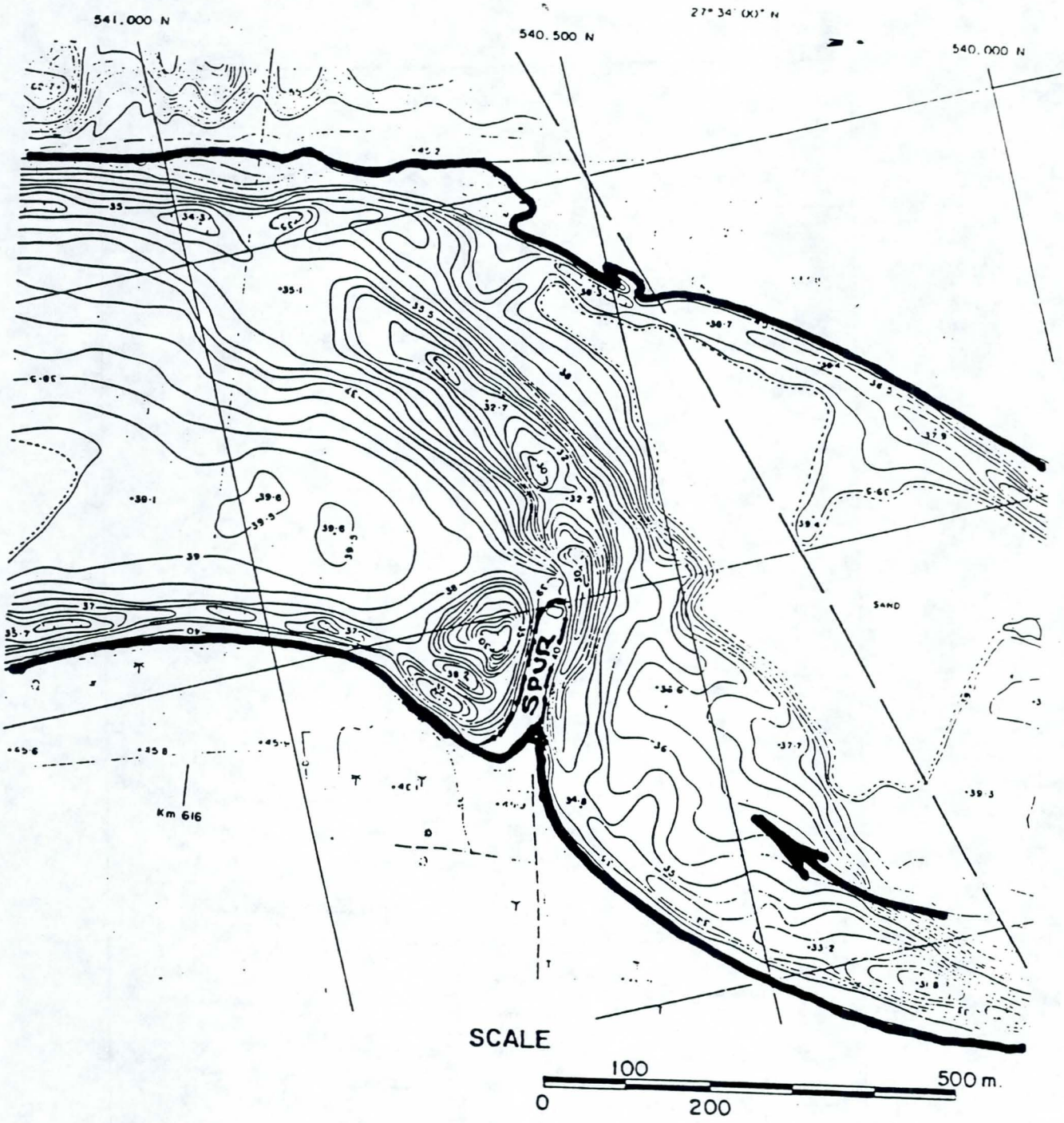

3 Hydrographic sounding of the River Nile in the vicinity of a spur constructed along the River Nile.

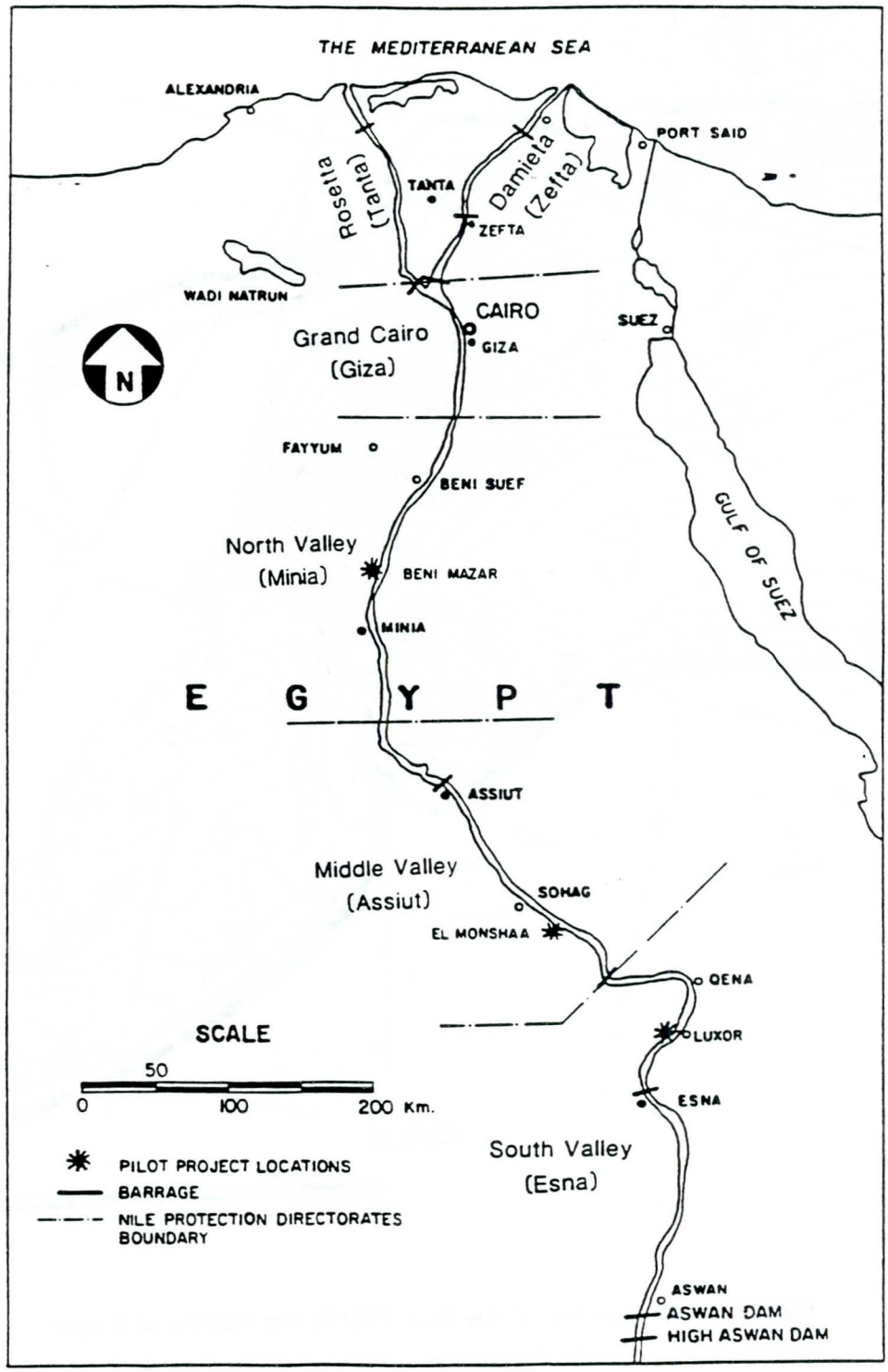

4 Comparison of traditional and RNPD Pilot Project designs.

	TRADITIONAL	RNPD	
		DESIGN A	DESIGN B
CROSS SECTION			
ALIGNMENT	NO	YES	YES
TOE	SMALL	BIG : UP TO LWL	BIG: UP TO 1.0 - 1.5 m ABOVE LWL
BACK FILL	STONE	SAND AND / OR BANK MATERIAL	BANK MATERIAL
FILTER	NO	GRAVEL OR STONE CHIPS	NO
FORMATION OF TERRACES AND GAIN OF NEW LAND	VERY LITTLE	YES , BY CONTRACT	YES, DEPENDING ON LAND OWNER
AVERAGE COST IN LE FOR ONE METER LENGTH OF BANK (PRICES OF 1990)	200 - 250*	170**	100**

* BASED ON PHASE I VOLUMES AT BENI MAZAR

** NET COST MAY BE REDUCED BY VALUE OF LAND GAINED

5 Comparison of traditional and RNPD Pilot Project designs.

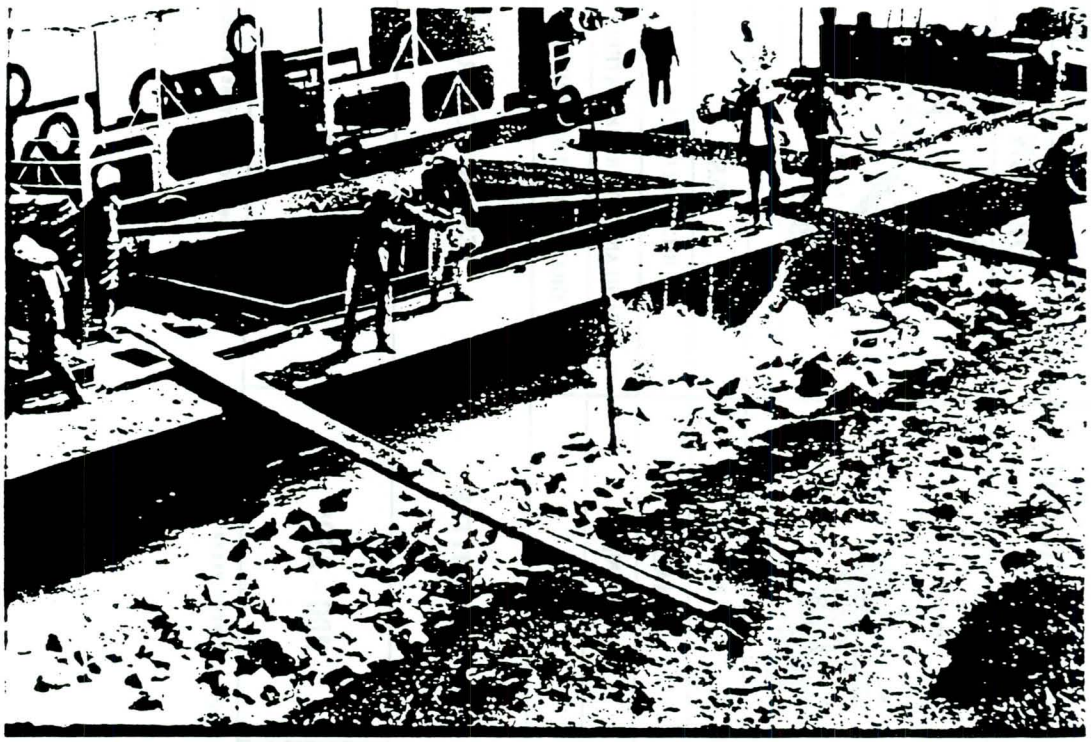

6 Dumping of toe stone along revetment at Beni Mazar Pilot Project.

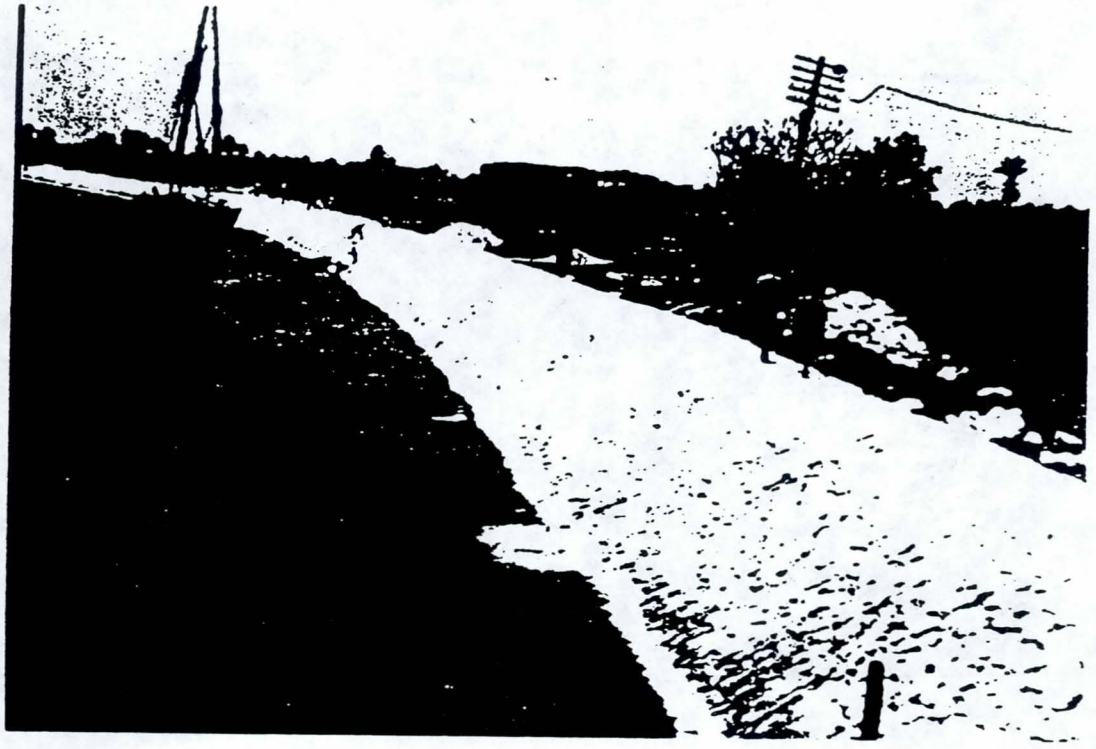

7 Completed stone revetment showing smooth alignment of the toe and slope at Beni Mazar. The stone has been hand placed.

8 Terrace under construction at Beni Mazar. The terrace can later be used for growing crops.

BIOTECHNICAL STABILIZATION OF COASTAL LANDFORMS

D.H. Gray and R.D. Hryciw
University of Michigan, Ann Arbor, MI 48109, USA

ABSTRACT

An alternative to rip rap protection is required where regulations prevent structural armoring of slopes in environmentally sensitive areas such as coastal dunes. This paper describes an alternative to structural armoring that is visually and physically non-intrusive but which could provide a comparable degree of protection. The system in question consists of a strong netting that is anchored to and stretched tightly over a sand slope. The tension in the netting imparts a confining stress to the sand that greatly increases its resistance to movement and detachment.

The netting is tensioned by passing the threaded ends of anchor rods through reinforced openings in the netting and tightening a nut and washer assembly down on the netting. The ground anchors consist of steel rods attached to screw plates or "duck bills" that are driven or inserted into the sand to a pre-determined depth. Guidelines are presented for the optimal anchor array (spacing, pattern, depth, etc) and best stretched shape for the netting.

An anchored netting system also lends itself to ancillary protection with soil bioengineering measures such as live staking and fascines. The objective of this integrated or combined approach is to increase the resistance to surficial erosion and to shallow sliding or sloughing in sandy coastal slopes. Improved resistance occurs as a result of both increased effective stress from developed compression on the ground surface and by an increase in apparent cohesion from fibrous root development around imbedded live stems and cuttings.

1.0 INTRODUCTION

Coastal communities often have regulations preventing the use of structural armor systems, e.g., rock rip rap, in environmentally sensitive areas such as coastal sand dunes. Coastal commissions in the State of Massachusetts, for example, often do not permit the use of revetments or sea walls for protecting areas designated as coastal dunes. A good example is shown in Figure 1 where a coastal property owner on the Cape Cod seashore was not allowed to build a rock revetment to protect his home in a reach of coast that has been designated as a "coastal dune" area. The protective sand berm system shown in Figure 1 will not withstand wave action in a major storm.

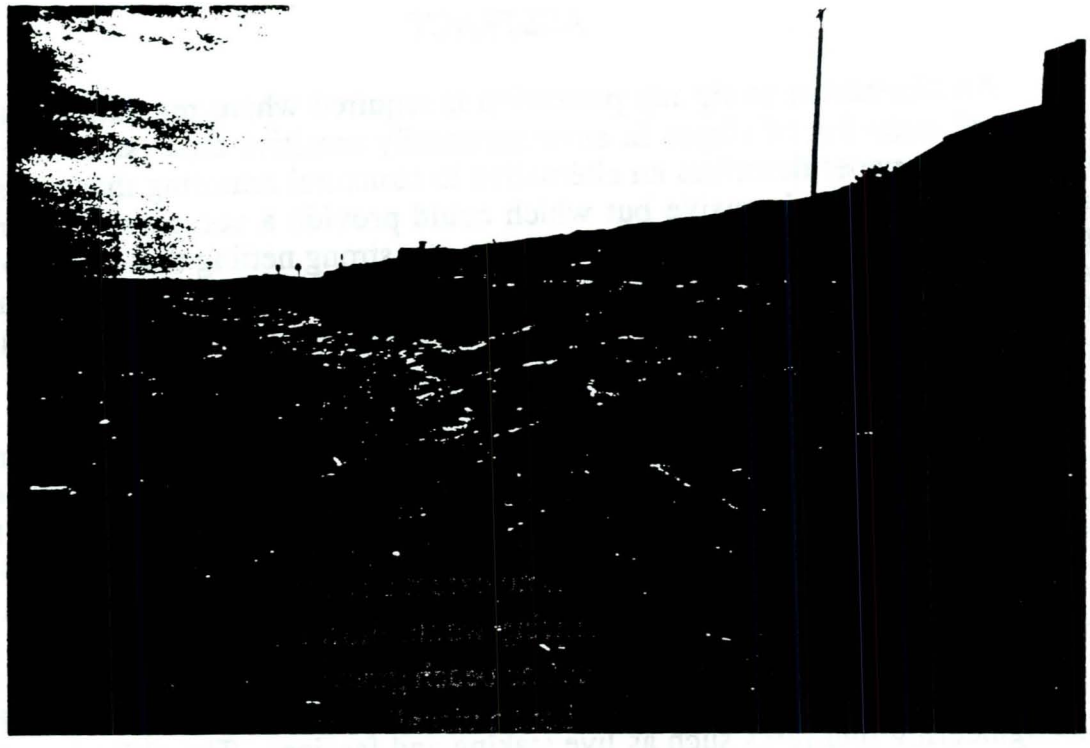

Figure 1. Because of classification as a "coastal dune" area, property owner has been restricted to use of a sand berm and sand bag system to protect his property.

This paper describes an alternative to structural rip rap that is visually and physically non-intrusive but which could provide a comparable degree of protection. The system in question consists basically of a strong netting that is anchored to and stretched tightly over a sand slope. The tension in the netting imparts a confining stress to the sand that greatly increases its resistance to movement and detachment. The anchored and tensioned netting in effect converts thousands of individual and cohesionless sand particles into a monolithic, and unitary mass that has sufficient weight and coherence to resist wave and current action.

Use of the anchored netting approach in areas subjected to wave action would require placement of a filter cloth behind the primary netting to prevent washout and piping of sand through the netting. The filter cloth serves the same purpose that it does when placed beneath a riprap or armor stone revetment, namely, restraining sand particles while permitting water to pass through and relieving pore pressure buildup in the slope behind. The openings in the filter fabric would have to be sized to match the particle size distribution of the sand in the slope.

The netting is tensioned by passing the threaded ends of the anchor rods through reinforced openings in the netting and tightening a nut and washer assembly down on the netting. The ground anchors consist of steel rods that are attached to screw plates or "duck bills" that are driven or inserted into the sand to a predeter-mined depth. The exact anchor array (spacing, pattern, depth, etc) has to be worked out for maximum efficiency. The edge treatment is also a critical consideration and requires burial and anchoring of the netting in a peripheral trench to prevent flanking of the protective system. This system stabilizes, strengthens, and armors a sand slope internally. There is no external structure placed or visible on the surface of the ground. Only the netting would show and this could be covered with sand or introduced vegetation such as beach grass. This attribute satisfies environmental and esthetic concerns about a visually intrusive revetment.

An anchored netting system also lends itself to ancillary protection with soil bioengineering measures such as live staking and fascines. The objective of this integrated or combined approach is to increase the resistance to surficial erosion and to shallow sliding or sloughing in sandy coastal slopes. Improved resistance occurs as a result of both increased effective stress from developed compression on the ground surface and by an increase in apparent cohesion from fibrous root development around imbedded live stems and cuttings. The compression from the netting also improves the frictional pullout resistance and tenacity of shallow roots.

2.0 EROSION RESISTANCE OF SANDY COASTAL LANDFORMS

The shear strength, or alternatively the resistance to particle detachment and displacement, in coarse textured, cohesionless soils depends upon the amount of confining or contact stress between particles. This stress increases with depth because of the weight of overlying soil or overburden stress. Accordingly, the shear strength of granular, cohesionless soils increases linearly with depth. Near the surface, where the confining stresses are very low, the shear strength will likewise be very low. These types of materials are very susceptible to surficial erosion and shallow mass wasting because in the absence of cohesion they offer little resistance to particle detachment and displacement under the influence of raindrop splash, overland flow, and wave erosion. Some sandy coastal areas are often droughty, slightly saline, or nutrient deficient and hence not capable of supporting a vegetative cover...at least not without some help. A vegetative cover protects the soil against raindrop splash; the roots provide some degree of reinforcement or cohesion near the surface.

The influence of cohesion and seepage on the factor of safety against sloughing (shallow face sliding) of a typical sandy slope is shown in Figures 2 and 3. The factor of safety is shown plotted as a function of depth for various seepage directions in Figure 2 for the case of zero cohesion. Note that the factor of safety is invariant with depth in this case. When seepage occurs parallel to the slope the factor of safety drops to about half that of the dry case (no seepage).

The presence of a small amount of cohesion (0.1 psi) significantly increases the factor of safety particularly near the surface. This is the region most vulnerable to tractive forces and displacement from seepage and raindrop splash. If some mechanism could be found to increase the confining stress near the surface the factor of safety could likewise be improved significantly. An equivalent confining stress can be calculated from the cohesion values used in the example from the following relationship:

$$\sigma_{equiv} = c / \tan \phi$$

for $c = 0.1$ psi and $\phi = 30$ degrees

$$\sigma_{equiv} = 0.1/0.577 = 0.173 \text{ psi } (25 \text{ psf})$$

One way to develop a confining stress on the ground surface is to place a fabric or membrane on the ground and pull it down tightly on the surface by means of anchors driven into the ground in some type of regular array. Geogrids or nets can also be used for this purpose; they have the additional advantage or permitting vegetation to be established in the interstices or opening of the net. An example of an anchored netting installation on a slope is shown in Figure 4.

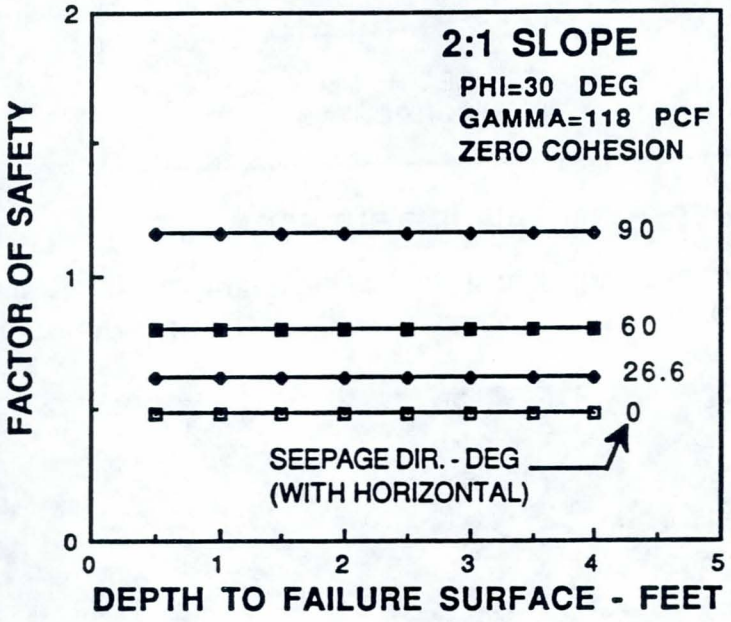

Figure 2. Factor of safety against shallow sloughing of a sandy, *cohesionless* slope as a function of depth and seepage direction.

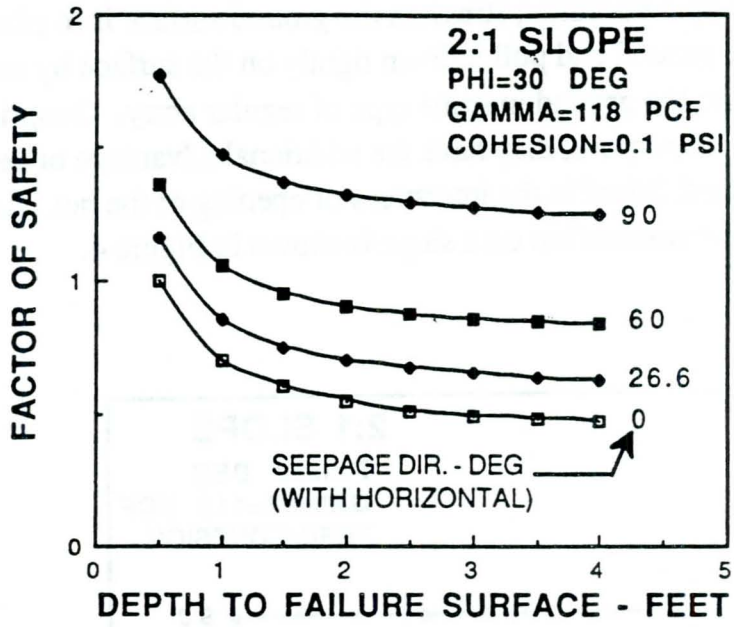

Figure 3. Factor of safety against shallow sloughing of a sandy slope with a *small amount of cohesion* as a function of depth and seepage direction

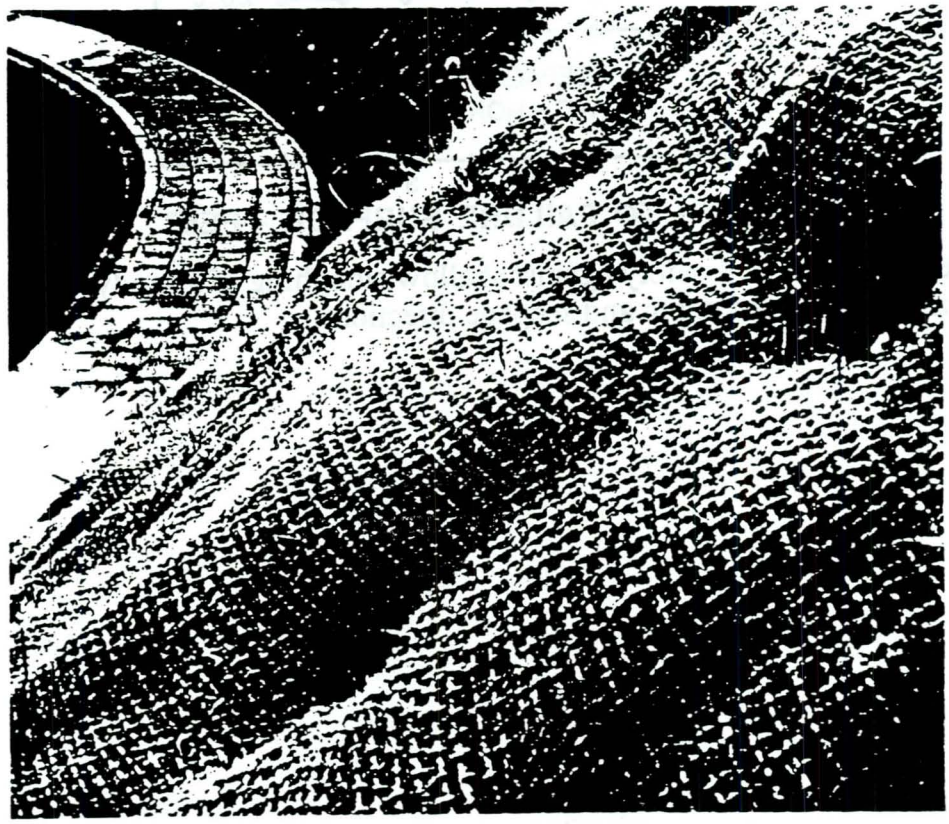

Figure 4. Natural coir netting or geotextile shown anchored tightly to a slope by means of metal rods driven through the netting into the ground.

Another way to develop apparent cohesion in a sandy soil is by the introduction of fibrous roots. Fiber or root cohesion can likewise make a significant difference in the resistance to shallow sliding or shear displacement in sandy soils with little or no intrinsic cohesion. Approximate contributions to increased shear strength from the presence of roots can be estimated from root biomass concentrations. Actual shear tests in the laboratory and field on root/fiber permeated sands (Gray and Ohashi, 1983; Maher and Gray, 1990) indicate a shear strength increase per unit fiber concentration ranging from 7 to 8 psi per lb of root biomass per cu.ft. of soil. Ziemer conducted in-situ shear tests on sandy soils permeated by pine roots with a maximum biomass concentration of 0.3 lbs of root per cu.ft. of soil. This root concentration translates into a maximum shear strength increase of approxi-mately 2.2 psi.

3.0 ANCHORED GEOTEXTILES AND GEONETS

3.1 Principles and Components of System

An anchored geotextile or geonet consists basically of a fabric or net that is stretched over and pulled down tightly on the ground surface by means of anchors that are inserted through and fastened to the geotextile. Driving or pushing the anchors into the ground causes the geotextile to go into tension, and this in turn imparts a slight compressive force on the ground surface. The compressive force increases shear strength and resistance to sliding. This additional shear strength is particularly critical in the case of sandy soils which have little resistance to sliding and particle detachment in the absence of any significant confining stress near the ground surface.

The use of anchored geotextile systems to improve the stability of slopes was suggested initially by Koerner(1985, 1986). The main function of the geotextile is to place the under lying soil into compression for reasons noted previously. The success of such a system depends upon a complex set of interactions, namely, the satisfactory transfer of load between the geotextile and the anchors, between the geotextile and soil, and between the anchor and soil. The nature and quantification of these interactions are still the subject of needed research, but enough is already known about the system to make rough performance estimates and preliminary recommendations with regard to installation.

3.2 Load Transfer from Geotextile/Geonet to Soil

An incremental length of stretched fabric or netting on a soil surface is shown schematically in Figure 5. The normal stress between soil and fabric acting over the increment Dq is given by the following expression:

$$\sigma_n = (T_2 + T_1)\ \Delta\theta / \Delta s$$

where Δs is the incremental curvilinear distance between points 1 and 2. Since $\Delta\theta/\Delta s$ is the radius of curvature (r), the normal stress at any point on the interface can be expressed simply as :

$$\sigma_n = T / r$$

where T is the developed tensile load per unit length in the fabric over the increment of interest. Accordingly, the stresses transferred from an anchored geotextile to the soil at a given point on the interface are only a function of the tension in the fabric and its local curvature. This holds true for both plane (2-D) curvature (from a line anchor) or axisymetric (3-D) curvature (from a geometric array of multiple anchor points).

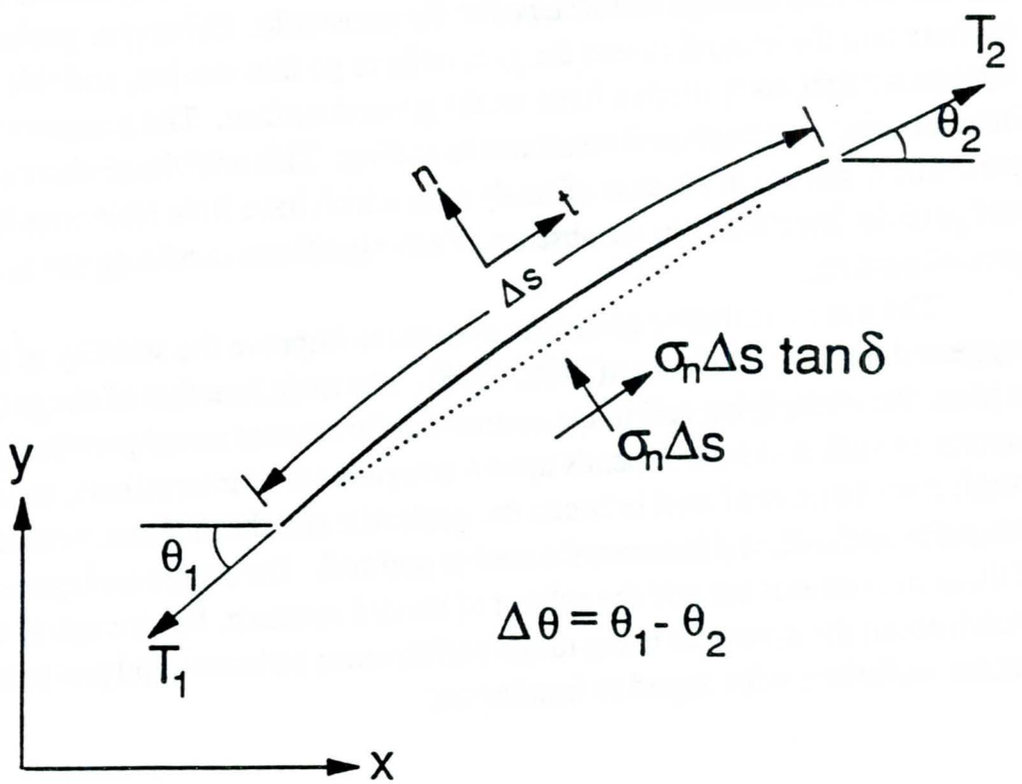

Figure 5. Load transfer between anchored geotextile and soil over an incremental fabric or netting length.

3.3 Conventional Netting Installations

Instructions for the installation of erosion control netting and fabrics typically emphasize the importance of not stretching the fabric. This warning is issued ostensibly to insure intimate contact with the ground surface and to avoid bridging over incipient rills and channels. The warning appears to be based on past experience with sites where rilling has been observed beneath tightly stretched netting.

This injunction not to stretch eliminates, however, the opportunity of exploiting an important stabilizing mechanism of a geotextile that is tightly stretched and anchored or staked securely to the ground. Furthermore, the problem of rilling and washout beneath a stretched fabric also is largely a function of the type of netting and the manner in which it is staked or fastened to the ground. Low tensile strength and modulus nettings should probably not be pulled down and stretched because they simply lack sufficient strength and stiffness to withstand the imposed tensile forces. Many synthetic nettings and some natural materials such as coir netting, on the other hand, have a relatively high unit tensile strength and do not suffer from this limitation.

The principles and advantages of anchored geotextiles are described in detail by Koerner (1986). Stretching of a geotextile on the ground by means of driven anchors imparts a slight compressive or confining stress on the surface. This confining stress in turn develops improved resistance to shallow sloughing and surficial erosion caused by downslope seepage forces. This additional shear strength is particularly critical in the case of sandy soils which have little shear strength and resistance to particle detachment in the absence of any significant confining stress near the ground surface.

Heavy duty nettings with sufficient unit tensile strength and stiffness should impart a substantial confining stress on the ground surface if they are properly stretched and anchored to the ground. If properly anchored, the netting should improve not only the shallow mass stability of a sandy slope but also its resistance to surface erosion or particle detachment. The operative word here is "properly" ....otherwise, the warnings about the adverse effects of stretching may apply.

Research at the University of Michigan (Hryciw, 1991; Hryciw and Ahmad, 1992) has shown that the effectiveness of anchored geotextiles is a function of the geometric arrangement, spacing, and inclination of the anchors in addition to the visco-elastic properties and stretched shape of the geotextile. The stretched shape of the geotextile is an important factor that depends upon the pull generated by the anchors, the geometry of the anchor array, and the prepared or groomed shape of the ground surface.

With regard to orientation, the natural tendency is install anchors normal to the slope in order to intersect potential failure surfaces with minimal anchor lengths. Hryciw (1991) has shown that this orientation is not optimal for increasing slope stability. Anchors inclined some 20 to 40 degrees with the slope normal typically give better results.

4.0 SOIL BIOENGINEERING

4.1 Principles

Soil bioengineering or biotechnical stabilization employs living plant material, namely, stems and branches, as the main structural components or reinforcements in a soil. Soil bioengineering techniques such as live staking, brush-layering, and contour wattling (or live fascines) work on this principle. Live cut stems and branches provide immediate reinforcement; secondary stabilization occurs as a result of adventitious rooting which develops along the length of buried stems.

The general principles and techniques of biotechnical slope protection and soil bioengineering have been presented elsewhere by Gray & Leiser (1982). Kropp (1989) describes the use of contour wattling in combination with subdrains to repair and stabilized a debris flow in California. Gray and Sotir (1992) discuss the use of soil bioengineering techniques to stabilize cut and fill slopes along highways.

4.2 Conjunctive Use of Soil Bioengineering and Anchored Netting

Live staking entails tamping short lengths of cut, woody plant material into the ground in a regular array. Species such as willow which root readily from cuttings are ideal for this purpose. A schematic illus-tration of live staking is shown in Figure 6. The combined or conjunctive use of live stakes and an anchored geonet are shown in Figure 7.

5.0 RESEARCH PROGRAM

5.1 Research Objectives

A research program has been undertaken to determine the effective-ness of anchored netting systems in resisting tractive stresses produced by water flowing down a slope and seepage stresses caused by water flowing through the sand. The research tasks consist of both analytical and experimental studies to determine the optimal anchorage design and installation procedure for netting and geofabrics that takes into account the influence of the following soil/slope/fabric variables:

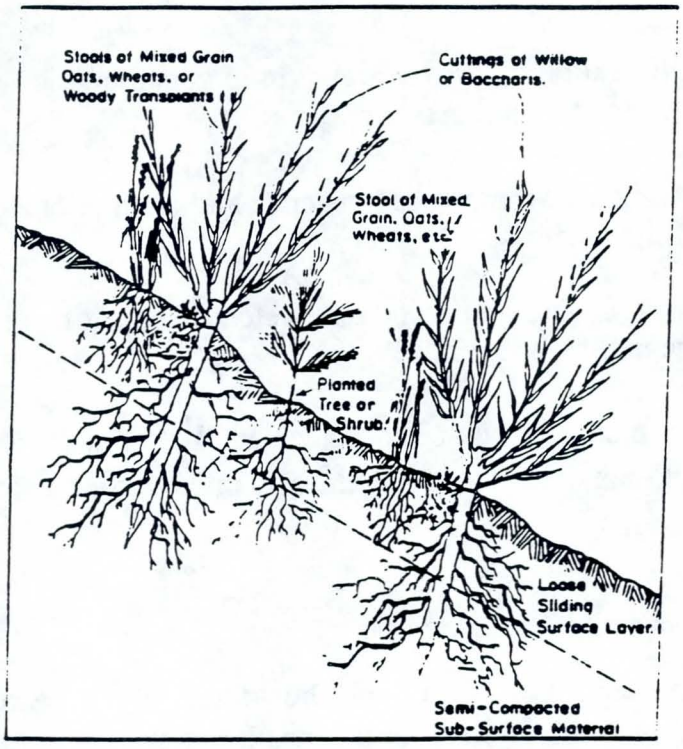

Figure 6. Schematic illustration of live staking using short lengths of woody plant material that roots readily from cuttings.

Figure 7. Illustration of live cut stakes used in conjunction with a ground net or anchored geotextile.

- geometric arrangement, spacing, and inclination of the anchors
- visco-elastic properties and stretched shape of the netting or geofabric

The influence of plant roots on performance will be simulated by introducing (mixing) discrete, randomly distributed fibers into the sand near the surface (below the netting).

5.2 Influence of Anchor Array or Pattern

Different anchor point arrays are shown in Figure 8. A relatively wide erosion channel of width S_e may form beneath a stretched, but uncurved fabric in a square pattern (Figure 8a). By offsetting alternate anchor rows (Figure 8b) into a triangular anchor pattern, the width of a direct downslope erosion channel can be reduced considerably, If the spacing between rows is also reduced (Figure 8c), a potential meandering erosion channel must follow a more tortuous path, and therefore, erosion resistance will be increased still further.

5.3 Influence of Initial Ground Shape

The initial shape of the ground surface also affect the efficiency of stress transfer. Pre-forming or plowing the ground surface across a slope as shown in Figure 9 can enhance performance by favorable modification of curvature and by providing a "contour terrace" effect. Plowing furrows in the slope and mounding the soil on either (uphill and downhill) side enlarges the zone of curvature beneath the netting. Anchors would be installed in the furrows in this case as shown schematically in Figure 9.

5.4 Influence of Anchor Inclination & Method of Emplacement

The inclination of the anchors and their method of emplacement affect the stress transfer between the netting and the ground surface. Different methods of transferring load to a sloping surface are shown schematically in Figure 10. A driven anchor system that relies on skin friction (e.g., ribbed metal rods) will

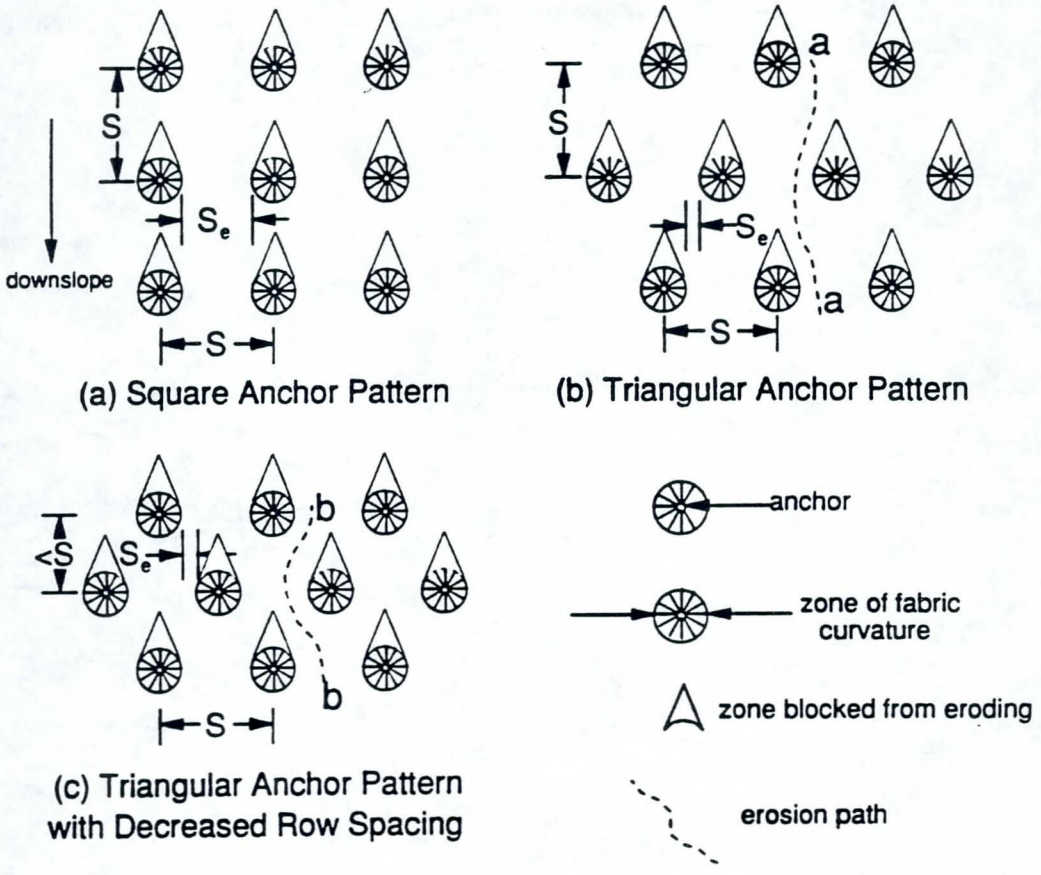

Figure 8. Anchor arrays for ground anchored netting systems (after Hryciw, 1990)

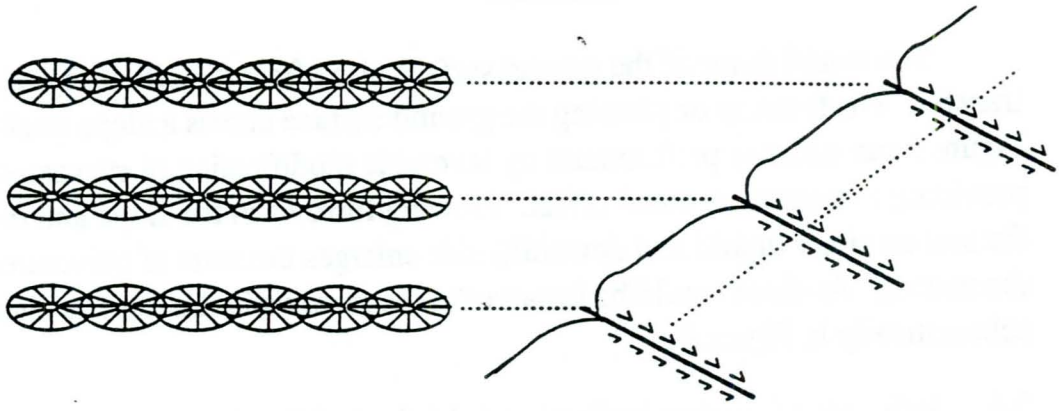

Figure 9. Pre-formed or furrowed surface for anchored netting (after Hryciw, 1990).

respond differently than anchors that are installed in other ways. The experiments will use thin wire anchors in order to mobilize only tensile resistance and not not unduly affect shear resistance along potential sliding surfaces by shear and bending resistance in the anchor.

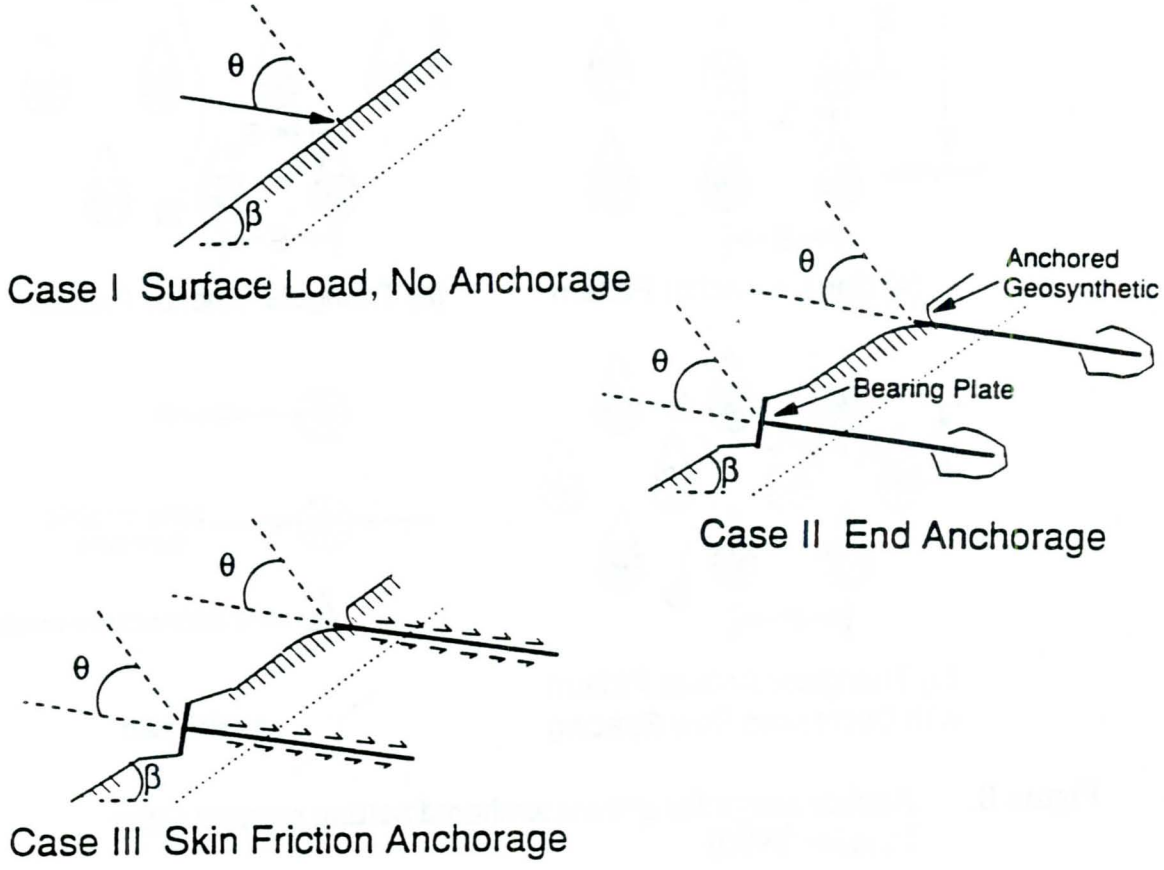

Figure 10. Anchor arrays for ground anchored netting systems (after Hryciw, 1990)

The anchors will also be connected to weights on pulleys as shown schematically in Figure 11. This arrangement is equivalent to the external anchor loading condition shown in Figure 10. This method of applying the anchor load permits sliding deformation to occur in the slope while maintaining a constant anchor load. It also permits easy detection and measurement of slope movement by simply monitoring and recording the position of the pulley weights.

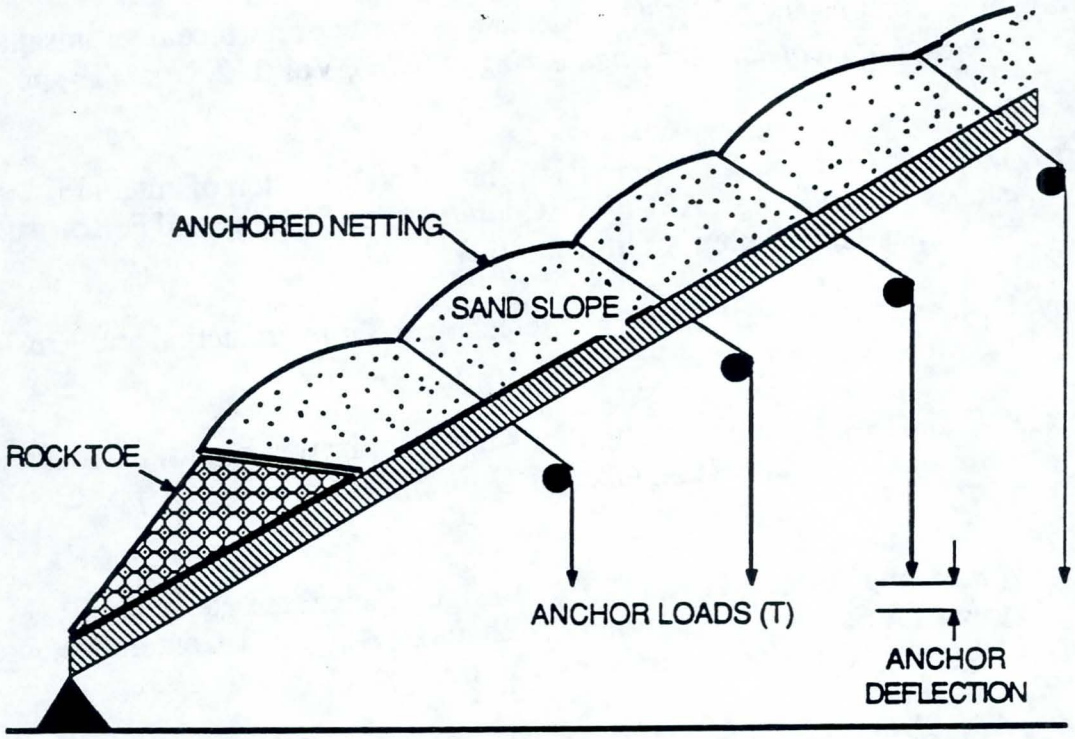

Figure 11. Schematic diagram of experimental test set-up showing inclined anchor forces applied to curved netting on surface via thin wire attached to pulley weights beneath.

6.0 CONCLUSIONS

An anchored geonet can be used to protect coastal landforms such as beach dunes where regulations prevent the use of structural armor systems. The geonet is stretched tightly on the slope and tensioned by means of ground anchors that pass through reinforced openings in the net. Guidelines are available to predict the optimal anchor array and stretched shape of the netting. Tests are presently

underway to corroborate these guidelines and examine the effectiveness of this approach. An anchored geonet system also lends iteself to ancillaruy protection with soil bioengineering measures such as live staking and fascines.

7.0 REFERENCES

Gray, D.H. and Ohashi, H. (1983). Mechanics of fiber reinforcement in sand. *Journal of Geotechnical Engineering* (ASCE), Vol. 112, No. GT3, pp. 335-353.

Gray, D.H. and Sotir, R.B. (1992). Biotechnical stabilization of cut and fill slopes. *Proceedings*, ASCE-GT Conference on Stability and Performance of Slopes-II, Berkeley, California, July, 1992

Gray, D.H. and Leiser, A.T. (1982). Biotechnical Slope Protection and Erosion Control. Van Nostrand Reinhold, New York, N.Y.

Hryciw, R.D. (1991). Anchor design for slope stabilization by surface loading. *Jour. of Geotechnical Engineering* (ASCE), Vol. 117, No. 8, pp. 1260-1276.

Hyrciw, R.D. and Ahmad, H.K. (1992). Design of anchored geosynthetic systems for slope stabilization. *Proceedings*, ASCE-GT Conference on Stability & Performance of Slopes-II, Berkeley, CA, July 1992.

Kropp, A. (1989). Biotechnical stabilization of a debris flow scar. *Proceedings*, XX Intl. Erosion Control Assoc. Conference, Vancouver, pp. 413-429.

Koerner, R.M. (1985). Slope Stabilization Using Anchored Geotextiles and/or Geogrids. *Proceedings*, Specialty Conf. on Geotechnical Engineering for Roads and Bridges, Harrisburg, PA.

Koerner, R.M. (1986). *Designing with Geosynthetics*. Prentice-Hall, Englewood Cliffs, New Jersey.

Maher, M. and Gray, D.H. (1990). Static response of sands reinforced with randomly distributed fibers. *J. of Geotechnical Engr.* (ASCE), Vol. 116, No. GT12, pp. 1661-1677.

PORE PRESSURES IN RIPRAP STRUCTURES DUE TO NON-STATIONARY LOADS

M.B. de Groot
Delft Geotechnics, Delft, The Netherlands
J. Lindenberg
Ministry of Public Works and Water Management, The Netherlands

ABSTRACT

The design of riprap structures often requires the prediction of the pore pressures due to non-stationary loads. These may be characterized by one or more potentially relevant phenomena. This paper presents "rules of the thumb" to assess the relevancy of the following phenomena: turbulence, phreatic storage, disconnection of phreatic surface at boundaries, internal phreatic set-up, elastic storage, excess pore pressures due to densification by cyclic loading.

1. INTRODUCTION

Pore pressures in and underneath a riprap structure may have a great influence on the design of the structure. This is illustrated with the breakwater of Figure 1. The stability against sliding of the front slope decreases, if the phreatic level inside the breakwater caused by wave run-up remains high during run-down. Excess pore pressures in the sand underneath the toe may also endanger this stability. The breakwater core must be separated from the sand by a filter of several carefully made filter layers, if high gradients occur along the interface between core and sub soil. With limited gradients, however, no filter is needed or just one filter layer. Finally, the groundwater table in the sand back-fill may become very high due to the internal phreatic set-up during a storm.

Pore pressures are the result of the interaction between external hydraulic loads, the geometry of the structure and the properties of riprap and subsoil. Depending on the characteristics of these elements, the pore pressures may be influenced by one or more of the following phenomena:

- turbulence of pore water flow
- phreatic storage (water level variation within the structure)
- disconnection of phreatic surface at boundaries
- internal phreatic set-up
- elastic storage by elastic compression of the pore water
- excess pore pressures due to densification (plastic volume decrease) of the soil skeleton by cyclic loading.

Mathematical equations and models generally take into account just one or two of these phenomena. This is usually justified, because one or two of the phenomena dominate in most cases. The question remains, however, to decide which phenomenon dominates in which situation. The paper will focuss the attention to this question. A brief explanation of some of the above mentioned phenomena will be given. "Rules of the thumb" will be presented to assess the importance of any phenomenon, and will be applied to the example of Figure 1.

2. TURBULENT PORE WATER FLOW

The flow inside a riprap structure is usually strongly influenced by turbulence. The influence of turbulence can be assessed among others with the following formula for the flow resistance of riprap (Shih, 1990; Burchart & Christensen 1991):

$$i = \alpha_0 \cdot \frac{(1-n)^2}{n^3} \cdot \frac{\nu}{g \cdot D_{15}^2} \cdot v + \beta_0 \cdot \frac{1-n}{n^2} \cdot \frac{1}{g \cdot D_{15}} \cdot v \cdot |v| \qquad [1]$$

where i is the head gradient due to hydraulic resistance, v the filter velocity, n the porosity, ν the kinematic viscosity of the water, g the acceleration of gravity, D_{15} a grainsize characteristic and α_0 and β_0 dimensionless, empirical constants with about the following values for steady flow: $\alpha_0 \approx 500$ and $\beta_0 \approx 2$. These values can also be used, as approximation, for cyclic flow with periods larger than 3 s.

The first term represents the laminar component, the second term the turbulent component. The second term divided by the first one yields:

$$\frac{\text{turbulent term}}{\text{laminar term}} = \frac{\beta_0}{\alpha_0}\cdot\frac{n}{(1-n)}\cdot Re = 0.003\cdot Re \qquad [2]$$

$$\text{with } Re = \frac{v\cdot D_{15}}{\nu}$$

Re is a Reynolds number. Where and when Re > 30, turbulence starts to be relevant. Where and when Re > 3000, turbulence dominates. This is the case with D_{15} = 0.01m, as soon as v > ca 0.1 m/s or i > ca 0.5 and with D_{15} = 0.1m, as soon as v > ca 0.01 m/s or i > ca 0.001.

With turbulent flow it is often practical to apply a linearised "Darcy" flow resistance, $k_0 = v/i$, which can by found from the second term in equation [1] by introducing a characteristic filter velocity v_0 or a characteristic gradient i_0:

$$k_0 = \frac{n\cdot g\cdot D_{15}}{\beta_0\cdot|v_0|} \quad \text{or} \quad k_0 = \sqrt{\left\{\frac{n\cdot g\cdot D_{15}}{\beta_0\cdot|i_0|}\right\}} \qquad [3]$$

3. PHREATIC STORAGE

3.1 General

Fluctuating external pressure conditions (e.g. tide or waves) cause the phreatic level in a riprap structure to rise and drop alternately which requires the flow of water to and from the phreatic surface. This process is attended by a phase lag in the propagation of the external pressure penetration in the structure and by simultaneous damping. This is due to the combination of drainage with 'phreatic storage', the phenomenon of temporarely storage of water by the fluctuating phreatic level.

Phreatic storage determines, for example, how far waves will penetrate into the breakwater of Figure 1. Analytical solutions are available for the simplified one-dimensional case with horizontal flow and linearized flow resistance.

One solution yields the phreatic level in the riprap structure after a sudden external waterlevel increase (CIRIA/CUR, 1991, section 5.2.8.1). Another yields the phreatic level due to a harmonically varying external waterlevel (Solitt & Cross, 1972; Hölscher et al., 1988). See Figure 2. These solutions may be characterized by a *characteristic period*, Tphs, or a *characteristic length*, Lphs, defined as follows:

$$Tphs = \pi \cdot n \cdot B^2/(h \cdot k_0) \quad [4]$$

$$Lphs = \sqrt{\{T \cdot h \cdot k_0/(\pi \cdot n)\}} \quad [5]$$

where B is the width of the structure, n the porosity, T the wave period, h the height of the structure and k_0 the (linearised) Darcy permeability. The physical meaning of Tphs and Lphs for the cases with dominating phreatic storage can be described as: Tphs is the order of time needed for a load variation at the front to penetrate over a distance B and Lphs is the distance from the front where such load is considerably damped. For example, the amplitude of the wave in the example of Figure 2 damps according to the negative exponential function exp(-x/Lphs), where x is the distance to the intersection of still water level and slope.

If the quotient $Tphs/T = B^2/Lphs^2$ is much smaller than unity, phreatic storage is not important and the load can be considered as quasi-stationary. If it is much larger than unity, phreatic storage is important in the part of the structure at a distance 1 to 3 times Lphs from the waterfront and the load variation at the front is not observed at the back: the construction width B does not influence the process any more.

3.2 Penetration of waterlevel variation through breakwater or dike

The characteristic parameters are calculated for the wind wave loaded rock fill breakwater of Figure 1, assuming B = 30 m; h = 10 m; n = 0.4; k_o = 0.4 m/s; T = 8 s:

Tphs = 300s

Lphs = 5 m.

Consequently: Tphs/T = $B^2/Lphs^2$ = 40 >> 1, from which it may be concluded that the phreatic level inside the dike only varies noticably in the outer few meters.

These parameters also allow the following conclusion for the case of a rock fill dike (without sand backfill) completely separating a water basin from the sea. With the same values for B, h, n, k and T, the same values for Tphs and Lphs are found and phreatic level variation is again only noticable in the outer few meters. Consequently, the waterlevel in the basin is not influenced by the windwaves at sea.

If instead of a wind wave, a tidal wave with T = 45 000 s is considered, the following values are found:

Tphs = 300s

Lphs = 400 m.

Now: Tphs/T = $B^2/Lphs^2$ = 0.007 << 1, from which it may be concluded that the tidal wave completely penetrates through the rock fill dike, as in a stationary situation.

If, however, the dike would be constructed of sand with a permeability of k = 0.000 1 m/s, whereas B, h, n would remain the same, then the following values are found with a tidal wave:

Tphs = 1 100 000s

Lphs = 6 m.

Now: Tphs/T = $B^2/Lphs^2$ = 25 >> 1, from which it may be concluded that the phreatic level inside the dike only varies noticably in the outer half of the dike and that the tidal variation will hardly induce any water level variation in the basin.

3.3 Maximum head gradient and filter stability

The value of Lphs can also be applied for the preliminary design of the filter underneath a breakwater as according to Figure 1. The number of filterlayers required between seabed sand and core may vary between zero and three, depending on the hydraulic gradient, i, along the seabed-breakwater interface (de Groot et al., 1992). The order of magnitude of the gradient can be found with the above mentioned analytical equation for harmonically varying outside waterlevel:

$$i = \frac{\frac{1}{2}H}{Lphs} \cdot \exp(-\frac{x}{Lphs}) \qquad [6]$$

With the above found value of Lphs = 5 m and a waveheight of H = 6 m, the gradient at the centre of the breakwater (x = 15m) is no more than a few percent and only one filter layer is needed.

Verification of this gradient with the help of a more sophisticated calculation model is required before deciding about the number and the extension of the filter layers. An example of a more sophisticated model is the MBREAK code, which is developed for the European program MAST from the HADEER code (Hannoura, 1978 and Hölscher et al., 1988).

4. DISCONNECTION OF PHREATIC SURFACE AT BOUNDARIES

The phreatic surface is supposed to be at the same level at both sides of the outer boundary in the above mentioned analytical solutions. In reality, however, different levels have often observed (Hannoura, 1978). Several phenomena, which have to do with the difference in flow regime outside and inside the structure, may be responsible for this 'disconnection'. The role of air in the water near the phreatic surface is probably different. Another relevant difference has to do with the influence of the different forces. Pressure gradients and gravity are important for both types of flow. Outside, these forces are hardly reduced by friction forces and may result in large accelerations. Inside, however, these forces are largely compensated by friction forces and no large scale accelerations occur.

This results, among others, in limited inside flow velocities, and, because the vertical velocity v_p of the phreatic surface is by continuity related to the vertical flow velocity (Figure 3), to limited values of v_p.

The largest downward velocities occur with the largest downward head gradient, which occurs with free falling water when the pore pressure is everywhere the same and equal to the atmospheric pressure. This gradient is equal to unity in downward direction. The consequent maximum downward velocity of the phreatic surface in the cases presented in Figure 3 is:

$$[v_p]_{max} = \frac{k_o}{n} \cdot \sin^2\alpha \qquad [7]$$

The upward velocity is limited as well and probably has the same order of magnitude.

This limit to the velocity may be compared with the velocity of the external waterlevel variation. For example, a 1:1.5 breakwater slope with a coarse armourlayer may be characterized by $k_o \approx 1$ m/s, $n \approx 0.4$ and, consequently, $[v_p]_{max} \approx 0.8$ m/s. If it is loaded by swell with a waveheight of 2m and a period of 18 s, the wavesteepness is small and the wave reflects to the slope, causing a harmonically varying waterlevel with maximum vertical velocity of about 0.6 m/s. Consequently, the waterlevel inside the armourlayer follows the external waterlevel easily.

A windwave with $H \approx 5$m, $T \approx 6$s, however, will break at the slope and cause maximum velocities of several meters per second. Then, the waterlevel in the armour layer remains behind and a discontinuity in the phreatic level at the outer boundary of a riprap structure occurs (Hölscher et al., 1988). Equation [7] makes clear that the maximum velocity, v_p, depends on the permeability and, consequently on the grain size of the riprap. Thus, the maximum velocity in the core of a breakwater is much smaller than in the armour layer. This may lead to disconnections of the phreatic level also at the interface between armour and core.

5. INTERNAL PHREATIC SET-UP

A second non-linear effect is the 'internal phreatic set-up'. This effect only occurs with a slope. It is due to the fact that the inflow surface along the slope under a wave crest is larger than the outflow surface under a wave trough, and to the fact that the average path for inflow is shorter than for outflow (Figure 4). Hence, during harmonic outside water level changes, more water enters the structure than it leaves. Eventually, a compensating outflow of the surplus of water is achieved by an average internal set-up and the consequent outward gradients. The set-up is particularly high (close to 0.5 times the wave height), if the water can only flow back in the direction of the sea. This is the case if the lee-side of the rock fill structure is closed, as in the case of a sand backfill behind a breakwater (Figure 1). It should be emphasized that 'internal' set-up is not due to asymmetry of the external load but must be added to the 'external' set-up by asymmetric wave load of the slope.

The governing equations have been formulated by Barends (1988) and he also found an analytical solution. This solution is a strong function of the ratios $H\cot\alpha/L_{phs}$ and B/L_{phs}. The relative set-up, the set-up divided by the waveheight H, is roughly proportional to $H\cot\alpha/L_{phs}$. It is also roughly proportional to B/L_{phs}, untill a certain maximum of B/L_{phs}, which equals 3 in case of a closed lee-side and 10 in case of an open lee-side. A rough estimate of the relative set-up for $B/L_{phs} > 3$, respectively $B/L_{phs} > 10$, reads:

$$\frac{\text{set-up}}{H} \approx 0.1 \cdot \frac{H \cdot \cot\alpha}{L_{phs}} \qquad [8]$$

With smaller values of B/L_{phs}, the value of the set-up found in [8] must be multiplied by $B/(3 \cdot L_{phs})$, respectively $B/(10 \cdot L_{phs})$.
Equation [8] is applied to the breakwater of Figure 1 with the properties given in the first example of section 3 ($B = 30$ m; $h = 10$ m; $n = 0.4$; $k_0 = 0.4$ m/s; $T = 8$ s; $L_{phs} = 5$ m), a sea slope of 1:3 and a waveheight of $H = 6$m. This yields: $B/L_{phs} > 3$ and a set-up ≈ 2 m. If this breakwater would not have a closed lee-side, the following values would be found: $B/L_{phs} < 10$, $B/(10.L_{phs}) = 0.6$ and the set-up ≈ 1.3 m.

6. ELASTIC STORAGE

6.1 General

In this paragraph attention is paid to the effects caused by the elastic compressibility of the pore fluid. Varying porepressures cause some variation of the volume of the porefluid. This variation is very small if the pore fluid is pure water without any air in it, because water is practically incompressible. However, in the region of varying water level, air is present in the water and the compressibility may be large enough to cause a significant quantity of water to flow in and out the mass of granular material.

When the period, T, of the head variation along the external boundary of the riprap structure is so short that this process of inflow and outflow cannot take place completely, then 'elastic storage' plays a role. It means that the change of pore pressure is retarded by the fact that the needed outflow of pore water is not possible. The soil is too impermeable and/or the pore fluid is too compressible in relation to the rate of boundary pressure changes. Like phreatic storage, elastic storage is attended by a phase lag in the propagation of cyclic phenomena in granular media and by damping.

Also here a *characteristic period*, Tes, and a *characteristic length*, Les, may be defined:

$$Tes = \frac{\pi \cdot B^2}{c_v} \qquad [9]$$

$$Les = \sqrt{(T \cdot c_v / \pi)} \qquad [10]$$

$$\text{with} \quad c_v = \frac{k_o \cdot Kw}{yw \cdot n} \qquad [11]$$

where B is the width of the structure or the thickness of the relevant layer or any other characteristic measure of the structure, T the wave period, c_v the consolidation coefficient for pore fluid compressibility (m^2/s), n the porosity, k_o the linearised permeability (m/s), γ_w the unit weight of the pore water (N/m^3) and Kw the modulus of compressibility of the air containing pore water (N/m^2).

The physical meaning of Tes and Les for the cases with dominating elastic storage can be described similarly to Tphs and Lphs: Tes is the time needed for a harmonic varying load at the boundary to penetrate over a distance B into the granular mass. Les is the distance from the boundary where any load variation is considerably damped: the amplitude of a harmonic wave damps according to the negative exponential function exp(-x/Les). If the quotient Tes/T = B^2/Les^2 is much smaller than unity, elastic storage is not important and the load can be considered as quasi-stationary. If it is much larger than unity, elastic storage is important and the load variation at the boundary is no longer observable at distance B: the construction width B does not influence the process any more.

6.2 Penetration of porepressure variation into riprap

The application of the characteristic parameters requires some knowledge about the air content in the pore water. Unfortunately, the air content is difficult to establish. The analyses of excess pore pressures measured in sand in some cases, gives the impression that the air content near the phreatic surface may reach values up to 10% and the air content in the sandy sea bed near the shore may reach values up to 1%. Even less is known about the air content in riprap.

For coarse riprap (k_o = 1 m/s) with an air content of 1%, c_v = 3000 m^2/s (order of magnitude). With B = 30m and T = 8 s, Tes = 1 s. Thus, Tes << T and elastic storage hardly plays a role and the load may be considered quasi-stationary. Only with higher load frequencies, as occurring with wave impacts, or very large structures, elastic storage may play a role.

With fine riprap (k_o = 0.2 m/s) and 5% air in the porewater, c_v = 100 m^2/s and Tes = 30s. Now elastic storage is important in case of waveloads (T = 8 s). The pressure head variations will not completely penetrate into a 30m wide structure, but only over a length with the order of magnitude of Les = 16 m.

One may wonder how important elastic storage is in relation to phreatic storage. This can be found out by comparing the characteristic periods or the characteristic lengths, as defined in the equations [4], [5], [9] and [10]. If the 30m wide breakwater of Figure 1 would be constructed of fine riprap, the assumptions of section 3.2 would need a small change: $k_o \approx 0.2$ m/s, which yields: Tphs ≈ 600s and Lphs ≈ 3.5 m. Now Tphs/Tes = Les²/Lphs² ≈ 20 >> 1, from which it may be concluded that phreatic storage dominates over elastic storage. There is no need to consider elastic storage here.

6.3 Upward pressure gradients in sea bed

Thus, elastic storage in the riprap of the breakwater of Figure 1 is not likely to be important. In the sand underneath the toe of this breakwater, however, it may be very relevant. The value of c_v for medium fine seabed sand with 1% of air in the porewater may be: $c_v \approx 0.1$ m²/s. With a wave period of T = 8s, this yields Les ≈ 0.25 m. The wave penetrates the soil over a depth of no more than some decimeters. This results in strong local outward pressure gradients in the sand and in a considerable reduction of the effective stress at the moment of a wave trough above the toe (Figure 5). Field observations confirm this theory (Zen and Yamazaki, 1991).

The risk of strong reduction of the effective stresses is often dangerous along a slope around the water level, where a high air content in the pore water may be expected. Sliding of a slope protection may be the result (Schulz & Köhler 1989).

6.4 Elastic storage by compressibility of soil skeleton

Another type of elastic storage is due to the compressibility of the soil skeleton. It is not important for riprap or sand directly in contact with the outside water. It may be important, however, if the external hydraulic loads reach the riprap indirectly, e.g. via a caisson. In those cases it is usually relevant if there is not much air in the porewater and the skeleton is rather loosely packed, circumstances which cause this type of elastic storage to dominate over the type discussed above. Analytical solutions for a combination of both types of elastic storage under harmonic loads are given by Yamamoto et al (1978), Verruyt (1982) and others.

7. EXCESS PORE PRESSURE DUE TO DENSIFICATION BY CYCLIC LOADING

Pore volume change in granular material may also be caused by dilation or contraction. Cyclic shear loading in loosely packed material calls for a continuous tendency for densification (contraction). As in the case of elastic storage this densification may be (partly) prevented by the pore fluid where the permeability and the compressibility of the pore water are too small in relation to the period of external loading (e.g. waveperiod). The result is a generation of excess pore water pressure in the granular mass which increases with each load cycle. Under special unfavourable conditions the excess pore water pressure may become so large that stability loss and liquefaction takes place. This phenomenon is sometimes referred to as "residual liquefaction" to distinguish from the possible "oscillatory" liquefaction due to the elastic storage.

The characteristic time period, Tpvs, and the characteristic length, Lpvs, may be defined as follows:

$$Tpvs = D^2/(N \cdot c_v^*) \quad [12]$$

$$Lpvs = \sqrt{(N \cdot T \cdot c_v^*)} \quad [13]$$

where D is the depth or length over which the shear stress works most heavily, N the number of stress cycles required for liquefaction in undrained conditions , $c_v^* = k_o/(\gamma \cdot mve)$ the consolidation coefficient for the skeleton during unloading, mve the coefficient of volume change during unloading and T the characteristic period of external loading. N can be established in laboratory tests as function of shearstress ratio (shear stress amplitude over mean effective stress) and relative density. At high stress ratios N may be 1 to 10 for loose sand and gravel, but may be 1000 or more for dense granular material.

As an example for which pore water generation due to plastic deformation is important, wave pressure penetration in loosely packed, fine sand at the toe of the breakwater of Figure 1 can be mentioned. The values Tpvs and Lpvs may be estimated assuming the shear stress to penetrate over a depth of $D = L/2\pi$ into the seabed. For example, with T = 10s, D = 10m, N = 10 and $c_v^* = 0.01 m^2/s$, Tpvs = 1000s and Lpvs = 1m. Clearly Tpvs >> T and, consequently, this phenomenon is important. Liquefaction may even occur (Figure 6). The resulting excess pore pressure should be added to the one due to elastic storage (Figure 5). Sophisticated computer codes are available to analyse such situations, including the influence of wave distribution (Barends & Calle, 1985) and the favourable effect of pre-loading or load history (de Groot et al., 1991).

More favourable is the case in which the layer thickness of the loosely packed silty sand would be smaller than 1m. Then D < 1m, Tpvs < T and a large part of the excess pore pressure drains away during every wave.

Riprap, with $c_v^* > 10$ m²/s, is hardly sensitive to this type of pore pressure generation due to wave loads, as can be concluded from the value of Tpvs/T. During earthquakes, however, the phenomenon may also be important in granular materials with $c_v^* \approx 10$ m²/s (e.g. gravel) as the value of T has the order of 0.1s. In many regions in the world earthquake is an important recurrent phenomenon and the degree of shaking may be very serious (LIQUEFACTION OF SOILS DURING EARTHQUAKES, 1985). The probability of earthquake induced liquefaction is generally higher than for wave loading because of the higher load frequency (in fine to medium sand the consolidation is only of minor importance during earthquake) and the fact that the influence depth can be very large (no geometric damping because of the fact that earthquake originate from deep layers).

CONCLUSIONS

Each of the phenomena discussed in this paper may be characterised by a characteristic parameter: turbulence by a Reynolds number, the disconnection of the phreatic surface by a maximum velocity, the internal set-up by two ratios of length parameters and the other three phenomena (phreatic storage, elastic storage and excess pore pressures due to densification by cyclic loading) by a characteristic time period or a characteristic length. The relevancy of each phenomenon can be assessed by considering the absolute value of the parameter or by comparing it with the corresponding parameter of the load or of another phenomenon.

REFERENCES

Barends FBJ and Calle EOF (1985). A method to evaluate the geotechnical stability of offshore structures founded on loosely packed sand in a wave loading environment. *BOSS´85*, Delft: 643-652.

Burchart HF and Christensen C (1991). On stationary and non-stationary porous flow in coarse granular materials. *MAST G6-S*. University of Aalborg.

Barends FBJ (1988). Discussion contribution. *BREAKWATERS 1988 - Design of breakwaters*. Thomas Telford, London.

CIRIA/CUR (1991). *Manual on the use of rock in coastal and shoreline engineering*. ISBN 0-86017-326-7. London and Gouda.

Groot MB de, Lindenberg J and Meijers P (1991). Liquefaction of Sand Used for Soil Improvement in Breakwater Foundations. *Geo-Coast´91*, Yokohama 5/4.

Groot MB de, Bakker KJ and Verheij HJ (1992). Design of geometrically open filters in hydraulic structures. *Geo-Filters´92*, Karlsruhe.

Hannoura AA (1978). *Numerical and experimental modelling of unsteady flow in rockfill embankments*. PhD thesis, Windsor, Ontario.

Hölscher P, Groot MB de and Meer JW van der (1988). Simulation of internal water movement in breakwaters. *Int Symp on Modelling of Soil-Water-Structure Interactions* 427-433. Rotterdam: Balkema.

Committee on Earthquake Engineering/National Research Council (1985). *LIQUEFACTION OF SOILS DURING EARTHQUAKES*. National Academy Press, Washington DC

Schulz H and Köhler HJ (1989). The developements in geotechnics concerning the dimensioning of revetments for inland navigable waterways. *PIANC-AIPCN Bulletin 1989 64*, 160-173.

Shih RWK (1990) Permeability Characteristics of Rubble Material - New Formulae. *Proc 22nd ICCE Delft & HR Published Paper No 38*, Hydraulic Research Wallingford.

Solitt CK and Cross RH (1972). Wave Reflection and Transmission at Permeable Breakwaters". Report 147, Parsons Laboratory, MIT.

Verruijt A (1982). Approximations of Cyclic Pore Pressures Caused by Sea Waves in a Poro-elastic Half Plane. *Soil Mechanics - Transient and Cyclic Loads*, Ch 3 Ed Pande and Zienkiewicz, John Wiley & Sons Ltd.

Yamamoto T, Koning HL, Sellmeyer H and Hijum E van (1978). On the response of a poro-elastic bed to water waves. *J Fluid Mech* (87), 193-206.

Zen K and Yamazaki H (1991). Field obsevation and analysis of wave-induced liquefaction in seabed. *Soils and Foundations* Vol 31-4: 161-179.

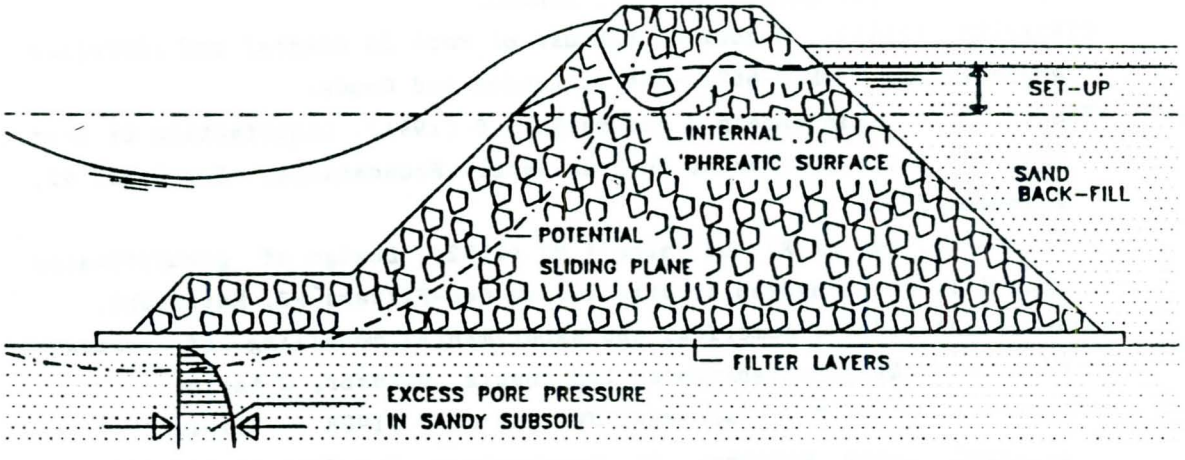

FIG.1 EXAMPLE OF RIPRAP STRUCTURE: BREAKWATER WITH BACK-FILL

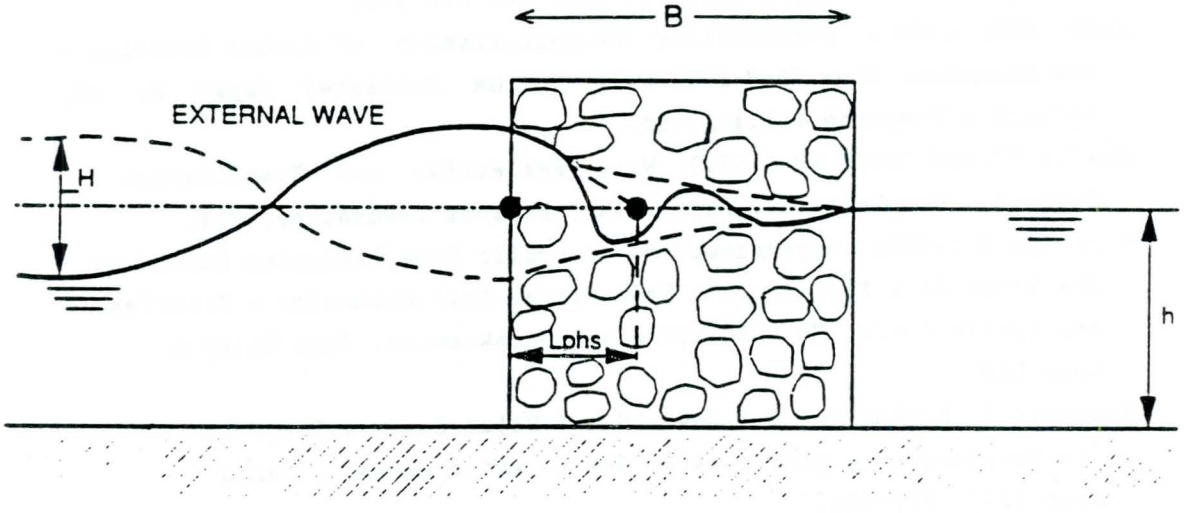

FIG.2 PHREATIC SURFACE IN SCHEMATIZED WAVE LOADED BREAKWATER

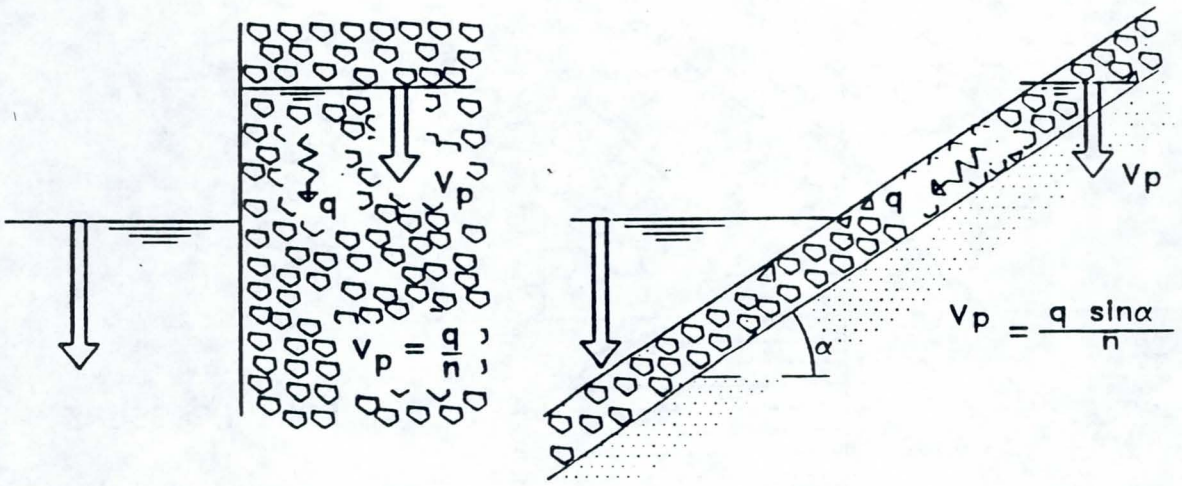

FIG.3 LIMITATION TO VERTICAL VELOCITY OF INTERNAL PHREATIC SURFACE

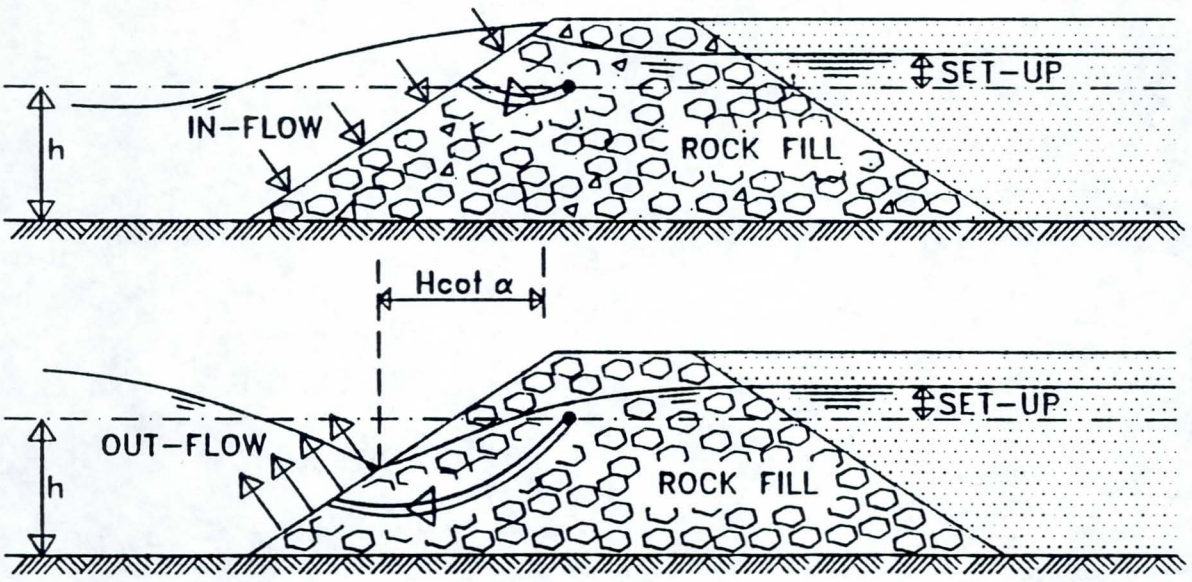

FIG.4 INTERNAL PHREATIC SET-UP DUE TO IN-FLOW DIFFERENT FROM OUT-FLOW

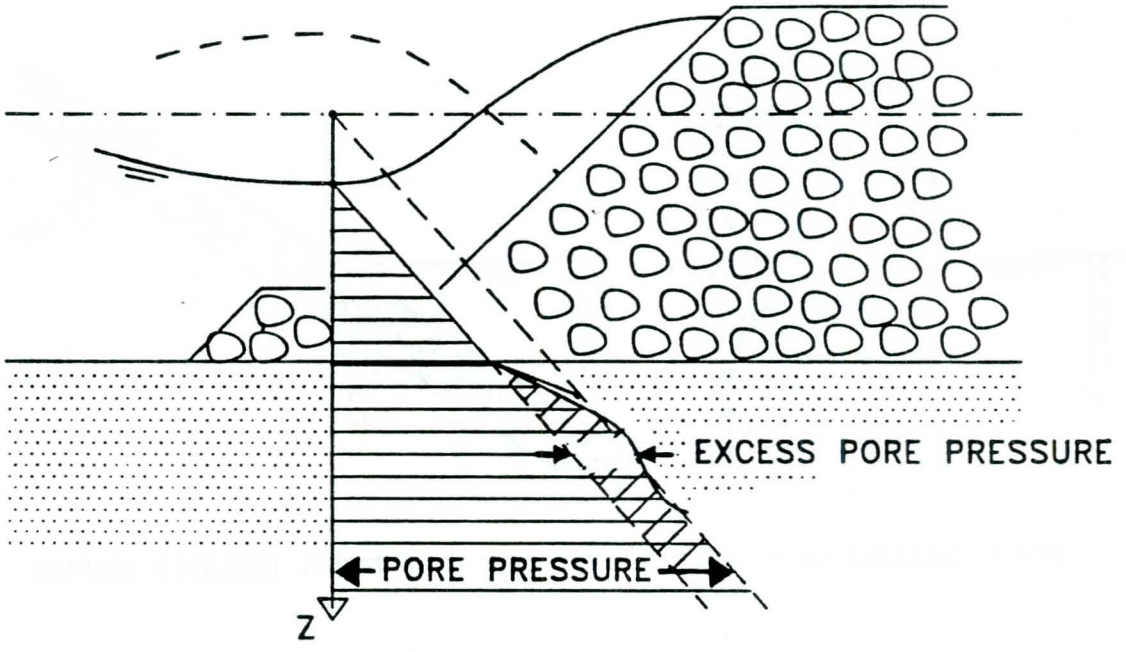

FIG.5 ELASTIC STORAGE INDUCED EXCESS PORE PRESSURE AT BREAKWATER TOE

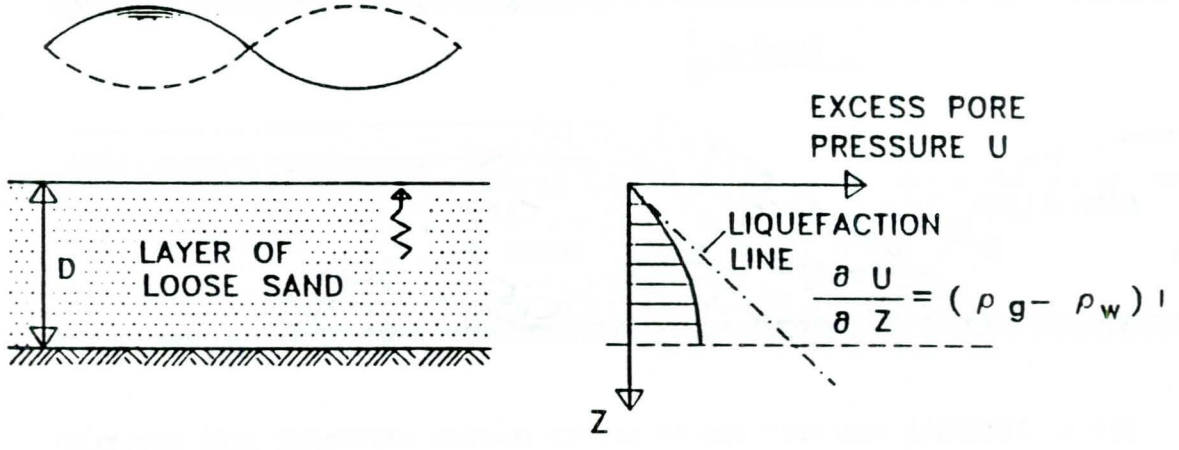

FIG.6 LIQUEFACTION OF SEABED DUE TO DENSIFICATION BY CYCLIC LOADS

WAVE INDUCED SLIDING OF REVETMENTS

M.B. de Groot and P. Meijers
Delft Geotechnics, Delft, The Netherlands

INTRODUCTION

This paper deals with the stability of wave loaded revetments against sliding along the slope. Both wind waves and ship waves are considered. According to traditional design rules, as the ones advocated by the PIANC (1987), the *local* sliding stability of each element of the revetment should be guaranteed. From an analysis of many well functioning revetments it can be learned, however, that the local sliding stability is often not met in the wave zone. Yet, no sliding occurs because the part of the revetment in the wave zone is supported by the adjacent parts of the revetment, the toe structure or an anchoring structure: the *overall* sliding stability is guaranteed. Revetment design based on local sliding stability would, in many cases, result in exceptional thick cover layers.

Assessment of the overall sliding stability is of particular interest for a structure like the one presented in Figure 1, where the permeability of the cover layer of the revetment is relatively low compared to the permeability of the riprap filter layer immediately underneath the cover layer. During wave attack large outward pressure head differences over the cover layer in the wave zone occur. These would cause local sliding, if this would not be prevented by load transfer parallel to the slope to the stable part of the revetment below the wave zone and eventually to the toe structure. A revetment with a mattress type of cover layer may be capable to transfer these forces upwards to an anchoring structure above the wave zone.

In many revetments with riprap cover layers no outward pressure head differences occur. If the subsoil consists of fine sand, however, large excess pore pressures may occur closely underneath the revetment and endanger the stability against sliding along an undeep plane nearly parallel to the slope (Köhler & Schulz, 1986). A revetment with a riprap cover layer usually cannot transfer large forces parallel to the slope and must meet the local sliding stability criterion, unless a strong geotextile is present anchored above the wave zone (Figure 2).

The main steps needed for the assessment of the overall sliding stability are discussed in this paper and some results are presented for the revetment types given in Figures 1 and 2.

METHOD TO ASSESS THE OVERALL SLIDING STABILITY

The assessment of the overall sliding stability along a plane parallel to the slope can be done in three steps:

1 Determination of external pressure along the slope

Breaking windwaves cause a strongly varying pressure distribution along the slope. The most dangerous moment for the higher part of the revetment is the moment just before breaking when the lowest head and the strongest head gradient downward along the slope occur at this part of the slope. For the lower parts of the revetment, however, the moment of lowest average head along this part is more dangerous. Which moment is critical for the overall sliding of the whole revetment depends on the type of revetment and its dimensions. Both moments can be analysed with the help of a schematised pressure head distribution over the whole slope.

The most dangerous component of ship waves is the waterlevel depression. The strongest head gradient downward along the slope occurs at the moment of maximum waterlevel depression. The pressure head distribution can be schematised accordingly.

2 Determination of pore pressures along potential sliding plane

Extensive research has been done on the response of the pore pressure along a potential sliding plane to the external pressure (Burger et al, 1990 Hjortnaes-Pedersen et al, 1987). Sophisticated models are available, but also simplified solutions. The latter can be applied here.

The response in cover layer and filter layer(s) can usually be considered quasi-stationary: the pressure distribution only depends on the momentaneous external pressure distribution and the permeabilities of the different layers. Analytical expressions of the pressure distribution in the filterlayer underneath a cover layer are available for the above mentioned schematised external pressure distributions.

A potential sliding plane may also be present in the sandy subsoil in a case like the one presented in Figure 2. The response of the pore pressure in the sand to the external load variation depends on the time: any pore pressure change at the revetment/sand interface gradually penetrates the sand and reduces with the distance to the interface. Most dangerous is a quick drop of the external pressure head in combination with a high air content and low permeability of the sand, when the porepressure close to the interface remains relatively high. An analytical expression is available to estimate this pore pressure distribution and, consequently, the depth of the potential sliding plane.

3 Response of the revetment

The combination of the external pressure distribution, the pressure distribution along the potential sliding plane and the weight of the revetment can be considered as the load of the revetment. The stability can be assessed by considering the equilibrium of forces perpendicular and parallel to the slope. The resistance against sliding parallel to the slope can be found from the effective stress perpendicular to the slope and the friction angle. At the interface between two materials this an is often smaller than within a material. Interfaces are, therefore, often potential sliding planes.

If the resistance against sliding is larger than the load component parallel to the slope, stability is guaranteed. In many situations, however, this is not the case and the toe or anchor structure must meet the difference between the load component parallel to the slope and the sliding resistance of the revetment.

EXAMPLES

Block revetment loaded by wind waves

Revetments with a cover layer of concrete blocks on top of a riprap filter layer (Figure 1) are widely used in the Netherlands to protect wave loaded sea dikes. Typical values of load and dimensions are: a design significant wave height of 2 m and a block thickness of 0.3 m. The interface between cover layer and filter is a potential sliding plane. The relatively low permeability of the cover layer causes considerable outward pressure head differences, and consequent low effective stresses, in the wave zone during wave run-down. The concrete-riprap friction angle may be less than 25°.

The presence of a solid toe appears to be essential to prevent sliding if the slope is steeper than approximately 1:6. With a more usual slope angle of 1:4 and a toe depth of about twice the significant wave height, the toe must meet a force of about 10 kN/m.

Inland waterway bank protection of riprap and geotextile on sand

Many bank protections in large inland waterways in Germany are constructed with riprap cover layers. The subsoil often consists of rather fine sand and a geotextile filter separates the riprap from the sand. Typical values of load and dimensions are: a waterlevel depression by ship waves of 0.8 m, a cover layer thickness of 0.3 m and a slope angle of 1:3.

Potentially dangerous is a sliding plane in the sand. Extensive research made clear that the local stability against sliding along an undeep sliding plane in the sand is often not met (Köhler and Schulz, 1986 and Bezuijen et al, 1990). The possible positive influence of a strong geotextile has been studied by calculating the tensile force associated with overall stability. It was found that a tensile strength of ca 40 kN/m is needed if the revetment extends to a depth of 3m below still water level.

REFERENCES

Bezuijen A, Köhler HJ and Schulz H (1990). Rip-rap revetments using geotextiles, measurements and numerical simulation. *Proc 4th Int Conf Geotextiles and Geomembranes*, Den Haag.

Burger AM, Klein Breteler M, Banach L, Bezuijen A and Pilarczyk KW (1990). Analytical Design Method for Relatively Closed Block Revetments. *ASCE J Waterways Port Coastal and Ocean Engineering*, 116-5: 525-543.

Hjortnaes-Pedersen AGI, Bezuijen A and Best H (1987). Non stationary flow under revetments using the Finite Element Method. *9th Eur Conf Soil Mech Found Eng*, Dublin.

Köhler HJ and Schulz H (1986). Use of geotextiles in hydraulic constructions in the design of revetments. Proc *3rd Int Conf Geotextiles*, Vienna.

PIANC (1987). *Guidelines for the design and construction of flexible revetments incorporating geotextiles for inland waterways.* Report Working Gr 4 of the Perm Techn Comm I. Supplement Bull 57.

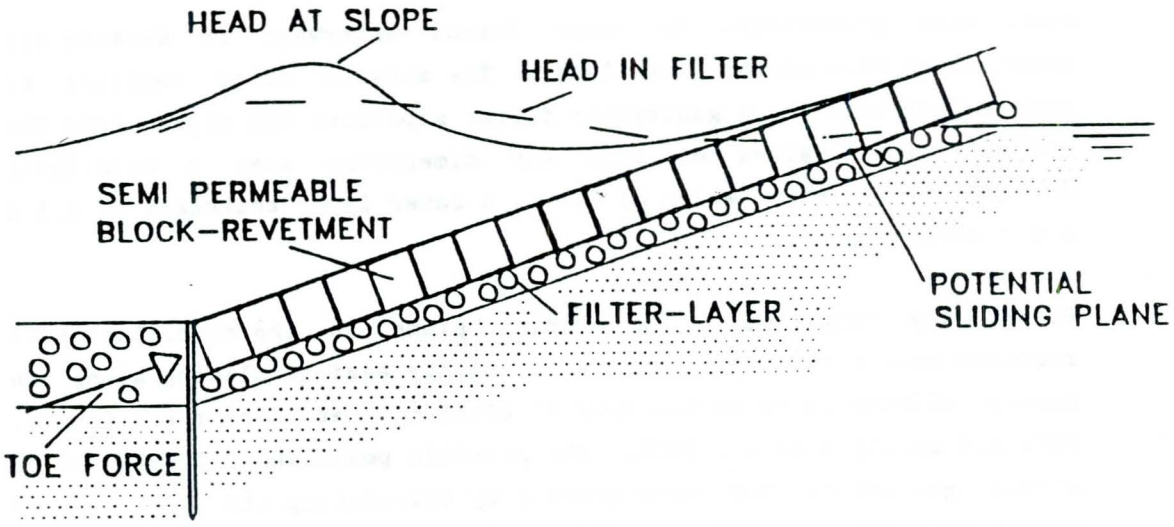

FIG.1 BLOCK REVETMENT LOADED BY WIND WAVES

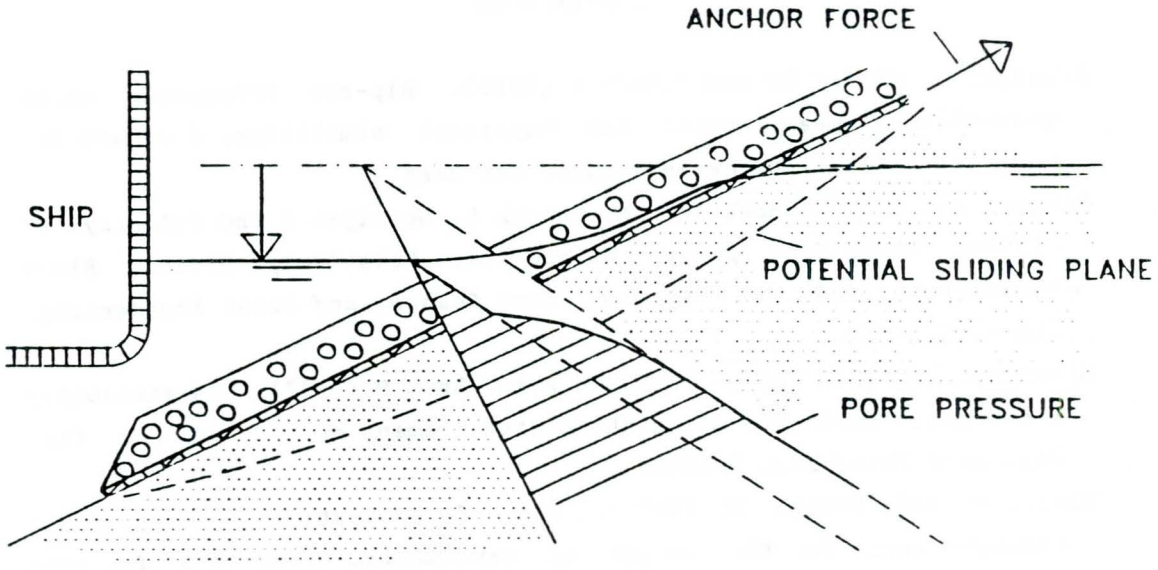

FIG.2 RIPRAP/GEOTEXTILE BANK PROTECTION LOADED BY SHIP WAVE

SEEPAGE EFFECTS IN RIPRAP ARMORED EMBANKMENTS

D.J. Hagerty and A.C. Parola
University of Louisville, Dept. of Civil Engineering
Louisville, KY 40292, USA

1. INTRODUCTION

As part of a general study of bank failure and erosion, the authors have made reconnaissance investigations along thousands of kilometers of banks, site-specific diagnostic investigations at hundreds of sites, and intensive, virtually continuous monitoring efforts on several sites. Mechanisms of instability were identified and evaluated. Erosion and instability were most severe and widespread on banks consisting of layered alluvial soils and occurred at locations and at times not consistent with tractive force scour (Ullrich et al., 1986; Hagerty 1992).

At bank reaches armored with riprap, instability and erosion were not forestalled in every case; in some cases, the banks retreated behind the rock armor and at other sites the rock sank through the banks which were to be protected. These failures appeared to be caused, at least in part, by seepage effects. Seepage emerging from a stream bank can be a major destabilizing influence even when the bank has been covered by a layer of riprap.

In the following paragraphs, information on bank failure mechanics will be presented, for the alluvial rivers studied by the authors, and the significance of those mechanics for riprap treatments will be analyzed. Performance of riprap protections will be examined in light of the importance influence of exfiltrating seepage and consequent bank instability. The layered and diverse character of alluvial deposits will be shown to be a very important influence on the success of riprap protections, even those protections provided with mineral or geotextile filters.

2. SEEPAGE-INDUCED EROSION

2.1 Field Studies - Ohio Valley

As part of the investigation of claims of accelerated erosion caused by dam construction on the Ohio River, made by riparian landowners (*Earl Loesch v. United States* 1981), twenty-three sites upstream from two of those dams were examined. Very comprehensive investigations were performed on each of these sites, and several reconnaissance studies were done throughout the lengths of the control reaches upstream from the two dams. These studies showed that much of the evident caving and erosion had not been caused by tractive force scour (Hagerty et al., 1981). Evidence of instability was found on the insides of bends and behind islands, where deposition (or

minimal net removal) would have been predicted on the basis of scour. Localized bank failures occurred at elevations well above preceding flood crests and long after flood recession. The instability at unexpected locations and times was being caused by piping and sapping (Hagerty, 1991a). Water recharged by floods into stream banks, or derived from non-stream sources such as infiltrating precipitation, invaded pervious alluvial layers and emerged from bank faces, moving particles out of those sandy layers. Removal of particles produced cavities in the banks, with eventual collapse of overlying strata by toppling, shearing or falling (Thorne and Tovey 1981).

Concern about Ohio River bank erosion generated a reconnaissance investigation throughout the entire 1300-km length of the Ohio River from Pittsburgh, Pennsylvania to Cairo, Illinois in 1978. In that investigation, attention was focused on the extent and severity of bank caving and erosion as evidenced by bare or disordered areas of bank. The Ohio River reconnaissance was supplemented by a similar reconnaissance for the entire navigable length of the Kanawha River in West Virginia, in 1979 (Huntington District 1979). Then monthly monitoring was done at eight sites on Sixmile Island on the Ohio River (Weigel and Hagerty 1983). More frequent and more detailed monitoring was done at six sites on and around Eighteenmile Island on the Ohio River (Hagerty et al., 1983). These investigations indicated that bank caving and erosion were initiated by piping and sapping. Tractive scour removed failed soil rather than *in situ* bank materials on most of the sites examined. Waves reworked and removed failed soils and recent sediments on the lower parts of the banks.

The results of these studies were confirmed when a second group of riparian landowners brought suit against the Corps of Engineers (*Avabelle Baskett v. United States* 1985), and the authors made detailed investigations of 98 sites in reaches controlled by six different dams. Not all of those sites showed evidence of active erosion, but on the apparently active sites, the dominant mechanism of caving and erosion was piping/sapping with consequent localized failures of overlying strata, and subsequent tractive force removal of failed soils. All of these studies were made on streams where stage was maintained at or above a level sufficient for commercial navigation. The topography at the active sites invariably included a gently sloping bench beneath the maintained stage level and a continuation of that feature for a variable distance above the maintained stage.

2.2 Additional Studies

The principal factors driving the mechanics of piping/sapping and localized failures have been identified (Springer et al., 1985; Ullrich et al., 1986; Hagerty et al., 1986). Other investigators have found evidence of piping/sapping erosion throughout the length of the Ohio River (Clough and Duncan, 1986) and on the Monongahela River in Pennsylvania (Hamel, 1988). The authors have found documentation of the occurrence of seepage-induced erosion on alluvial streams in more than two dozen countries around the world (Hagerty, 1991a).

The authors re-examined 106 of the sites they had studied from 1977 through 1983, in 1986 because dry weather and a period of infrequent and minor floods had characterized the Ohio River valley between 1982 and 1986. Two-thirds of the sites on which the banks had been eroded and bare after wet weather and frequent floods in 1977-1981 were covered thickly in vegetation in 1986 and sediment accumulations were found on the lower bank areas at many sites (Hagerty, 1986; Hagerty and French, 1987). The reconnaissance survey done on the Kanawha River in 1979 was repeated in 1986, with results similar to those found on the Ohio River (Huntington District, 1986; Spoor, 1986).

In 1988, the 1978 reconnaissance of both banks of the Ohio River from Pittsburgh to Cairo was repeated (Hagerty and Spoor, 1989). As a supplement to the bank reconnaissance, 113 cross-sections were obtained at sites of apparent bank erosion, and investigations were made at locations where bank protection had been constructed. At none of those sections was evidence of undercutting by currents or waves found. In a companion investigation, the authors conducted reconnaissance bank surveys of 286 miles of the Illinois Waterway from near Chicago to the waterway junction with the Mississippi River at Grafton, Illinois. The reconnaissance studies were supplemented by intensive investigations on thirty-one sites. None of the 51 cross-sections obtained during 1988 showed any evidence of undercutting by scour below the maintained stage level (Spoor and Hagerty, 1989). Data from earlier studies (Bhowmik and Schicht, 1980) were used to develop 189 additional cross-sections, none of which showed any evidence of undercutting.

In 1990, the authors returned to Sixmile Island to investigate conditions on the island banks (Parola et al., 1991). Monitoring during winter 1990 and spring 1991 showed that sediments were deposited over much of the middle and lower banks of the island during a flood of 10 year recurrence interval in December 1990 - January 1991 (Parola and Hagerty, 1992; Parola et al., 1992). The south side of the island, adjacent to the thalweg of the river, showed significant caving and retreat of the upper part of the bank height, little or no erosion of the lower parts of the banks, and slight deposition on the lower third of the bank height. The bank caving and retreat on the island appeared to have been initiated by piping/sapping (Hagerty, 1991b) with removal of failed soil by current action. During summer and early fall 1991, sediments were reworked by waves (principally on the south banks) and moved by currents; sediment plumes were noted along the island banks during frequent visits to the island, particularly when wind wave action was significant.

2.3 Summary on Prior Studies

The significance of the field and analytical studies, described herein, for riprap protection systems lies in the mechanism by which bank failures occurred, in the topography observed on the eroded banks, and in the character of the deposits in which bank failure and erosion were severe and widespread. Most of the failed banks studied by the authors did not fail as a result of tractive force scour or wave attack; it is questionable whether or not riprap was necessary or large rock was required at many of the sites where the authors have seen it used. At many sites, the actual function of the riprap was to hold a filter in place over a bank where piping/sapping was the mechanism initiating failures, and the riprap treatment failed to hold the filter on a number of sites. Even on banks where wave attack and/or flood flow forces were significant, seepage exit was an important factor in the overall instability and erosion process. Riprap treatment *must* be designed against seepage effects, if possible. Current designs using mineral or fabric filters have not been successful in all applications, and the causes of failures beneath filters should be examined.

The topography found on failed and eroding banks is significant in that it indicates the area of bank attack. On the rivers studied by the authors, stage is maintained to provide a depth adequate for commercial towboat navigation (approximately 3 m). The failed and eroding banks almost without exception include, beneath the retained pool level, a gently sloping bench which extends channelward as much as 20 m. This feature clearly shows that the failed banks have not been oversteepened by scour at the bank toe. Toe scour has been given as a primary cause of failure in riprap treatments (Brown 1984; Heerten and Muhring 1984), but very few of the failures seen by the authors were caused by toe scour. A number of the failed riprap treatments had experienced bulging near the toe of the treatment, and in some cases the filter fabric had become dislodged near the bank toe, but in other failed treatments, the bank simply retreated landward and the riprap slumped down on itself. How these latter failures occurred should be examined.

The vast majority of the failures seen by the authors have occurred in alluvial soils consisting of layered and lensed deposits. Typically, relatively thin (2 to 10 cm) layers of silts or clayey silts separated sandy layers 1 to 50 cm thick. The sandy layers were more pervious and were the locations of piping/sapping removal. The mode of failure in these deposits (piping with subsequent collapse of overlying cohesive layers) itself is significant, but the variation in bank soil properties also has important implications for riprap treatment. Not all riprap revetments on layered alluvial soils necessarily will fail; in some instances, outflow seepage will not be concentrated sufficiently to cause piping/sapping, while in other cases recharge to the bank (or groundwater sources) will not provide enough water to drive the piping mechanism. Wherever recharge or groundwater outflow is copious and is concentrated by large differences in hydraulic conductivity between adjacent soil layers, however, seepage will have detrimental effects on riprap revetments, either through buildup of water pressures or through loss of soil out of the bank, with consequent instability of overlying layers. Designers typically rely on a filter layer to prevent soil loss from out-of-bank seepage, but effective filtration of layered soil banks may be virtually impossible.

3. SEEPAGE THROUGH RIPRAP

Some revetments have failed for lack of a proper filter below riprap, others have failed because of inadequate performance of a filter (mineral or fabric), and others have provided the desired protection. Features of each of these situations merit examination.

3.1 Riprap Without Filter

Some riprap treatments have failed because they were designed with attention to current tractive forces and wave action but without consideration of seepage-induced failure mechanisms. The importance of piping/sapping and associated mechanisms has been recognized; thus, failures due to these mechanisms should become very rare. One aspect of this situation--riprap without a filter--should be examined, however, even though the situation may become uncommon. That aspect can be expressed in a question: If a bank were subject to failure and erosion by piping/ sapping and consequent localized failure mechanisms, would placement of riprap on that bank decrease, increase or fail to affect the extent and severity of failure and erosion of that bank? What factors pertain to this evaluation?

3.1.1. Hydraulic Gradient for Internal Erosion

In times past, an apparent controversy arose between empiricists who gathered evidence on failures by internal erosion (piping/sapping) in dams and dikes, and theorists who declared that flow net analysis would indicate if and where seepage forces would be sufficient to cause sudden mass soil movement and instability (hydraulic heave). In brief, earth structures had failed by piping in circumstances which should have been stable according to flow net analyses. Moreover, flow net theory indicated that failure would occur as soon as the hydraulic gradient reached a critical value, and that the failure would be total; many of the observed failures occurred many years after flow was initiated and as the result of a gradual loss of soil at points of concentrated groundwater flow. The controversy was resolved when engineers realized that the internal erosion mechanism was driven by the local hydraulic gradients at seepage exfiltration faces, that most dam or dike foundations consisted of layered and lensed soils, and that, therefore, the gross gradient developed from a flow net drawn for homogeneous soil was not a valid measure of danger from internal erosion. The sequential nature of soil loss by groundwater seepage also has been described (Howard and McLane 1988). Unfortunately, theoretical presentations in textbooks emphasize the hydraulic gradient which is *critical* for mass movements in uniform soils. For typical *in situ* soil densities, that gradient is in the range of 0.8 to 1.1. Many engineers have failed to recognize that soil loss at an exfiltration face can occur at a much lower hydraulic gradient. In experiments in the authors' laboratory, using uniform sand (d_{10} = 0.40 mm and d_{60} = 0.62 mm), active erosion of a sloped face was initiated at gradients as low as 0.2. These laboratory experiments are in agreement with field evidence obtained at sites where piezometers were installed to measure porewater pressures; on those sites, soil loss from seepage exfiltration in sandy layers continued for long periods of time when gradients were low, and the cumulative effect of that loss was collapse of overlying cohesive layers. In experiments by Faure et al. (1984), soil loss through filter materials was almost as great at hydraulic gradients of unity as under gradients as high as 40. All of these results indicate that even low hydraulic gradients are sufficient to cause soil loss at seepage faces; this conclusion is significant because placing riprap on a bank is likely to increase local gradients at seepage exits.

3.1.2. Blockage by Riprap/Filter

Placement of riprap or any other type of block over a bank from which seepage occurs will concentrate flow at the seepage faces in the interstices between blocks. Bezuijen at al. (1986) reported uplift pressures as high as 3.0 kN/m^2 under a block revetment equipped with a geotextile filter; water pressure fluctuations as high as 9.0 kN/m^2 were observed under the influence of wave impact. The blocks used in the monitored revetment produced a joint opening ratio (ratio of opening between blocks to width of blocks) of 0.006, and the investigators used a flow analysis to predict a flow velocity between the blocks equal to 170 times the mass flow velocity toward the block layer, as a result of constriction of flow lines in the vicinity of the spaces between blocks. Of significance to riprap revetments were the observation of a definite phase shift between the wave overpressure on the top surface of the revetment and the pore pressure developed within the soil under the revetment, and the resultant uplift pressures on the revetment. In laboratory tests using a wave generator in a flume, Muskatirovic and Batinic (1986) measured

water pressures within a model revetment equal to 90 percent of wave generated pressures, at depths of 30 to 70 cm inside the revetment under a block protection layer. Hjortnaes-Pedersen et al. (1987) used a finite method flow analysis to verify the phase shift observed by Bezuijen et al. and to demonstrate that a granular filter layer produces very different pore pressure fluctuations than will a geotextile filter. This last consideration could be of great significance to riprap revetments equipped with geotextile filters, if riprap treatments respond in the same way as do block revetments. Bezuijen et al. (1990) developed equations to describe pore pressure fluctuations in the soil beneath a riprap revetment produced by changes in water level in the stream adjacent to the revetment, and demonstrated that the factors which determine the magnitude and variation in pore pressure are the velocity with which the water surface falls, the coefficient of hydraulic conductivity of the soil below the filter and the degree of saturation of the soil.

In prototype tests along the Hartel Canal, hydraulic gradients as high as 0.5 were measured under sections of bank where block revetments had been constructed without a bedding layer, during the impact of waves from passing vessels (Blaauw et al. 1984). Uplift pressures as high as 1.8 kN/m^2 were measured under blocks placed on a gravel underlayer. Hydraulic gradients sufficient to cause subsoil instability were calculated from these measurements of pressure (Pilarczyk 1984). Gradients transverse to the bank treatments averaged about 0.15 for the first half-meter depth below the subsoil surface, while gradients parallel to and down the slope of the soil surface were as high as 0.5. If such high localized gradients were caused by wave impact, it is reasonable to expect even higher gradients between blocks or pieces of riprap on banks with sustained seepage discharge.

3.1.3. Macro/micro Phenomena

Placement of riprap on a river bank causes changes in the flow system around the pieces of rock. Some of these changes are macroscopic and some are microscopic. On the macroscopic level, the bank resistance to overland flow with the riprap in place is much higher than for the bank without riprap. This change in flow resistance retards runoff down the bank, causes more temporary retention, and causes more infiltration of surface water into the bank; the increase in infiltration leads to more outflow seepage and more consequent soil loss at the exfiltration face. The riprap blocks part of the outflow seepage face, and thereby causes local accelerations of groundwater flow. The local accelerations are caused by the constriction of streamlines through the reduced outflow areas. When waves break over a riprap revetment, return flow is retarded, infiltration is increased, and return flow is concentrated in the channels between the pieces of rock and is effective in removing sediments or piped-out soils accumulated within the riprap layer. On a microscopic level, groundwater flow is significantly different at the interface between soil and rock than in the soil at locations remote from the rock. The size and configuration of voids between soil particles are quite different from the voids at the boundary between soil and rock; larger voids and less tortuous interstices exist along the soil/rock interface. Hydraulic conductivity consequently is much higher at the soil/rock interface. Such interface flow has been studied by the authors in laboratory experiments using impermeable blocks and pieces of actual riprap. Whenever an obstacle was placed on a sand slope from which seepage was induced, the loss of soil was observed to occur preferentially at the interface between the sand and the

impermeable obstacle or piece of rock. Even when raprip is placed on cohesive soils, a zone of higher conductivity is likely to occur at the interface between the soil and the rock; if the cohesive soil is dry and firm, numerous gaps will exist between the rock pieces and the soil, and if the soil is wet and soft, it is likely to shrink away from the rock in an uneven way when it dries. Any separation between the rock and the soil will produce high hydraulic conductivity and seepage-induced loss at the interface separation.

Notwithstanding all of the possibilities for detrimental interplay of riprap and seepage from a bank, is it not the case that concern for such interplay is not warranted? Cannot the detrimental effects of seepage on riprap be eliminated through the use of a filter beneath the riprap?

3.2 Riprap With Filter

The function of a filter below a revetment is to allow water to flow safely out of the revetted bank while retaining the soil of that bank. Mineral filters are evaluated on the basis of grain size and size distribution, on the assumption that soil void sizes are related to grain size and texture; criteria for permeability and soil retention were developed by Terzaghi (Bertram 1940). Terzaghi's soil retention criterion was verified in part by Sherard et al. (1984), but Heerten and Wittmann (1985) have shown that that criterion is applicable only if the protected soil is relatively uniform.

Fabric filters have been evaluated on the basis of some indicative pore size or opening in the fabric compared to a characteristic particle size of the soil to be protected. Criteria for geotextile filters have been presented (Calhoun 1972; Carroll 1973; Faure et al. 1984; Giroud 1982; Ingold 1984a; Office, Chief of Engineers 1986; Ogink 1975; Schrober and Teindl 1979) and reviewed (Bakker et al. 1990; Giroud 1988; Koerner 1990; Lawson 1982). Differences still exist on how to characterize filter openings (Lawson 1982; Montero and Overmann 1990) and on criteria relating filter opening to soil particle size.

3.2.1. Filters Under Riprap

The difficulties of obtaining and placing mineral aggragates suitable for filters long ago drove engineers to seek alternative filter media. Experiments with glass fiber mats were done as early as 1957 in the laboratory and 1958 in the field (Agerschou 1961) and plastic fabrics were utilized soon thereafter (Barrett 1966). Sheets of geotextiles are easy to transport and place, have considerable tensile strength, and are relatively inexpensive. Under conditions of unidirectional flow, geotextile filters are very effective in retaining uniform soils and allowing free exit of seepage from retained soil. In situations of reversing flow, over non-uniform soils, geotextile filtration can be problematic.

Contrary to widely held belief, filters do not retain soil by forming a "filter cake" of fines at the interface between filter and soil. Fine particles wash into filter pores and soil loss will continue until a filtration zone is developed within the soil where gradually a network of larger particles forms and acts to retain smaller particles (Heerten 1984; Montero and Overmann 1990; Williams and Abouzakhm 1989). This network typically is only a few millimeters thick and is easily disturbed. Filtration length (filter thickness) is important; experiments with different thicknesses show that with increasing filter thickness, the pore-size distribution measured by passing uniform glass spheres or soil grains through the filter become apparently smaller (Heerten and Wittmann 1985). Recognition of the effect of filter thickness is evident in the large thicknesses of multi-layer fabrics used in Europe

compared to fabrics used in North America. Excavation of filters after long use has shown considerable penetration of fines into thick fabrics (Heerten et al. 1984). This penetration causes changes in filter performance which can affect riprap revetments adversely.

3.2.2. Problems With Filters Under Riprap

Mineral filters and geotextile filters alike are subject to some degree of clogging; this clogging usually is slight with uniformly sized protected soil (Faure et al. 1986). However, in gap-graded soils (fine particles and coarse particles with few intermediate-size grains) and in silty soils, filter clogging may be severe (Fluet and Luettich 1993; Heerten et al. 1984; Koerner and Ko 1982; Lawson 1982; Rollin et al. 1988). Ogink (1975) recommended a drastic reduction in filter opening to retain gap-graded soils, as did Heerten and Wittmann (1985); the latter authors showed the necessary reduction to be a function of filter thickness, and recommended that the filter thickness should be at least 25 times the average pore size of the filter. Ingold (1984b) showed also that the reduction is dependent on gradient. Koerner (1990) recommended that geotextile filters be tested by using a sample of bank soil and the candidate geotextiles in gradient ratio tests (Haliburton and Wood 1982) or long-term flow tests (Koerner and Ko 1982). However, Koerner warned against a high likelihood of complete clogging of geotextiles over cohesionless soils where high gradients occur. Fluet and Luettich (1993) recommended selecting filter fabrics to retain the sand component of flat-graded silty sands containing less than 20 percent silt by weight, and allowing loss of the silt, only because they felt that loss of the silt would not cause settlement since the sand grain-grain structure would be stable without the silt. Their approach may be acceptable for soils with the narrow limits and conditions on gradation they specify, but it would not be applicable to the situation of layered alluvial soils under a revetment. For gap-graded soils, Koerner recommended (p. 122-3) that use of geotextiles should be avoided altogether or the geotextile should be so coarse that some soil loss occurs. Soil loss is not advisable under a revetment, so some clogging must be accepted if the bank soils are not uniform. What are the consequences of such clogging?

Heerten et al. (1984) have tested the hydraulic conductivity of geotextile samples excavated from canal banks after years of use and have reported reductions in coefficient of permeability from 0.01 cm/s to 0.0005 cm/s as a result of clogging. In a comprehensive laboratory study, Bhatia et al. (1990) found that filter clogging by fine sand reduced filter coefficient of permeability from 0.003 cm/s to less than 0.0002 cm/s. When silt was added to the protected soil (20 percent by weight silt), the final permeability was 0.00009 cm/s. Similar results have been obtained by Williams and Abouzakhm (1989). In the model revetment tests done by Muskatirovic and Batinic (1986), a ten-fold reduction in system permeability was noted within 90 minutes after flow was initiated, when suspended sediments clogged the geotextile filter used in the model revetment.

If the riprap treatment is not maintained properly, clogging and reduction in permeability of a filter may occur by siltation and vegetation growth between pieces of riprap. Goldworthy (1984) described such a case and the authors have studied such a situation. In the latter case, a mineral filter on the bank of the Tombigbee River at a paper mill became clogged by sediments and vegetation, water pressures increased within the revetment, and soil loss out the ends of the treatment endangered a tank complex above the revetment.

Clogging and reduction in filter permeability can generate significant uplift pressures under riprap layers

as well as cause soil loss through the ends of a revetment. If the filter layer over a 5 m-high bank becomes clogged and the hydraulic conductivity of the filter is reduced to one-tenth of that of the bank soil, uplift pressures will be sufficient to displace 30-cm riprap at the toe of the bank. Because of the high tensile strengths of some geotextiles, large uplift pressures are likely to pull the filter fabric loose and/or to cause a void between the fabric and the bank soil. If the filter is displaced from the face of the bank, flow of soil out of piping layers and down the bank face would occur. Interstreaming of soil grains along the face of the bank also would be likely to occur if the separation of filter and soil were extensive (Brown 1984).

3.2.3. Failures in Riprap Revetments With Filters

Distress and failures in filter systems under riprap treatments have been described by several investigators (Brown 1984; Calhoun 1969; Fairley et al. 1970; Goldworthy 1984; Heerten and Wittmann 1985; Keown and Dardeau 1980; Keown and Oswalt 1984; McCormick 1984; Muhring 1984; Pilarczyk 1984). The authors have observed the types of failures due to seepage reported by others; those failures can be grouped in two general classes--the bank soil was lost through the treatment, or the bank distorted behind the treatment. The conditons observed by the authors on failed banks may explain why some of these failures occurred.

For those treatements which failed by soil loss, either the filter did not retain the soil (or there was no filter) or the loss occurred out the ends of the treatment where the filter was not anchored sufficiently. What factors could have caused failure of the filter to retain the soil? The flow conditions under the revetment may have caused the failure. Ingold (1984b) noted a "dearth of information relating to geotextile filter performance under the alternating and turbulent flow conditions often prevailing beneath a revetment." Periodic bank inundation during floods, as well as rapid flow reversal during wave impact, may prevent the formation of a stable bridging network in the protected soil and/or destroy any filtering zone developed within the bank soil immediately beneath the filter.

Another likely cause of soil loss is an inability to suit the fabric filter to the bank soil. By far, the situation most commonly encountered by the authors on eroded banks was thinly layered alluvium, with large variations in grain size and permeability between layers. A filter selected to be sufficiently pervious to pass flows from coarser bank layers would be too open to retain finer particles from intervening bank layers.

Many of the distressed treatments seen by the authors or described by others did not fail by soil loss through the filter below the riprap. Rather, the bank shape changed under the revetment, with subsidence of the upper part of the bank and bulging of the treatment near the bank toe (Fairley et al. 1970; Heerten 1986; Keown and Dardeau 1980; Miller 1978; Muhring 1984). Such a situation would be very likely to occur for a layered alluvial bank if the filter had been selected to retain the finer soils or even the average grain size for the layered bank. Clogging of the filter by migrating fines would be very likely to occur. Liftoff of the clogged fabric caused by pressure buildup within the bank would allow downslope movement of piped-out fines. Measured downslope gradients (Blaauw et al. 1984) would be adequate to cause such transport of fines, and such displacement has been observed (Heerten 1986; Muhring 1984). Concentration of fines near the toe of the revetment would aggravate filter clogging there and cause bulging of the toe; soil loss in the upper bank would lead to the revetment subsidence noted

at numerous sites.

The mechanisms of failure of less pervious cohesive bank layers are significant in the assessment of pressure buildup in a bank. Undermined cohesive layers crack vertically when subjected to the tension incident on their bending downward when undermined. The authors have observed such cracks in many banks, to distances of as much as two meters from the bank face. The occurrence of such cracks in impervious layers serves to connect all the bank layers as a single hydraulic system so that water pressures at the toe of a revetment may correspond to depth below the uppermost phreatic surface in the bank layers.

Does this evaluation mean that all bank revetments on layered soils are likely to fail? Certainly, the variation in soil sizes and permeabilities in a layered bank makes that bank roughly equivalent to a bank of gap-graded soil, with all the attendant problems. However, the variation in soil permeability may not be so great as to cause uplift of the clogged geotextile. Heerten (1984) suggested that if the original permeability of the geotextile is at least 50 times the permeability of the protected soil, clogging would not be a serious problem. Additionally, the source of the water which drives the piping/sapping mechanism is important. If the water in the bank is derived mainly from bank recharge during floods, then recharge will occur preferentially into coarser layers, flow into fine-grained soils will be minimal, and subsequent outflow will occur mainly from coarser layers. In such a situation, loss of fines would be much less than if flow from less pervious layers was persistent. Where the source of the seepage is general groundwater flow, or leakage from a water conduit, eventually all bank layers will exhibit flow and soil loss will occur from finer layers. It can be seen that predicting long-term performance of a revetment filter over an alluvial riverbank is complicated and difficult.

3.3 Flow Over/Through Riprap

In the foregoing remarks, the role of tractive forces during floods, and waves, has been described as that of reworking and transport of failed soils away from banks being affected dominantly by piping/sapping. Placing riprap over a bank failing by such a mechanism will affect the action of currents and waves on the subject bank.

3.3.1. Erodibility of Piped Soils

If a riprap revetment is equipped with a filter which does retain bank soil, no soil will be piped through the filter. If soil loss does occur, the piped-out soils will be much more erodible than the same materials in place in the undisturbed bank. Soil layer structure and particle interaction in the disturbed soils will be minimal. Fines most probably will be transported completely out of the riprap layer, while sandy particles will be deposited by the erosion from the seepage face in a very loose condition. During floods, it is very likely that this failed soil will be eroded from among the pieces of riprap even if more soil is piped out and sediments are deposited on the riprap during and after flood recession. On the bench below the retained pool level at sites examined by the authors, piped-out soils and sediments did not dry and harden, so they remained very erodible.

No systematic monitoring and testing has been done on the physical properties, especially relative erodibility, of failed soils on the lower portions of banks where seepage outflow has caused piping/sapping and localized failures in middle and upper bank zones. Moreover, the interaction of failed soils and sediments deposited

over and around those soils is complex and should be investigated. Virtually continuous monitoring of a failing site is required and the bank under examination should consist of layered alluvial soils.

3.3.2. Local Turbulence Effects

The irregular surface produced by placing riprap on a bank interacts vigorously with the stream flow, especially incipient flows during floods (Maynord 1989). The increase in surface roughness increases energy transfer at the riprap layer, and the transferred energy is expended in very turbulent flow around the individual pieces of riprap. This localized turbulent flow is much more erosive than the flow along a relatively smooth bank of *in situ* soil. The energy which would have been expended in attacking the *in situ* soil is dissipated in flow around the riprap. If the riprap is sized properly, it is not displaced by this transfer of energy and the bank is protected (Maynord 1988). Any soil particles resting between the pieces of riprap, however, would be subject to localized turbulence and erosion.

The turbulent flow field around a piece of riprap should be examined in a prototype revetment. Continuous monitoring of flow fluctuations are necessary in order to evaluate the dependence of local turbulence on size of riprap, thickness of riprap layer, and gradation of riprap. It may be feasible to reduce the size of riprap used on many sites by using a mixture of rock sizes to interfere constructively with the local turbulent flow fields around the individual pieces of rock in a revetment.

3.3.3. Water Pressure Effects

Flow of water around obstacles such as bridge piers is distorted by the obstacle so that vortices develop. These vortices form and move with the current around the obstacle. As a result, pressure fluctuations alternately drive water into the stream bed around the obstacle and then pull that water back out of the soil. Such pressure fluctuations have been measured in model studies by Hjorth (1975). The localized turbulence around pieces of riprap also should produce pressure fluctuations and reversing gradients similar to those noted at larger obstacles. Although the gradients caused by these fluctuations are likely to be quite small, the soils on which they would act is highly erodible and even small gradients have been shown to be sufficient to cause seepage-induced erosion.

The occurrence and variations in porewater pressures under a filter in a riprap revetment should be monitored through the use of piezometers installed in the protected bank. The piezometers should be very small transducer units capable of measuring the rapid pressure fluctuations under a filter cloth, in thin soil layers; since seepage outflow erosion is most severe, and consequent problems with soil loss or filter clogging are most serious in banks where relatively thin soil layers show very significant differences in grain size and permeability, it is necessary that such layers be treated as discrete hydraulic units and monitored appropriately.

4. RECOMMENDATIONS

In addition to the measurements described in the preceding sections, a prototype study should be done to evaluate the possibility of stabilizing banks failing as a result of seepage outflow mechanisms, by using positive

drainage. Many of the failures caused by outflow seepage in riprap revetments appear to have been caused by clogging of filter layers and buildup of pressure under the clogged filter layers. Ironically, even pieces of riprap much larger than what would be required to resist actual current and wave forces on certain sites have proved to be too small to hold filters in place when those filters clogged and could not pass the water emerging from bank layers. It may be possible to achieve economies by providing more extensive drainage systems *within* revetments under filter layers, thereby reducing pressures under clogged filters, so that much smaller riprap would suffice to retain the filter in place. Obviously, since filter clogging is the reason why uplift pressures occur in such situations, any drainage system would require filters around the pipes or conduits used to drain the bank, and those filters would be subject to the same clogging problems which affect the filters under the riprap. How could this problem be avoided? Consideration should be given to using small drain pipes situated against the more pervious bank layers in such a way that the filters around the drain pipes could be sized for the relatively narrow range of grain sizes in the immediately adjacent soil layers.

In the prototype installation used to test the feasibility of positive drainage to prevent water pressure buildup and filter uplift, a variety of filter fabrics should be used to test the susceptibility of different types and thicknesses of filter fabric to clogging by layered alluvial soils. Riprap sizes and thicknesses should be varied to see if it would be possible to reduce riprap sizes by using positive drainage and/or selected filter materials. During a prototype study, areas of bank adjacent to the revetment should be monitored continuously using devices such as the automatic erosion monitoring system (PEEP) (Lawler 1992), and time-lapse photography, to determine when and how bank failure and erosion occur.

Another factor which merits investigation is the role of vegetation in bank protection/erosion. If a bank is failing principally by seepage outflow erosion and associated failure mechanisms, can vegetation be used to retard or prevent that erosion? It is unlikely that vegetation could prevent piping/sapping *per se*, but vegetation may be effective in retarding the removal, by waves and current forces, of failed soils and recent sediments, and so could interrupt the material transport sequence on the bank (Parola and Hagerty 1992; Parola et al. 1992). If failed soils and sediments accumulated to form a lower-bank berm, piping/sapping action would become much less intense. Vegetation growing in sediments on and in a riprap layer has been observed to cause drainage problems and failure in revetments. It might be possible, however, to use woody vegetation (Shields and Gray 1992) in combination with smaller riprap over filters to effect economies in bank protection, if positive drainage can be provided under the filters. Such combined treatments would enhance the bank ecosystem and aesthetics, compared to revetments of riprap only over filters.

5. SUMMARY

Seepage-induced erosion is widespread, and is severe in alluvial banks consisting of layered sands and silts. A characteristic topography is produced by outflow seepage from such alluvial banks; on rivers where stage is maintained to retain depth sufficient for commercial navigation, this topography includes a gently sloping bench at

and just below the retained pool stage. The presence of this bench indicates that tractive force scour during floods does not undercut the toes of these banks; riprap has been placed on many sites where tractive forces and waves are not sufficient to require riprap protection. Nevertheless, not all of these riprap treatments have been successful.

Placement of riprap on a bank failing as a result of seepage outflow causes outflow to be concentrated, and does not retard or lessen soil loss compared to the situation in which no riprap is present. Only small hydraulic gradients are required to cause soil loss at seepage exit faces, and field measurements have confirmed that such gradients occur under revetments. Soil loss is a function of the concentrated flow which occurs at the interface between soil and rock.

Filters under riprap over silty or gap-graded soils easily become clogged. Layered alluvial banks present just such conditions. Penetration of geotextile filters by fines reduces filter permeability. Reduction in filter permeability leads to buildup of water pressures under the filter, with consequent bulging of the revetment toe and subsidence of the upper part of the revetment, or soil loss out of the ends of the revetment and collapse of the structure. If filters are made sufficiently open to avoid clogging, loss of soil fines through the filter will lead to bank retreat behind the revetment.

The flow system around the pieces of riprap on a bank is highly turbulent and effective in removing failed soils, which are extremely erodible, and sediments deposited in the interstices in the riprap. The turbulent flow around the riprap augments the hydraulic gradients causing seepage outflow. Consideration should be given to prototype studies of seepage-induced effects on filters under riprap revetments, and to the use of positive drainage as well as vegetation in more cost-effective bank protection systems.

6. REFERENCES

Agerschou, H. A. (1961). "Synthetic material filters in coastal protection." *Journal of the Waterways and Harbors Division*, ASCE, 87 (WW1) 111-124.

Avabelle Baskett v. United States, 8 Cl.Ct. 201 (1985), *affirmed* 790 F2d93, *cert. denied*, 106 S.Ct. 3300 (1986).

Bakker, K. J., Breteler, M. Klein, and den Adel, H. "New criteria for granular filters and geotextile filters under revetments." *Proc., 22nd Int. Conf. Coastal Engrg.*, Delft, 2, 1524-1537.

Barrett, R. J. (1966). "Use of plastic filters in coastal structures." *Proceedings of the 16th Int. Conf. Coastal Eng.*, Tokyo, 1048-1067.

Bertram, G. E. (1940). "An experimental investigation of protective filters." *Soil Mech. Series No. 7*, Graduate School of Engrg., Harvard Univ., Cambridge.

Bezuijen, A., Klein Breteler, M. and Pilarczyk, K. W. (1986). "Large-scale tests on a block revetment placed on sand with a geotextile as separation layer." *Proc., 3rd Int. Conf. Geotextiles*, Vienna, II, 501-505.

Bezuijen, A., Kohler, H. J. and Schulz, H. (1990). "Rip-rap revetments using geotextiles, measurements and numerical simulation." *Proc., 4th Int. Conf. Geotextiles and Geomembranes*, The Hague.

Bhatia, S. K., Qureshi, S. and Kogler, R. M. (1990). "Long-term clogging behavior of non-woven geotextiles with

silty and gap-graded sands." *Geosynthetic Testing for Waste Cont. Appli., ASTM STP 1081*, Am. Soc. Test. Matls., 285-297.

Bhowmik, N. G. and Schicht, R. J. (1980). "Bank erosion of the Illinois River." *Report of Investigation 92*, Ill. St. Water Survey, Champaign.

Blaauw, H. G., deGroot, M. T., van der Knaap, F. C. M., and Pilarczyk, K. W. (1984). "Design of bank protection of inland navigation fairways." *Proc., Int. Conf. Flex. Arm. Revetments Inc. Geotextiles*, London, Thomas Telford Ltd., 39-65.

Brown, C. T. (1984). "Flexible revetments--theory and practice." *Proc., Int. Conf. Flex. Arm. Revetments Inc. Geotextiles*, London, Thomas Telford Ltd., 1-12.

Calhoun, C. C., Jr. (1969). "Summary of information from questionnaires on uses of filter cloths in the Corps of Engineers." *Misc. Paper S-6-46*, US Army Eng. Waterways Exp. Sta., Vicksburg.

Calhoun, C. C. (1972). "Development of design criteria and acceptance specifications for plastic filter cloths." *Technical Report S-72-7*, US Army Eng. Waterways Exp. Sta., Vicksburg.

Carroll, R. G. (1983). "Geotextile filter criteria." *Transportation Research Record 916, Engineering Fabrics in Transportation Construction*, TRB, 46-53.

Clough, G. W. and Duncan, J. M. (1986). "Ohio River bank stability reconnaissance and evaluation." *Report to Huntington District*, Corps of Engineers.

Earl Loesch v. United States, 227 Ct.Cl. 34, 645 F.2d 905, *cert. denied*, 454 US 1099, 102 Sct. 672, 70 L.Ed. 2d 640 (1981).

Fairley, J. G., Easley, R. T., Bowman, J. H., and Littlejohn, B. J. (1970). "Use of plastic filter cloth in revetment construction." *Potamology Inv. Rpt. 21-4*, US Army Waterways Exp. Sta., Vicksburg.

Faure, Y., Gourc, J. P. and Sundias, E. (1984). "Influence of the filtration opening size on soil retention capacity of geotextiles." *Proc., Int. Conf. Flex. Arm. Revetments Inc. Geotextiles*, London, Thomas Telford Ltd., 95-107.

Faure, Y., Giroud, J. P., Brochier, P. and Rollin, A. (1986). "Soil-geotextile interaction in filter systems." *Proc., 3rd Int. Conf. Geotextiles*, Vienna, 1207-1212.

Fluet, J. E., Jr. and Luettich, S. M. (1993). "Geotextile filter criteria for gap-graded silty sands." *Proc., Geosynthetics '93 Conf.*, Vancouver, IAFI (in press).

Giroud, J. P. (1982). "Filter criteria for geotextiles." *Proc., 2nd Int. Conf. Geotextiles*, Las Vegas, IFAI, 103-108.

Giroud, J. P. (1988). "Review of geotextile filter criteria." *Proc., 1st Indian Geotextiles Conf.*, Bombay, 1-6.

Goldworthy, M. H. (1984). "Discussion on geotechnical aspects." *Proc., Int. Conf. Flex. Arm. Revetments Inc. Geotextiles*, London, Thomas Telford Ltd., 111-112.

Hagerty, D. J. (1986). "Ohio River site investigations--1986." *Summary Report to Louisville District*, Corps of Engineers.

Hagerty, D. J. (1991a). "Piping/sapping erosion. I: Basic considerations." *J. Hydr. Engrg.*, ASCE, 117(8), 991-

1008.

Hagerty, D. J. (1991b). "Piping/sapping erosion. II: Identification–diagnosis." *J. Hydr. Engrg.*, ASCE, 117(8), 1009-1025.

Hagerty, D. J. (1992). "Identification of piping and sapping erosion of streambanks." *Contract Rpt. HL-92*, US Army Eng. Waterways Exp. Sta., Vicksburg.

Hagerty, D. J. and French, M. N. (1987). "Ohio River bank caving--an investigation of factors affecting bank instability." *Report to Louisville District*, Corps of Engineers.

Hagerty, D. J. and Spoor, M. F. (1989). "Alluvial streambank erosion--a ten-year study." *Proc., Int. Symp. Sediment Transport and Modeling*, ASCE, 594-599.

Hagerty, D. J., Spoor, M. F., and Ullrich, C. R. (1981). "Bank failure and erosion on the Ohio River." *Engrg. Geol.*, 17, 141-158.

Hagerty, D. J., Sharifounnasab, M., and Spoor, M. F. (1983). "Riverbank erosion--a case history." *Bull., Assoc. Engrg. Geol.*, 20(4), 411-437.

Hagerty, D. J., Spoor, M. F., and Kennedy, J. F. (1986). "Interactive mechanisms of alluvial-stream bank erosion." *Proc., 3rd Int. Symp. River Sedimentation*, Jackson, MS, 1160-1168.

Haliburton, T. A. and Wood, P. D. (1982). "Evaluation of the U.S. Army Corps of Engineers gradient ratio test for geotextile performance." *Proc., 2nd Int. Conf. Geotextiles*, Las Vegas, IFAI, 97-101.

Hamel, J. V. (1988). "Geotechnical failure mechanisms in alluvial banks." *Mechanics of Alluvial Channels*, Water Resources Publ., Littleton, CO, 369-386.

Heerten, G. (1984). "Discussion on geotechnical aspects." *Proc., Int. Conf. Flex. Arm. Revetments Inc. Geotextiles*, London, Thomas Telford Ltd., 112.

Heerten, G. (1986). "Functional design of filters using geotextiles." *Proc., 3rd Int. Conf. Geotextiles*, Vienna, IV, 1191-1196.

Heerten, G. and Muhring, W. (1984). "Proposals for flexible toe design of revetments," *Proc., Int. Conf. Flex. Arm. Revetments Inc. Geotextiles*, London, Thomas Telford Ltd., 25-37.

Heerten, G., Meyer, H. and Muhring, W. (1984). "Experience with a flexible interlocking revetment system of the Mittellandkanal in Germany since 1973." *Proc., Int. Conf. Flex. Arm. Revetments Inc. Geotextiles*, London, Thomas Telford Ltd., 179-192.

Hjorth, P. (1975). "Studies on the nature of local scour." *Bulletin Series A, No. 46*, Dept. Water Res. Engrg., Lund Inst. Technology, University of Lund, Sweden.

Hjortnaes-Pedersen, A. G. I., Bezuijen, A. and Best, H. (1987). "Non-stationary flow under revetments using the finite element method." *Proc., 9th Eur. Conf. Soil Mech. Fdn. Engrg.*, Dublin, 435-438.

Howard, A. D. and McLane, C. F. III (1988). "Erosion of cohesionless sediment by groundwater seepage." *Water Resources Research*, 24(10), 1659-1674.

Huntington District. (1979). *Kanawha River Reconnaissance*. Corps of Engineers.

Huntington District. (1986). *Kanawha River Bank Failure and Erosion: Confluence to Head of Navigation*. Corps of Engineers.

Ingold, T. S. (1984a). "Geotextiles as filters beneath revetments." *Proc., Int. Conf. Flex. Arm. Revetments Inc. Geotextiles*, London, Thomas Telford Ltd. 83-94.

Ingold, T. S. (1984b). "Discussion on geotechnical aspects." *Proc., Int. Conf. Flex. Arm. Revetments Inc. Geotextiles*, London, Thomas Telford Ltd., 116.

Keown, M. P. and Dardeau, E. A. Jr. (1980). "Utilization of filter fabric for streambank protection applications." *Tech. Rpt. HL-80-12*, US Army Eng. Waterways Exp. Sta., Vicksburg.

Keown, M. P. and Oswalt, N. R. (1984). "US Army Corps of Engineers experience with filter fabric for streambank protection applications." *Proc., Int. Conf. Flex. Arm. Revetments Inc. Geotextiles*, London, Thomas Telford Ltd., 227-237.

Koerner, R. M. (1990). *Designing with Geosynthetics*, 2nd Ed., Prentice Hall, Englewood Cliffs, NJ.

Koerner, R. M. and Ko, F. K. (1982). "Laboratory studies on long-term drainage capability of geotextiles." *Proc., 2nd Int. Conf. Geotextiles*, Las Vegas, IFAI, 91-95.

Lawler, D. M. (1992). "Process dominance in bank erosion systems." Chap. 5 in *Lowland Floodplain Rivers: Geomorphological Perspectives*, Ed. P. A. Carling and G. E. Potts, Wiley, London, 118-143.

Lawson, C. R. (1982). "Filter criteria for geotextiles: relevance and use." *Jour., Geotech. Engrg. Div.*, ASCE, 108 (GT10) 1300-1317.

Maynord, S. T. (1988). "Stable riprap size for open channel flow." *Tech. Rpt. HL-88-4*, US Army Eng. Waterways Exp. Sta., Vicksburg.

Maynord, S. T. (1989). "Riprap stability in channel bends." *Proc., 1989 Nat. Conf. Hyd. Engr.*, Ed. M. A. Ports, ASCE, 206-211.

McCormick, W. N., Jr. (1984). "Use of geotextiles under riprap." *Engr. Tech. Ltr. 1110-2-286*, Corps of Engineers, Washington.

Miller, S. P. (1978). *Bank Distress of Low Water Weirs on Big Creek, La., Misc. Paper S-78-2*, US Army Eng. Waterways Exp. Sta., Vicksburg.

Montero, C. M. and Overmann, L. K. (1990). "Geotextile filtration performance test." *Geosynthetic Testing for Waste Cont. Appl., ASTM STP 1081*, R. M. Koerner, Ed., Am. Soc. Test. Matls., 273-284.

Muhring, W. (1984). "Discussion on construction." *Proc., Int. Conf. Flex. Arm. Revetments Inc. Geotextiles*, London, Thomas Telford Ltd., 374-377.

Muskatirovic, D. and Batinic, B. (1986). "Some hydraulic properties of geotextile filters built into river engineering structures." *Proc., 3rd Int. Conf. Geotextiles*, Vienna, III, 769-774.

Office, Chief of Engineers. (1986). "Civil works construction, guide specification, geotextiles used as filters."

CW 02215, OCE, Washington.

Ogink, H. J. M. (1975). "Investigations on the hydraulic characteristics of synthetic fabrics." *Publ. No. 146*, Delft Hydraulics Laboratory, Delft, The Netherlands.

Parola, A. C. and Hagerty, D. J. (1992). "Evaluation of Palmiter erosion remediation techniques--a case study." *Proc., Water Forum '92*, ASCE, 660-665.

Parola, A. C., Hagerty, D. J., and Schaefer, D. A. (1991). "Study of extent of stream bank failure and erosion on Sixmile Island, Ohio River mile 597.7." *Report to Louisville District*, Corps of Engineers.

Parola, A. C., Hagerty, D. J., and Schaefer, D. A. (1992). "Evaluation of Palmiter non-structural bank stabilization technique." *Report to Louisville District*, Corps of Engineers.

Pilarczyk, K. W. (1984). "Prototype tests of slope protection systems." *Proc., Int. Conf. Flex. Arm. Revetments Inc. Geotextiles*, London, Thomas Telford Ltd. 239-254.

Rollin, A., Andre, L. and Lombard, G. (1988). "Mechanisms affecting long-term filtration behavior of geotextiles." *Geotextiles and Geomembranes*, 7, 119-145.

Schober, W. and Teindl, H. (1979). "Filter criterion for geotextiles." *Proc., 7th Eur. Conf. Soil Mech. Found. Engrg.*, 2, 121-129.

Sherard, J. P., Dunnigan, L. P. and Talbot, J. R. (1984). "Basic properties of sand and gravel filters." *Jour. Geotech. Engrg.*, ASCE, 110 (6) 684-700.

Shields, F. D., Jr. (1992). "Effects of woody vegetation on sandy levee integrity." *Water Res. Bull.*, 28(5) 917-931.

Spoor, M. F. (1986). "Kanawha river reconnaissance." *Report to Huntington District*, Corps of Engineers.

Spoor, M. F. and Hagerty, D. J. (1989). "Bank failure and erosion on the Illinois Waterway." *Proc., Int. Symp. Sediment Transport and Modeling*, ASCE, 600-605.

Springer, F. M., Jr., Ullrich, C. R., and Hagerty, D. J. (1985). "Streambank stability." *J. Geotech. Engrg.*, ASCE, 111(5), 624-640.

Thorne, C. R. and Tovey, N. K. (1981). "Stability of composite riverbanks." *Earth Surf. Proc. Land.*, 6, 469-484.

Ullrich, C. R., Hagerty, D. J., and Holmberg, R. W. (1986). "Surficial failures of alluvial streambanks." *Can. Geot. J.*, 23(3), 304-316.

Weigel, T. A. and Hagerty, D. J. (1983). "Riverbank change--Sixmile Island, Ohio River, U.S.A." *Engrg. Geol.*, 19, 119-132.

Williams, N. D. and Abouzakhm, M. A. (1989). "Evaluation of geotextile/soil filtration characteristics using the hydraulic conductivity ratio approach." *Geotextiles and Geomembranes*, 8(1), 1-26.

ENVIRONMENTALLY SENSITIVE APPROACHES TO RIVER CHANNEL MANAGEMENT

J. Haltiner and P.E.P. Williams
Philip Williams & Associates, Ltd

ABSTRACT

Traditional engineering approaches to river channel erosion and flood hazards have focused on single purpose, structurally intensive solutions such as monolithic rip-rap or concrete-lined channels, and drop structures. While often successful in reducing erosion, these approaches have serious technical and land-use drawbacks. They provide little or no environmental, aesthetic or recreational values. Designed as single-purpose systems, they destroy the biotic habitat value of what is typically the richest ecological zone in a region. To expand the range of channel management solutions, two concepts are emphasized: watershed-based, regional planning approaches, in which localized problems and solutions are evaluated in the broader context of changes in the watershed (runoff, sediment, vegetation, etc.) and channel processes; and, integrated design, in which the at-a-point solutions are based on a multiple-objective design, combining engineering design with biotic, aesthetic, and land-use values. This latter element emphasizes the concept of stream restoration as a viable alternative to channelization or other traditional solutions. Essential to this approach is the design of a stable channel. Often, this channel must respond to the altered catchment hydrology resulting from urbanization, logging, etc. Biotechnical approaches integrating rip-rap or other structural measures with vegetation provide a range of bank and channel stabilization methods consistent with a multi-objective approach.

1. INTRODUCTION

During the past two centuries, attitudes towards urban streams have changed dramatically in the American West. Throughout the history of native American settlement and early colonization by Mexican and European settlers, streams were vitally important. They provided a source of drinking and irrigation water, food, and navigation. Often, these early settlements were named after the local streams. As these small villages expanded into urban centers, use of local streams for water supply and irrigation was replaced by projects located hundreds of miles away. River navigation lost importance and local food gathering ceased. In many instances, the encroachment of cities destroyed the very streams from which they derived their names. Rising land values pushed urban development to the river's edge.

As a consequence of urban and agricultural encroachment, periodic flooding, erosion, and lateral channel migration, all natural phenomena, now resulting in extensive damage and suffering. Forestry, agricultural practices, and urban development in the watershed, increased the severity of flood flows, and often resulted in substantial channel downcutting and bank erosion. These problems of flooding and erosion/sedimentation resulted in urban streams being perceived as more of a hazard and less of a resource to the local population. Local, state and federal agencies were expressly funded to combat these problems, and the approach was clear: rivers were a threat to life and property, requiring control.

2. TRADITIONAL CHANNEL PROTECTION METHODS

The perceived need for river channel/bank protection projects results when geomorphic processes produce undesirable channel changes which represent a threat to structures, agricultural land, etc. The traditional responses to these problems have included stream channelization, with bank stabilization being accomplished by rip-rap, concrete lining, and a variety of other revetment materials. Erosive flow velocities and channel incision have been controlled using vertical or cascade grade control/drop structures to reduce scour velocity. The design and construction of

channel protective works has been based on a combination of trial and error, supported by some theoretical and experimental studies (cf: State of California, 1970). These approaches have focused on at-a-site solutions, based on the capability of the revetment to withstand the hydraulic forces during a flood event. The design issues include selection of revetment type, initial bank/channel grading, slope, use of geotextile fabric, stone parameters (size, weight, durability), with some discussion of end tie-in, depth of toe below channel to accommodate scour, and revetment height.

While these types of 'channel improvements' have reduced flood hazards in many areas, they have a variety of engineering, environmental, and land-use planning deficiencies. The engineering design is typically based primarily on hydraulic ('clear-water') principles, and does not include the effects of debris and sediment conveyed during high flows. The extent of revetment is often over-designed, based on an incomplete understanding of the erosive forces. This is particularly true concerning the height of rip-rap on the bank. Toe protection, on the other hand has often been too shallow, resulting in undercutting and collapse of the revetment. Likewise, end protection and tie-in to the banks has frequently been a source of failure. As a consequence, recent engineering research has focused on improving and refining the technical aspects of revetment design.

In addition to the technical deficiencies, however, these traditional solutions provide little or no environmental or land-use values. Designed as single-purpose systems, they destroy the habitat value of what is typically the richest ecological zone in a city. The high-velocity flows and turbulent conditions at hydraulic structures are a safety hazard, and despite fencing and signs, numerous drownings occur. Maintenance costs are often higher than anticipated. Channelized streams lack a riparian canopy to shade out understory species, and the channel may become choked with vegetation, requiring expensive and destructive ongoing maintenance. Failure to manage sediment transport adequately results in either costly sediment removal, or erosion control costs. As a result of these deficiencies, there appear to be a number of key areas where an expansion beyond traditional approaches is warranted, as discussed in the following sections.

3. WATERSHED AND RIVER CORRIDOR PERSPECTIVE

When bank or channel erosion occurs, the immediate response is to develop a local protection scheme. Experienced river engineers will conduct analyses to identify the erosion cause to improve the protection design. However, the problem is rarely viewed in the broader context of regional processes and regional solutions. This results both from the nature of land ownership (an individual landowner is concerned only with on-site issues) and with the cost and complexity of a larger scale study. However, experience has shown that channel changes do not occur in isolation, and that the effect of channel modifications will extend up and/or downstream. It is not uncommon along an incising urban creek in California for each property owner to install a different type of channel protection scheme, without coordination, knowledge of potential success, impacts on others etc. Consequently, it is the responsibility of the local, state, or federal agency with permitting or regulatory responsibility to ensure regional perspective and coordination. This planning is preferably done on a watershed basis, and in this paper will be referred to as *Integrated River Basin Management*. This approach has been applied most widely in England (Gardiner, 1988), where river management has been shifted from county-based planning to management based on watershed boundaries. The two technical areas that distinguish this approach from traditional at-a-point methods are the regional spatial perspective, and a multi-disciplinary analysis, which incorporates geomorphic perspectives both on the channel dynamics and on the time frames over which changes occur.

This multi-disciplinary approach extends beyond the technical realm. In defining goals, objectives, and parameters on which to base river management decisions, the traditional goals of structure or land protection and cost/benefit ratio are expanded to include biotic values (vegetation, wildlife, and fishery), recreational, land-use, public safety, aesthetic, and water quality benefits. While recognition of many of these additional values has been widespread among various planning and regulatory authorities, their inclusion in the engineering design process has been slow. The reasons include the lack of constructed and monitored examples of integrated management, the perception of higher costs, the goal to maximize developable land, and a lack of confidence that federal agencies will participate in cost sharing. Engineering, a

construction-based profession, is conservative by nature. This is understandable, considering the importance of public safety and the magnitude of costs involved in river projects. However, considerable progress has been achieved during the past several decades in the planning and implementation of some multi-objective river projects, and the need exists to integrate these into engineering education and practice in a more systematic manner.

Figure 1 presents a flow chart describing how this broader approach may be applied to channel stability problems. The initial phase focuses on problem identification. The type of problem and extent/severity is assessed, and both local and regional causes are pursued. For example, localized erosion may result from direct flow impingement on a bank, channel incision, channel migration or as a result of bank properties (groundwater seepage, bank material properties, etc.). However, these local causes may be the result of a modified hydrologic regime (urbanization, logging, grazing), regional channel aggradation or degradation, or a modified sediment regime. The goals and parameters to be addressed expand beyond the on-site protection and minimal cost. They include the potential need for regional channel protection, preserving or restoring local or regional biotic environment, land use/recreation components, water quality degradation, aesthetics, public safety, and a broader cost analysis (which includes both short- and long-term costs, and off-site as well as on-site costs). A range of alternatives can be developed from this expanded array of goals. It may be determined that it is wisest to accommodate the change, abandon or relocate any structures, and provide setbacks to accommodate future channel changes. The alternatives may also include regional channel approaches (bypass channels, rock check dams, etc.) which provide solutions over an extended reach. At a truly regional scale, watershed modifications represent an important tool, particularly in urbanizing areas. These may include detention basins, maintaining floodplain storage, or other design parameters (porous paving, maintenance of open space, seepage pits, drainage swales, etc.). Increasingly, urban developments are being prohibited from increasing post project flood peaks, necessitating the inclusion of detention basins. However, these are still relatively rare, and there is a strong need for monitoring and the development of design criteria for multi-objective detention basins. The selection of a preferred approach should be based on a comparison of the effectiveness of the alternatives in meeting the goals. The regulatory and permitting agencies must take a much

stronger role, if regional approaches are to be effective. In addition, this involvement must be proactive and consistent. In general, landowners don't want detention basins or other land-use constraints. Finally, the implementation and management phase of the project requires the same level of involvement and commitment that typically ends at the design/planning phase. Construction should be consistent with the design unless the impacts of any proposed modifications are thoroughly analyzed. Once built, a completed project will evolve over a period of perhaps decades, particularly the vegetative and sediment-affected components. An adaptive management structure must be in place, capable of responding to the system evolution. Performance criteria should be established, and steps taken if a project component fails. In particular, the response of the system to an episodic extreme event should be monitoring. Although occurring irregularly, major flood events are often the critical test of project success or failure. It is crucial that performance in these events be evaluated.

4. INTEGRATED ON-SITE CHANNEL STABILIZATION

Where the above planning approach recommends on-site solutions, a multi-objective approach is also stressed. Figure 2 presents a schematic of a recommended planning process. The problem identification phase (Existing Conditions) is similar to that in Figure 1. However, the selection of goals and the identification of key parameters are focused on optimizing the design at a single point. Thus, available materials and local expertise are stressed, the risk of failure (likelihood and consequences) are assessed, and the riparian corridor boundaries established. Issues of cost, access, and maintenance are included at this early planning stage. Similarly, the design process focuses on the selection of the stabilization approach, design details (such as cross-section, configuration and construction materials). Subsequent implementation stages are similar to those in Figure 1, but also include the recognition that evolving values and needs may result in future additional modifications to the project.

Perhaps the greatest need in the implementation of environmentally sensitive on-site channel protection schemes is the development of design parameters, pilot projects, and

monitoring/documentation of constructed systems. In our work on California streams, we have developed a variety of bank and channel stabilization approaches which range from the use of vegetation to increasingly structural solutions. Figure 3 depicts the general design approach followed to identify the most suitable method. As before, the initial step is to develop an understanding of the local and regional processes, including the watershed hydrology, geomorphological trends and any land-use changes. These include the local channel morphology (including shape, aggradation/degradation, sediment load/size distribution), hydraulic parameters (channel-forming and 100-year discharge, velocity and water depths), substrate characteristics (size distribution, nutrient availability, groundwater depth/variability), and water quality issues (presence of hazardous materials, high salinity, etc). This knowledge of the local and regional physical processes is then combined with a similar analysis of the biotic environment to identify an appropriate stabilization approach. The selected method must provide the required protection, while being compatible with the local biological and land-use needs. Key factors in the design process include the design of the channel cross-section, identification of the appropriate structural components, and selection of the optimal vegetation component. The construction then proceeds with initial grading, installation of the structural elements, followed by planting. In some cases (such as the installation of willow poles in the rip-rap), the structural and planting proceed simultaneously. Obviously, this requires additional care to prevent damage to the vegetation. Management includes a monitoring program to track the success of the project, maintain the vegetation until it is self-sustaining, control weeds and exotic, invasive vegetation, and the replacement of vegetation or structural elements as needed. Typically, this establishment/monitoring period extends about five years. While this should be suitable to ensure that the vegetation will survive, it is not adequate to track the evolution of the site to maturity (which may take thirty to fifty years), or determine performance and stability during a catastrophic event.

Schematic depictions of a number of different design approaches are shown in Figures 4 through 12. Figure 4 emphasizes the importance of establishing a stable channel cross-section prior to the installation any bank protection schemes. Based on research in England (cf: Hydraulic Research, 1988), we have emphasized the creation of multi-stage channels either where severe

incision has occurred or where significant flood hazard reduction is important. Typically, in incised California streams, the existing channel is deep, often broad, and lacks a defined or stable low-flow channel. The banks are over-steep and subject to on-going failure. The channel incision results in a lowering of the groundwater table, precluding the establishment of riparian trees along the top of bank. Once a channel becomes destabilized, it will continue incising (often, for hundreds of years) until the longitudinal slope becomes sufficiently flattened to reduce the bed shear stress below erosive levels, or until the channel thalweg encounters bedrock. Restoration of these streams is often impossible without significant modification to create a stable cross-section. The multi-stage channel allows establishment of a defined low-flow channel, while higher terraces can accommodate various riparian species. During flood events, the overflow onto the upper terraces at least partially simulates the natural overbank/floodplain flow. Often, even a regraded channel requires additional bank and channel bed stabilization to prevent future degradation.

Figure 5 depicts a number of different vegetative bank stabilization approaches. Where sufficient bank or bed erosive forces exist, a combined vegetation/rip-rap approach such as that shown in Figure 6 has been used. In this approach, willow pole cuttings are inserted between the rip-rap (and through the underlying filter fabric) as the rock is being placed. Over time, the tree roots extend around the rock, providing additional stability. The rip-rap is shown extending from the estimated scour depth up to the elevation of the 5-year flood event. Above this height, it is assumed that vegetation, stabilized with some type of matting, will prevent erosion.

Where a more extensive and uniform layer of rip-rap is required, or to retrofit existing rip-rap, planting collars can be installed through the rock layer (Figure 7). Typically, sections of 24- or 36-inch plastic or concrete pipe have been used. The pipes are backfilled with topsoil and trees or shrubs are planted. An irrigation system can be included during installation. Depending on the vegetation used, the planting collars are located on 5- to 15-foot centers. While this technique does not actually represent "biostabilization", the resulting vegetation cover does provide wildlife and aesthetic benefits.

Where the available corridor width is not sufficient to allow resloping the banks to accommodate rock and vegetation, more structural approaches are required. Figures 8 through 11 depict the use of log cribwalls, gabions, and vertical rock walls in an environmentally acceptable manner. The key stability factors include adequate tie-in to the banks on the upstream and downstream ends, and extension of the structure (or protection with rip-rap) to the depth of toe scour.

Local channel bed incision has typically been controlled with monolithic concrete drop structures. Figure 12 depicts the use of boulder clusters and in-channel check dams to prevent channel downcutting. These are installed at more frequent intervals to minimize the gradient drop at each individual structure. This is essential, both to prevent failure of the structure from excessive energy dissipation and to allow fish passage. In our experience, grade control structures stabilizing a drop of 2- to 4-feet are most stable.

5. RESEARCH NEEDS

Most of the techniques and approaches described above are not new. Some have been implemented in rural areas (particularly by the United States Soil Conservation Service) for many years. However, their application in conjunction with an integrated river basin management approach requires a much more sophisticated understanding of fluvial processes. In addition, their application in urban areas, with significantly altered hydrologic, hydraulic and geomorphic regimes is not well-established. These approaches have generally not been subject to rigorous, controlled experimentation, testing and design refinement. The interaction of tree roots and rip-rap, the level of erosion protection offered by vegetation, the behavior of vegetated channels during large floods, the size of rock to be used in check dams all represent major areas of uncertainty. Multiobjective environmental approaches will not be adopted by local agencies and engineers until sufficient theoretical, laboratory, pilot project, and full-scale installations are conducted to provide a basis reliable design. Where feasible, standard design specifications and details should be developed.

The extension of modern river understanding in conjunction with a commitment to maximize the use of multi-objective techniques offers the opportunity to revive the degraded value of our urban streams. The result can provide cost-effective flood hazard reduction and channel stabilization as well as a network of urban parks and open space.

6. REFERENCES

Gardiner, J.L. (1988). Environmentally Sound River Engineering: Examples from the Thames Catchment. Regulated Rivers: Research and Management, Vol.2, 445-469.

Hydraulics Research Ltd. (1988). Assessing the Hydraulic Performance of Environmentally Acceptable Channels. Report EX 1799, Wallingford, Oxfordshire, England. Sept. 1988

State of California-Department of Transportation (1970). Bank and Shore Protection in California Highway Practice. Publication no. 78704-500 3-79, 423.

Figure 1.

CONCEPTUAL APPROACH TO RESOLVING CHANNEL STABILITY PROBLEMS

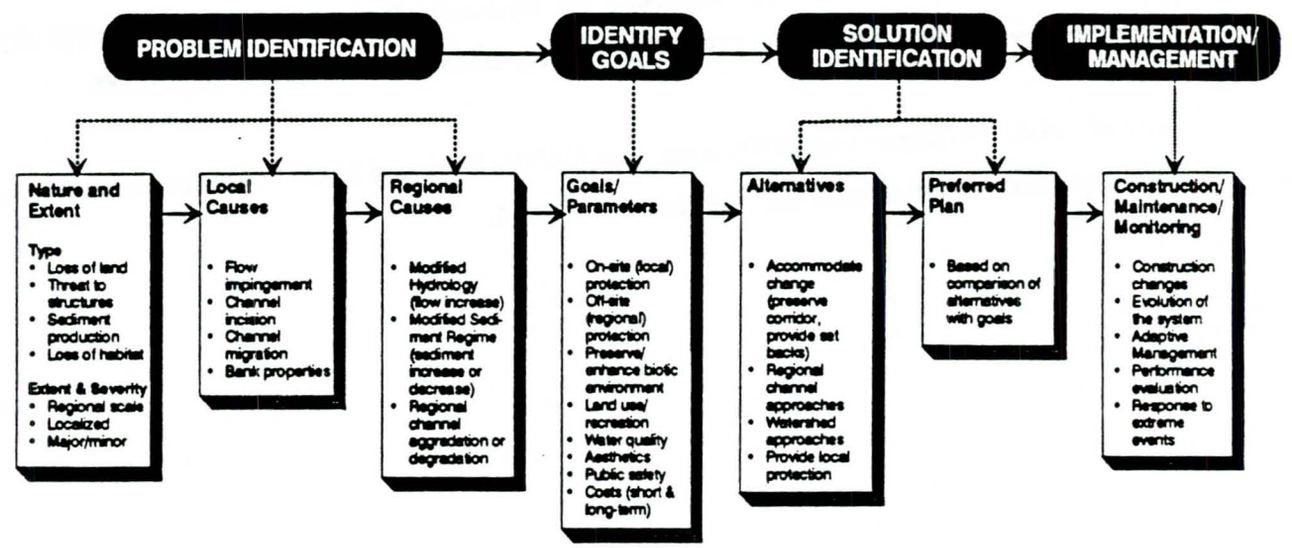

Figure 2.

Design Process for On-Site Channel Modification

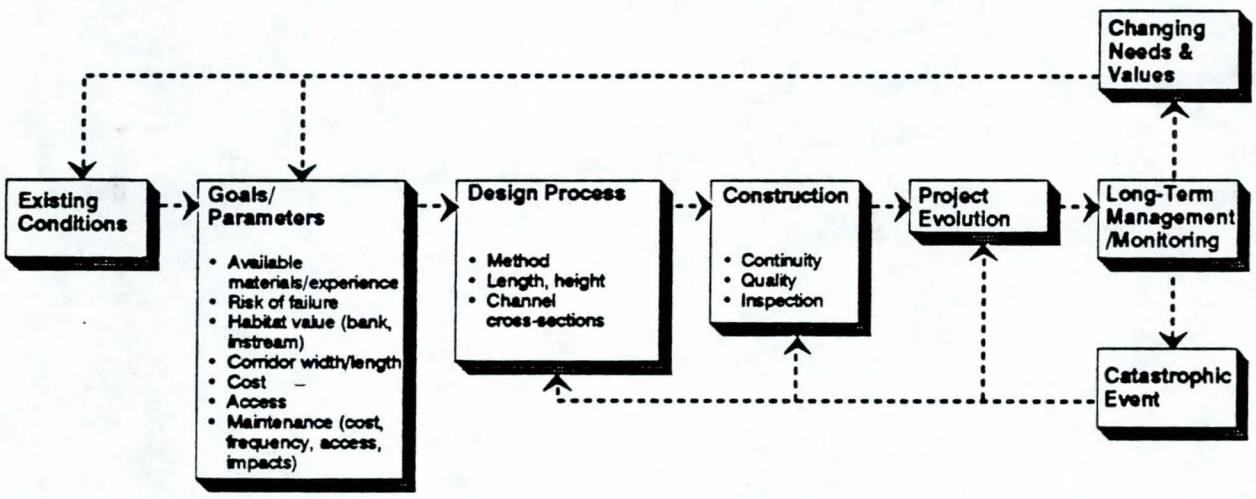

Figure 3.

Integrating Physical and Biological Systems in Channel Stabilization

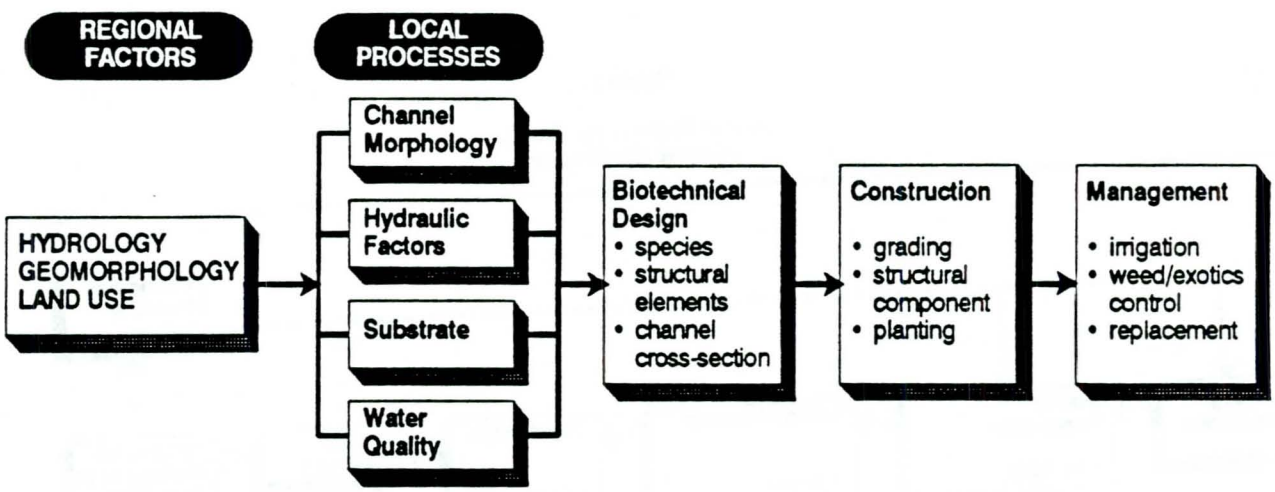

Fig. 4: Slope Stabilized by Creating Terraced Banks

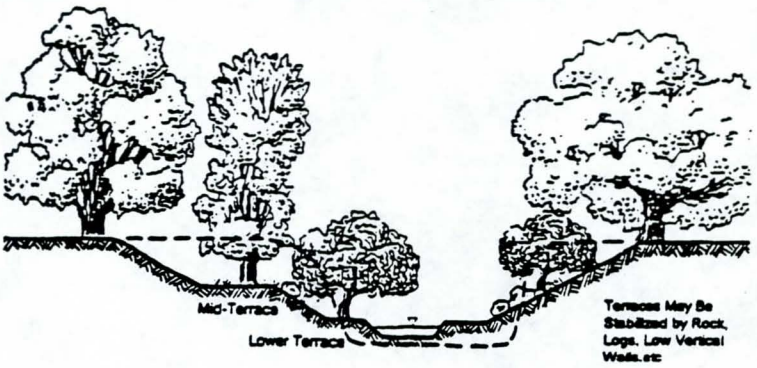

Fig. 5: Existing Banks Modified and Revegetated

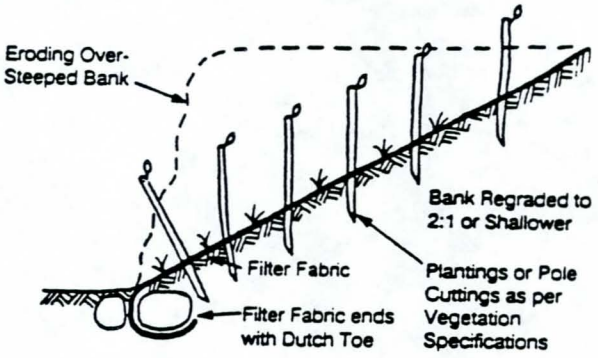

Brush Layering

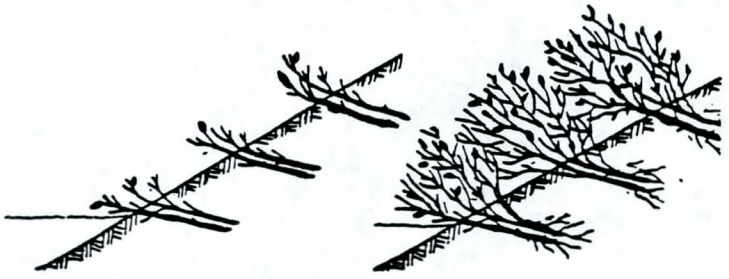

Fig. 6: Toe of Slope Stabilized with Rip-Rap and Planted

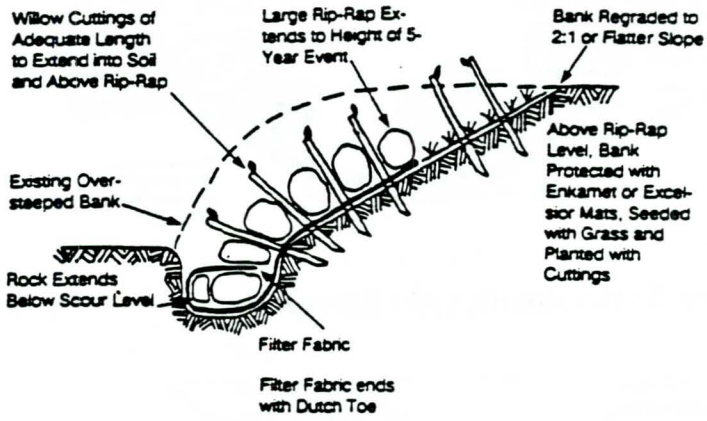

Fig. 7: Rip-Rap with Planting Collar

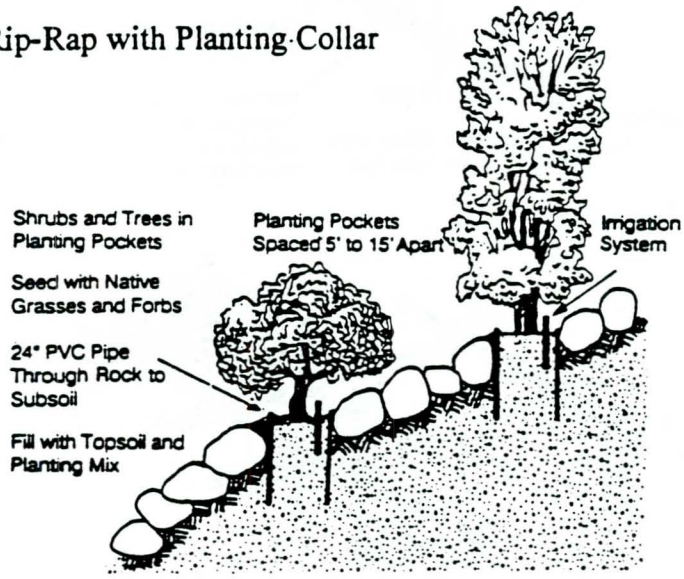

Fig. 8: Log Cribwall

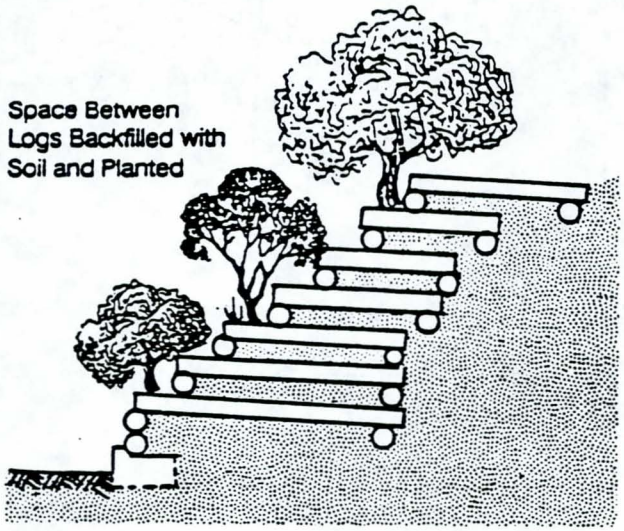

Fig. 9: Gabions

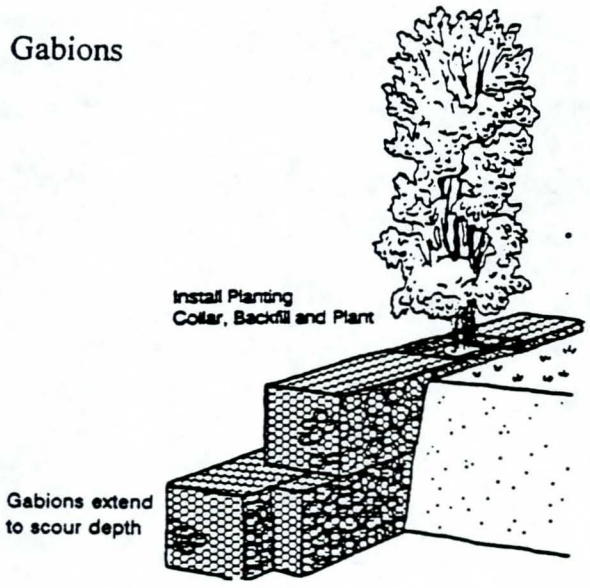

Fig. 10: Vertical Retaining Wall Used to Stabilize Bank

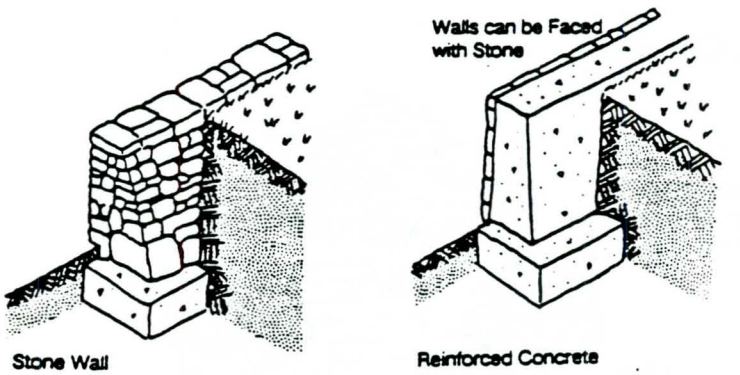

Fig. 11: Multiple Walls Used to Stabilize a Steep Bank, Rather Than a Single High Wall

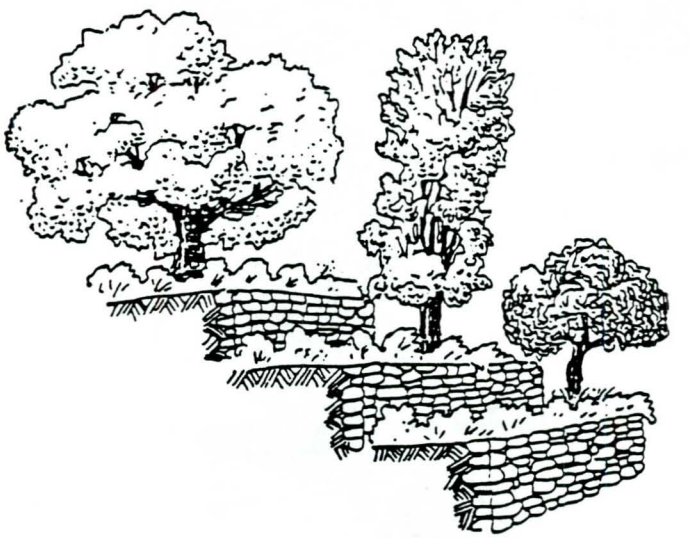

Fig. 12: Channel Stabilization, Fish Habitat Enhancement

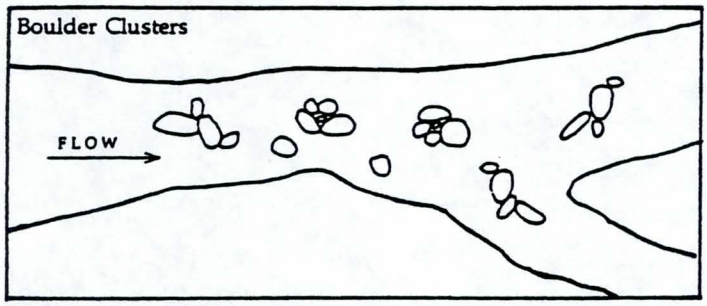

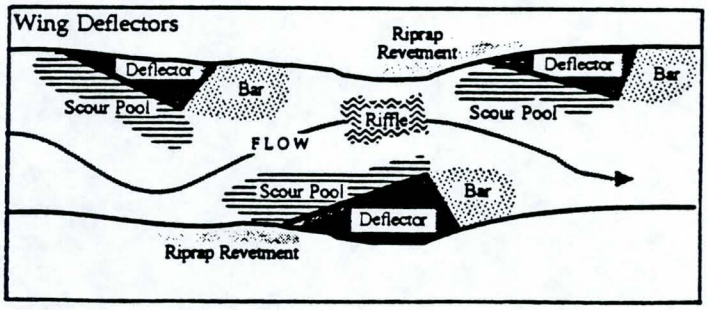

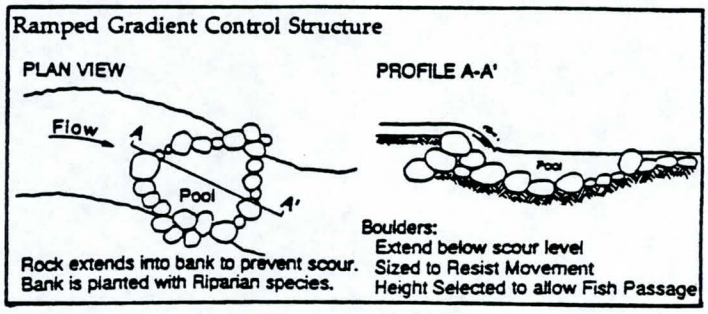

CASE STUDY RISK ANALYSIS CLOSURE WORKS SAEMANKEUM

F.Th. Heezen
DHV Environment and Infrastructure,
P.O. Box 1075, 3800 BB Amersfoort, The Netherlands

ABSTRACT

A Technical risk analysis is done on closure works for a land reclamation project. The analysis focuses on design criteria for sill, closure dam and bottom protection. A fault tree analysis is done, identifying failure mechanisms and design formula. A deterministic design is made and compared with a probabilistic design, using stochastic parameters. For the sill a design is chosen with a certain acceptable probability of failure, derived from the fault tree analysis. For the bottom protection an economical optimal probability of failure is determined.

1 INTRODUCTION

In this Case Study a risk analysis of a closure operation is carried out. The objective of the risk analysis is to realize a technical safe closure operation, with an optimum probability of failure of the components. The method is illustrated in this Study.

The closing procedure, the geometry of the structures involved and the geotechnical and hydraulic boundary conditions are based on an existing design for a land reclamation project in the Republic of Korea. The Study focuses on the failure mechanisms during the closure operation and the relevant dimensions of the structures (i.e relative weight of the stones or length of the bottom protection). In view of the objective of this Study, some simplifications and assumptions are made. Therefore results do not apply to the real project. Important starting points are:

- the Study partially uses assumed input data;
- not all possible failure mechanisms are analyzed;
- only one closure gap of three is discussed;
- the stability of the top layer of the sill and the length of the bottom protection are treated more in detail; a limited analysis is made concerning the closure dam;
- only the construction stage is considered, not the final situation.

The case Study comprises the following sections:

1. introduction;
2. a description of the project, the closing procedure, the main dimensions of the structures and the boundary conditions;
3. a fault analysis in which relevant failure mechanisms are determined;
4. the relevant failure mechanisms and formulas;
5. a deterministic design using the formulas given in section 4;

6. probabilistic calculations resulting in probabilities of failure for different design values;
7. comparison of the deterministic and the probabilistic calculations and optimal probabilistic design.

2 DESCRIPTION OF THE PROJECT AND THE DESIGN

2.1 The project

The closure operation is part of the Saemankeum land reclamation project, located at the west coast of the Republic of Korea. The situation is given in Figure 1. The total area to be closed is 40.000 ha. The sea dikes have a total length of about 30 km. The hydraulic conditions are severe: a tidal amplitude of up to 3.5 m and a tidal prism of 3.10^9 m^3. The bottom level varies between 4 and 20 m below sea level, and consists of layers of sand, silt and clay. At a depth of MSL - 35 to 40 m a rock zone is present (MSL = Mean Sea Level).
The overall length of the three final closure gaps is 4100 m. The length of gap 1 is 1300 m.

Closing of the final gaps of the sea dikes is done in stages (see Figure 2):
1. at an early stage a bottom protection is laid, made of a fascine mattress, on which stones are dumped. The bottom protection prevents that the stability of the sill is endangered by slide planes, caused by scour holes.
2. a sill made of quarry stone is constructed using marine equipment. The sill is gradually heightened over the total length of the gap, until it is too difficult to work with marine equipment.
3. A horizontal closure dam is constructed on top of the sill, starting from the sides of the gap. The dam is constructed using quarry stones, tipped at the head of the dam using dump trucks.

2.2 The geometry of the closure structures

Levels are given in meters, relative to Mean Sea Level (MSL).

Sill (see Figure 3):
- top level: - 6 m
- bottom level: -16 m
- the sill consists of a core and a top layer. The stones in the top layer are relatively large.

Closure dam (see Figure 3):
- top width: 10 m
- top level: + 5 m
- bottom level: - 6 m
- seaward slope: 1:2 (vertical to horizontal)
- no different gradations of quarry stones are used in a cross section.

Bottom protection (see Figure 4):
- length from the toe of the sill to the mattress edge: 114 m
- bottom level: - 16 m

2.3 Boundary conditions

The fetch length from the South-West direction is not limited by islands nearby and is dominant for wave attack. The final closure is planned in the summer season, therefore the statistics of this season are used. The Probability of Exceedence P_E of the windspeed u_{10} (10 minutes duration) for the 3 month summer season is:

Windspeed [m/s]	P_E (summer)
20	$1.8*10^{-2}$
22	$8.6*10^{-3}$
24	$4.0*10^{-3}$
26	$1.9*10^{-3}$
28	$8.9*10^{-4}$
30	$4.2*10^{-4}$

The P_E of the windspeed averaged over a year is about 6 m/s higher than the value given for the summer season. The windspeed for 5-hour duration is about 85 % of the 10-minutes windspeed.

The bottom level in the gap studied is MSL-16 m. At 2 km in South-West direction from the gap, a relatively shallow area is present with a bottom level of MSL-9 m. At larger distances the sea gradually becomes deeper. The following depth contour is used:

Distance from gap, SW direction:	0	2	10	100 [km]
Bottom level:	-16	-9	-20	-40 [m]

The maximum depth of the sea in SW direction is 80 m.

The tidal range varies from 3.60 m at neap tide to 6.40 m at spring tide. The characteristics of the amplitude A of spring tide are: $\mu(A) = 3.20$ m and $\sigma(A) = 0.14$ m (per spring tide).

Wind can cause a change in the mean water level during a storm. The change depends on the characteristics of the wind field and of the basin. A first rough indication of the setup S, without taking characteristics of the basin into consideration is given by

$$S = 3 \cdot 10^{-6} \cdot u^2 \cdot \frac{L}{10D} \qquad (1)$$

With: u = windspeed [m/s]
L = fetch length [m]
D = depth [m]

With typical values for windspeed = 19 m/s (5-hours windspeed, P(exceedence) = 0.01 per season, SW direction), fetch length = 300 km and an average depth of 60 m, the set-up is about 0,5 m. This set-up is relatively small, compared to the variation in tidal water levels. The influence on the relevant mechanism (wave attack at the closure dam) is neglected within the scope of this Study, but should be incorporated in the final design.

The tidal prism depends on the intertidal area which changes from neap to spring tide. The flooded area varies from about $18*10^7$ m^2 at MSL-4 m to $40*10^7$ m^2 at MSL+4 m, according to a storage curve.

Waves have been calculated coming from a South-Western direction. In the relatively deep water parts the Bretschneider wave generation formula has been used. Wave propagation in the shallow parts has been calculated using a model incorporating both wind influence and energy decay caused by friction. The calculations present a rough indication only, because possible two-dimensional effects have not been included and a simplified depth contour is used.

Wind speed[m/s]	H_s [m]	T_m[s]
20	3.4	8.5
22	3.6	9.2
24	3.7	9.5
26	3.7	9.8
28	3.8	10.2
30	3.8	10.4

From a limited amount of boreholes the following could be concluded:

- The bottom level in the centre of the gap is MSL-16, with a standard deviation σ of 1 m.
- the grain size (d_{50}) of the upper layers is fine (80 - 100 μm)
- bottom material consists of layers of sand and layers of clay and silt mixed with sand.
- relative density of sand layers is mostly 0.5 (medium); at one location a thin layer of loose sand (relative density of 0.3) was found, 3 m below the bottom level.
- A weathered bedrock zone is present from MSL - 35 m (average μ),with a standard variation σ of 2 m.

fig 1 Situation

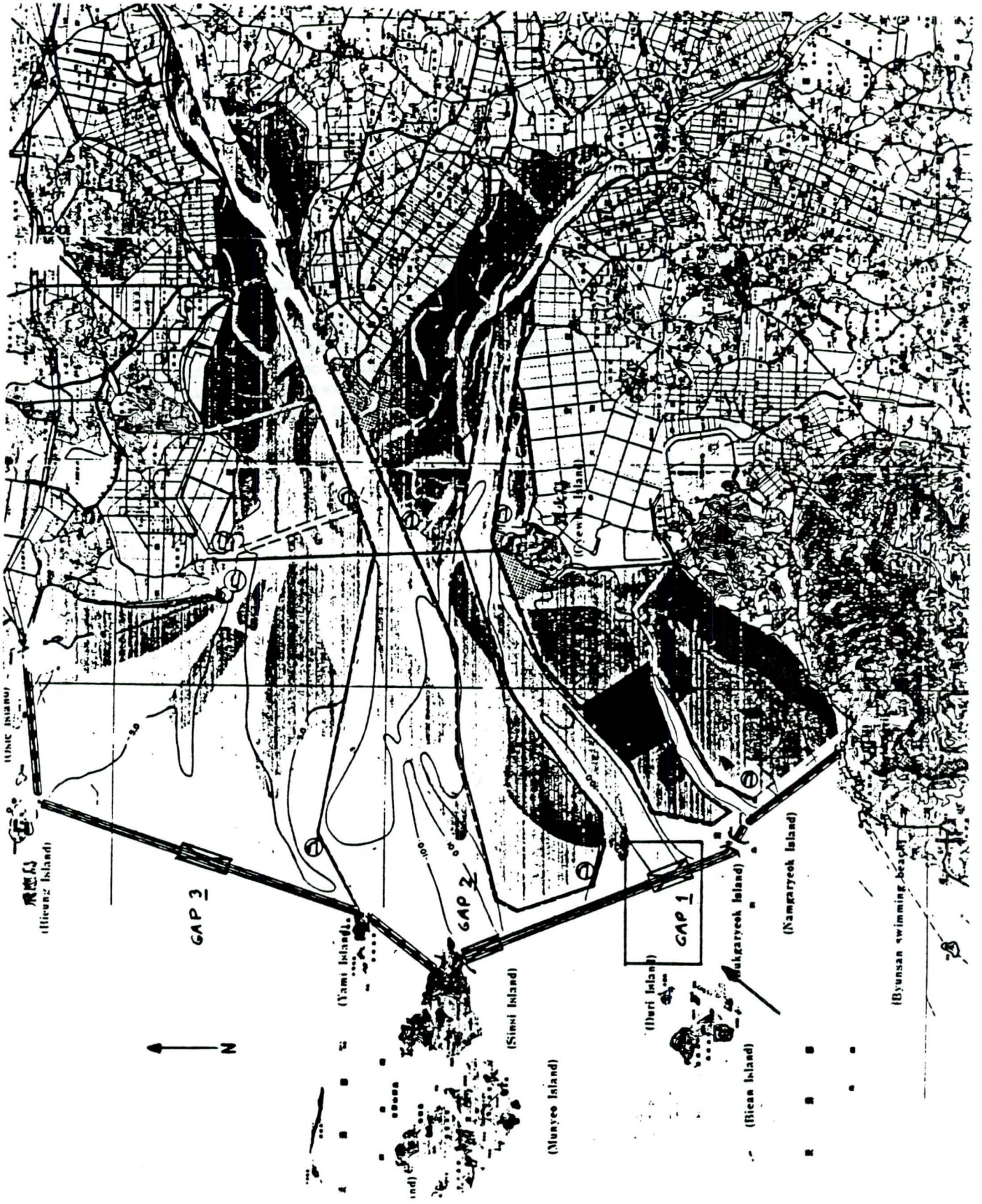

fig 2 Combined closing

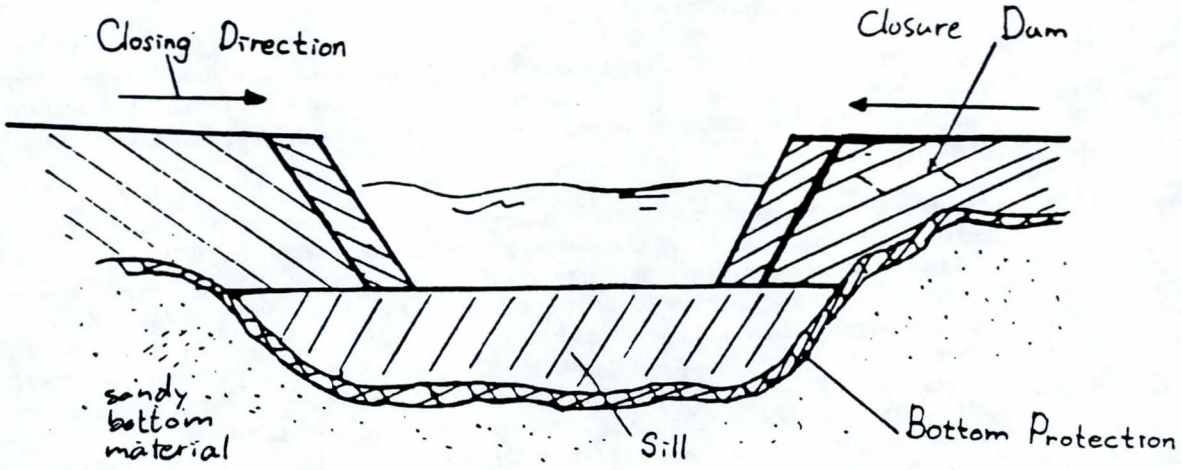

fig 3 Cross section of the gap

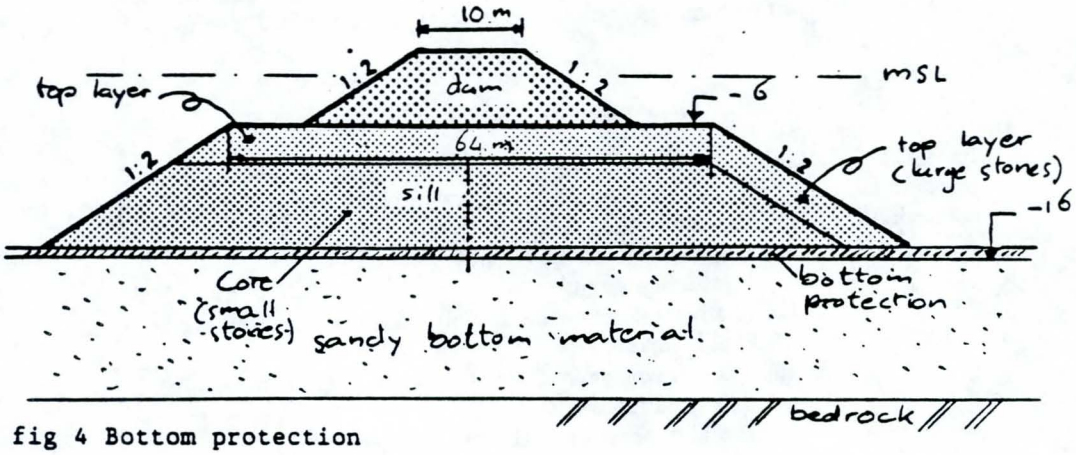

fig 4 Bottom protection

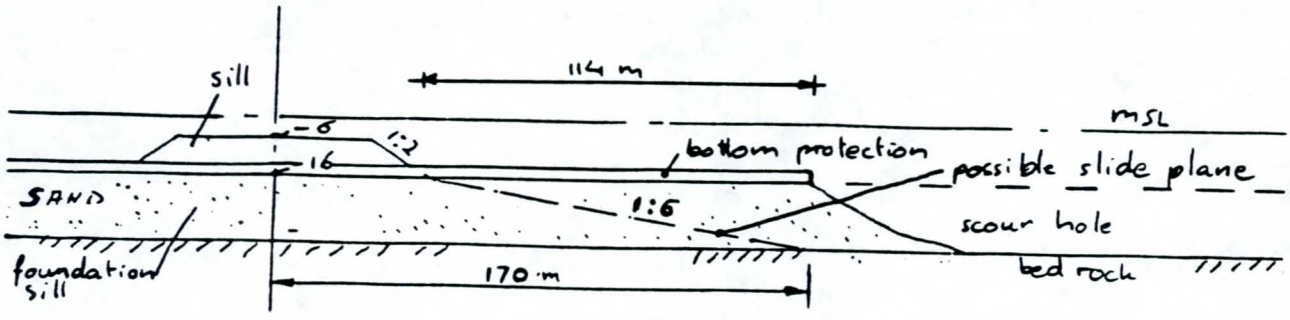

3 FAULT ANALYSIS

3.1 Failure and its consequences

Unwanted initial events and situations may lead to the unwanted consequence, failure of the closure gap. By organizing all the relevant elements in a fault tree it is possible to assess the influence of the elements on this unwanted consequence. In Figure 5 the main fault tree is given.

An important unwanted consequence is failure during construction and it's consequential losses. In this Study, the failure of a closure gap and the extra costs caused by a failure is the unwanted consequence. Failure may lead to a breach with a width up to several hundred meters. In this gap high flow velocities up to 6 - 7 m/s may occur because of the large tidal range, requiring the use of large stones from bedrock zone to the top of the dam (total height about 40 m) when closing the new gap. Often it is necessary to construct a new dam around the scour hole. Consequences of the breach both in time and costs are therefore significant. Failure can be caused by sill, dam or bottom protection (Figure 3 and 4):

- failure of the sill exposes the relatively small stones of the core and the bottom protection to heavy current attack. This may result in erosion of the sill and the bottom protection, followed by scour reaching the weathered bedrock zone at about MSL - 35 m.
- failure of the dam has serious consequences especially near the side of the gap. The heavy current attack occurring in a breach may erode the relatively small stones of both the dam and the sill at this location. After a breach, the same processes as described for the sill may occur.
- failure of the bottom protection leads to instability of the foundation of the sill. At the location of this instability, the same processes as described for the sill may occur.

3.2 Sill

In Figure 6 the fault tree of the sill is given. Important failure mechanisms for the sill are pore pressure induced slides of the rock body and erosion of the stones at the top of the sill during horizontal closing. This Study concentrates on erosion only, which can be caused by:

- the top layer of the sill is not up to specifications:
  - top layer not present;
  - the relative density or the diameter of the stones used not as specified;
  - sill level incorrect;
- the hydraulic load (mainly current induced) is too high because of:
  - extreme conditions;
  - horizontal dimensions of the gap(s) are wrong;

Events as the top layer not present and wrong dimensions of the gap should be prevented using surveys and measurements. Important normal uncertainties are fluctuations of the sill level, extreme hydraulic conditions and fluctuations in density or diameter of the stones. These are accounted for in the probabilistic calculations.

3.3 Closure dam

Important failure mechanisms of the closure dam are:
a) erosion of the head (tip) of the dam;
b) breach on the trunk of the dam during construction by wave action.

The stones are designed to be stable under normal tidal conditions. Erosion of the head only occurs if hydraulic load is too high (for instance during an extreme spring tide), and can cause

some retreat of the head. The retreat halts when the hydraulic load has decreased, and repairs can be made. Only production is slowed down and no total failure of the closure gap happens. Breaching of the trunk of the closure dam (just completed though not protected) may be initiated by wave action, followed by rapid erosion of dam, sill and bottom protection, resulting in a large breach. If the flow conditions during closure are used as the design load for the stones, the most probable location of this event is near the starting points of the dam at the sides of the gap, where the flow velocities and therefore also the stone dimensions are still relatively small.

As far as the dam is concerned, this Study is limited to a review of calculations with the mechanism wave action and an indicative deterministic design for current attack at the head tip. For a complete risk analysis, other mechanisms may be important (erosion, overtopping, slide planes, filter problems).

3.4 Foundation and bottom protection

In Figure 7 the fault tree of the foundation of the sill and bottom protection is given. The unwanted consequence in this subtree is instability of the foundation underneath the sill. Events possible of leading to failure are:

- direct instability caused by earthquakes. In this area earthquakes may occur, but are too small to cause damage;
- instability caused by scour induced slides. Two mechanisms are possible: flow slides and slide planes caused by geotechnical failure. Flow slides only occur in loosely packed sand having a hight porosity. In only one location this sand was found, 3 m below the sea bottom with a thickness of a few meters. Considering the limited depth and limited number of locations measured with sand capable of flow slides, the effect is considered to be neglectable compared to slide planes. Because of the limited information available, it is advisable to do a more extensive geotechnical survey before a detailed design is made.

Two situations can be distinguished concerning scour and slide planes:

- slide planes caused by scour inside the bottom protection area. This can happen for example after erosion of the bottom protection because of current attack or damage caused by anchors.
- slide planes caused by scour at the end of the bottom protection area. This can happen if the scour hole at the end of the bottom protection becomes to deep and the upstream slope of the hole becomes too steep. This mechanism is analyzed more in detail in section 4.

Fig 5 Main fault tree

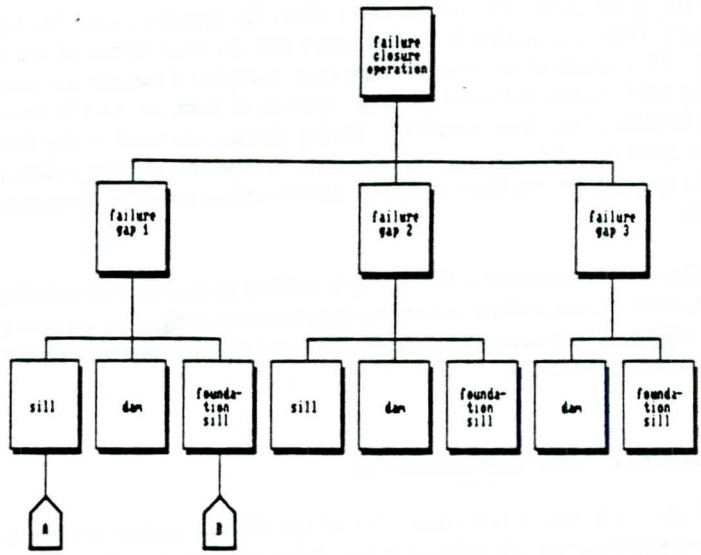

Fig 6 Fault tree sill

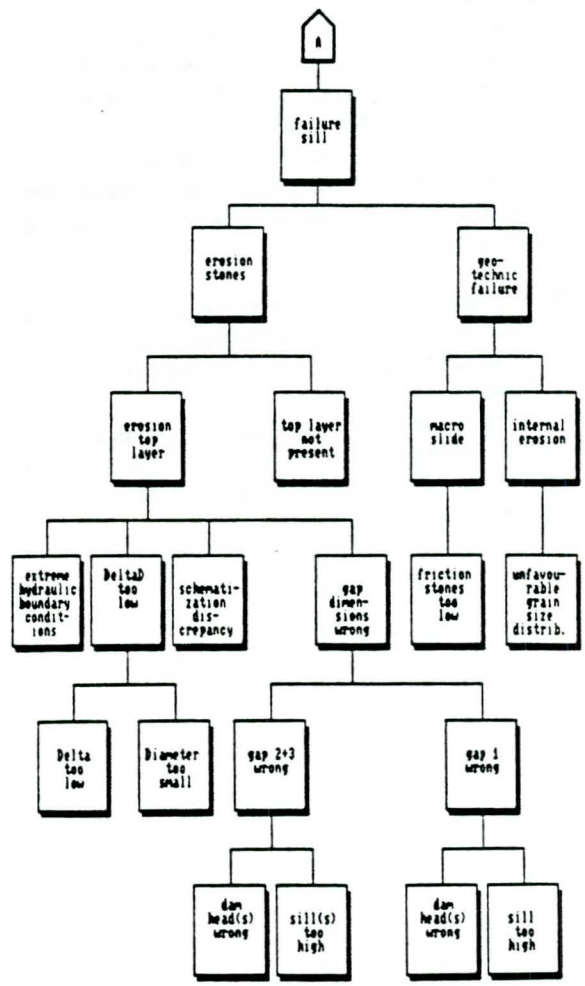

Fig 7 Fault tree bottom protection

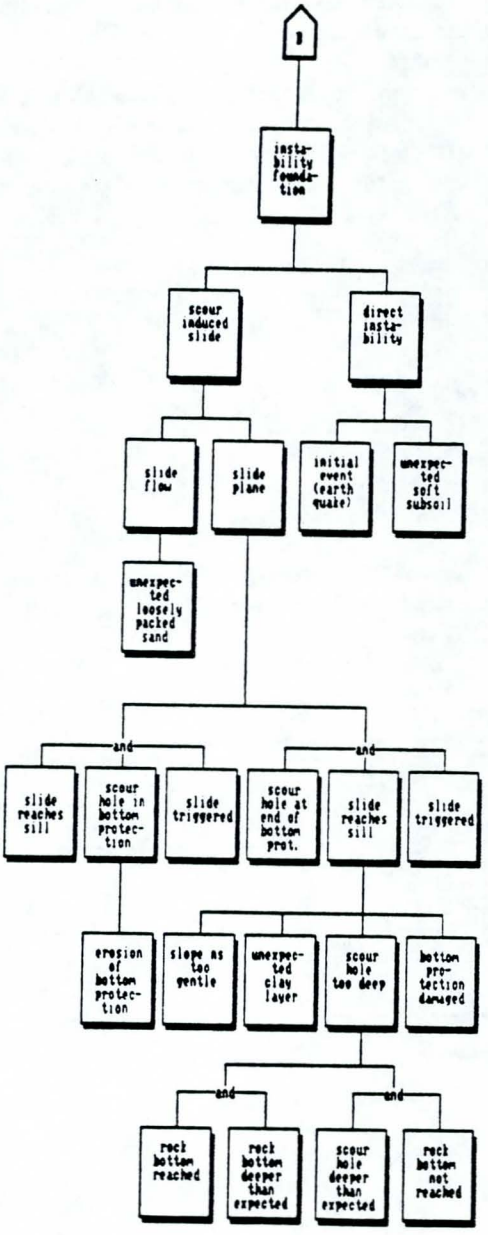

4 FAILURE MECHANISMS AND RELIABILITY FUNCTIONS

4.1 Hydraulic conditions

Both the stability of the sill and the scour at the end of the bottom protection depend on the hydraulic conditions in the gaps. As a first approximation, a basin storage model is used to calculate the conditions during the closure stages.

The system is schematized as a reservoir, surrounded by a dike with three closure gaps. An important load parameter for the sill and the bottom protection is the flow rate Q through the closure gap. The flow rate depends on the geometry of the gaps and the water level in the reservoir and at sea. The water level in the reservoir depends on the flow rate through the gaps and the area of the reservoir. The flow rate Q is calculated using the following relations:

$$Q = B \cdot m \cdot h \cdot \sqrt{(2 \cdot g \cdot (H-h))} \quad [m^3/s] \quad \text{(subcritical flow)} \tag{2}$$

$$Q = B \cdot m \cdot 1.7 \cdot H^{1.5} \quad [m^3/s] \quad \text{(critical flow)} \tag{3}$$

With:

B	=	width of the gap		[m]
m	=	discharge parameter = 0.7 - 1.1	[-]	
g	=	acceleration of gravity = 9.81	[m/s^2]	
H	=	upstream water level above sill	[m]	
h	=	downstream water level above sill		[m]

For the discharge parameter a value of 0.9 is adopted. In Figure 8 hydraulic conditions are presented when the gap is nearly closed: width of the gap is 100 m, sill level is MSL-6 m and spring tide conditions.

Fig. 8a Hydraulic conditions in closure gap: water levels

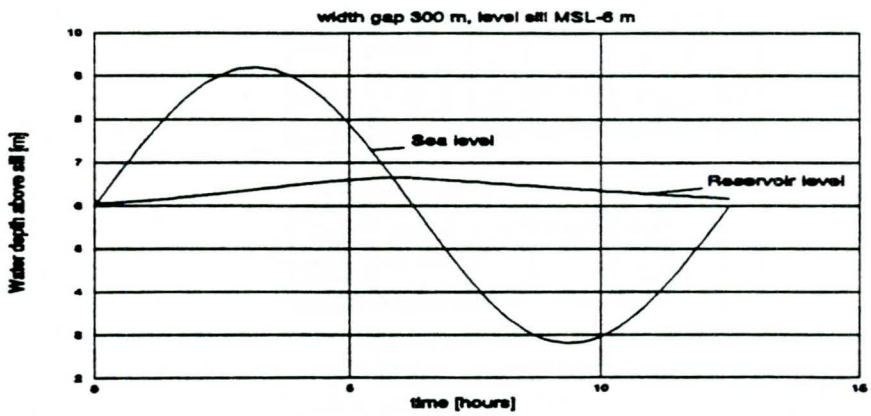

4.2 Stability of the sill

The stability of stones against wave or flow attack is characterized by the factor ΔD_n: the product of the relative density of the stones under water and the nominal diameter of the stones D_n.

The flow attack on the stones in the sill depends primarily on the difference between the

Figure 8b Hydraulic conditions closure gap: flow parameters

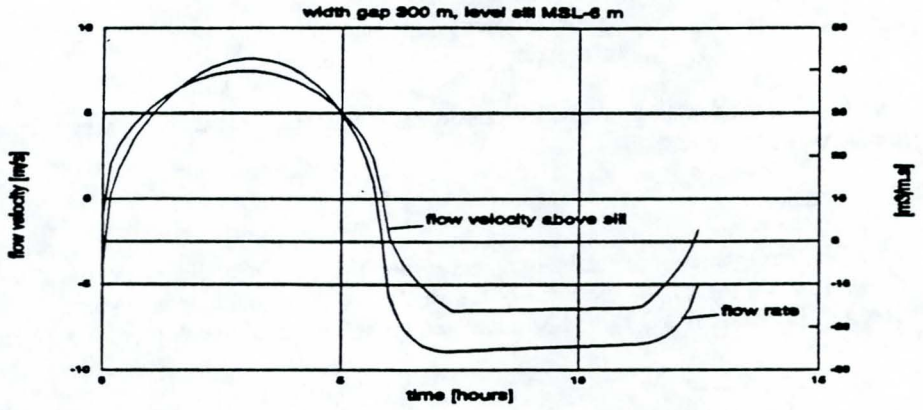

upstream and downstream water levels. Using the criterion established by Delft Hydraulics, the stability of the stones of the sill can be checked. The boundary between stable and not stable is described as:

$$\frac{H}{\Delta D_n} = a + b\frac{h}{\Delta D_n} + c\left(\frac{h}{\Delta D_n}\right)^2 + d\left(\frac{h}{\Delta D_n}\right)^3 + e\left(\frac{h}{\Delta D_n}\right)^4 \qquad (4)$$

With: a = 2.00061
b = 0.75595
c = 0.05705
d = -0.00353
e = 0.00007

The area above the boundary represents an unstable situation, the area below the line represents a stable situation.

4.3 Erosion of the trunk of the closure dam by wave attack and of the tip of the dam by flow attack

Wave attack

The stability of the closure dam against wave attack is calculated using the formula of Van der Meer:

$$\frac{H_s}{\Delta D_n} = 6.2 \cdot P^{0.18} \cdot \left(\frac{S}{\sqrt{N}}\right)^{0.2} \cdot \frac{1}{\sqrt{\xi}} \qquad (5)$$

$$\xi = \frac{\tan\alpha}{\sqrt{\frac{H_s}{1.56 T_m^2}}} \qquad (6)$$

With: P = parameter for permeability depending on the design. For the permeable, homogeneous core of the closure dam, a value of 0.6 can be adopted.
S = 12 = parameter for damage, related to the cross section of the damage
N = 3000 = number of waves in storm

α = slope of dam; tanα = 0.5
H_s = significant wave height [m]
T_m = wave period [s]

The value of S adopted accounts for considerable damage. This is acceptable as repair during the construction is easy.

Flow attack

As a first impression of the stability of the stones against flow attack at the tip of the dam, the design formula (4) for the top layer of the sill (at the corresponding cross section) may be used. The calculated ΔD should be corrected for influence of the slope with a slope factor m_s:

$$m_s = \frac{1}{\sqrt{1-(\frac{\sin\alpha}{\sin\phi})^2}} = 1.35 \qquad (7)$$

With: α = slope angle of the tip of the dam; a typical value of tanα = 0.5 is used
ϕ = 40° to 45°; a value of 42.5° is chosen

4.4 Slides and the length of the bottom protection

Scour of the original bottom occurs at the ends of the bottom protection. It is caused by higher flow velocities and extra turbulence during the construction stages of the dikes and closure gaps. Scour holes threaten the stability of the foundation of the closure structures and a bottom protection has to be applied in an early stage of the closing operation and with sufficient length. When a bottom protection is present, the sill can only be damaged when L caused by a slide is larger then the length of the bottom protection L_b. The length of the bottom L which may be moved during a slide is determined by the geometry of the scour hole and the post-slide slopes. In Figure 9 a typical geometry after a slide is given, based on experience from the Delta project in the Netherlands. Because of limited information available, the post-slide geometry is schematized as a straight plane. Length L is determined by:

$$L = \alpha D \cdot (n_a - n_b) \qquad (8)$$

With: n_a = cotangent of average slope after slide [-]
n_b = cotangent of average slope before slide [-]
D = depth of scour hole [m]
α = quotient of depth of intersection of slopes before and after the slide, and the depth of the scour hole

Three criteria have to be fulfilled to cause failure:

a. A scour hole has to be present. This is certain in this case.
b. The slide has to be initiated. This happens when the upstream slope ß of the scour hole is steeper than a certain critical slope. Calculations using a indicative formula, based on DElft Hydraulics tests indicate that this is the case.
c. The slide has to reach the sill.

Because of the long construction period, it is probable that the scour hole reaches the rock zone. Calculations indicate this. The thickness D is then determined by the level of the sea bottom (h_{bottom}) and the rock zone (h_{rock}). Information about slide planes related to scour holes is limited to measurements in local sands for the Eastern Scheld Storm Surge Barrier in the Netherlands [4], [6]. The data indicate that:

- the damaged area upstream of the scour hole L ranges from about 0.5 to 2 times the thickness of soft bottom material layer D above the bedrock;

- n_s ranges from 3 to 7; for 85% of the measurements $n_s \leq 6$;
- n_b ranges from 1.7 to 6;

The following values are used for the parameters in formula 8, which agree fairly well with the measurements mentioned in [6]:

parameter	μ	σ	distribution
n_s	5	1	normal
n_b	3	1	normal
α	0.5	0	deterministic

Several events are possible that increase the probability of a slide reaching the sill:

a. The calculation represents only the mechanism of a slide plane in rather homogeneous sand, comparable to the geotechnic situation in the Zeeland (The Netherlands); the effect - for instance - of slide flows, soft clay layers or the bottom protection being damaged by a slide is in this case assumed to be neglectable. In detailed design more elaborate geotechnical studies should verify this assumption

b. After a slide the bottom protection covers the remaining soil. If the protection is damaged, bottom material may be exposed to the current. The following scouring process can take place very quickly, possibly resulting in more dangerous slide planes nearer to the sill. The probability of a second slide reaching the sill is much larger, because the distance to the sill is reduced. For example, when the length of the protection equals two average slides, the probability of the second slide reaching the sill is near to 1 if the bottom protection fails; the probability of failure then becomes about equal to the probability of failure of the bottom protection. Because of this, some aspects considering the bottom protection are:
   - it should be constructed as a "falling apron", flexible enough to follow the scour holes and strong enough to withstand the friction forces caused by the slides under the protection;
   - the protection should be anchored in the sill;
   - the maximum friction force per meter caused by slides can be approximated by $\tan\phi * L * q$ (ϕ = friction angle bottom material, q = weight of mattress in N/m2). This maximum occurs near the toe of the sill, decreasing with increasing distance from the sill.

Because of the risks that no measuring will be done after a slide, or the possibility of a damaged bottom protection after a slide, it may be advisable to reduce the probability of a slide by monitoring the scour hole and dumping extra stones along the edge before a slide can happen, preventing the upstream slope to become critical. In this way the probability of the occurrence of a slide is also reduced.

Fig 9 Slide mechanism

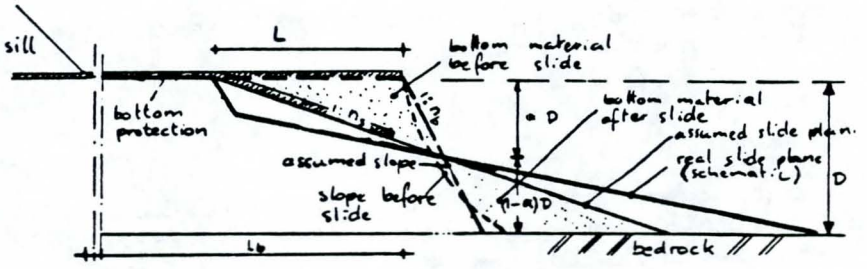

5 DETERMINISTIC DESIGN

5.1 Sill

The increase of the flow attack during construction of the sill is accounted for by gradually using larger stones. Final closure is realized by constructing closure dams on top of the sill, simultaneously from two sides. During final closure the flow attack on the top layer of the part of the sill still open increases. Therefore the largest stones are necessary at the last stage, in the centre of the gap.

A safety factor is used to determine de design ΔD_n. A typical value of 1.4 is adopted. The following ΔD_n values are calculated using formula (4):

Width remaining gap [m]	ΔD_n calculated [m]	ΔD_n design [m]
1300	1.15	1.61
550	1.97	2.76
100	2.05	2.87

5.2 Closure dam

For the wave conditions given in section 2 the minimal ΔD_n is calculated using formula (5):

H_s [m]	T_m [s]	ΔD_n [m]
3.4	8.5	1.41
3.6	9.2	1.50
3.8	10.4	1.66

The calculations indicate that for high wind velocities the wave height is relatively insensitive for the wind speed. The maximum calculated significant wave height is H_s = 3.8 m, with a P_E = $4*10^{-4}$ per summer season. This seems acceptable and safe for a construction stage. Using formula (5), the minimal ΔD_n is 1.66 m.

For a first indication of the stability of the tip of the dam against current attack during closure, formula (4) and (7) are used. The stability during spring tide is calculated. Because duration of spring tide is short and possible damage is limited to some erosion at the tip, no safety factor is needed. The following ΔD_n values are calculated:

Width remaining gap [m]	ΔD_n design [m]
1300	1.55
550	2.66
100	2.77

At the starting points of the dam, wave attack is the dominant design criterion. Nearer to the centre of the dam current attack is dominant.

5.3 Bottom protection

Using formula (8) the average length of the bottom L which is moved during a slide is 17 m. The traditional method of calculating the length of the bottom protection is illustrated in Figure 4. The design slope is 1:6. The length is calculated starting at the toe of the post-slide slope vertically under the end of the bottom protection. With a depth of the soft soil layer of 19 m, the length of the bottom protection becomes 114 m.

6 RESULTS OF PROBABILISTIC CALCULATIONS

6.1 Introduction

A central concept in probabilistic design is the reliability function Z. This function Z represents the difference between strength or resistance parameter R and load or action parameter S: Z = R-S. When the load is larger than the resistance the construction fails: Z < O. When stochastic variables are used in R and S, the probability of Z < O represents the Probability Of Failure (Pf) of a mechanism. Generally more than one variable influences the Z-function. The calculation of the Pf then can be done by integration (level III) or by approximation (level II) calculations. The approaches are dealt with extensively in literature. The calculations done for this design are based on the level II approach. Basically the procedure for a probabilistic calculation is:

1. The Z-function is formulated, using the physical relations determining the failure mechanisms (see section 4)
2. The stochastic parameters are determined; uncertainties often can be described using a "normal distribution". This distribution is characterised by a mean value μ and a standard deviation σ. The standard deviation is the value, which has a probability of exceedence P_E of 16%.
3. Several design values are taken (for instance ΔD_n = 0.9, 1.0 and 1.1). These values represent the resistance parameter R.
4. Using a computer program, Z = 0 (equivalent to R = S) is calculated for the different design values by varying the stochastic variables. Results are the Pf of the design and the contribution of each stochastic variable in the Pf.

6.2 Stability of stones in the top layer of the sill

The probability of erosion of the top layer of the sill is calculated using a Z-function based on formula (4):

$$Z = \frac{H}{\Delta D_n} - \left(a + b\frac{h}{\Delta D_n} + c\left(\frac{h}{\Delta D_n}\right)^2 + d\left(\frac{h}{\Delta D_n}\right)^3 + e\left(\frac{h}{\Delta D_n}\right)^4\right) \qquad (9)$$

The function is iteratively calculated for a given value of ΔD_n. The relevant stochastic variables are:

- Relation:
  The design formula is based on measurements, which often deviate from the ideal line given by formula (4). Uncertainties in the relationship are represented by making parameter "a" of the formula a stochastic variable. Variation of "a" results in vertical translation of the ideal line. A range of $1.2 < a < 3$ covers almost all measurements. Assuming these lines to represent the P_E = 1% (as a rough first estimate), the uncertainty in the relationship is accounted for with $\mu(a) = 2.00061$ and $\sigma(a) = 0.26$.
- Tidal amplitude:
  The tidal range is the most important boundary condition for the flow attack at the sill. The largest variations occur during spring tide. The amplitude of each individual spring tide a_i is described with $\mu(a_i) = 3.2$m and $\sigma(a_i) = 0.14$ m. More spring tide exposures of a certain construction stage result in a larger probability of an extreme amplitude. This can be accounted for by an increase in the standard deviation: $\sigma = \sqrt{(T/N_T)} * 0.14$, with T = duration of the construction stage in days and N_T = number of days between spring tide. However, between two spring tides the remaining gap width is reduced by construction activities, and the flow conditions change. If the total closure operation takes place within a few spring tides, flow conditions increase considerably each tide, and only one - the last - tide contributes significantly to the Pf of the remaining open part of the sill. Since no special equipment is used for construction and rock material is abundant, it is assumed that no significant delay will occur during closure and the σ = 0.14 is in this case acceptable. Analysis of possible causes of delays (Special Events)

could verify this assumption.

- Sill height:
  Discrepancies in the height of the sill:
  1. A variation in the hydraulic load: a higher sill causes a difference in water level between sea and reservoir which is larger than assumed, because the amount of water flowing in and out of the reservoir is reduced. This increases the difference in water level between sea and reservoir, resulting in a heavier attack than accounted for.
  2. A variation in the stability situation as defined with the relation given in section 4.2. The stability situation of a given design is represented by the position of the design point relative to the design line. For $h/(\Delta D_n) > \approx 2$ a variation in the depth of the sill causes a translation almost parallel to the line. The distance to the design line doesn't change, therefore the stability situation is not changed. For $h/(\Delta D_n) < \approx 2$ this is not the case: a sill lower than assumed causes a less stable situation and a higher sill causes a more stable situation.
  The discrepancies mentioned above give opposite effects on the stability. In the calculations they are accounted for in the water depths above the sill, using a typical uncertainty level $\sigma(h_{sill}) = 0.61$ m.
- Material:
  The material uncertainty is the diameter D and the relative density Δ of the stones. Typical values for sorted stones from an approved quarry are: $\sigma(\Delta) = 0.03$ and $\sigma(D) = 4.8\%$ of the D_n.

Calculations have been done for widths of the closure gaps each of 1300 m (completely open), 550 and 100 m.

Summary of stochastic variables:

	μ	σ
a	2.00061	0.26
a_t	3.2	0.14
h_{sill}	-6	0.61
Δ	1.53	0.03
D_n	variable	4.8%

Results of calculations[1]:

Width gap	ΔD_n	Pf	Contribution stoch. variables α					Design point X^*				
[m]	[m]		a	a_t	h_{sill}	Δ	D_n	a	a_t	h_{sill}	Δ	D_n
100	4.0	1.5E-4	0.86	0.03	0	0.02	0.10	1.14	3.30	-6.02	1.51	2.46
	3.5	1.1E-3	0.82	0.04	0	0.02	0.12	1.28	3.28	-6.02	1.51	1.89
	3.0	1.0E-2	0.78	0.05	0	0.02	0.15	1.47	3.27	-6.01	1.52	1.89
	2.5	9.1E-2	0.74	0.06	0	0.03	0.17	1.70	3.25	-6.01	1.52	1.59
550	3.5	6.4E-4	0.79	0.05	0.03	0.02	0.11	1.25	3.30	-5.67	1.52	2.18
	3.0	6.0E-3	0.75	0.07	0.03	0.02	0.14	1.45	3.29	-5.60	1.52	1.89
	2.5	6.8E-2	0.69	0.09	0.04	0.03	0.16	1.67	3.27	-5.81	1.52	1.59
1300	3.0	1.2E-5	0.7	0.05	0.16	0.01	0.08	1.08	3.34	-4.97	1.52	1.85
	2.5	1.9E-4	0.62	0.07	0.21	0.01	0.09	1.28	3.33	-5.01	1.52	1.55
	2.0	4.6E-3	0.52	0.09	0.27	0.02	0.11	1.52	3.31	-5.17	1.52	1.26
	1.75	2.4E-2	0.44	0.10	0.33	0.02	0.11	1.66	3.29	-5.31	1.52	1.11

[1]
- Pf per closure operation, assuming no delay in the production of each dam head more than a period of 1 to 1.5 weeks (see stochastic variable "relation").
- α represents the relative importance of a stochastic variable in the calculation of the probability
- X^* gives the most probable combination of values of the stochastic variables for a given probability

The deterministic ΔD_n has a P_f of about 0.02.

No separate probabilistic calculations of the dam have been done. For design criterion, see

section 7.

6.3 Length of bottom protection

The probability of a slide plane reaching the sill is calculated using a Z-function based on formula (8):

$$Z = L_b - \frac{1}{2}(h_{bottom} - h_{rock}) \cdot (n_s - n_b) \qquad (10)$$

L_b is the design value of the length of the bottom protection. The relevant stochastic variables are:

- Relation:
  The uncertainty is incorporated in the values for n_s and n_b. These are already treated in section 4.4 of this study.
- Geotechnic boundary conditions:
  From measurements the following values are calculated: $\sigma(h_{bottom}) = 1$ m and $\sigma(h_{rock}) = 2$ m.

Summary of stochastic variables:

	μ	σ
n_s	5	1
n_b	3	1
h_{bottom}	MSL-16	1
h_{rock}	MSL-35	2

Results of the calculations are:

Length	Pf	Contribution stoch. variables				Design point X*			
[m]		n_s	n_b	h_{bottom}	h_{rock}	n_s	n_b	h_{bottom}	h_{rock}
114	<1E-8	0.39	0.39	0.04	0.18	8.9	0	-14.5	-40
100	2.8E-7	0.39	0.39	0.04	0.18	8.2	0	-14.9	-39.2
80	4.2E-5	0.41	0.41	0.04	0.14	7.5	0.5	-15.2	-38.1
60	2.8E-3	0.43	0.43	0.03	0.11	6.8	1.2	-15.5	-36.9
55	7.0E-2	0.43	0.43	0.03	0.11	6.6	1.4	-15.6	-36.6
50	2.0E-2	0.44	0.44	0.02	0.10	6.4	1.6	-15.7	-36.3
40	7.0E-2	0.46	0.46	0.02	0.07	6.0	2.0	-15.8	-35.8

The lengths of 100 m and more (including the traditionally designed bottom protection of section 5, length 114 m) result in a very low probability of failure. These extremely low values are rather theoretical. In reality the other uncertainties or special events will become dominant, resulting in a higher Pf of the bottom protection.

7 PROBABILISTIC DESIGN USING DIFFERENT DESIGN CRITERIA

The acceptable probability of failure Pf is a main design parameter. Three important methods to determine this parameter are (lit. [1]): personally acceptable risk, socially acceptable risk and economic optimal risk. The personally and socially acceptable risks are related to casualties. For a construction phase, the financial risks are more relevant.

For a structure with a distinct relation between investment costs, damage costs and the Pf, the optimal Pf can be determined using the results of the probabilistic calculations. For main cost-determining structures the costs of a higher safety (i.e. lower Pf) are at a certain point not justified by the lowering of the risk. As an example, the optimal Pf is calculated in section 6.3 for the length of the bottom protection. Sometimes this exercise is difficult or time consuming to perform. In that case a top-down method can be used, with the acceptable Pf based upon experience of previous projects and calculations. Typical Pf values for final situations are small,

often 10^{-3} to 10^{-4} per year. During construction a higher Pf (equivalent to a smaller safety factor) is generally acceptable, mainly because lower costs of damage and lower risks for casualties. As an example of the top-down method, the sill and the dam are dealt with in section 7.

In a probabilistic design, taking a calculated risk is rewarded by a cheaper design. Because the costs of failure can be significant, attention should be paid to which of the parties involved is responsible for the risks and the connected benefits.

7.1 Design of the top of the sill

For this closing operation Pf = 1/50. In Figure 5 the main structure components of the closing operation were given. The relation between the Pf of each individual gap and the Pf of the total operation is:

$$\max(Pf_1, Pf_2, Pf_3) \leq Pf(\text{operation}) \leq Pf(\text{gap 1}) + Pf(\text{gap 2}) + Pf(\text{gap 3}) \qquad (11)$$

When each gap is designed with the same Pf and failure mechanisms are independent, the right hand side of formula (11) is valid. The maximal allowable Pf_1 then becomes: $Pf_1 = 1/3 * 1/50 = 0.0067$. If the mechanisms are 100% dependent Pf_1 = Pf(operation) = 1/50.

Each gap consists of 2 or 3 main components (dam, bottom protection, and sill), and each component is subjected to several failure mechanisms. All independent mechanisms contribute to the Pf of a gap. However, only the mechanisms that contribute significantly to costs should be designed in such a way that the lowest costs, i.e highest possible Pf, is obtained. Section 6 shows that the traditionally designed bottom protection has a Pf which can be ignored compared to the sill. So, only the dam and the sill contribute significantly to the Pf. Because the two mechanisms are independent the Pf of the sill and the dam should be each $0.0034 \leq Pf \leq 0.01$.

As a starting point the Pf of the two main failure mechanisms of the sill (geotechnical failure and erosion of the stones) are chosen to be equal. The element "top layer not present" is a special event and is not incorporated in the probabilistic calculation. This makes the acceptable Pf for erosion of the top layer $0.0017 \leq Pf \leq 0.005$. Combining this with the results of section 6.2, the design value of the ΔD_n of the stones of the top layer of the sill are:

Width remaining gap	ΔD_n
1300 m	about 2 m
550 m	3.0 to 3.25 m
100 m	3.25 to 3.5 m

Comparison of the deterministic and probabilistic calculations shows the latter to result in a 20% higher ΔD_n. Important causes for this difference are:

- the influence of the uncertainty in the relation is high. Neglecting this results in a 20% lower ΔD_n;
- the average spring tide is used in the deterministic calculations. Instead, the highest average tide within a certain period should be used. For example the tidal range with a P_E once a year results in an ΔD_n about 40% higher.

Possibilities for optimization still exist. For example, the ΔD_n for a remaining gap width of 100 and 550 is high, and could be lower when the closing is planned outside a spring tide window. Then also production delays may cause failure of the closure operation, making it essential to consider the elements causing delays in the production.

7.2 Design of closure dam

As stated above the Pf of the dam should be $0.0034 \leq Pf \leq 0.01$. From wind statistics and wave calculations can be concluded that the corresponding wave heights are H_s = 3.6 to 3.7 m in the summer season and H_s = 3.8 m for a total year. The ΔD_n of the stones needed for construction in the summer season is 1.50 to 1.56 m. This is slightly lower than the ΔD_n = 1.66 m in the deterministic design.

As stated in section 3.3, current attack at the head tip is not able to cause breaching and is therefore not considered here.

7.3 Optimum economic length of bottom protection

A rational method to determine the optimal Pf is to find the economic optimum design. This is done for the length L of the bottom protection.

The optimal length is the length with the lowest total costs of the bottom protection. The costs consist of:

- the investments I: construction of the bottom protection (costs increase with larger lengths) and optional measures to prevent slides (a fixed sum)
- the risk R, defined as Pf * repair costs. The repair costs after a breach can be assumed fixed sum. The Pf decreases with increasing length of the protection, causing the risk to decrease also, along with the Pf.

The sum of the investments and risks I + R has a minimum for a certain Pf which represents the optimal length. Two scenarios are analyzed:

I without preventive measures to avoid a slide;

II with preventive measures to avoid slides. The effect of these measures are (arbitrarily) assumed to lower the probability of a slide from 1 to 0.2.

Costs are in this particular case assumed to be:

- measures to prevent slides: 550,000 US$
- investment in the bottom protection: 50,000 US$ per extra meter length;
- repair costs of a complete breach (assumed 200 m wide): 30 million US$.

Summary of formulas used to calculate optimum length:

Scenario I: $I = 50{,}000 * Lb$
$R = 30{,}000{,}000 * Pf$

Scenario II: $I = 50{,}000 * Lb + 550{,}000$
$R = 30{,}000{,}000 * Pf$
$Pf(II) = Pf(I) * 0.2$
Pf(I): see section 6.3

The results are presented hereafter and Figure 10 (costs in 10^6 US$, Pf per closure operation).

	Scenario I				Scenario II			
L	Pf	I	R	I+R	Pf	I	R	I+R
114	<1E-8	5.70	0	5.70	<1E-8	6.25	0	6.25
100	2.8E-7	5.00	0	5.00	5.6E-8	5.55	0	5.55
80	4.2E-5	4.00	0	4.00	8.4E-6	4.55	0	4.55
60	2.8E-3	3.00	0.1	3.10	5.6E-4	3.55	0.02	3.57
55	7.0E-3	2.75	0.2	2.95	1.4E-3	3.30	0.04	3.34
50	2.0E-2	2.50	0.6	3.10	4.0E-3	3.05	0.10	3.15
40	7.0E-2	2.00	2.1	4.10	1.4E-2	2.55	0.4	2.95
35	1.3E-1	1.75	3.9	5.65	2.6E-2	2.30	0.8	3.10

Fig. 10 Optimal length of bottom protection

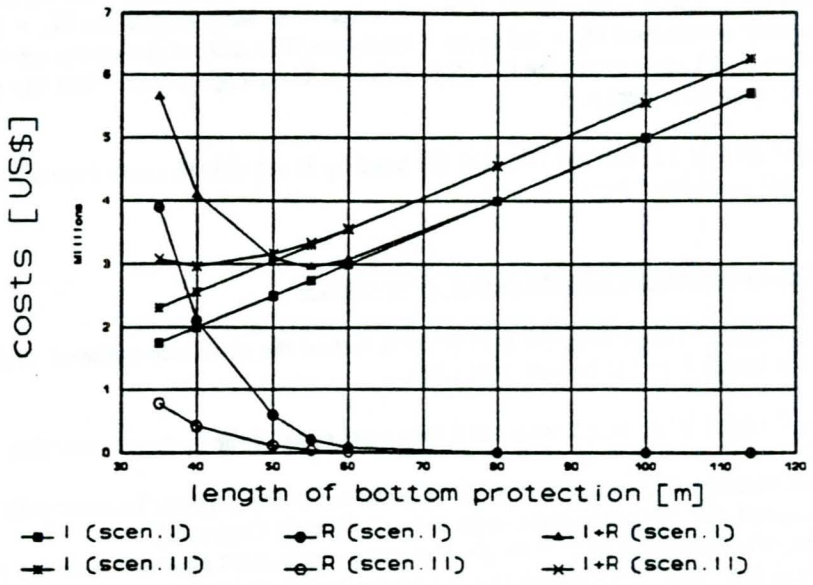

For scenario I a length of 55 m is optimal, corresponding with a Pf of about 0.007. This Pf is somewhat higher than deduced for the sill, but the order of magnitude is comparable. To minimize the influence on the Pf of the top event, a length of about 80 m or more should be chosen.

For scenario II a length of 40 m is optimal, corresponding with a Pf = 0.014. The sum of investment and risk I+R and the investment for scenario II is somewhat lower. Therefore in this particular case it is recommended to take preventive measures to avoid slides. The advantages are lower investment costs and a more predictable behaviour of the structure (see section 4.4).

It is important to realise that the suggested optimization scenarios in reality are not always viable: for instance monitoring of the bottom protection could be very difficult, making scenario I unacceptable, or preventive measures could be unreliable, making scenario II unacceptable.

In this case study analyses have been given as an example and are partially based on assumed data. Therefore the results can differ from reality. Generally, for a design analyzes should be based on actual project data. Consequences of construction procedures, effects of all special events and all mechanisms should be analyzed.

LITERATURE

[1] Probabilistic design of flood defences, report 141, TAW / Cur, the Netherlands 1990.
[2] Closure of tidal basins, Delft University Press, Delft - the Netherlands 1984.
[3] Coastal defences, editor W. Pilarczyk, A.A Balkema, Rotterdam 1990.
[4] Design report Eastern Scheld Storm Surge Barrier, volume 2, Ministry of transport and Public Works (in Dutch)
[5] Design report Closure of the Krammer, Rijkswaterstaat, 1986 (in Dutch)
[6] Eastern Scheld Storm Surge Barrier, nota 22RABO-N-81023 app. B

DESIGN, REPAIR AND REHABILITATION OF SCOUR PROTECTION DOWNSTREAM FROM INLAND NAVIGATION DAM STILLING BASINS

J.E. Hite, Jr.
US Army Engineer Waterways Experiment Station,
3909 Halls Ferry Road, Vicksburg, USA

ABSTRACT

Scour of the streambed downstream from inland navigation dams has occurred at numerous projects within the Corps Of Engineers (CE) jurisdiction. A research work unit was initiated in 1984 to develop better guidance for repair and rehabilitation of scoured areas downstream from navigation dam stilling basins. Previous methods used for scour protection at existing projects were identified. Riprap protection was used at nearly every project. Guidance for designing riprap protection for new projects had been developed based on physical model tests performed for site specific Corps projects built in the 1970's and 1980's. A research model was constructed in 1985 to evaluate and improve the existing riprap design guidance. Physical model tests were performed for different stilling basin designs and riprap placement. This paper discusses the current method used by the Corps of Engineers to design riprap protection downstream from navigation dam stilling basins and methods to repair or rehabilitate existing scoured areas.

1. INTRODUCTION

1.1 Background

The Corps of Engineers began building navigation dams in the early 1900's and continues to do so today. They have built or operated 185 such projects. These dams have normal heads from a few feet to 100 ft and often provide flood control, hydropower, and recreation benefits as well as navigation benefits. A navigation dam provides the water depth needed for towboats with barges to navigate the river. The navigation project usually consists of the dam, a spillway (gated and/or ungated) to control the flow, a stilling basin downstream from the spillway, a navigation lock, and sometimes hydropower capability. The stilling basin dissipates the energy of the spillway flow to minimize the scour downstream from the structure.

1.2 Scour Problem

Over years of operation, numerous projects have experienced scour downstream from the dam. The extent and severity varies from one project to the next. Many of these dams were built before 1950 and will be required to operate for many future years. Extensive scour can undermine and possibly threaten the integrity of the project. The scour damage at some projects must be repaired or rehabilitated to continue operation.

Site specific model studies have been conducted on many projects to determine a practical and economical method for repairing the scoured areas. The cost of repairing these scoured areas often runs in the millions of dollars. Realizing general design guidance needed to develop scour protection methods for stabilizing the scoured areas was limited, the Corps of Engineers undertook a research effort to gather design information. This

study was performed by the Hydraulics Laboratory of the US Army Engineer Waterways Experiment Station. The study focused on navigation projects since the problem was prevalent at many of these projects and the cost of these repairs was often more than the original project cost.

2. RIPRAP DESIGN FOR NEW NAVIGATION DAMS

Project operation schedules are an essential consideration in stilling basin and riprap design. The stilling basins for projects constructed 30 years ago or more, were designed based on an equal distribution of flow through the spillway gates. Experience has shown that this type of operation is not always possible. Often times the gated spillway is used to pass ice or debris required to keep the navigation channel open. Navigation accidents have also caused situations where equal gate operations were not possible. Other circumstances that have caused unusual operating conditions are malfunction of the gate hoisting mechanism and even vandalism. Many projects have been severely damaged as a result of these types of operating conditions.

2.1 Criteria From EM 1110-2-1605

Guidance for the design of navigation dam stilling basins found in EM 1110-2-1605 (Office, Chief of Engineers 1987) states that unusual or emergency operation must be considered. New project stilling basin and downstream riprap design must consider the following conditions

a. Uniform discharge through all the spillway gates for a range of headwaters and tailwaters expected during project life.

b. Single gate fully opened with normal headwater and minimum tailwater. This is considered gate misoperation and would only occur for an emergency condition. Minor damage to the downstream scour protection is acceptable as long as the integrity of the structure is not jeopardized. Single gate fully opened with above normal pool (perhaps the 50- to 100-year pool) should be considered. This condition could occur as a result of a navigation accident.

c. Single gate open sufficiently wide to pass floating ice or drift at normal headwater and minimum tailwater. During preliminary design, a gate half opened can be used

to approximate this ice- or drift-passing condition. No damage is acceptable for this condition. Final design usually requires model studies to determine the proper gate opening.

The three conditions above are used to optimize stilling basin length and downstream riprap protection thickness ,size, and length.

2.2 Design Procedure from EM 1110-2-1605

Existing riprap design guidance downstream from navigation dam stilling basins suggests the use of a form of the Ishbash equation for determining the stone size. The stone size determined from this equation is

$$V = C\left[2g\left(\frac{\gamma_s - \gamma_w}{\gamma_w}\right)\right]^{0.5} D_{50}(\text{min})^{0.5} \qquad (1)$$

where

V = Velocity in ft/sec

C = Coefficient

γ_s = Specific weight of stone in lb/ft^3

γ_w = Specific weight of water in lb/ft^3

D_{50} = Stone diameter, ft, of which 50% is finer by wt.

g = Acceleration due to gravity in ft/sec^2

Past practice for design has been to use $C = 0.86$ for turbulent areas downstream from stilling basins. A review of stone sizes developed from recent model studies of navigation dam stilling basins designed for single gate operations with minimum tailwater suggested that C should be 1.12. Also, 80 percent of the velocity over the riprap could be used for V in Eq. (1) for determining downstream riprap size for basins designed according to the criteria in EM 1110-2-1605. Guidance for gradations, thickness, length, and placement is also given in EM 1110-2-1605.

2.3 Additional Design Guidance

Hite (1988a) used a laboratory model to investigate riprap stability downstream from a navigation dam stilling basin designed according to criteria presented in EM 1110-2-1605 for a gated

navigation dam. Research model test results indicated that the depth of flow over the end sill and the average velocity over the end sill were important parameters for analyzing riprap stability downstream from navigation dam stilling basins. Neill (1967) in his work with coarse uniform bed material gives

$$\frac{d_s}{D} = \text{function of} \left[F, \left(\frac{\gamma_w}{\gamma_s - \gamma_w} \right)^{0.5} \right] \quad (2)$$

where

d_s = particle size of which a certain percent is finer by weight

D = flow depth

γ_w = specific weight of water

γ_s = specific weight of stone

F = Froude number = $V/(gD)^{0.5}$

Many researchers, Grace et al. (1973), Maynord (1988), and Reese (1984) have used forms of Eq. (2) to evaluate riprap stability. According to Maynord (1988) determining which velocity to use is an important step in developing a riprap sizing method based on velocity. Mean velocity is the easiest to calculate using both numerical and physical modeling techniques. To analyze the laboratory results, Eq. 2 was modified to give

$$\frac{d_{50}}{D'} = C \left[F_{es} \left(\frac{\gamma_w}{\gamma_s - \gamma_w} \right)^{0.5} \right]^b \quad (3)$$

where

d_{50} = stone size of which 50 percent is finer by weight

D' = depth of flow over the end sill

F_{es} = Froude number over the end sill = $V_{es}/(gD')^{0.5}$

V_{es} = Velocity over end sill

C and b = Coefficients determined from experimental tests

A characteristic stone size of d_{50} was used in this relationship

because a literature search revealed this value was known for several previous model tests and results could be compared.

The following equation was developed from the research results for a horizontal riprap blanket sized according to EM 1110-2-1605 for a stilling basin designed for normal pool, a single fully open gate, and minimum tailwater.

$$\frac{d_{50}}{D'} = 0.15 \left[\left(\frac{\gamma_w}{\gamma_s - \gamma_w} \right)^{0.5} F_{es} \right]^{1.5} \qquad (4)$$

To compare the research results from the model tests with Eq. (1), the average velocity of flow over an end sill was determined for flow depths of 10, 20, and 30 ft and Froude numbers over the end sill of 0.2, 0.4, 0.6, 0.8, and 1.0. The stable riprap size was then determined using Eq. (1) with C = 0.86 for the Ishbash criteria, Eq. (1) with C = 1.12 and 0.8 V for EM 11102-1605 criteria for stilling basins designed for single gate operations with minimum tailwater, and Eq. (4). Fig. 1 shows a comparison of the stable stone sizes determined from these three methods. The Ishbash equation with C = 0.86 is conservative for stilling basins designed according to EM 1110-2-1605. Eq. (4) and Eq. (1) with C = 1.12 are in close agreement for velocities up to 16 ft/sec which is a practical upper limit for velocities exiting a stilling basin. Test results used to develop Eq. (4) verified the guidance in EM 1110-2-1605 for riprap design downstream from navigation dam stilling basins.

3. REPAIR AND REHABILITATION DESIGN GUIDANCE

Many of these navigation dams including both uncontrolled fixed-crest and gated types have significant scour downstream from them. In most cases, the scour has resulted from operating conditions and/or flow conditions changing from the original project design and from inadequate energy dissipation in the stilling basin.

3.1 Uncontrolled Fixed-Crest Navigation Dams

Most of the Corps' uncontrolled fixed-crest dams were designed and constructed more than four decades ago and will be required to operate for several more years. Observations of flow conditions at these types of structures revealed that the worst attack on the streambed occurs when the flow transitions from one regime to another. The two regimes of interest were designated plunging flow and riding flow. These two types of flows are illustrated in Fig. 2. Plunging flow occurs when the trajectory of the flow jet issued from the upper pool travels in a downward direction usually adhering to the face of the spillway. Plunging flow is not dominated by the tailwater and is generally considered to be free uncontrolled flow. Riding flow occurs when high tailwater causes the flow jet to remain near the water surface. Riding flow is generally considered to be submerged uncontrolled flow.

During the transition from plunging to riding flow and back to plunging, the high velocity jet attacks the streambed below the dam and can cause scour. The maximum scour caused by the transitional flow is not always known. It is analogous to scour around a bridge pier during a design flow event. Scour measurements obtained after the event probably do not reflect the degree of scour that was present during the peak of the flow event.

3.1.1 Repair and Rehabilitation Guidance

Length and flow parameters mentioned in the following discussion are shown in Fig. 3. To develop a repair design, the maximum discharge where plunging flow occurs must be determined. The design ratio h/H which involves the tailwater referenced to the crest, h, and the head on the crest, H is used to determine this

discharge. Hite (1988b) modeled several uncontrolled fixed-crest navigation dams and found a h/H value of 0.7 to be a good indicator of the maximum plunging discharge and developed the following procedure to assist in developing a repair design.

1) Using the project discharge and tailwater rating curves, determine the discharge that gives an h/H value of 0.7

2) Divide this value by the weir length to determine the unit discharge

3) Determine the theoretical hydraulic flow parameters d_1, v_1, F_1, and d_2 for the project, Fig. 4. The Froude number of flow entering the spillway apron is computed according to

$$F_1 = \frac{v_1}{\sqrt{gd_1}} \tag{5}$$

The momentum equation is used to determine the ratio between the depths before and after the hydraulic jump according to

$$\frac{d_2}{d_1} = \frac{1}{2}\left(\sqrt{1 + 8F_1^2} - 1\right) \tag{6}$$

4) Knowing d_1 and d_2, the parameters d_1/L and TW/d_2, where L is the length of the spillway apron and TW is the depth of tailwater above the spillway apron for the discharge determined in step 1, can be determined for the project

5) Enter plot shown in Fig. 5 with d_1/L and TW/d_2 to determine scour potential caused by hydraulic flow conditions for this project

Fig. 5 was developed based on a very limited amount of model and prototype data but the general approach is a logical one. The logic considers that a large value of d_1/L is not desirable and will probably result in high scour potential. Values of d_1/L less than 0.1 are desirable and the lower the ratio the better. The lower this ratio is, the more length of apron is available for flow streamlines to straighten and become parallel with the spillway apron. The logic also considers values of TW/d_2 less than 1.0 are not desirable for a spillway apron with no baffle blocks or end sill to aid in energy dissipation. The higher value of TW/d_2 for a

constant d_1/L the less scour potential exists. The dividing zones among the areas of scour potential are certainly not exact and much research would be required to better define the dividing lines.

A survey of the existing conditions below the project is also needed to determine the extent of the scour protection required. Large scour holes generally indicate inadequate energy dissipation is occurring in the existing stilling basin. Scour holes progressively enlarging indicate flow conditions that have high or moderate scour potential occur frequently, and the streambed is an erosive material. This structure will need a structural modification. If the soundings indicate slight scour and hydraulic flow conditions capable of causing moderate or excessive scour are experienced frequently, the streambed is probably an erosion resistant material. However, most streambeds will scour if adequate energy dissipation is not achieved.

Structures that have ratios of TW/d_2 greater than 1.0 and ratios of d_1/L less than 0.1 can probably be repaired using large riprap, derrick stone, or grout-filled fabric bags for scour protection. These materials armor the upstream slope of the existing scour hole. Those with low TW/d_2 ratios and high d_1/L ratios will probably need structural modifications such as a secondary stilling basin, end sill, spillway extension, or a combination of these.

3.2 Gated Navigation Dams

Investigations by Hite (1988a) of gated navigation dams revealed that scour downstream from the stilling basin is usually caused from one or more of the following conditions;

a. Exposure to excessive hydraulic flow conditions involving velocity, pressure, and turbulence

b. Leaching and/or piping of the underlying natural bed material through the scour protection material

c. Undercutting and raveling of the scour protection material due to scour at the end of the protection

The following discussion concerns scour caused by hydraulic flow

conditions. Adverse hydraulic flow conditions generally occur at gated low-head navigation dams due to improper gate operation and/or inadequate energy dissipation. Improper gate operation can be caused by any one or more of the following: operator error, equipment malfunction, vandalism, navigation accidents, or operating the structure beyond its normal operating range to pass ice or debris. The stilling basin and scour protection for projects built before 1970 were usually designed based on equal gate operations. All gates were utilized to pass increasing discharges and adjacent gate setting were no more than 1 or 2 ft different. This provided desirable hydraulic flow conditions in the stilling basin and scour caused by these operations was minimal.

3.2.1 Scour Caused from Gate Operations

Experience gained from years of operation has shown many occasions when the gates can not be raised and lowered symmetrically. Often in colder regions of the country, ice must be passed through the spillway and stilling basin to maintain the navigation channel, as well as, reduce adverse structural loads on the dam. Ice that forms in the river during periods of low flow must be passed with low tailwater. When the gates have to be raised to pass ice, much more discharge is released through the spillway and stilling basin due to the low tailwater. Many times, the tailwater is insufficient to maintain a hydraulic jump in the stilling basin. The jump will occur in the downstream channel causing high velocity, turbulent flow which attacks the channel bottom and causes scour. This same operation is often required to pass debris, and can also result in severe scour. These increased discharges through the spillway gates can also occur from operator error, gate malfunction, vandalism, and navigation accidents. A navigation accident in this sense refers to tows or barges that become impinged against the spillway gates and normal operation of the spillway gates is altered.

3.2.2 Scour Caused from Inadequate Energy Dissipation

Inadequate energy dissipation in the stilling basin can result from improper basin design and/or existing project conditions

differing from those anticipated when the stilling basin was designed. Stilling basins that are too short or not set low enough for a jump to form in them are examples of improper basin design. A scoured streambed resulting in lower tailwaters and changing hydrologic conditions are examples of changing project conditions.

3.2.3 Guidance for Repair and Rehabilitation of Gated Dams

The repair or rehabilitation of existing stilling basins and scour protection depend on the flow conditions (discharge, pool elevation, gate setting, and tailwater elevation) for which the protection must remain stable. The condition and composition of the exit channel downstream from the stilling basin are also factors. A definition sketch for theoretical hydraulic flow parameters for a gated navigation dam stilling basin is shown in Fig. 6. Hite (1988a) developed the following steps to assist Corps Of Engineers personnel designing scour protection for gated navigation dams.

1) Determine the design flow condition
   a. Normal or above normal pool
   b. Gate operation ie, one gate fully open, one gate partially opened, or all gates operated equally
   c. Normal or minimum tailwater elevation

2) Determine the unit discharge exiting the stilling basin. If single gate criteria is adopted, use the unit discharge through the gate bay in operation for the unit discharge through the stilling basin.

3) Compute d_1, v_1, F_1, and d_2 as in step 3) of section 3.1.1. Eq. (6) is used to determine the ratio between the depths before and after the hydraulic jump. This form of the momentum equation ignores the forces on baffle blocks in the analysis. Basco (1970) provides a comprehensive treatment of these forces.

4) Determine the tailwater depth, TW, over the stilling basin floor for the scour protection design condition.

5) Compare the tailwater depth, TW, with the value for d_2 computed in step 3 and compute the ratio TW/d_2.

6) Use Table 1 as a guide in selecting the scour protection.

3.2.3.1 Stilling Basin Rehabilitation

The stilling basin will probably need rehabilitation if sufficient tailwater is not present for the flow condition for which the scour protection is designed. This could be the case for basins with TW/d_2 less than 1.0. Severe scour downstream from a stilling basin with this flow condition indicates that structural modifications are usually necessary. These structural modifications could consist of installing a secondary stilling basin immediately downstream from the existing one or possibly constructing a tailwater dam to increase the depth of water over the basin. Construction of a tailwater dam is usually not feasible for a navigation project unless the tailwater dam contains a navigation lock.

Secondary stilling basins can be constructed in a number of ways. The most effective, and costly, is to dewater and construct a newly designed basin. A design procedure very similar to the one used for construction of a new basin according to guidance in EM 1110-2-1605 has been model tested by Hite (1989) for Morgantown Dam and was effective in improving energy dissipation.

Secondary stilling basins can also be constructed using other methods. A basin constructed of riprap and tremie concrete may be a viable alternative. Utilizing abandoned barges and sinking them below the existing basin has been discussed for some projects. The barges could then be filled with concrete or riprap and tremie concrete. Another method could be driving sheet piling downstream from the existing basin at an appropriate location and back filling from the sheet piling to the existing basin with concrete or riprap and tremie concrete. Since baffle blocks and end sills can not always be used in basins of this type, an additional length for the secondary basin should be considered. The apron elevation should be low enough to allow a depth of flow equal to d_2. Very large grout-filled fabric bags could possibly be used if they can be anchored to the streambed and reinforced within themselves and to one another. Some form of scour protection is needed downstream

from the secondary stilling basins and graded riprap is usually adequate.

3.2.3.2 Graded Riprap for Scour Repair

Computations may indicate the existing stilling basin is acceptable for the design flow conditions for scour protection. Severe scour below a basin of this type usually means the original scour protection was inadequate. The protection may have failed due to leaching of the subgrade material causing the scour protection (usually riprap) to sink and/or raveling at the termination of the protection causing the riprap to move downstream. Guidance for sizing riprap below new gated navigation dam stilling basins is suitable for this type repair work.

3.2.3.3 Alternatives to Riprap for Repair

If riprap can not be used to repair an existing scoured area due to the extreme size or cost of transport, alternative scour protection is necessary. Scour protection consisting of materials such as grout-filled fabric bags, concrete cubes, dolos, tetrapods, quadrapods, and tremie concrete have been considered for use at various projects. Dolos, tetrapods, and quadrapods are generally designed as armor units in a coastal environment and use in turbulent flow downstream of an energy dissipator would require additional research to determine design criteria. Generally, the thickness of the underlying layers needed with these units along with the size of the units themselves, preclude their use in the shallow depths typically found downstream from a navigation dam stilling basin. If an inland navigation dam requires scour protection material so large that riprap is not feasible, serious consideration should be given to stilling basin rehabilitation or replacement.

Previous physical model tests, Hite (1982) and Murphy and Hite (1988), of two site-specific projects have indicated grout-filled fabric bags 20 ft long by 6.75 ft wide by 2.75 ft thick could be used instead of 4- to 5-ft diameter riprap. The alignment of the bags was found to affect their stability with certain flow conditions. Previous model tests have also shown that 4- ft

concrete cubes provided the same degree of protection as 4- to 5-ft diameter stones. An example of concrete cubes model tested for scour protection at Dam No. 26 on the Mississippi River is shown in Fig. 7. The precast concrete cubes were more stable when placed in an orderly and controlled manner rather than random placement. If large precast units are used as scour protection material in a highly turbulent area, the top layer of filter material underneath the units has to be larger than the voids in the precast units to prevent piping. The orderly and controlled placement of the units minimizes the voids.

4. SUMMARY

4.1 Non Structural Alternatives

Many methods of protecting the area downstream from navigation dam stilling basins have been discussed. Non structural alternatives include those designs which do not require dewatering or structural changes to the stilling basin. The most universal scour protection material is riprap and the majority of the time it is the most economical. Markussen and Wilhelms (1987) give examples of riprap repair work modeled for projects on the Upper Mississippi River. Guidance for repair work using riprap was discussed in sections 2.2, 2.3, 3.1, and 3.2. In cases when riprap can not be used, an alternative such as large grout-filled bags may be economically feasible. The grout-filled bags were used to repair an area downstream from Emsworth Dam on the Ohio River. The advantage of the bags is they provide a large mass resistant to the forces of the flowing water. If the bags should crack, they no longer provide the large mass. Good foundations and efforts to reinforce the bags within themselves and to each other will reduce cracking tendencies.

The use of concrete cubes has been considered for cases where riprap could not be used. The cubes perform better when placed in a neat and orderly manner such as shown in Fig. 7. Random dumping of the cubes such as shown may cause large voids which increases the potential for piping and movement of the cubes to occur. In cases where extra stability is needed, the cubes could be cabled or

tied together to form a large mass. Concrete spheres have been considered due to reduced drag forces, but existing scoured areas generally have a downward slope and the spheres tend to roll downstream unless they are keyed in carefully.

The use of scour protection materials such as gabions, articulated concrete mattress, and other materials typically used for streambank protection were not considered suitable for use in a highly turbulent area downstream from a stilling basin. The use of materials such as tetrapods, quadrapods, and dolos as scour protection downstream from stilling basins has also been considered. However, their use in a turbulent area downstream from a stilling basin has not been thoroughly investigated in the United States.

4.2 Structural Alternatives

Structural alternatives are those which require structural changes to the dam to improve the energy dissipation of the stilling basin. This might include modifying the original structure or installing a secondary stilling basin. Modifications to the existing basin could be lengthening to provide additional energy dissipation or adding an end sill. An end sill was installed by the New Orleans District under water at the Old River Control Structure after the 1973 flood. This was done to repair damage sustained during the flood and to improve performance of the stilling basin. The end sill also helped alleviate a problem encountered by debris causing abrasive damage upstream from the end sill. The basin was inspected in the dry in August 1987, 15 years after the end sill was installed, and the end sill was still in good condition. The structural alternatives were discussed in sections **3.1.1 and 3.2.3.1.**

5. CONCLUSIONS

Repair of scour damage or rehabilitation of the stilling basin for existing navigation dams is often a large scale engineering effort that requires considerable planning, design, construction, and expenditures. The site-specific nature of the problem does not permit detailed guidance for all projects. This paper summarized general guidance for the selection of preliminary designs for scour protection methods and materials. Sections 2, 3 and 4 provide information for use in the design of scour protection downstream from inland navigation dams. Physical model studies have proven to be quite effective in developing a suitable scour protection design, especially when severe flow conditions are anticipated.

6. ACKNOWLEDGEMENT

The tests described and the resulting data presented herein, unless otherwise noted, were obtained from research sponsored by the Headquarters, U.S. Army Corps of Engineers (USACE). The tests were conducted by the U.S. Army Engineer Waterways Experiment Station. Permission was granted by the Chief of Engineers to publish this information.

7. REFERENCES

Basco, D. R. 1970 (May). "An Experimental Study of Drag Force and Other Performance Criteria of Baffle Blocks in Hydraulic Jumps," Miscellaneous Paper H-70-4, US Army Engineer Waterways Experiment Station, Vicksburg, MS.

Grace, J. L., Jr., Calhoun, C. C., Jr., and Brown, D. N. (1973). "Drainage and Erosion Control Facilities, Field Performance Investigation," Miscellaneous Paper No. H-73-6, US Army Engineer Waterways Station, Vicksburg, MS.

Hite, J. E., Jr. 1982 (January). "Model Tests of Scour Protection for Emsworth Locks and Dams," Summary Report 20 January 1982, US Army Engineer Waterways Experiment Station, Vicksburg, MS.

Hite J. E., Jr. 1988a, "Scour Protection Downstream from Gated Low-Head Navigation Dams," REMR Technical Note No. HY-N-1.6, US Army Engineer Waterways Experiment Station, Vicksburg, MS.

Hite, J. E., Jr. 1988b, "Scour Protection Downstream from Uncontrolled Fixed-Crest Dams," REMR Technical Note No. HY-N-1.5, US Army Engineer Waterways Experiment Station, Vicksburg, MS.

Hite, J. E., Jr. (1989). "Scour Protection for Morgantown Dam, Monongahela River, West Virginia," Miscellaneous Paper HL-89-4, US Army Engineer Waterways Experiment Station, Vicksburg, MS.

Markussen, J. V. and Wilhelms, S. C. (1987). "Scour Protection for Locks and Dams 2-10, Mississippi River," Technical Report No. HL-87-4, US Army Engineer Waterways Experiment Station, Vicksburg, MS.

Maynord, S. T. 1988. "Stable Riprap Size for Open Channel Flows," Technical Report No. HL-88-4, US Army Engineer Waterways Experiment Station, Vicksburg, MS.

Murphy, T. E., Jr., and Hite, J. E., Jr. (1988). "Scour Protection for Dam No. 7, Monongahela River, Pennsylvania," Miscellaneous Paper HL-88-3, US Army Engineer Waterways Experiment Station, Vicksburg, MS.

Neill, C. R. (1967). "Mean-Velocity Criterion for Scour of Coarse Uniform Bed-Material. International Association on Hydraulic Research, 12th Congress, Paper C6, 3, C6.1-C6.9.

Office, Chief of Engineers, US Army. 1987 (May). "Hydraulic Design of Navigation Dams," EM 1110-2-1605, US Government Printing Office, Washington, DC.

Reese, A. (1984). "Riprap Sizing - Four Methods," Proceedings of the ASCE Hydraulics Speciality Conf., Cour d'Alene, ID, 397-401.

Table 1. Scour Protection for Gated Navigation Dams

TW/d_2 at design flow	Existing Scour	Scour Protection Needed
<0.85	Severe	Rehabilitate existing stilling basin and repair or replace existing scour protection (suggest model study)
<0.85	Questionable	Determine the extent of scour and repair accordingly. If severe scour, suggest above procedure, if not, see below
<0.85	Minimal	Determine if or how many times the design flow condition for scour protection has occurred. If the flow condition has occurred yearly, scour protection is probably not needed. If the flow condition has never occurred and the streambed is not scour resistant, some form of scour protection is necessary.
0.85-1.0	Severe	Check basin design and possibility of leaching. Check original filter design. If basin is OK, use riprap for scour protecion. If basin is not adequate, consider basin rehabilitation, and repair or replacement of scour protection. Provide good filter.
0.85-1.0	Questionable	Determine extent of scour and provide protection accordingly .
0.85-1.0	Minimal	Determine if flow condition for design of scour protection has occurred. If it has occurred regularly, no additional scour protection is necessary. If it has not occurred, use a scour protection material.
>1.0		Follow guidelines for TW/d_2 ratios for 0.85-1.0.

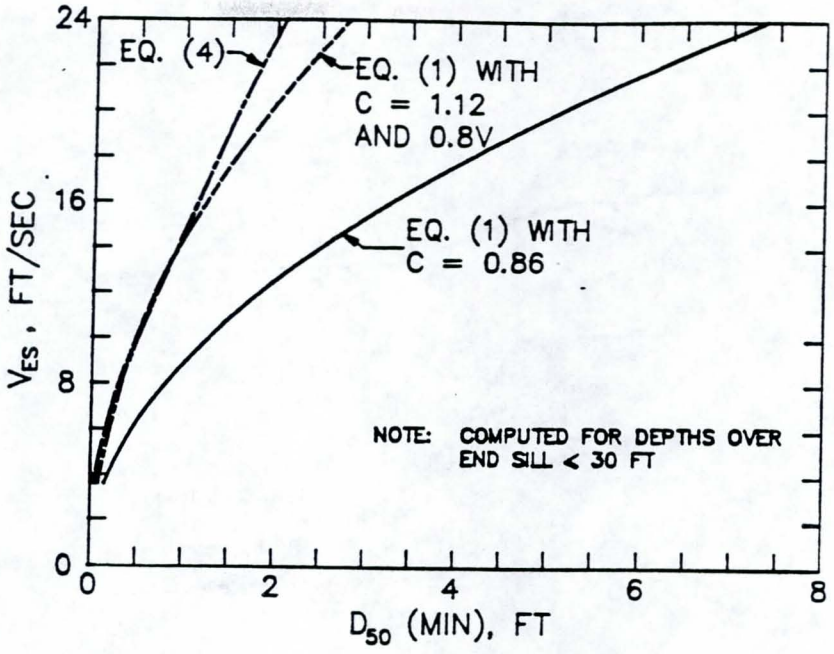

Fig. 1. Comparison of Stable Stone Sizes

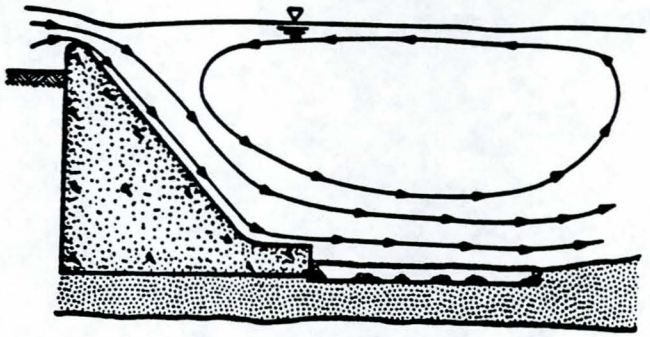

a. PLUNGING FLOW

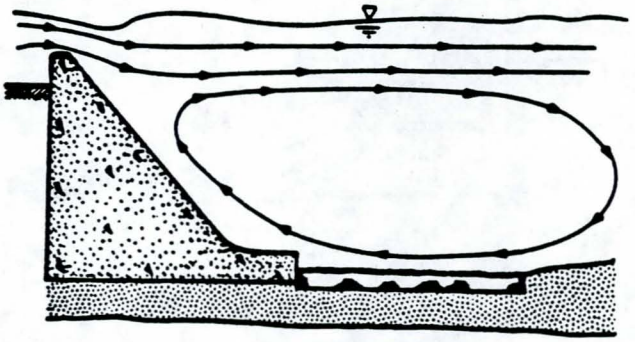

b. RIDING FLOW

Fig. 2. Transition Flow Regimes

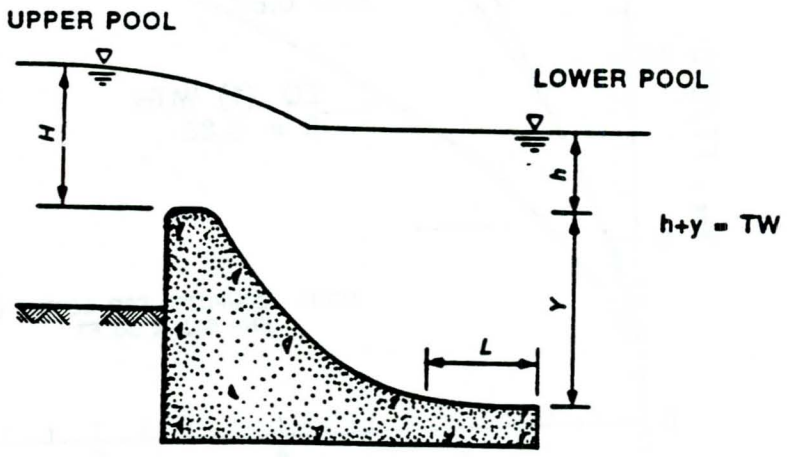

Fig. 3. Length and Flow Parameters, Uncontrolled Fixed-Crest Dam

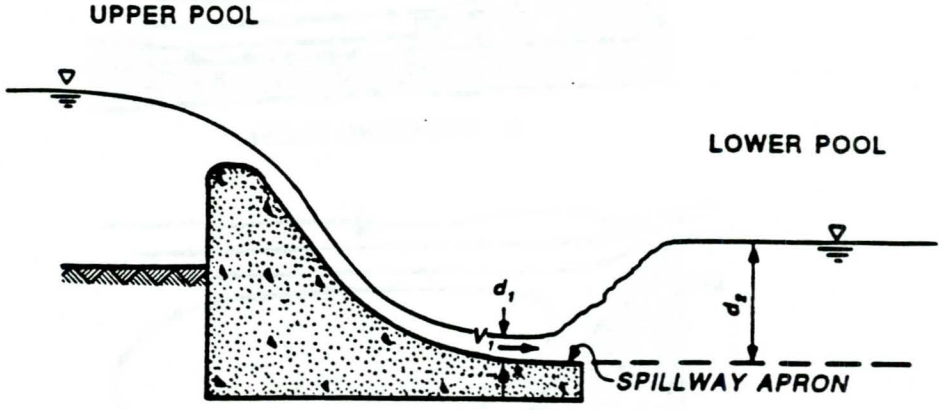

Fig. 4. Theoretical Flow Parameters, Uncontrolled Fixed-Crest Dam

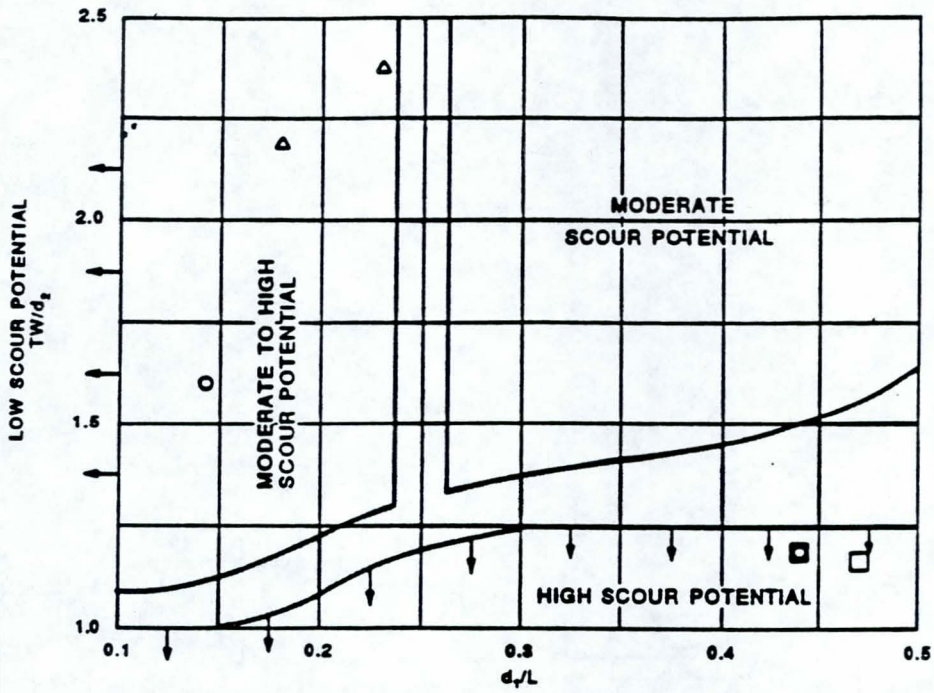

Fig. 5. Scour Potential for Uncontrolled Fixed-Crest Dam

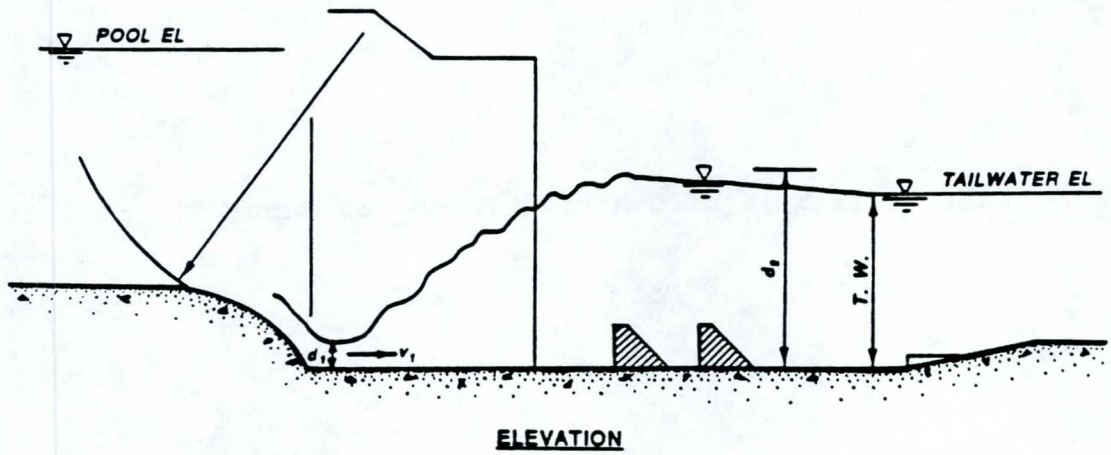

Fig. 6. Theoretical Flow Parameters, Gated Navigation Dam

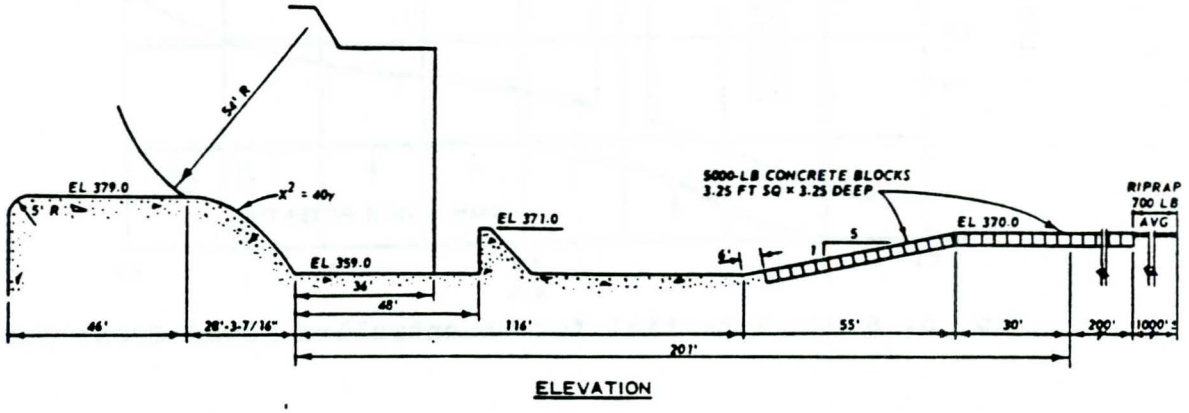

Fig. 7. Example of Concrete Cubes for Scour Protection

CONSTRUCTION ASPECTS OF ROCK STRUCTURES

J. van 't Hoff
Dredging and Hydraulic Engineering Consultancy
M. Lindo
Van Oord ACZ Dredging and Marine Constractors
W.H. Tutuarima
Boskalis Zinkcon BV

1 INTRODUCTION

In this paper a brief review is given of commonly used equipment for placing stone in rockfill structures, followed by a summary on position accuracies and tolerances. The paper concludes with a few examples of construction methods of some typical hydraulic structures including the consequences of these methods for the design of the structure.

2 REVIEW OF TYPES OF EQUIPMENT AND THEIR APPLICATIONS

2.1 General

When considering equipment used for construction of rock structures [1], distinction can be made between landbased operations and sea borne operations. Landbased operations may also include the placing of stone below the waterline. An important factor in selecting equipment, whether landbased or water based, is the distinction between *direct dumping* of bulk material such as in the core of a breakwater and *controlled placement* of stone as in primary and secundary layers of revetments. According to these distinctions a summary of common equipment is given in table 1.

	direct dumping	controlled (individual) placement
land based	dumptrucks often combined with bulldozers, loaders and cranes	cranes
water based	split barges; bottom door barges.	side stone dumping vessel; flat deck barge with bulldozer; crane pontoon; fall pipe vessel.

table 1 Typical types of equipment and applications.

2.2 Landbased equipment: direct dumping of bulk material

Placement of rockfill is carried out by direct dumping of bulk material with trucks or loaders, or by crane.

Dumptrucks
Placement is most simply done by direct dumping from trucks carrying 20 to 50 tonnes, often assisted by a bulldozer. Dumptrucks require haul tracks at least 4 m wide. In case of a single lane "passing places" have to be provided at least 7 m wide.
When used on public roads a maximum wheel load has to be observed.

Loaders
Loaders may be used when the stone can be obtained from a stockpile directly adjacent to the work site. For instance in case of small breakwaters or for the construction of embankments. Compared to trucks, stone can be placed further away from the crest in a more controlled manner. The use of loaders for placing stone in bulk is limited to gradings upto 60 kg (e.g. core material and secondary layers).

Cranes
Stone can also be placed by cranes, with material supplied by dump trucks. In case of placing bulk material these cranes are provided with skips or rock trays. They are filled by a loading shovel at the quarry or stockpile and carried by trucks to the construction site, or trays loaded directly at the construction site. In these cases heavy cranes are required and much space is needed.

The production of cranes is determined by the lifting capacity of the crane and the rotation and lifting speed.
For dumping core material with skips, trays or wire nets, large skip cranes are required.

2.3 Landbased equipment: controlled placement

Controlled placement is carried out using cranes.

Cranes
Controlled placement is defined here as the placement of individual larger stones or stones in relatively small quantities per cycle, for which backhoes can be used. For this purpose cranes are provided with a simple hook for the individual handling of armor provided with eyebolts or can be equipped with a clamshell or orange peel grab to dig into the stock of core material dumped by trucks.
The smaller cranes require a work platform of at least 5 m wide (no passing possible).

Also here the production capacity of the cranes depends on the volume of the grab and on the rotation and lifting speed.
For conventional dragline cranes 20 cycles per hour is a good average. For hydraulic cranes an increase to about 30 to 40 cycles per hour can be realized.

Typical examples and some characteristics of landbased equipment is given in figure 1.

type		capacity [m^3]	weight [ton]	width [m]
(off high way) dumptruck	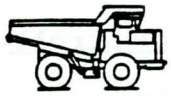	20 - 80	empty: 30 - 110 loaded: 60 - 270	wheel base: 3.7 - 5.7
articulated dumptruck		12 - 27	empty: 20 - 40 loaded: 40 - 90	wheel base: 5.7 - 6.8
wheel loader		2.5 - 9	15 - 86	bucket width: 2.7 - 4.7
track loader		2.5 - 3	25	bucket width: 2.7
backhoe crane		0.5 - 15	15 - 200	track gauge: 2 - 5
front shovel		2 - 15	40 - 200	track gauge: 2 - 5
bulldozer		blade width: 2.5-5 m	10 - 80	track gauge: 2 - 3

figure 1 Summary of typical landbased equipment.

2.4 Waterborne equipment: direct dumping of bulk material

Split barges, bottom door barges, (tilting barges)
These types of barges are usually employed for dumping of large quantities of bulk material in shallow water (approx. two times the maximum draught of the barge). This material is used in core constructions of breakwaters, sills or closure dams etc., where initially less accuracy in the levels is required.
After the opening in the bottom of the barge exceeds a certain limit, the stone is dumped in a short time as one big mass. Dumping usually takes less than one minute. The mass of the stone stays together in a "cloud", resulting in a fall velocity exceeding the equilibrium fall velocity of each individual stone. As a result the cloud of stones and water

will reach the bottom with a velocity two to three times the equilibrium velocity of an individual falling stone. The impact of this kind of dump is very heavy and may result in damage when covering pipelines or cables, in particular in freespan sections.
After hitting the bottom the material usually shifts sideways, leaving a minor quantity at the desired spot. Therefore this dumping is not utilized in jobs requiring accurate placement of stone, such as for the protection of pipelines in deeper water.
Tilting barges are less preferable because of uncontrolled lateral movement when discharging.
Common available self-unloading types have load capacities in the order of 500 to 800 tonnes.

2.5 Controlled placement with waterborne equipment

Side stone dumping vessel or barge
With these barges large quantities of stone can be dumped in a controlled manner. The stone is gradually pushed overboard in a sideways direction using sliding shovels placed on the loading deck. Alternatively a chain transport system or a vibrating floor system are used. Depending on constructional requirements, the stone can either be placed in particular prescribed layer weight (bottom protection works) or in relatively narrow ridges with prescribed thickness (pipeline covers etc.).
In the first case the vessel will slowly be moved in a lateral direction at a controlled speed allowing placing in rather thin layers (0.5 m). In the second case the vessel is kept in a stationary position or slowly moved forward, or in a lateral direction, depending on required dimensions and the local water depth. For that purpose these vessels are usually equipped with shottels for lateral control or even with a dynamic positioning system. This is related to the velocity of the shovels.
Essential for this type of discharging is that the stones are dumped slowly. Each stone may be considered to fall individually. For a side stone dumping vessel of 1000 tonnes the actual dumping time is approximately 15 minutes.
The deck of the barge is usually divided in a number of sections which can be unloaded separately. It enables the placing of different types of rock per section which may be required when a bottom layer of smaller stones has to be covered with bigger stones during the same operation to ensure stability of the layer against high currents.
The loading capacity of these type of vessels roughly varies from 500 tonnes to 1500 tonnes for the larger vessels.

Because of mutual interaction between the stones and the waves and currents, the stone will spread in directions parallel and perpendicular to the barge. Following contact with the seabed, the stones will spread further along the seabed, depending on bottom slope and characteristics of the stones and the seabottom. The extent of this spreading depends very much on the method of dumping, see figure 2.

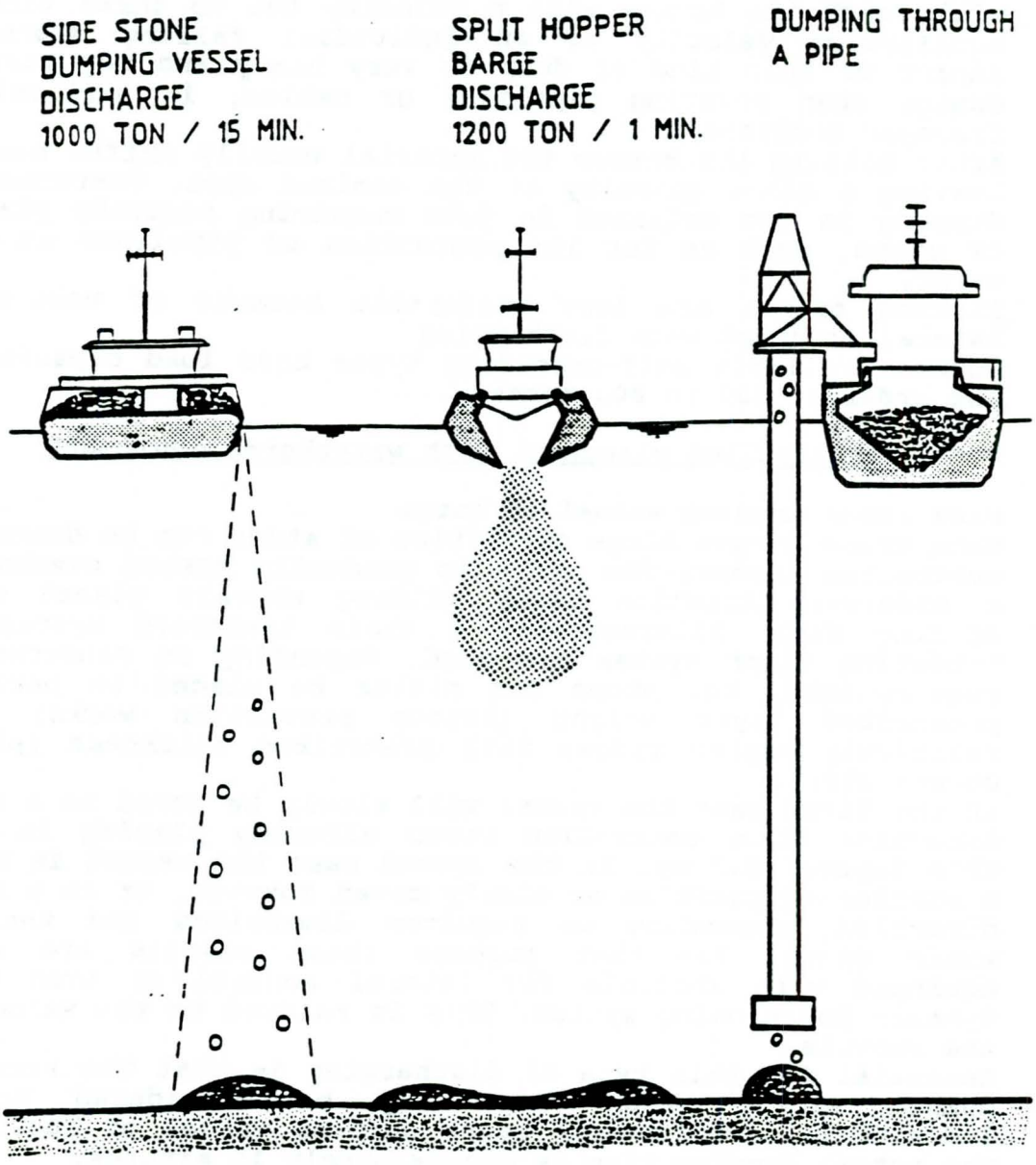

figure 2 Placement of stone for different types of floating equipment.

Fall pipe vessel

This type of dumping system is employed to achieve greater accuracy in deeper water. The system guides the rock to a level of only some meters above the seabed and is therefore especially suitable for accurate dumping in deeper water (over 50 m).

The system consists of a vessel from which a (flexible) pipe can be lowered down to some meters above the sea bed. The end of the pipe can be positioned using either an independent working propulsion unit, or a free moving Remote Operating Vehicle (R.O.V.), both fitted out with equipment capable of making pre- and post-dump surveys. The dumping material aboard

is transported by means conveyor belts from the hoppers into the fall pipe or steel wire tube. An example for the use of this type of equipment is the covering of pipelines with stones at great water depths. The vessel moves along the pipeline with a constant speed while the stone is placed on top of the pipe.

Reverse operating hopper dredge
Placing of gravel sized gradings can be done using modern trailing suction hopper dredgers. Such hoppers are equipped with systems to pump the mixture back through the suction pipe, with the draghead suspended only a few meters above the seabed. Following the dumping, the layers can also be levelled by lowering the draghead to the proper level and dozing-off the high spots.

Flat deck barges with bulldozers
Also with these type of barges relatively large quantities of stone can be placed with a high degree of accuracy. Again these barges may be equipped with shottels for lateral movement or with a dynamic positioning system. Compared to the other described type of barges the flat deck barges have the advantage of less specialized equipment involved (apart from a possibly employed dynamic position system). For that reason it can be used in circumstances where specialized equipment is less readily available. Also here different sizes of stone may be placed during the same dumping operation. Another advantage is the possibly much higher capacity of these barges, typically reaching 5000 tonnes.

Pontoon with a derrick or crane
With this type of equipment small quantities of stone are placed each cycle, or, larger stones are placed individually. An example of stone placement in controlled quantities is the bottom protection for bridge abutments where the use of dumping barges has a lesser preference because of limitations in manoeuvrability. Another example is trimming of side slopes of breakwaters or embankments as an alternative to operation with landbased equipment (figure 3).

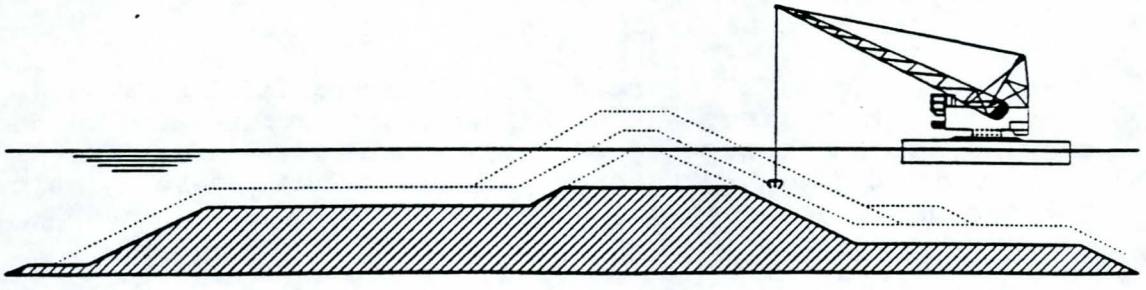

figure 3 Shaping of core material.

Also the building up of a stone dam through the water level in horizontal layers may be carried out with a floating crane. Cranes are also used when accurate placement of individual stones is required. In that case rock is placed piece by piece like the building of a proper two layer construction in a breakwater. The availability of accurate position systems akllow for accurate manoeuvring of the grabs.
Usually the crane operates from its own pontoon and remains stationary on the site on an anchorage system and stone supply is taken care of by separate barges. However, rock supply and placement may also be combined aboard the same vessel.

3 WORKING CONDITIONS

3.1 Working conditions for landbased operations

With direct dumping natural slopes will be achieved of 1:1 to 1:2, which is rather steep. This applies especially to dumping with dumptrucks and loaders. Also a rather irregular finishing of the outer slope will result. Therefore direct dumping is usually carried out only in cases like core constructions of breakwaters or stone bunds enclosing sandfill area's. These may be trimmed at a later stage or covered with other layers. The trimming can best be done by hydraulic (backhoe) cranes provided the slope is not too long and the stone weight is not too large (less than 2 tonnes). When the trimming is carried out in combination with direct placement by trucks, sufficient space has to be provided to allow for passing of these trucks aside the hydraulic crane in operation.

For direct dumping outside the natural slopes, cranes with a long reach will have to be used.

Direct dumping of wide gradings generally involves the problem of segregation. There will be a tendency of larger stones to roll down and smaller fractions to stay on top. Consequently a poor filter will be obtained. This segregation is a lesser problem when large volumes of stone are required i.e. the core of a breakwater, stone quays supporting a seawall structure etc.

More accurate direct placement is obtained using cranes with rock trays or skips by which stone is directly placed at the required location. Even better results are achieved with cranes using clamshells or orange peel grabs.

Placing of stones by crane is often controlled by using a grid system. With modern CAD techniques the cross-section design drawing can automatically be transformed into co-ordinates for the crane driver, presented on a screen, where particular volumes of stones must be dumped.

A landbased method is normally more economic than marine placing, particularly if material is hauled directly from the quarry to the construction site and for working on the seaward side of a breakwater where workability is more limited.

3.2 Working conditions for waterborne operations

For operations the following site conditions will have to be observed:

- current, wave and wind conditions
- available water depth and manoeuvring space
- vertical currency velocity profile
- seasonal influences
- shipping
- tidal variation
- visibility

Current, waves and wind conditions
Dumping is preferably carried out around slack tide. Positioning is achieved either by a roundabout anchoring system (usually 6 anchors), or a combination of 2 anchors and 2 sideways oriented thruster propulsion units, or a dynamic positioning system using a computerized thruster propulsion. Despite an obvious preference for dumping at minimum if not zero current velocity, operations sometimes cannot avoid dumping under current conditions. These (tidal) currents should not exceed maximum values of 1.5 to 2.0 m/s. This maximum obviously depends very much on the dimensions of the vessel or barge, on the anchorage possibilities and on the installed capacity of the propulsion system.

Down time caused by waves and wind is mainly due to their influence on the positioning accuracy of the stone dumping vessel and thus on the accuracy of stone placement, rather then on operational limitations of the equipment.
Locally generated short waves (period 3 to 6 sec.) have less impact on the vessel or barge and thus on the stone dumping process than swell conditions having longer periods. Generally wind waves should not exceed 1 to 1.5 m corresponding with wind force 6 on the Beaufort scale, whereas swell conditions beyond 0.5 m can already impose restrictions on the dumping.

Waterdepth
For building up structures to a relatively shallow depth the maximum elevation of the construction for dumped material is governed by two criteria:

- The maximum draught of barges or pontoons, plus a safety clearance for heave (vertical motion). The highest practical level is about 3.0 m below water level. However bottom door barges, which require a greater clearance, will need the level to be lowered. Hence this draught restriction applies to shallow bottom protections, aprons for closure works, embankments etc.

- For "winter constructions", the need to limit the loss of material to acceptable values where reshaping within the contours of the final core is clearly acceptable.

Also the available manoeuvering space and presence of structures may restrict the use of floating equipment.

Vertical current velocity profile
Displacement of individual stones under water depends on the velocity of the current, waterdepth, stone size and stone shape.

Seasonal influences
Construction may not be allowed during the winter season or during the monsoon period with high river discharges and severe wave conditions.

Shipping
Special care must be given to safe passage of other shipping. in busy water ways hindrance to shipping usually is not permitted at all.

Tidal variation
Tidal conditions may vary from moderate tidal ranges of say 1.0 to 1.5 m occurring along most of the oceanic coasts upto considerable ranges from 5 to 10 m as in the English Channel with current velocities upto 3 to 4 m/s, or even higher, causing down time of waterborne operations. Good use can be made of high and low water during the construction of embankments.

Visibility
Although modern radar and position systems usually enable stone placement to proceed at reduced visibility, operations in confined areas and close to structures will be very risky during fog occurrence.

An alternative to placement using dumping methods is placement close above the bed using a clamshell or orange peel grab, especially when small quantities of stone are required.

4 TOLERANCES

4.1 Tolerances for landbased operations

The acceptable tolerance of stone placement is first of all set by the functional requirements of the structure and can therefore be either more or less strict. These requirements relate to:

- stability of the structure (currents, waves)
- smoothness of the surface (e.g. foundations for caisson structures)
- guaranteed navigation depth
- visual aspects

The construction method must be selected accordingly. For instance because of optical reasons rather strict accuracies of placement of the outer layer of a waterfront structure may be wanted whereas the accuracy applied to the primary layer of a breakwater structure exposed to oceanic swells, will be

mainly dictaded by functional requirements.

The tolerances which can be achieved depend on the type of equipment and on the stone size. With respect to the latter, distinction is made between broken stone (gravel), usually a filter underneath coarser stone gradations or a support layer for closed block revetments, and stone gradations from say 10 to 60 kg upward.

When using standard type of equipment, the following tolerances apply in practise:

gravel
- above water: upto ± 0.05 m
- below water: ± 0.10 to 0.15 m

stone 10 to 60 kg and beyond
- above and below water: 0.25 to 0.5 times D_{50} with a minimum of ± 0.20 m for the smaller gradations

In which:

$$D_{50} = \sqrt[3]{\frac{W_{50}}{F_s \rho_s g}}$$

D_{50} = median sieve size diameter (m)
W_{50} = median weight (kN)
ρ_s = density of solids (kg)
F_s = shape factor: 0.6

In slope protections the cross-sectional tolerance is generally defined as the variation perpendicular to the designed slopes of the different layers.

Stricter tolerances than indicated here can only be achieved with gravel or carefully selected stone for landbased operations with manual assistance. Tolerances of 0.05 to 0.10 m can be achieved with special placement of rock stone (pitching). This is applied when large accuracies are required for aesthetic reasons. However in a technical sense this type of "finishing" is less recommendable.

4.2 Tolerances for waterborne operations

As mentioned already for landbased equipment, the placing tolerance should be related to the functional requirements of the structure and the working method should be selected accordingly. The more strict the requirements, the more sophisticated the working method shall be.
Particularly under water also the measuring techniques play an important role in defining the acceptable tolerance.
Contrary to constructions above water, visual aspects are not relevant. However, it is important that a bed protection is stabilized with the required weight of stone with a sufficiently smooth finishing where individual stones do not

protrude the design level in case of navigation requirements. To achieve sufficient weight, tolerances related to the layer thickness must be observed because they eliminate the possible accumulation of opposite deviations from the design profile, thus preventing unacceptable thin layers. Also with respect to filter requirements a minimum layer thickness must be ensured.

Using the right type of equipment, generaly the same vertical tolerances as mentioned for landbased operations should be achievable.

The accuracy of placement in a horizontal direction (see 5) depends on:
- type of equipment (manoeuvring characteristics, presence of dynamic position system etc.)
- accuracy of positioning system
- external conditions such as waves and currents

Generally in sheltered water (no currents and waves) a horizontal accuracy of ± 1 m can be achieved. In exposed conditions this accuracy will be less.
In order to reduce possible occurrence of open spaces the flow of material leaving the vessel should be as continuous as possible. Dumping of adjacent sections should either be overlapping or, when possible, be carried out in layers in a "brick stone" fashion.

5 ACCURACY OF POSITIONING AND OF POSITION SYSTEMS

5.1 Accuracy of equipment positioning

The accuracy of stone placing operations not only depends on the accuracy of a position system but also on the ability of bringing the equipment in the desired position. For land based operations it is usually no problem to bring equipment in the desired position, however, for water born equipment this depends very much on external site conditions and on the possibilities of the equipment itself.
Maintaining a position of a vessel can either be the manoeuvering of the equipment in the right position and maintaining this position or, for discharging while sailing, keeping the vessel on its right course.

For the various types of equipment a summary of the positioning accuracy is given in table 2 as a function of wave height. These parameters depend furthermore on the weather, the currents, experience of the crew etc. Consequently they cannot be regarded as generally applicable. It should further be stated that the mentioned positioning accuracies apply to the relevant equipment and not to the discharged stone.
The determination of position and the surveying of this position in the field are idealized in this table. Hence, inaccuracies in the determination of the position have to be superimposed on these values.

equipment	position accuracy for H_s < 1.0 m [m]	position accuracy for H_{smax} [m]	wave height H_{smax} [m]
vessel + dp*	2 - 5	5 - 10	1 - 1.5
vessel + bow thruster	5 - 10	10 - 20	1 - 1.5
vessel or barge, self propelled	10 - 20	20 - 30	0.5 - 1
barge on wires	1	1	0.5
barge on spud	0.5	0.5	0.3
barge with tug	± 20	± 30	0.5 - 1
pontoon on wires	1	1	0.5

H_{smax}: maximum allowable wave height [m]
H_s: significant wave height [m]
vessel: side stone dumping vessel, hopper dredger, fall pipe vessel
barge/pontoon split barge , tilting barge, flat top barge
* dynamic positioning system

table 2 Indicative positioning accuracy for discharge equipment (no currents).

5.2 Accuracy of position systems

In table 3 a review is given of commonly used position systems and accuracies. The medium and long range systems are generally used for water borne operations. The micro wave systems and range bearing systems can both be used for land based and water borne equipment.

5.3 Accuracies of depth measurements

The operating frequency of the transducer is variable and varies between 20 and 250 kHz. For water depth upto 200 m usually a frequency is chosen between 20 to 80 kHz while for shallow water a frequency is selected of 100 to 250 kHz. High frequencies allow less penetration of the beam (sound pulse) into the sea bed, hence (soft) silt layers will not be penetrated and will be included in the measurement. Low frequencies will penetrate through soft silt layers and will measure the depth upto the hard (sub)-layer. Therefore the selection of the frequency is strongly related to the purpose of the depth sounding.
The sound pulse is transmitted with a specific beam width. Within this width of the beam the most shallow section of the sea bed will be recorded. Therefore when measuring slopes or a strongly undulating sea bed, the level is most accurately measured with a narrow beam width. The beam width is strongly related to the size of the transducer and the selected frequency: a narrow beam width is obtained when increasing the frequency.
Generally for all types of echosounders an accuracy of ± 0.10 m can be obtained. However when measuring slopes this accuracy will be less with increasing water depth due to the increasing

influence of the beam width.
In addition to the accuracy of the echosounder the accuracy of the reference level (chart datum + tidal measurement) should be added. For modern depth survey systems the influence of wave action and swell is minimized by an electronic heave compensator.

system	reach	accuracy	remarks
medium and long range systems			
Global Positioning System (GPS)	worldwide	long range: 5 - 6 m short range: < 1 m	accuracies apply to differential GPS
Omega	international		US Navy system
Loran C	international	± 100 m	US Navy system
Decca	international	± 100 m ± 30 - 150 m	US Navy system accuracy dependant on location
Pulse 8	± 400 km		
Hyper-fix	± 300 km	± 30 m	
Syledis	100 km		
		± 2 - 5 m	partly North Sea
		± 5 m	North Sea/ Wadden Sea
micro wave systems			
Trisponder	± 80 km	± 1 m	
Motorola miniranger	± 35 km	± 3 m	
Microfix	± 60 km	± 1 - 2 m	
range bearing systems			
Artemis	± 30 km	0.5 m/km	
Polarfix	± 5 km	0.5 m/km	
visual systems			
Sextant	max. 1 km	5 m	
flagpole + distancemeter	max. 1 km	5 m	
Transit	max. 1 km	5 m	
markers			
Laser + distancemeter	3 - 5 km	< 0.5 m	

table 3 Position systems and accuracies.

The influence of the beam width on the accuracy when measuring slopes is illustrated with figure 4.
For a slope of 1:2 and a beam width of 15 degrees, the difference between the actual depth and the measured depth

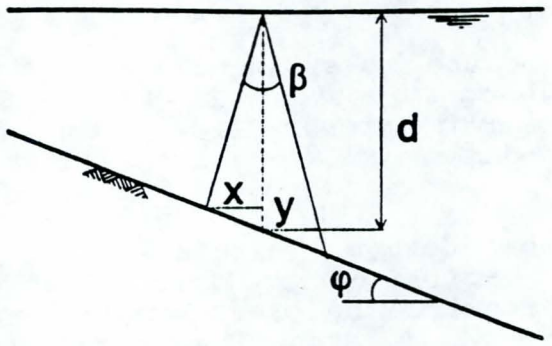

figure 4 Influence of beam width on slope measurement.

amounts to 0.6 m at a depth of 5 m. For measuring of structures of limited width, such as trenches and (stone) berms (e.g. cover layers on pipe lines off shore) use is often made of scanning profilers as an alternative to the echosounder. The scanning profiler is equipped with a rotating transducer which emits sound pulses perpendicular to the vessel's course. The scanning head may rotate through an arc of upto 180°. The measured profile is displayed either on a video monitor or printed out on a recorder for subsequent analysis. The frequency of the printout may vary between 0.5 to 2 minutes.
The advantage of the scanning profiler compared to the echosounder is that profiles are measured continuously in a cross-sectional direction when sailing parallel to the structure, whereas with the echosounder the structure has to be crossed for measuring each seperate profile. With the scanning profiler the process of stone placement, e.g. on a pipeline through a fall pipe system, may be continuously monitored from the bridge of the dumping vessel and adjusted if needed.

5.4 Diver inspection

The echo sounding survey may not be sufficiently accurate for inspection of the dumping results. Within the aims of Quality Assurance, the control of the stone placing process should direct the results within the formulated quality requirements. However, if the analysis of the discharge process give rise to additional investigation it may be decided to carry out a diver inspection in the relevant area.

6 SOME EXAMPLES OF CONSTRUCTION METHODS

6.1 Construction of seawalls

Seawalls are mostly constructed as a protection of already existing or newly reclaimed land. Two examples of the construction of a seawall with identical functional requirements are shown in figure 5 and in figure 6. The ultimate shape depends on the chosen workmethod which is

influenced by the water depth, wave action and equilibrium slope during construction. In figure 5 the basic required design is shown: armour layer, two filter layers and a geotextile between the secondary filter layer and the sand core.

The theoretical design, which allows for a minimum volume of stone, can hardly be realized. Exposed, or semi-exposed conditions, require the steep outer slope to be built up by placing alternately stone bunds and sand backfill. Stone quantities can be reduced by accurate placement. At shallower depth, placement accuracy increases and narrower bunds should be possible. Once this part of the revetment structure is realized, the geotextile is placed followed by the subsequent cover layers.
In figure 6 a design is shown where it is anticipated that placement of the geotextile cannot be carried out on the outer slope because of high wave conditions. Also placement of stone in shallow water with barges is prohibited by wave action. Therefore the design provides for a geotextile at the inner side of a protective rock bund to be included in the structure. The lower reach of the geotextile should only be extended to such a level that the influence of the tide, waves and currents on washing out of sand is negligible and can be coped with by placing a sufficiently thick layer of quarry stone.
As for waves, currents will require a rapid cover of under layers with a minimum exposure to current action. In addition to this, from a morphological point of view, preference should be given to carry out the construction in a down stream direction in order to reduce siltation of the working area.

Construction stages of seawall in figure 5.

phase I
Placement of stone bunds using water born equipment (side stone dumping vessel, fall pipe vessel) combined with sand backfill. The upper reach of the slope is placed with landbased equipment making use of the tidal variation. This section is raised by using extra geotextile.

phase II
Trimming of outer slope and placement of geotextile.

phase III
Subsequent placement of secondary and primary sublayer and armour layer.

phase IV
Not shown: completion of top section of the structure.

Construction stages of seawall in figure 6

phase I
Placement of sufficiently broad bunds with water borne equipment (side stone dumping vessel, fall pipe vessel) combined with sand backfill.

phase II
Placement of quarry run dam upto half tide level (depending on workability) with land based equipment and placement of secondary stone layer at upper reach of the slope. Because of exposed conditions the geotextile fabric is now placed at the lee side of the upper stone bund.

phase III
Placement of primary and armour stone layer on top of secondary stone bunds.

phase IV
Not shown: completion of top section of the structure.

6.2 Construction of rockfill closure dams

A closure gap is defined as that part of a closure structure in which the velocities of the passing flow are such that the closure can only be realized with special means.

For closures using rock [2], sufficient quantities of rock of suitable size have to be available to be able to realize the closure. Construction plant is either land based or water based or a combination of these. The type of equipment to be used depends on the required volumes of stone, handling capacity and limitations with respect to the circumstances under which the closure has to be performed.

The current velocity through the closure gap and the available water depth have to be known for all stages of a tidal closure. This will enable the determination of the operational conditions for water borne equipment for the closure.

The dimensions of the final closure gap should take into account the actual current velocities near the bed or bed protection, including material to be dumped in the closure gap to avoid excessive erosion and enable operations with floating equipment.
In figure 7 a typical example is given of the maximum velocities during a vertical closure and during a horizontal closure (crest level of -3 m). During vertical closure the velocity is determined by the crest level (free fall situation). After reaching its maximum value at a crest level of approximately -1 m the velocity gradually decreases to zero when the crest is further raised. During horizontal closure the velocity is determined by the difference in water level upstream and downstream of the gap and continues to increase until the gap is closed.

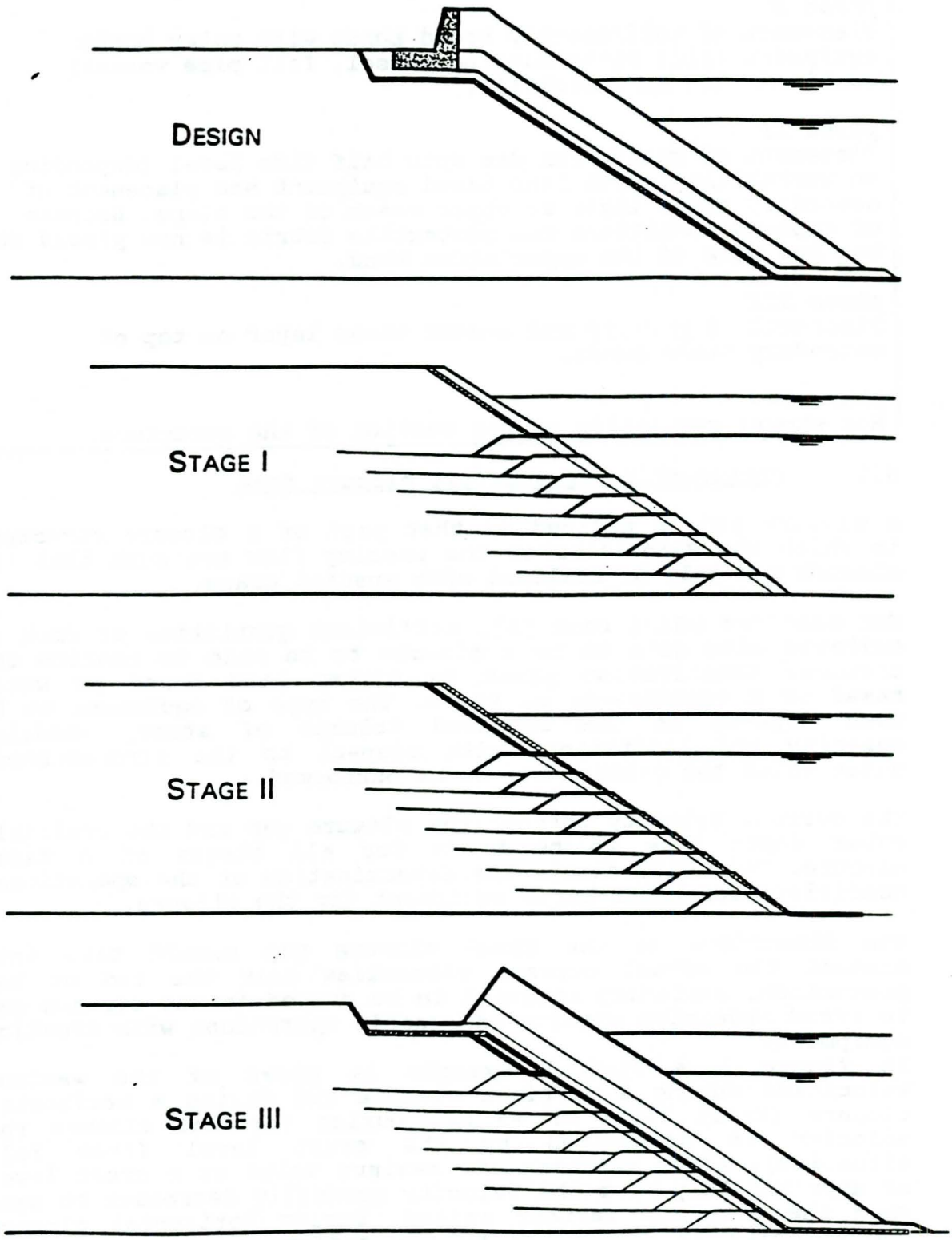

figure 5 Theoretical design of seawall and construction aspects, seaward position of geotextile.

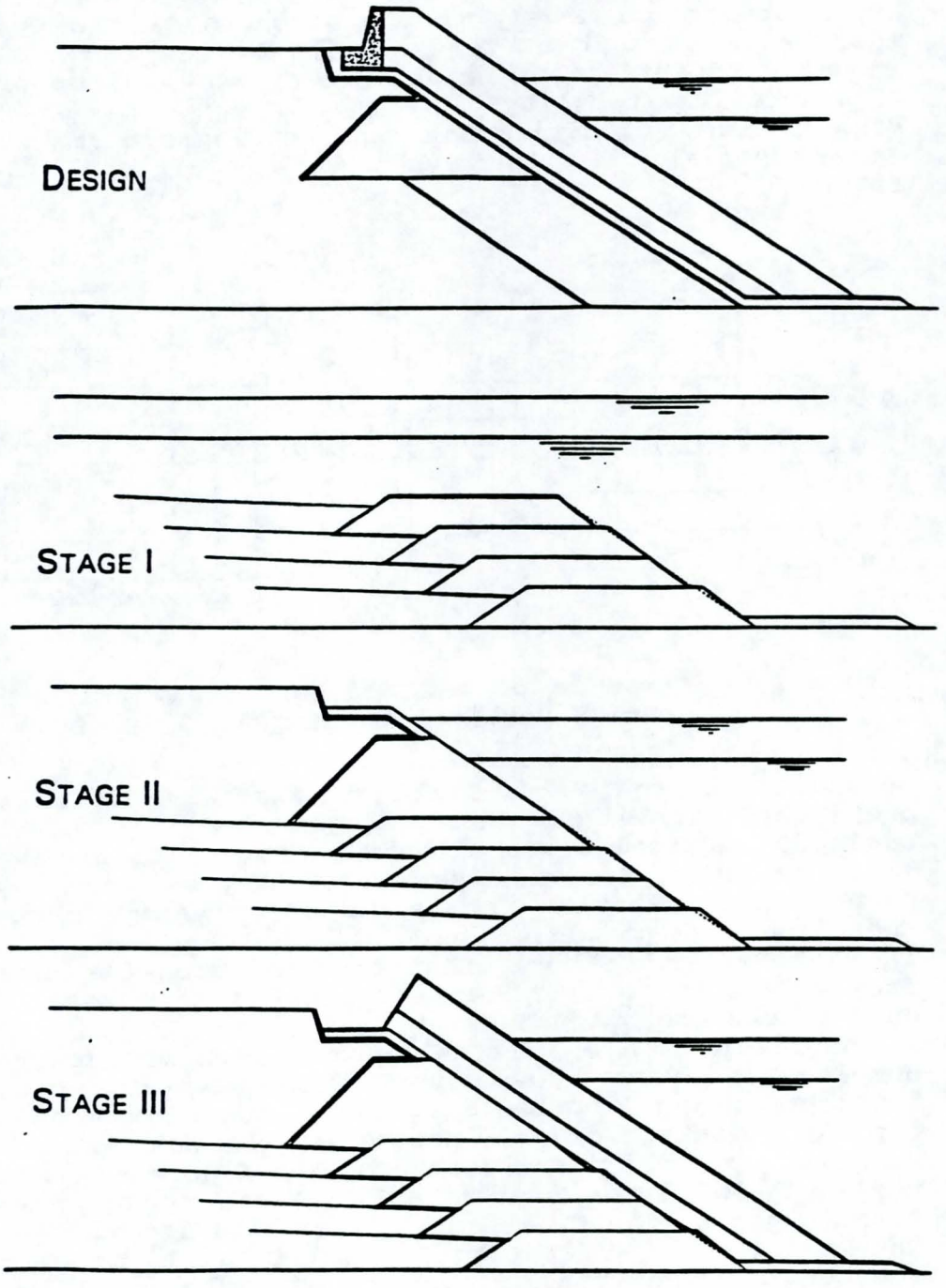

figure 6 Practical design of seawall taking into account exposed wave conditions, landward position of geotextile.

The weight of the stones used for the closure of the gap must be adapted continuously to the strength of the current. Care must be taken that at the location of the final closure also stones with sufficient weight are present on top of the crest to ensure its stability.
High current velocities may occur during closure of the final gap, especially in the event of a horizontal closure (see figure 7).

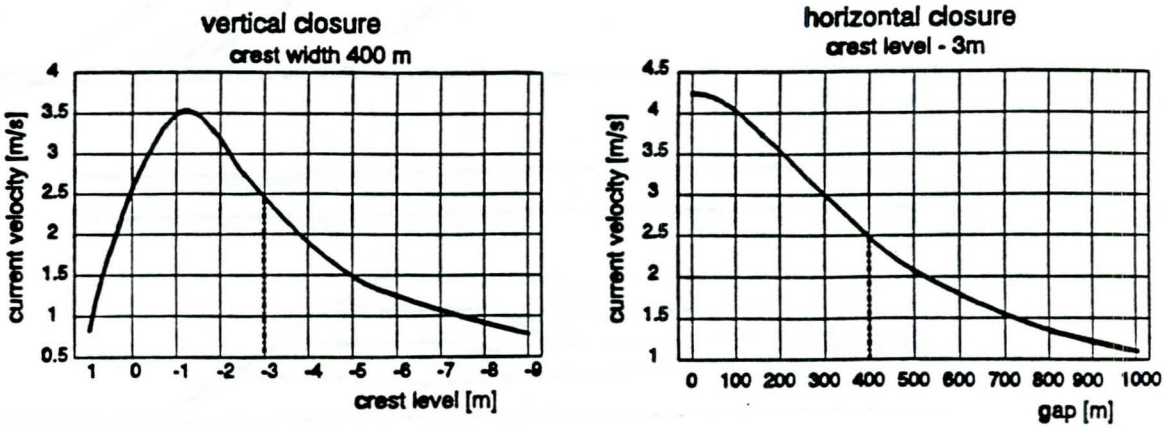

figure 7 Example of maximum current velocities occurring during vertical and horizontal closure.

Depending on the required quantities, the final closure is preferably carried out during slack tide.
During a vertical closure the closure dam is gradually raised layer by layer. For this dump barges may be used, a cable way, dump trucks operating from a temporary bridge or grab cranes operating from pontoons.
In the event of a horizontal closure, stone is dumped either from one side or from two sides using land based equipment: dump trucks and bulldozers.
A combination of a vertical and horizontal closure includes dumping of layers using water borne equipment upto a certain level and using land based equipment for closing the remaining gap. An advantage of this method is that the retaining dam can be built up in horizontal layers (see figure 8), thus avoiding the need for large quantities of stone to be dumped in the closure gap at the final critical closing stage.
The capacity of floating equipment will be hampered and reduced in the final stages of the closure. Due to their draught and the highly increased current velocities, stone dumping vessels are able to float over the retaining dam at high tide only. Floating cranes have a relatively low dumping capacity and are unable to anchor behind the closure gap without special mooring pontoons or anchor poles due to the high current velocities. The use of floating equipment (split barges, elevator barges or stone dumping vessels) for vertical closure, is quite an easy and cheap solution until the crest of the embankment reaches about 2 to 3 m below low water. The use of floating equipment has to be adapted to the increasing

current velocities during the final stage of a gradual closure, see figure 9.

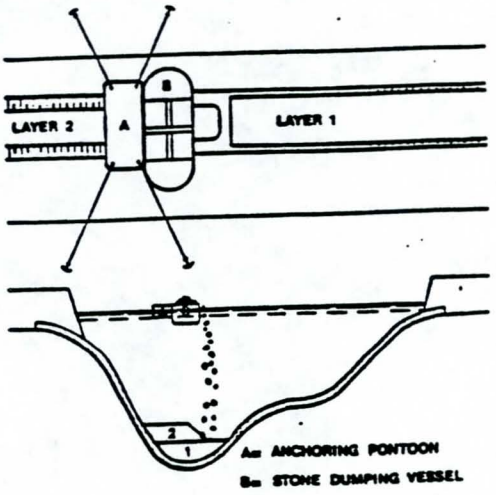

figure 8 Side stone dump barge placing stone in horizontal layers.

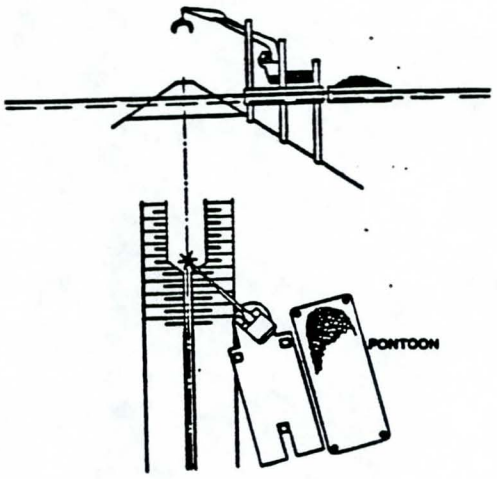

figure 9 Floating crane during final closure stage.

References:

1 CIRIA/CUR, Manual on the use of rock in coastal and shoreline engineering. CIRIA special publication 83, CUR report 154, London, Gouda, 1991.

2 Huis in 't Veld J.C., J.Stuip, A.W. Walther, J.M. van Westen, The closure of tidal basins. Delft University press, 1987.

DESIGN OF THE BED PROTECTION OF THE ROTTERDAM STORM SURGE BARRIER

R.E. Jorissen and D.P. De Wilde
Ministry of Transport, Public Works and Water Management,
Civil Engineering Div., Utrecht, The Netherlands
E. Berendsen
Ministry of Transport, Public Works and Water Management,
Road and Hydraulic Engineering Div., Delft, The Netherlands

ABSTRACT

In 1989 the Dutch government decided to build a storm surge barrier in the New Waterway near Rotterdam. This barrier will be closed if a storm surge level is predicted that might threaten the safety of an economically very important region of the Netherlands. Contrary to earlier similar projects the design has largely been contracted out to the builder of the barrier. Only some components of the design, like the bed protection, are solved by a joint effort of the builder and the Ministry of Transport and Public Works.

The design of the bed protection is based on two conditions to be fulfilled : the permissible probability of failure and the required lifetime of the construction.

Based on model tests a relation between the stability of the toplayer of the bed protection and the hydraulic loads has been developed. This relation has been integrated into a model, that describes the probability distributions of the hydraulic loads. As a result of this integration the probability distribution of the required toplayer diameter can be calculated.

1. INTRODUCTION

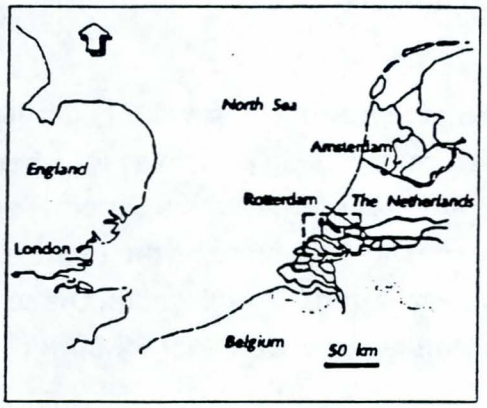

Figure 1

The project area is in the southwest of the Netherlands as shown in the figures 1 and 2. Figure 2 shows the dikes, which were to be reinforced as a consequence of the Delta plan. This plan was developed after the flood of 1953. It included shortening of the coast line by closing several tidal inlets and strengthening remaining dikes. In 1985 most of this plan has been completed, when a re-examination of design conditions led to higher values than those originally calculated. This implied very costly construction works in densely populated areas. Therefore, in 1987 the Dutch government initiated a study to consider a storm surge barrier near Rotterdam. This barrier should significantly reduce design conditions to avoid problems related to dike reconstruction works. The prescribed reduction of design conditions is based on those areas, which would be most affected by the reconstruction works. These areas are within the cities of Rotterdam and Dordrecht. From several predesigns a final choice was made at the end of 1989. The selected barrier design features two semi-circular doors with a length of about 220 meters.

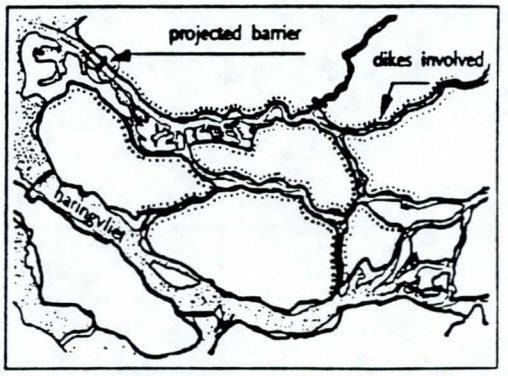

Figure 2

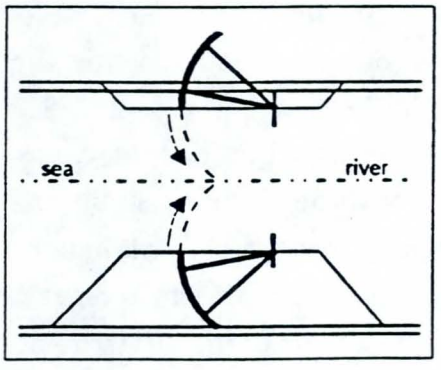

Figure 3

The barrier is closed by rotating the floating doors into the river as shown in figure 3 and lowering the entire construction to the river bottom by filling ballast tanks with water. This operation is completed in 2.5 hours. If closed, the doors will rest on a threshold, that consists of concrete elements placed on a riprap filter construction. On both sides of the barrier a riprap bed protection is necessary to prevent scouring in the immediate environment of the barrier and threshold. Based on the operational behaviour of the barrier the bed protection had to be designed to withstand hydraulic loads during the closure operation (flood) and the opening

operation (ebb). If the doors are entirely closed, the hydraulic loads on the bed protection are negligible.

This paper deals with the design of the bed protection and the related hydraulic aspects. The design of the bed protection is based on two main principles : the permissible probability of failure and the required lifetime of the construction. The contribution of the bed protection to the total probability of failure of the barrier is set at a value of 10^{-8} per year. Because the required lifetime is 200 years, the use of geotextiles as a essential part of the bed protection is not considered. Both the filter and the toplayer of the bed protection will be made of riprap.

2. MODEL INVESTIGATIONS

The stability of the riprap was investigated in two scale models, both a section (2D) model and a 3D model. The section model was scaled 1:30 and the 3D model was scaled 1:60. All numbers presented in this paper are based on the prototype.

gap [m]	head [m]
10.0	0.40
7.50	1.40
5.00	2.90
3.00	4.10
1.00	5.80

Table 1

Based on the operation of the barrier the bed protection had to be designed to withstand hydraulic loads during the closure operation (flood) and the opening operation (ebb). The barrier will be closed as soon as a certain water level has actually been exceeded and the predicted maximum sea level exceeds a critical level. Due to the duration of the closing process (2.5 hours) a head will gradually develop. This head will be influenced by the development of the water levels in front of the barrier and by wind effects. The head will, together with the effects of waves, cause a hydraulic load on the bed protection at the riverside of barrier. To give an impression of the order of magnitude of these hydraulics loads the head at 10^{-8} per year conditions is shown in table 1 as a function of the barrier gap h_s. The effect of these loads were investigated in the model tests.

The barrier will be opened if the water levels on both sides of the barrier are equal and the predicted maximum sea level does not exceed the critical level any more. Mostly due to the duration of the opening process (2.5 hours) again a head will develop. However this head is much smaller than the heads mentioned in table 1. A typical design head for this situation is about 1 meter.

In closed condition the hydraulic loads on the bed protection are negligible. Therefore the model tests were focused on the stability of the toplayer of the bed protection at several stages of the closing and opening operation. In table 2 an overview of the tests, which were carried out, is shown.

The stability of the riprap was tested by measuring the number of displaced stones from each section of the bed protection. The sections correspond with the planned sections in the prototype.

At the beginning of each test a small head was applied. This head was increased step by step until the design head was exceeded or the riprap construction had failed. The head was kept constant during a period of 2 hours (prototype). After each step the total number of displaced stones was counted. These data were collected in a relation between head and the total damage.

Based on these relations the critical head for each investigated geometry has been determined. The critical head is defined as the head at which the damage to the toplayer exceeds the number of 100 stones per 1000 m^2 during 2 hours.

Test	2D/3D	h_s [m]	flood /ebb
T 403	3D	1.0	flood
T 3	2D	1.0	flood
T 6	2D	1.0	flood
T 408	3D	1.0	ebb
T 19	2D	1.0	ebb
T 405	3D	3.0	flood
T 405F	3D	3.0	flood
T 420	3D	3.0	flood
T 4	2D	3.0	flood
T 5	2D	3.0	flood
T 409	3D	3.0	ebb
T 409F	3D	3.0	ebb
T 17	2D	3.0	ebb
T 406	3D	6.0	flood
T 410	3D	6.0	ebb
T 411F	3D	10.0	flood

Table 2

Also the streamprofiles during the mentioned phases were investigated. The results of this part of the model tests proved to be very useful, because of the limited number of stability tests which were carried out.

The values for the critical heads were used to determine the value of K in the following stability formula. This formula is based on the well-known Shields relation with a correction factor K to account for the distorted velocity profile (see Franken, Jorissen and Klatter, [1]).

$$\Delta * D_n = \frac{(K * U_0)^2}{C^2 * \Psi} \qquad (1)$$

$$U_0 = \sqrt{2 * g * (h_1 - h_2)} \qquad (2)$$

Δ relative density riprap [-] = $(\rho_s - \rho_w)/\rho_w$
D_n nominal diameter riprap [m] = $\sqrt[3]{(M_{50}/\rho_s)}$
U_0 reference velocity [m/s]
K correction factor or stability parameter [-]
C roughness parameter [$m^{0.5}/s$] = $25 * (h_x/D_n)^{1/6}$
Ψ damage parameter [-]
h_1 water level upstream [m]
h_2 water level downstream [m]
h_x local flow depth (see figure 5) [m]

The damage parameter Ψ is taken to be 0.056 at the described failure conditions.

In figure 4 the results of the model tests are shown as values of K as a function of the distance x from the barrier and the gap between the floating doors and the threshold (h_s). In this figure the results for the riverside (flood) and the seaside (ebb) of the barrier are both shown.

The lacking information at some distances is clearly visible in figure 4. Also the situation with a gap of 10 meters was not investigated for the riverside (flood) of the barrier. This situation was only investigated for the seaside (ebb).

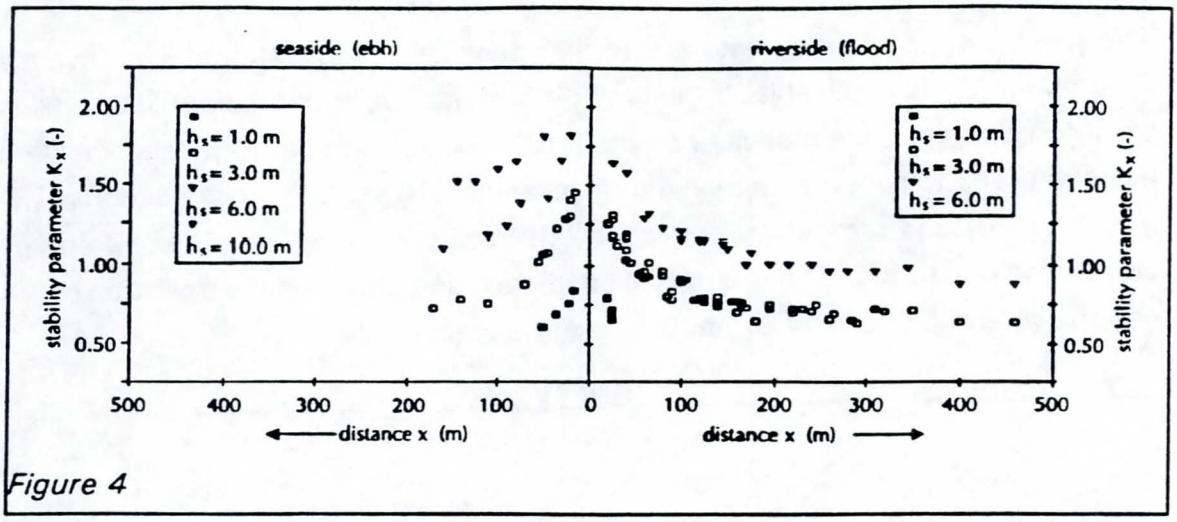

Figure 4

The values of K turn out to be a function of barrier gap (h_s in figure 5) and the distance x from the barrier. It is believed that this behaviour of K is dominated by the behaviour of the velocity U_x. At $x=0$ this velocity equals more or less the reference velocity U_0. This led to the assumption that if the local velocity U_x is used in relation (1) K becomes more or less a constant. This assumption is shown in equation (3).

$$K_x * U_0 = K_0 * U_x \qquad (3)$$

K_0 stability parameter at $x=0$
K_x stability parameter at x
U_0 reference velocity
U_x flow velocity at x

The further analysis of the test results is be based on this assumption.

3. FURTHER ANALYSIS OF TEST RESULTS

The results of the model tests are further analyzed to investigate whether the assumption (3) is applicable. If the result is satisfactory it can be applied to fill in the lacking data on the stability parameters K. For this reason the streamline data has been used to construct a momentum balance between the cross-section at the barrier (x=0) and a other cross-section (x). In this balance the effect of energy dissipation due to friction has been included. Based on this balance a relation between the reference velocity U_0 and a velocity U_x can be derived.

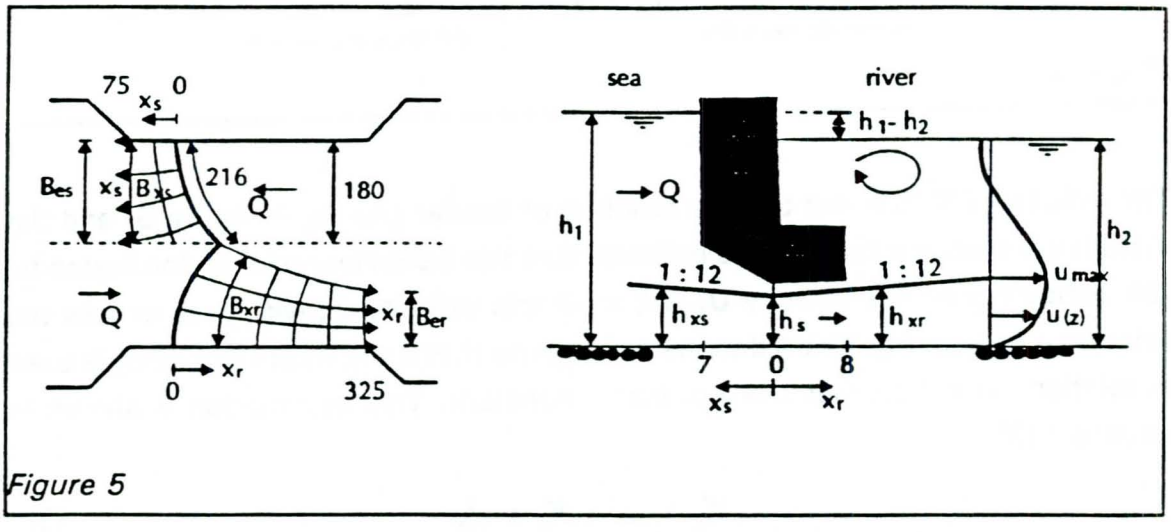

Figure 5

The available streamline information is shown in figure 5. From the model tests the parameters h_x and B_x could be expressed as follows. The suffix s stands for seaside (ebb), while r stands for riverside (flood).

$$h_x = h_s + \frac{x}{12} \tag{4}$$

$$B_{xr} = 216 - \frac{(216 - B_{er}) * x}{325} \tag{5}$$

$$B_{er} = 90 + 9 * h_s \tag{6}$$

$$B_{xs} = 216 - \frac{(216 - B_{es}) * x}{75} \tag{7}$$

$$B_{es} = 180 \tag{8}$$

The momentum balance between the cross-section at the barrier (x = 0) and another cross-section (x) yields equation (9).

$$\frac{\varrho * g * h_{TX}^2}{2} + \varrho * Q_X * U_X + F_{friction} = \frac{\varrho * g * h_{T0}^2}{2} + \varrho * Q_0 * U_0 \tag{9}$$

If the total water depths downstream of the barrier h_{TX} and h_{T0} are assumed to be equal, equation (9) can be written as equation (10).

$$B_0 * h_s * U_0^2 = B_x * h_x * U_x^2 + \sum_0^x (\tau * B_x * \Delta X) \tag{10}$$

Combined with a friction law, equation (10) can be written as equation (11) or (12).

$$B_0 * h_s * U_0^2 = B_x * h_x * U_x^2 + \sum_0^x (\lambda * U_x^2 * B_x * \Delta X) \tag{11}$$

$$\frac{U_x}{U_0} = \sqrt{\frac{B_0 * h_s}{B_x * h_x + \sum_0^x (\lambda * B_x * \Delta X)}} \tag{12}$$

If the assumption (3) and equation (12) are combined, a relation between K_x, K_0, U_0 and x has been derived.

$$K_X = K_0 * \sqrt{\frac{B_0 * h_s}{B_x * h_x + \sum_0^x (\lambda * B_x * \Delta X)}} \tag{13}$$

λ friction parameter
B_0 flow width at x = 0 (= 216 m, see figure 5)
B_x flow width at x
h_s flow depth at x = 0
h_x flow depth at x

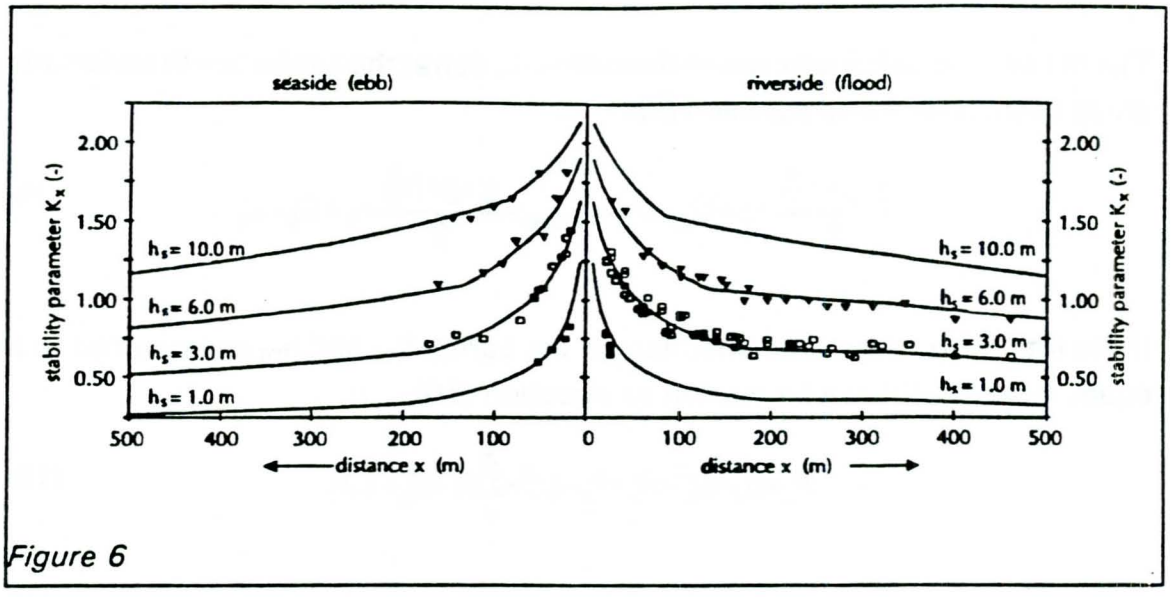

Figure 6

In this relation only one variable (λ) remains, because K_0, B_0, h_s, B_X, h_x are known from the model tests and U_0 represents the hydraulic load. This remaining variable has been fitted to the data. The results of this procedure are shown in figure 6 and table 3.

gap h_s [m]	K_0	λ	situation
10.0	2.2	0.05	ebb
6.00	2.0	0.05	ebb + flood
3.00	1.8	0.05	ebb + flood
1.00	1.6	0.05	ebb + flood

Table 3

Regarding to the values for K_0 and λ the following remarks can be made.

First of all it seems that the direction of the flow doesn't influence the value of K_0. This is logical, because immediately downstream of the barrier the flow direction doesn't influence the stability of the riprap. It is only further away from the barrier that due to a different horizontal velocity profile the stability of riprap will be influenced differently. This means that the test results for the ebb situation can be used to predict stability of riprap at the riverside of the barrier or vice versa.

The value of λ turns out to be constant. The value of λ can be related to the hydraulic roughness parameter with equation (14).

$$\lambda = \frac{g}{C^2} \qquad (14)$$

For a λ of 0.05 the hydraulic roughness is about 15 $m^{0.5}/s$, which is rather low. But based on the very large diameter of riprap and the small values of h_x immediately downstream of the barrier this value seems to be reasonable. Further downstream this value of C is too low, but the influence of this error in the cumulative type of formula like equation (13) is relatively small.

4. DESIGN APPROACH

Based on the model tests a relation between the stability of the toplayer of the bed protection and the hydraulic loads has been derived. This relation has been integrated into a model, which generates the probability distributions of these hydraulic loads. The procedure of determining these distributions has been treated by Janssen and Jorissen [2, 3]. In this paper only a brief summary of this procedure will be given based on the calculation scheme shown in figure 7.

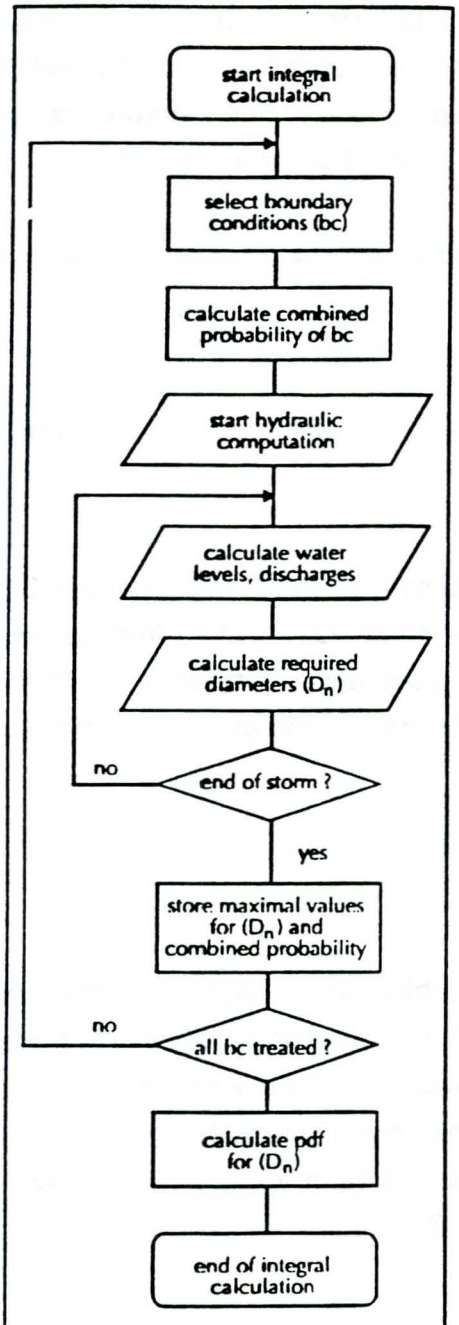

Figure 7

The hydraulic conditions in the project area are determined by two boundary conditions : the storm surge level at the river entrance and the upstream river inflow. These boundary conditions have a stochastic nature. The probability distribution functions of these boundary conditions are known. Also, the occurance of storm surge can supposed to be independent of the occurrence of a river flood.

The hydraulic model is used as a transfer function from the boundary conditions mentioned above to hydraulic conditions at various locations. For each relevant combination of storm surge and river discharge a hydraulic computation has been made. During that computation not only the time development of water levels and discharges are calculated, but also the required diameter for each section of the bed protection. This calculation is based on the equations (1) and (13). Of each combination and each section the maximum required diameter is stored together with the probability of occurrence of the combination of storm surge and river discharge. As a result of this procedure the probability distribution of required toplayer diameter can be calculated. From this distribution the design diameter, which has a permissible probability of failure, can be determined.

The bed protection consists of various sections in which different riprap diameters are applied. The question remains if these sections can be assumed to be correlated or not. If they can be assumed to be correlated, each section is allowed to have a probability of failure equal to the total probability of failure. If the required diameter in the various sections are independent, the total probability of failure has to be divided by the total number of sections.

From the design calculations it showed, that the hydraulic loads ($\div$ K*U) on each section of the bed protection were completely correlated. This and the fact that the standard deviation of the stability relation is large compared to the standard deviation of the actual strength (= Δ*D), made the assumption of a complete correlation between all sections acceptable. Also because of the relatively large standard deviation of the hydraulic loads it was decided to treat the strength parameter ΔD as a deterministic parameter. This means that the stochastic variables are the value of K_x and the reference velocity U_0. For K_x relation (13) has been used. This relation is shown in figure 6 as the collection of solid lines. This relation has been included in the hydraulic model mentioned earlier. The reference velocity U_0 is determined with equation (2) based on data directly derived from the hydraulic model.

5. RESULTS

If the probability distribution functions of the required riprap diameter D_n are known, the final design values for the diameter in each section can easily be determined by looking for that diameter, which has a frequency of exceedance that is equal to the demanded probability of failure.

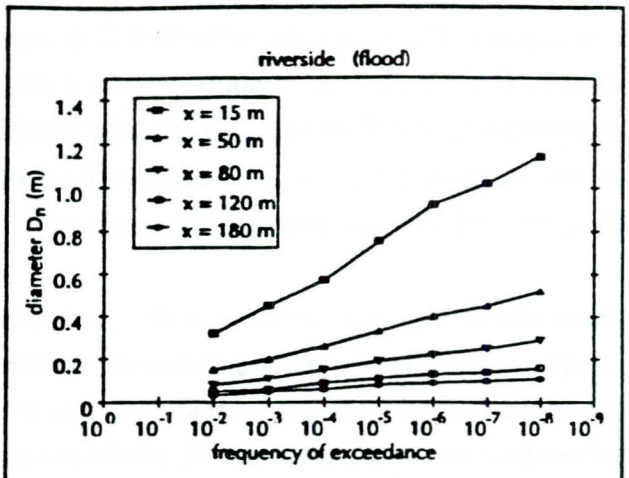

Figure 8

In figure 8 the calculated frequency exceedance curves for the required diameter at various distances x are shown for the riverside only. These results show that immediately downstream of the barrier the required diameter is about 1.20 metres. Also it shows, that the required diameter will decrease rapidly with increasing distance from the barrier.

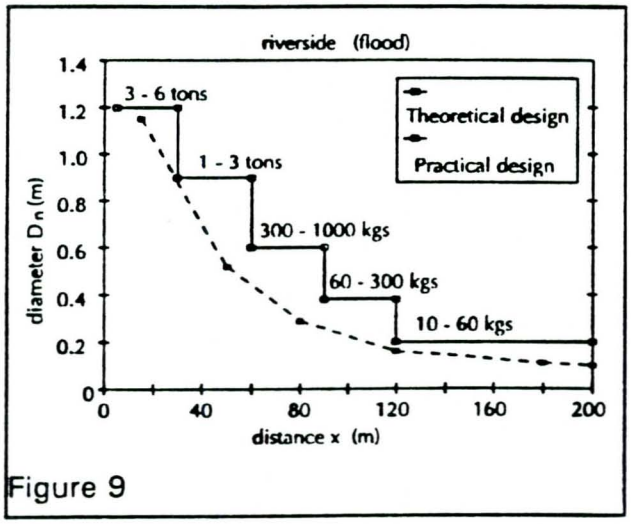

Figure 9

In figure 9 both the theoretical and the practical design of the bed protection at the riverside are shown. This practical design is based on available riprap, various loads during construction phases, filter rules and minimum section width, construction method.

6. CONCLUSIONS

The calculation of various hydraulic loads on a bed protection within a hydraulic model is a relatively small task. The results of such an addition prove to be very useful if the hydraulic model is used for an overall probabilistic design. In the case of this project similar additions to a hydraulic model have been made, like the development of a scour hole and the hydraulic forces due to head, velocities and waves.

If model tests are carried out to investigate the stability of riprap, it is essential to acquire reliable velocity profiles. These prove to be necessary if a relation between the hydraulic loads and the strength of the bed protection has to be derived. Such a relation will contribute to the development of stability models and will reduce the number of model tests to be carried out.

7. REFERENCES

[1] Design rules for the use of riprap in closure works, A. Franken, R.E. Jorissen and H.E. Klatter, to be presented at The International Riprap Workshop, Fort Collins, Colorado USA, 12-16 july 1993.

[2] Modelling storm surges and forecast effect in designing the Rotterdam storm surge barrier, J.P.F.M. Janssen and R.E. Jorissen, workshop STORM'91, Hamburg, 1991.

[3] Integrating forecast effects and operational behaviour in designing the Rotterdam storm surge barrier, J.P.F.M. Janssen and R.E. Jorissen, 3rd International Conference on FLOODS AND FLOOD MANAGEMENT, Florence, Italy, 24-26 November 1992.

QUALITY AND QUALITY CONTROL OF STONE FOR HYDRAULIC STRUCTURES

G.J. Laan
Ministry of Transport, Public Works and Water Management,
Road and Hydraulic Engineering Div., Delft, The Netherlands

1. INTRODUCTION

In 1988 the CEN (Comité Européen de Normalisation) established the TC154 technical committee for the development of European standards for aggregates.
Co-operation between the Netherlands and the UK on the production of a *Manual of the use of rock in coastal and shoreline engineering* [1] prompted TC154 to turn to the standardisation of armourstone, and early 1991 it commissioned a 'Group of Experts' to prepare this standard. The group includes representatives from Austria, Belgium, France, Germany, Ireland, the Netherlands, Norway, Sweden and the United Kingdom.
The importance of a European standard for stone in hydraulic structures is generally recognised. Specifications for hydraulic structures often include requirements for rock materials and test methods whose real usefulness is at best doubtful. Requirements for gradings are often impossible to comply with during production, and methods of controlling grading may not even be given. The introduction of EC standards is important not only technically, but also as a means of removing trade restrictions. The second point is highly relevant to stone in hydraulic structures, since many countries import and export stone.

Together with the development of European standards, specifications are being developed for factory production control for use by the manufacturers of construction products, if their products shall be provided with the European conformity mark consisting of the symbol CE.
In general quality assurance for armourstone is poorly developed. Recent advances in design and materials science have greatly increased the performance of structures and allowed them to be built more economically; but there is still much room for improvement in the quality of the materials used. The existing, often casual, approach to the quality of stone for hydraulic structures, with a strong emphasis on experience and visual assessment, does not meet the demands of modern structures.
This paper presents some ideas which have been gained through practical experience of quality assurance in the supply of armourstone for hydraulic structures in the Netherlands.

2. TEST METHODS AND POSSIBLE REQUIREMENTS

The Experts Group has established test methods for a European standard for stone in hydraulic structures. This section outlines the reasoning behind their choices. The description of each test method is accompanied by a summary of the conditions with which they must comply. Formal requirements have not yet been established; for the time being, the following comments should be of use.
The standard should consider stone requirements under three headings:

(i) intrinsic characteristics, which depend primarily on the nature of the stone and cannot be significantly altered in the manufacturing process;

(ii) manufactured characteristics, which result from the manufacturing process;

(iii) additional characteristics, which do not clearly fall into either of the first two categories.

2.1. Intrinsic characteristics

Density

Requirements and test methods for determining the density of stone vary widely from one country to another. For the purpose of the standard two types of density are defined:

(i) density of stone (particle density), representing the relationship between the dry mass of the stone and its volume, *including* pores;

(ii) density of stone matter, representing the relationship between the dry mass of the stone and its volume, *excluding* pores.

The density of stone (ρ_r) is used in formulae for armour stability design. The relative buoyant density (Δ) is employed, and is defined as $\Delta = \rho_r/\rho_w - 1$, in which ρ_w is the density of water. Using denser rock of the same grading in armour-layer size increases stability and reduces layer thickness, but at the same time increases the total mass of material required. The use of denser material for fill, core and filter applications also leads to orders for increased tonnage for the same volumes of stone. Density is importantly correlated with durability. The minimum average density quoted as acceptable in the UK is 2600 kg/m^3, for Germany 2300 kg/m^3, and for the Netherlands 2500 kg/m^3.

Density can vary fairly widely in a quarry. For this reason there should be a requirement for both average density and the 90% exceedance value. In general, when only one type of rock is involved, this value is not more than 100 kg/m^3 less than the average density. These requirements make it necessary to determine the density stone by stone, by weighing the dry stone and determining its mass above and under water after is has been soaked. If the density of the water used is not 1000 kg/m^3, the difference is corrected for.

Determination of the density of stone matter makes it possible to determine porosity, provided that the density of the stone is known. On the basis of porosity, a certain water absorption can be expressed as a degree of saturation. Porosity is also important in determining the index of continuity (see 2.1: 'Breakage index and index of continuity'). However, no requirement will be set for the density of stone matter.

Intact strength to resist breakage

The intact strength of the mineral fabric, which indicates resistance to breakage along new fractures, is most often measured in term of uniaxial compressive strength (UCS), which the group therefore takes as the primary rating of intact strength. Low intact strength could result in the removal of corners, edges and asperities, leading to a reduction in angularity and, for finer gradings, a significant loss of mass.

The simplest measurement of intact strength is the point load strength index. This measurement can be performed in the laboratory, or in the field with portable equipment. Whenever possible, use of the corresponding ISRM-suggested test method for point load strength should be allowed for quality approval. But in this case the point load strength result must be translated into a rating of compressive strength via an existing correlation, as the specification will quote values of UCS.

The compressive strength test method, in common with the point load method, will use only water-saturated specimens that do not have discontinuities such as cracks and seams. In view of the fairly wide spread in measurement results, a sufficiently large number of stones will have to be examined to obtain a reliable average value.

Breakage index and index of continuity

Block integrity of 'wholeness' indicates resistance to breakage along partial or traversing flaws such as cracks, veins, and bedding planes (Fig. 1).

Block integrity can be determined directly by means of a drop test, the result of which can be expressed in a breakage index. The breakage index is a measurement of the reduction in D_{50} (coarse gradings) or in M_{50} (light and heavy gradings) (see Section 2.2: 'Standard gradings'). The drop test (Fig. 2) must be performed in a way that is both generally practicable and reproducible. Various factors are involved here, such as the extent to which the samples are representative, and monitoring the height of the drop and the surface onto which the material falls. The last of these is especially important in the case of heavy gradings, because damping resulting from the elastic or plastic properties of the floor, and from crushing of the floor, may have an important influence on the result of the test.

An indirect non-destructive method is to measure the velocity of sonic waves through blocks. The index of continuity (Ic) indicates the ratio of real speed to theoretical maximum speed through material without discontinuities. A low index figure corresponds to a low real speed due to extensive discontinuities, and so a high susceptibility to breakage. Porosity affects the Ic, but not the block integrity. This effect can be eliminated by making use of an established linear relationship between porosity and the effect on the Ic.
The drop test and the sonic velocity test are the only objective methods of measuring block integrity, and their importance is generally recognised. Susceptibility to breakage can vary very widely, and is of primary importance during the handling of stone materials. It can lead to rejection of certain rock sources, or to a modification in the handling and/or design to be adopted.
The drop test can be used for all grading types; the sonic velocity test only for light and heavy gradings (see 2.2: 'Standard gradings').
The problem with both test methods is that experience with standardized methods has been very limited. A certain amount of experience has been gained in the Netherlands [2]. In France, the sonic velocity test is used more extensively than the drop test. In fact, the velocity test has been developed in that country into a standardised, operational test method [3]. All this makes it necessary to undertake a research programme before deciding to include any test methods and requirements in the European standard.

Resistance to wear

Resistance to abrasion in service is most important on sites where foreshore attrition agents such as shingle or sand can attack the armour. Also, for structures using dynamic design concepts, the increased risk that stones will slide and roll means that only highly wear-resistant materials should be used.
The non-standard abrasion mill test [1] is one of the best ways to measure resistance to wear.
For the standard for armourstone preference has been expressed for the wet Deval test armourstone [4]. This test is often criticised for poor reproducibility and discrimination, but its abrasion simulation is comparable in type to that of the mill abrasion test.

Freeze/thaw resistance

For stone affected by freezing and thawing, a freeze/thaw test has been chosen. This test needs to be performed only if water absorption exceeds a certain value - say, 0,5% by mass - at atmospheric pressure.
The test conditions set out by the 'Group of Experts' are as follows.

(i) The mass of the stones to be tested should be 10-20 kg, unless the grading is lighter. These are manageable sizes, in spite of the large freezers required. The ideal would be real-scale tests.

(ii) The test should have 25 cycle numbers.

Resistance to salt crystallisation

Resistance to salt crystallisation is important in salt water in warm climates. A magnesium sulphate test has been proposed. The test should preferably be performed on larger pieces, for example between 63 and 125 mm. It is necessary only if water absorption exceeds a certain value, to be agreed upon.

2.2. Manufactured characteristics

Standard gradings

Access to standard gradings offers several advantages.

(i) The designer can be confident that these gradings can be and have been produced.

(ii) There can be a workable system of quality control (for mass or particle size distribution) because the standard gradings are defined through experience with the production process, in such a way that control is as easy as possible.

(iii) Materials can be more easily produced, as a result of coordinating the system of standard gradings with production methods involving blasted rock, breaking and screening equipment, and visual selection methods. This coordination also allows the greatest use of blasted rock at the same time as the production of the largest number of gradings. There is less need to change crushing and screening equipment.

(iv) Production is more continuous, because the producer is certain of the demand for gradings and can therefore safely build up stockpiles.

(v) Prices can be lower.

A disadvantage is that designers have only a limited choice of gradings. In some circumstances it is highly desirable to deviate from the standard gradings. This should not be ruled out, especially with heavy gradings, where sizes can be changed with little detriment to production. Standard gradings are not needed for temporary dedicated quarries supplying single projects where it is necessary to make the greatest use of blasted rock.
In connection with the above, several conditions need to be built into the system of standard gradings, their requirements and test methods.
First of all, it is useful to split gradings into three categories:

(i) Heavy gradings, which are usually selected by eye.

(ii) Light gradings, which can be made by machine - these are gradings weighing up to 300 kg, but gradings with a nominal upper mass of between 200 and 300 kg may also be selected visually.

(iii) Coarse gradings made by breaking and screening, and whose measurements are expressed in millimetres.

This categorisation is useful for various reasons. Every production method for sorting and selecting stone for grading and shape is associated with a particular precision. Each of these methods therefore has a limiting effect on the tolerances that can realistically be imposed as regards of stone shape. Selection for shape is most effectively done by eye. In the case of gradings produced by machine, the equipment now available offers very little scope for influencing or monitoring the shape of the stones during production.
Finer gradings are expressed in terms of size (mm) rather than mass, because in the production process sieves with round or square openings are used, and because control is easiest with test sieves.

Light and heavy gradings

The 'Group of Experts' has reached agreement on the principles of the test method, and on a number of standard gradings. These are the light gradings of 5-40 kg, 10-60 kg, 40-200 kg and 60-300 kg; and the heavy gradings 300-1000 kg, 1000-3000 kg, 3000-6000 kg, 6000-10000 kg and 10000-15000 (Fig. 3).

A wide light grading for use in underlayers is still being discussed; such gradings are in common use and perform satisfactorily on the whole, but there have been problems with segregation.

Proposals from the UK and the Netherlands for requirements for light and heavy gradings correspond with the guidance presented in the CIRIA/CUR *Manual* [1]. Some of its principles are discussed below taking grading 1000-3000 kg as an example. Requirements for mass distribution are stated in terms of percentage exceedance allowed above or below nominal masses, as defined by class limits. For the upper class limit (UCL, e.g. 6000 kg) and the lower class limit (LCL, e.g. 3000 kg), maximum exceedance levels of 30% by mass and 10% by mass respectively have been proposed. To restrict the inclusion of very heavy stones and very light material that is unusable, an extreme upper class limit (EUCL, e.g. 9000 kg) and an extreme lower class limit (ELCL, e.g. 2000 kg) have been defined. The exceedance requirements proposed for them are 3% by mass and 2% by mass respectively. The EUCL for heavy gradings is one and a half times the UCL. The ELCL is about two-thirds of the LCL. For light gradings wider limits are in force, the width increasing with lightness.

Gradings are further limited by requirements for the average mass (M_{av}) of stones, excluding 'fragments' (pieces weighing less than the ELCL). M_{av} can be monitored much more easily than median mass (M_{50}), though the latter is the more important parameter from the point of view of design. The ratio between M_{50} and M_{av} can be calculated from mass distributions, and is determined by examining quality control. The M_{50}/M_{av} ratio for the range 10-60 kg to 6000-10000 kg varies from 1.3 to 1.0.

Some training is necessary for visual selection, and the gradings are fairly narrow. However, gradings defined in this way have been easily produced, and offer several advantages:

(i) segregation is less likely;

(ii) the minimum thickness of layers is relatively small;

(iii) the fields of application are numerous.

To test the grading, the mass distribution is determined by weighing stones drawn from a representative sample. For accuracy, a sample of at least 200 stones must be taken. Testing will take some time. A lifting device is necessary for gradings of 60-300 kg and above. A fast test method is to weigh the total sample and fragments in bulk and to determine the number of stones exceeding the ELCL.

Coarse gradings

The coarseness of coarse standard gradings should be between that of standard aggregate gradings (for concrete, roads, etc.) and that of light gradings. Three or four gradings would be a suitable number. The gradings could be broader than mass gradings, because the thickness of layers is determined more by practical considerations than on the basis of a theoretical minimum thickness.

The test sieves consist of standard sieves for aggregates and large steel sieves with meshes of 63, 90, 125, 180 and 250 mm (Fig. 4).

Shape

The shape of stones can be practically determined only by measuring their thickness (d) and length (l). For coarse gradings a measurement could also be made of the sieve size, which could be related to the thickness measurement to provide extra information about shape.

The requirements will apply to elongate and tabular stones with a d/l less than 1/3. Whether a stone meets the criterion can usually be determined by eye. Thickness and length should be checked with the help of a calliper if the d/l value is about 1/3, because no clear visual assessment can then be made.

2.3. Additional requirements

Resistance to wetting and drying

Schistose and weathered rock, and rock containing clay minerals, may be susceptible to deterioration as a result of in-service weathering. A wetting/drying test can provide relevant information. Such a test could include boiling and cyclical testing.

'Sunburn'

Sunburn (Sonnenbrand) is a type of rock decay that may be present in relatively young alkaline basalts. It is usually attributed to the transformation of nepheline and albite into analcite during the solidification and cooling of magma. Owing to the accompanying changes in density and forces obstructing volume change, internal stresses are set up in the rock. Alternating stresses caused by hot days and cold nights, or by the boiling test, may then degrade the rock.

Other researchers attribute the phenomenon to the presence of deleterious minerals such as swelling clay. In either case, a boiling test will reveal it.

Unsoundness of slags

Slag material contain various forms of unsoundness, such as the lime and iron unsoundness of blast furnace slag and the lime unsoundness of steel slag. Specific test methods can detect these phenomena.

Petrographic description

It is very important that petrographic information is available for rock that is to be supplied for hydraulic structures. This is especially true for the presence of deleterious minerals that can cause degradation during the lifetime of a structure. Such information may lead to specific extra tests to further determine the activity of these minerals.

3. QUALITY CONTROL

3.1. Principles

Quality control is much concerned with variation in rock properties and the margin between the requirements - i.e. the thresholds set for a certain test result - and the available or producible quality. Rock formations are often far from homogeneous; a fact which is of particular concern when dealing with the required intrinsic material properties. Compared with quality control for industrial production, in the production and selection of armourstone the human factor is important. This applies particularly to blasting and to the visual selection of gradings, shape and block integrity.

Quality control should anticipate these matters. The accuracy of its results depends on various factors, such as the representativeness of the samples, processing of the samples to prepare them for analysis, and the margin of error in testing.

The representativeness of the samples depends on the variability in the batch to be inspected, and the sampling method and sample size, which will depend on the degree of variation. The more the quality of a batch varies, the more samples must be taken. The sampling method should be non-

selective: every piece of stone should have an equal chance of being included in a sample. This is impossible, or extremely difficult, if the batch is static (as in a stockpile or ship's cargo). It is therefore better to take samples during handling. With a static batch particular attention must be paid to the possibility of segregation. While prevention of segregation is desirable for structural reasons, sampling must allow for the fact that it does happen.

The precision of quality control determines the degree of risk of erroneous rejection or acceptance for producer and client respectively. For both these parties the cost of quality assurance must be weighed against the magnitude of these risks. In the case of the producer, a margin must be maintained between the actual quality and the limit values laid down in specifications taking the intensity of the inspection into account. For example, a specification of maximum 3% for the proportion of the heaviest stones in a mass distribution to be above a certain mass, effectively means that in production 0% has to be aimed at. The client should take quality risks into account in the design. This can be done by using safety factors, or by adopting a probabilistic approach to a design.

3.?. Quality control of armourstone properties

3.2.1. Intrinsic characteristics

Density

Density is determined for the rock source or for a batch of material produced from it.

Consider the former case, which is part of the appraisal process to investigate the suitability of the rock mass for production of the desired material and to detect any variation in the quality of the rock. For this samples are taken for analysis from cores from boreholes if available, or from the quarry faces. In the case of rock which has been blasted, samples are taken from points evenly distributed through the mass, in order to obtain a true representation of the entire face. Pieces of rock for analysis are broken off at random from larger blocks. If there are visually identifiable differences in quality, different parts of the quarry faces are tested separately. The results should be fed back to the production process in order to meet the density requirements.

Testing of produced materials also involves samples broken off blocks. Any small fragments which may be present must not be used.

Visible phenomena which indicate a possible variation in density require a sampling technique that is unaffected by conscious or unconscious human choice. Various methods are available for this, such a numbering stones and drawing lots; or taking out pieces of rock at predetermined intervals during handling, or from predetermined locations in static batches.

Monitoring of density during the whole supply period is important because the stability and the bulk density of the material used in the structure depend primarily on it. Density monitoring is also important, however, because variation in density may indicate variations in other intrinsic characteristics. These variations may be due to a variation in the composition of the rock and/or the degree of weathering. Such variations can generally be detected satisfactory by density tests. These tests can be carried out quickly, and are cheaper than the tests for most other intrinsic properties. The frequency of examination of intrinsic properties can therefore be made to depend on the results of a relatively intensive density check. When analyzing the results of density measurements, allowance must be made for the fact that the statistical distribution is skewed towards the higher values. If different types of stone are mixed in the rock mass, the distribution is complex.

The frequency and extent of acceptance tests for density may depend on various factors, such as the degree of variation in density and the margin between the minimum or maximum required and the actual density.

Resistance to weathering

The check on resistance to weathering can include various tests and examinations: petrographic description, identification of the presence of swelling clay, a boiling test to determine the resistance to wetting and drying and the presence (in volcanic rock) of signs of 'sunburn' (*Sonnenbrand*), freezing/thawing tests, and salt crystallisation tests.

Petrographic description should always be performed as the first stage to identify the presence of deleterious minerals and thus sensitivity to weathering. If the rock is suspected of containing clay minerals, a methylene blue test [6] may give definite answers on the presence of swelling clay or other possibly deleterious water-absorbent minerals. The effect of any such minerals can be ascertained subsequently by, for instance, a boiling test.

The number of samples to be covered by the petrographic description depends on the variation in the quality of the rock formation and the likelihood that it includes material susceptible to weathering. This likelihood has to do with the type of rock. Experience of rock behaviour in different conditions is also important. Visual assessment and the results of density measurements may give indications of the degree of quality variation.
In visual assessment it is particularly important to detect the presence of weathered rock and to correlate its location with the degree of weathering. The petrographic description can then be concentrated on suspect areas in the rock mass. This examination is generally carried out relatively infrequently, say once every two years. In subsequent analyses the survey can be confined to possible changes in comparison with the previous examination.
If cores from boreholes were examined in the first analysis, a single analysis now may suffice. On the other hand, rock sources with a relatively large variation in quality may need more frequent analysis.
The above observations on the frequency of petrographic description also apply to freezing/thawing resistance tests and salt crystallisation tests. Only one of these tests is carried out, depending on the conditions in which the stone is to be used.
The presence of sunburn in volcanic rock for instance calls for intensive testing. If this phenomenon is widespread throughout the entire rock source, it may prove impossible to select any useful stone. Generally the phenomenon is concentrated in certain zones, in which case an inspection of the blast pile generated in or near these zones is necessary. Quite a large number of stones will need to be tested to establish the exact location of the material susceptible to weathering. Generally only a small percentage of stones with sunburn is permitted in a batch. This too means that inspection involving tests on a large number of rock blocks is necessary. The criterion for acceptability may be that 20 specimens should be tested and none of these found to be affected. If one affected specimen is found, a further 20 must be examined, and the batch is accepted only if all of these prove to be sound. Such criterion should be based on an operating characteristic (Fig. 5).

Strength

The aspects of strength which are important for armourstone are resistance to crushing, to abrasion, and to breakage. The integrity of blocks, which determines resistance to breakage, is generally the most important strength property in heavy gradings, but no standard tests for integrity are in practical use except in France.

There are, however, various possibilities for ascertaining resistance to breakage of stone from a specific quarry. Earlier practical experience may be helpful, especially if supported by test data.

For large projects it is sometimes possible to obtain trial deliveries before supply contracts are concluded, in which case breakage resistance is studied by determining the mass distribution immediately after production and after delivery. It is important that the handling conditions should be as similar as possible to those during actual delivery. Tests on trial deliveries have the advantage of establishing the amount of fines produced, which can be taken into account in the design; and also give an indication of possible additional fining during working of the stone in the structure.

Drop tests can give an idea of breakage during handling of armourstone. The drop should be as faithful a representation as possible of the total influence of impacts due to handling. With a standard test, the result should be translated to take account of the actual conditions. Until standard tests are available in a European context, use can be made of French experience with the drop test and sonic velocity measurements [3] and the information in the CIRIA/CUR Manual [1].

Strength test need not be performed frequently. If there is no obvious variation in quality in the rock source, one test every two years may suffice. Changes in quality in the quarry face revealed by density tests and visual assessment may make it advisable to repeat the tests sooner. In visual assessment, it is particularly important to pay attention to discontinuities and flaws in the blasted blocks.

Resistance to breakage in the manufactured material can be influenced during production. This requires constant attention. Blocks with severe blast-induced and natural discontinuities, flaws and cracks which could lead to breakage are to be rejected. Blocks of dubious quality may be subjected to a drop during selection. The method of handling and storage may have a considerable influence on the amount of breakage. This should be considered in planning, and should receive constant attention during execution (see 3.2.2: 'Visually selected gradings').

3.2.2. Manufactured characteristics

Manufactured characteristics are properties which are determined wholly or largely by the production process. These include the particle size distribution of coarse gradings, the mass distribution of light and heavy gradings, and the shape of stones. Quality control therefore includes supervision, and adjustments and refinements in production and handling; this aspect is known as process control. The quality of products should be monitored at various stages of production and working, which calls for labour-intensive tests.

Mechanically produced gradings

Coarse gradings are produced mechanically, as are most light gradings. Mechanical production has the advantage that the particle or mass distribution of the product is relatively constant. This is less so when grizzlies (passive grids) are used. The screening efficiency of these grids is imperfect and may be unsatisfactory. It also depends very much on how the material to be screened is fed onto the grid. Continuous process control and intensive product control are therefore necessary.

With mechanically produced gradings, process control means constant attention, particularly in respect to breakage and wear of the screens, wear on the crusher, steady feed of material to the crusher and the screens, and the size distribution of the material to be processed. Breakage due to handling, and contamination with material from the floor of the stockpile, may cause inadmissible deviations from the grading specifications. It is therefore necessary to ensure that drop heights are limited, and to pay attention to the quality of the stockpile floor and the way in which stone is picked up from stockpiles. It may be necessary when collecting light gradings to carry out a secondary screening with a grizzly.

Product control concerned with acceptance may be fairly infrequent. With large batches a check may be carried out every 10000 to 30000 tonnes. Inspection of a coarse grading comprises measurement of the particle size distribution of at least six samples from a stockpile or a shipload, and at least three samples from a conveyor belt or falling stream. The mass distribution of a light grading is checked on a sample of which at least 200 pieces are not fragments. Depending on whether a static or non-static

batch is being examined, this sample is composed of at least six or three increments.
The samples should be as representative as possible. Particular attention must be paid to this in the case of stockpiles and shiploads, in view of possible inhomogeneity due to segregation or other causes. This problem can be avoided to some extent by sampling a batch during handling. When samples are taken from a stockpile, some material should first be removed before a sample is taken. During collection from a stockpile or discharging of a shipload, if the material lower down looks different from the material first examined, it may be necessary to repeat the inspection.

Visually selected gradings

Quality assurance for armourstone starts with the producer, with the drafting of production, handling and transport plans, because these affect the quality of the armourstone to be supplied. This applies in particular to breakage of blocks in heavy gradings.
From production to placing, armourstone may be subjected to many operations leading to breakage or contamination with other materials (fig. 6). Various factors involved in this are discussed below.

(i) Scale of project

For large-scale projects, transport is generally designed for large capacity and continuity of supply. This requires large vehicles and equipment and offers little opportunity for time-consuming inspection on arrival or dispatch, or for secondary selection.

(ii) Means of transport

In large-scale operations there is a higher risk of breakage. This is reduced if the stone is taken immediately from production to the project by wheeled transport and is then handled with grabs or cranes. Avoidance of tipping of truckloads places restrictions on transport capacity but considerably reduces the risk of breakage.
With wheeled transport the degree of breakage is influenced by the size of the loads, and by the method of tipping if this is practised. Tipping damage can be reduced if the truck tips the load onto stone which has been discharged previously. 'Roll on-roll off' pontoons offer the advantage that loading and unloading can be done from trucks and wheeled loaders.

The disadvantage here is the lack of opportunity for secondary selection, which grabs or cranes perform more or less automatically by leaving fine material behind (fig. 7). However, such an opportunity can be provided by loading the incoming material onto the pontoon by using a hydraulic machine with a grab. The need for this depends on the specifications laid down for the grading, and on the extent to which fining has occurred.
In loading material onto a ship, the drop height must be restricted. There is unlikely to be a risk of too great a drop height with very heavy gradings, as this would also damage the vessel.

(iii) Handling equipment
Wheeled loaders are attractive because of their handling capacity. By comparison with grabs, their disadvantage is the lack of opportunity for secondary selection, as already mentioned. They also pick up material from the substrate.

(iv) Stockpiles
Transferring material from one stockpile to another should be done as seldom as possible. Direct transport from production to the loading point, for example, gives better quality than transport via an intermediate stockpile in the quarry. To save space on the ground, stockpiles tend to be built up fairly high. This may cause stone to fall down when material is removed from the base of the pile.

As in the case of mechanically produced gradings, it is useful to distinguish two types of quality control: production control and acceptance control.

(i) Production control
The selection of narrow gradings requires some training. Accuracy of selection improves through feedback from test results. As an aid, specimen stones may be provided near the selection site. For feedback it is not necessary to carry out full tests in which every stone is weighed individually. It is often enough to weigh truckloads on a weighbridge. The average mass can be checked by this bulk weighing and by counting the number of stones. The range of the grading can also be roughly checked by weighing the stones evaluated visually as the lightest and heaviest.

Counting and weighing stones is a suitable inspection method for gradings heavier than 1000 kg nominal. It can be used to establish the average mass of partial or even full batches. The same method can also be used for lighter gradings, but in this case truckloads have to be tipped so that the number of stones can be counted. It should be borne in mind that stones with a low mass (less than ELCL) should not be included in the determination of the average mass (M_{av}), as they would affect the average mass measured by this method.

The client may require in the specification that the producer should check the mass distribution at certain intervals, using standard test methods. To provide feedback on selection it is advantageous to carry out this check on the material immediately after production. However, the mass distribution will change between that moment and delivery, through breakage during handling. The extent of this change will need to be researched. Breakage can be compensated for by maintaining a certain margin over specified minimum limits during production. An alternative is secondary selection during loading to exclude broken-down blocks.

(ii) Acceptance inspection

On the face of it, it would seem sensible to carry out acceptance control at the time of loading for transport to the construction site, because rejection after delivery can involve considerable cost and may delay work. On the other hand, such timing may disrupt operations if, as is generally the case, all the available manpower, transport and handling equipment are being used to achieve rapid loading. Another possible time for inspection by or on behalf of the client is immediately after production. This would also act as a check on the producer's production control. The research into breakage already mentioned should certainly be carried out at this point. Inspection by the client could also take place immediately before loading, if the material to be loaded is waiting at the dispatch site. Inspection from a stockpile offers limited possibilities, however, since only the material on the outside of the pile is accessible. A genuinely reliable inspection by the client at the production and dispatch site is not feasible for various reasons, and would involve the risk of shifting responsibility for quality from producer to customer. The time of delivery, when the material arrives at or near the construction site, will remain the official time to decide whether the producer has complied with the

specifications.

For non-routine projects, in any event, it is essential in practice for the client to be involved in inspections during production and until dispatch. The absence of a tradition of effective quality assurance for armourstone means that communication between the parties involved is indispensable. From the foregoing it is clear that acceptance control after delivery is necessary. This will always include visual inspection. Control tests should be carried out at random, or on the basis of results of visual inspection.

(iii) General guidance for quality control of block mass

The confidence that can be gained by testing about the actual form of the mass distribution depends mainly on the frequency of test weighings, the representativeness of the samples, the size of the samples and the accuracy of weighing. Weighing accuracy may be roughly 1-2%. The size of the samples determines the fundamental error [5]. This error is a function of the degree to which the limited sample can represent the population, which in turn is a function of the variation of stone properties within the population. An example for a grading of 1000-3000 kg based on weighing 200 or 100 blocks is given in table 1.

Property	Real value	95% confidence interval	
		200 blocks	100 blocks
<ELCL (650 kg) %	0,0		
<LCL (1000 kg) %	7,5	4,8 - 10,2	3,6 - 11,4
<UCL (3000 kg) %	80,0	72,2 - 87,8	69,0 - 91,0
<EUCL (4500 kg) %	98,0	94,8 - 100,0	93,5 - 100,0
average mass (M_m) kg	1764	1648 - 1880	1601 - 1927
M_{50} kg	1910	1760 - 2100	1705 - 2200

Table 1 Fundamental errors for a grading of 1000-3000 kg.

Shape of blocks

The shape of stones from mechanical production can be influenced to some extent by provisions in the crushing and screening equipment. If necessary, the accuracy of visual selection can be improved by sample blocks marked with aspect ratios. In practice the shape control test can be carried out

on the same blocks used for tests on particle or mass distribution.
In performing a test on block shapes, only those blocks which appear to the eye to be on the borderline of the required shape need be measured. If the specification states that no blocks are allowed to exceed a certain aspect ratio - a tight requirement - checks during production should include measuring all blocks that appear possibly to exceed that aspect ratio.

3.3 Practical Experience

3.3.1. Standard specification clauses in the Netherlands

In the Netherlands standard specification clauses are used for delivery of stone for hydraulic structures. These clauses were drawn up in consultation between clients and contractors, represented on an equal footing in and *ad hoc* body.
The clauses refer to Dutch standards for quality requirements, sampling and test methods.
The specification clauses on quality control comprise four main elements: a preliminary examination, control by or on behalf of the contractor during production, control by or on behalf of the management (client) during production, and acceptance controls on delivery.
The preliminary examination comprises an inspection by or on behalf of the producer, followed by release by the management for delivery from the quarry in question. The inspection takes the form of internal control of all applicable quality requirements. The data should be no more than two years old. The main purpose of the preliminary examination is to demonstrate that it is possible to supply material of the desired quality.
Control during production concerns the manufactured characteristics. These control requirements generally apply to large deliveries. The frequency of control is stated in the specification.
Acceptance control on delivery is carried out by or on behalf of the client. The contractor will assist in taking samples, and in transporting the samples if necessary.
Checks on particle size distribution or mass distribution, the shape of the stones, and any contamination may be carried out within a specified time before discharge of a shipload begins.

In practice these specification clauses provide a broadly satisfactory method of quality control. However, clients' casualness in enforcing the clauses, including the standards, does detract somewhat from ideal performance.

3.3.2 The Storm Surge Barrier in the Eastern Scheldt

Some 5 million tonnes of armourstone was supplied between 1980 and 1986 for the construction of the Storm Surge Barrier in the Eastern Scheldt. Large deliveries came from five quarries in Finland, Sweden and Germany.
The gradings ranged from 5-40 kg to 10000-15000 kg. Before the supply contracts were signed preliminary examinations were carried out. These included trial deliveries, in which the breakage of the stone during handling was studied.
The contracts contained requirements for density, durability, crushing strength, mass distribution and shape of the stones, and also for discontinuities. The specifications for mass distribution after delivery were somewhat less stringent than those for control in the quarries, to allow for breakage.
Continuous monitoring of the specifications by the producers was stipulated. The producers' quality control was verified by having an independent body carry out control during production.
A specific component of the control provided for frequent testing of small samples, the results of which were totalled and evaluated every 12 weeks. The producer was required to check the density of 10 blocks and the mass of at least 10 blocks in every week of production. The test results were totalled up over periods of 12 production weeks (fig. 8). If the requirements were not complied with, and depending on the number of periods of non-compliance, a warning was given, followed successively by a small or large price reduction, and eventually the option of terminating delivery.
When shiploads arrived the material was inspected visually, and the mass distribution checked if necessary, by or on behalf of the client. The results were as follows.

During the order acquisition and production planning stages the producers were not sufficiently aware of the requirements for quality assurance, or of their consequences. These consequences related to cost, integration of

the quality plan into the production and transport plans, and organisational preparation.

An industrial enterprise with no experience in the production of armourstone was most successful in adapting rapidly to the quality requirements and the system of control.

Intensive consultation at an early stage between all the parties involved in production, transport, and quality assurance were seen to be necessary to ensure the success in quality terms of a non-routine order. Coordination of production, transport and handling with quality proved highly important here. As a result of the large scale of the handling operation and the need to establish stockpiles in the quarry and at the dispatch point, there was a good deal of breakage during the supply stage: with resistant types of rock the measured reduction in M_{50} was 5-10%. The susceptibility to breakage of light gradings and very heavy gradings was less than that in the intermediate gradings such as 300-1000 kg and 1000-3000 kg. In the case of light gradings this was due to the lower number of discontinuities in the stone on account of their smaller size, and possibly to the less severe impacts on the material, since single blocks were subjected to more handling.

It was apparent that the demand for continuity of supply of large quantities of materials in large-scale projects may tend to reduce concern for quality.

The cost of quality assurance amounted to 2.75% of the supply costs for armourstone. The costs were divided among the parties as follows: producers 60%, client 13%, and independent inspection body 27%. The return on the quality assurance was described as high.

3.4 Conclusions

Practical experience with quality assurance for armourstone has led to the following conclusions.

(i) Quality and quality assurance for stone for hydraulic structures can be coordinated with engineering requirements in a scientifically sound manner. Excuses for defective quality on the grounds that armourstone is a 'natural product' are untenable.

(ii) The case for quality assurance is an economic one. In general the return on the effort expended in quality assurance is underestimated.

(iii) Quality assurance of armourstone should be based on an understanding of risk, sampling and testing.

(iv) Regulations on quality specifications, test methods and contractual obligations require further development.

(v) An exchange of information between all parties is necessary in order to speed up the development of quality assurance.

(vi) Import and export of stone for hydraulic structures require the development both of international quality standards and of internationally accepted rules for quality assurance. These can be based on existing general standards [7].

REFERENCES

1. CIRIA/CUR (1991). Manual on the use of rock in coastal and shoreline engineering.

2. Niese, M.S.F. (1988). Classification of large armourstone using an acoustic velocity analysis method. Memoir of the Centre of Engineering Geology in The Netherlands, No. 65. Delft University of Technology.

3. LCPC (1989). Les Enrochements. Paris: Ministère de l'Equipement, du Logement, des Transports et de la Mer, Laboratoire Central des Ponts et Chaussées, 107 pp.

4. Afnor (1990). Essai Deval, P. 18-577. Essai d'usure micro-Deval, P. 18-572.

5. Gy, P.M. (1979). Sampling of particulate materials: theory and practice. Amsterdam: Elsevier, 431 pp.

6. Stapel, E.E. and Verhoef, P.N.W. (1989). The use of the methylene blue absorption test in assessing the quality of basaltic tuff rock aggregate. Engineering Geology, 26, 233-246.

7. EN 29000 (1989). Quality management and quality assurance standards - guidelines for selection and use. Related standards: EN 29001-4.

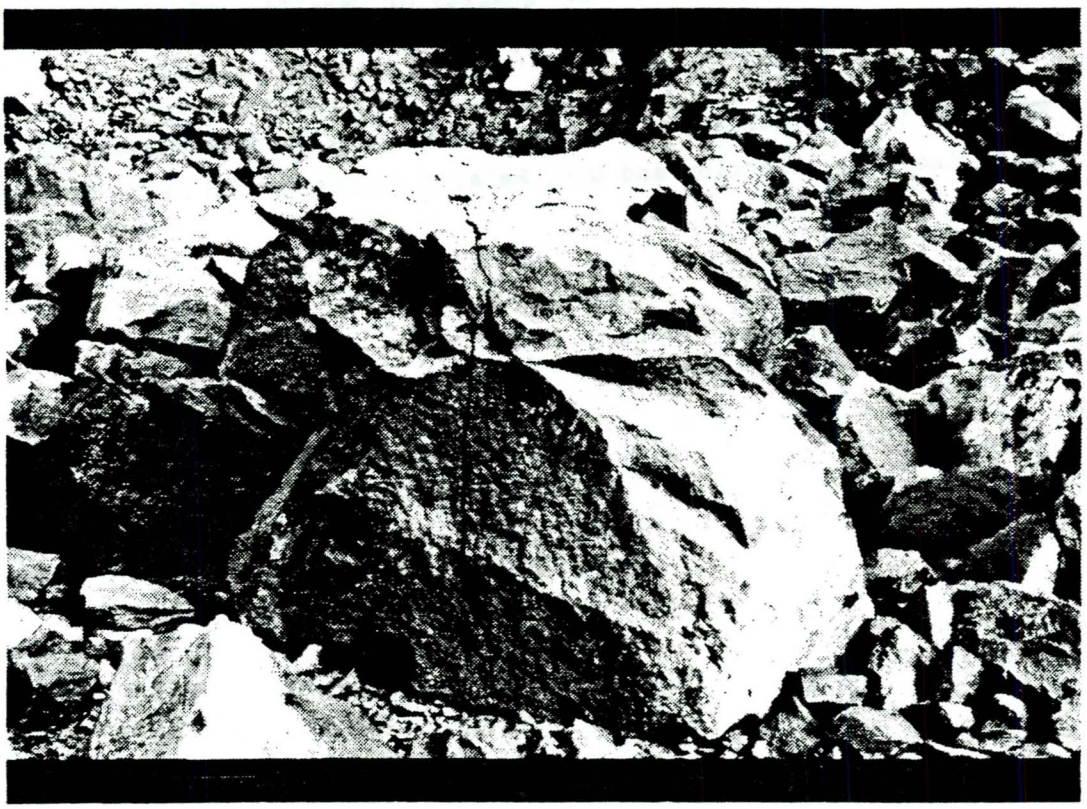

Figure 1 A block of poor integrity

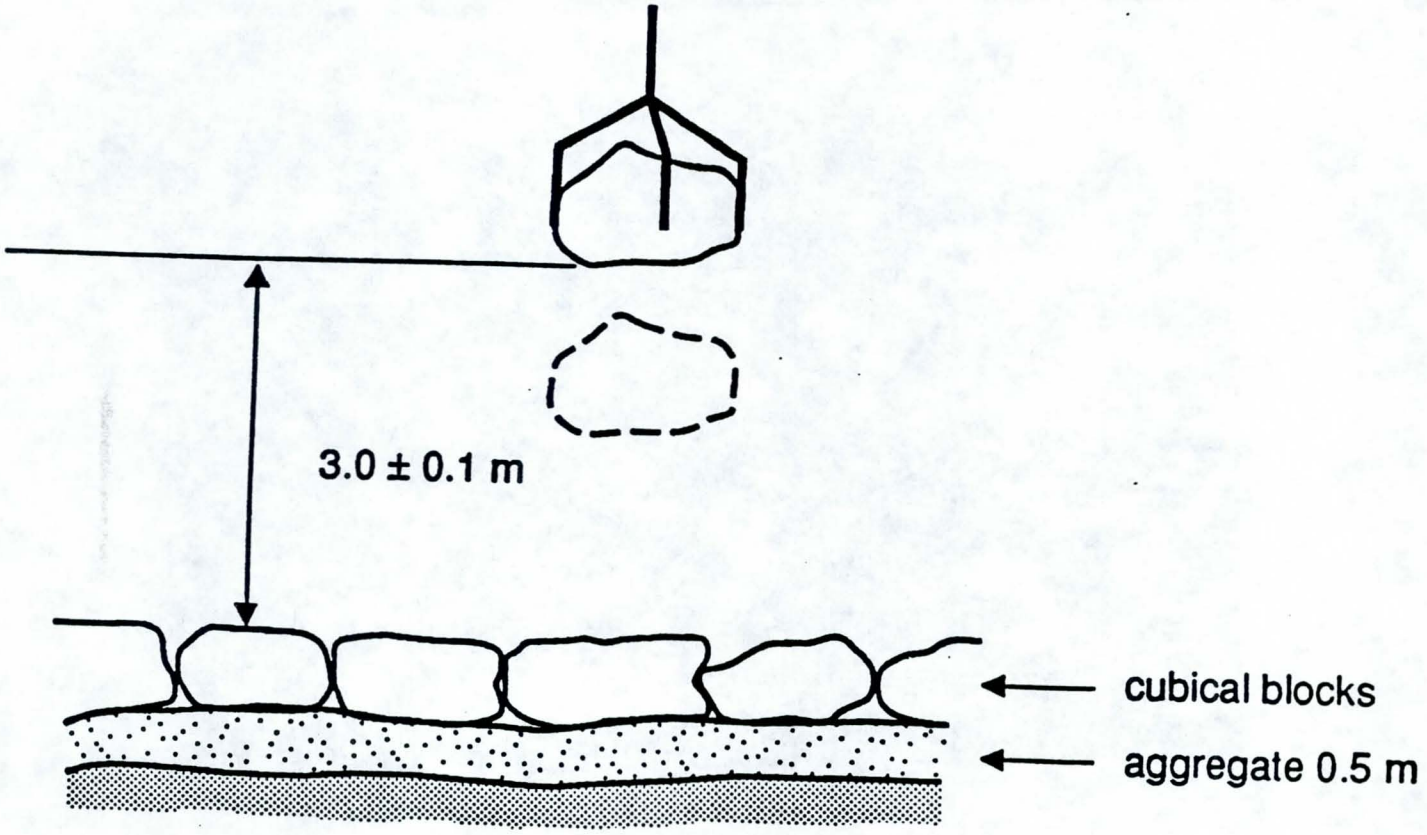

Figure 2 The proposed drop test

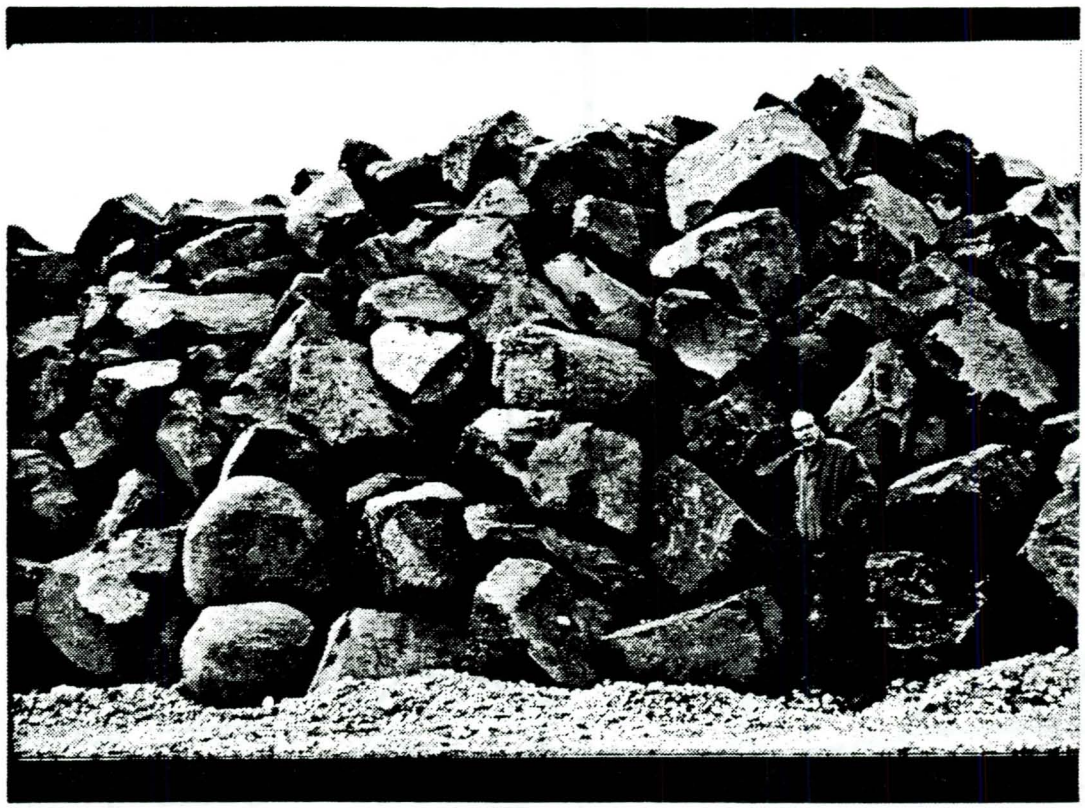

Figure 3 Grading 1000-3000 kg

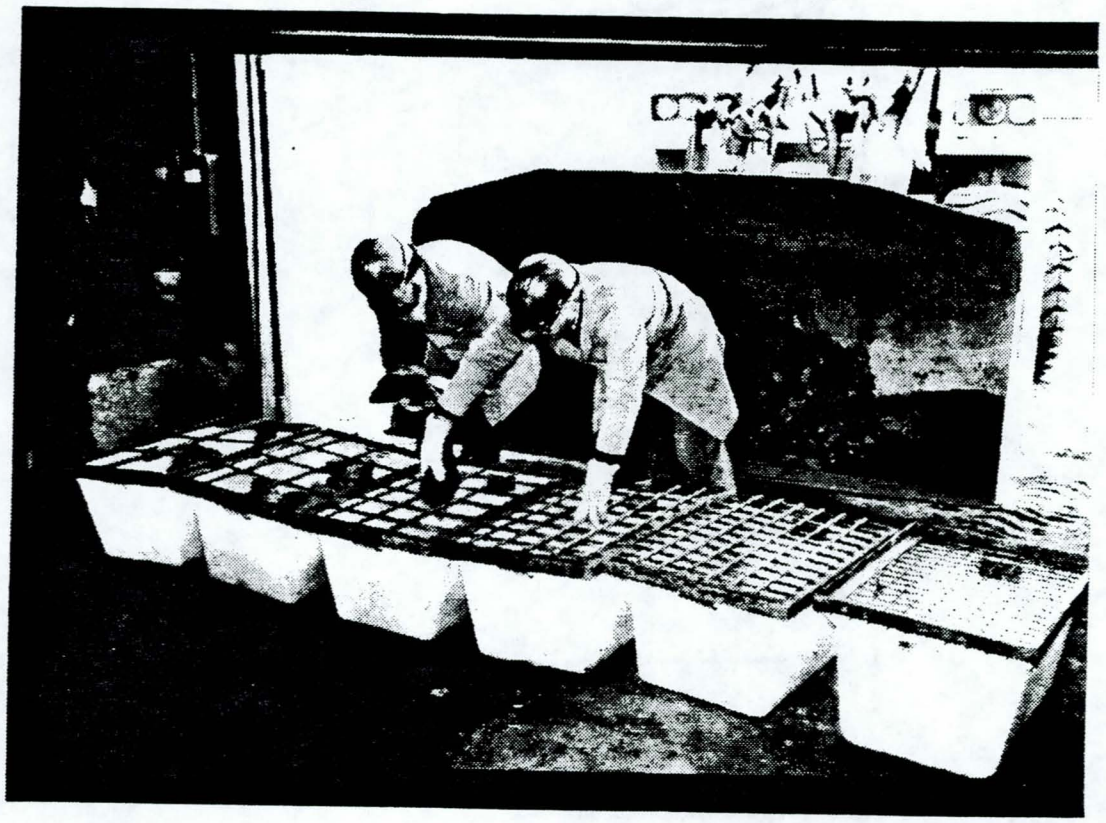

Figure 4 Sieve test on a coarse grading

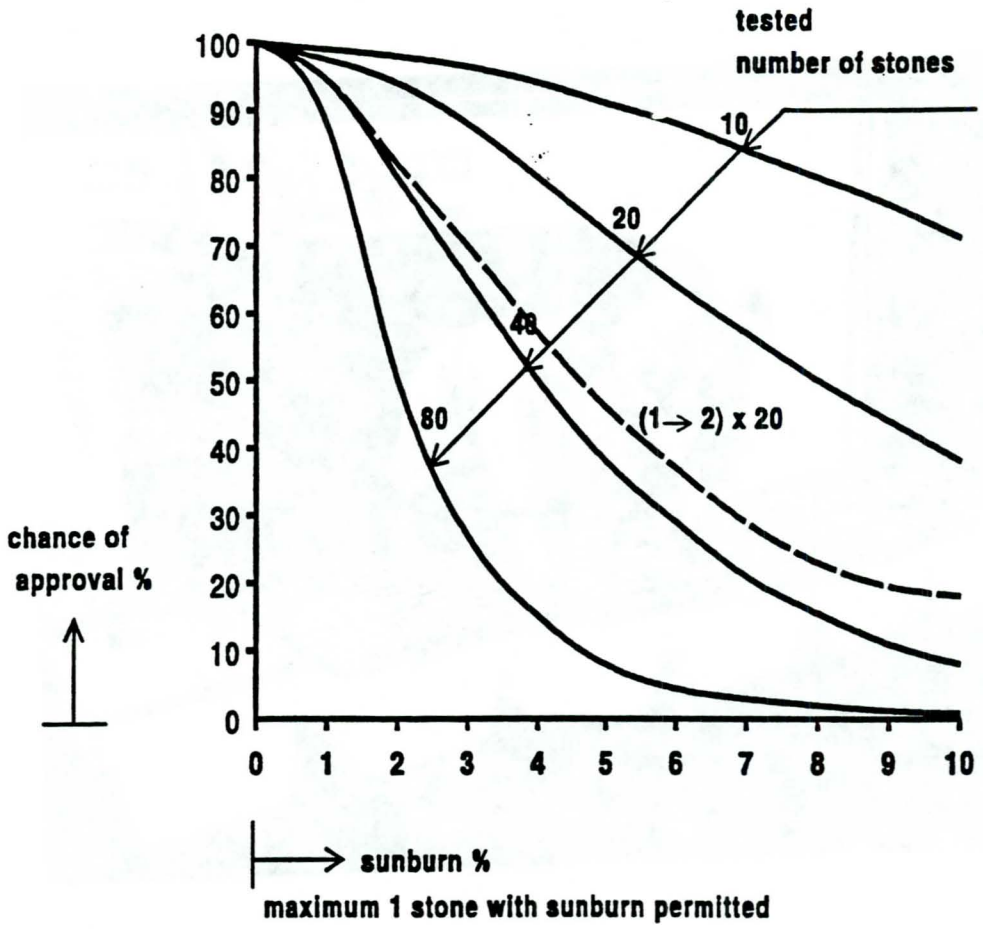

Figure 5 Operating characteristics for testing on sunburn

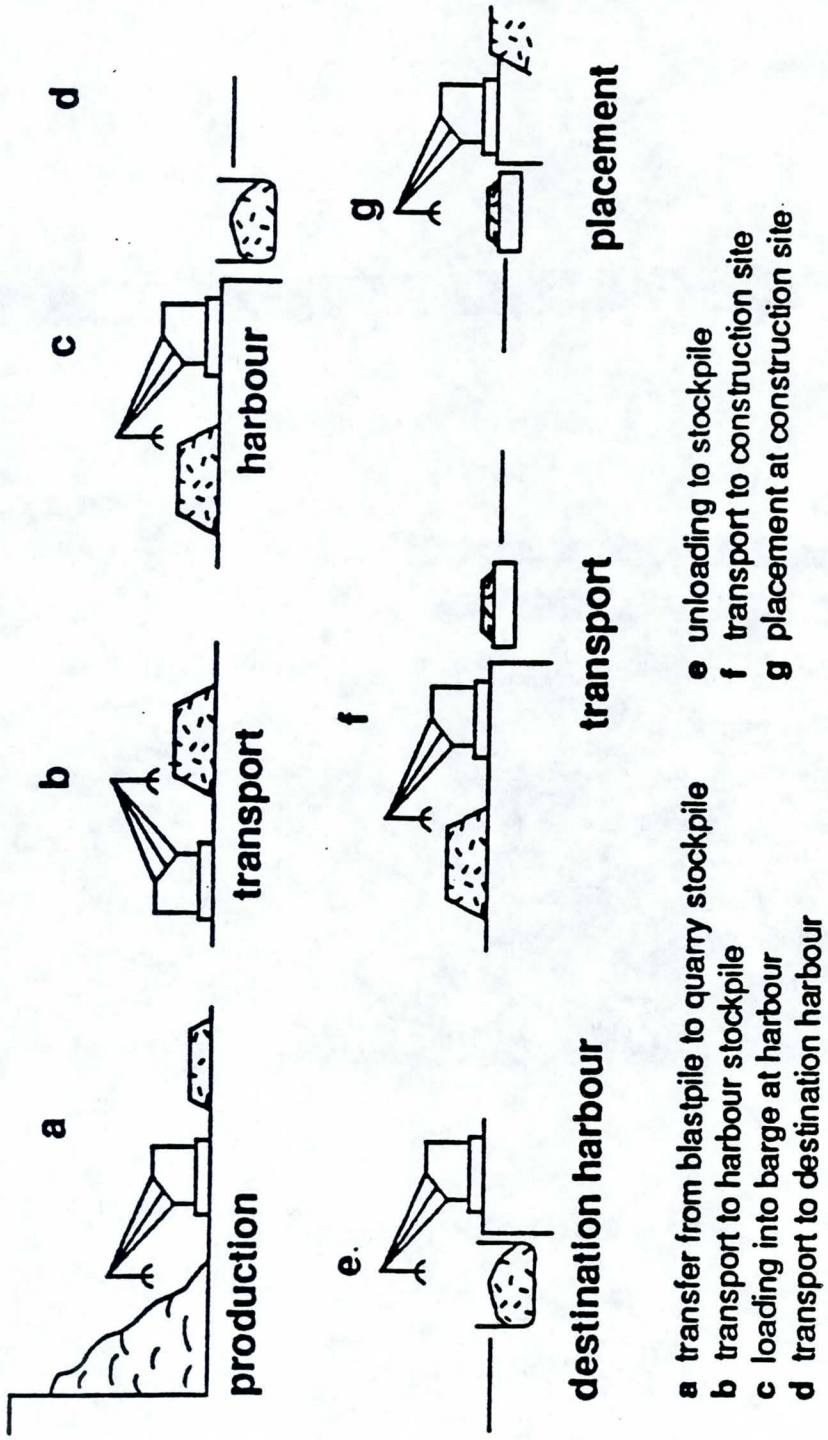

Figure 6 Phases of transport and handling

Figure 7 Fine material left behind during unloading

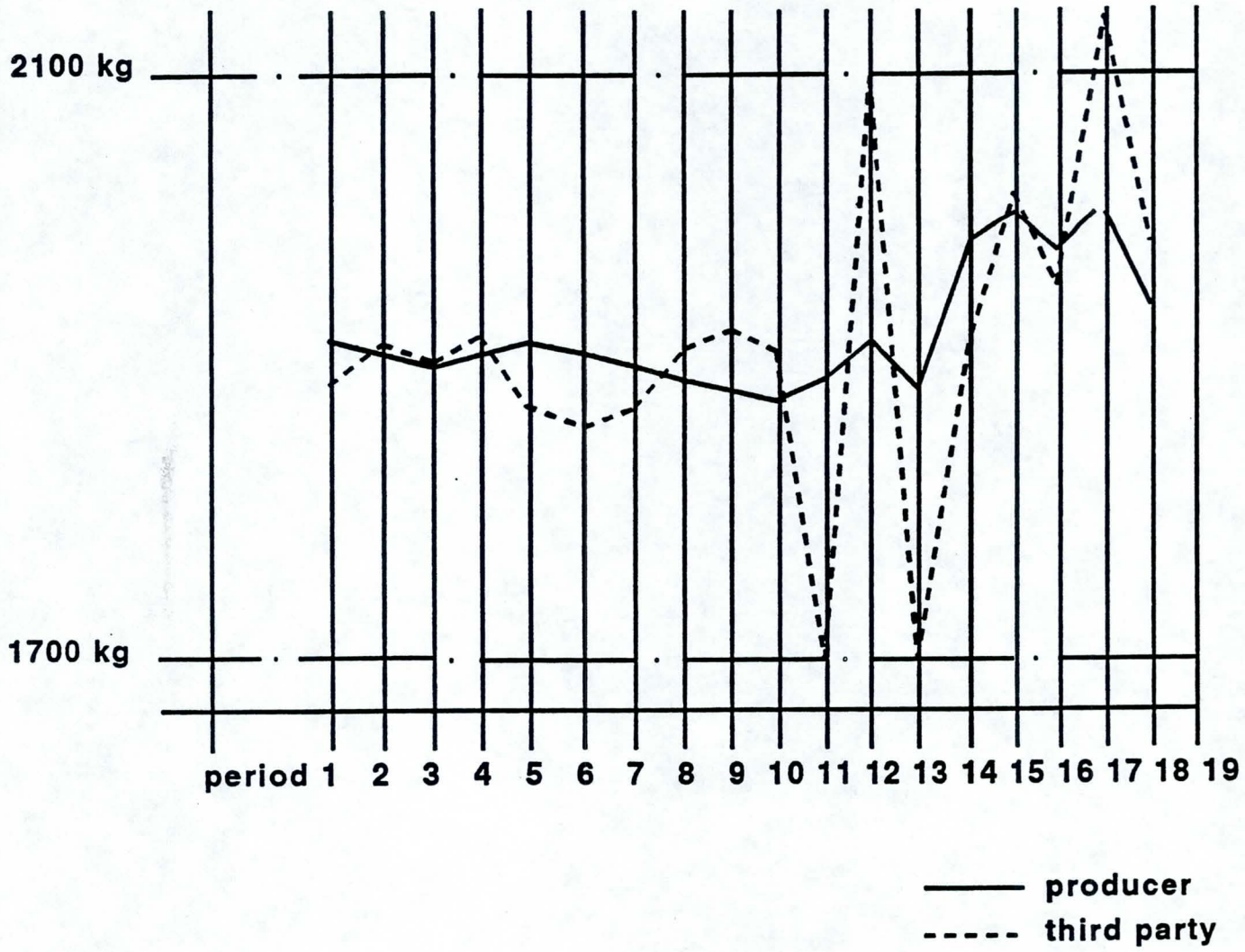

Figure 8 Results of mean mass measurements for a grading 1000-3000 kg

DURABILITY INDEX FOR PROTECTION STONE: A CONCEPT

R.J. Larson and G.A. Nicholson
US Army Engineer Waterways Experiment Station

Prediction of protection stone durability and longevity currently relies, for the most part, on the results of index tests. Such tests attempt to model either conditions causing stone failure (e.g. freeze/thaw) or measure engineering properties thought to be related to stone performance (e.g. rock strength). Selection of protection stone based on this approach is deficient in several respects. First, there is no prescribed recipe of which set of tests to conduct for varying site conditions nor do the tests directly account for differing environmental conditions. Second, the tests do not directly account for geologic features present in many rock (e.g. distance between weak bedding planes) or the size and shape of the quarried stone. Finally, the method of quarry excavation and handling (i.e. transportation and emplacement practices) are seldom addressed in the selection process. In this respect, the U.S. Army Engineer Waterways Experiment Station is currently conducting research to develop a Durability Index for selecting protection stone. Conceptually, the index system will consist of key index tests that provide a combined quantitative base index value intended to measure stone quality. The base index value will then be adjusted to account for differing environmental and geologic conditions as well as differing stone excavation and handling processes. Finally, the adjusted index value will be integrated with performance/longevity criteria developed from case histories to provide the final Durability Index.

THE DROP TEST FOR ARMOURSTONE INTEGRITY

J-P. Latham
London University, Queen Mary & Westfield College,
London E1 4NS, UK
G.A. Gauss
Martindale, Penrose, St. Ervan,
Wadebridge, Cornwall, UK

Abstract

The background to the subject of armourstone block breakage is presented. The particular problems of specifying the real strength of blocks for coastal engineering is tackled using an objective direct method -- the drop test. The CIRIA/CUR (1991) drop test method is outlined and recent applications of this test to three rock sources are described. A detailed account of the test on Larvik armourstone is given whilst Carboniferous limestone from both the Mendip and Calais regions of UK and France are mentioned briefly. The analysis of drop test results examines the shift in the cumulative weight distribution curve of 50 blocks before and after they are subjected to a standardized fall of 3 metres. The drop test breakage index, defined in the CIRIA/CUR (1991) drop test, is shown to be an unsuitable index and a number of alternatives are defined which show more promise for discriminating block integrity.

1. INTRODUCTION

1.1 Background

Massiveness, density and durability are the most essential properties of armourstone that the designer will seek to control. Indeed, massiveness and density appear directly in design equations for stability. Armourstone massiveness, and its ability to interlock when in service in armour layers, will be seriously and rapidly reduced during handling, transportation, placing, and in service if the rock is essentially of a weak mineral fabric and poor durability for the engineering environment to which it is subjected. Fortunately a number of tests are available to assess this potential for progressive breakdown or wear.

This paper is, however, addressed to a somewhat more dramatic process of size and weight reduction of armourstones -- that which accompanies the sudden or progressive splitting of blocks. This form of breakdown presents a much more difficult phenomenon to predict and control by means of objective test methods, not least because of the sizes of the blocks that would be involved in determining the real resistance to breakage of full-sized armourstone blocks. Neither can the full-sized strength be reliably extrapolated from hand-sized specimens because of the unsystematic strength-scale effects for different rocks.

Not only do blocks crack in transit to site, causing a reduction in average weight and the production of mostly unusable fragments, but cracks may open up on the structure while in service. Citing the worst case of structures maintained by the US Army Corps of Engineers (USACE) in which an alarming 33% and 40 - 50% of outer layer stones were cracked, Ward (1992) discussed the planning of a physical model testing programme, to be commissioned by the USACE, in order to investigate the influence of broken blocks on the stability of armour layers. This proposed flume study, believed to be commencing in 1993, was considered necessary in order to compare the risks of failure with the costs of replacing blocks that have cracked open. Currently, the detrimental effect of broken blocks on stability is poorly understood and remains to be proven for different proportions of cracked blocks in the layer.

There is nonetheless, a general consensus of opinion that the costs of controlling and preventing cracked blocks from reaching the structure is money well spent. Laan (1992) noted that during a test delivery of 6 to 10 tonne armourstone, the 50% passing weight, W_{50}, dropped by nearly one tonne due to rough handling and transport by barge. Such reductions of W_{50} of 10 to 20% are certainly unsatisfactory and clearly indicate unacceptable block integrity.

As discussed repeatedly at the workshop on Durability of Stone for Rubble Mound Breakwaters, held in Cleveland, Ohio in May 1991, the Great Lakes area of North America has experienced considerable problems with major block breakages due to poor integrity i.e., those termed type 2 breakages below. In this area, the high incidence of cracked blocks seen within armourlayers is partly in consequence of the local necessity of using relatively weak, porous or microporous sedimentary rocks which are sometimes of marginal quality (typically dolomitic limestones are most problematic). This is compounded by the severe freezing winter climates. However, more important perhaps are the weakness planes such as blast induced cracks and geological flaws, including stylolite seams, sedimentary structures and weakly cemented veins or joints. These fragile blocks with poor 'integrity' or 'wholeness' resulting from cracks and geological flaws often go undetected during quality control and almost certainly contribute to most of the cracks seen on breakwaters; see for example Marcus (1992), for an account of experiences with cracked blocks in the Buffalo district.

Lutton and Erickson (1992) reviewed the sudden and progressive nature of throughgoing and pervasive cracking phenomena in the Great Lakes area. They summarized the following causes of cracking deterioration within blocks as: stratification and joints, quarry damage (i.e. cracking resulting from use of high shock energy explosives and blast designs typical of aggregates' production), ineffective quality control, construction damage, stress relief and pore-water freezing.

Clark and Palmer (1991) illustrated some examples of igneous and metamorphic armourstone blocks delivered to the UK from Scandinavia where at one stage 25% of blocks were deemed to be of unsatisfactory integrity or shape on arrival at site with significant cost implications to the contractor. Many of the unsatisfactory cracked and flawed blocks could probably just as easily have been rejected on visual criteria at the quarry. However, the subjectivity of visual criteria remains a potential source of contractual problems. Before considering how specification clauses are used to control block integrity, it will be helpful to briefly discuss the types of breakage phenomena.

1.2 Types of breakage

Breakage of armourstone often occurs during handling, and apart from occasional crushing and bruising, experience suggests there are two extreme types of breakage.

Type 1 breakage: blocks break into major pieces along cracks and geological flaws;
Type 2 breakage: blocks break along new fractures through the mineral fabric of the rock. Usually this results in edges and corners of insignificant weight being knocked or sheared off.

In general, for large pieces of rock, the possibility of major flaws is increased and their overall resistance to breakages is likely to be reduced, the intact strength of the mineral fabric being less significant. For riprap and armourstone blocks greater than about 50 kg or 300 kg (depending on the discontinuity pattern in the quarry), type 1 breakage is more common. Cracks and geological flaws in armourstone blocks that are likely to lead to whole block failure, constitute a major problem for quality control as subjective assessment criteria still prevail.

Type 2 breakages, which often result in rounding during bulk handling, can be minimised or kept within acceptable limits by using rocks which exceed a minimum intact strength as given by fracture toughness (ISRM 1988), compressive, tensile or point-load strength (ISRM 1985) test results. Intact strength tests on hand-sized specimens are usually preferred to aggregate strength tests because of the poor performance during testing of many excellent coarse grained igneous rocks. (Further explanation of block integrity and intact strength tests such as fracture toughness and point load strength are given in CIRIA/CUR, 1991). The two extreme types of breakage behaviour require that both the intact strength of the mineral fabric and the block integrity should be assessed for contract purposes.

1.3 Specification of resistance to type 1 breakage

The prevailing approach in the USA and most of Europe is to include qualitative statements that outline what is or is not acceptable stone and to have quality control inspectors at the quarry and/or job site (e.g. see Marcus 1992; BS 6349, 1984). That the acceptance control is to be at the job site should be clearly stated because of possible transit damage. Such acceptance clauses are well known to contractors. They typically state that 'the stone shall be free from detrimental cracks, seams and other defects that could lead to breakage during handling and/or placing'. These may be supplemented with other more objective clauses such as that the stone is to be stockpiled in the quarry for a set period, for example 90 days, before delivery. The problem is that all qualitative statements regarding integrity require judgements to be made about the seriousness of cracks and flaws. In general, poor integrity blocks can be eliminated on visual inspection given both sufficient time and experienced inspectors. Sometimes, however, the most serious flaws are so fine as to be invisible to the eye whilst in contrast, the most obvious veins may constitute no significant weakening so that the rejection of blocks can be disputed even amongst experienced geologists.

The often quoted simple practice of 'proving' the integrity of blocks by rough handling in the quarry prior to selection can unfortunately also lead to excessive and unnecessary damage to blocks and therefore cannot be recommended for general practice. Dropping suspected weak or cracked blocks off the back of a lorry (Fookes & Poole, 1981), or using a more controlled set of drop conditions than this, remains a practical rejection method for individual suspect blocks. But, for specification purposes, the individual testing of subjectively selected marginal blocks is not likely to gain future acceptance and more objective methods representative of a given source will no doubt have to be developed.

1.4 Objective tests for type 1 breakage

For a given production method and source of rock there will tend to be a characteristic degree of fragility or expected amount of breakage for any given large scale handling operation. This degree of fragility, or resistance to type 1 breakage, if defined in a practical and meaningful way, is of great interest to the designer, for example:

(i) for comparing the large scale strength of different sources;

(ii) for predicting likely changes to the weight distribution as supplied at the quarry and as available for construction on site;
(iii) for predicting amounts of undersize or unusable fragments.

Test methods available for assessing representative samples of armourstones may be divided into the indirect methods (e.g. non-destructive, such as sonic velocity methods) and direct methods (e.g. direct full-scale impact testing - the drop test methods). Some considerable progress has been made in France and Holland (LCPC 1989, Niese et al. 1990) with the indirect methods.

The French method operates on the principle that sonic velocities measured in a full-scale block will be reduced by the presence of cracks and flaws from the values expected or measured for a typical unflawed hand-sized specimen of the same rock. Only three perpendicular velocity measurements are made per block and the degree of cracking is assessed by normalising these values relative to the hand specimen values, or even the theoretical velocity calculated using the known sound velocities of the individual minerals and their proportions obtained from petrographic analysis.

The Dutch method relies upon taking between 10 and 20 velocity readings per block and analysing the velocities using two statistical parameters of the velocity distribution. The first is to account for the possible spread of results; this will be wider when several low velocities, associated with poor acoustic coupling across cracks and flaws, are intersected. The second is an averaged velocity for the block which is used to normalize the first parameter, and thus provide a comparative index for all rock types that may have fundamentally differing sound velocities due to their mineralogy.

Although the sonic velocity method is reported to be in use in France for assessing integrity of armourstone, further research and experience is needed to correlate these methods with performance such as might be measured by drop testing. The question of how many blocks are to be tested for a sample evaluation to be representative of the source and how often a source should be tested for integrity must also be tackled.

2. DROP TESTING - CIRIA/CUR METHOD

2.1 Introduction

Until the publication of the CIRIA/CUR Rock Manual (1991), there had been no suggested objective test method for the direct measurement of block integrity or fragility that could be used in contract specifications, inspite of LCPC's (1989) reference to a drop test suggested for calibrating sonic velocity methods. A test method for the determination of the drop test breakage index was recently given in the Rock Manual where the relative lack of experience with this new test method was remarked upon openly. Early experiences with this particular test method are now presented below.

2.2 Summary of Determination of the Drop Test Breakage Index (CIRIA/CUR 1991, Appendix A2.11)

By chosing a large number of representative armourstone blocks with known weight distribution, subjecting each one to a 'standardized drop' and determining the new weight distribution of the fallen blocks, it is possible to obtain a measure of integrity (or fragility) by comparing statistical parameters such as W_{50} from the initial and final weight distribution.

The sample contains 50 pieces taken at random from above the extreme lower class limit (ELCL) of the grading class in question. The CIRIA/CUR class limit system for defining standard gradings may be illustrated for a 6 to 10 tonne grading as follows:

> 97%	by weight must be lighter than 15 tonne
70 - 100%	by weight must be lighter than 10 tonne
10 - 30%	by weight must be lighter than 6 tonne
< 2%	by weight must be lighter than 4 tonne

In this example the four class limits: EUCL, UCL, LCL and ELCL are 15, 10, 6 and 4 tonnes respectively. All blocks and pieces in the grading that are less than the ELCL weight of 4 tonnes are termed the 'fragments'.

The drop is to be executed by a suitable hydraulic grab (e.g. orange peel type). Weighing equipment should be accurate to 2% of the ELCL. The bed of rocks receiving the falling blocks is to made of blocks of the same grading as the sample to be tested and a 0.5 +/- 0.05 m thick bed of crushed rock aggregate is layed to support this bed of rocks.

The individual weights of the rock sample are determined according to the CIRIA/CUR test for weight distribution. Each block is subjected to a fall height of 3 +/- 0.1 m onto the bed of rocks and qualitative results recorded. After the drop, each block is removed together with any broken pieces. All resulting pieces greater than, or close to, the ELCL weight are set aside for further individual weighing to an accuracy of 2% of the LCL weight.

The cumulative weight distribution is calculated for blocks and pieces heavier than the ELCL both before and after the drop testing and the drop test breakage index is calculated from the percentage change in the 50% passing weight.

2.3 Available data

The authors were aware of three full data sets which yielded drop test results. The test at Larvik Quay was the most extensively documented and includes qualitatitive observations. It is described in detail below, followed by brief accounts of two tests on different Carboniferous limestones.

3. THE DROP TEST AT LARVIK QUAY

3.1 Armourstone stocking operations at Larvik

Larvik armourstone is obtained from two sources in the Larvik area known as Tverdal and Tjolling. Both areas produce dimensionstone blocks exported for cutting and polishing which often eventually are sold for ornamental uses and for cladding of buildings. Extraction of stone is by wire sawing and by closely spaced drilling with low velocity pre-split blasting to define rectangular prismatic dimensionstone shapes. The Tverdal rock is a homogeneous light to medium grey coarse grained (~10mm) igneous rock usually classified as syenite because of its characteristically high feldspar content. It exhibits the schillerization effect producing the attractive blue colouration to a greater or lesser degree which in turn determines its quality class as a dimensionstone product. The Tjolling area produces dimensionstone blocks of another distinctive but altogether darker more coarsely crystalline (~15mm) syenite with similar schillerization effects usually best seen on cut surfaces. From the point of view of supplying armourstone from dimensionstone rejects, the Tverdal and Tjolling areas operate on a similar scale and in very comparable ways. These are the only two quarry areas said to have supplied armourstone material to the Larvik Armourstone quayside operations; it was stated that for any 10,000 tonne consignment over the last 3 years, the proportion of material from Tverdal has ranged from one to two thirds of the total.

Blocks arriving at the quayside are of known weight, as recorded from the weight indicated in the loading machines during selection in the quarry areas. They are unloaded and placed in appropriate piles usually 3 to 4 blocks high. These stockpiles were found to be well ordered over a large stocking area, reasonably accessible and classified into weight ranges of only 1 tonne. Beginning with a 3-4 tonne class, successive piles were inspected with classes rising to 11-12 tonnes. Larger blocks

could also be seen in other piles. This stockpiling arrangement is of considerable practical benefit as it enables blending to produce specific or standard gradings and allows colour coding for extra control during construction if the client so wishes. Quality control by rejection of blocks with poor shape or integrity can be applied at a later stage during the loading of barges, but judging from the stockpiles, this proportion would normally be less than 5% and rejected due to shape rather than integrity.

Two machines were seen operating together most effectively; a Komatsu 500 of 16 tonne capacity and a CAT 988 of 30 tonne capacity, both fitted with fork-lifts and able to pass blocks to each other to speed up the weighing and drop testing.

3.2 Sampling

The 50 block sample was selected so as to represent the distribution and range of sizes considered likely to be dispatched in a consignment of the 6-10 tonne standard grading. The distribution was as follows.

6-7 tonne stockpile	10 blocks
7-8 tonne stockpile	15 blocks
8-9 tonne stockpile	15 blocks
9-10 tonne stockpile	10 blocks

The ratio of Tverdal (Tv) rock to Tjolling (Tj) rock was found to vary in the stockpiles, with a larger proportion of Tj in the piles containing stones above 9 tonnes and a notebly larger proportion of Tv in the 6-7 and 7-8 tonne piles.

From a 'walk-over survey', the top and back areas of these four stockpiles were compared visually with the blocks in the accessible parts at the front; no significant differences were noted. The homogeneity within Tv blocks and within Tj blocks was remarkable although a small percentage, perhaps 1-3%, of the Tj blocks appeared to have significant signs of weathering indicating a possible reduction in strength. Very few blocks appeared to have flaws, these being the occasional crack or vein.

The appropriate number of blocks were chosen at random from each stockpile by selecting and numbering every third block on ground level and working back along the second level if necessary to obtain the required number.

3.3 Floor Preparation

Conditions of the substrate and floor blocks at the quay in preparation for the test were reported to be from the top down:

15 tonne floor block(s).
0.2m of 4-8mm chippings
0.5m of 150-350mm bedstone blinded with 0.1m of fines
bedrock.

These conditions vary in minor details from those stated in the CIRIA/CUR test procedure. A ramp was prepared for the CAT to drive up so as to give the extra height and control over the correct drop position (Fig. 1). For the first 25 drops, using 6-8 tonne blocks, only one floor block was used (Fig. 1). With the second 25 drops, two new square sectioned floor blocks were pushed into position to make a wide flat platform so as to prevent falling blocks from landing on corners of floor blocks (Fig. 2). These floor blocks sustained no damage until block 50 when one of them split vertically in two (Fig. 3). (Note there are very few chippings surrounding the floor blocks after completion of the drops. Broken pieces of one tonne or more were taken for weighing and piled elsewhere.)

3.4 Drop height control and block release

It was, unfortunately, not possible to obtain an orange-peel type grab locally for use in the planned drop test. Experience was gained with dropping blocks from forks by practising with some ten blocks prior to the test since accuracy with height and aim was important.

A rope was attached to the back of the forks such that a knot would just touch the floor block when the forks were held horizontally but in a position 3.0 m vertically above the floor block. Releasing a block from the forks was achieved by repeated tilting and jolting. To varying degrees, the tilting causes the back of the forks to rise while the front also drops a little. To ensure the drop height was a minimum of 3.0 m each block was held in the horizontal forks and lifted so that the knot was judged to be at 0.5 m (within +/- 0.1m) above the floor block prior to tilting. This procedure was judged to give a free-fall height (depending somewhat on block size and shape) of 3.3 +/- 0.3m with some additional velocity due to sliding along the forks prior to falling (See Fig.1).

3.5 Weighing of blocks

The Komatsu and CAT both have weigh cells based on hydraulic pressure measurement. Usually these are considered to be of unreliable accuracy when weighing armourstones inside buckets or shovels. However, with the fork attachments and a consistent weighing position, the accuracy is much greater. The Komatsu's weight readings were said to have been compared recently with weighbridge values obtained for armourstones brought from the quarry area and the two weights were reported to be consistently within 50 kg of each other. A value of 50 kg was also said to be the smallest division on the Komatsu's weight reading instrument. For the purpose of the drop test, it was considered that an accuracy of about 50 kg was achieved which for a 4 tonne block is well under 2%. The CAT was said to be of similar accuracy but with a systematic bias and was, therefore, not used for the test weighing.

4. RESULTS

4.1 Qualitative Observations

These were recorded together with the weight measurements using a drop test data proforma. For each of the 50 blocks tested on the 16th and 17th July 1992, notes were made on the following:

(i) the type of rock (Tv or Tj);
(ii) if visible partial flaws (ones affecting minor parts of the block and/or are non-traversing) or, traversing flaws (ones affecting major parts and are fully traversing) are present;
(iii) if the block is estimated to have a length/thickness > 3;
(iv) the type of breakage observed, if any;
(v) if the block landed with a face to face contact.

The qualitative results from the drop test on 50 randomly sampled blocks were as follows:

(i) the Tv and Tj blocks showed no significant difference in breakage behaviour;
(ii) the first 25 blocks contained 7 Tj blocks while the second 25 blocks contained 14 Tj blocks;
(iii) eight blocks with visible partially or fully traversing flaws did not break open along these flaws upon impact, see block 9 after testing, Fig. 4;
(iv) two blocks with visible partial and fully traversing flaws did break on impact;
(iv) significant breakage occurred in five blocks with no visible flaws detected, see block 23 which split into two major pieces, probably along an undetected crack, Fig. 5;

(v) only one of the 50 blocks broke completely into fragments of less than 4 tonnes (the ELCL weight referred to in the test method);
(vi) the blocks falling from the forks tended to spin in the air with unpredictable consequences upon impact;
(vii) a face to face impact appears to be more likely to cause breakage than a point or edge on face impact which tends to produce crushing at the impact point (usually of minor significance) and resultant rolling of the fallen block.

The visibility of pre-existing flaws and fine veins would have been enhanced by wetting of blocks. This practice was not used for the preliminary examination of blocks for this drop test. It should be noted that in about 80% of the 50 blocks selected at random, there was no visible indication of the slightest flaw of any significance in these homogeneous crystalline blocks. This, in the authors' experience, is a high proportion for an armourstone stockpile prepared for loading.

4.2 Calculation of the drop test breakage index, I_{d50}

The cumulative curves of the weight distribution before and after drop testing, together with the total weight before testing and the total weight after testing greater than the ELCL (4 tonnes), is all that is required for the calculation of I_{d50}. The cumulative curves and total weights can be calculated rapidly with the aid of a calculator using class intervals such as 6.0 to 6.5, 6.5 to 7.0 etc. as set out on a pro-forma. Alternatively, most computer spread sheet programs with sort routines can give the precise cumulative data points, one for each of the blocks. This procedure was not adopted in this paper as the use of class intervals is the recommended practical procedure for generating cumulative plots from the weight distribution test (CIRIA/CUR). It is not clearly stated but is implicit in the test method that interpolation should be used to obtain W_{50} from cumulative curves derived from class intervals. The test description does not specify whether W_{50} should be calculated from a linear interpolation between numeric data, or be estimated from a graph. The latter would not be sufficiently accurate.

Applying the definitions given below (Section 6.1), the drop test breakage index is given by the following equation:

$$I_{d50} = (W_{50i} - W_{50f})/W_{50i}$$

The cumulative curves for the Larvik test are shown in Figs. 7 and 8. The class interval data has been used to interpolate W_{50} values from which I_{d50} was calculated to be 3.9%.

5. DROP TESTS ON CARBONIFEROUS LIMESTONE

5.1 Mendip limestone

The quarry did not have sufficiently accurate weighing equipment to perform the test in the quarry. Carboniferous limestone blocks in the 6 to 10 tonne standard grading were supplied from the Mendip area and transported to the coastal site of Elmer, W Sussex where a sample was subjected to the CIRIA/CUR drop test on 24th February 1992.

A Caterpillar 245 with grab and weigh cell accurate to 10 kg was used. A bedstone layer (10-200 kg) was laid out to 0.5 m thick on top of which 6 pieces of armourstone were laid. The sample of 54 stones consisted of blocks mostly between 8 and 8.5 tonnes in weight. The 3 m drop height was controlled with the aid of an EDM. It was reported that the sample blocks appeared to have no planes of weakness, however, 3 blocks completely shattered and personnel took cover to avoid being hit by flying rock. The "windscreen" of the machine operator's cabin was also fitted with a metal grille for protection.

The I_{d50} value was calculated to be 3.0%.

5.2 Calais limestone

Carboniferous limestone blocks, evenly distributed within the 6 to 10 tonne standard grading, were drop tested in the quarry (Fig. 6) on 15th and 16th December 1992. A bucket attachment had to be used with the hydraulic excavator and the drop height was set with a calibrated metre staff. The extension of the loaded excavator at 3 m height was noted and used for subsequent guidance with re-calibration as necessary. An accuracy in fall height of +/- 0.1m was a difficult tolerance to meet with the quarry plant available.

Out of 50 blocks tested, 4 were reduced to pieces less than the ELCL weight of 4 tonnes. However, perhaps surprisingly, the I_{d50} value was calculated to be only 2.2%.

6. DISCUSSION OF DROP TEST RESULTS

6.1 Alternative Indices of breakage

Definitions:

W_{50i}	50 % passing wt. from the initial sample containing only blocks > ELCL
W_{50f}	50 % passing wt. after drop testing but containing only blocks > ELCL
W_{50ft}	50 % passing wt. after drop testing containing all pieces including < ELCL
N	Number of blocks > ELCL
W_{em}	Average weight of blocks > ELCL
ΣW	Total weight of blocks > ELCL
W_{15}	15% passing weight

Alternative Indices of breakage:

$$I_{d50t} = (W_{50i} - W_{50ft}) / W_{50i}$$

The index I_{d50t} takes account of the true shift in W_{50} resulting from impacts because the final weight distribution includes all pieces less than the ELCL weight. Assuming that no secondary selection is possible, this would be the true W_{50} in the built armour layer, although in practice, most fragments are left behind or used elsewhere.

$$I_{dem} = (W_{emi} - W_{emf}) / W_{emi}$$

The index I_{dem}, is useful and simple to determine, if the test is to be carried out on smaller gradings than say 1 to 3 tonnes, since a bulk weighing and block counting procedure is all that is required before and after the 50 drops.

$$I_{dloss} = (\Sigma W_i - \Sigma W_f) / \Sigma W_i$$

The percentage of rock by weight that is no longer in the original grading class (or < ELCL) after the test, i.e. the % that is potentially out of weight specification or unusable, is identified by the index I_{dloss}.

$$I_{d15} = (W_{15i} - W_{15ft}) / W_{15i}$$

The shift in the 15% weight is given by the index I_{d15} which probably most accurately reflects the tendency to produce breakages and fragments principally resulting from type 2 breakages. These indices are now considered alongside the cumulative curves for the three rocks tested, (see Figs. 7, 8 and 9).

5.2 Comparison of drop test results from Larvik syenite, Mendip and Calais limestone -- discussion.

The breakage performance of the different rock sources, the alternative indices of breakage and the test method problems can now be discussed.

Breakage of different rock sources

Cumulative curves given in Fig. 8 for the initial weights and the total final weights i.e. including all the broken pieces, indicate clearly that breakage and the generation of under-weight pieces is most pronounced in the Calais stone (30% less than 6 tonnes which is well out of specification for a standard 6 to 10 tonne grading), while considerably fewer breakage losses occur in the Larvik and Mendip stone (10% less than 6 tonnes).

Fig. 9 (individual block weight loss data was not available for Calais), emphasises some important differences in types of breakage. The Larvik stone only rarely generates any fragments of more than a few kilograms and the weight loss data plotted practically within the precision of the weighing apparatus. Occasionally however (8 blocks), significant pieces, amounting to losses of about 1 tonne or more, broke off mainly in type 1 breakages. For the Mendip stone, the total weight of pieces breaking off, most probably by type 2 breakages, is typically 100 to 1000 kg. However, only 3 blocks appeared to give significant type 1 breakage and these were plotted for convenience as having final weights of 2 tonnes (i.e. losses of about 6 tonnes) although they were reported to have 'completely shattered'. The Calais stones tested suffered 4 block breakages in which the final weights fell below the 4 tonnes value; from Fig. 8 and it may be suggested that Calais stone suffered somewhat more type 1, and significantly more type 2 breakages than Larvik and Mendip stone.

TABLE 1 Summary of results

Parameter	Larvik Syenite	Mendip Limestone	Calais Limestone
W_{50i}	8.17	8.30	7.78
W_{50f}	7.87	8.05	7.61
W_{50ft}	7.71	7.95	7.33
N_i	50	53	50
N_f	49	50	46
W_{emi}	8.06	8.31	7.57
W_{emf}	7.73	7.92	7.06
ΣW_i	402.85	440.49	378.47
ΣW_f	378.55	395.82	324.71
W_{15i}	6.95	8.02	6.51
W_{15f}	6.70	7.60	5.97
W_{15ft}	6.55	7.29	4.09
I_d	3.9	3.0	2.2
I_{dt}	5.6	4.2	5.8
I_{dem}	4.1	4.7	6.7
I_{dloss}	6.0	10.1	14.2
I_{d15t}	5.8	9.1	37.2

Note: Results are calculated using interval data for the weight distributions.

All three samples of armourstone exhibited at least good block integrity with few type 1 breakages. The tendency to produce fragments from type 2 breakages could however become significant for a real armourstone project using the limestones especially the Calais limestone if it transpired that the 3 tonne drop height is representative of the cumulative loads during handling and placement.

It is to be expected for reasons relating to dimensionstone production methods that blast-induced damage will be minimized in the Larvik stone. Also, quarries producing armourstone as a specialist product often will be able to minimize blast damage. However, where armourstone is a by-product to aggregate production, as with both limestone quarries, blast induced cracking of big blocks will arguably be more common.

For the Mendip limestone, which was tested on site, the sample was checked to remove cracked and flawed blocks. Also, the test blocks have undergone 'proving' during handling and transport by lorry to site and the weakest blocks may already have been broken and are thus not available for testing. For these reasons, results for tests at site and in the quarry cannot be compared directly when assessing different sources of material. The sampling method chosen for the Larvik drop test was designed to be representative of the material in stockpiles and a further selection is possible during loading. A further selection is always possible during loading of barges, although every block brought to the quay is already selected as fit for armourstone export.

The mineral fabric strength due to the strong coarse minerals in the Larvik syenite tend to inhibit both type 2 breakages and catastrophic propagation from tips of partially traversing cracks during the drop test, unless the landing geometry gives a face to face or other optimal contact on impact. Only one Larvik block split up totally into pieces below 4 tonnes. In fact this block was slightly slabby and was dropped twice because the first fall was inaccurate and only glanced the corner of the floor block. It shattered on the second drop probably because of the highly damaging tensile bending stresses from the first impact. Such impacts were not intended in the test method and therefore this block should not perhaps have been included in the results. Nonetheless, this result was included because it was considered probable that the effect of variations in drop conditions were averaged out sufficiently when the overall result was expressed using the various statistical breakage indices based on these 50 blocks.

Alternative breakage indices

All the indices in Table 1 were calculated from interval (see Fig. 7) rather than continuous (Fig. 8) cumulative data. Considering the index I_{d50} alone, Larvik, Mendip and Calais stones have performed very well in the drop test (all < 4%), especially since 6-10 tonne gradings are extremely heavy and considerable breakage might be expected. It is interesting to note that the tentative suggested acceptance value given in the CIRIA/CUR Rock Manual for I_{d50} is 5%. This value was chosen for the expected breakage of blocks in the 3-6 tonne range, also to be dropped from a height of 3 m, for which the energy to be dissipated on impact is about half that for the 6-10 tonne range.

The very low value of I_{d50} for Calais stone is somewhat fortuitous because several blocks weighing less than 4 tonnes after testing are excluded from the analysis. On the basis of I_{d50t}, the percentage losses are slightly greater, and probably more meaningful, with the performances of all three rock samples being about the same. However, these two indices (based on 50% passing values), when taken in isolation, can be somewhat misleading. Other indices tell a different story. For example, results for I_{dloss} indicate a greater proportion of Calais stone (14.2%) and Mendip stone (10.1%) becomes 'unusable' when compared with Larvik stone (6.0%). In other words, within the specified 6-10 tonne grading class, these percentages (in perethesis) by weight fall below 4 tonnes.

The practical implication, assuming that the test simulates damage during transport and construction, is that, while removal of pieces less than 4 tonnes (for example by secondary selection after delivery to site) will retain a grading in which W_{50}

has been reduced by only 3.9 and 3.0 and 2.2%, for Larvik, Mendip and Calais stone respectively, the equivalent losses of material from the specified grading are about 6.0, 10.1 and 14.2%.

An appropriate and sensitive index definition might be one based on the shift in the cumulative curve at the 15% passing value based on the total weights and not just the pieces > ELCL. In Table 1 above, I_{d15t} (as well as I_{dloss}) indicates that Calais limestone is significantly weaker than Larvik syenite.

From the above discussion it is suggested that I_{dloss} tends to measure susceptibility to type 2 breakage whilst I_{d50t} measures type 1 breakages, or block integrity more effectively. This also suggests that a good relationship might existbetween I_{dloss} or $I_{d1<}$ and intact strength measures such as fracture toughness or point load strength .

Problems with the test method

The sample must be representative. There will always be some scope for removing blocks which show cracks and flaws prior to testing. Consistency must be applied so that drop test results from a given source should refer to armourstone stocks prepared for dispatch and already screened for cracks etc. The sample should span the full range of weights in the grading evenly.

Many quarries do not have the ideal type of grab (orange peel) for accurate drop height control, nor the apparatus for weighing blocks with appropriate accuracy. Fork attachments and buckets lead to uncertainties in drop height but can help randomize the way in which the stones are dropped and the consequent type of impact resulting. Face on face contacts are more damaging and are potentially more easily avoided, or contrived, by the operator of a grab. Preparation of the substrate layer of rocks must be carried out carefully according to a precise description to reproduce impact damping conditions and in order to produce a large enough, approximately flat surface, so that blocks cannot fall onto edges.

The test appears dangerous but need not be if proper precautions are taken. It is already expensive to perform and for the test to be completed in one day, the number of blocks should not exceed 50. However, 50 blocks is surely the minimum number from which a statistically discriminating index can be derived, particularly as the way the block falls can affect the result.

The treatment of results poses certain problems. The cumulative curves from continuous data and interval data can differ significantly for the range of accuracies required (compare Figs. 7 and 8 for Larvik stone which give a value for I_{d50} of about 7% for continuous data rather than the 3.9% obtained). The indices derived from interval data are very sensitive to mistaken interval classification of block weights suggesting that continuous data analysis would be preferable.

Drop testing of light and heavy gradings from 6 - 10 tonnes down to 10 - 60 kg could give invaluable information on fragility that could not be measured by other means such as intact tests. Details of testing conditions such as fall heights and substrate conditions remain to be established for the lighter gradings.

Not until a significant build-up of experience with these methods has occured will drop tests and their acceptance values for a particular index become common usage. It is strongly urged that research into direct and indirect test methods for block integrity and their correlations is undertaken. This would provide objective practical solutions for quality control problems that are repeatedly met when left to subjective criteria.

6 CONCLUSIONS

The CIRIA/CUR drop test is an important step towards objective controls on block integrity. There are however a number of problems that require further research before the test can be used routinely for quality assesment.

The CIRIA/CUR Drop Test Breakage Index, I_{d50}, is likely to be an unreliable indication of block integrity and there are better ways of analysing the results of the drop test.

Test conditions of sampling, fall height, and substrate were not entirely comparable for the three tests but it is unrealistic to expect much greater control of testing conditions for a practical quarry test.

The drop test is a promising test principle for assessing the resistance to breakage of armourstone and riprap blocks during handling and in service, with the probable exception of freeze-thaw breakage mechanisms that can sometimes occur in porous rock types that do not have cracks and flaws.

The results of this preliminary research are not conclusive but point towards the possible use of alternative indices based on changes in the weight distribution before and after testing, as defined in this paper. For example, the 15% passing index, I_{d15t}, and the 50% passing index, I_{d50t}, may provide the best indicators of damage by type 2 and type 1 breakage respectively, while as an overall indication of fragility, I_{dloss} appears to be the most suitable parameter.

7 ACKNOWLEDGEMENTS

The authors wish to thank Larvik Armourstone, Robert West and Partners and the owners of the French limestone quarry for granting thempermission to publish the results of drop tests in this paper. We are extremely grateful for the work of Gerard Laan in the generation of ideas and the promotion of research in this subject. Through his involvement with the CIRIA/MANUAL, Jonathan Simm of Hydraulics Research, Wallingford, has assisted greatly in pushing the drop test into the practical domain from where we can begin to learn.

8 REFERENCES

British Standards Institution (1984), Code of Practice for maritime structures: Part 1 General Criteria, BS 6349.

Clark A R & Palmer J S (1991), The problem of quality control and the selection of armourstone *Q. J. Engng. Geol. London.* **24**, pp. 119-122.

CIRIA/CUR (1991), Manual for the Use of Rock in Coastal and Shoreline Engineering. Published jointly by the Construction Industry Research and Information Association in the UK and the Centre for Civil Engineering Research, Codes and Specifications in the Netherlands.

Fookes P G & Poole A B (1981). Some preliminary considerations on the selection and durability of rockand concrete materials for breakwaters and sea defence works. *Q. J. Engng. Geol. London.* **14** pp. 97-128.

ISRM, (1985), Suggested method for determining point load strength: Intl. Soc. Rock Mech. Comm. on Testing Methods, *Int. J. Rock Mech. Min. Sci. & Geomech. Abstr.* 22, pp. 51-60.

ISRM, (1988), Suggested methods for determining the fracture toughness of rock. F. Ouchterlony (Co-ordinator): Intl. Soc. Rock Mech. Comm. on Testing Methods, *Int. J. Rock Mech. Min. Sci. & Geomech. Abstr.* 25, pp. 71-96.

Laan, G J, (1992), Quality assurance of armourstone in practice. Report on the Proceedings of the Seminar on Armourstone. Queen Mary and Westfield College, London University.

LCPC, (1989), Les Enrochments, Ministere de L'Equipement, du Logement, des Transports et de la Mer, Laboratoires Central des Ponts et Chaussees, 107 pp.

Lutton R J & Erickson R L, (1992), Problems with armor-stone quality on Lakes Michigan, Huron and Erie. Proceedings of the Workshop on Durability of Stone for Rubble Mound Breakwaters. Eds. O.T. Magoon and W. F. Baird. ASCE publication. pp. 115-136.

Marcus D W (1992). Recent experience with armor stone cracking in the Buffalo District. Proceedings of the Workshop on Durability of Stone for Rubble Mound Breakwaters. Eds. O.T. Magoon and W. F. Baird. ASCE publication. pp. 222-237

Niese M S J, Van Eijk F C A A, Laan G J & Verhoef P N W (1990). Quality assessment of large armourstone using an acoustic velocity analysis method, *Bulletin of the International Association of Engineering Geology*, **42**, pp 55-65.

Ward D L (1992). Physical Model Testing of Broken Armor Stone. Proceedings of the Workshop on Durability of Stone for Rubble Mound Breakwaters. Eds. O.T. Magoon and W. F. Baird. ASCE publication. pp 34-39.

Figure Captions

Figure 1 The Drop test set-up showing the floor block used for the first 25 drops with ramp and CAT position at the moment of drop testing. Note also the measuring rope and the armourstone stockpile in the background.

Figure 2 Floor blocks and set-up used for the second 25 blocks.

Figure 3 Breakage to floor block giving two broken halves but these remain within the required grading for floor blocks. This break became apparent only after testing block 50.

Figure 4 Block 9 after testing, showing a partially traversing flaw consisting of a rare type of wavy joint surface, which remained intact.

Figure 5 Block 23 which landed with a nearly face to face contact and split into two major pieces of 4.45 and 3.10 tonnes along an undetected crack.

Figure 6 Drop test set-up at the quarry in the Calais region of France. Block fall height is more difficult to control from a bucket attachment than a grab.

Figure 7 Cumulative weight distribution plots calculated from 0.5 tonne interval data for the three armourstone samples tested. The initial and final cumulative curves W_i, W_f and W_f of total, are explained in the text.

Figure 8 Cumulative weight distribution plots calculated from continuous data using each of the 50 block weights directly, for the same three armourstone samples tested in Fig. 7. The initial and final cumulative curves W_i, W_f and W_f of total, are explained in the text.

Figure 9 Weight losses for each of the Mendip and Larvik blocks tested.

Figure 1

Figure 2

Figure 3

Figure 4

Figure 5

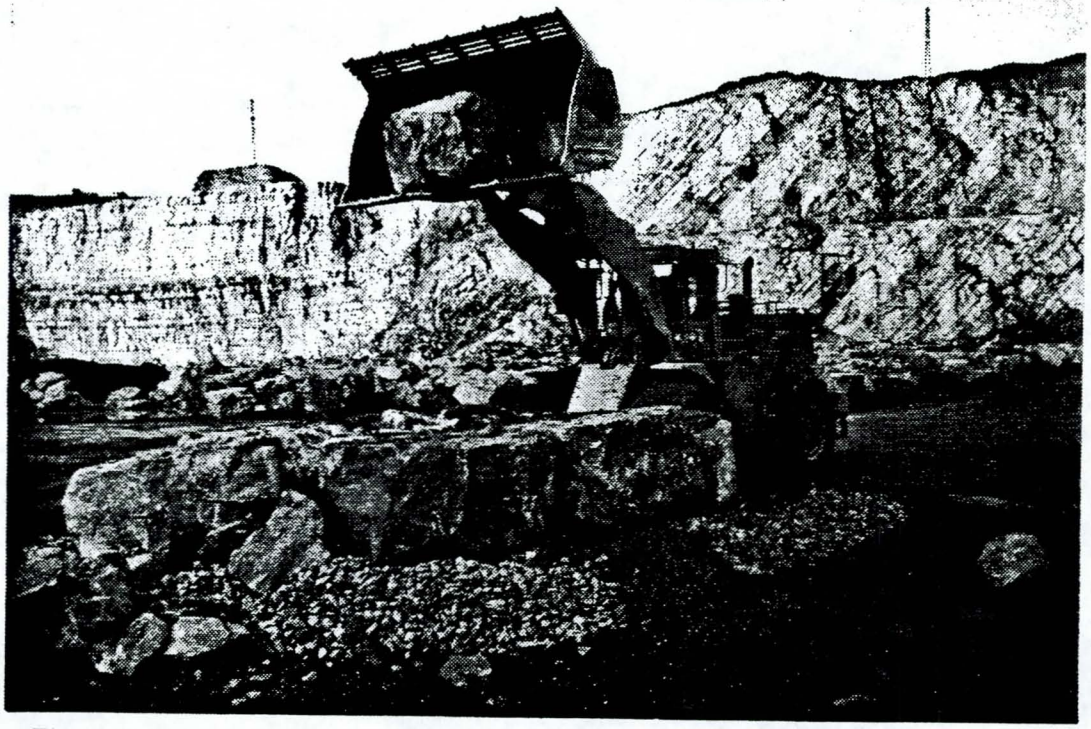

Figure 6

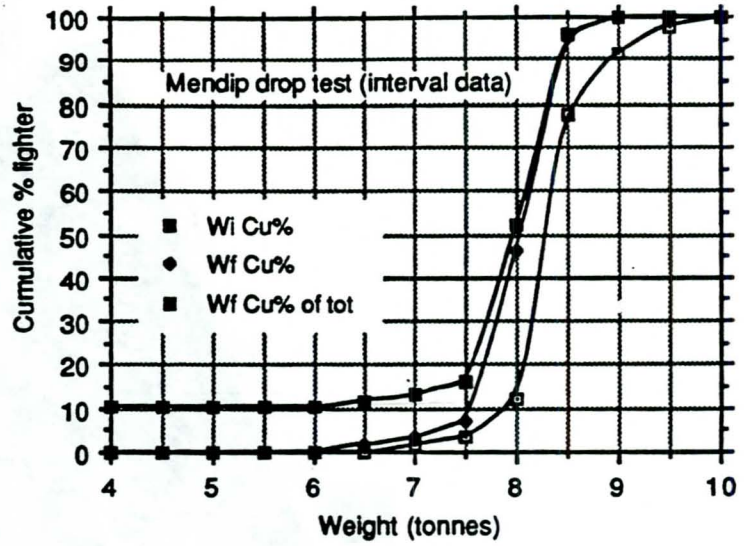
Mendip drop test (interval data)
Cumulative % lighter
Wi Cu%
Wf Cu%
Wf Cu% of tot
Weight (tonnes)

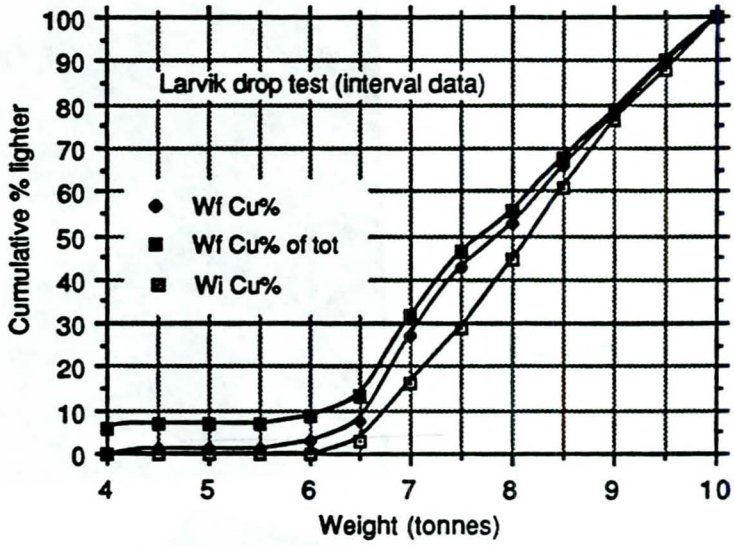
Larvik drop test (interval data)
Cumulative % lighter
Wf Cu%
Wf Cu% of tot
Wi Cu%
Weight (tonnes)

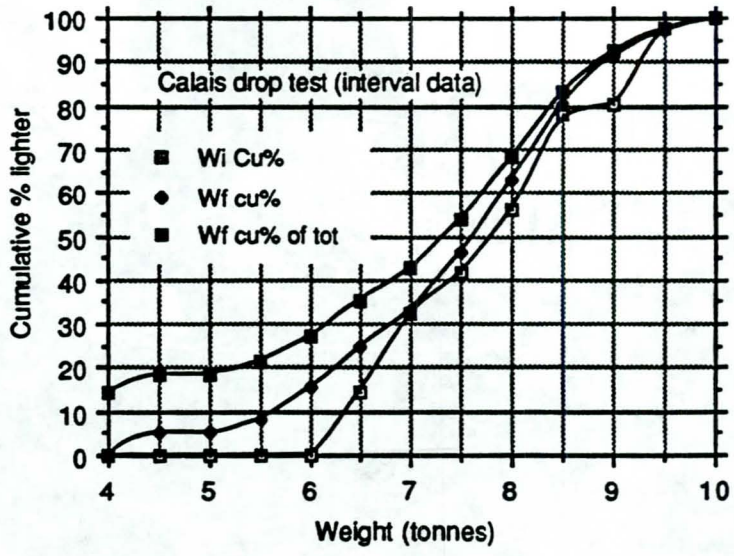
Calais drop test (interval data)
Cumulative % lighter
Wi Cu%
Wf cu%
Wf cu% of tot
Weight (tonnes)

Figure 7

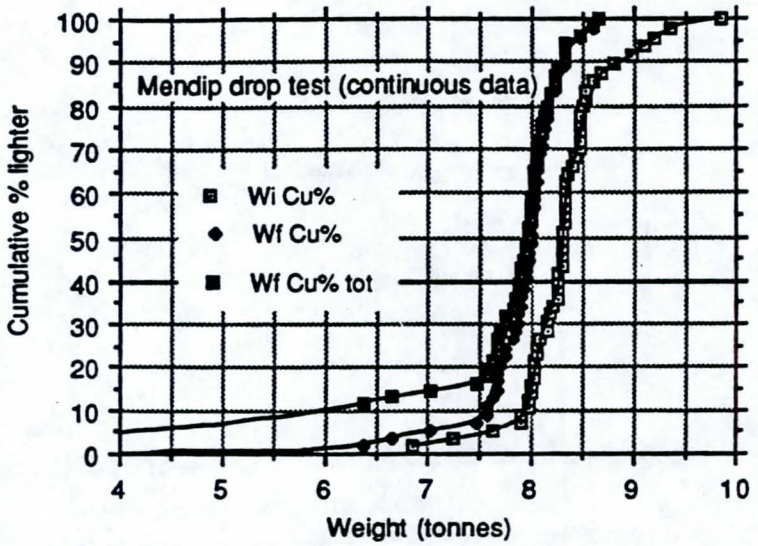
Mendip drop test (continuous data)
Cumulative % lighter
Weight (tonnes)
Wi Cu%
Wf Cu%
Wf Cu% tot

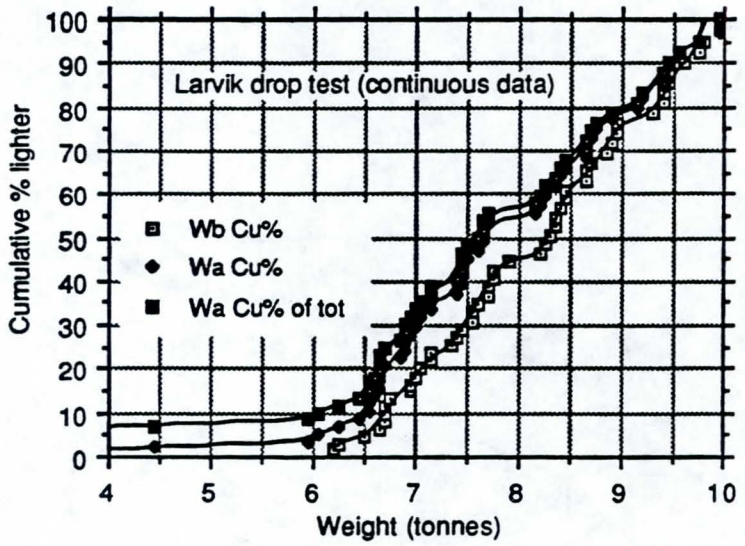
Larvik drop test (continuous data)
Cumulative % lighter
Weight (tonnes)
Wb Cu%
Wa Cu%
Wa Cu% of tot

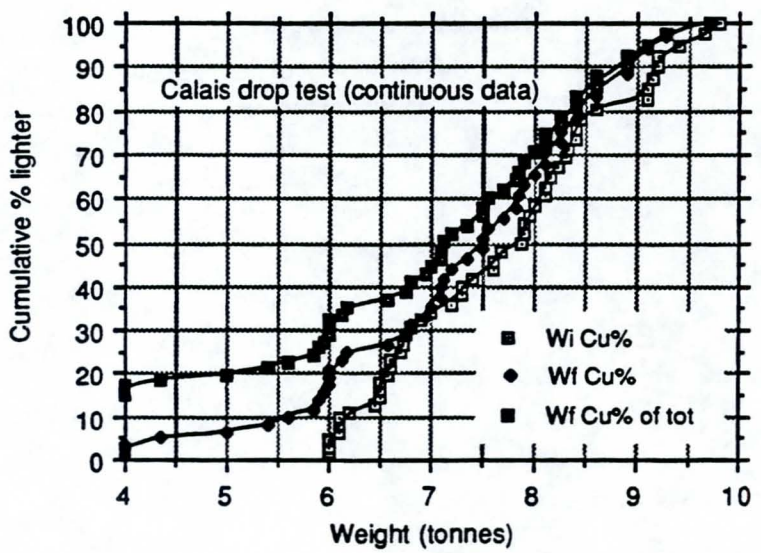
Calais drop test (continuous data)
Cumulative % lighter
Weight (tonnes)
Wi Cu%
Wf Cu%
Wf Cu% of tot

Figure 8

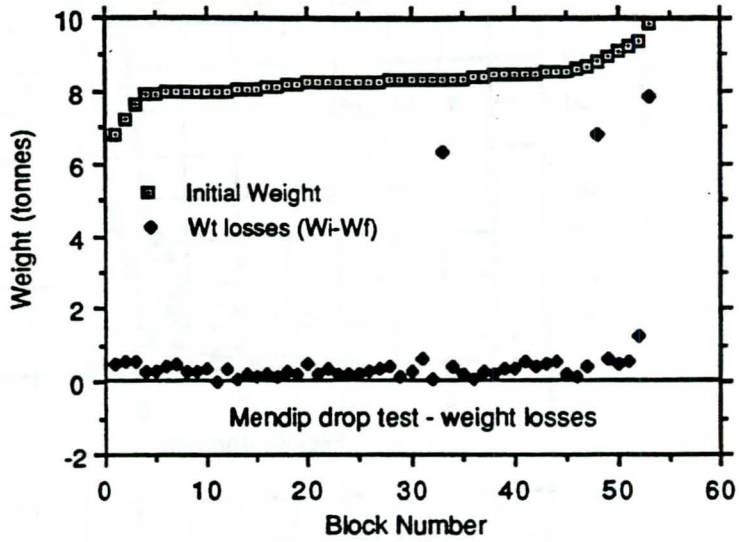
Weight (tonnes)
Initial Weight
Wt losses (Wi-Wf)
Mendip drop test - weight losses
Block Number

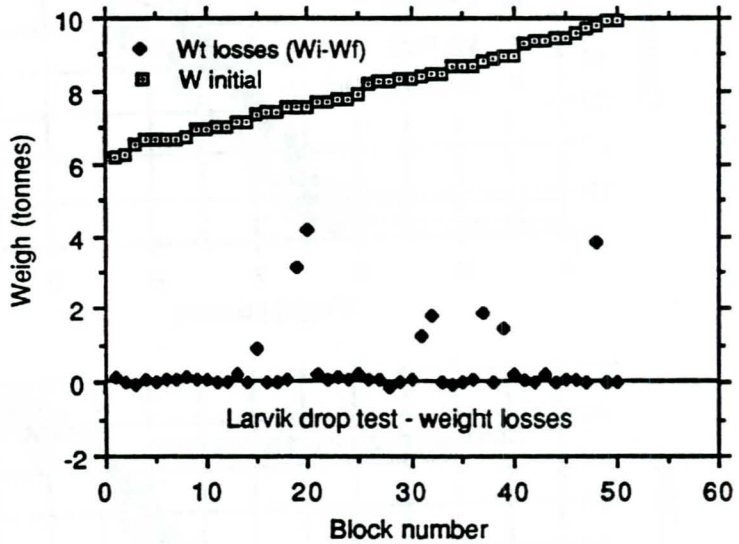
Weigh (tonnes)
Wt losses (Wi-Wf)
W initial
Larvik drop test - weight losses
Block number

Figure 9

MINIMIZING COSTS OF STREAMBANK PROTECTION USING RIPRAP

By Warren J. Mellema, P.E.
Deputy Director, HTRW and Engineering Directorate
Missouri River Division, Corps of Engineers
Omaha, Nebraska USA

ABSTRACT

The advantages of using stone riprap as a means of controlling streambank erosion are well known and accepted, and many successful projects have been built over the years under a wide variety of field conditions. The well documented advantages of using stone riprap (availability, low cost, ease of construction, ease of repair, flexibility, etc.) are well known and accepted; however, these features in and of themselves do not ensure a low cost project that will withstand required economic tests. Streambank protection techniques must be both technically effective and economically feasible in order to be acceptable to the local entity required to pay for the installation.

This paper will discuss several techniques that have been developed in an attempt to provide streambank protection at the least cost. Primary emphasis will be on streams with high vertical banklines where streambank protection costs are often excessive, and where pressure is put on the designer to minimize costs. Techniques that will be discussed will include stone windrow revetment, intermittent streambank protection techniques,

using riprap, composite riprap and vegetation revetments and sand filled dikes protected by riprap. The above techniques have proven to keep erosion within tolerable limits at the least cost.

The paper will develop thesis that streambank protection schemes do not have to hold every grain of soil on the bankline to be successful, and design engineers are encouraged to use their ingenuity to develop techniques that will pass both the engineering and cost tests associated with a project.

Abstract

Deterioration of Carbonate Breakwater Stones on Lake Michigan Shoreline

by
Kevin R. Stank[1]
and Mirsa M. Baig[2]

The U.S. Army Corps of Engineers has been inspecting and providing maintenance of breakwaters along the southern Lake Michigan shoreline since the late 19th century. During the last 100 years significant changes have been made in breakwater structure designs and construction materials. Rubble mound breakwater commonly in use today allow for reduced construction costs through quick placement of low cost locally produced materials. However, maintenance costs have increased due to rapid deterioration of the materials. In some cases the entire structures were required to be rehabilitated after only 10 years. The alternative is to use higher cost materials and tighten the QA and QC criteria.

Lake Michigan is located on the western flank of the Michigan Basin. Silurian aged rocks subcrop beneath glacial sediments on the west side of Lake Michigan, gently dipping 10-15° east into the Michigan Basin. Some of these rocks, such as dolomite have been utilized in breakwater construction.

During the early part of the 20th century the large expansion of the steel industry created a need for sources of steel flux. The subcrops of Silurian aged carbonate rocks (dolomite) provided excellent flux material to the steel industry. As a result the economics eventually shifted, favoring purchase of less expensive dolomite stone for breakwaters. Dolomite quarries are now providing the bulk of material being used to rehabilitate old breakwaters utilizing rubble mound designs, and to build new rubble mound structures.

The selection of breakwater stone sources is driven by two

1.Civil Engineer, Geotechnical and Coastal Branch, Army Corps of Engineers, Chicago District, 111 N. Canal St., Chicago, IL 60606

2.Geologist, Geotechnical and Coastal Branch, Army Corps of Engineers, Chicago District, 111 N. Canal St. Chicago Il 60606

MAR 19 '93 08:44 CH60 DIST INFO_MGT OFC_CENCC-IM P.2

factors; cost and supply. A number of problems have been encountered with the use of Silurian dolomite stone because of premature deterioration caused by brittle behavior, and thin interbedded laminations. Delamination, cracking, and disintegration have been observed in dolomite stones after only 3 years of service. The quarry operators generally do not have adequate quality control measures to exclude such stones from delivery. It is also difficult to convince quarry operators to perform adequate quality control, in the absence of having a clear definition of unsuitable stones. Laboratory durability tests are costly and limited and, therefore, do not give a statistically accurate picture of durability from a particular source as a whole. There are sources of highly durable stone, but high cost and an inadequate supply have prevented these sources from being utilized.

Premature stone deterioration has created a maintenance problem for those areas where highly durable stone cannot compete with less durable locally produced stone. Accurate maintenance costs are being developed to evaluate the economic feasibility of using more expensive materials. If expensive materials are not warranted, the design life of the rubble mound structures should be reduced to 10 years. New breakwater designs specifying durable materials in the freeze thaw environment and less durable materials below the water line, may provide an alternative solution to this problem.